



Improving antifungal properties of *Bacillus* spp.

Stancheva, Bodil Kjeldgaard

Publication date:
2023

Document Version
Publisher's PDF, also known as Version of record

[Link back to DTU Orbit](#)

Citation (APA):
Stancheva, B. K. (2023). *Improving antifungal properties of Bacillus spp.* DTU Bioengineering.

General rights

Copyright and moral rights for the publications made accessible in the public portal are retained by the authors and/or other copyright owners and it is a condition of accessing publications that users recognise and abide by the legal requirements associated with these rights.

- Users may download and print one copy of any publication from the public portal for the purpose of private study or research.
- You may not further distribute the material or use it for any profit-making activity or commercial gain
- You may freely distribute the URL identifying the publication in the public portal

If you believe that this document breaches copyright please contact us providing details, and we will remove access to the work immediately and investigate your claim.

Improving antifungal properties of *Bacillus* spp.

Bodil Kjeldgaard Stancheva

Ph.D. thesis

July 2023

Technical University of Denmark
Department of Biotechnology and Biomedicine
Bacterial Interactions and Evolution group



Chr. Hansen A/S
Research & Development



Preface

This Ph.D. thesis serves as partial fulfilment of the requirements to obtain a Ph.D. degree from the Technical University of Denmark (DTU). The work described in the thesis was conducted from December 2018 to July 2023 in collaboration between the Bacterial Interactions and Evolution group at the Department of Biotechnology and Biomedicine, DTU and Chr. Hansen A/S, Research & Development, Discovery.

The Ph.D. project was supervised by Professor Ákos T. Kovács at DTU, Principal Research Scientist Patricia Dominguez-Cuevas and Department Manager César Fonseca at Chr. Hansen.

The Ph.D. project was funded by the Innovation Fund Denmark (8053-00109B) and Chr. Hansen A/S.

Bodil Kjeldgaard

July, 2023

Acknowledgements

I would like to express my gratitude to my exceptional supervisor team, Professor Ákos Kovács at DTU, Principal Research Scientist Patricia Dominguez-Cuevas, and Department Manager César Fonseca at Chr. Hansen. Your constant support, encouragement and the countless scientific discussions throughout the project have been instrumental for completing my PhD research work. I am truly grateful for the guidance you have provided and the knowledge that you have shared with me. Working under your supervision has been a great pleasure and I have learned a lot.

For their invaluable scientific contribution, I would like to acknowledge following people: Birgit for her Hamilton expertise and fantastic job running the high throughput screening, Ricardo for all biochemical analyses, Anna for whole genome sequencing, Tammi and Kosai for SNP analysis, Martin and Tammi for RNA sequencing analysis, Corinna and Signe for the local AntiSMASH analysis, Stjepan for protease activity assays, Raquel for root colonization guidance, and Iuliana for her great help running experiments, while I attended courses.

To the members of the Bacterial Interactions and Evolution group at DTU, thank you for creating a friendly and supportive environment in the beginning of my PhD journey. Especially, thanks to my office mates Heiko and Carlos, and to Anna for being a true friend. For always making a good atmosphere in the office at Chr. Hansen, I would like to acknowledge former and current office colleagues. Special thanks to Sophia for being a true companion throughout the challenges of the PhD journey. I am also grateful to Signe and Jildau for the many coffee breaks and shared drives to work in good company.

Special thanks to my mother for being a great babysitter during the thesis writing process. Lastly, I am deeply grateful to my husband, Lyubo, for supporting me throughout the entire process and taking so good care of our daughter in my absence.

Abstract

The plant root growth niche is a hotspot for microbial life and interactions of different character between species and kingdoms, ranging from mutualistic and synergistic to antagonistic. The multispecies microbial communities that inhabit the rhizosphere greatly impact plant health. Among the microbial inhabitants, plant growth-promoting rhizobacteria (PGPR) offer beneficial effects to the plant through various mechanisms. Members of the *Bacillus* genus are regularly isolated from the rhizosphere, rhizoplane or phylloplane and possess plant beneficial properties including modulation of nutrient availability, phosphate solubilization, enhancement of abiotic stress tolerance, and plant growth promotion. In addition, *Bacillus* spp. have the potential to produce a vast array of bioactive compounds potentially inhibitory to plant pathogens, positioning these bacteria as promising candidates for biological control strategies in agriculture, particularly for combating fungal phytopathogens.

Alike *Bacillus* spp., the black mold fungus *Aspergillus niger* is frequently identified in soil samples, however, little is known about the interaction between these species. Using bacterial-fungal co-cultures, we investigated the hyphal colonization by *Bacillus subtilis* biofilm mutants and demonstrated that extracellular matrix components are essential for robust biofilm formation on the mycelium. Furthermore, we showed that matrix components are shared, as defective biofilm formation can be rescued by addition of a producing strain. The interaction between the species was further explored by adaptive laboratory evolution of *B. subtilis* in the presence of *A. niger*. The repeated bacterial-fungal co-cultivation promoted enhanced *B. subtilis* niche colonization facilitated by increased colony expansion. The spreading behavior was attributed to increased biosynthesis of the lipopeptide surfactin, which caused fungal cell wall stress and reduced acidification of the medium by the fungus. This phenotype was correlated to genetic changes of the regulatory system DegS-DegU.

Inspired by these results, we explored experimental evolution of natural *Bacillus* isolates in co-culture with phytopathogenic fungi as a strategy to improve the antifungal properties of the bacteria for biocontrol applications. To assess the inhibitory potency of evolved strains, we developed two high throughput screening methods, allowing quantification of antifungal properties and facilitating easy comparison to the respective ancestors. The methods provided insights of the antifungal potency of culture supernatant components or accounted for all the antagonistic mechanisms by co-inoculation of the species.

The *Bacilli* subjected to iterative planktonic growth cycles, in the presence or absence of the grey mold fungus *Botrytis cinerea*, accumulated flagellum-related mutations, conferring loss of motility to the evolved strains. Repetitive growth on solid medium, in the presence or absence of the filamentous fungus *Fusarium culmorum*, fostered adaptation of the quorum sensing system ComP-ComA associated with enhanced niche colonization in confrontation with the fungus, reduced production of antifungal lipopeptides, and increased volatilome effect on fungal growth. In both experimental evolution campaigns, further adaptive changes were detected in transcriptional regulators and cell differentiation pathways, which were associated with multiple phenotypic changes such as altered biofilm morphology, modulated biosynthesis of specialized metabolites and fungal growth inhibition potency. Several adaptation mechanisms focused on energy preservation effects by compromising carbon- and energy-demanding metabolic pathways, demonstrating an evolutionary selection for growth.

In summary, this Ph.D. project contributed to the knowledge of bacterial-fungal interactions and understanding of the *Bacillus* adapted response to fungal co-cultivation. The evaluation of *Bacillus* antifungal potency highlighted the importance of specialized metabolites and additional alternative fungal inhibition mechanisms. Furthermore, the project investigated experimental evolution as a tool for strain improvement for biocontrol purposes.

Danish summary

Vækstnichen omkring planteroden er et hotspot for mikrobielt liv og interaktioner af forskellig karakter mellem arter og kongeriger, lige fra gensidige og synergistiske til antagonistiske. De mangeartede mikrobielle samfund, der bebor rhizosfæren, har stor indflydelse på plantesundhed. Blandt de mikrobielle arter har plantevækstfremmende rhizobakterier (PGPR) gavnlige virkninger på planten gennem forskellige mekanismer. Medlemmer af *Bacillus*-slægten isoleres regelmæssigt fra rhizosfæren, rhizoplanet eller phylloplanet og besidder plantegavnige egenskaber, herunder modulering af næringsstoftilgængelighed, fosfatsolubilisering, forbedring af abiotisk stresstolerance og promovering af plantevækst. Derudover har *Bacillus*-arter potentialet til at producere en bred vifte af bioaktive stoffer, der potentielt hæmmer plantepatogener, hvilket gør disse bakterier lovende kandidater til biologiske kontrolstrategier i landbruget, især til bekæmpelse af plantepatogene svampe.

Ligesom *Bacillus*-arter bliver den sorte skimmelsvamp *Aspergillus niger* ofte identificeret i jordprøver. Dog vides meget lidt om interaktionen mellem disse arter. Ved hjælp af bakterie-svampe co-kulturer undersøgte vi hyfekoloniseringen af *Bacillus subtilis* biofilmmutanter og demonstrerede, at ekstracellulære matrixkomponenter er essentielle for robust biofilmdannelse på myceliet. Desuden viste vi, at matrixkomponenter deles, da defekt biofilmdannelse kan reddes ved tilsætning af en producerende stamme. Interaktionen mellem arterne blev yderligere udforsket ved adaptiv laboratorieudvikling af *B. subtilis* under tilstedeværelsen af *A. niger*. Den gentagne samdyrkning af bakterie og svamp fremmede forbedret nichekolonisering af *B. subtilis*, som blev faciliteret af øget koloniudvidelse. Den udbredende adfærd kunne tilskrives øget biosyntese af lipopeptidet surfactin, som forårsagede stress i svampecellevæggen og reducerede vækstmedieforsuring af svampen. Denne fænotype var relateret til genetiske ændringer af det regulatoriske system DegS-DegU.

Inspireret af disse resultater udforskede vi eksperimentel evolution af naturlige *Bacillus*-isolater i samkultur med plantepatogene svampe som en strategi til at forbedre bakteriernes svampehæmmende egenskaber til biokontrolanvendelse. For at vurdere den svampehæmmende styrke af de udviklede stammer, genererede vi to screeningsmetoder med høj kapacitet, hvilket faciliterede kvantificering af svampehæmmende egenskaber og lettede sammenligning med de respektive bakterielle forfædre. Metoderne gav indsigt i den svampehæmmende styrke af komponenter i kultursupernatanten eller medregnede alle de antagonistiske mekanismer ved samdyrkning af arterne.

Bacillus-bakterierne, der blev udsat for gentagne planktoniske vækscyklusser, i nærvær eller fravær af gråskimmelsvampen *Botrytis cinerea*, akkumulerede flagel-relaterede mutationer, hvilket medførte tab af motilitet til de udviklede stammer. Gentagne vækscyklusser på fast medium, i nærvær eller fravær af svampen *Fusarium culmorum*, fremmede tilpasning af quorum sensing-systemet ComP-ComA. Dette var forbundet med øget nichekolonisering i konfrontation med svampen, reduceret produktion af svampehæmmende lipopeptider og øget effekt volatilomet på svampevæksten. I begge eksperimentelle evolutionskampagner blev yderligere adaptive ændringer påvist i transkriptionelle regulatorer og celledifferentieringsprogrammer, som var forbundet med flere fænotypiske ændringer, såsom ændret biofilmmorfologi, moduleret biosyntese af specialiserede metabolitter og styrke af svampevæksthæmning. Adskillige tilpasningsmekanismer drejede sig om energibevarelse ved at kompromittere kulstof- og energikrævende metaboliske veje, hvilket demonstrerede en evolutionær selektion for vækst.

Sammenfattende har dette Ph.D.-projekt bidraget til vores viden om interaktioner mellem svampe og bakterier samt forståelsen af den tilpassede respons fra *Bacillus* ved samdyrkning med svampe. Evalueringen af *Bacillus*' svampehæmmende styrke fremhævede vigtigheden af specialiserede metabolitter samt yderligere alternative mekanismer for hæmning af svampevækst. Endvidere undersøgte projektet eksperimentel evolution som et værktøj til stammeforbedring til biokontrolformål.

Table of content

Preface.....	I
Acknowledgements	II
Abstract	III
Danish summary.....	V
Table of content	VII
Publications and studies.....	IX
Chapter 1 General introduction and thesis outline	1
1.1 Agricultural challenges	1
1.2 Purpose and specific aims	3
1.3 Thesis content and structure.....	4
Chapter 2 <i>Bacillus</i> -fungus interactions	5
2.1 Introduction to <i>Bacillus</i>	5
2.3 Bacterial-fungal interactions	9
<i>Bacillus</i> interactions with <i>Aspergillus niger</i>	11
Chapter 3 Fungal inhibition properties of <i>Bacillus</i> spp.....	16
3.1 Bioactive metabolites and modes-of-action against fungal phytopathogens.....	17
Cyclic lipopeptides.....	17
Lytic enzymes.....	23
Nutrient and niche competition	24
Volatile organic compounds.....	25
Priming of plant defense	26
3.2 Methods for assessing fungal inhibitory potential of <i>Bacillus</i> spp.....	27
3.3 Evaluation of fungal inhibitory potential of natural <i>Bacillus</i> isolates.....	30
Chapter 4 Cell differentiation in <i>Bacillus</i>	34
4.1 Quorum sensing.....	34

Sensing and responding to a community	34
Quorum sensing mutants emerge during experimental evolution	36
4.2 Developmental pathways	37
Competence development	37
Sporulation and cannibalism	38
Biofilm, the natural bacterial growth form	39
Regulation of biofilm formation	40
Biofilm matrix components	41
Matrix components are shared among community members and enable fungal attachment	42
Quorum sensing mutants display altered biofilm	43
Degradative enzyme production and motility.....	45
Experimental evolution in suspension selects against motility.....	47
Chapter 5 <i>Bacillus</i> adaptation to fungi	49
5.1 Adaptive laboratory evolution (ALE)	49
5.2 Experimental design of microbial ALE	50
5.3 Bacterial ALE with fungi and different modes-of-action for fungal inhibition	53
5.4 <i>Bacillus</i> -fungi ALE dynamics and trends	60
Chapter 6 Conclusions and perspectives	64
References	67
Research articles.....	97

Publications and studies

The Ph.D. thesis is based on following studies:

Study 1: Kjeldgaard, B., Listian, S. A., Ramaswamhi, V., Richter, A., Kiesevalter, H. T., and Kovács, Á. T. (2019). Fungal hyphae colonization by *Bacillus subtilis* relies on biofilm matrix components. *Biofilm* 1, 100007. doi:10.1016/j.bioflm.2019.100007.

Study 2: Richter, A., Blei, F., Hu, G., Schwitalla, J. W., Lozano-Andrade, C. N., Jarmusch, S. A., Wibowo, M., ***Kjeldgaard, B.**, Surabhi, S., Jautzus, T., Phippen, C. B. W., Tyc, O., Arentshorst, M., Wang, Y., Garbeva, P., Larsen, T. O., Ram, A. F. J., Hondel, C. A. M., Maroti, G., and Kovacs, A. T. (2023). Enhanced niche colonisation and competition during bacterial adaptation to a fungus. To be submitted, preprint deposited in bioRxiv, 2023.03.27.534400. doi:10.1101/2023.03.27.534400.

Study 3: Kjeldgaard, B., Neves, A. R., Fonseca, C., Kovács, Á. T., and Domínguez-Cuevas, P. (2022). Quantitative High-Throughput Screening Methods Designed for Identification of Bacterial Biocontrol Strains with Antifungal Properties. *Microbiology Spectrum*. Vol. 10, Issue 2. doi:10.1128/spectrum.01433-21.

Study 4: Kjeldgaard, B., Fonseca, C., Kovács, Á. T., and Domínguez-Cuevas, P. Assessment of antifungal potential of natural *Bacillus* spp. isolates. To be submitted.

Study 5: Kjeldgaard, B., Fonseca, C., Kovács, Á. T., and Domínguez-Cuevas, P. Improving biocontrol ability of *Bacillus* spp. against *Fusarium culmorum*. To be submitted.

Study 6: Kjeldgaard, B., Fonseca, C., Kovács, Á. T., and Domínguez-Cuevas, P. Adaptive evolution of *Bacillus* spp. against *Botrytis cinerea*. To be submitted.

**minor contribution*

Chapter 1 | General introduction and thesis outline

1.1 Agricultural challenges

In 2022, the global population reached 8 billion putting on unprecedented productivity pressure on agriculture. Projections indicate that by 2050, the aggregated global consumption of agricultural products is expected to surge by 60% compared to the levels observed in 2005/2007 (1). Consequently, the agricultural sector faces extraordinary challenges to meet the increased demand for food and ensure global food security. The Food and Agriculture Organization of the United Nations (FAO) estimates an annual crop production loss of 20-40% due to plants pests, including plant pathogenic fungal species. Annually, plant diseases lead to economic losses of approximately US\$220 billion globally (2). Furthermore, it is estimated that global climate changes will entail an increased threat to agriculture crops by plant pests, including plant pathogenic fungi, due to altered pathogen distribution, pathogen abundance, and disease severity (3). Fungal phytopathogens contribute to detrimental crop damages and cause massive economic losses to agricultural production worldwide (4, 5). Species from the *Fusarium graminearum* complex comprise phytopathogens that infect important cereal crops including barley, oat, rice and, in particular, wheat (6), whereas the generalist pathogen *Botrytis cinerea* infects soft tissues such as fruits, vegetables, and flowers in a range of more than 200 plant varieties (7). Specifically, *Fusarium* phytopathogens contribute to post-harvest yield losses or harvest quality deterioration by accumulation of mycotoxins in grains, thereby rendering the crop unfit for human or animal consumption (8, 9), while *B. cinerea* often manifests post-harvest in seemingly healthy plants leading to drastically reduced yield (10, 11).

Commonly, plant diseases caused by fungal pathogens are prevented or treated using chemical fungicides, accounting for 17.5% of the global pesticide usage. Although,

application of pesticides remedy plant diseases, leading to increased yield and quality, the chemicals constitute a potential risk to ecosystems. Especially heavy use of pesticides leads to leaching into soil and water bodies affecting microflora, insects, and wildlife (12). These chemicals potentially pollute groundwater supplies, magnify in food chains, or remain as residuals in food (13, 14). Besides being environmentally hazardous, pesticides also imply potential short-term as well as chronic impacts on human health. Moreover, fungicide-resistant phytopathogenic fungi arise globally. *Botrytis cinerea* overcomes fungicide sensitivity by genetic changes of target genes or by increased expression of drug efflux transporters (15, 16), an adaptation also employed by fungicide-resistant *Fusaria* (17). The emergence of fungicide resistance, together with the environmental- and human health threat of these chemicals, question their sustainable use.

The usage of microbial agents to control plant pathogens represents a safe and environmentally friendly alternative to conventional pesticides (18). These microbes naturally occur in the soil environment and have the capacity to reduce plant diseases. Microbial biocontrol agents employ various mechanisms against plant pathogens such as induction of systemic resistance in plants, competition for ecological niche and nutrients or direct antagonism by secretion of specialized compounds. Species from the *Bacillus subtilis* taxonomic group hold great potential as biocontrol agents (19). These bacteria have the ability to synthesize a remarkable arsenal of bioactive compounds with low toxicity against mammals and most are generally recognized as safe (GRAS) (20–24). The inhibitory capacity of *Bacillus* spp. against fungi relies on mechanisms such as induced systemic resistance, secretion of volatile organic compounds (VOCs), siderophore chelation of iron, production fungal cell-wall degrading enzymes and, especially, the biosynthesis of cyclic lipopeptides (25–28).

Despite the promising features of biological control agents, the development and implementation of biocontrol products enclose multiple challenges. Aside from troublesome market execution due to legislation, especially in Europe (29), the laboratory performance of biocontrol strains often does not translate to field trials, which results in

inconsistent product effectiveness (30–33). Therefore, quantitative and complementary screening methods are needed to identify potent and robust plant pathogen inhibitors (34).

Furthermore, for identification and further development of potent antifungal biocontrol strains, a better understanding of bacterial-fungal interactions is required. Adaptive laboratory evolution (ALE) is a powerful tool that allows the study of microbial adaptation to certain conditions under a specific selective regime, while developing potentially better strains for specific applications. Thus, experimental evolution may be used as an approach for studying the adaptation of *Bacillus* spp. to the presence of fungi and, at the same time, providing novel insights of the bacterial-fungal interactions. In addition, ALE is a potential tool for natural strain improvement and has for instance been employed to enhance the root colonization abilities of *B. subtilis* strains (35), but is yet to be explored for the development of biocontrol strains with improved antifungal properties.

1.2 Purpose and specific aims

The overall purpose of this Ph.D. project was to develop potent antifungal *Bacillus* biocontrol strains and gain a better understanding of bacterial-fungal interactions as well as *Bacillus* adaptive responses to fungi. This was achieved by studying the short-term colonization by *Bacillus* on fungal mycelium as well as the acquired genetic adaptation of *Bacilli* during experimental evolution in co-culture with fungi. Furthermore, to allow the identification of improved fungal inhibitor strains, quantitative and high throughput methods were developed. The specific aims of the project were the following:

- To generate mechanistic knowledge on the molecular interaction between strains of *Bacilli* and filamentous fungi
- To develop quantitative methods to assess fungal inhibitory potential of bacteria
- To evolve *Bacillus* strains with improved inhibitory potential against plant-pathogenic fungi

- To identify the genetic alterations responsible for the evolved phenotypes and correlate these changes with the metabolic and physiological adaptations

1.3 Thesis content and structure

The theoretical part of this thesis starts in **Chapter 2** with a general introduction to the *Bacillus* genus, its natural habitats, and discusses *Bacillus* interactions with fungi. The impressive capacity of *Bacillus* to produce specialized metabolites, their potent antifungal properties, and mechanisms underlying plant protecting are described in **Chapter 3**. The chapter further discusses common methods used to assess and evaluate the antifungal potential of biocontrol candidate strains. In **Chapter 4**, the *Bacillus* quorum sensing system and cell differentiation pathways are introduced with emphasis on important response regulatory players. **Chapter 5** delves into genetic changes emerging in such regulatory systems during experimental evolution and *Bacillus* adaptation to fungi. In **Chapter 6**, a summary and the main conclusions of the findings in the thesis are presented.

The experimental studies and manuscripts are disclosed after the theoretical chapters at the end of the thesis.

In **Study 1**, the interaction between *B. subtilis* and *Aspergillus niger* or *Agaricus bisporus*, provided by the colonization of the fungal mycelium by bacterial biofilm mutants, was investigated. The study clarified the specific biofilm components needed for *Bacillus* biofilm formation associated with the fungal hyphae and showed that matrix components can be shared between biofilm producers and non-producing mutants.

The interaction between *B. subtilis* and *A. niger* was further explored in **Study 2** by establishing a co-cultivation system with the species and evolve the bacterial strain in the presence of the fungus under laboratory conditions. The study discloses the primary

adaptation of *B. subtilis* to the fungus by increased specialized metabolite production and enhanced space colonization.

In **Study 3**, two quantitative- and high throughput screening methods of biocontrol candidate strains were developed. The methods assessed the antifungal potency of secreted compounds into the supernatant or measured the antagonistic mechanisms by direct co-cultivation of the bacterial and fungal species. These methods were evaluated using selected prominent fungal phytopathogens and *Bacillus* spp. originating from the Chr. Hansen strain collection. Furthermore, the novel methods were employed in **Study 4** in combination with genome mining of biosynthetic gene cluster and analytical chemistry of specialized metabolites to enable selection of candidate strains for experimental evolution campaigns.

Inspired by Study 2, different adaptive laboratory evolution systems (in liquid or solid medium) were established and employed to investigate the adaptation of *Bacillus* spp. to the filamentous fungi *F. culmorum* in **Study 5** and *B. cinerea* in **Study 6**. In addition, the studies explored adaptive laboratory evolution as a tool for biocontrol strain optimization by co-cultivating *Bacillus* spp. with the respective fungi and identified improved evolved derivatives. Acquired genetic changes in evolved *Bacillus* strains were identified in regulatory genes as well as motility-related genes, which were linked to phenotypic traits.

Chapter 2 | *Bacillus*-fungus interactions

2.1 Introduction to *Bacillus*

The *Bacillus* genus belongs to Bacillota (previously Firmicutes) phylum of the bacterial kingdom and are rod-shaped, spore-forming, Gram-positive bacteria. Within the *Bacillus* genus, the *B. subtilis* clade is the most intensively studied group and is the focus of this thesis as well. The clade encompasses *Bacillus* of the major classifications *subtilis*,

licheniformis, *pumilus* and *amyloliquefaciens*, which each comprise further species (19, 21) (Table 1). *Bacillus* spp. reside in various environments ranging from the rhizosphere and marine sediment to the human or animal gastrointestinal tract (36), but have predominantly been considered soil-dwelling organisms due to their frequent isolation from rhizosphere and soil samples. An interesting trait of *Bacillus* spp. is their stunning capacity to produce a variety of specialized metabolites. *B. subtilis* strains delegate 4-5% of their genome to the potential production of specialized metabolites (22), whereas *B. velezensis* strains may devote up to 8.5% of the genome for this purpose (37). Owing to their antimicrobial properties, specialized metabolites have been proposed to function as microbial warfare compounds. However, the diversity of the specialized metabolites suggests that the natural purpose of these molecules may be more complex and include functions such as bio-emulsification, surface attachment and intra- or interspecies community signaling (22, 38, 39). *Bacillus* specialized metabolites and their antifungal properties are further described in **Chapter 3**.

Table 1. Species from the *Bacillus subtilis* complex. *Bacillus* species from the subtilis clade listed according to relatedness to the first original member of the group (bold). Inspired by (40).

<i>B. subtilis</i>	<i>B. amyloliquefaciens</i>	<i>B. pumilus</i>	<i>B. licheniformis</i>
<i>B. gibsonii</i>	<i>B. siamensis</i>	<i>B. safensis</i>	<i>B. hayensis</i>
<i>B. vallismortis</i>	<i>B. velezensis</i>	<i>B. zhangzhouensis</i>	<i>B. aerius</i>
<i>B. intestinalis</i>	<i>B. nakamurai</i>	<i>B. australimaris</i>	<i>B. paralicheniformis</i>
<i>B. cabrialesii</i>		<i>B. altitudinis</i>	<i>B. swezeyi</i>
<i>B. tequilensis</i>		<i>B. areophilus</i>	<i>B. sonorensis</i>
<i>B. halotolerans</i>		<i>B. cellulasensis</i>	<i>B. glycinifermentans</i>
<i>B. mojavensis</i>		<i>B. stratosphericus</i>	<i>B. globiensis</i>
<i>B. atrophaeus</i>		<i>B. xiamenensis</i>	

Another remarkable feature of the *Bacillus* bacterium is its ability to differentiate into functionally distinct cell types. The flagellated bacterium is capable of switching from the motile lifestyle to a sessile lifestyle encapsulated in a self-produced matrix, which is altogether termed biofilm. As the biofilm matures, the bacteria may differentiate into

distinct cell types by engaging in, for instance, competence development, degradative enzyme production or endospore-formation. The spore formation enables *Bacillus* spp. to endure extreme environments by entering a dormant state until conditions favor active growth, while the secretion of enzymes allows the bacterium to liberate nutrients from the environment and the development of competence permits the uptake of foreign DNA that may benefit survival through gain of functions (41). The highly intertwined differentiation pathways and functionally distinct cell types are further assessed in **Chapter 4**.

Bacillus subtilis is a well-studied model of Gram-positive organisms due to its metabolic diversity, genetic amenability and industrial relevance (42). Over the years, several databases (Subtilist, BsubCyc, BSGAtlas, SubtiWiki) have been dedicated to this organism, comprising curated data for gene organization and function, metabolic pathways, transcriptomic data under different condition, and links to relevant literature (43–46). In industrial settings, *Bacillus* bacteria are widely employed for their production of degradative enzymes in for instance biomass conversion to fuels and chemicals, animal feed (47), chitin bioconversion (48), detergents, or textile processing (49). Other applications of *Bacillus* spp. include their use as human or animal probiotics (50), food preservatives (51), and biocontrol agents in agriculture (23).

Bacillus spp. are predominantly found in the rhizosphere. In the soil, 1 gram may harbor up to 10^8 bacteria comprising up to 10^3 diverse species (52) and a spatial soil ecology study suggests that a single cell interacts with up to 100 species in the near vicinity (53). The rhizosphere i.e., the soil surrounding the plant root, constitutes a microbial hotspot forming the base for interactions between kingdoms and a myriad of species. The rhizosphere forms the habitat of plant pathogens as well as plant beneficial microbes commonly referred to as Plant Growth-Promoting Rhizobacteria (PRGP) and includes species from the *B. subtilis* group. The success of any PGPR depends on proper root

colonization, which *Bacillus* spp. ensures via matrix production and biofilm formation. *Bacillus* spp. are known to promote plant growth, increase nutrient availability, or enhance abiotic stress tolerance; amenities that are exchanged for various root exudates beneficial to the bacterial growth. In addition, *Bacillus* spp. exert biological control and reduce disease severity by inducing systemic resistance, rendering the plant less prone to infection, or by directly inhibiting growth of plant pathogens (Fig. 1) (54–56). Mechanisms by which *Bacillus* spp. inhibit phytopathogenic growth are described in **Chapter 3**.

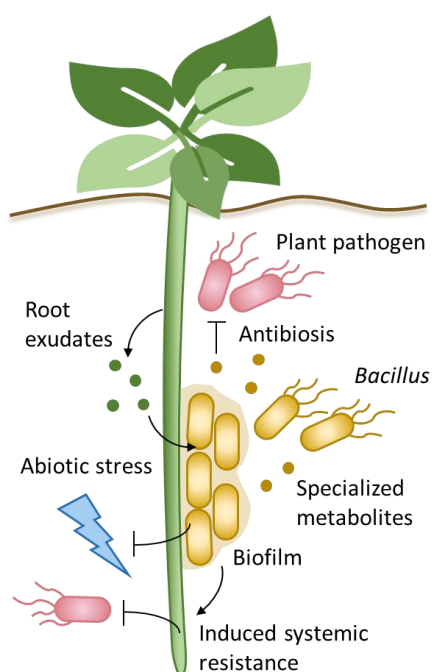


Fig. 1. *Bacillus* biocontrol and biofertilization. *Bacilli* colonize plant roots by biofilm formation and secrete bioactive compounds that directly inhibit the growth of plant pathogens. Additionally, the bacteria induce plant systemic resistance, rendering the plant entirely less susceptible to pathogen attack. Other beneficial properties include growth promotion and enhanced tolerance to abiotic stresses such as drought and salt. The bacteria in turn benefit from the plant root exudates. Inspired by (57).

2.3 Bacterial-fungal interactions

Bacterial and fungal species are ubiquitously widespread and often share habitats. Therefore, bacterial-fungal interactions are varied and range from antagonistic to symbiotic relationships. These different relationships may be established by indirect contact between the species, direct physical association, or most likely as a combination (58, 59). Indirect contact occurs by means of secreted compounds such as metabolites, volatiles, quorum sensing molecules, or specialized metabolites. These secreted compounds have various functions including antibiosis, metabolite exchange, cross-kingdom signaling, induction of chemotaxis towards the fungal hyphae, and growth stimulation (59–62). An example of volatile mediated antibiosis is given by the compounds 2-nonanone and 2-heptanone produced by a *B. amyloliquefaciens* strain showing strong antifungal effects on the phytopathogen *F. oxysporum* f.sp. *niveum* (63). In contrast, volatiles released by the *Pseudomonas aeruginosa* PAO1 led to growth induction of the fungus *Aspergillus fumigatus*, where both species are pathogenic to humans and especially to cystic fibrosis patients (64). In addition, di-rhamnolipids secreted by *P. aeruginosa* induce production of *A. fumigatus* extracellular matrix (ECM), which aids bacterial attachment and demonstrates that bacteria and fungi can alter the metabolism of one another (65). Direct interaction is established for the purpose of nutrient acquisition, but also as a mean for the bacteria to travel along the hyphae reaching favourable growth niches, exemplified by the *in situ* migration of *Bacilli* along *Mortierella* hyphae (66). Physical association may be manifested as bacterial settlement on the mycelium produced by a filamentous fungus or as endophytic bacterial colonization. For instance, the soil-dwelling bacteria *Burkholderia* was shown to settle on the mycelium of the co-isolated fungi *Alternaria alternata* or *Fusarium solani* and thrive on the secreted fungal compounds to the benefit of the bacteria (67), while *Paraburkholderia rhizoxinica*, also from the *Burkholderiaceae* family, is known to engage in endophytic colonization of *Rhizopus microspores*, where the bacterium supplies the

fungus with toxins that facilitate rice pathogenesis (68). Such mutualistic relations presumably have adapted over millions of years (59) and suggest that bacterial and fungal species shape the evolution of one another.

Nutrient competition between bacteria and fungi over millions over years have resulted in the development and natural selection of genetic biosynthetic pathways encoding a plethora of antibacterial and antifungal compounds (59). The well-established biocontrol potential of *Bacillus* spp. derives from their impressive capacity to produce an arsenal of bioactive compounds, where in particular the cyclic lipopeptides display antifungal activity. Consequently, interaction studies between fungi and *Bacillus* spp., from the *subtilis* group, have been mainly centered around the biocontrol field, with *Bacillus* antifungal activities against phytopathogens being extensively documented and reviewed (20, 23, 28, 69–72). Nevertheless, due to the prominent antifungal properties of *Bacillus* spp., their application has also been suggested in the field of medicine to treat fungal infections by human pathogens, such as *Candida albicans* (73). Specifically, the lipopeptide surfactin was shown to inhibit growth, reduce adhesion and morphogenesis of *C. albicans* and enhance susceptibility to the fungicide fluconazole, making *Bacilli* promising candidates for complementary therapies (74).

During interaction with phytopathogenic fungi, *Bacillus* spp. may respond by altering specialized metabolite production. Not only may the fungal interaction lead to an increase in bioactive lipopeptides biosynthesis, but also alter the lipopeptide profile and redirect the production towards a specific compound (75). Such metabolic response was observed in *B. velezensis* SQR9 that increased production of the siderophore bacillibactin, when encountering a range of phytopathogenic fungi (*V. dahliae*, *S. sclerotiorum*, *F. oxysporum*, *R. solani*, *F. solani*, and *P. parasitica*) (76), suggesting that these organisms may compete for iron with *Bacilli* engaging in iron scavenging. The opposite scenario was observed in co-culture of *B. subtilis* 168 with *Fusarium tricinctum*, which led to the induction of fungal bioactive metabolites hampering bacterial growth (77). These studies

show that fungal and *Bacillus* species interaction may contribute to the potentiated or hampered production of specific specialized compounds. In addition, *Bacillus* spp. may benefit from interactions with fungi by cross-feeding mechanisms. For example, *B. amyloliquefaciens* is able to metabolize secreted oxylipins, i.e. oxygenated natural products, from *Aspergillus oryzae* leading to reduced production of bacterial bioactive lipopeptides (78).

Bacillus* interactions with *Aspergillus niger

Like *Bacillus* spp., the black mold fungus *A. niger* is prevalent in soil samples. However, little is known about the interaction between these two species in the environment. A previous study showed that during *in vitro* interaction of *B. subtilis* with *A. niger*, the species altered their metabolism. Both species downregulate transcription of genes related to antibiosis (79). In **Study 1**, the interaction between *B. subtilis* and *A. niger* was explored as well as the interaction between *B. subtilis* and the basidiomycete mushroom *Agaricus bisporus*, commonly used for human consumption. In this study, it was shown that biofilm formation by *B. subtilis* enabled colonization of *Aspergillus niger* and *Agaricus bisporus* hyphae (Fig. 2). The essential biofilm matrix components, which are required for successful colonization were further elucidated. These components are described in **Chapter 4**.

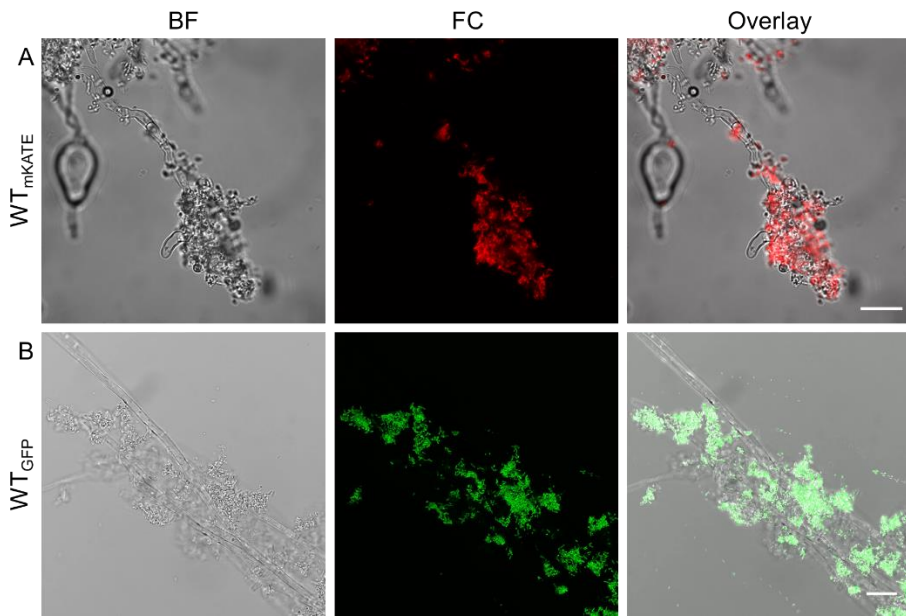


Fig. 2. Colonization of fungal hyphae by *B. subtilis*. *B. subtilis* attachment to the hyphae of the fungi A) *Aspergillus niger* or B) *Agaricus bisporus*. FC: fluorescent channel. BF: bright field. WT: wildtype. Scale bars indicate 20 μm . Adapted from (80), **Study 1**.

In **Study 2^a**, the interaction between *B. subtilis* and the filamentous fungus *Aspergillus niger* was further explored by experimental evolution. Using a co-cultivation system on agar growth medium, the adaptation of *B. subtilis* to the fungus was investigated. The species were co-inoculated from a fungal spore suspension and from diluted bacterial culture in a hashtag and square pattern, respectively (Fig. 3). Following incubation, an agar plug was excised and transferred to a new growth plate. *Bacillus* outgrowth was used for culture inoculum, and a new co-cultivation cycle was initiated with fresh fungal spores to avoid co-evolution of *A. niger* and selectively focus on *Bacillus* adaptation.

^a *Minor contribution*

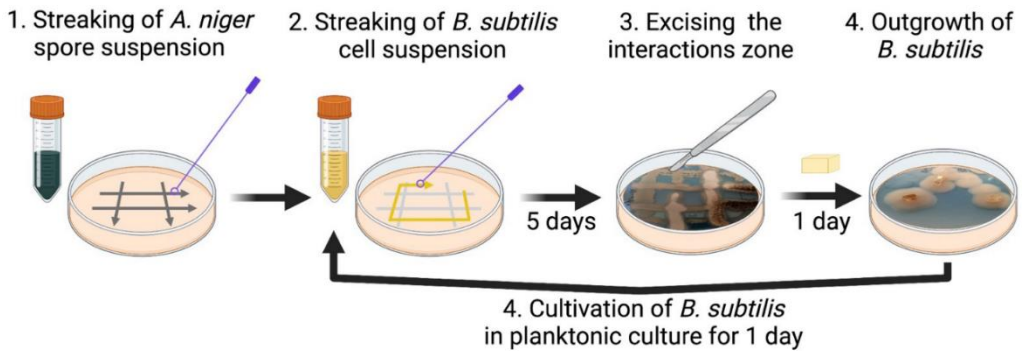


Fig. 3. Design of experimental evolution of *B. subtilis* with *A. niger*. *B. subtilis* was adapted to the presence of *A. niger* by co-inoculation the species on agar growth medium, transferring the bacteria and engaging another co-cultivation round.

Co-cultivation of *B. subtilis* with *A. niger* selected for enhanced bacterial surface colonization leading to fungal growth restraint. The enhanced colonization was attributed to increased levels of the biosurfactant and specialized metabolite surfactin that enables multicellular motility (Fig. 4). Surfactin also mediated cell-wall stress in *A. niger*, which was reflected by bulbous hyphal cells and transcriptional upregulation of α -1,3-glucanase synthase, an enzyme related to stress response. In addition, the adaptation resulted in *Bacillus*-mediated disruption of fungal medium acidification. The altered characteristic of *B. subtilis* were assigned to mutations of the two-component regulatory system DegS-DegU. In conclusion, the antifungal properties were enhanced during the adaptation of *B. subtilis* to presence of *A. niger* by potentiated production of a bioactive compound, surfactin.

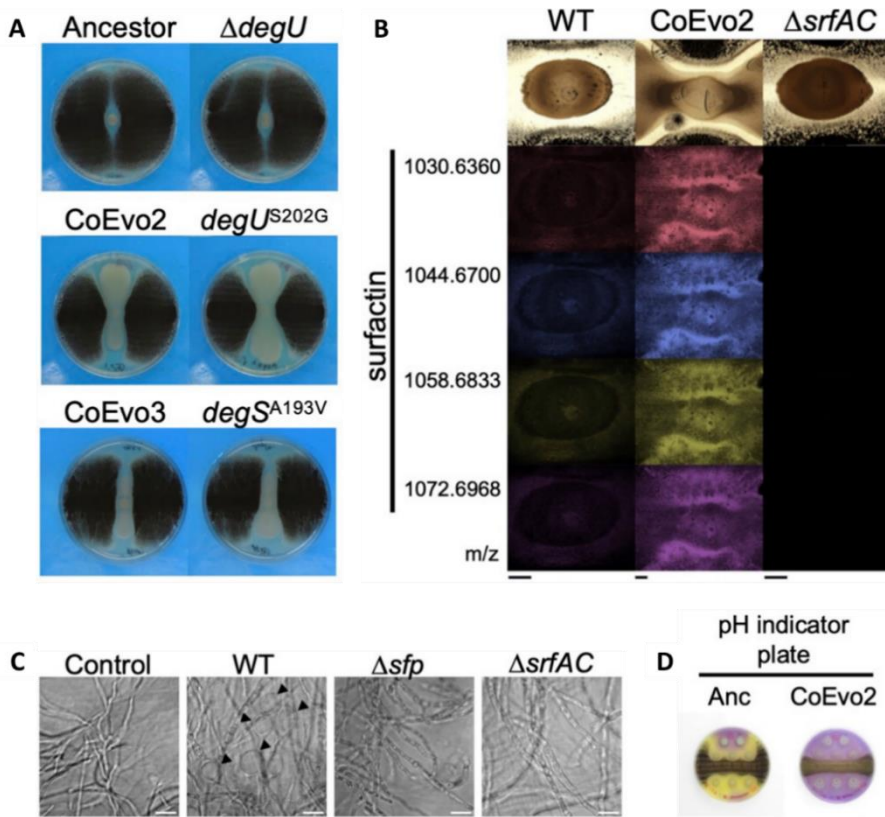


Fig. 4. Altered phenotypes of *B. subtilis* and impact on fungal growth and morphology. A) Confrontation assay against *A. niger* of evolved strains CoEvo2 and CoEvo3 harboring *degU*^{S202G} or *degS*^{A193V} substitution mutations, respectively. B) MALDI-MSI spatial detection of surfactin isoforms in colonies of *B. subtilis* wild-type, CoEvo2, and the *srfAC* mutant grown in between streaks of *A. niger*. Scale bar = 2mm. C) Hyphal morphology upon inoculation with cell-free supernatants of wild-type *B. subtilis* NCIB3610, and respective *sfp* and surfactin mutant (*srfAC*). D) *A. niger* medium acidification in the presence of wt *B. subtilis* and CoEvo2. Modified from (81), **Study 2**.

The experimental evolution of *B. subtilis* in the presence of *A. niger* inspired **Study 5** and **Study 6**. Encouraged by the finding that repeated co-cultivation cycles lead to enhanced fungal inhibition properties, a co-cultivation system mimicking the experimental design of **Study 2** was established with *Bacillus* spp. and the phytopathogen *Fusarium culmorum*. In

addition, experimental evolution of *Bacillus* spp. with *Botrytis cinerea* was explored in **Chapter 5**, for the purpose of strain improvement against this grey mold fungus.

The following chapter addresses the antifungal properties of the *B. subtilis* species complex and highlights the commonly employed methodologies used to assess the antifungal potency of biocontrol candidate strains.

Chapter 3 | Fungal inhibition properties of *Bacillus* spp.

Specialized metabolites derive their name from their specialized functions that potentially provide the producing strain with physiological or ecological benefits in distinct niches. Originally, these compounds were referred to as secondary metabolites, making a clear distinction from the primary metabolism that sustains growth of an organism. Although not essential for growth, these small molecules are hypothesized to fulfil functions in signaling, antibiosis, nutrient acquisition, or interspecies interactions. Owing their outstanding bioactive capacity, specialized metabolites are widely employed as therapeutic agents in cancer treatment and as antibiotics in the medicine field. Driven by the early discoveries of penicillin and streptomycin, researchers have explored microbiomes for specialized metabolites in search for new efficient antibiotics in the race against the emerging drug resistance (82, 83).

Approximately 5% of the any given *B. subtilis* genome is devoted to specialized metabolite production (22), while 8.5% of the genome of the well-studied biocontrol strain *B. velezensis* FZB42 is assigned for this purpose (37). Specialized metabolites and exoproducts of *Bacillus* spp. display remarkable chemical and structural diversity. Among others, these include siderophores, polyketides, lipopeptides, volatiles, and lytic enzymes with bioactive capacity. Especially, cyclic lipopeptides display antifungal activity, while polyketides and some ribosomally synthesized peptides, such as bacteriocins, have prolific antibacterial activity (21). Owing the structural diversity and bioactivity of specialized metabolites produced by *Bacillus* species, they present an intriguing source for the discovery of antibiotic candidates (84, 85) and are promising for biocontrol against bacterial, insectile, and plant pathogens (23). The following sections focus exclusively on metabolites relevant for biocontrol of fungal phytopathogens.

3.1 Bioactive metabolites and modes-of-action against fungal phytopathogens

Cyclic lipopeptides

The non-ribosomal peptide synthases (NRPS) that facilitate lipopeptide biosynthesis are encoded by genes co-localized in large biosynthetic gene clusters (BGCs) that also comprise genes for transcriptional regulation, secretion, and resistance to the respective biosynthetic product. The NRPS requires the 4-phosphopantetheinyl transferase Sfp for post-translational conversion from its apoform to the catalytic active form (86). Once active, these large multi-enzymes have a modular structure comprised by domains that stepwise incorporate the amino acids into the lipopeptide chain. In this sense, the NRPS modules share co-linearity to the amino acid chain in the lipopeptide. The first adenylation domain (A) phosphorylates the amino acid, which is subsequently transferred by the peptidyl carrier protein (PCP) to the condensation domain (C) that forms the C-N bond between the amino acid and the growing oligopeptide (Fig. 5). Structure variety occurs by means of auxiliary domains like the cyclisation- (Cy), methylation- (MT), or epimerization domains (E) placed in the elongation modules. The final module contains a thioesterase domain (TE) that releases the peptide from the module assembly and in most cases cyclizes the lipopeptide (21, 23, 27, 38).

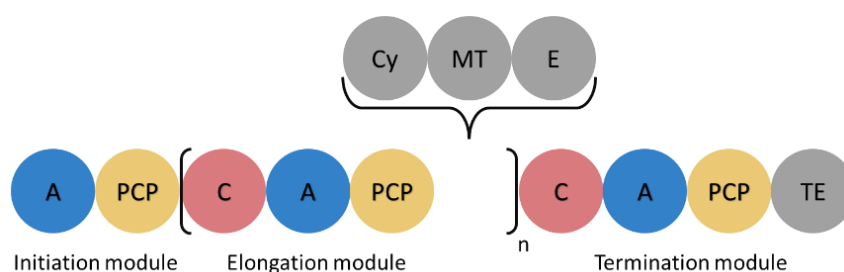


Fig. 5. Schematic NRPS structure. The structure of a non-ribosomal peptide synthase with the core adenylation (A), peptidyl carrier protein (PCP), condensation (C) and the terminal thioesterase domain. The chemical and structural diversity of these molecules is facilitated by the cyclization (Cy), N-methylation (MT), and epimerization (E) auxiliary domains. Figure inspired by (21).

Surfactins are cyclic heptapeptides attached to a β -hydroxy fatty acid chain of varying length (13-15 carbons) (Fig. 6) (27). The metabolite exhibits eminent biosurfactant properties that enable cell migration across a surface (87). Due to its amphipathic nature, surfactin integrates and transiently destabilizes biological membranes providing the metabolite with antibacterial but also antiviral properties. Sterol content in membranes opposes this effect and possibly explains, why surfactins do not exhibit strong antifungal properties (23). However, against certain filamentous fungi such as *A. niger*, surfactin causes fungal cell wall stress, hyphal bulging, and mislocalization of secretory vesicles, as shown in **Study 2** (81). Furthermore, surfactins pose a synergistic effect in combination with other lipopeptides potentiating the antifungal potency of a strain (88–90). Notably, lichenysin, produced by *B. licheniformis* and *B. paralicheniformis* species, shares similar structure and properties to surfactin (Harwood et al., 2018).

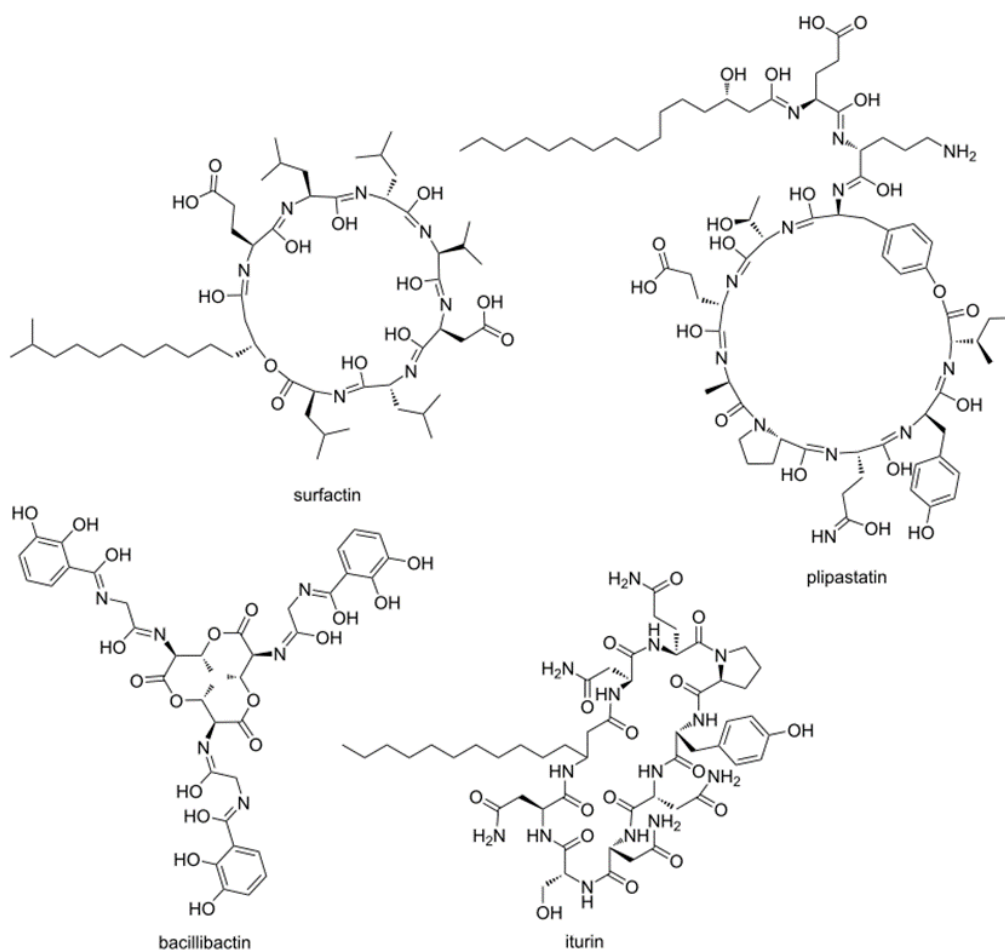


Fig. 6. Structure of *Bacillus* spp. lipopeptides and bacillibactin. The siderophore bacillibactin and the cyclic lipopeptides iturin, plipastatin and surfactin. Modified from (91).

The surfactin NRPS is encoded by the *urf* operon and comprises the four enzymatic units SrfAA, SrfAB, SrfAC, and SrfAD required for surfactin biosynthesis (92). The operon is regulated by the quorum sensing system ComQXPA interlinking competence and sporulation (Fig. 7) (93–95). Surfactin NRPS transcription is induced upon activation of the two-component system ComP-ComA by extracellular accumulation of the pheromone ComX at high cell densities. Another regulatory pathway involves CSF (PhrC) that inactivates the phosphatase RapC and prevents it from dephosphorylating ComA (38, 96).

Due to the cell-density based regulation, surfactin is produced in the transition from exponential to stationary growth phase (97).

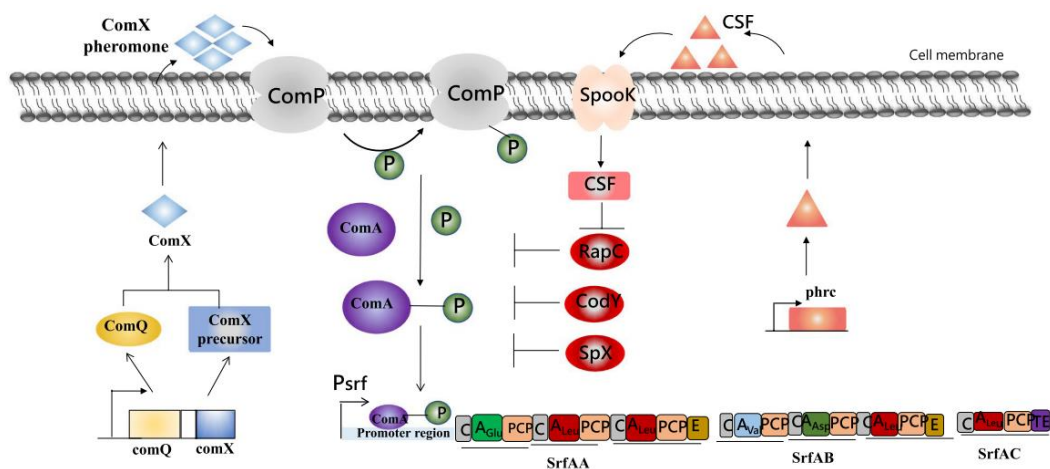


Fig. 7. Regulation of surfactin biosynthesis. The complex network of surfactin biosynthesis regulation involves two peptides (ComX, CSF) mediated signaling pathways induced by cell density and several regulators. T-bars indicate negative regulation by dephosphorylation or inhibition at transcriptional level. Bent arrows indicate gene transcription. Figure adapted from (Hu et al., 2019).

Like surfactins, iturins are cyclic heptapeptides, but they differ in the amino acid composition and contain a β -amino fatty acid chain of 14-17 carbons (Fig. 6). Iturinic compounds are commonly found in *B. amyloliquefaciens* and *B. velezensis* species, with a single cluster being confined to each strain (98, 99). Among others, this lipopeptide family includes mycosubtilin, bacillomycins, and iturins (27). The NRPS for biosynthesis of iturin A is encoded by the *itu* operon (100), which requires the presence of DegQ for activation of DegU to induce expression (101, 102).

Fengycins are lipodecapeptides containing a lactone ring incorporated into the cyclized peptide and a β -hydroxy fatty acid chain of 14-19 carbons (Fig. 6). The fengycin family comprises the nearly identical plipastatins. The difference lies in the positioning of L-

tyrosine and D-tyrosine at either position 3 and 9, or reversed (103, 104). Distinction between fengycins and plipastatins cannot be facilitated by liquid chromatography-mass spectrometry (LC-MS), but nuclear magnetic resonance (NMR) provides a reliable method for differentiation. The reliance on LC-MS has led to numerous instances of misidentification and misreporting of these compounds. Like iturins, the biosynthesis of fengycins/plipastatins is regulated by DegQ activity via DegU (105–107). Moreover, loss of surfactin production was shown to negatively impact fengycin/plipastatin biosynthesis, providing a link between the regulation of these lipopeptide families (105).

Members from both the iturin and fengycin/plipastatin lipopeptide families exhibit notable inhibitory activity against multiple filamentous fungi and reduce plant disease severity caused by fungal phytopathogens. For instance, disease severity in mango caused by *Colletotrichum gloeosporioides* was reduced by bacillomycin D to greater extent than application of common fungicides (108). Studies with mutant strains impaired in lipopeptide biosynthesis indicate that iturins, fengycins, or a combination of the two are required for inhibition of several filamentous fungi including *Cladosporium cucumerinum*, *F. oxysporum* and *B. cinerea* (28). The application of iturin and fengycin/plipastatin lipopeptides cause various morphological abnormalities to the fungal structures. For example, fengycins/plipastatins in quantities below the minimal inhibitory concentration (MIC) were shown to induce chlamydospore formation in *Fusaria*, while higher concentrations caused hyphal swelling and conidia lysis (109). Another study reported membrane and cell wall disruption in addition to cytoskeleton breakage of *Fusarium oxysporum* induced by fengycins/plipastatins (107). Furthermore, a comparative study of the morphological effects on *F. graminearum* hyphae and conidia by iturin A and plipastatin A indicated that, although both compounds damaged conidia and caused loss of cell viability, iturin A led to restricted hyphal branching, bulging and condensed structure formations, whereas plipastatin A led to bulging, vacuolation in young hyphae and at the hyphal tip (110). In line with these findings, we showed in **study 2** that the

induction of hyphal bulging in *F. culmorum* and *F. graminearum* was dependent on the presence of plipastatin in *B. subtilis* culture (Fig. 8) (81). Hyphae conglobation, enlarged vacuoles, and reduced branching was also observed for *Colletotrichum gloeosporioides* mycelium when treated with bacillomycin D (108). Multiple studies propose that iturins (108, 111–114) and fengycins (115–118) exert their molecular mode-of-action through membrane destabilization and pore formation, resulting in the leakage of ions or cell content. Besides, disruption of membrane integrity, lipopeptides may cause fungal metabolic changes. For example, the iturinic compound bacillomycin D not only contributed to inhibition of *F. graminearum* conidia germination, leading to formation of swollen hyphae structures, but also induced the production of the mycotoxin deoxynivalenol (119). In *Aspergillus carbonarius*, iturin A caused metabolic changes related to transport, energy metabolism, and osmotic imbalance, likely related to swelling of hyphal structures (120). Interestingly, *Bacilli* may modulate the biosynthesis of specialized metabolites when encountering fungal species dependent on the nature of the fungus. For example, the amount of iturins and fengycins were increased by *Bacilli* upon interaction with *Pythium aphanidermatum* and *F. oxysporum* compared to control cultures (28).

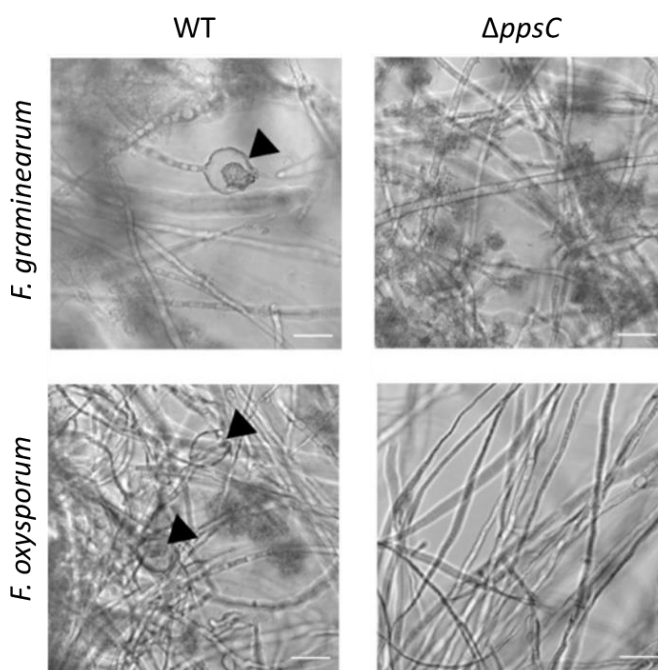


Fig. 8. Influence of plipastatin on *Fusaria* hyphae. Microscopy visualization of bulging *Fusaria* hyphae with wild type (WT) and a mutant strain lacking surfactin plipastatin (Δ *ppsC*). Scale bar = 25 μ m. Adapted from Study 2.

Lytic enzymes

Bacilli are efficient producers of degradative enzymes widely used in various industrial applications such as detergent formulation, animal feed digestive treatments, food manufacturing, and chitin waste conversion (47–49, 121). Owing to their high stability, efficient cellular secretion, and remarkable tolerance to pH, temperature and solvents, *Bacillus* proteases account for 60% of the enzyme market share (49). The degradative enzyme activity also benefits the biocontrol properties of *Bacilli* (122). Fungal cell walls consist of chitin, a linear polymer composed of (1→4) β -linked N-acetyl-D-glucosamine (GlcNAc) residues, which can be hydrolyzed by chitinases (EC 3.2.1.14), chitosanases (EC 3.2.1.132), and β -N-acetylglucosaminidases (EC 3.2.1.52) such as NagZ (123, 124). Fungal

cell wall material can effectively induce the secretion of *Bacillus* chitinases and proteases to obtain carbon for sustaining bacterial growth (125). Specifically, the secretion of chitinolytic and proteolytic enzymes by *Bacillus* spp. has been demonstrated to be an antibiosis mechanism against fungal and oomycete plant pathogens like *Fusaria*, *B. cinerea*, *Rhizoctonia solani* and *Pythium* by inhibition of hyphal extension, induction of hyphal abnormalities, inhibition of germination, and conidia lysis (126–131).

Nutrient and niche competition

Competition for ecological niche colonization is hypothesized to be an antagonistic mode-of-action of bacteria from the rhizosphere against phytopathogens, although evidence is scarce (54). Theoretically, the pathogen is outcompeted by fast colonizing biocontrol bacteria that reduce nutrient availability and occupy niches potentially colonized by the pathogen (56). *In vitro*, competition between *Bacillus* spp. and filamentous fungi by space colonization was observed in **Study 2 and 5**, where increased surface spreading facilitated by surfactin, and possibly changes to biofilm production, conferred restricted fungal growth expansion. These observations suggest that under laboratory conditions, fungal growth may be controlled by niche colonization competition.

Furthermore, efficient competition for nutrients can contribute to the biocontrol capacity of a bacterial strain by production and secretion of iron-chelating compounds, like bacillibactin (Fig. 6). For instance, *B. amyloliquefaciens* MBI600 subjected to iron starvation induced expression of the *dhb* operon, encoding the siderophore bacillibactin synthetase, and potentiated antifungal activity. The observed enhanced antifungal potency was abolished upon iron addition, illustrating that the fungal inhibition was caused by iron scavenging (132). Further supporting the role of bacillibactin in fungal antibiosis, a study identified that *B. subtilis* CAS15, a proficient producer of bacillibactin, effectively controlled *Fusarium* disease *in planta*, which was alleviated upon iron supplementation (133).

Volatile organic compounds

Bacterial volatiles have been proposed to serve as nutrient sources, act as chemical signals in microbial communities, or play a role in antibiosis (60). Certain *Bacillus*-derived volatiles, such as 2,3-butanediol and acetoin, have the capacity to induce plant growth and enable the bacterium to persist in the rhizosphere microbiome (134, 135). In addition to promoting plant growth, volatiles produced by *Bacilli* may contribute to the biocontrol properties by inhibiting the growth of plant pathogens. For example, several volatile compounds, especially small ketones, produced by *B. amyloliquefaciens* NJN-6, effectively inhibited *Fusarium oxysporum* mycelial growth (136), while the volatilome of *B. subtilis* JA inhibited *B. cinerea* growth, and generated retraction of the protoplast within hyphae during germination (137). Other volatiles with antifungal effect include *O*-anisaldehyde, secreted by *Bacillus atrophaeus* CAB-1, which exhibited 70% growth reduction of *Sphaerotheca fuliginea*, the causative agent of cucumber powdery mildew (138), and the volatiles 5-nonylamine and 3-methylbutanoic acid, produced by *Bacillus velezensis* CE 100, suppressing spore germination of the fungus *Colletotrichum gloeosporioides* (139). Interestingly, *Bacillus* volatilome changes have been observed in response to co-cultivation with the fungal pathogen *Setophoma terrestris* (140). During the bacterial-fungal interaction, *Bacilli* acquired mutations in the quorum sensing systems, resulting in alterations in the volatile profile and enhanced antifungal properties, which were attributed to the volatile ketone compounds 2-heptanone and 2-octanone. These findings share great resemblance to **Study 5**, where we show that experimental evolution of *Bacillus* spp. with *Fusarium culmorum* led to genetic changes in *comP* encoding part of the two component quorum sensing pair ComP-ComA. Those genetic changes were correlated with improved volatile effect on the fungal growth inhibition (Fig. 9).

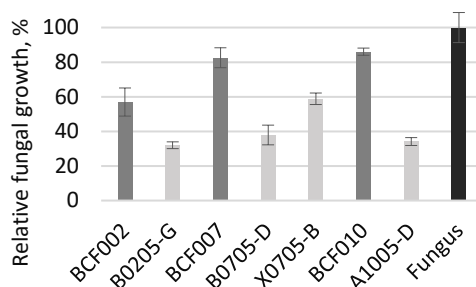


Fig. 9. Inhibition of *F. culmorum* by *Bacillus* spp. volatilome. *Bacillus* strains or *F. culmorum* spore suspension was inoculated in the center of a petri dish on a filter paper disc. The plates were incubated 1.5 days before sandwiching the bottoms of plates with each strain (one *Bacillus* strain and *F. culmorum*). The plate sandwich was sealed to prevent escape of volatiles and incubated at 25°C. The VOC blends effect of ALE derivatives (light grey) was calculated in relation to the fungal control (fungus grown in a petri dish compartment without bacteria) (black) and compared to the ancestor strains (BCF010, BCF007, BCF002, BCF001) (dark grey) after 48h. Figure adapted from Study 5.

Priming of plant defense

Aside from direct pathogen inhibition, *Bacilli* elicit plant defense systems that confer enhanced pathogen resistance in the entirety of the plant including distal tissues from the microbial induction site. Induced systemic resistance (ISR) relies on recognition of microbial molecules and molecular patterns, or direct invasive damage. ISR is transmitted to the plant body by phytohormone signaling pathways via ethylene or jasmonic acid (141). Examples of *Bacillus*-derived molecular triggers of plant innate immune responses include the iturinic compound mycosubtilin, conferring enhanced resistance to *Botrytis* in grapevine (142), phenylacetic acid, leading enhanced protection against *Fusarium* in tomato (143), or surfactin that was demonstrated to stimulate plant defense in tobacco and tomato conferring reduced *Botrytis* grey mold disease severity seemingly in a concentration dependent manner (144–146). In addition, volatile organic compounds,

such as butanediol, acetoin, or dimethyl disulfide, effectively trigger plant defense systems in plants (134, 147).

3.2 Methods for assessing fungal inhibitory potential of *Bacillus* spp.

Assessing the inhibitory potential of microbial biocontrol strains is a crucial step in the development and application of effective biological control strategies against plant diseases. As field trials are costly and demanding (148), and the efficacy of potent pathogen inhibitors observed under laboratory conditions does not always directly correlate with their performance in the field (30–33), it is important to have reliable screening methods to assess fungal inhibitory potential of microbial biocontrol strains. The most accurate system for assessing inhibition potential is undoubtedly *in planta*, which accounts for host-pathogen-antagonist interactions and responses. However, this system is not suitable for screening of large libraries. Classical antagonistic assays evaluate the impact of a potential biocontrol strain by *in vitro* co-inoculation with the phytopathogen, on solid medium (34, 149, 150). While these assays account for all antagonistic mechanisms i.e., nutrient competition, niche competition, and secretion of bioactive compounds, the accuracy and throughput are limited. Other antagonistic methods or proxies of fungal inhibition include evaluation of volatile effect, lytic enzyme activity, efficacy of bacterial supernatants or microscopy of fungal morphology in response to antagonistic treatment (34, 149, 151, 152).

To address the need for experimental approaches to identify and rank potential biocontrol microbial strains from large libraries, we developed two high-throughput (HT) and quantitative screening methods in **Study 3** (153). The methods were developed with *F. culmorum* and further validated using the fungal phytopathogens *B. cinerea* and *F. graminearum*. In brief, bacterial cultures were adjusted by optical density (OD₆₀₀) and sequentially diluted. Fungal spore suspensions with a fixed concentration were co-inoculated with each bacterial culture dilution on solid growth medium in a microtiter

plate, assigning a column for each candidate strain (Fig. 10A). The co-inoculated plate was incubated for 5 days and the minimal inhibitory cell concentration (MICC) that abolished fungal growth was determined as a measure of inhibitory potency. The second developed method assessed inhibition by secreted compounds. Specifically, bacterial cultures were added in increasing volumes to microtiter plates with fungal spore suspensions with fixed concentration and bacteriostatic antibiotics. The fungal growth in response to bacterial culture addition was measured by OD₆₀₀, which was previously described as an accurate indicator of fungal growth (154) (Fig. 10B).

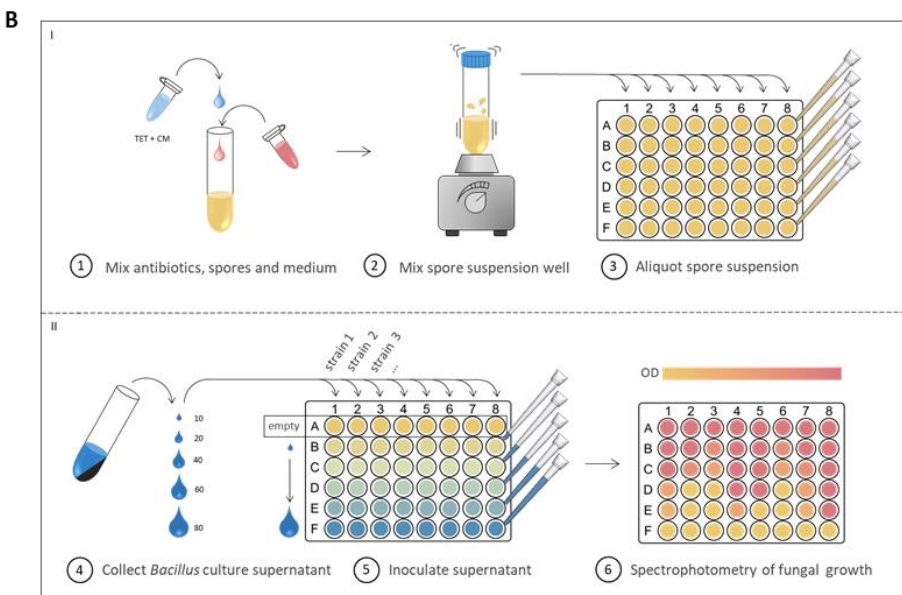
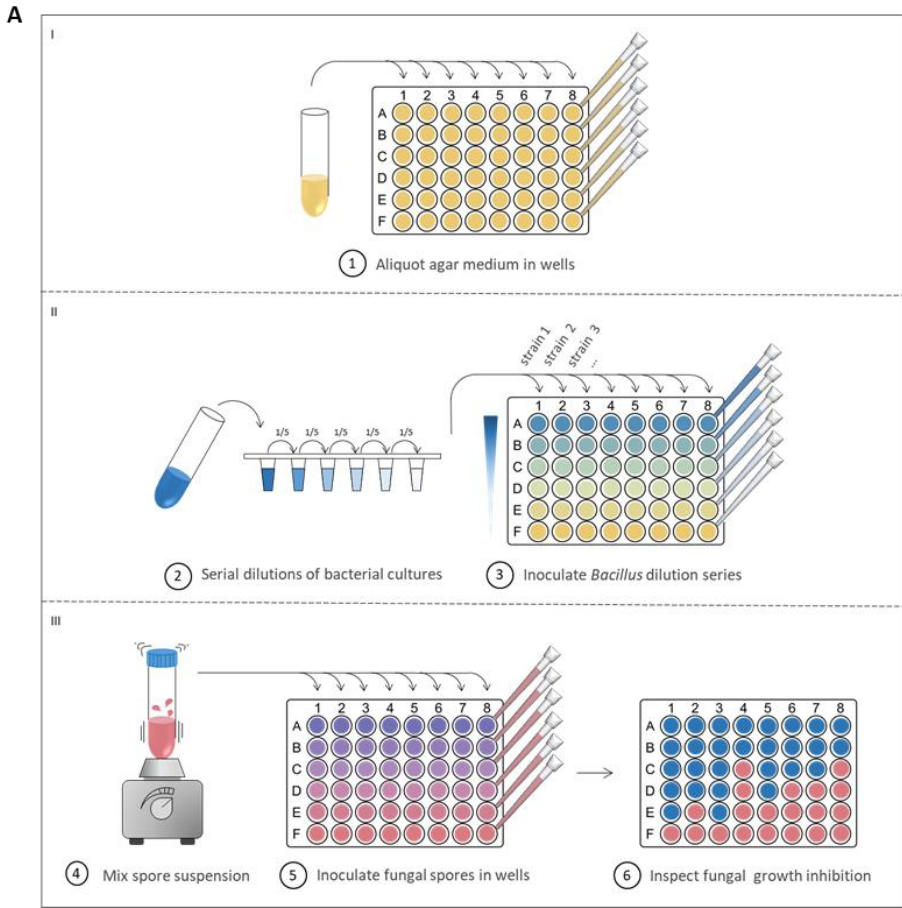


Fig. 10. High throughput screening of fungal inhibition potency of *Bacillus* strains. The minimal inhibitory culture or supernatant dilution that suppressed fungal growth was determined for *Bacillus* strains by HT-screens. AI) molten agar medium was poured into a 48-well microtiter plate and let to solidify. AII) Bacterial culture dilution series were prepared on inoculation onto the agar assigning a column for each *Bacillus* strain. AIII) A fixed spore concentration was co-inoculated in each well with bacterial dilution series. The fungal growth was evaluated by visual inspection after 5 days at 25°C. BI) Fungal spore suspension was prepared with bacteriostatic antibiotics and aliquoted into each well of a 48-microtiter plate. BII) Bacterial culture was co-inoculated in each well ranging from 10-80 μ l and incubated at 25°C. Figure adapted from Kjeldgaard et al., 2022.

The antagonistic co-cultivation method accounts for all direct inhibitory mechanisms and provides easy scoring of inhibitory potency. As several studies documented that *Bacilli* modify biosynthesis of specialized metabolites upon encounter with fungi (28, 76, 155), it is valuable to assess the direct interaction between the biocontrol candidate strain and the fungal phytopathogen. Contrasting classical antagonistic assays, the method assesses inhibition of both spore germination and mycelial growth, enabling ranking of inhibition potency, and facilitates HT-screening. In combination with the supernatant assay that assesses the secreted compounds, the methods provide different results fueling further investigation of inhibition mechanism.

3.3 Evaluation of fungal inhibitory potential of natural *Bacillus* isolates

The *in vitro* assessment of fungal inhibition by *Bacillus* spp. can be combined with analyses of both the genetic potential for the biosynthesis of specialized metabolites and the chemical quantification of such metabolites in cultures used for evaluation of fungal inhibition (88). In **Study 4**, the described HT screening methods (Kjeldgaard et al., 2022, Study 3) were used in combination with genome mining of biosynthetic gene clusters (BCGs) and biochemical analysis of specialized metabolites to assess the inhibition potential of selected *Bacillus* species from the Chr. Hansen strain collection. In all strains, genome mining identified BGCs for fengycin/plipastatin and surfactin, or lichenysin in

case of *B. paralicheniformis* (Fig. 11). Furthermore, species-specific BGCs were identified in accordance with literature i.e., diffidicin in *B. velezensis* strains, macrolactin and iturin in *B. velezensis* and *B. amyloliquefaciens* strains, in addition to co-occurrence of lichenysin, fengycin and bacitracin BGCs in *B. paralicheniformis* strains (98, 156, 157). Liquid Chromatography-Mass Spectrometry (LC-MS) analysis confirmed the presence of the respective specialized metabolites in correlation with the genome mining results.

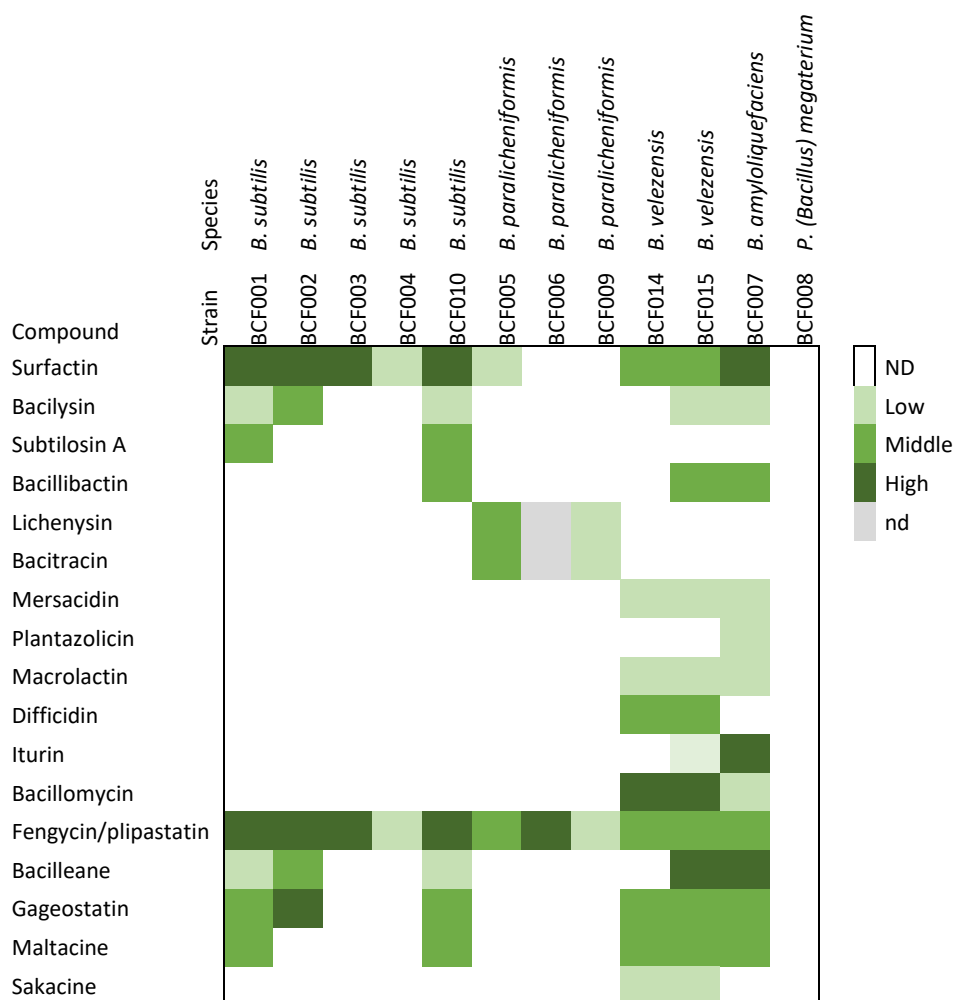


Fig. 11. Relative levels of specialized metabolites in supernatants of cultures from *Bacillus* isolates. LC-MS analysis of culture supernatants from *Bacillus* spp. grown for 24-48 h in PDB, LB, M2 or MSgg media at 37 °C. Color gradient, from light green (low levels) to dark green (high levels), refers to relative levels of bioactive metabolites from average peak areas of biological duplicates. Nd = no data.

The *in vitro* antifungal potency of the undomesticated *Bacilli* was addressed against the fungal phytopathogens *F. culmorum*, *F. graminearum*, and *B. cinerea* by classic antagonistic plate assays in combination with the quantitative and HT-inhibition methods described in **Study 3**. Minor differences were observed between results obtained by the respective methods, underlining that the assays reveal different inhibitory traits, and that the combination of assays provides insight of the nature of inhibition mechanism. In summary, *B. amyloliquefaciens*, *B. velezensis* and specific *B. subtilis* strains displayed prominent inhibition of all three fungal phytopathogens, whereas other *B. subtilis* and *B. paralicheniformis* strains inhibited fungal growth to a minor extent (Fig. 12).

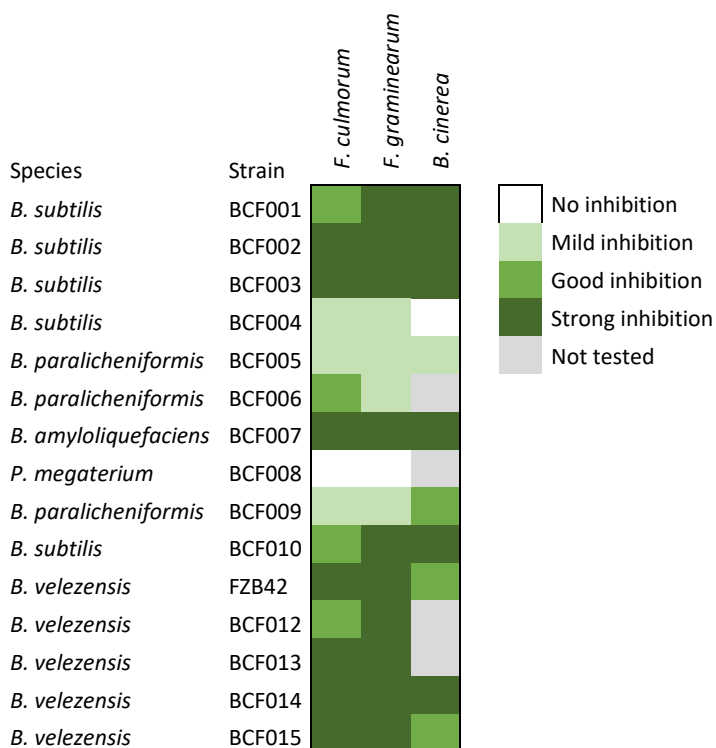


Fig. 12. Summary and conclusion of fungal inhibition capacity of *Bacillus* isolates. A summarizing conclusion on fungal inhibition potency was drawn from the three types of fungal inhibition assays (plate confrontation, co-inoculation, culture supernatants).

Study 4 showed that genome mining of BGCs in combination with biochemical analysis of specialized metabolite production and different antagonistic assays is a valuable approach for assessing the biocontrol potential of a strain. This approach offers a comprehensive estimate of the fungal inhibition potency, also hinting to the inhibition mechanism provided by the results from the different antagonistic assays.

Chapter 4 | Cell differentiation in *Bacillus*

Upon reception of external cues, *Bacilli* differentiate into distinct cell types controlled by complex and highly intertwined regulatory networks. The nature of these cues may be accumulation of self-produced signals (e.g., autoinducer peptides) or changes to the environment such temperature fluctuations, variation in pH, and nutrient availability. The diverse cell differentiation pathways are coordinated by regulators that repress genes committed to a specific development, while simultaneously inducing the expression of other genes. Although many differentiations are mutually exclusive, the commitment to a specialized cell type is not definitive and engagement in developmental pathways may occur sequentially. Within a genetically homogenous population, multiple specialized cell types may co-exist concurrently in subpopulations, conferring phenotypic heterogeneity to the community. Differentiation pathways are varied and comprise for example matrix production, sporulation, motility, competence, and degradative activity (95, 158, 159). This chapter briefly introduces *Bacillus* developmental programs and the regulation thereof.

4.1 Quorum sensing

Sensing and responding to a community

The ability to differentiate enables bacteria to survive under variable conditions. The differentiation of individual cells depends on the reception of external signals that activate or repress specific pathways (95). The process of monitoring and responding to the bacterial population is referred to as quorum sensing and grants bacteria features similar to those of a multicellular organism (160). Quorum sensing relies on secretion, extracellular accumulation, and reception of small signaling molecules (161), but can also be activated by pH, nutrient limitation, temperature, or specific metabolites (95). When a signal molecule reaches a certain threshold, behaviors such as biofilm formation,

competence development, or sporulation are triggered by alteration of gene expression (162). In Gram-positive bacteria, oligopeptides constitute quorum sensing signaling molecules, which are received by membrane-bound two-component sensor histidine kinases (160). In *Bacillus*, the ComP-ComA two-component system plays part in a complex regulatory network that determines the fate of the cells within a culture or biofilm. Upon increase in cell density, extracellular accumulation of the signal molecule ComX, activates ComP-ComA leading to a coordinated responsive behavior across multiple cells (163, 164) (Fig. 13). The pheromone ComX binds to ComP, residing in the cell membrane, and triggers the sensor histidine kinase to autophosphorylate, thereby activating the response regulator ComA (165, 166). Another quorum sensing system comprises the Phr peptides and the oligopeptide permease (Opp), which receives and internalizes the signal peptides upon reaching high threshold concentrations (167, 168). Intracellularly, Phr peptides bind to specific Rap phosphatases, preventing them from antagonizing the target regulators Spo0F, DegU, or ComA (169–171).

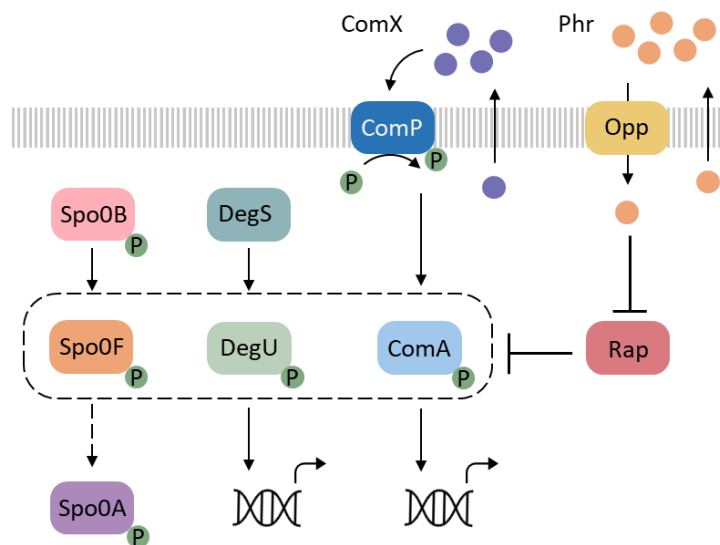


Fig. 13. Schematic representation of the *Bacillus* quorum sensing mechanism. Extracellular accumulation of the pheromone ComX induces autophosphorylation of ComP, which in turn

activates the transcription regulator ComA. Phr peptides are internalized by the oligopeptide permease Opp and inhibit specific Rap proteins. Rap phosphatases target the regulators ComA, DegU, or Spo0F (boxed). Bent arrows indicate gene expression, whereas dashed arrows indicate multiple steps.

Quorum sensing mutants emerge during experimental evolution

Interestingly, experimentally evolved strains from **Study 5** acquired mutations in the genes *comP*, *comA*, *oppB*, and *oppC* encoding the two-component quorum sensing system and the oligopeptide permease that facilitates signal molecule transport into the cell. *comP* appeared as most frequently mutated open reading frame and mutations persisted throughout the time course of the evolution experiment (Fig. 14). Also, several mutations were identified in the regulatory network enabling cell differentiation (Fig. 15). The abundant mutations affecting genes related to quorum sensing and cell differentiation highlight their significant role in the experimental evolution. These genetic changes had a strong impact on the final phenotype, enabling adaptation to cultivation conditions and fungal pathogen exposure.

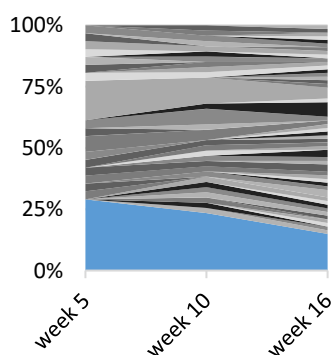


Fig. 14. Relative frequency of specific mutations. Relative frequency of all mutations in genetic regions were determined relative to the total number of mutations at the given timepoints in the evolution experiment (week 5, 10 and 16) across all ancestors. Each black and white shade area correspond to a mutation, while *comP* is indicated in blue. Figure adapted from **Study 5**.

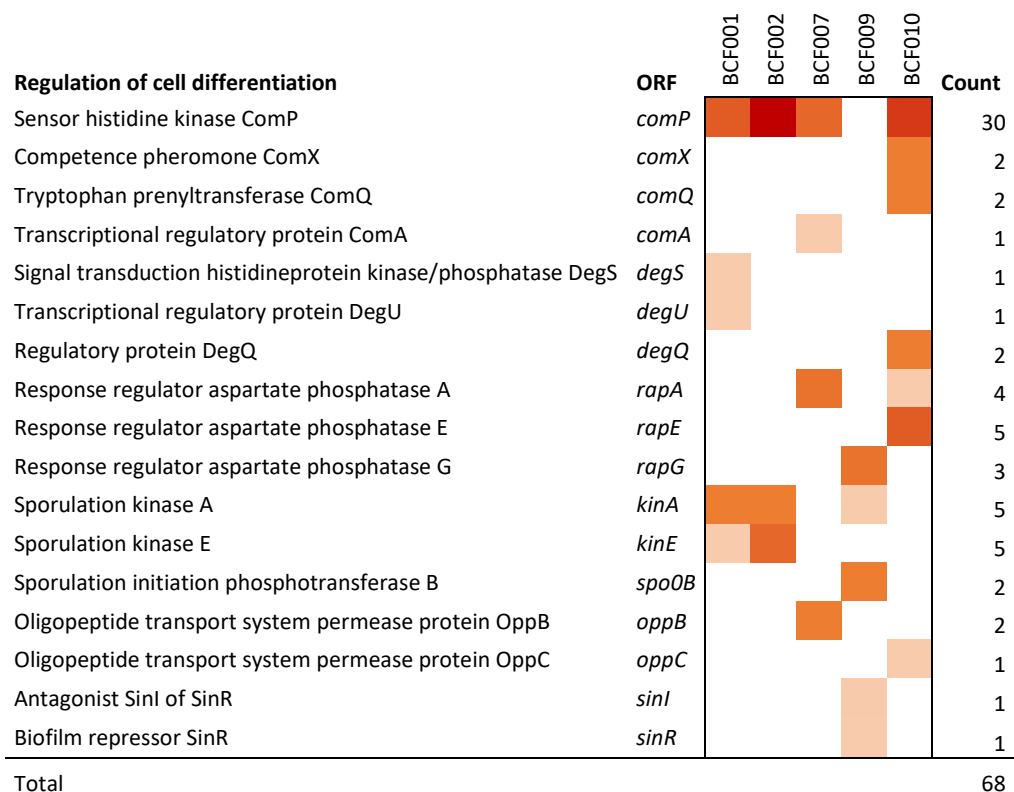


Fig. 15. Mutations affecting ORFs related to cell differentiation. Multiple mutations were identified that affected the open reading frames (ORFs) of proteins involved in various cell differentiation pathways. Count denotes number of occurrences across evolved strains from the ancestors BCF001, BCF002, BCF007, BCF009 and BCF010. Adapted from **Study 5**.

4.2 Developmental pathways

Competence development

Natural competence is the ability of a bacterial cell to take up extracellular DNA from the environment, in a process called transformation, and incorporate it in its genome by homologous recombination. *Bacillus* spp. can become naturally competent upon induction by the quorum sensing system ComP-ComA. When phosphorylated by ComP, the transcription regulator ComA triggers expression of ComS embedded in the *srfA*

operon (93, 172, 173). ComS prevents the degradation of the competence regulator ComK (174) and thereby onsets expression of genes related to uptake and assimilation of exogenous DNA (175). Development of genetic competence requires functional flagella, correlating motility differentiation with transformability, and underlining the connectivity of cellular processes (176, 177).

The ability to integrate foreign DNA in the genome enables horizontal gene transfer and constitutes an alternative adaptation mechanism to evolution driven by mutations. Natural competence allows the uptake of DNA that confers multiple changes to the genome simultaneously, potentially resulting in the gain of new functions with a consequent evolutionary advantage to the bacterium (178, 179).

Sporulation and cannibalism

Bacillus cell differentiation into the sporulation pathway enables survival under harsh conditions such as oxygen deprivation, desiccation, extreme temperatures, or nutrient limitation. The spore constitutes a dormant and durable life form that effectively preserves DNA until conditions once again permit vegetative growth (180). From an industrial perspective, the ability to undergo sporulation render *Bacilli* attractive for biocontrol product formulation and application. From an evolutionary perspective, sporulation confers an advantage to *Bacilli* by enabling persistency and survival under detrimental conditions for vegetative cell growth. Thus, this mechanism increases the chances of long-term survival of the bacteria.

Sporulation is governed by the master regulator Spo0A, which directly controls the expression of more than 100 genes (181). Spo0A activity depends on its phosphorylation state; at high levels, phosphorylated Spo0A triggers the onset of sporulation, whereas low phosphorylation levels trigger matrix production (182–184). Sporulation is an irreversible commitment and begins with genome replication followed by asymmetric division by the formation of an endospore within the mother cell, which subsequently lyses to release the spore (158, 180).

Sporulation is preceded by cannibalistic behavior that delays the irreversible and energy demanding spore formation process. Cannibalism is considered a mechanism of programmed cell death (PCD) that modulates differentiation. The phenomenon is initiated by low Spo0A activity in a subpopulation that induces the production of toxins (bacteriocins), killing sibling cells through lysis and fostering nutrient release to sustain the growth of the immune toxin producers. Thus, the toxin producers cannibalize their neighboring cells and provisionally postpone onset of sporulation (159, 185, 186).

Biofilm, the natural bacterial growth form

In natural environments, bacterial growth is widely considered to occur in the form of biofilm (187–189). The biofilm lifestyle enables bacteria to withstand harsh environments and provides the community with protection from, for instance, UV radiation, pH, and antimicrobial compounds (189, 190). Biofilms are complex single- or multispecies communities embedded in a self-produced matrix comprised of extracellular polysaccharides (EPS), DNA, and structural proteins (Fig. 16). These matrix components enable biofilm attachment to diverse abiotic and biotic surfaces such as plant roots (191), lung tissue (190) or even fungal hyphae (80), as shown in **Study 1**. Within the *Bacillus* biofilm, phenotypic distinct subpopulations co-exist. Both motile, matrix-producing, and sporulating cells inhabit the biofilm, which confers heterogeneity to the community (192).

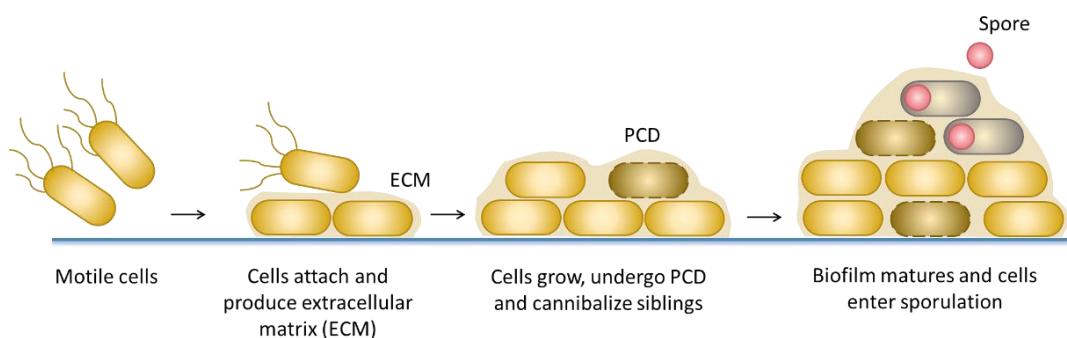


Fig. 16. Initiation of biofilm formation by *Bacillus*. Motile cells attach to a surface and differentiate into extracellular matrix (ECM) producers. The biofilm forms as cells embed in the self-produced matrix. As the biofilm matures, some cells enter the sporulation pathway, whereas other undergo programmed cell death (PCD). Figure inspired by (187).

Regulation of biofilm formation

Biofilm formation is costly and thus tightly controlled by an intricate regulatory network, which has been thoroughly reviewed (57, 193, 194). This section describes selected regulatory pathways. Biofilm formation begins as motile cells differentiate into sessile matrix-producing cells (Fig. 15). The initiation of biofilm formation depends on accumulation of external signals, such as surfactin and ComX, to induce expression of matrix genes governed by the master regulator Spo0A (195). Extracellular accumulation of ComX induces the biosynthesis of surfactin through the quorum sensing system ComP-ComA. Surfactin sequentially activates the kinase KinC that phosphorylates Spo0A. In addition, the ComP-ComA system influences the sporulation/biofilm pathway via induction of RapA/C/E/F protein expression (169, 196). Rap proteins are a part of the phosphorelay system that inhibit phosphorylation of the response regulator Spo0A and DegU (170, 197), while the histidine kinases KinA/B/C/D and the phosphotransferases Spo0F/B activate Spo0A (198). External cues activate the kinases, resulting in phosphorylation and sequential transfer of the phosphoryl group from Spo0F to Spo0B and finally to Spo0A. Low levels of Spo0A-P trigger biofilm formation by inducing transcription of the anti-repressor *sinI* and repressing transcription of *abrB*, encoding the global regulator that represses genes for stationary growth phase (183, 199). SinI relieves the repression by binding the repressor SinR, which controls the expression of the matrix genes encoded by the *epsA-O* and *tapA-sipw-tasA* operons (200–202). The transcription regulator AbrB also negatively regulates matrix genes encoded by the *tapA-sipw-tasA* and *epsA-O* operons, as well as expression of the matrix protein BslA. Upon repression of *abrB* by Spo0A, biofilm production is initiated (203, 204).

Another regulatory pathway of importance to biofilm formation comprises the DegS-DegU system. Moderate levels DegU~P enhance biofilm formation and are required for complex biofilm architecture, while high DegU phosphorylation state induces lytic enzyme production (204–207). The pleiotropic regulator DegQ activates DegU and its cognate histidine kinase DegS, while expression of DegQ itself is induced by the quorum sensing system ComP-ComA upon high cell-densities (207, 208). Specifically, DegU controls the expression of the biofilm hydrophobin BslA (205, 209) as well as the biofilm polymer poly- γ -glutamic acid (γ -PGA) (210). BslA is also regulated by Rok, the transcription factor and repressor of *comK*, during complex biofilm architecture formation (211).

Biofilm matrix components

The ability of *Bacilli* to form multicellular communities relies on the production of extracellular polysaccharides (EPS) and the structural protein TasA that ensure the biofilm integrity by holding the cells together (212). The EPS is encoded by the 15-gene operon *epsA-O* (213) and contributes with water retention, as well as structural properties of the biofilm (205, 214). Poly- γ -glutamic acid (γ -PGA) content also correlates with water retention and the polymer confers a mucoid biofilm phenotype (215, 216). The γ -PGA matrix levels vary depending on the producing strain (194). TasA proteins form fibers within the biofilm, which are associated with structural biofilm integrity. The protein TapA anchors the TasA fibers to the cell wall, and aids the fiber assembly (217, 218). The biofilm surface is covered by the hydrophobin BslA that creates a hydrophobic and protective coat resistant to, for instance, chemicals (219–221). In addition, BslA confers architectural complexity, although the protein is dispensable for biofilm establishment (209), as also shown in **Study 1** (80). Furthermore, extracellular DNA contributes to biofilm structure (222), although its function is less explored compared to other biofilm components. Traditionally, biofilm composition has been correlated with macroscopic differences in colony structure, as observed in **Study 5 and 6**. Structure formation, such as

wrinkles, arise from localized cell death, that creates a lateral pressure leading to vertical bulging (223), and synthesis of the biofilm components, as described above.

Matrix components are shared among community members and enable fungal attachment

The matrix components EPS and TasA are known to be essential for biofilm formation on the air-liquid interphase (pellicle), on agar medium, as well as on plant roots (213, 224). In **Study 1**, *Bacillus* biofilm associated with fungal hyphae of *Aspergillus niger* and *Agaricus bisporus* was shown to be dependent on TasA and EPS production. Interestingly, TasA- or EPS-defective mutants failed to colonize the fungal hyphae, a phenotype that could be rescued by the addition of a TasA/EPS producing strain (Fig. 17). The hydrophobin BslA conferred no change on hyphal colonization ability. The study demonstrated that the matrix components EPS and TasA are indeed required for settlement on fungal mycelia, and that the *Bacillus* community share matrix components, as was previously established for *B. subtilis* biofilms (212, 225, 226).

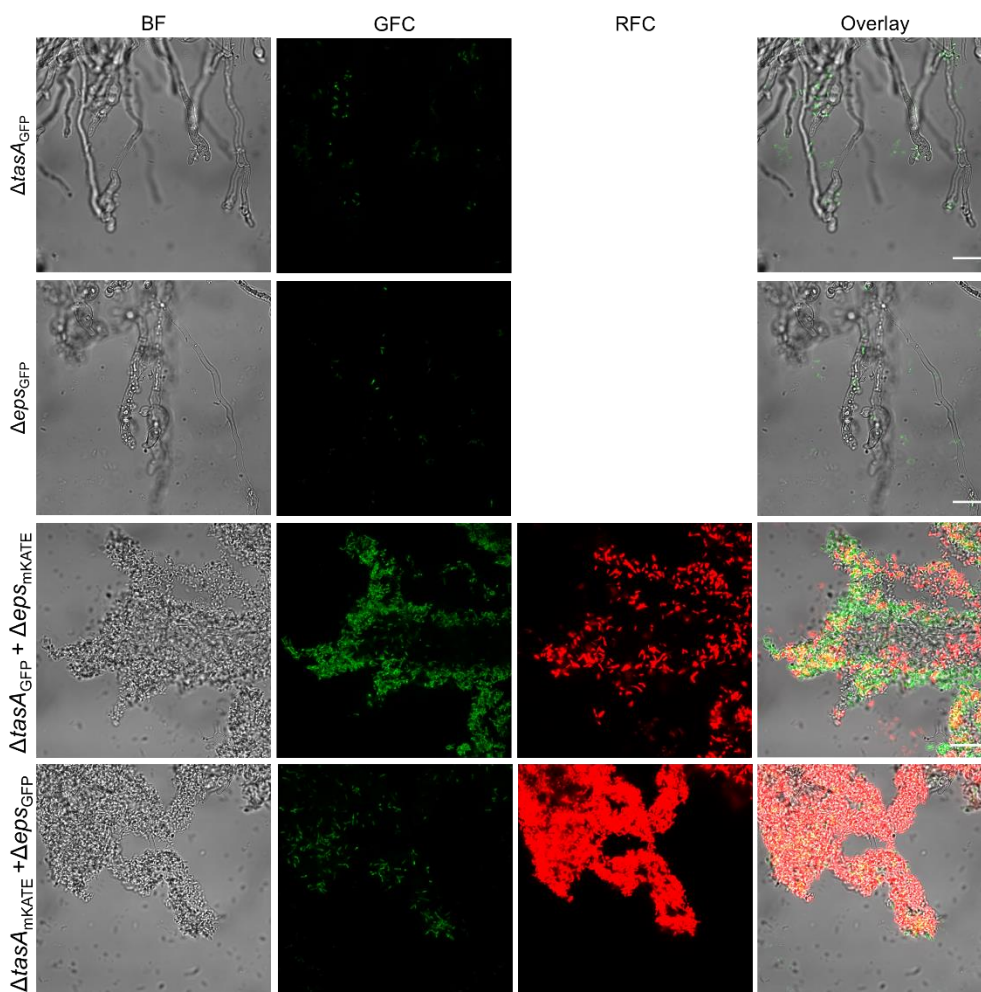


Fig. 17. Fungal hyphae colonization by matrix defective *Bacillus* mutants and biofilm complementation. The biofilms of TasA- or EPS-defective mutants of *B. subtilis* NCIB3610 on *A. niger* hyphae were rescued when co-inoculated. GFC: green fluorescence channel; RFC: red fluorescence channel. Scale bars indicate 20 μm . Figure modified from **Study 1** (80).

Quorum sensing mutants display altered biofilm

Evolved *Bacillus* strains from **Study 5** acquired predominantly mutations in the quorum sensing regulator ComP, but also adapted cell differentiation pathway regulators such as

DegS. Interestingly, the evolved strains displayed altered colony morphology on biofilm inducing medium when compared with to the parental strain (Fig. 18). Loss of biofilm complexity was associated with *comP* mutants from all *Bacillus* species used (*B. subtilis* BCF001, BCF002, BCF010, and *B. amyloliquefaciens* BCF007), regardless of their genetic background, while enhanced surface colonization was exclusively observed in *comP* mutants derived from *B. subtilis* strains (BCF001, BCF002, BCF010). Previous studies associated loss of biofilm complexity and flat colony formation with disruption of the *tapA* operon (*tapA*, *sipW*, *tasA*), or impaired production of EPS and BslA (57). Albeit the quorum sensing system ComP-ComA does not control the formation of these biofilm components directly, the response regulator ComA may influence matrix production, as suggested (227). ComP-ComA indirectly modulate the phosphorylation level of DegS-DegU through *degQ* transcription (207, 208), leading to biofilm formation and development of biofilm complexity (204–207, 227). In addition, ComP-ComA induce transcription of Rap proteins that are involved in the phosphorelay controlling the activity of the master regulator Spo0A (169, 196), which governs the entry into sporulation or biofilm formation dependent on its phosphorylation state. The additional loss of structure conferred by changes of ComA suggests that the transcription regulator may retain some activity in absence of ComP, and further supports the critical role of ComA activity in biofilm formation, as supported by previous studies (227).

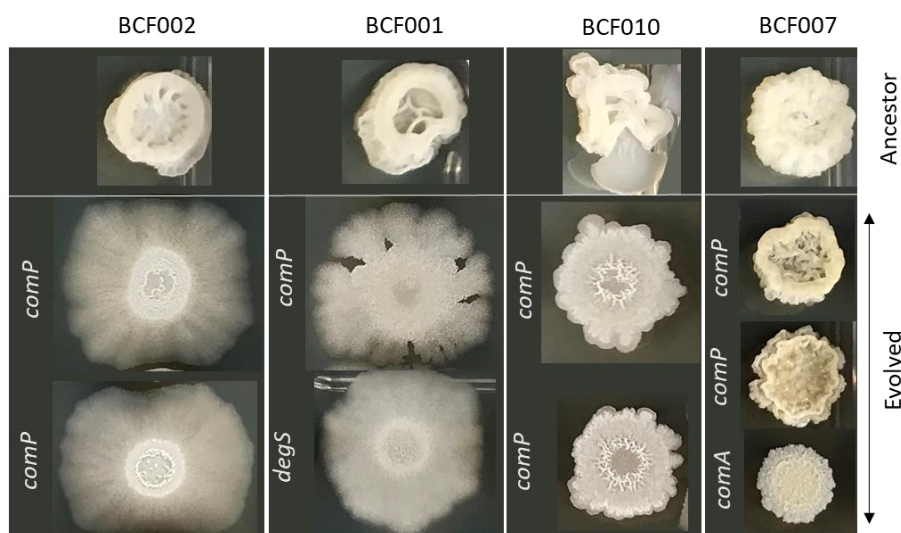


Fig. 18. Colony morphology of quorum-sensing and cell differentiation mutants. Derivatives from ancestors *B. subtilis* BCF001, BCF002, BCF010 and *B. amyloliquefaciens* BCF007 acquired mutations in quorum sensing and cell differentiation related genes (*comP*, *comA*, *degS*) among others, and displayed altered colony morphology on biofilm inducing medium. Adapted from **Study 5**.

Degradative enzyme production and motility

Within a bacterial community, a subpopulation may engage in production of degradative enzymes to scavenge amino acids and sugars by degrading proteins and polysaccharides from dead cells or secreted material (159, 228). The major extracellular proteases, bacillopeptidase and subtilisin, as well as the levansucrase (encoded by *bpr*, *aprE* and *sacB*, respectively), constitute degradative enzymes that are induced by the response regulator DegU at high phosphorylation state (229) (Fig. 19). DegU activity is controlled by the cognate sensor kinase DegS, which is activated by nutrient scarcity and salt stress (230). In addition, DegU activity is modulated by other quorum sensing systems. The extracellular accumulation of PhrG leads to its internalization, where the signal peptide inhibits the phosphatase RapG, preventing DegU dephosphorylation (231) Furthermore, the ComP-ComA quorum sensing system affects DegS-DegU activity by inducing

expression of DegQ at high cell densities (207, 208). Subsequently, the accumulation of DegU~P promotes lytic enzyme production (232, 233). Moreover, degradative enzyme production is repressed by the stationary gene regulator AbrB (234), which is relieved upon high levels of Spo0A~P (235), allowing transcription of the genes encoding extracellular degradative enzymes.

While high DegU activity triggers lytic enzyme production, moderate DegU activity is required for biofilm formation. Expression of matrix genes and γ -PGA induced by DegU is inversely correlated to swarming, indicating a reciprocal relation between the motility and biofilm developmental programs (215, 236, 237). Low phosphorylation of DegU and Spo0A relieves the transcriptional repression of flagella genes, and favors motile planktonic cell growth (181, 207, 238). The flagellar biosynthesis and chemotaxis receptors, both critical for the bacterial motility, are encoded by 30 genes in the large *fla-che* operon in addition to other genes (i.e. *hag*, *motA*, *motB*), which are expressed during exponential phase (238). These genes encode the flagellum apparatus that enable individual bacteria to swim within a liquid, but also facilitates multicellular migration across a surface, a phenomenon known as swarming (239). In addition to the flagella biosynthesis, swarming motility is dependent on the production of amphipathic surfactant molecules to reduce surface tension, like surfactin (239, 240).

The complex regulatory networks emphasize that cell differentiation pathways are intertwined and highly connected. Thus, the alteration of one developmental program may severely impact others. This was exemplified in **Study 5 and 6**, where adaptation of single regulators impacted multiple phenotypic traits in evolved strains such as biofilm development, colony morphology, motility, and lytic enzyme activity.

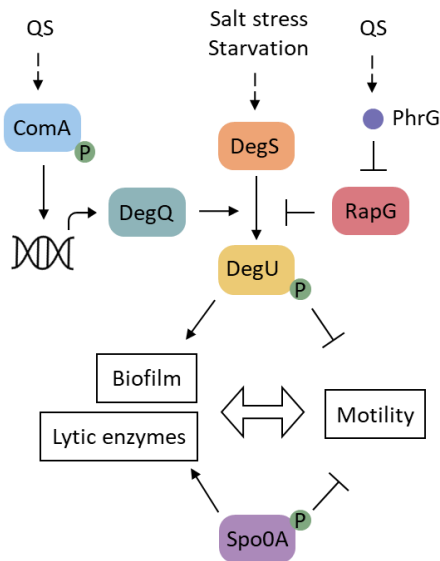


Fig. 19. Motility and biofilm regulation by DegU in *B. subtilis*. During planktonic growth, the levels of phosphorylated DegU are low, which favors transcription of flagellar genes. Upon high cell densities, the ComP-ComA induces *degQ* expression, which in turn stimulates phosphorylation of DegU by DegS. Moreover, the signal peptide PrhG binds to the phosphatase RapG and prevents it from inhibiting DegU. DegU induces its own transcription, the transcription of genes encoding degradative enzymes, involved in antibiotic synthesis, required for γ -PGA, and biofilm formation. Simultaneously, high level of DegU~P also represses transcription of flagellar genes. QS = quorum sensing. Figure and text inspired by (207).

Experimental evolution in suspension selects against motility

In **Study 6**, the propagation of *Bacillus* spp. under planktonic growth conditions predominantly promoted genetic changes in flagellar genes, conferring loss of motility in the evolved strains. In fact, experimental evolution of *Bacillus* culture suspensions has, on several occasions, promoted loss of motility, as for example observed in the adaptation of *Bacillus* to plant root colonization under mild agitation conditions (35, 241). Furthermore, the evolved strains derived from the ancestor *B. subtilis* BCF002 displayed mucoid biofilm morphology, which was attributed to increased γ -PGA production. This correlates with

the inverse relation between biosynthesis of the polymer and motility, which is regulated by DegU at different phosphorylation level (215, 237). These results underline that changes towards one cell differentiation pathway and phenotypic trait may lead to alterations of other developmental systems, as the regulatory networks are complex and intertwined.

Chapter 5 | *Bacillus* adaptation to fungi

5.1 Adaptive laboratory evolution (ALE)

Mutations constitute the foundation for adaptability and arise from spontaneous faulty DNA replication and errors in DNA repair mechanisms. If a specific mutation confers a fitness advantage to the cell, the subsequent positive selection pressure is expected to favor that genetic change, leading to its persistence and amplification within the population. Experimental evolution is a tool for studying such adaptive changes in populations propagated under specific and controlled growth conditions. Microorganisms are excellent candidates for the purpose of studying adaptation mechanisms owing their easy cultivation under simple conditions, rapid multiplication, and small size, allowing evolution for numerous generations. Particularly, the short generation time enable the observation of adaptation processes within limited time spans, while their small size and easy cultivation enable handling of several parallel populations and a large number of evolved individuals (242). The indefinite storage possibilities of cryogenic samples enable the investigation of emergence and persistence of genetic changes throughout the timeline of an evolution experiment (243). Furthermore, the reduced cost and increased throughput of genome sequencing technologies have greatly advanced the possibilities for examination of adaptive laboratory evolution experiments. Whereas early studies of microbial evolution were unable to establish connection between phenotype and genotype, the invention of modern sequencing methods has revolutionized adaptive laboratory evolution by facilitating effortless whole-genome sequencing of individual isolates, amplicon sequencing to track multiple lineages, and metagenomic sequencing of entire populations (244). Since Lenski and colleagues engaged the famous long-term experimental evolution of *E. coli* in 1988, currently exceeding 75,000 generations (245), microorganisms have been widely employed to test evolution theories. Microbial evolution under laboratory conditions facilitated the study of evolutionary hypotheses

and phenomena such as genetic drift, clonal interference, parallel evolution, evolutionary trade-off, mutation hitchhiking, and epistasis (243, 246).

5.2 Experimental design of microbial ALE

The simplest experimental design for microbial adaptive laboratory evolution entails inoculation of cells into growth medium and cultivation until the population density increases, followed by the regular transfer of cells to engage a new cultivation cycle (discontinuous batch cultivation), or the continuous supply of fresh nutrients and equal culture volume removal (continuous batch cultivation) (247). An identical selection pressure can be maintained over several generations, while additional selection pressure may be introduced in the form of increasing/decreasing pH, temperature, and nutrient concentration or by sequential addition of carbon sources for improved utilization (248). More intricate experimental evolution designs achieve higher degree of environment complexity through growth on beads, exposure to antibiotics, utilization of microcosms, or interaction with higher eukaryotic hosts such as plants, the gut of animals or worms. The inclusion of multiple microbial species in experimental evolution introduces further complexity compared to the propagation of a single clone (249). In **Study 5**, *Bacilli* were propagated in the presence of the phytopathogenic fungus *F. culmorum* on solid growth medium, according to the previously established bacterial-fungal experimental evolution system in **Study 2** (Fig. 20A). In **Study 6**, the experimental evolution design was modified so that *Bacilli* were co-cultured with the grey mold fungus *B. cinerea* under planktonic growth conditions (Fig. 20B).

As evidenced by numerous studies, filamentous fungi readily adapt to the specific environment, when subjected to controlled selective pressures under laboratory growth conditions (250–252). For example, the experimental evolution of the wild *Penicillium* molds demonstrated that within few serial passages, the fungal strains rapidly adapted to the growth niche in fermented foods and acquired phenotypic and metabolic traits alike

the domesticated relatives used in the cheese industry (253). The domestication entailed reduced mycotoxin production, decreased specialized metabolite biosynthesis, and altered volatilome profile. Therefore, to avoid the inadvertent evolution of the fungi and exclusively focus on *Bacillus* adaptation, the bacterial populations evolved in **Studies 5 and 6** underwent serial passages, while new fungal inoculum was applied in each cultivation cycle. The application of new fungal cells ensured consistent selective pressure in each experimental cycle, and represents an established approach for the experimental evolution of an inhibitor against a pathogen (254).

When applicable, the inclusion of control trajectories to experimental evolution is valuable for monitoring adaptation to the specific growth conditions, as demonstrated by previous studies (Zhou et al., 2018; Richter et al., 2023, Study 2). For instance, the addition of *Pseudomonas putida* control lineage in the experimental evolution study of *Acinetobacter* and *P. putida* biofilm associations accounted for the adaptations to growth in flow chambers (256), the repeated sole passage of *Streptomyces clavuligerus* served as an control lineage for the adaptative evolution of *S. clavuligerus* in competition against *Staphylococcus aureus* (254), and the parallel monoculture evolution of *Staphylococcus equorum* constituted a control to co-evolution of the bacterium with *Penicillia* (257). A corresponding approach was implemented in **Studies 5 and 6** to identify mutations solely arising from the selective pressure imposed by laboratory growth conditions and to pinpoint specific mutations resulting from co-cultivation with the fungus. Specifically, *Bacilli* were evolved in the absence of the fungi under identical cultivation conditions.

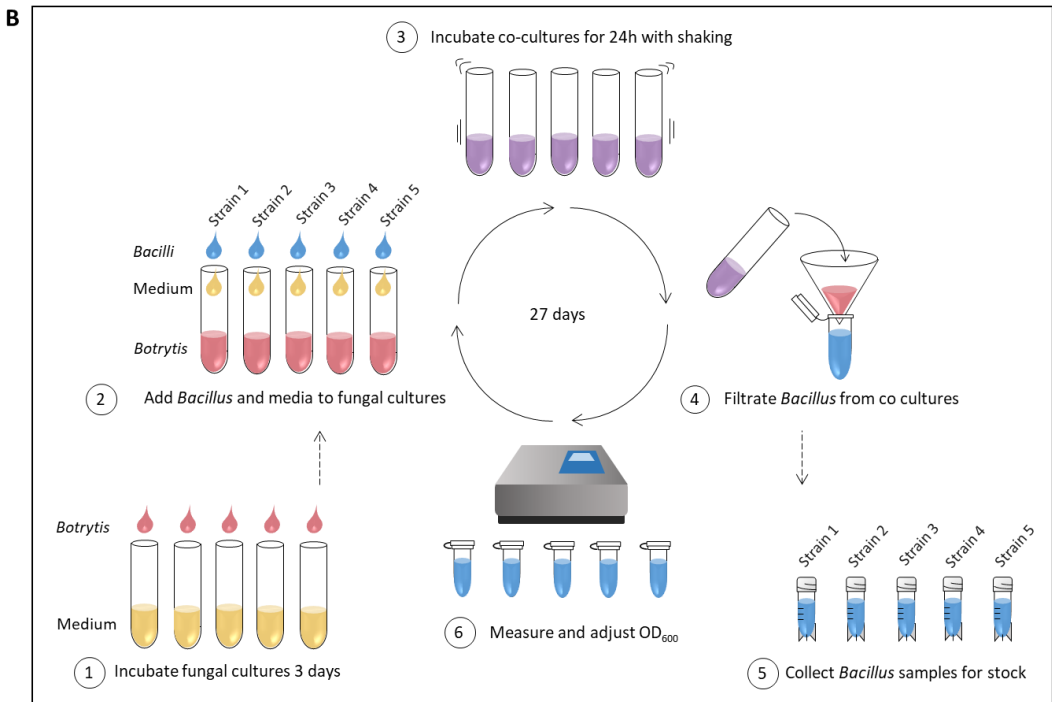
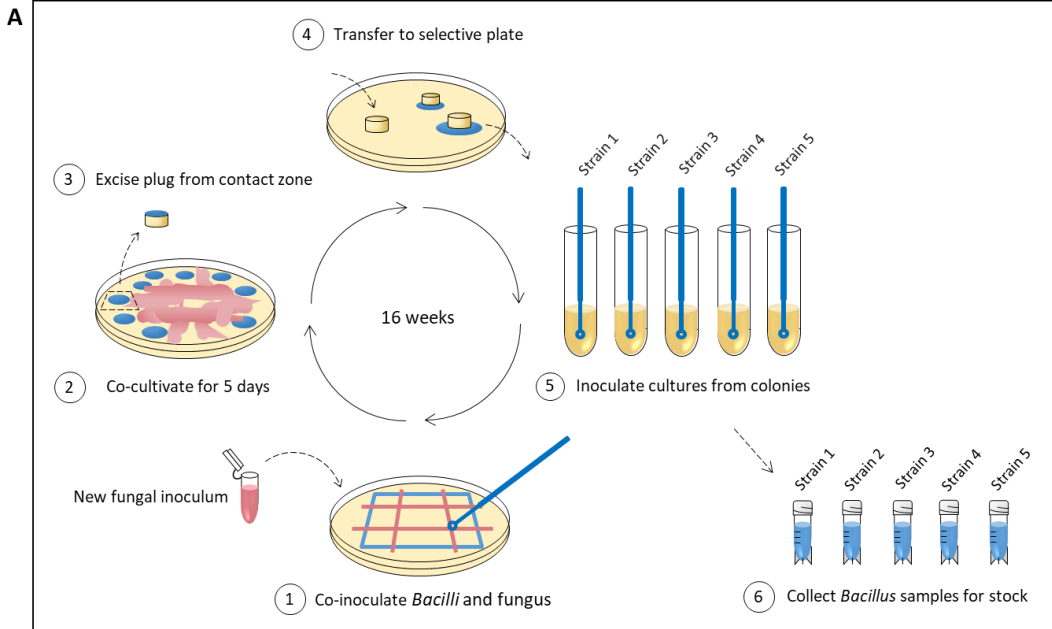


Fig. 20. Design of bacterial-fungal experimental evolution systems. **A)** *Bacillus* spp. were co-cultivated with *F. culmorum* for 16 consecutive cycles on solid medium (**Study 5**). The species were co-inoculated in a hashtag pattern onto the surface of a PDA growth plate and co-cultivated for 5 days at room temperature. An agar plug was excised from the growth contact zone and transferred to a bacterial selective medium. Overnight cultures (37°C) were inoculated from the outgrowing bacteria and stocks were prepared for later fitness screening. **B)** *Bacillus* spp. were co-cultivated with *Botrytis cinerea* for 27 cycles (approximately 200 bacterial generations) in liquid medium (**Study 6**). Fungal spores were suspended in PDB medium and incubated 3 days prior to addition of *Bacillus* cultures. The co-cultures were incubated with agitation for 24 h at 26°C. Following, the bacteria were separated from the fungal mycelium by passing the co-culture through a filter and discarding the mycelium. The bacterial filtrate was adjusted to OD₆₀₀ 0.01 prior to co-inoculation with fresh fungal cultures. In both experimental evolutions, the evolved populations were sampled by each passage and fresh fungal spores were used for the co-inoculations to prevent simultaneous evolution of the fungal strain. Bacterial evolution control lineages were grown under the same conditions, but in the absence of fungi.

5.3 Bacterial ALE with fungi and different modes-of-action for fungal inhibition

To the best of our knowledge, limited research has been conducted on the experimental adaptation of bacterial-fungal co-cultures, as was carried out in **Studies 2, 5 and 6**. Previous bacterial evolution in the presence of fungi includes for instance the adaptation of the cheese bacterium *S. equorum* in the presence of *Penicillium* spp., leading to out-competition of the bacterium in most co-evolved communities (257). The adaptation of bacterial persistors comprised few genetic changes, while evolved *S. equorum* control lineages acquired changes to a phosphoesterase, conferring reduced fitness against the *Penicillium chrysogenum* in comparison with the ancestor. Another study investigated the adaptation of *Saccharomycetaceae* to the sequential presence of a variety of bacterial competitors including *B. subtilis*, with the focus on increasing yeast fitness (255). This

study found that the cross-kingdom competition promoted large-scale genomic rearrangements and phenotypic diversification of yeast. Interestingly, an evolution experiment with *B. subtilis* and the phytopathogen *Setophoma terrestris* resulted in increased biofilm formation and colony structure complexity, impaired swarming, declined biosynthesis of the lipopeptides plipastatin and surfactin, as well as increased secretion of the ketones conferring enhanced inhibition of fungal growth (140). These findings exhibit striking similarities to the results obtained in **Study 5**, further discussed in the subsequent section.

In **Studies 5 and 6**, adaptive laboratory evolution of six undomesticated *Bacillus* spp., co-cultured with phytopathogenic fungi, was explored for the purpose of developing strains with improved fungal inhibition properties. In both studies, a large quantity of evolved isolates (1083 in **Study 5** and 293 in **Study 6**) from different time points, and derived from co-evolved or control populations, was assessed by high-throughput screening for fungal inhibition capacity by bacteria-fungal co-inoculation according to (153, **Study 3**). Additional primary phenotypic characterization (colony morphology, inhibition potency score, sporulation capacity) facilitated strain selection for whole genome sequencing and subsequent genotypic analysis. In **Study 6**, *Bacilli* subjected to experimental evolution under planktonic growth conditions predominantly accumulated genetic changes in flagellar genes, resulting in severely compromised motility, both in derivatives from control lineages and from co-cultivation with *B. cinerea* (Table 2). Impaired motility arising from adaption in shaken cultures has been documented multiple times and supposedly confers a growth advantage owing the shed energy burden (258–261). The obtained motility mutants produced colonies with reduced structure, in contrast to previous reports of hampered motility promoting evolution of wrinkled phenotypes (262).

Table 2. Motility-related mutations in evolved *Bacillus* strains. Genetic alterations related to motility genes were identified across ancestor (*B. subtilis* BCF001, BCF002, BCF010, *B. amyloliquefaciens* BCF007, *B. velezensis* BCF015) lineages in 52 out 193 of total mutations (Study 6).

Protein	Gene	Occurrences
Flagellar basal body rod protein FlgC	<i>flgC</i>	1
Flagellar basal body rod protein FlgG	<i>flgG</i>	1
Flagellar hook associated protein 1	<i>flgK</i>	1
Flagellar biosynthetic protein FliP	<i>fliP</i>	1
Flagellar stator protein MotB	<i>motB</i>	1
Flagellar stator protein MotA	<i>motA</i>	1
Flagellar protein required for flagellar formation	<i>fliL</i>	1
Flagellum assembly	<i>fliR</i>	1
Flagellum and nanotube assembly	<i>fliQ</i>	1
Flagellar assembly protein	<i>fliH</i>	1
Flagellar FliJ protein	<i>fliJ</i>	2
Flagellar biosynthesis protein FlhA	<i>flhA</i>	3
Two-component response regulator DegU	<i>degU</i>	4
Flagellar basal body rod protein FlgB	<i>flgB</i>	4
Swarming motility protein	<i>swrAA</i>	4
Flagellar hook-length control	<i>fliK</i>	8
Flagellar-specific ATPase	<i>fliI</i>	8
Flagellar motor switch protein FliM	<i>fliM</i>	9
Total		52

In addition to motility related genes, bacterial adaptations to *B. cinerea* comprised changes to metal ion transport proteins and regulators, identified in the ancestor *B. subtilis* BCF002 background, which may be indicative of growth medium specific adaptation or ion competition with the fungus. These strains also displayed increased γ -PGA production conferring a mucoid biofilm morphology, as previously evidenced and inversely linked to flagellar motor function (215). Other adaptations comprised the DegS-DegU regulatory system. An amino acid change in proximity to the response regulator

phosphorylation site conferred phenotypes previously associated with hyperactive DegU variants (206, 233, 263–265) i.e., loss of motility, reduced biofilm structure complexity, and strongly increased protease activity, suggesting altered phosphorylation pattern of the regulator. Another substitution within the DegU DNA-binding domain, potentially affecting the regulatory activity, conferred deterioration of biofilm structure complexity, reduced mucoidity, and lower production of the specialized metabolites fengycins and iturins, which led to reduced fungal inhibition potency. Additionally, a frameshift *degS* mutation was linked to diminished lipopeptide production and reduced biocontrol potency, which is in accordance with the proposed involvement of DegU-DegS in specialized metabolite biosynthesis through the pleiotropic regulator DegQ (106, 266, 267). Furthermore, the DegS mutant displayed insignificant protease activity, consistent with previous studies indicating reduced degradative enzyme production in absence of DegS phosphorylation (268). Despite the reported antifungal activity of *Bacillus* degradative enzymes (128, 129), protease activity of the evolved strains showed no direct correlation to antifungal potency. In comparison with the ancestors, most evolved strains showed reduced or comparable biosynthesis of specialized metabolites to their ancestors, consistent with diminished or comparable fungal inhibition potency, respectively. These results indicate that lipopeptides are intrinsic to the antifungal properties of *Bacillus* spp., especially fengycins and iturins, but also surfactins, as inferred from previous studies (28, 88, 138). Indeed, two strains derived from *B. amyloliquefaciens* BCF007 with amino acid modifications in the plipastatin subunit C and PksJ, the first module of the bacillaene hybrid PKS/NRPS (269), reached higher fungal inhibitory potency against *B. cinerea* growth compared with the ancestor. This phenotype is likely associated with the increased amounts of iturin, fengycin, or siderophores, and changed bacillaene, produced by those strains. This suggests a metabolic rewiring in biosynthesis of specialized metabolites, in accordance with previous observations of modified lipopeptide and polyketide production in response to fungi (28, 75). Furthermore, derivatives from *B. velezensis* BCF015 acquired modifications in carbon catabolite repression genes,

putatively conferring improved growth under conditions similar to those applied during the experimental evolution. These changes suggest selection for improved growth. Consistent with the adaptation of carbon catabolism, the transcriptomic response of *Bacilli* to co-cultivation with *F. culmorum* entailed differential expression of multiple genes belonging to the CcpA regulon (Carbon Catabolite Control Protein) (data not shown). Specifically, genes related to carbohydrate acquisition and utilization were downregulated, indicating the presence of the preferred carbon source, glucose (270). Higher expressed genes comprised the operon assigned for biosynthesis of branched-chain amino acids, the N-acetylglucosaminidase NagZ for recycling of linked sugars, the extracellular serine proteases subtilisin E, and the minor protease encoded by *vpr*. Potentially, these degradative enzymes could facilitate acquisition of carbohydrates and amino acids derived from fungal debris, fungal cell wall material, or complex media polymers made available by extracellular fungal enzymes (121, 124, 125, 271).

In **Study 5**, *Bacilli* subjected to repeated cultivation on solid medium adapted to the growth conditions predominantly through the functional loss of ComP, both in the presence and absence of *F. culmorum*. The two-component system ComP-ComA responds to cell-density dependent external signals and participates in a complex regulatory network that determines cell fate (159, 272). Furthermore, *Bacilli* adapted other key components of the quorum sensing system (ComQXPA) in addition to several regulators (Table 3) gating cell differentiation pathways i.e., development of genetic competence, onset of motility, initiation of biofilm formation, production of degradative enzymes, and biosynthesis of specialized metabolites.

Table 3. Cell differentiation mutations in evolved Bacillus strains. Genetic alterations related to cell differentiation genes were identified across ancestor (*B. subtilis* BCF001, BCF002, BCF010, *B. amyloliquefaciens* BCF007, *B. paraliceniformis* BCF009,) lineages in 73 out of 145 total mutations (**Study 5**). Count denotes number of occurrences across strains, where intergenic mutations are shown in brackets.

ORF	Protein	Count
<i>comP</i>	Sensor histidine kinase ComP	30
<i>comX</i>	Competence pheromone ComX	2
<i>comQ</i>	Tryptophan prenyltransferase ComQ	2
<i>comA</i>	Transcriptional regulatory protein ComA	1
<i>degS</i>	Cytoplasmic sensor histidine kinase DegS	1
<i>degU</i>	Transcriptional regulatory protein DegU	1
<i>degQ</i>	Regulatory protein DegQ	2
<i>rapA</i>	Response regulator aspartate phosphatase A	4(5)
<i>rapE</i>	Response regulator aspartate phosphatase E	(5)
<i>rapG</i>	Response regulator aspartate phosphatase G	3
<i>kinA</i>	Sporulation kinase A	5
<i>kinE</i>	Sporulation kinase E	5
<i>spoOB</i>	Sporulation initiation phosphotransferase B	2
<i>oppB</i>	Oligopeptide permease protein OppB	2
<i>oppC</i>	Oligopeptide permease protein OppC	1
<i>sinR</i>	Antagonist of SinR	1
<i>sinI</i>	Biofilm repressor SinR	1
Total		73

Derivatives that acquired genetic changes in *comP* were mainly associated with improved inhibition in the high-throughput screening for antifungal potency. Surprisingly, this improved inhibitory activity could not be ascribed to increased biosynthesis of specialized metabolites. Relative levels of fengycins and iturins, the most important antifungal lipopeptides for *Fusarium* inhibition (28, 88, 107, 109, 110, 119), were reduced, indicating an alternative mode of action for these specific derivatives. In correlation with the lower lipopeptide contents, the supernatant fungal inhibition potencies were diminished. Instead, enhanced fungal inhibition potency was associated with improved surface colonization capacity and increased volatilome inhibitory effect on fungal growth. In confrontation with *F. culmorum*, the improved colony expansion led to enhanced plate colonization, suggesting that loss of ComP function provided the evolved strains with improved abilities for space competition. A similar phenotype was observed in **Study 2** (81), leading to enhanced growth inhibition of *A. niger*, which was ascribed to increased

secretion of surfactin. In contrast, surfactin production was not improved, dismissing the involvement of the biosurfactant in surface spreading and growth inhibition of *F. culmorum*. Surface expansion could potentially arise from passive motive forces of a growing colony and the secretion of biofilm exopolysaccharides (273). The quorum sensing system ComP-ComA may modulate biofilm formation through the regulation of Rap protein expression (169, 171, 196), which in turn controls the phosphorylation of the master regulator Spo0A, (170), that gates entry to sporulation or matrix production. In addition, ComP-ComA induce transcription of DegQ (208), which activates the regulatory system DegS-DegU (207), influencing biofilm synthesis and complexity (57, 267, 274, 275). Indeed, phenotypic characterization of quorum sensing mutants unveiled reduced biofilm structure complexity, desiccated colony appearance, and enhanced surface spreading. The dry colony appearance was linked to decreased γ -PGA production, in accordance with prior research establishing the involvement of ComP-ComA function in biosynthesis of the polymer (227, 276, 277). As documented on several occasions, the importance of robust biofilm formation for root colonization and rhizosphere persistence correlates with the biocontrol capacity of a strain (224, 278). Therefore, the root colonization capacity of *A. thaliana* seedlings by quorum sensing mutants was investigated. However, owing the high variability of this type of assays (35, 197, 241), further experimental repetitions are required to draw any conclusions.

In addition to improved surface colonization, derivatives with *comp* mutations displayed enhanced fungal inhibitory effect by volatile organic compounds. Interestingly, similar results were obtained for a *B. subtilis* strain subjected to experimental evolution in co-culture with the fungus *S. terrestris* on solid growth medium (140). The bacterial-fungal co-cultivation promoted adaptation of the quorum sensing system (ComQPXA), which resulted in decreased biosynthesis of antifungal lipopeptides and elevated production of the ketones, 2-heptanone and 2-octanone, conferring improved fungal growth inhibition (140). Unlike the experimental design of **Study 5**, no control lineage was included. In **Study 5**, the inclusion of control lineages enabled us to conclude that the adaptation of

the quorum sensing system owes the growth condition selection pressure rather than the fungal presence. In **Study 5**, the improved fungal inhibition by volatile compounds observed for *comP* mutants requires further volatilome analysis to determine which specific volatile compounds are responsible for this trait.

5.4 *Bacillus*-fungi ALE dynamics and trends

In both experimental evolution campaigns, mutations in *comP* and motility genes were identified in derivatives from the first timepoint studied, consistent with the fast adaptation reported for *Bacilli* (262, 279, 280). Genetic changes in the respective genes emerged within just 15 days of adaptation to planktonic growth and 5 weeks of cultivation on potato dextrose agar. In addition, global- and specific regulators were targeted during the adaptation in both experimental evolution campaigns. Such substantial adaptation enabled by regulatory changes rather than genetic changes affecting single protein functions, is a phenomenon that has been extensively documented in diverse microorganisms including *E. coli*, *Candida albicans*, and *Saccharomyces cerevisiae* (243). Indeed, adaptation of the regulators DegU-DegS, ComP-ComA, CcpA, CzrA, or SwrAA among others, resulted in changes to specialized metabolite biosynthesis, protease activity, motility, γ -PGA production, biofilm structure complexity, and antifungal volatilome effect, demonstrating that adaptation of single regulators may impose drastic changes to multiple phenotypes.

In **Study 5**, a decreasing number of improved derivatives was selected as the evolution experiment progressed, except for derivatives originating from the less effective fungal inhibitor *B. paralicheniformis* BCF009. This finding suggests that strains with lower initial fitness comprise more room for improvement compared to prolific fungal inhibitors (BCF001, BCF002, BCF007, BCF010). Consistent with this hypothesis, *E. coli* strains adapted to glucose-based growth with low initial fitness on maltose improved their growth on maltose more and reached same fitness level as those strains already adapted

to maltose (281). In **Study 6**, no common trend in improvement was observed across ancestors. Noteworthy, results in **Study 6** built on screening of roughly 300 evolved strains, whereas in **Study 5** close to 1100 *Bacillus* evolved derivatives were screened. Hence, the limited numbers of screened strains in **Study 6** may explain the lack of an apparent trend in antifungal potency improvement/reduction.

Intriguingly, in both laboratory evolution experiments, mutations specific to the laboratory growth conditions (*comP*/motility genes) represented the most prevalent genetic changes and heavily dominated the adaptation. These results suggest that the experimental designs selected for fast domestication. Given the rapid adaptation of microorganisms, model microbes have likely and inadvertently undergone evolutionary changes in response to the laboratory conditions during routine cultivation and freeze-storing cycles (282). For example, the *B. subtilis* model strain 168 lost distinguished phenotypic features of an undomesticated strain, such as robust biofilm formation with complex structures, exopolysaccharides production, γ -PGA biosynthesis, swarming motility, and the specialized metabolite surfactin, owing mutations in *degQ*, *epsC*, *rapP*, *swrAA*, and *sfp* (213, 227, 274, 283–286). Further laboratory evolution studies identified the sporulation pathway and the regulators DegU and SinR as targets of domestication in *Bacilli*, leading to impaired of swarming motility, altered biofilm formation, loss of biofilm structure, reduced extracellular protease activity, and hampered sporulation capacity (279, 287–290, **Study 2**). Several of these phenotypes were observed as a result of serial passages of the undomesticated *Bacillus* spp. in **Studies 5 and 6**, suggesting strong selection for adaptation to the laboratory growth condition. While most growth conditioned changes were represented in both fungal-adapted lineages and control lineages, genetic changes targeting the sporulation pathway and sporulation-deficient derivatives were exclusively identified in evolved control populations. This observation suggests that preservation of sporulation is required in fungal co-culture, but not detrimental to *Bacillus* laboratory single-species cultures. The selection pressure to maintain functional sporulation in co-culture could be related to accelerated nutrient

consumption and initiation of sporulation at an earlier timepoint compared to single-species culture, resulting in transfer of a higher spore quantity. Despite the strong laboratory adaptation, improvement of antifungal properties was observed in derivatives from both control lineages and populations evolved in the presence of fungi. For example, the functional loss of ComP arose across all populations in **Study 5**, and yet resulted in enhanced fungal inhibition by volatiles and improved competition for growth space under laboratory growth conditions. These findings suggest that the adaptation of the evolved strains to the laboratory environment confers an advantage in co-culture with the respective fungi under these specific growth conditions.

Experimental evolution to achieve enhanced specialized metabolite production has previously been explored by species co-cultivation. For instance, a study focused on developing prolific antibiotic producers by examining the repeated competition between methicillin-resistant *S. aureus* (MRSA) N315 and *S. clavuligerus* (254). This led to the enhanced constitutive production of holomycin by *S. clavuligerus*, effectively inhibiting the growth of MRSA. In contrast, both experimental evolutions presented in this thesis mainly led to reduced secretion of the major antifungal lipopeptides i.e., iturins and fengycins, suggesting decreased antagonism in response to repeated cultivation under the specific conditions. The reduction of antifungal compounds in combination with the high number of mutations specific to laboratory growth adaptation suggest that fungal co-cultivation imposed a weak selection pressure for antagonistic improvement on the bacteria. In natural populations, the removal or weakening of a selection pressure results in reduction or loss of traits that were maintained by the specific selection (291). The competition for resources between fungi and bacteria over million years is hypothesized to have promoted the development and diversification of bioactive compounds (59). Under the laboratory conditions employed in **Studies 2, 5 and 6**, resources were plentiful and regularly renewed. Hence, it is plausible that the nutrient abundance imposed a relaxed selection for antifungal properties and instead selected for growth. Indeed, in

both studies several adaptation strategies concerned energy conservation i.e., through mutations in the costly flagellum machinery leading to loss of motility, reduction of specialized metabolite biosynthesis, declined protease activity, or alterations to carbon catabolite repression enabling improved growth. Collectively, the results suggest that in absence of competitive stimulation, the antifungal properties wither in progression with adaptation to laboratory conditions. For future endeavors in improving antifungal properties of *Bacillus* spp., modifications to the experimental design may be required. It would be interesting to explore the adaption of *Bacilli* to fungal co-culture under nutrient limitation. However, this approach may be challenging, as these conditions could potentially result in reduced growth or loss of one of the species, consistent with the experimental evolution of the cheese bacterium *S. equorum* in the presence of *Penicillia* (257). Alternative strategies for improving antifungal capacity of *Bacillus* spp. may yield more fruitful results, such as chemical mutagenesis for enhanced natural product biosynthesis followed by the implementation of high-throughput screening methods tailored to identify potent candidate strains.

Chapter 6 | Conclusions and perspectives

Bacillus spp. naturally inhabit the rhizosphere and confer plant growth promoting benefits to crop cultivars, positioning them as excellent options for biological products in agricultural applications. In addition, *Bacilli* are potent producers of specialized metabolites with bioactivity against diverse microorganisms. Numerous studies document the proficient antifungal properties of natural *Bacillus* isolates, attributed to biosynthesis of cyclic lipopeptides and other antifungal compounds. For this reason, members of the *Bacillus* genus are promising candidates for biocontrol of fungal phytopathogens in agricultural settings. The employment of microbial biocontrol solutions offers a sustainable alternative to the heavy usage of chemical pesticides and addresses the increasing fungicide resistance. However, the efficient implementation of biocontrol agents to combat fungal phytopathogens requires a better understanding of bacterial-fungal interactions.

We explored the interaction between *Bacillus* spp. and filamentous fungi by co-cultivation and adaptive laboratory evolution with focus on the *Bacilli*. Co-cultivation of *B. subtilis* with *A. niger* or *A. bisporus* demonstrated that the biofilm components EPS and the structural protein TasA are essential for successful bacterial colonization of the hyphae. The study further exemplified division of labor between subpopulations deficient in the production of matrix components, as biofilm formation was restored upon mixing of *Bacillus* mutants with complementary biofilm mutations (*tasA/eps*).

The adapted response of *B. subtilis* to *A. niger* was investigated by a simple experimental evolution system that resulted in increased surfactin production, conferring enhanced fungal inhibition by surface spreading, fungal cell wall stress, and reduced medium acidification by the fungus. The study provided insights of the primary adaptation path of *B. subtilis* to *A. niger*.

The indication that repetitive cycles of bacterial-fungal co-cultivation fosters increased inhibition potency inspired us to explore adaptive laboratory evolution as a tool for biocontrol strain improvement against fungal phytopathogens. Undomesticated *Bacillus* spp. were co-cultivated in the presence of *F. culmorum* or *B. cinerea* in repetitive cycles on solid growth medium or under planktonic growth conditions, respectively. For benchmarking the evolved strains to their ancestors, we developed two novel quantitative high-throughput screening methods that facilitated easy comparison and scoring of fungal inhibition potency by co-inoculation of the species or by assessment of the bacterial supernatant effect on fungal growth. We propose a combination of these methods for screening of large libraries, as an innovative strategy to identify biocontrol strains. The methods were employed to screen a great number of evolved *Bacillus* strains and enabled selection of derivatives for further phenotypic and genotypic characterization.

During experimental evolution with *F. culmorum*, we found that *Bacilli* readily adapted to the laboratory growth conditions by loss of ComP function, which conferred improved fungal inhibition in the initial screening of evolved strains. Surprisingly, the improved *comP* derivatives were associated with reduced production of the lipopeptide specialized metabolites and employed alternative antagonistic mechanisms i.e., enhanced surface colonization and altered volatilome composition. The nature of the antifungal compounds and whether the improved competition for space confers enhanced growth niche colonization on plant roots remains to be investigated.

During experimental evolution with *B. cinerea*, *Bacilli* adapted to the planktonic growth conditions by acquiring mutations in flagellar genes, leading to compromised motility. In both experimental evolution campaigns, further genetic alterations were identified in genes related to regulation and cell differentiation, conferring multiple phenotypic changes such as altered colony morphology, changed biofilm matrix production, rewired specialized metabolite production, modified protease activity, and adapted fungal inhibition. Most adaptation strategies concerned energy preservation through various

mechanisms such as loss of motility, reduced specialized metabolite production, and modified carbon catabolism control. The findings of these studies suggest that experimental evolution of *Bacilli* in the presence of filamentous fungi imposes a weak selection pressure for classical antagonism provided by the lipopeptidic specialized metabolites. On the contrary, we showed that *Bacilli* readily adapted to the laboratory growth conditions by modulating costly cellular and biosynthetic pathways, indicative of an evolutionary selection for growth.

Although it is generally accepted that the antifungal properties of *Bacilli* greatly rely on the production of cyclic lipopeptides, the experimental evolution studies indicate the presence of multiple pathways for achieving effective antifungal potency, such as volatile-mediated antibiosis, competition for growth space, or improved growth under the specific conditions. For future strain improvement endeavors to achieve improved production of antifungal lipopeptides, we suggest rethinking the bacterial-fungal experimental evolution design or engaging in alternative approaches such as chemical mutagenesis followed by suiting screening methods.

In conclusion, this Ph.D. project contributed to the knowledge of bacterial-fungal interactions and understanding of the *Bacillus* adapted response to fungal co-cultivation. The investigation of *Bacillus* antifungal potency highlighted the importance of specialized metabolites and additional alternative fungal inhibition mechanisms. Furthermore, the project examined experimental evolution as a tool for strain improvement for biocontrol purposes.

References

1. Alexandratos N, Bruinsma J. 2012. World Agriculture Towards 2030 / 2050: The 2012 Revision. ESA Work Pap 12:146.
2. FAO. 2019. New standards to curb the global spread of plant pests and diseases. <http://www.fao.org/news/story/en/item/1187738/icode/>. Retrieved 28 March 2020.
3. Secretariat I. 2021. Scientific review of the impact of climate change on plant pests. Scientific review of the impact of climate change on plant pests. FAO on behalf of the IPPC Secretariat. <https://doi.org/10.4060/cb4769en>. Retrieved 17 May 2023.
4. Savary S, Ficke A, Aubertot J-N, Hollier C. 2012. Crop losses due to diseases and their implications for global food production losses and food security. *Food Secur* 4:519–537.
5. Savary S, Willcoquet L, Pethybridge SJ, Esker P, McRoberts N, Nelson A. 2019. The global burden of pathogens and pests on major food crops. *Nat Ecol Evol* 3:430–439.
6. Aoki T, O'Donnell K, Geiser DM. 2014. Systematics of key phytopathogenic *Fusarium* species: Current status and future challenges. *J Gen Plant Pathol* 80:189–201.
7. Bi K, Liang Y, Mengiste T, Sharon A. 2023. Killing softly: a roadmap of *Botrytis cinerea* pathogenicity. *Trends Plant Sci* 28:211–222.
8. Sobrova P, Adam V, Vasatkova A, Beklova M, Zeman L, Kizek R. 2010. Deoxynivalenol and its toxicity. *Interdiscip Toxicol* 3:94–99.
9. Rocha O, Ansari K, Doohan FM. 2005. Effects of trichothecene mycotoxins on eukaryotic cells: A review. *Food Addit Contam* 22:369–378.
10. Hua L, Yong C, Zhanquan Z, Boqiang L, Guozheng Q, Shiping T. 2018. Pathogenic mechanisms and control strategies of *Botrytis cinerea* causing post-harvest decay

References

- in fruits and vegetables. *Food Qual Saf. Oxford Academic*
<https://doi.org/10.1093/fqsafe/fyy016>.
11. Williamson B, Tudzynski B, Tudzynski P, Van Kan JAL. 2007. *Botrytis cinerea*: The cause of grey mould disease. *Mol Plant Pathol* 8:561–580.
 12. Sharma A, Kumar V, Shahzad B, Tanveer M, Sidhu GPS, Handa N, Kohli SK, Yadav P, Bali AS, Parihar RD, Dar OI, Singh K, Jasrotia S, Bakshi P, Ramakrishnan M, Kumar S, Bhardwaj R, Thukral AK. 2019. Worldwide pesticide usage and its impacts on ecosystem. *SN Appl Sci* <https://doi.org/10.1007/s42452-019-1485-1>.
 13. Kim KH, Kabir E, Jahan SA. 2017. Exposure to pesticides and the associated human health effects. *Sci Total Environ. Elsevier B.V.*
<https://doi.org/10.1016/j.scitotenv.2016.09.009>.
 14. Syafrudin M, Kristanti RA, Yuniarto A, Hadibarata T, Rhee J, Al-onazi WA, Algarni TS, Almarri AH, Al-Mohaimeed AM. 2021. Pesticides in Drinking Water—A Review. *Int J Environ Res Public Health* 18:468.
 15. Hahn M. 2014. The rising threat of fungicide resistance in plant pathogenic fungi: *Botrytis* as a case study. *J Chem Biol. Springer Verlag*
<https://doi.org/10.1007/s12154-014-0113-1>.
 16. Harper LA, Paton S, Hall B, McKay S, Oliver RP, Lopez-Ruiz FJ. 2022. Fungicide resistance characterized across seven modes of action in *Botrytis cinerea* isolated from Australian vineyards. *Pest Manag Sci* 78:1326–1340.
 17. Hellin P, King R, Urban M, Hammond-Kosack KE, Legrève A. 2018. The adaptation of *Fusarium culmorum* to DMI fungicides is mediated by major transcriptome modifications in response to azole fungicide, including the overexpression of a PDR transporter (*FcABC1*). *Front Microbiol* 9:1385.
 18. Nguyen PA, Strub C, Fontana A, Schorr-Galindo S. 2017. Crop molds and mycotoxins: Alternative management using biocontrol. *Biol Control. Academic Press* <https://doi.org/10.1016/j.biocontrol.2016.10.004>.
 19. Dunlap C. 2019. Phylogeny and Taxonomy of Agriculturally Important *Bacillus*
-

References

- Species, p. 143–150. *In* Bacilli in Climate Resilient Agriculture and Bioprospecting. Springer, Cham.
20. Cawoy H, Bettiol W, Fickers P, Ongena M. 2011. Bacillus-Based Biological Control of Plant Diseases. *Pestic Mod World - Pestic Use Manag* 1849:273–303.
 21. Caulier S, Nannan C, Gillis A, Licciardi F, Bragard C, Mahillon J. 2019. Overview of the Antimicrobial Compounds Produced by Members of the *Bacillus subtilis* Group. *Front Microbiol* 10:302.
 22. Stein T. 2005. *Bacillus subtilis* antibiotics: Structures, syntheses and specific functions. *Mol Microbiol* 56:845–857.
 23. Ongena M, Jacques P. 2008. Bacillus lipopeptides: versatile weapons for plant disease biocontrol. *Trends Microbiol* 16:115–125.
 24. Klich MA, Arthur KS, Lax AR, Bland JM. 1994. Iturin A: A potential new fungicide for stored grains. *Mycopathologia* 127:123–127.
 25. Fazle Rabbee M, Baek KH. 2020. Antimicrobial Activities of Lipopeptides and Polyketides of *Bacillus velezensis* for Agricultural Applications. *Molecules*. Multidisciplinary Digital Publishing Institute (MDPI) <https://doi.org/10.3390/molecules25214973>.
 26. Legein M, Smets W, Vandenneuvel D, Eilers T, Muyschondt B, Prinsen E, Samson R, Lebeer S. 2020. Modes of Action of Microbial Biocontrol in the Phyllosphere. *Front Microbiol*. *Frontiers Media S.A.* <https://doi.org/10.3389/fmicb.2020.01619>.
 27. Harwood CR, Mouillon JM, Pohl S, Arnau J. 2018. Secondary metabolite production and the safety of industrially important members of the *Bacillus subtilis* group. *FEMS Microbiol Rev* <https://doi.org/10.1093/femsre/fuy028>.
 28. Cawoy H, Debois D, Franzil L, De Pauw E, Thonart P, Ongena M. 2015. Lipopeptides as main ingredients for inhibition of fungal phytopathogens by *Bacillus subtilis*/*amyloliquefaciens*. *Microb Biotechnol* 8:281–295.
 29. Robin DC, Marchand PA. 2019. Evolution of the biocontrol active substances in the framework of the European Pesticide Regulation (EC) No. 1107/2009. *Pest Manag*
-

References

- Sci 75:950–958.
30. Droby S, Wisniewski M, Macarasin D, Wilson C. 2009. Twenty years of postharvest biocontrol research: Is it time for a new paradigm? *Postharvest Biol Technol* 52:137–145.
 31. Droby S, Wisniewski M, Teixidó N, Spadaro D, Jijakli MH. 2016. The science, development, and commercialization of postharvest biocontrol products. *Postharvest Biol Technol* 122:22–29.
 32. Besset-Manzoni Y, Joly P, Brutel A, Gerin F, Soudière O, Langin T, Prigent-Combaret C. 2019. Does in vitro selection of biocontrol agents guarantee success in planta? A study case of wheat protection against *Fusarium* seedling blight by soil bacteria. *PLoS One* 14:e0225655.
 33. Folman LB, Postma J, Van Veen JA. 2003. Inability to find consistent bacterial biocontrol agents of *Pythium aphanidermatum* in cucumber using screens based on ecophysiological traits. *Microb Ecol* 45:72–87.
 34. Pliego C, Ramos C, de Vicente A, Cazorla FM. 2011. Screening for candidate bacterial biocontrol agents against soilborne fungal plant pathogens. *Plant Soil* <https://doi.org/10.1007/s11104-010-0615-8>.
 35. Blake C, Nordgaard M, Maróti G, Kovács ÁT. 2021. Diversification of *Bacillus subtilis* during experimental evolution on *Arabidopsis thaliana* and the complementarity in root colonization of evolved subpopulations. *Environ Microbiol* 23:6122–6136.
 36. Hong HA, To E, Fakhry S, Baccigalupi L, Ricca E, Cutting SM. 2009. Defining the natural habitat of *Bacillus* spore-formers. *Res Microbiol* 160:375–379.
 37. Chen XH, Koumoutsi A, Scholz R, Schneider K, Vater J, Süßmuth R, Piel J, Borriss R. 2009. Genome analysis of *Bacillus amyloliquefaciens* FZB42 reveals its potential for biocontrol of plant pathogens. *J Biotechnol* 140:27–37.
 38. Raaijmakers JM, de Bruijn I, Nybroe O, Ongena M. 2010. Natural functions of lipopeptides from *Bacillus* and *Pseudomonas*: More than surfactants and
-

References

- antibiotics. *FEMS Microbiol Rev* <https://doi.org/10.1111/j.1574-6976.2010.00221.x>.
39. Romero D, Traxler MF, López D, Kolter R. 2011. Antibiotics as signal molecules. *Chem Rev* 111:5492–5505.
 40. Gupta RS, Patel S, Saini N, Chen S. 2020. Robust demarcation of 17 distinct *Bacillus* species clades, proposed as novel Bacillaceae genera, by phylogenomics and comparative genomic analyses: description of *Robertmurraya kyonggiensis* sp. nov. and proposal for an emended genus *Bacillus* limiting it o. *Int J Syst Evol Microbiol* 70:5753–5798.
 41. Hamoen LW, Venema G, Kuipers OP. 2003. Controlling competence in *Bacillus subtilis*: Shared use of regulators. *Microbiology* <https://doi.org/10.1099/mic.0.26003-0>.
 42. Kovács ÁT. 2019. *Bacillus subtilis*. *Trends Microbiol* <https://doi.org/10.1016/j.tim.2019.03.008>.
 43. Moszer I, Jones LM, Moreira S, Fabry C, Danchin A. 2002. SubtiList: The reference database for the *Bacillus subtilis* genome. *Nucleic Acids Res* 30:62–65.
 44. Zhu B, Stülke J. 2018. SubtiWiki in 2018: From genes and proteins to functional network annotation of the model organism *Bacillus subtilis*. *Nucleic Acids Res* 46:D743–D748.
 45. Geissler AS, Anthon C, Alkan F, González-Tortuero E, Poulsen LD, Kallehauge TB, Breüner A, Seemann SE, Vinther J, Gorodkin J. 2021. Bsgatlas: A unified *bacillus subtilis* genome and transcriptome annotation atlas with enhanced information access. *Microb Genomics* 7.
 46. Barbe V, Cruveiller S, Kunst F, Lenoble P, Meurice G, Sekowska A, Vallenet D, Wang T, Moszer I, Médigue C, Danchin A. 2009. From a consortium sequence to a unified sequence: The *Bacillus subtilis* 168 reference genome a decade later. *Microbiology* 155:1758–1775.
 47. Payling L, Woyengo TA, Nielsen M, Stein HH, Walsh MC, Romero L, Arent S. 2019.
-

References

- Microscopy and protein solubilization of digesta from pigs fed wheat, corn, or soybean meal-based diets, with or without protease and a *Bacillus* spp. direct-fed microbial. *Anim Feed Sci Technol* 247:183–193.
48. Wang D, Li A, Han H, Liu T, Yang Q. 2018. A potent chitinase from *Bacillus subtilis* for the efficient bioconversion of chitin-containing wastes. *Int J Biol Macromol* 116:863–868.
 49. Contesini FJ, Melo RR de, Sato HH. 2018. An overview of *Bacillus* proteases: from production to application. *Crit Rev Biotechnol* 38:321–334.
 50. Lee NK, Kim WS, Paik HD. 2019. *Bacillus* strains as human probiotics: characterization, safety, microbiome, and probiotic carrier. *Food Sci Biotechnol*. Springer <https://doi.org/10.1007/s10068-019-00691-9>.
 51. Abriouel H, Franz CMAP, Omar N Ben, Galvez A. 2011. Diversity and applications of *Bacillus* bacteriocins. *FEMS Microbiol Rev* 35:201–232.
 52. Torsvik V, Goksoyr J, Daae FL. 1990. High diversity in DNA of soil bacteria. *Appl Environ Microbiol* 56:782–787.
 53. Raynaud X, Nunan N. 2014. Spatial ecology of bacteria at the microscale in soil. *PLoS One* 9.
 54. Blake C, Christensen MN, Kovács ÁT. 2021. Molecular Aspects of Plant Growth Promotion and Protection by *Bacillus subtilis*. *Mol Plant Microbe Interact* 34:15–25.
 55. Backer R, Rokem JS, Ilangumaran G, Lamont J, Praslickova D, Ricci E, Subramanian S, Smith DL. 2018. Plant growth-promoting rhizobacteria: Context, mechanisms of action, and roadmap to commercialization of biostimulants for sustainable agriculture. *Front Plant Sci*. Frontiers Media S.A. <https://doi.org/10.3389/fpls.2018.01473>.
 56. Lugtenberg B, Kamilova F. 2009. Plant-growth-promoting rhizobacteria. *Annu Rev Microbiol* 63:541–556.
 57. Vlamakis H, Chai Y, Beaugerard P, Losick R, Kolter R. 2013. Sticking together:
-

References

- Building a biofilm the *Bacillus subtilis* way. *Nat Rev Microbiol*
<https://doi.org/10.1038/nrmicro2960>.
58. Frey-Klett P, Burlinson P, Deveau A, Barret M, Tarkka M, Sarniguet A. 2011. Bacterial-Fungal Interactions: Hyphens between Agricultural, Clinical, Environmental, and Food Microbiologists. *Microbiol Mol Biol Rev* 75:583–609.
 59. Deveau A, Bonito G, Uehling J, Paoletti M, Becker M, Bindschedler S, Hacquard S, Hervé V, Labbé J, Lastovetsky OA, Mieszkin S, Millet LJ, Vajna B, Junier P, Bonfante P, Krom BP, Olsson S, van Elsas JD, Wick LY. 2018. Bacterial-fungal interactions: Ecology, mechanisms and challenges. *FEMS Microbiol Rev* 42:335–352.
 60. Effmert U, Kalderás J, Warnke R, Piechulla B. 2012. Volatile Mediated Interactions Between Bacteria and Fungi in the Soil. *J Chem Ecol* 38:665–703.
 61. Lowery CA, Dickerson TJ, Janda KD. 2008. Interspecies and interkingdom communication mediated by bacterial quorum sensing. *Chem Soc Rev* 37:1337–1346.
 62. Steffan BN, Venkatesh N, Keller NP. 2020. Let’s get physical: Bacterial-fungal interactions and their consequences in agriculture and health. *J Fungi*. Multidisciplinary Digital Publishing Institute <https://doi.org/10.3390/jof6040243>.
 63. Wu Y, Zhou J, Li C, Ma Y. 2019. Antifungal and plant growth promotion activity of volatile organic compounds produced by *Bacillus amyloliquefaciens*. *Microbiologyopen* 8:1–14.
 64. Briard B, Heddergott C, Latgé JP. 2016. Volatile compounds emitted by *Pseudomonas aeruginosa* stimulate growth of the fungal pathogen *Aspergillus fumigatus*. *MBio* 7.
 65. Briard B, Rasoldier V, Bomme P, Elaouad N, Guerreiro C, Chassagne P, Muszkieta L, Latgé JP, Mulard L, Beauvais A. 2017. Dirhamnolipids secreted from *Pseudomonas aeruginosa* modify anjpeungal susceptibility of *Aspergillus fumigatus* by inhibiting β 1,3 glucan synthase activity. *ISME J* 11:1578–1591.
 66. Simon A, Hervé V, Al-Dourobi A, Verrecchia E, Junier P. 2017. An in situ inventory
-

References

- of fungi and their associated migrating bacteria in forest soils using fungal highway columns. *FEMS Microbiol Ecol* 93:217.
67. Stopnisek N, Zuhlke D, Carlier A, Barberan A, Fierer N, Becher D, Riedel K, Eberl L, Weisskopf L. 2016. Molecular mechanisms underlying the close association between soil Burkholderia and fungi. *ISME J* 10:253–264.
 68. Mondo SJ, Lastovetsky OA, Gaspar ML, Schwardt NH, Barber CC, Riley R, Sun H, Grigoriev I V., Pawlowska TE. 2017. Bacterial endosymbionts influence host sexuality and reveal reproductive genes of early divergent fungi. *Nat Commun* 8:1–9.
 69. Khan N, Martínez-Hidalgo P, Ice TA, Maymon M, Humm EA, Nejat N, Sanders ER, Kaplan D, Hirsch AM. 2018. Antifungal activity of bacillus species against fusarium and analysis of the potential mechanisms used in biocontrol. *Front Microbiol* 9:2363.
 70. Fira D, Dimkić I, Berić T, Lozo J, Stanković S. 2018. Biological control of plant pathogens by Bacillus species. *J Biotechnol* 285:44–55.
 71. Santoyo G, del Orozco-Mosqueda MC, Govindappa M. 2012. Mechanisms of biocontrol and plant growth-promoting activity in soil bacterial species of Bacillus and Pseudomonas: A review. *Biocontrol Sci Technol* <https://doi.org/10.1080/09583157.2012.694413>.
 72. Khan N, Maymon M, Hirsch A. 2017. Combating Fusarium Infection Using Bacillus-Based Antimicrobials. *Microorganisms* 5:75.
 73. Wang W, Zhao J, Zhang Z. 2022. Bacillus Metabolites: Compounds, Identification and Anti-Candida albicans Mechanisms. *Microbiol Res (Pavia)*. Multidisciplinary Digital Publishing Institute <https://doi.org/10.3390/microbiolres13040070>.
 74. Jakab Á, Kovács F, Balla N, Tóth Z, Ragyák Á, Sajtos Z, Csillag K, Nagy-Köteles C, Nemes D, Bácskay I, Pócsi I, Majoros L, Kovács ÁT, Kovács R. 2022. Physiological and transcriptional profiling of surfactin exerted antifungal effect against Candida albicans. *Biomed Pharmacother* 152.
-

References

75. Andrić S, Meyer T, Ongena M. 2020. *Bacillus* Responses to Plant-Associated Fungal and Bacterial Communities. *Front Microbiol* 11:1350.
76. Li B, Li Q, Xu Z, Zhang N, Shen Q, Zhang R. 2014. Responses of beneficial *Bacillus amyloliquefaciens* SQR9 to different soilborne fungal pathogens through the alteration of antifungal compounds production. *Front Microbiol* 5:636.
77. Ola ARB, Thomy D, Lai D, Brötz-Oesterhelt H, Proksch P. 2013. Inducing secondary metabolite production by the endophytic fungus *Fusarium tricinctum* through coculture with *Bacillus subtilis*. *J Nat Prod* 76:2094–2099.
78. Singh D, Lee SH, Lee CH. 2022. Non-obligate pairwise metabolite cross-feeding suggests ammensalic interactions between *Bacillus amyloliquefaciens* and *Aspergillus oryzae*. *Commun Biol* 5:1–12.
79. Benoit I, van den Esker MH, Patyshakuliyeva A, Mattern DJ, Blei F, Zhou M, Dijksterhuis J, Brakhage AA, Kuipers OP, de Vries RP, Kovács ÁT. 2015. *Bacillus subtilis* attachment to *Aspergillus niger* hyphae results in mutually altered metabolism. *Environ Microbiol* 17:2099–2113.
80. Kjeldgaard B, Listian SA, Ramaswamhi V, Richter A, Kiesewalter HT, Kovács ÁT. 2019. Fungal hyphae colonization by *Bacillus subtilis* relies on biofilm matrix components. *Biofilm* 1:100007.
81. Richter A, Blei F, Hu G, Schwitalla JW, Lozano-Andrade CN, Jarmusch SA, Wibowo M, Kjeldgaard B, Surabhi S, Jautzus T, Phippen CBW, Tyc O, Arentshorst M, Wang Y, Garbeva P, Larsen TO, Ram AFJ, Hondel CAM van den, Maroti G, Kovacs AT. 2023. Enhanced niche colonisation and competition during bacterial adaptation to a fungus. *bioRxiv* 2023.03.27.534400.
82. Harvey AL, Edrada-Ebel R, Quinn RJ. 2015. The re-emergence of natural products for drug discovery in the genomics era. *Nat Rev Drug Discov* <https://doi.org/10.1038/nrd4510>.
83. Traxler MF, Kolter R. 2015. Natural products in soil microbe interactions and evolution. *Nat Prod Rep* 32:956–970.

References

84. Cochrane SA, Vederas JC. 2016. Lipopeptides from *Bacillus* and *Paenibacillus* spp.: A Gold Mine of Antibiotic Candidates. *Med Res Rev* 36:4–31.
85. Malit JJJ, Leung HYC, Qian PY. 2022. Targeted Large-Scale Genome Mining and Candidate Prioritization for Natural Product Discovery. *Mar Drugs*. Multidisciplinary Digital Publishing Institute (MDPI) <https://doi.org/10.3390/md20060398>.
86. Lambalot RH, Gehring AM, Flugel RS, Zuber P, LaCelle M, Marahiel MA, Reid R, Khosla C, Walsh CT. 1996. A new enzyme superfamily — the phosphopantetheinyl transferases. *Chem Biol* 3:923–936.
87. Kinsinger RF, Shirk MC, Fall R. 2003. Rapid surface motility in *Bacillus subtilis* is dependent on extracellular surfactin and potassium ion. *J Bacteriol* 185:5627–5631.
88. Kiesevalter HT, Lozano-Andrade CN, Wibowo M, Strube ML, Maróti G, Snyder D, Jørgensen TS, Larsen TO, Cooper VS, Weber T, Kovács ÁT. 2021. Genomic and Chemical Diversity of *Bacillus subtilis* Secondary Metabolites against Plant Pathogenic Fungi. *mSystems* 6.
89. Li Y, Héloir MC, Zhang X, Geissler M, Trouvelot S, Jacquens L, Henkel M, Su X, Fang X, Wang Q, Adrian M. 2019. Surfactin and fengycin contribute to the protection of a *Bacillus subtilis* strain against grape downy mildew by both direct effect and defence stimulation. *Mol Plant Pathol* 20:1037–1050.
90. Maget-Dana R, Thimon L, Peypoux F, Ptak M. 1992. Surfactin/iturin A interactions may explain the synergistic effect of surfactin on the biological properties of iturin A. *Biochimie* 74:1047–1051.
91. Kiesevalter HT, Lozano-Andrade CN, Strube ML, Kovács ÁT. 2020. Secondary metabolites of *Bacillus subtilis* impact the assembly of soil-derived semisynthetic bacterial communities. *Beilstein J Org Chem* 16:2983–2998.
92. Peypoux F, Bonmatin JM, Wallach J. 1999. Recent trends in the biochemistry of surfactin. *Appl Microbiol Biotechnol* 51:553–563.

References

93. Nakano MM, Xia L, Zuber P. 1991. Transcription initiation region of the *srfA* operon, which is controlled by the *comP-comA* signal transduction system in *Bacillus subtilis*. *J Bacteriol* 173:5487–5493.
94. Nakano MM, Magnuson R, Myers A, Curry J, Grossman AD, Zuber P. 1991. *srfA* is an operon required for surfactin production, competence development, and efficient sporulation in *Bacillus subtilis*. *J Bacteriol* 173:1770–1778.
95. López D, Kolter R. 2010. Extracellular signals that define distinct and coexisting cell fates in *Bacillus subtilis*. *FEMS Microbiol Rev* <https://doi.org/10.1111/j.1574-6976.2009.00199.x>.
96. Hu F, Liu Y, Li S. 2019. Rational strain improvement for surfactin production: enhancing the yield and generating novel structures. *Microb Cell Fact* 18:42.
97. Touré Y, Ongena M, Jacques P, Guiro A, Thonart P. 2004. Role of lipopeptides produced by *Bacillus subtilis* GA1 in the reduction of grey mould disease caused by *Botrytis cinerea* on apple. *J Appl Microbiol* 96:1151–1160.
98. Steinke K, Mohite OS, Weber T, Kovács ÁT. 2020. Phylogenetic Distribution of Secondary Metabolites in the *Bacillus subtilis* Species Complex. *mSystems* 6.
99. Dunlap CA, Bowman MJ, Rooney AP. 2019. Iturinic Lipopeptide Diversity in the *Bacillus subtilis* Species Group – Important Antifungals for Plant Disease Biocontrol Applications. *Front Microbiol* 10.
100. Tsuge K, Akiyama T, Shoda M. 2001. Cloning, Sequencing, and Characterization of the Iturin A Operon. *J Bacteriol* 183:6265–6273.
101. Tsuge K, Inoue S, Ano T, Itaya M, Shoda M. 2005. Horizontal transfer of iturin a operon, *itu*, to *Bacillus subtilis* 168 and conversion into an iturin A producer. *Antimicrob Agents Chemother* 49:4641–4648.
102. Koumoutsis A, Chen XH, Vater J, Borriss R. 2007. DegU and YczE positively regulate the synthesis of bacillomycin D by *Bacillus amyloliquefaciens* strain FZB42. *Appl Environ Microbiol* 73:6953–6964.
103. Wang J, Liu J, Wang X, Yao J, Yu Z. 2004. Application of electrospray ionization

References

- mass spectrometry in rapid typing of fengycin homologues produced by *Bacillus subtilis*. *Lett Appl Microbiol* 39:98–102.
104. Hussein W. 2019. Fengycin or plipastatin? A confusing question in *Bacilli*. *BioTechnologia* 100:47–55.
 105. Vahidinasab M, Lilge L, Reinfurt A, Pfannstiel J, Henkel M, Morabbi Heravi K, Hausmann R. 2020. Construction and description of a constitutive plipastatin mono-producing *Bacillus subtilis*. *Microb Cell Fact* 19:205.
 106. Tsuge K, Matsui K, Itaya M. 2007. Production of the non-ribosomal peptide plipastatin in *Bacillus subtilis* regulated by three relevant gene blocks assembled in a single movable DNA segment. *J Biotechnol* 129:592–603.
 107. Gao L, Han J, Liu H, Qu X, Lu Z, Bie X. 2017. Plipastatin and surfactin coproduction by *Bacillus subtilis* pB2-L and their effects on microorganisms. *Int J Gen Mol Microbiol* 110:1007–1018.
 108. Jin P, Wang H, Tan Z, Xuan Z, Dahar GY, Li QX, Miao W, Liu W. 2020. Antifungal mechanism of bacillomycin D from *Bacillus velezensis* HN-2 against *Colletotrichum gloeosporioides* Penz. *Pestic Biochem Physiol* 163:102–107.
 109. Li L, Ma M, Huang R, Qu Q, Li G, Zhou J, Zhang K, Lu K, Niu X, Luo J. 2012. Induction of chlamydospore formation in *fusarium* by cyclic lipopeptide antibiotics from *bacillus subtilis* C2. *J Chem Ecol* 38:966–974.
 110. Gong AD, Li HP, Yuan QS, Song XS, Yao W, He WJ, Zhang JB, Liao YC. 2015. Antagonistic mechanism of iturin a and plipastatin a from *Bacillus amyloliquefaciens* S76-3 from wheat spikes against *Fusarium graminearum*. *PLoS One* 10:e0116871.
 111. Maget-Dana R, Ptak M, Peypoux F, Michel G. 1985. Pore-forming properties of iturin A, a lipopeptide antibiotic. *BBA - Biomembr* 815:405–409.
 112. Maget-Dana R, Peypoux F. 1994. Iturins, a special class of pore-forming lipopeptides: biological and physicochemical properties. *Toxicology* 87:151–174.
 113. Aranda FJ, Teruel JA, Ortiz A. 2005. Further aspects on the hemolytic activity of the
-

References

- antibiotic lipopeptide iturin A. *Biochim Biophys Acta - Biomembr* 1713:51–56.
114. Zhao X, Zhou Z, Han Y. 2017. Antifungal Effects of Lipopeptide Produced by *Bacillus amyloliquefaciens* BH072. *Adv Biosci Biotechnol* 08:295–310.
 115. Deleu M, Paquot M, Nylander T. 2005. Fengycin interaction with lipid monolayers at the air–aqueous interface—implications for the effect of fengycin on biological membranes. *J Colloid Interface Sci* 283:358–365.
 116. Zakharova AA, Efimova SS, Malev V V., Ostroumova OS. 2019. Fengycin induces ion channels in lipid bilayers mimicking target fungal cell membranes. *Sci Rep* 9:16034.
 117. Sur S, Romo TD, Grossfield A. 2018. Selectivity and Mechanism of Fengycin, an Antimicrobial Lipopeptide, from Molecular Dynamics. *J Phys Chem B* 122:2219–2226.
 118. Patel H, Tscheka C, Edwards K, Karlsson G, Heerklotz H. 2011. All-or-none membrane permeabilization by fengycin-type lipopeptides from *Bacillus subtilis* QST713. *Biochim Biophys Acta - Biomembr* 1808:2000–2008.
 119. Gu Q, Yang Y, Yuan Q, Shi G, Wu L, Lou Z, Huo R, Wu H, Borriss R, Gao X. 2017. Bacillomycin D produced by *Bacillus amyloliquefaciens* is involved in the antagonistic interaction with the plantpathogenic fungus *Fusarium graminearum*. *Appl Environ Microbiol* 83:e01075-17.
 120. Jiang C, Li Z, Shi Y, Guo D, Pang B, Chen X, Shao D, Liu Y, Shi J. 2020. *Bacillus subtilis* inhibits *Aspergillus carbonarius* by producing iturin A, which disturbs the transport, energy metabolism, and osmotic pressure of fungal cells as revealed by transcriptomics analysis. *Int J Food Microbiol* 330:108783.
 121. Azrin NAM, Ali MSM, Rahman RNZRA, Oslan SN, Noor NDM. 2022. Versatility of subtilisin: A review on structure, characteristics, and applications. *Biotechnol Appl Biochem*. John Wiley & Sons, Ltd <https://doi.org/10.1002/bab.2309>.
 122. Prashar P, Kapoor N, Sachdeva S. 2013. Biocontrol of Plant Pathogens Using Plant Growth Promoting Bacteria, p. 319–360. *In* Lichtfouse, E (ed.), *Sustainable Agriculture Reviews*.
-

References

123. Choi YJ, Kim EJ, Piao Z, Yun YC, Shin YC. 2004. Purification and Characterization of Chitosanase from *Bacillus* sp. Strain KCTC 0377BP and Its Application for the Production of Chitosan Oligosaccharides. *Appl Environ Microbiol* 70:4522–4531.
124. A. Veliz E, Martínez-Hidalgo P, M. Hirsch A. 2017. Chitinase-producing bacteria and their role in biocontrol. *AIMS Microbiol* 3:689–705.
125. Schönbichler A, Díaz-Moreno SM, Srivastava V, McKee LS. 2020. Exploring the Potential for Fungal Antagonism and Cell Wall Attack by *Bacillus subtilis* natto. *Front Microbiol* 11:521.
126. Wang S-L, Shih I-L, Liang T-W, Wang C-H. 2002. Purification and Characterization of Two Antifungal Chitinases Extracellularly Produced by *Bacillus amyloliquefaciens* V656 in a Shrimp and Crab Shell Powder Medium. *J Agric Food Chem* 50:2241–2248.
127. Chang W-T, Chen C-S, Wang S-L. 2003. An Antifungal Chitinase Produced by *Bacillus cereus* with Shrimp and Crab Shell Powder as a Carbon Source. *Curr Microbiol* 47:102–108.
128. Huang C-J, Wang T-K, Chung S-C, Chen C-Y. 2005. Identification of an Antifungal Chitinase from a Potential Biocontrol Agent, *Bacillus cereus* 28-9. *BMB Rep* 38:82–88.
129. Kishore GK, Pande S. 2007. Chitin-supplemented foliar application of chitinolytic *Bacillus cereus* reduces severity of *Botrytis* gray mold disease in chickpea under controlled conditions. *Lett Appl Microbiol* 44:98–105.
130. Liu Y, Tao J, Yan Y, Li B, Li H, Li C. 2011. Biocontrol Efficiency of *Bacillus subtilis* SL-13 and Characterization of an Antifungal Chitinase. *Chinese J Chem Eng* 19:128–134.
131. Pang Y, Yang J, Chen X, Jia Y, Li T, Jin J, Liu H, Jiang L, Hao Y, Zhang H, Xie Y. 2021. An Antifungal Chitosanase from *Bacillus subtilis* SH21. *Molecules* 26:1863.
132. Dimopoulou A, Theologidis I, Benaki D, Koukounia M, Zervakou A, Tzima A, Diallinas G, Hatzinikolaou DG, Skandalis N. 2021. Direct Antibiotic Activity of

References

- Bacillibactin Broadens the Biocontrol Range of *Bacillus amyloliquefaciens* MBI600. mSphere 6.
133. Yu X, Ai C, Xin L, Zhou G. 2011. The siderophore-producing bacterium, *Bacillus subtilis* CAS15, has a biocontrol effect on *Fusarium* wilt and promotes the growth of pepper. *Eur J Soil Biol* 47:138–145.
 134. Ryu C-M, Farag MA, Hu C-H, Reddy MS, Wei H-X, Paré PW, Kloepper JW. 2003. Bacterial volatiles promote growth in *Arabidopsis*. *Proc Natl Acad Sci* 100:4927–4932.
 135. Trivedi P, Leach JE, Tringe SG, Sa T, Singh BK. 2020. Plant–microbiome interactions: from community assembly to plant health. *Nat Rev Microbiol*. Nature Publishing Group <https://doi.org/10.1038/s41579-020-0412-1>.
 136. Yuan J, Raza W, Shen Q, Huang Q. 2012. Antifungal activity of *Bacillus amyloliquefaciens* NJN-6 volatile compounds against *Fusarium oxysporum* f. sp. *cubense*. *Appl Environ Microbiol* 78:5942–5944.
 137. Chen H, Xiao X, Wang J, Wu L, Zheng Z, Yu Z. 2008. Antagonistic effects of volatiles generated by *Bacillus subtilis* on spore germination and hyphal growth of the plant pathogen, *Botrytis cinerea*. *Biotechnol Lett* 30:919–923.
 138. Zhang X, Li B, Wang Y, Guo Q, Lu X, Li S, Ma P. 2013. Lipopeptides, a novel protein, and volatile compounds contribute to the antifungal activity of the biocontrol agent *Bacillus atrophaeus* CAB-1. *Appl Microbiol Biotechnol* 97:9525–9534.
 139. Choub V, Won S-J, Ajuna HB, Moon J-H, Choi S-I, Lim H-I, Ahn YS. 2022. Antifungal Activity of Volatile Organic Compounds from *Bacillus velezensis* CE 100 against *Colletotrichum gloeosporioides*. *Horticulturae* 8:557.
 140. Albarracín Orio AG, Petras D, Tobares RA, Aksenov AA, Wang M, Juncosa F, Sayago P, Moyano AJ, Dorrestein PC, Smania AM. 2020. Fungal–bacterial interaction selects for quorum sensing mutants with increased production of natural antifungal compounds. *Commun Biol* 3:1–9.
 141. Pieterse CMJ, Zamioudis C, Berendsen RL, Weller DM, Van Wees SCM, Bakker
-

References

- PAHM. 2014. Induced systemic resistance by beneficial microbes. *Annu Rev Phytopathol* 52:347–375.
142. Farace G, Fernandez O, Jacquens L, Coutte F, Krier F, Jacques P, Clément C, Barka EA, Jacquard C, Dorey S. 2015. Cyclic lipopeptides from *Bacillus subtilis* activate distinct patterns of defence responses in grapevine. *Mol Plant Pathol* 16:177–187.
143. Akram W, Anjum T, Ali B. 2016. Phenylacetic Acid Is ISR Determinant Produced by *Bacillus fortis* IAGS162, Which Involves Extensive Re-modulation in Metabolomics of Tomato to Protect against *Fusarium Wilt*. *Front Plant Sci* 7.
144. Ongena M, Jourdan E, Adam A, Paquot M, Brans A, Joris B, Arpigny J-L, Thonart P. 2007. Surfactin and fengycin lipopeptides of *Bacillus subtilis* as elicitors of induced systemic resistance in plants. *Environ Microbiol* 9:1084–1090.
145. Cawoy H, Mariutto M, Henry G, Fisher C, Vasilyeva N, Thonart P, Dommes J, Ongena M. 2014. Plant Defense Stimulation by Natural Isolates of *Bacillus* Depends on Efficient Surfactin Production. *Mol Plant-Microbe Interact* 27:87–100.
146. Stoll A, Salvatierra-Martínez R, González M, Araya M. 2021. The role of surfactin production by *bacillus velezensis* on colonization, biofilm formation on tomato root and leaf surfaces and subsequent protection (ISR) against *botrytis cinerea*. *Microorganisms* 9:2251.
147. Huang C-J, Tsay J-F, Chang S-Y, Yang H-P, Wu W-S, Chen C-Y. 2012. Dimethyl disulfide is an induced systemic resistance elicitor produced by *Bacillus cereus* C1L. *Pest Manag Sci* 68:1306–1310.
148. Russels K, Merriman P. 1990. Screening Strategies for Biological Control, p. 427–435. *In* Hornby, D (ed.), *Biological Control of Soil-Borne Plant Pathogens*. CAB International.
149. Raymaekers K, Ponet L, Holtappels D, Berckmans B, Cammue BPA. 2020. Screening for novel biocontrol agents applicable in plant disease management – A review. *Biol Control* <https://doi.org/10.1016/j.biocontrol.2020.104240>.
150. Knudsen IMB, Hockenhull J, Funck Jensen D, Gerhardson B, Hökeberg M,

References

- Tahvonen R, Teperi E, Sundheim L, Henriksen B. 1997. Selection of biological control agents for controlling soil and seed-borne diseases in the field. *Eur J Plant Pathol* 103:775–784.
151. Oh HS, Lee YH. 2000. A target-site-specific screening system for antifungal compounds on appressorium formation in *Magnaporthe grisea*. *Phytopathology* 90:1162–1168.
152. Mota MS, Gomes CB, Souza Júnior IT, Moura AB. 2017. Bacterial selection for biological control of plant disease: criterion determination and validation. *Brazilian J Microbiol* 48:62–70.
153. Kjeldgaard B, Neves AR, Fonseca C, Kovács ÁT, Domínguez-Cuevas P. 2022. Quantitative High-Throughput Screening Methods Designed for Identification of Bacterial Biocontrol Strains with Antifungal Properties. *Microbiol Spectr* 10.
154. Broekaert WF, Terras FRG, Cammue BPA, Vanderleyden J. 1990. An automated quantitative assay for fungal growth inhibition. *FEMS Microbiol Lett* 69:55–59.
155. Defilippi S, Groulx E, Megalla M, Mohamed R, Avis TJ. 2018. Fungal Competitors Affect Production of Antimicrobial Lipopeptides in *Bacillus subtilis* Strain B9–5. *J Chem Ecol* 44:374–383.
156. Olajide AM, Chen S, LaPointe G. 2021. Markers to Rapidly Distinguish *Bacillus paralicheniformis* From the Very Close Relative, *Bacillus licheniformis*. *Front Microbiol* 11:3367.
157. Du Y, Ma J, Yin Z, Liu K, Yao G, Xu W, Fan L, Du B, Ding Y, Wang C. 2019. Comparative genomic analysis of *Bacillus paralicheniformis* MDJK30 with its closely related species reveals an evolutionary relationship between *B. paralicheniformis* and *B. licheniformis*. *BMC Genomics* 20:283.
158. Qin Y, Angelini LL, Chai Y. 2022. *Bacillus subtilis* Cell Differentiation, Biofilm Formation and Environmental Prevalence. *Microorganisms*. Multidisciplinary Digital Publishing Institute <https://doi.org/10.3390/microorganisms10061108>.
159. Lopez D, Vlamakis H, Kolter R. 2009. Generation of multiple cell types in *Bacillus*

References

- subtilis*. FEMS Microbiol Rev <https://doi.org/10.1111/j.1574-6976.2008.00148.x>.
160. Waters CM, Bassler BL. 2005. Quorum sensing: Cell-to-cell communication in bacteria. *Annu Rev Cell Dev Biol* 21:319–346.
 161. Camilli A, Bassler BL. 2006. Bacterial small-molecule signaling pathways. *Science* (80-). NIH Public Access <https://doi.org/10.1126/science.1121357>.
 162. Miller MB, Bassler BL. 2001. Quorum Sensing in Bacteria. *Annu Rev Microbiol* 55:165–199.
 163. Magnuson R, Solomon J, Grossman AD. 1994. Biochemical and genetic characterization of a competence pheromone from *B. subtilis*. *Cell* 77:207–216.
 164. López D, Vlamakis H, Losick R, Kolter R. 2009. Paracrine signaling in a bacterium. *Genes Dev* 23:1631–1638.
 165. Weinrauch Y, Penchev R, Dubnau E, Smith E, Dubnau D. 1990. A *Bacillus subtilis* regulatory gene product for genetic competence and sporulation resembles sensor protein members of the bacterial two-component signal-transduction systems. *Genes Dev* 4:860–872.
 166. Tortosa P, Logsdon L, Kraigher B, Itoh Y, Mandic-Mulec I, Dubnau D. 2001. Specificity and genetic polymorphism of the *Bacillus* competence quorum-sensing system. *J Bacteriol* 183:451–460.
 167. Perego M, Higgins CF, Pearce SR, Gallagher MP, Hoch JA. 1991. The oligopeptide transport system of *Bacillus subtilis* plays a role in the initiation of sporulation. *Mol Microbiol* 5:173–185.
 168. Rudner DZ, LeDeaux JR, Ireton K, Grossman AD. 1991. The *spo0K* locus of *Bacillus subtilis* is homologous to the oligopeptide permease locus and is required for sporulation and competence. *J Bacteriol* 173:1388–1398.
 169. Auchtung JM, Lee CA, Grossman AD. 2006. Modulation of the ComA-dependent quorum response in *Bacillus subtilis* by multiple *rap* proteins and Phr peptides. *J Bacteriol* 188:5273–5285.
 170. Pottathil M, Lazazzera BA. 2003. The extracellular PHR peptide-*rap* phosphatase
-

References

- signaling circuit of bacillus subtilis. *Front Biosci* <https://doi.org/10.2741/913>.
171. Gallegos-Monterrosa R, Kovács ÁT. 2023. Phenotypic plasticity: The role of a phosphatase family Rap in the genetic regulation of Bacilli. *Mol Microbiol* <https://doi.org/10.1111/mmi.15060>.
 172. Roggiani M, Dubnau D. 1993. ComA, a phosphorylated response regulator protein of *Bacillus subtilis*, binds to the promoter region of *srfA*. *J Bacteriol* 175:3182–3187.
 173. Hahn J, Dubnau D. 1991. Growth stage signal transduction and the requirements for *srfA* induction in development of competence. *J Bacteriol* 173:7275–7282.
 174. Turgay K, Hahn J, Burghoorn J, Dubnau D. 1998. Competence in *Bacillus subtilis* is controlled by regulated proteolysis of a transcription factor. *EMBO J* 17:6730–6738.
 175. Berka RM, Hahn J, Albano M, Draskovic I, Persuh M, Cui X, Sloma A, Widner W, Dubnau D. 2002. Microarray analysis of the *Bacillus subtilis* K-state: Genome-wide expression changes dependent on ComK. *Mol Microbiol* 43:1331–1345.
 176. Hölscher T, Schiklang T, Dragoš A, Dietel AK, Kost C, Kovács ÁT. 2018. Impaired competence in flagellar mutants of *Bacillus subtilis* is connected to the regulatory network governed by DegU. *Environ Microbiol Rep* 10:23–32.
 177. Diethmaier C, Chawla R, Canzoneri A, Kearns DB, Lele PP, Dubnau D. 2017. Viscous drag on the flagellum activates *Bacillus subtilis* entry into the K-state. *Mol Microbiol* 106:367–380.
 178. Slomka S, Françoise I, Hornung G, Asraf O, Biniashvili T, Pilpel Y, Dahan O. 2020. Experimental evolution of *Bacillus subtilis* reveals the evolutionary dynamics of horizontal gene transfer and suggests adaptive and neutral effects. *Genetics* 216:543–558.
 179. Brito PH, Chevreux B, Serra CR, Schyns G, Henriques AO, Pereira-Leal JB. 2018. Genetic competence drives genome diversity in *Bacillus subtilis*. *Genome Biol Evol* 10:108–124.
-

References

180. Piggot PJ, Hilbert DW. 2004. Sporulation of *Bacillus subtilis*. *Curr Opin Microbiol*. Elsevier Current Trends <https://doi.org/10.1016/j.mib.2004.10.001>.
181. Molle V, Fujita M, Jensen ST, Eichenberger P, González-Pastor JE, Liu JS, Losick R. 2003. The Spo0A regulon of *Bacillus subtilis*. *Mol Microbiol* 50:1683–1701.
182. Fujita M, Losick R. 2005. Evidence that entry into sporulation in *Bacillus subtilis* is governed by a gradual increase in the level and activity of the master regulator Spo0A. *Genes Dev* 19:2236–2244.
183. Hamon MA, Lazazzera BA. 2001. The sporulation transcription factor Spo0A is required for biofilm development in *Bacillus subtilis*. *Mol Microbiol* 42:1199–1209.
184. Fujita M, González-Pastor JE, Losick R. 2005. High- and Low-Threshold Genes in the Spo0A Regulon of *Bacillus subtilis*. *J Bacteriol* 187:1357–1368.
185. González-Pastor JE, Hobbs EC, Losick R. 2003. Cannibalism by sporulating bacteria. *Science* (80-) 301:510–513.
186. López D, Vlamakis H, Losick R, Kolter R. 2009. Cannibalism enhances biofilm development in *Bacillus subtilis*. *Mol Microbiol* 74:609–618.
187. Claessen D, Rozen DE, Kuipers OP, Sogaard-Andersen L, Van Wezel GP. 2014. Bacterial solutions to multicellularity: A tale of biofilms, filaments and fruiting bodies. *Nat Rev Microbiol* 12:115–124.
188. Branda SS, Vik Å, Friedman L, Kolter R. 2005. Biofilms: the matrix revisited. *Trends Microbiol* 13:20–26.
189. Davey ME, O’toole GA. 2000. Microbial Biofilms: from Ecology to Molecular Genetics. *Microbiol Mol Biol Rev* 64:847–867.
190. Hall-Stoodley L, Costerton JW, Stoodley P. 2004. Bacterial biofilms: From the natural environment to infectious diseases. *Nat Rev Microbiol* 2:95–108.
191. Ramey BE, Koutsoudis M, Bodman SBV, Fuqua C. 2004. Biofilm formation in plant-microbe associations. *Curr Opin Microbiol* 7:602–609.
192. Vlamakis H, Aguilar C, Losick R, Kolter R. 2008. Control of cell fate by the formation of an architecturally complex bacterial community. *Genes Dev* 22:945–953.

References

193. Cairns LS, Hobley L, Stanley-Wall NR. 2014. Biofilm formation by *Bacillus subtilis*: New insights into regulatory strategies and assembly mechanisms. *Mol Microbiol* 93:587–598.
194. Arnaouteli S, Bamford NC, Stanley-Wall NR, Kovács ÁT. 2021. *Bacillus subtilis* biofilm formation and social interactions. *Nat Rev Microbiol* 19:600–614.
195. López D, Fischbach MA, Chu F, Losick R, Kolter R. 2009. Structurally diverse natural products that cause potassium leakage trigger multicellularity in *Bacillus subtilis*. *Proc Natl Acad Sci* 106:280–285.
196. Comella N, Grossman AD. 2005. Conservation of genes and processes controlled by the quorum response in bacteria: Characterization of genes controlled by the quorum-sensing transcription factor ComA in *Bacillus subtilis*. *Mol Microbiol* 57:1159–1174.
197. Nordgaard M, Mortensen RMR, Kirk NK, Gallegos-Monterrosa R, Kovács ÁT. 2021. Deletion of Rap-Phr systems in *Bacillus subtilis* influences in vitro biofilm formation and plant root colonization. *Microbiologyopen* 10:e1212.
198. Jiang M, Shao W, Perego M, Hoch JA. 2000. Multiple histidine kinases regulate entry into stationary phase and sporulation in *Bacillus subtilis*. *Mol Microbiol* 38:535–542.
199. Pisithkul T, Schroeder JW, Trujillo EA, Yeesin P, Stevenson DM, Chaiamarit T, Coon JJ, Wang JD, Amador-Noguez D. 2019. Metabolic remodeling during biofilm development of *Bacillus subtilis*. *MBio* 10:2021.
200. Chai Y, Chu F, Kolter R, Losick R. 2008. Bistability and biofilm formation in *Bacillus subtilis*. *Mol Microbiol* 67:254–263.
201. Chu F, Kearns DB, Branda SS, Kolter R, Losick R. 2006. Targets of the master regulator of biofilm formation in *Bacillus subtilis*. *Mol Microbiol* 59:1216–1228.
202. Kearns DB, Chu F, Branda SS, Kolter R, Losick R. 2005. A master regulator for biofilm formation by *Bacillus subtilis*. *Mol Microbiol* 55:739–749.
203. Hamon MA, Stanley NR, Britton RA, Grossman AD, Lazazzera BA. 2004.

References

- Identification of AbrB-regulated genes involved in biofilm formation by *Bacillus subtilis*. *Mol Microbiol* 52:847–860.
204. Kobayashi K. 2007. *Bacillus subtilis* pellicle formation proceeds through genetically defined morphological changes. *J Bacteriol* 189:4920–4931.
205. Verhamme DT, Murray EJ, Stanley-Wall NR. 2009. DegU and Spo0A Jointly Control Transcription of Two Loci Required for Complex Colony Development by *Bacillus subtilis*. *J Bacteriol* 191:100–108.
206. Verhamme DT, Kiley TB, Stanley-Wall NR. 2007. DegU co-ordinates multicellular behaviour exhibited by *Bacillus subtilis*. *Mol Microbiol* 65:554–568.
207. Kobayashi K. 2007. Gradual activation of the response regulator DegU controls serial expression of genes for flagellum formation and biofilm formation in *Bacillus subtilis*. *Mol Microbiol* 66:395–409.
208. Msadek T, Kunst F, Klier A, Rapoport G. 1991. DegS-DegU and ComP-ComA modulator-effector pairs control expression of the *Bacillus subtilis* pleiotropic regulatory gene degQ. *J Bacteriol* 173:2366–2377.
209. Ostrowski A, Mehert A, Prescott A, Kiley TB, Stanley-Wall NR. 2011. YuaB Functions Synergistically with the Exopolysaccharide and TasA Amyloid Fibers To Allow Biofilm Formation by *Bacillus subtilis*. *J Bacteriol* 193:4821–4831.
210. Ohsawa T, Tsukahara K, Ogura M. 2009. *Bacillus subtilis* response regulator DegU is a direct activator of pgsB transcription involved in γ -poly-glutamic acid synthesis. *Biosci Biotechnol Biochem* 73:2096–2102.
211. Kovács AT, Kuipers OP. 2011. Rok Regulates yuaB Expression during Architecturally Complex Colony Development of *Bacillus subtilis* 168. *J Bacteriol* 193:998–1002.
212. Branda SS, Chu F, Kearns DB, Losick R, Kolter R. 2006. A major protein component of the *Bacillus subtilis* biofilm matrix. *Mol Microbiol* 59:1229–1238.
213. Branda SS, González-Pastor JE, Ben-Yehuda S, Losick R, Kolter R. 2001. Fruiting body formation by *Bacillus subtilis*. *Proc Natl Acad Sci U S A* 98:11621–11626.
214. Epstein AK, Pokroy B, Seminara A, Aizenberg J. 2011. Bacterial biofilm shows

References

- persistent resistance to liquid wetting and gas penetration. *Proc Natl Acad Sci U S A* 108:995–1000.
215. Chan JM, Guttenplan SB, Kearns DB. 2014. Defects in the flagellar motor increase synthesis of poly- γ -glutamate in *Bacillus subtilis*. *J Bacteriol* 196:740–753.
216. Kesel S, Grumbein S, Gümperlein I, Tallawi M, Marel AK, Lieleg O, Opitz M. 2016. Direct comparison of physical properties of *Bacillus subtilis* NCIB 3610 and B-1 biofilms. *Appl Environ Microbiol* 82:2424–2432.
217. Romero D, Vlamakis H, Losick R, Kolter R. 2011. An accessory protein required for anchoring and assembly of amyloid fibres in *B. subtilis* biofilms. *Mol Microbiol* 80:1155–1168.
218. Mammeri N El, Hierrezuelo J, Tolchard J, Cámara-Almirón J, Caro-Astorga J, Álvarez-Mena A, Dutour A, Berbon M, Shenoy J, Morvan E, Grélard A, Kauffmann B, Lecomte S, de Vicente A, Habenstein B, Romero D, Loquet A. 2019. Molecular architecture of bacterial amyloids in *Bacillus* biofilms. *FASEB J* 33:12146–12163.
219. Arnaouteli S, Ferreira AS, Schor M, Morris RJ, Bromley KM, Jo J, Cortez KL, Sukhodub T, Prescott AR, Dietrich LEP, MacPhee CE, Stanley-Wall NR. 2017. Bifunctionality of a biofilm matrix protein controlled by redox state. *Proc Natl Acad Sci U S A* 114:E6184–E6191.
220. Kobayashi K, Iwano M. 2012. BslA(YuaB) forms a hydrophobic layer on the surface of *Bacillus subtilis* biofilms. *Mol Microbiol* 85:51–66.
221. Hopley L, Ostrowski A, Rao F V, Bromley KM, Porter M, Prescott AR, MacPhee CE, Van Aalten DMF, Stanley-Wall NR. 2013. BslA is a self-assembling bacterial hydrophobin that coats the *Bacillus subtilis* biofilm. *Proc Natl Acad Sci U S A* 110:13600–13605.
222. Peng N, Cai P, Mortimer M, Wu Y, Gao C, Huang Q. 2020. The exopolysaccharide-eDNA interaction modulates 3D architecture of *Bacillus subtilis* biofilm. *BMC Microbiol* 20:1–12.
223. Asally M, Kittisopikul M, Rué P, Du Y, Hu Z, Çağatay T, Robinson AB, Lu H, Garcia-

References

- Ojalvo J, Süel GM. 2012. Localized cell death focuses mechanical forces during 3D patterning in a biofilm. *Proc Natl Acad Sci U S A* 109:18891–18896.
224. Beaugregard PB, Chai Y, Vlamakis H, Losick R, Kolter R. 2013. *Bacillus subtilis* biofilm induction by plant polysaccharides. *Proc Natl Acad Sci* 110:E1621–E1630.
225. Lemon KP, Earl AM, Vlamakis HC, Aguilar C, Kolter R. 2008. Biofilm Development with an Emphasis on *Bacillus subtilis*, p. 1–16. *In* *Current Topics in Microbiology and Immunology*. NIH Public Access.
226. Dragoš A, Kiesewalter H, Martin M, Hsu CY, Hartmann R, Wechsler T, Eriksen C, Brix S, Drescher K, Stanley-Wall N, Kümmerli R, Kovács ÁT. 2018. Division of Labor during Biofilm Matrix Production. *Curr Biol* 28:1903-1913.e5.
227. Stanley NR, Lazazzera BA. 2005. Defining the genetic differences between wild and domestic strains of *Bacillus subtilis* that affect poly- γ -DL-glutamic acid production and biofilm formation. *Mol Microbiol* 57:1143–1158.
228. Veening JW, Igoshin OA, Eijlander RT, Nijland R, Hamoen LW, Kuipers OP. 2008. Transient heterogeneity in extracellular protease production by *Bacillus subtilis*. *Mol Syst Biol* 4:184.
229. Msadek T. 1999. When the going gets tough: Survival strategies and environmental signaling networks in *Bacillus subtilis*. *Trends Microbiol.* *Trends Microbiol* [https://doi.org/10.1016/S0966-842X\(99\)01479-1](https://doi.org/10.1016/S0966-842X(99)01479-1).
230. Kunst F, Rapoport G. 1995. Salt stress is an environmental signal affecting degradative enzyme synthesis in *Bacillus subtilis*. *J Bacteriol* 177:2403–2407.
231. Ogura M, Shimane K, Asai K, Ogasawara N, Tanaka T. 2003. Binding of response regulator DegU to the *aprE* promoter is inhibited by RapG, which is counteracted by extracellular PhrG in *Bacillus subtilis*. *Mol Microbiol* 49:1685–1697.
232. Kunst F, Pascal M, Lepesant-Kejzlarova J, Lepesant JA, Billault A, Dedonder R. 1975. Pleiotropic mutations affecting sporulation conditions and the syntheses of extracellular enzymes in *Bacillus subtilis* 168. *Biochimie* 56:1481–1489.
233. Dahl MK, Msadek T, Kunst F, Rapoport G. 1991. Mutational analysis of the *Bacillus*

References

- subtilis* DegU regulator and its phosphorylation by the DegS protein kinase. *J Bacteriol* 173:2539–2547.
234. Strauch MA, Spiegelman GB, Perego M, Johnson WC, Burbulys D, Hoch JA. 1989. The transition state transcription regulator *abrB* of *Bacillus subtilis* is a DNA binding protein. *EMBO J* 8:1615–1621.
235. Strauch M, Webb V, Spiegelman G, Hoch JA. 1990. The SpoOA protein of *Bacillus subtilis* is a repressor of the *abrB* gene. *Proc Natl Acad Sci U S A* 87:1801–1805.
236. Dergham Y, Sanchez-Vizueté P, Coq D Le, Deschamps J, Bridier A, Hamze K, Briandet R. 2021. Comparison of the genetic features involved in *Bacillus subtilis* biofilm formation using multi-culturing approaches. *Microorganisms* 9:1–17.
237. Cairns LS, Marlow VL, Bissett E, Ostrowski A, Stanley-Wall NR. 2013. A mechanical signal transmitted by the flagellum controls signalling in *Bacillus subtilis*. *Mol Microbiol* 90:6–21.
238. Mukherjee S, Kearns DB. 2014. The structure and regulation of flagella in *Bacillus subtilis*. *Annu Rev Genet* 48:319–340.
239. Kearns DB. 2010. A field guide to bacterial swarming motility. *Nat Rev Microbiol*. NIH Public Access <https://doi.org/10.1038/nrmicro2405>.
240. Angelini TE, Roper M, Kolter R, Weitz DA, Brenner MP. 2009. *Bacillus subtilis* spreads by surfing on waves of surfactant. *Proc Natl Acad Sci U S A* 106:18109–18113.
241. Nordgaard M, Blake C, Maróti G, Hu G, Wang Y, Strube ML, Kovács ÁT. 2022. Experimental evolution of *Bacillus subtilis* on *Arabidopsis thaliana* roots reveals fast adaptation and improved root colonization. *iScience* 25:104406.
242. Van den Bergh B, Swings T, Fauvart M, Michiels J. 2018. Experimental Design, Population Dynamics, and Diversity in Microbial Experimental Evolution. *Microbiol Mol Biol Rev* 82.
243. Elena SF, Lenski RE. 2003. Evolution experiments with microorganisms: The dynamics and genetic bases of adaptation. *Nat Rev Genet*. Nature Publishing

References

- Group <https://doi.org/10.1038/nrg1088>.
244. Bruger EL, Marx CJ. 2018. A decade of genome sequencing has revolutionized studies of experimental evolution. *Curr Opin Microbiol*. Elsevier Current Trends <https://doi.org/10.1016/j.mib.2018.03.002>.
245. Lenski RE. 2023. Revisiting the Design of the Long-Term Evolution Experiment with *Escherichia coli*. *J Mol Evol* <https://doi.org/10.1007/s00239-023-10095-3>.
246. Kawecki TJ, Lenski RE, Ebert D, Hollis B, Olivieri I, Whitlock MC. 2012. Experimental evolution. *Trends Ecol Evol*. Elsevier Current Trends <https://doi.org/10.1016/j.tree.2012.06.001>.
247. McDonald MJ. 2019. Microbial Experimental Evolution – a proving ground for evolutionary theory and a tool for discovery. *EMBO Rep* 20.
248. Dragosits M, Mattanovich D. 2013. Adaptive laboratory evolution - principles and applications for biotechnology. *Microb Cell Fact*. BioMed Central <https://doi.org/10.1186/1475-2859-12-64>.
249. Remigi P, Masson-Boivin C, Rocha EPC. 2019. Experimental Evolution as a Tool to Investigate Natural Processes and Molecular Functions. *Trends Microbiol* 27:623–634.
250. Schoustra SE, Debets AJM, Slakhorst M, Hoekstra RF. 2006. Reducing the cost of resistance; experimental evolution in the filamentous fungus *Aspergillus nidulans*. *J Evol Biol* 19:1115–1127.
251. de Crecy E, Jaronski S, Lyons B, Lyons TJ, Keyhani NO. 2009. Directed evolution of a filamentous fungus for thermotolerance. *BMC Biotechnol* 9:74.
252. Fisher KJ, Lang GI. 2016. Experimental evolution in fungi: An untapped resource. *Fungal Genet Biol* 94:88–94.
253. Bodinaku I, Shaffer J, Connors AB, Steenwyk JL, Biango-Daniels MN, Kastman EK, Rokas A, Robbat A, Wolfe BE. 2019. Rapid phenotypic and metabolomic domestication of wild penicillium molds on cheese. *MBio* 10.
254. Charusanti P, Fong NL, Nagarajan H, Pereira AR, Li HJ, Abate EA, Su Y, Gerwick WH,

References

- Palsson BO. 2012. Exploiting adaptive laboratory evolution of streptomyces clavuligerus for antibiotic discovery and overproduction. *PLoS One* 7.
255. Zhou N, Katz M, Knecht W, Compagno C, Piškur J. 2018. Genome dynamics and evolution in yeasts: A long-term yeast-bacteria competition experiment. *PLoS One* 13:e0194911.
256. Hansen SK, Rainey PB, Haagenen JAJ, Molin S. 2007. Evolution of species interactions in a biofilm community. *Nature* 445:533–536.
257. Ye R, Tomo C, Chan N, Wolfe BE. 2023. Penicillium molds impact the transcriptome and evolution of the cheese bacterium *Staphylococcus equorum*. *mSphere* <https://doi.org/10.1128/MSPHERE.00047-23>.
258. Ni B, Ghosh B, Paldy FS, Colin R, Heimerl T, Sourjik V. 2017. Evolutionary Remodeling of Bacterial Motility Checkpoint Control. *Cell Rep* 18:866–877.
259. Sher AA, Jerome JP, Bell JA, Yu J, Kim HY, Barrick JE, Mansfield LS. 2020. Experimental Evolution of *Campylobacter jejuni* Leads to Loss of Motility, *rpoN* (σ^{54}) Deletion and Genome Reduction. *Front Microbiol* 11:2781.
260. Edwards RJ, Sockett RE, Brookfield JFY. 2002. A simple method for genome-wide screening for advantageous insertions of mobile DNAs in *Escherichia coli*. *Curr Biol* 12:863–867.
261. Cooper TF, Rozen DE, Lenski RE. 2003. Parallel changes in gene expression after 20,000 generations of evolution in *Escherichia coli*. *Proc Natl Acad Sci U S A* 100:1072–1077.
262. Richter A, Hölscher T, Pausch P, Sehr T, Brockhaus F, Bange G, Kovács ÁT. 2018. Hampered motility promotes the evolution of wrinkly phenotype in *Bacillus subtilis*. *BMC Evol Biol* 18:1–11.
263. Dahl MK, Msadek T, Kunst F, Rapoport G. 1992. The phosphorylation state of the *degU* response regulator acts as a molecular switch allowing either degradative enzyme synthesis or expression of genetic competence in *Bacillus subtilis*. *J Biol Chem* 267:14509–14514.

References

264. Msadek T, Kunst F, Henner D, Klier A, Rapoport G, Dedonder R. 1990. Signal transduction pathway controlling synthesis of a class of degradative enzymes in *Bacillus subtilis*: Expression of the regulatory genes and analysis of mutations in *degS* and *degU*. *J Bacteriol* 172:824–834.
265. Amati G, Bisicchia P, Galizzi A. 2004. *DegU*-P represses expression of the motility *fla-che* operon in *Bacillus subtilis*. *J Bacteriol* 186:6003–6014.
266. Tsuge K, Ano T, Hirai M, Nakamura Y, Shoda M. 1999. The genes *degQ*, *pps*, and *lpa-8* (*sfp*) are responsible for conversion of *Bacillus subtilis* 168 to plipastatin production. *Antimicrob Agents Chemother* 43:2183–2192.
267. Wang P, Guo Q, Ma Y, Li S, Lu X, Zhang X, Ma P. 2015. *DegQ* regulates the production of fengycins and biofilm formation of the biocontrol agent *Bacillus subtilis* NCD-2. *Microbiol Res* 178:42–50.
268. Tanaka T, Kawata M, Mukai K. 1991. Altered phosphorylation of *Bacillus subtilis* *DegU* caused by single amino acid changes in *DegS*. *J Bacteriol* 173:5507–5515.
269. Butcher RA, Schroeder FC, Fischbach MA, Straight PD, Kolter R, Walsh CT, Clardy J. 2007. The identification of bacillaene, the product of the PksX megacomplex in *Bacillus subtilis*. *Proc Natl Acad Sci U S A* 104:1506–1509.
270. Fujita Y. 2009. Carbon catabolite control of the metabolic network in *Bacillus subtilis*. *Biosci Biotechnol Biochem* 73:245–259.
271. Schoffemeer EAM, Klis FM, Sietsma JH, Cornelissen BJC. 1999. The cell wall of *Fusarium oxysporum*. *Fungal Genet Biol* 27:275–282.
272. Kunst F, Msadek T, Bignon J, Rapoport G. 1994. The *DegS/DegU* and *ComP/ComA* two-component systems are part of a network controlling degradative enzyme synthesis and competence in *Bacillus subtilis*. *Res Microbiol* 145:393–402.
273. Harshey RM. 2003. Bacterial Motility on a Surface: Many Ways to a Common Goal. *Annu Rev Microbiol*. Annual Reviews 4139 El Camino Way, P.O. Box 10139, Palo Alto, CA 94303-0139, USA
<https://doi.org/10.1146/annurev.micro.57.030502.091014>.

References

274. McLoon AL, Guttenplan SB, Kearns DB, Kolter R, Losick R. 2011. Tracing the Domestication of a Biofilm-Forming Bacterium. *J Bacteriol* 193:2027–2034.
275. Murray EJ, Kiley TB, Stanley-Wall NR. 2009. A pivotal role for the response regulator DegU in controlling multicellular behaviour. *Microbiology* <https://doi.org/10.1099/mic.0.023903-0>.
276. Tran L-SP, Nagai T, Itoh Y. 2000. Divergent structure of the ComQXPA quorum-sensing components: molecular basis of strain-specific communication mechanism in *Bacillus subtilis*. *Mol Microbiol* 37:1159–1171.
277. Nagai T, Phan Tran L-S, Inatsu Y, Itoh Y. 2000. A New IS 4 Family Insertion Sequence, IS 4Bsu 1, Responsible for Genetic Instability of Poly- γ -Glutamic Acid Production in *Bacillus subtilis*. *J Bacteriol* 182:2387–2392.
278. Chen Y, Yan F, Chai Y, Liu H, Kolter R, Losick R, Guo J. 2013. Biocontrol of tomato wilt disease by *Bacillus subtilis* isolates from natural environments depends on conserved genes mediating biofilm formation. *Environ Microbiol* 15:848–864.
279. Leiman SA, Arboleda LC, Spina JS, McLoon AL. 2014. SinR is a mutational target for fine-tuning biofilm formation in laboratory-evolved strains of *Bacillus subtilis*. *BMC Microbiol* 14:1–10.
280. Dragoš A, Lakshmanan N, Martin M, Horváth B, Maróti G, García CF, Lieleg O, Kovács ÁT. 2018. Evolution of exploitative interactions during diversification in *Bacillus subtilis* biofilms. *FEMS Microbiol Ecol* 94.
281. Travisano M, Mongold JA, Bennett AF, Lenski RE. 1995. Experimental tests of the roles of adaptation, chance, and history in evolution. *Science* (80-) 267:87–90.
282. Sandberg TE, Salazar MJ, Weng LL, Palsson BO, Feist AM. 2019. The emergence of adaptive laboratory evolution as an efficient tool for biological discovery and industrial biotechnology. *Metab Eng. Academic Press Inc.* <https://doi.org/10.1016/j.ymben.2019.08.004>.
283. Aguilar C, Vlamakis H, Losick R, Kolter R. 2007. Thinking about *Bacillus subtilis* as a multicellular organism. *Curr Opin Microbiol* 10:638–643.

References

284. Kearns DB, Losick R. 2003. Swarming motility in undomesticated *Bacillus subtilis*. *Mol Microbiol* 49:581–590.
285. Patrick JE, Kearns DB. 2009. Laboratory strains of *Bacillus subtilis* do not exhibit swarming motility. *J Bacteriol* 191:7129–7133.
286. Nakano MM, Corbell N, Besson J, Zuber P. 1992. Isolation and characterization of *sfp*: a gene that functions in the production of the lipopeptide biosurfactant, surfactin, in *Bacillus subtilis*. *MGG Mol Gen Genet* 232:313–321.
287. Maughan H, Masel J, Birky CW, Nicholson WL. 2007. The Roles of Mutation Accumulation and Selection in Loss of Sporulation in Experimental Populations of *Bacillus subtilis*. *Genetics* 177:937–948.
288. Brown CT, Fishwick LK, Chokshi BM, Cuff MA, Jackson JM, Oglesby T, Rioux AT, Rodriguez E, Stupp GS, Trupp AH, Woollcombe-Clarke JS, Wright TN, Zaragoza WJ, Drew JC, Triplett EW, Nicholson WL. 2011. Whole-genome sequencing and phenotypic analysis of *Bacillus subtilis* mutants following evolution under conditions of relaxed selection for sporulation. *Appl Environ Microbiol* 77:6867–6877.
289. Zeigler DR, Nicholson WL. 2017. Experimental evolution of *Bacillus subtilis*. *Environ Microbiol* 19:3415–3422.
290. Barreto HC, Cordeiro TN, Henriques AO, Gordo I. 2020. Rampant loss of social traits during domestication of a *Bacillus subtilis* natural isolate. *Sci Rep* 10.
291. Lahti DC, Johnson NA, Ajie BC, Otto SP, Hendry AP, Blumstein DT, Coss RG, Donohue K, Foster SA. 2009. Relaxed selection in the wild. *Trends Ecol Evol*. Elsevier Current Trends <https://doi.org/10.1016/j.tree.2009.03.010>.

Research articles

Study 1

Kjeldgaard, B., Listian, S. A., Ramaswamhi, V., Richter, A., Kiesevalter, H. T., and Kovács, Á. T.
(2019).

Fungal hyphae colonization by *Bacillus subtilis* relies on biofilm matrix components

Biofilm 1, 100007. doi:10.1016/j.bioflm.2019.100007.



Fungal hyphae colonization by *Bacillus subtilis* relies on biofilm matrix components

Bodil Kjeldgaard^{a,1}, Stevanus A. Listian^{a,1}, Valliyammai Ramaswamhi^b, Anne Richter^{a,b}, Heiko T. Kiesealther^a, Ákos T. Kovács^{a,b,*}

^a Bacterial Interactions and Evolution Group, Department of Biotechnology and Biomedicine, Technical University of Denmark, Kongens Lyngby, Denmark

^b Terrestrial Biofilms Group, Institute of Microbiology, Friedrich Schiller University Jena, Jena, Germany



ARTICLE INFO

Keywords:

Bacillus subtilis
Aspergillus niger
Agaricus bisporus
 Fungal hyphae
 Biofilm matrix

ABSTRACT

Bacteria interact with their environment including microbes and higher eukaryotes. The ability of bacteria and fungi to affect each other are defined by various chemical, physical and biological factors. During physical association, bacterial cells can directly attach and settle on the hyphae of various fungal species. Such colonization of mycelia was proposed to be dependent on biofilm formation by the bacteria, but the essentiality of the biofilm matrix was not represented before. Here, we demonstrate that secreted biofilm matrix components of the soil-dwelling bacterium, *Bacillus subtilis* are essential for the establishment of a dense bacterial population on the hyphae of the filamentous black mold fungus, *Aspergillus niger* and the basidiomycete mushroom, *Agaricus bisporus*. We further illustrate that these matrix components can be shared among various mutants highlighting the community shaping impact of biofilm formers on bacteria-fungi interactions.

1. Introduction

Biofilm development by a plethora of bacteria and fungi has been pragmatically studied separately in the laboratory. Biofilm formation is abundant in the environment [1] and these biofilm communities likely comprise both bacteria and fungi in addition to higher eukaryotes grazing or residing these habitats. Interaction among bacteria and fungi extends physical associations, and furthermore includes chemical communications, ranging from antibiosis and metabolic exchange to specific signaling and chemotaxis [2]. These direct or indirect interactions among bacteria and fungi alters the physiology, growth, movement, differentiation, pathogenesis, reproduction and/or survival of either or both partners [2]. During physical interaction between bacteria and fungi, stable association is possibly facilitated by the production of a viscous biofilm matrix. Indeed, the production of a biofilm matrix has been suggested for various bacterial isolates on the hyphae of the ectomycorrhizal fungus, *Laccaria bicolor* [3], however, the essentiality of the biofilm matrix in long term attachment has not been confirmed before. Several molecular determinants have been described to be important for bacteria-fungi interactions, including motility, quorum sensing, bacterial

secretion system, secondary metabolites (see an extended list reviewed in Ref. [4]). Here, we examined the role of biofilm components of *Bacillus subtilis* during association with filamentous Ascomycota and Basidiomycota. *B. subtilis* is a soil-derived Gram-positive bacterium and long-studied model for physiology, genetics and differentiation, including motility, sporulation, biofilm formation [5]. Phenotypic diversification of this bacterium is influenced by intertwinement of global regulators, including Spo0A that has been originally described to be involved in production of heat and pressure resistant spores [6]. In addition, Spo0A has been later shown to impact protease secretion, toxin production, and biofilm development, thus involved in regulation of genes related to cell fate decision of the bacterium [7]. Formation of biofilm in *B. subtilis* requires a complex matrix composed of exopolysaccharide (EPS), TasA amyloid fiber, and a surface localized hydrophobin, BslA [8–13]. The former two matrix components are essential for the establishment of a floating biofilm on the air-medium interface (referred to as pellicle), the creation of complex vein-like structures on agar medium, or attachment to the root surface of plants [8–10,14,15]. BslA protein creates a shield around the pellicle and colony biofilm to avoid penetration of hydrophobic fluids and its deletion alters

* Corresponding author. Bacterial Interactions and Evolution Group, Department of Biotechnology and Biomedicine, Technical University of Denmark, Kongens Lyngby, Denmark.

E-mail address: atkovacs@dtu.dk (Á.T. Kovács).

¹ Contributed equally.

<https://doi.org/10.1016/j.biofilm.2019.100007>

Received 1 August 2019; Received in revised form 15 October 2019; Accepted 19 October 2019

Available online 24 October 2019

2590-2075/© 2019 The Author(s). Published by Elsevier B.V. This is an open access article under the CC BY license (<http://creativecommons.org/licenses/by/4.0/>).

Table 1

Bacterial and fungal strains used in this study. Cm^R, Spec^R, Km^R, and Tet^R denote chloramphenicol, spectinomycin, kanamycin, and tetracycline resistance cassettes, respectively.

Bacterial strains		
<i>B. subtilis</i> strains	Characteristics	Reference
DK1042	NCBI3610 <i>comI</i> ^{Q121}	[31]
TB34	DK1042 <i>amyE::P_{hyperspank}-gfp</i> , Cm ^R	[32]
TB35	DK1042 <i>amyE::P_{hyperspank}-mKATE2</i> , Cm ^R	[33]
TB36	DK1042 Δ <i>hag::Km^R</i> ; <i>amyE::P_{hyperspank}-gfp</i> , Cm ^R	[34]
TB37	DK1042 Δ <i>hag::Km^R</i> ; <i>amyE::P_{hyperspank}-mKATE2</i> , Cm ^R	[34]
TB421	DK1042 Δ <i>spo0A::Km^R</i> ; <i>amyE::P_{hyperspank}-gfp</i> , Cm ^R	[32]
TB524	DK1042 Δ <i>eps::Tet^R</i> ; <i>amyE::P_{hyperspank}-gfp</i> , Spec ^R	[11]
TB525	DK1042 Δ <i>eps::Tet^R</i> ; <i>amyE::P_{hyperspank}-mKATE2</i> , Spec ^R	[11]
NRS2097	NCIB3610 Δ <i>bslA::Cm^R</i>	[35]
TB526	DK1042 Δ <i>bslA::Cm^R</i> ; <i>amyE::P_{hyperspank}-gfp</i> , Spec ^R	This study
TB538	DK1042 Δ <i>tasA::Km^R</i> ; <i>amyE::P_{hyperspank}-gfp</i> , Spec ^R	[11]
TB539	DK1042 Δ <i>tasA::Km^R</i> ; <i>amyE::P_{hyperspank}-mKATE2</i> , Spec ^R	[11]
Fungal strains		
Species name	Strain and collection numbers	Reference
<i>A. bisporus</i>	H39/CBS 122262	[36]
<i>A. niger</i>	N402/ATCC 64974/CBS 132248	[37]

microstructure of colonies [12,13,16], but it is not indispensable for establishment of floating biofilms [17,18]. The ability and degree of biofilm matrix production correlates with attachment to the plant root surface in hypotonic cultures and also with the ability of the bacterial

strains to protect tomato plant against wilt disease caused by *Ralstonia solanacearum* [10,19]. As the matrix components are secreted from the cells, mutants lacking either EPS or TasA are able to complement each other and create a functional biofilm both *in vitro* and on the plant root [10,11,20].

A previous study demonstrated that attachment of *B. subtilis* to the mycelia of *Aspergillus niger* leads to metabolic alterations in both partners [21]. Microarray experiments revealed that genes responsible for single cell motility in *B. subtilis* are downregulated 3 h after attachment [21], suggesting settlement of the bacterial cells on the fungal hyphae. However, transcriptions of biofilm-related genes were not altered at such an early stage of interaction compared to planktonic cells.

Here, we revisited the interaction of *B. subtilis* with *A. niger* dissecting the co-cultures after 24 h of incubation. We demonstrate that long-term attachment depends on the genes required for exopolysaccharide and amyloid fiber production, but neither the synthesis of hydrophobin nor the ability for single cell motility are required for the bacterial settlement on the fungal mycelium. Moreover, the secreted matrix components can complement single gene deletion mutants. Finally, we show that such a matrix-dependent colonization of fungal hyphae is not only restricted to *A. niger*, but similarly required for biofilm formation on the mycelia of the basidiomycete, *Agaricus bisporus*.

2. Material and methods

2.1. Strains, media composition and culturing conditions

All the bacterial and fungal strains used in this study are listed in Table 1. Bacterial strains were cultivated in Lysogeny Broth medium (LB-

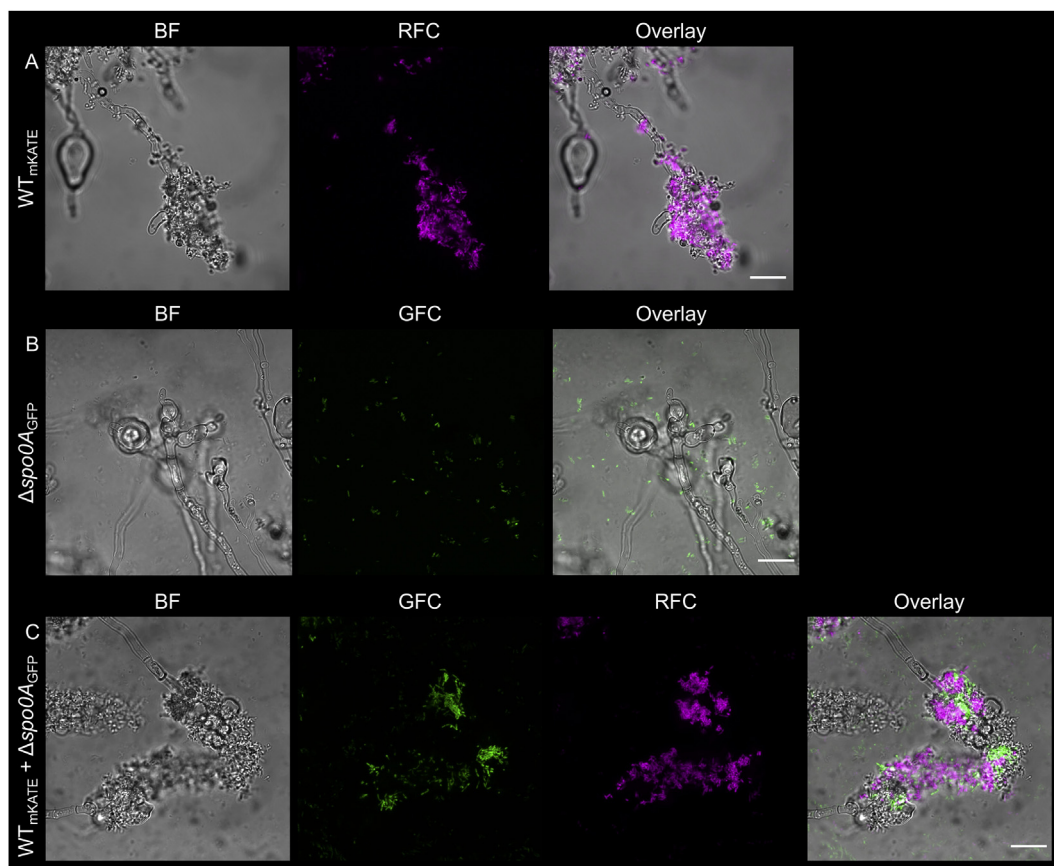


Fig. 1. Colonization of the *A. niger* hyphae by *B. subtilis* (A) wild type, (B) *spo0A* mutant and (C) the co-culture of 10:1 GFP-labeled *spo0A* mutant and mKATE-labeled wild type. GFC: green fluorescent channel; RFC: red fluorescent channel. Scale bars indicate 20 μ m. The images presented are representative examples selected from independent samples repeated on different days. (For interpretation of the references to color in this figure legend, the reader is referred to the Web version of this article.)

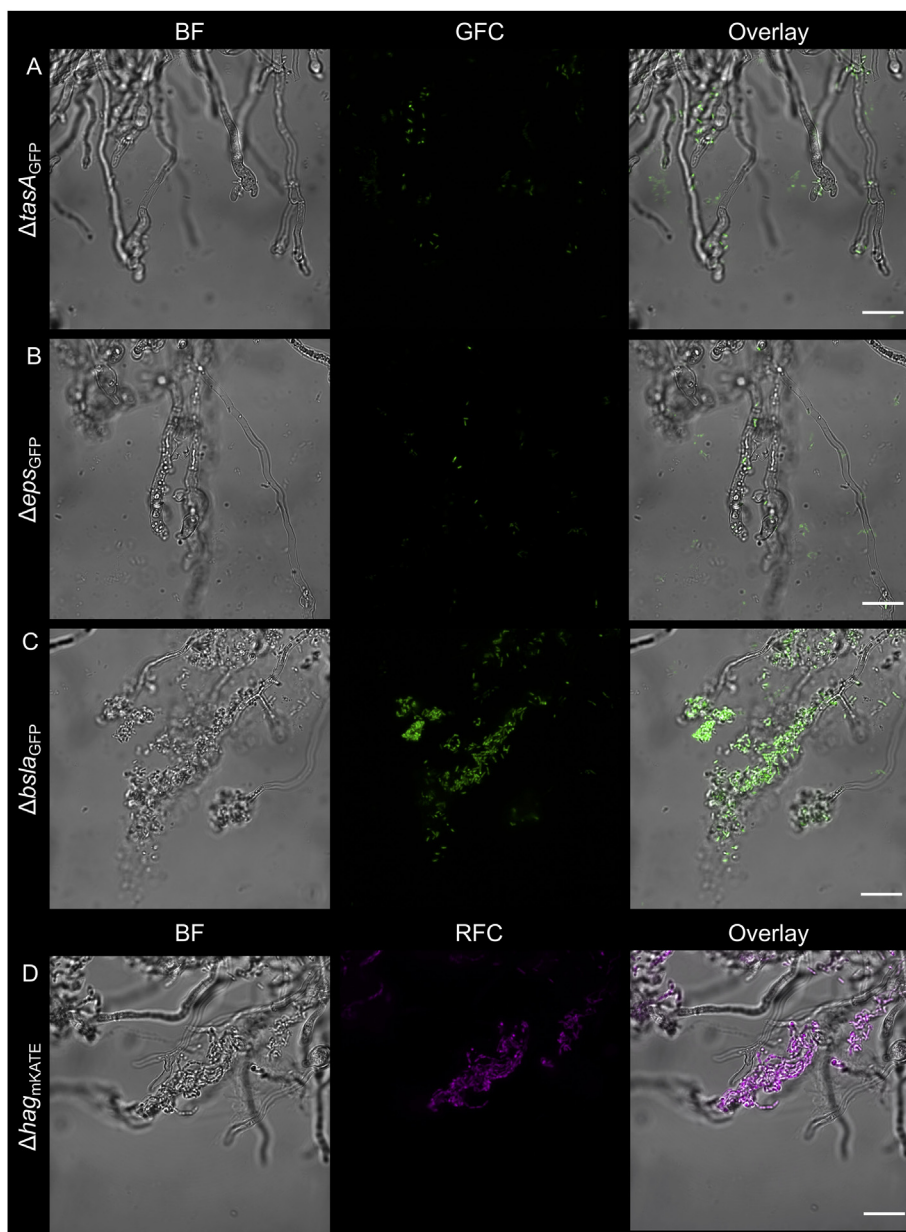


Fig. 2. *B. subtilis* lacking biofilm components, (A) TasA or (B) EPS are unable to grow on the *A. niger* hyphae, while strains lacking (C) the production of hydrophobin, BslA or (D) motility established stable colonization on the mycelia. GFC: green fluorescent channel; RFC: red fluorescent channel. Scale bars indicate 20 μm . The images presented are representative examples selected from independent samples repeated on different days. (For interpretation of the references to color in this figure legend, the reader is referred to the Web version of this article.)

Lennox, Carl Roth, Germany; 10 g l^{-1} tryptone, 5 g l^{-1} yeast extract and 5 g l^{-1} NaCl) supplemented with 1.5% Bacto agar if required. Supplemented LB medium was prepared by adding 1% 1 mol l^{-1} MgSO_4 and 0.1% 0.1 mol l^{-1} MnCl_2 to basic LB medium. *A. niger* was cultivated on potato dextrose glucose agar (PDA) medium (Carl Roth, Germany; potato infusion 4 g l^{-1} , glucose 20 g l^{-1} , agar 15 g l^{-1} , pH value 5.2 ± 0.2) to harvest spores and in LB medium for formation of macro-colonies. *A. bisporus* was cultivated on PDA plates or potato dextran glucose broth (PDB) medium (Carl Roth, Germany; potato infusion 4 g l^{-1} , glucose 20 g l^{-1} , pH value 5.2 ± 0.2).

TB526 was obtained using natural competence [22] by transforming genomic DNA extracted from NRS2097 to TB34 and selecting for chloramphenicol resistance, followed by verifying the mutation by PCR. To select for resistant bacterial colonies after transformation, 5 $\mu\text{g l}^{-1}$ chloramphenicol was used.

2.2. Hyphal colonization assay of *A. niger*

Spores of *A. niger* cultures grown at 28 $^{\circ}\text{C}$ for 7–12 days on PDA plates were harvested using 10 ml saline tween solution (8 g l^{-1} NaCl and 0.05 ml l^{-1} Tween 80) and filtered through Miracloth (Millipore; Billerica, USA) following the protocol described in Ref. [21]. The spore solution was centrifuged 5000 rpm for 10 min and resuspended in saline tween solution. Spores were stored at 4 $^{\circ}\text{C}$ until use, but no more than 14 days. Around 3×10^5 spores ml^{-1} were inoculated into 25 ml of LB medium and shaken at 120 rpm at 28 $^{\circ}\text{C}$ for 24 h 4–5 macro-colonies were transferred into a single well of a 24-well plate and culture was supplemented with 0.01 mol l^{-1} MgSO_4 and 0.1 mmol l^{-1} MnCl_2 as indicated for supplemented LB medium. 10 μl of *B. subtilis* overnight culture grown at 37 $^{\circ}\text{C}$ was inoculated into each well (single or mixed culture). The co-cultures were incubated at 28 $^{\circ}\text{C}$ with shaking at 170 rpm for 24 h.

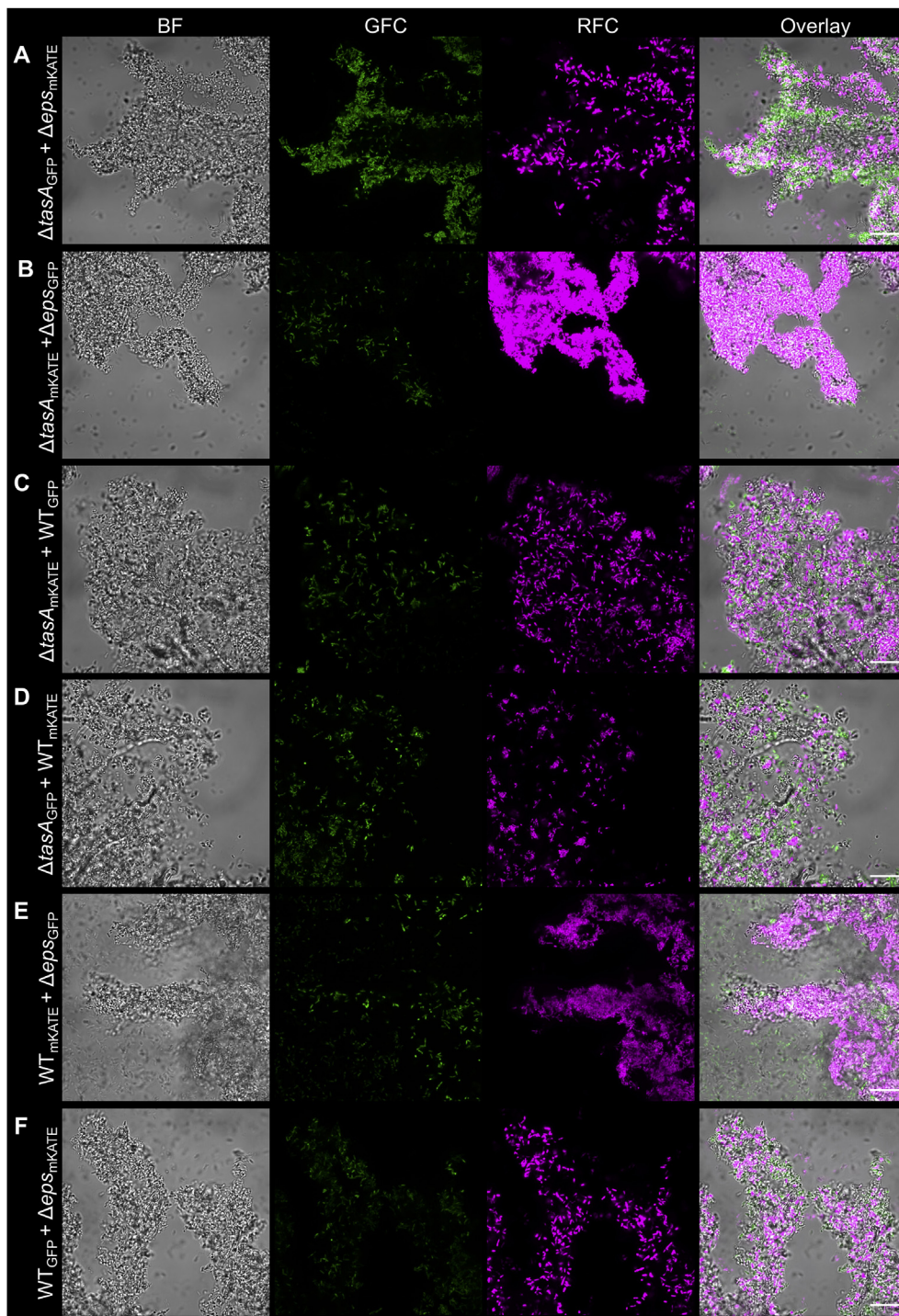


Fig. 3. Mutations in *tasA* and *eps* genes were complemented by the co-inoculation of the mutants (A and B), and by the wild type strain (C–F) including a fluorescent marker swap, resulting in fungal colonization by the mutants. GFC: green fluorescent channel; RFC: red fluorescent channel. Scale bars indicate 20 μm . The images presented are representative examples selected from independent samples repeated on different days. (For interpretation of the references to color in this figure legend, the reader is referred to the Web version of this article.)

Following incubation, the pellicle biofilm formed at the air-liquid interface was removed from each well. Subsequently, *A. niger* macro-colonies were washed two times with sterile MilliQ water before imaging.

2.3. Hyphal colonization assay of *A. bisporus*

Three-week old *A. bisporus* culture, grown on PDA plates at 25 °C was wetted with 10 ml of physiological saline and scraped thoroughly with a spreader. Afterwards, 1 ml of the hyphal suspension was incubated in 25 ml PDB at 25 °C without agitation for 8–14 days. After eight days, *A. bisporus* macro-colonies were floating within the media. One macro-colony each was transferred into a well of a 24-well microtiter plate.

Remaining PDB was removed and the macro-colonies were washed once with physiological saline. 1 ml of supplemented LB medium was added to each macro-colony and inoculated with 10 μl of *B. subtilis* overnight culture grown at 37 °C (single or mixed culture). The microtiter plate was incubated at 25 °C with shaking at 170 rpm for 22–24 h. Subsequently, *A. bisporus* macro-colonies were washed three times with physiological saline.

2.4. Sample preparation and confocal laser scanning microscopy (CLSM)

Washed fungal macro-colonies were transferred to microscope slides and gently sealed with cover slips. Fungal hyphae colonization was

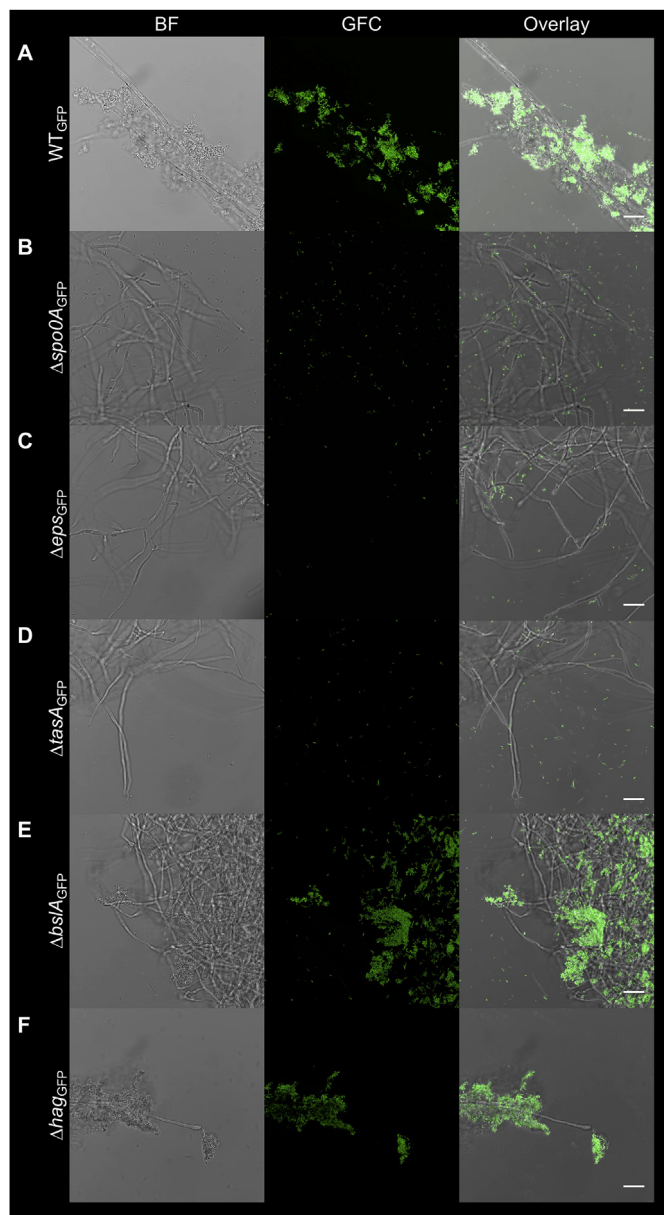


Fig. 4. Attachment of *B. subtilis* on *A. bisporus* hyphae. *B. subtilis* wild type (A) and its corresponding mutants were co-cultivated with *A. bisporus* macro-colonies. Fungal macro-colonies were subsequently washed and visualized with CLSM. The images were recorded at the edge of the fungal macro-colonies. GFC: green fluorescent channel. Scale bars represent 20 μm . The images presented are representative examples selected from different positions of the fungal macro-colonies on independent samples repeated on different days. (For interpretation of the references to color in this figure legend, the reader is referred to the Web version of this article.)

analysed with two confocal laser scanning microscopes (LSM 710 (Carl Zeiss) or TCS SP8 (Leica) both equipped with an argon laser and a Plan-Apochromat 63x/1.4 Oil objective). Fluorescent reporter excitation was performed at 488 nm for green fluorescence and at 561 nm for red fluorescence, while the emitted fluorescence was recorded at 540/40 nm and 668/86 nm (Zeiss) or 520/23 nm and 700/90 nm (Leica) for GFP and mKATE, respectively, (wavelength/bandwidth). For generating multi-layer images, Z-stack series with 1 μm steps were acquired and processed with the software ImageJ (National Institutes of Health). Maximum intensity was used to merge five chosen stacks of the green fluorescent, red fluorescent and overlay channel. Merging of the five stacks was done to integrate signals from the bacterial cells at different

focus planes. The bright field channel is represented by only one brightness-adjusted image from one of the stacks used to obtain the fluorescent images.

3. Results and discussion

3.1. Colonization of the *A. niger* hyphae by *B. subtilis* depends on the global regulator, *Spo0A*

Transcriptome analysis of attaching *B. subtilis* cells on *A. niger* mycelia has revealed that expression of genes related to single cell motility is reduced compared to non-attached cells [21] suggesting that the bacterial cells switch from planktonic to sessile state of growth. The global transcriptional regulator, Spo0A influences hundreds of genes in *B. subtilis* that determine bacterial cell fate, e.g. differentiation into swimming, biofilm forming, or sporulating cell types [7]. Therefore, the impact of *spo0A* gene deletion in *B. subtilis* was first assayed during colonization of the hyphae of *A. niger*. As expected, bacterial cells of the *spo0A* strain showed reduced hyphal colonization compared to the wild type and only planktonic cells were observed around *A. niger* (Fig. 1A and B). Driven by the observation that colonization of plant root by *B. subtilis* requires secreted biofilm matrix components [10,19], we have inspected if addition of wild type strain restores attachment of *spo0A* mutant cells on the fungal hyphae. Indeed, co-inoculation of wild type and *spo0A* cells in 1:10 ratio rescued attachment of *spo0A* strain to the hyphae, suggesting that secreted factors by the wild type strains are sufficient for the establishment of biofilm by the two strains on the fungal mycelia (Fig. 1C). Alternatively, signaling molecules produced by the wild type strain, but absent in the *spo0A* mutant could induce the molecular factors responsible for hyphal biofilms.

3.2. Hyphal colonization depends on *B. subtilis* biofilm matrix components, *EPS* and *TasA*

Biofilm formation of *B. subtilis* depends on various secreted components, including EPS, TasA and BslA. The transcription of these operons involved in the production of matrix is indirectly dependent on Spo0A. Therefore, we have tested how single deletion of *eps* operon, *tasA* or *bslA* genes impacts fungal colonization by *B. subtilis*. Unlike the *bslA* mutant, removal of either EPS or TasA hindered the bacterial biofilm development on the hyphae of *A. niger* (Fig. 2A–C). This suggests that both core components of the matrix, EPS and TasA contribute to establishment of stable biofilm on the mycelia, while the hydrophobin BslA is not necessary for stable attachment. In accordance, previous studies found that BslA is not essential for the establishment of floating pellicle biofilm of *B. subtilis*, but is required for its repellency and the microstructure of colonies [12,13,17,18]. Finally, gene deletion in the flagellin coding gene was assayed for biofilm establishment during mycelia colonization. Although motility is not essential for generation of biofilms, it has been described to be critical for fast formation of *B. subtilis* biofilm [23]. Cells lacking single cell motility could colonize the hyphae of *A. niger* (Fig. 2D), similar to the wild type strain (Fig. 1A). The importance of bacterial flagella and type 4 pili was previously described during co-migration of *Burkholderia terrae* with fungal hyphae through soil [24], suggesting that essentiality of bacterial motility for fungal interaction could depend on the environment, bacterial physiology or specific properties of the fungal and bacterial cell surfaces. In addition, other examples highlight that fungal hyphae could facilitate bacterial swimming along the hyphae and therefore niche colonization [25,26]. In our simple laboratory system, the bacterium-fungus co-cultures are mildly agitated, which allows firm contact of the bacterial cells and the mycelia. Under these conditions, motility is plausibly not essential.

3.3. Secreted biofilm matrix components are shared among mutants

To complement the mutations and lack of biofilm formation ability of

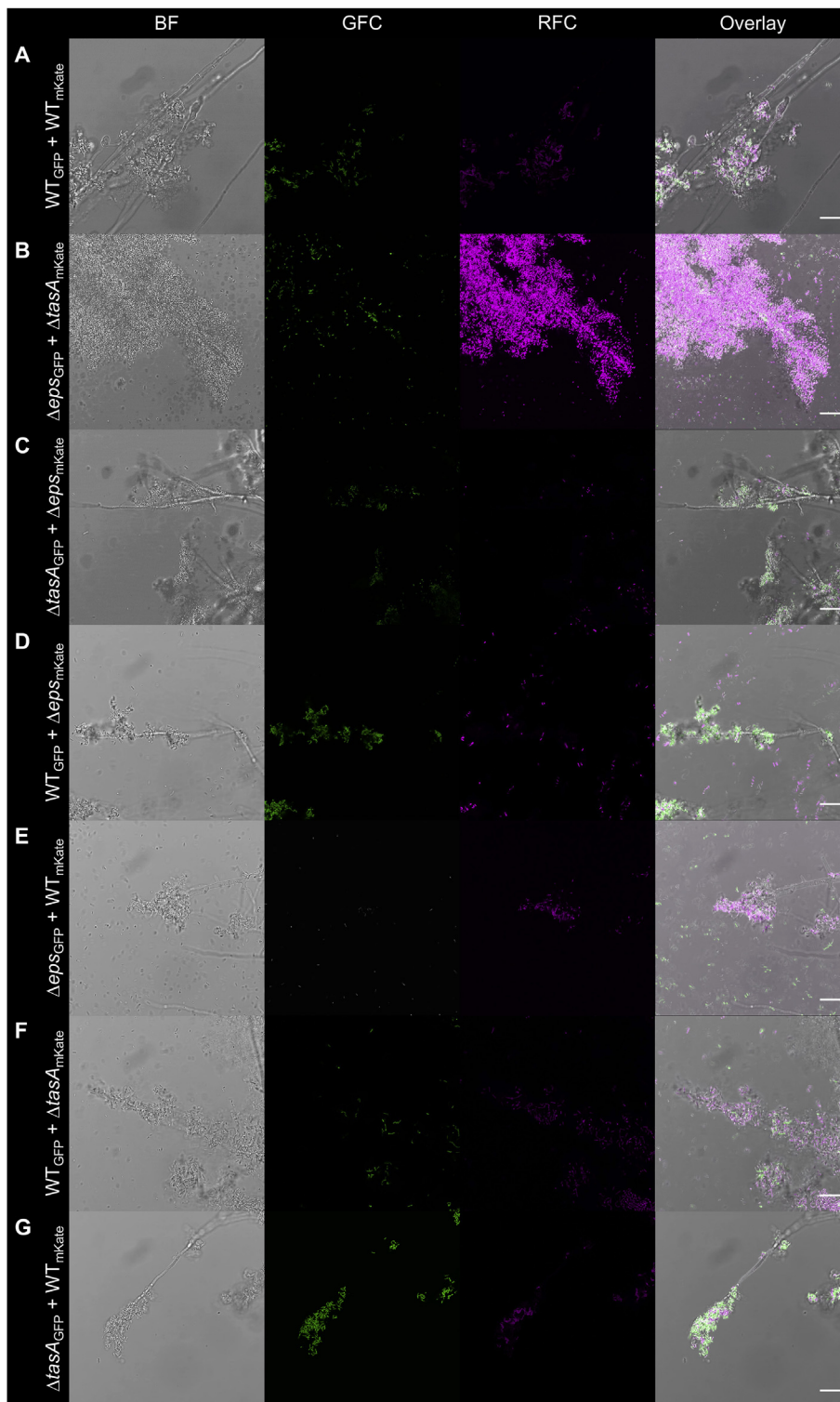


Fig. 5. Attachment of mixed-culture *B. subtilis* strains to *A. bisporus* hyphae. Overnight cultures of different *B. subtilis* strains were mixed and co-cultivated with *A. bisporus* macro-colonies. Fungal macro-colonies were subsequently washed and visualized with CLSM; pictures were taken approximately near the edge of the macro-colonies. GFC: green fluorescent channel; RFC: red fluorescent channel. Scale bars represent 20 μm . The images presented are representative examples selected from different positions on independent samples. (For interpretation of the references to color in this figure legend, the reader is referred to the Web version of this article.)

the bacterial strains on the hyphae of *A. niger*, various co-cultivations were tested. Deficiency in EPS or TasA production was complemented either by co-cultivation of mutant strains together or by addition of the wild type strain to biofilm matrix mutant *B. subtilis*, irrespective of fluorescent labeling (Fig. 3). Previous studies demonstrated that secreted biofilm matrix components complement pellicle biofilm formation [20, 27] as well as plant colonization [10,11]. Notably, mixing *eps* and *tasA* mutant *B. subtilis* strains results in genetic division of labor, thus increased population productivity both during pellicle biofilm formation

at the air-liquid interface and during plant root colonization [11,28].

3.4. Biofilm formation of *B. subtilis* on the basidiomycete mycelia

The above described simple co-culture system comprises a bacterium, *B. subtilis* and an Ascomycota fungus, *A. niger* that can be both isolated from soil, however, their co-occurrence in nature has never been reported according to our knowledge. Therefore, we examined fungus-attached biofilm formation by *B. subtilis* on a more ecologically relevant host. *In*

in vitro laboratory experiments suggest that *B. subtilis* cells can colonize the hyphae of the ectomycorrhizal fungus, *L. bicolor* [3] and the basidiomycete *Coprinopsis cinerea* [29]. In addition, *B. subtilis* has been isolated from the soil directly underneath a troop of growing *Paxillus involutus* mushrooms [30] and below an *Agaricus* sp. fruiting body (Kiesewalter and Kovács, unpublished observation). Therefore, we set out to examine the importance of biofilm matrix components during mycelia colonization of button mushroom, *A. bisporus*. In agreement with the above observations on *A. niger* from this study, hyphal biofilm formation by *B. subtilis* was diminished by deletion of *spo0A*, *epsA-O*, or *tasA* genes, while removal of *bslA* or *hag* genes did not impact colonization properties (Fig. 4).

Further, complementation of the matrix mutants, *eps* and *tasA* strains was performed using a co-culture of the mutants or by addition of wild type to the mutants (Fig. 5). The experiments with the basidiomycete, *A. bisporus* strengthens the observation that fungal hyphae colonization and biofilm formation by *B. subtilis* depends on secreted biofilm components. This suggest that production of a matrix by biofilm-proficient bacterial species in nature could potentially facilitate the establishment of multi-species biofilms on fungal hyphae. Indeed, the presence of biofilm matrix and extracellular DNA has been demonstrated for a numerous bacterial species during colonization of ectomycorrhizal fungi, including *L. bicolor* [3]. Our genetic approach further supports the importance of bacterial biofilm matrix production during long term colonization of fungal mycelia.

4. Conclusion

Bacterial biofilms in the laboratory have been mostly studied using inert substrates, however, during infections or in the environment, bacteria also interact with eukaryotes, including their hosts (from humans and animals to plants) or the co-habitants of their milieu. Here, we demonstrate that biofilm matrix components of *B. subtilis* are essential for colonization of the hyphae of *A. niger* and *A. bisporus*. In addition, the secretion of these matrix components is sufficient to rescue biofilm formation of matrix deficient strains suggesting that social interaction likely shapes the co-evolution of fungi and bacteria in the environment. This leads to the appearance of specific interactions, including primary metabolite cross-feeding, molecular recognition, and potential induction of secondary metabolite production.

Funding information

This work was supported by the Danish National Research Foundation (DNRF137) within the Center for Microbial Secondary Metabolites.

Declaration of competing interest

The authors declare that there are no conflicts of interest.

Acknowledgement

We thank Nicola Stanley-Wall for the comments on our bioRxiv submission.

References

- Flemming HC, Wuertz S. Bacteria and archaea on Earth and their abundance in biofilms. *Nat Rev Microbiol* 2019;17:247–60.
- Frey-Klett P, Burlinson P, Deveau A, Barret M, Tarkka M, Sarniguet A. Bacterial-fungal interactions: hyphens between agricultural, clinical, environmental, and food microbiologists. *Microbiol Mol Biol Rev* 2011;75:583–609.
- Guennoc CM, Rose C, Labbé J, Deveau A. Bacterial biofilm formation on the hyphae of ectomycorrhizal fungi: a widespread ability under controls? *FEMS Microbiol Ecol* 2018;94:fiy093. <https://doi.org/10.1093/femsec/fiy093>.
- Deveau A, Bonito G, Uehling J, Paoletti M, Becker M, Bindschedler S, et al. Bacterial-fungal interactions: ecology, mechanisms and challenges. *FEMS Microbiol Rev* 2018;42:335–52. <https://doi.org/10.1093/femsec/fuy008>.
- Kovács Á. *Bacillus subtilis*. *Trends Microbiol* 2019;27:724–5. <https://doi.org/10.1016/j.tim.2019.03.008>.
- Trowsdale J, Chen S, Hoch J. Evidence that *spo0A* mutations are recessive in *spo0A*-*spo0A*+ merodiploid strains of *Bacillus subtilis*. *J Bacteriol* 1978;135:99–113.
- López D, Vlamakis H, Kolter R. Generation of multiple cell types in *Bacillus subtilis*. *FEMS Microbiol Rev* 2009;33:152–63. <https://doi.org/10.1111/j.1574-6976.2008.00148.x>.
- Branda SS, González-Pastor JE, Ben-Yehuda S, Losick R, Kolter R. Fruiting body formation by *Bacillus subtilis*. *Proc Natl Acad Sci U S A* 2001;98:11621–6.
- Romero D, Aguilar C, Losick R, Kolter R. Amyloid fibers provide structural integrity to *Bacillus subtilis* biofilms. *Proc Natl Acad Sci U S A* 2010;107:2230–4. <https://doi.org/10.1073/pnas.0910560107>.
- Beauregard PB, Chai Y, Vlamakis H, Losick R, Kolter R. *Bacillus subtilis* biofilm induction by plant polysaccharides. *Proc Natl Acad Sci U S A* 2013;110:E1621–30.
- Dragoš A, Kiesewalter H, Martin M, Hsu C-Y, Hartmann R, Wechsler T, et al. Division of labor during biofilm matrix production. *Curr Biol* 2018;28:1903–13.
- Kobayashi K, Iwano M. BslA(YuaB) forms a hydrophobic layer on the surface of *Bacillus subtilis* biofilms. *Mol Microbiol* 2012;85:51–66.
- Hobley L, Ostrowski A, Rao FV, Bromley KM, Porter M, Prescott AR, et al. BslA is a self-assembling bacterial hydrophobin that coats the *Bacillus subtilis* biofilm. *Proc Natl Acad Sci U S A* 2013;110:13600–5.
- Branda SS, González-Pastor JE, Dervyn E, Ehrlich SD, Losick R, Kolter R. Genes involved in formation of structured multicellular communities by *Bacillus subtilis*. *J Bacteriol* 2004;186:3970–9.
- Gallegos-Monterrosa R, Mhatre E, Kovács Á. Specific *Bacillus subtilis* 168 variants form biofilms on nutrient-rich medium. *Microbiology* 2016;162:1922–32.
- Kovács ÁT, van Gestel J, Kuipers OP. The protective layer of biofilm: a repellent function for a new class of amphiphilic proteins. *Mol Microbiol* 2012;85:8–11.
- Ostrowski A, Mehert A, Prescott A, Kiley TB, Stanley-Wall NR. YuaB functions synergistically with the exopolysaccharide and TasA amyloid fibers to allow biofilm formation by *Bacillus subtilis*. *J Bacteriol* 2011;193:4821–31. <https://doi.org/10.1128/JB.00223-11>.
- Kovács ÁT, Kuipers OP. Rok regulates *yuaB* expression during architecturally complex colony development of *Bacillus subtilis* 168. *J Bacteriol* 2011;193:998–1002. <https://doi.org/10.1128/JB.01170-10>.
- Chen Y, Yan F, Chai Y, Liu H, Kolter R, Losick R, et al. Biocontrol of tomato wilt disease by *Bacillus subtilis* isolates from natural environments depends on conserved genes mediating biofilm formation. *Environ Microbiol* 2013;15:848–64.
- Branda SS, Chu F, Kearns DB, Losick R, Kolter R. A major protein component of the *Bacillus subtilis* biofilm matrix. *Mol Microbiol* 2006;59:1229–38.
- Benoit I, van den Esker MH, Patyshakuliyeva A, Mattern DJ, Blei F, Zhou M, et al. *Bacillus subtilis* attachment to *Aspergillus niger* hyphae results in mutually altered metabolism. *Environ Microbiol* 2015;17:2099–113. <https://doi.org/10.1111/1462-2920.12564>.
- Anagnostopoulos C, Spizizen J. Requirements for transformation in *Bacillus subtilis*. *J Bacteriol* 1961;81:741–6.
- Hölscher T, Bartels B, Lin Y-C, Gallegos-Monterrosa R, Price-Whelan A, Kolter R, et al. Motility, chemotaxis and aerotaxis contribute to competitiveness during bacterial pellicle biofilm development. *J Mol Biol* 2015;427:3695–708.
- Yang P, Zhang M, Van Elsas JD. Role of flagella and type four pili in the co-migration of *Burkholderia terrae* BS001 with fungal hyphae through soil. *Sci Rep* 2017;7:2997. <https://doi.org/10.1038/s41598-017-02959-8>.
- Ingham CJ, Kalisman O, Finkelshtein A, Ben-Jacob E. Mutually facilitated dispersal between the nonmotile fungus *Aspergillus fumigatus* and the swarming bacterium *Paenibacillus vortex*. *Proc Natl Acad Sci U S A* 2011;108:19731–6. <https://doi.org/10.1073/pnas.1102097108>.
- Kohlmeier S, Smits THM, Ford RM, Keel C, Harms H, Wick LY. Taking the fungal highway: mobilization of pollutant-degrading bacteria by fungi. *Environ Sci Technol* 2005;39:4640–6. <https://doi.org/10.1021/es047979z>.
- Martin M, Dragoš A, Hölscher T, Maróti G, Bálint B, Westermann M, et al. *De novo* evolved interference competition promotes the spread of biofilm defectors. *Nat Commun* 2017;8:15127.
- Kovács Á, Dragoš A. Evolved Biofilm: review on the experimental evolution studies of *Bacillus subtilis* pellicles. *J Mol Biol* 2019. <https://doi.org/10.1016/j.jmb.2019.02.005>. in press.
- Stanley CE, Stöckli M, Van Sway D, Sabotić J, Kallio PT, Künzler M, et al. Probing bacterial-fungal interactions at the single cell level. *Integr Biol* 2014;6:935–45. <https://doi.org/10.1039/c4ib00154k>.
- Tauber JP, Gallegos-Monterrosa R, Kovács Á, Shelest E, Hoffmeister D. Dissimilar pigment regulation in *Serpula lacrymans* and *Paxillus involutus* during inter-kingdom interactions. *Microbiology* 2018;164:65–77. <https://doi.org/10.1099/mic.0.000582>.
- Konkol MA, Blair KM, Kearns DB. Plasmid-encoded comI inhibits competence in the ancestral 3610 strain of *Bacillus subtilis*. *J Bacteriol* 2013;195:4085–93. <https://doi.org/10.1128/JB.00696-13>.
- Seccareccia I, Kovács Á, Gallegos-Monterrosa R, Nett M. Unraveling the predator-prey relationship of *Cupriavidus necator* and *Bacillus subtilis*. *Microbiol Res* 2016;192:231–8. <https://doi.org/10.1016/j.micres.2016.07.007>.
- Hölscher T, Dragoš A, Gallegos-Monterrosa R, Martin M, Mhatre E, Richter A, et al. Monitoring spatial segregation in surface colonizing microbial populations. *J Vis Exp* 2016;2016:e54752. <https://doi.org/10.3791/54752>.
- Richter A, Hölscher T, Pausch P, Sehr T, Brockhaus F, Bange G, et al. Hampered motility promotes the evolution of wrinkly phenotype in *Bacillus subtilis*. *BMC Evol Biol* 2018;18:155.

- [35] Verhamme DT, Murray EJ, Stanley-Wall NR. DegU and Spo0A jointly control transcription of two loci required for complex colony development by *Bacillus subtilis*. *J Bacteriol* 2009;191:100–8. <https://doi.org/10.1128/JB.01236-08>.
- [36] Sonnenberg ASM, Gao W, Lavrijssen B, Hendrickx P, Sedaghat-Telgerd N, Foulongne-Oriol M, et al. A detailed analysis of the recombination landscape of the button mushroom *Agaricus bisporus* var. *bisporus*. *Fungal Genet Biol* 2016;93:35–45. <https://doi.org/10.1016/j.fgb.2016.06.001>.
- [37] Bos CJ, Debets AJM, Swart K, Huybers A, Kobus G, Slakhorst SM. Genetic analysis and the construction of master strains for assignment of genes to six linkage groups in *Aspergillus niger*. *Curr Genet* 1988;14:437–43. <https://doi.org/10.1007/BF00521266>.

Study 2

Richter, A., Blei, F., Hu, G., Schwitalla, J. W., Lozano-Andrade, C. N., Jarmusch, S. A., Wibowo, M., ***Kjeldgaard, B.**, Surabhi, S., Jautzus, T., Phippen, C. B. W., Tyc, O., Arentshorst, M., Wang, Y., Garbeva, P., Larsen, T. O., Ram, A. F. J., Hondel, C. A. M., Maroti, G., and Kovacs, A. T. (2023).

Enhanced niche colonisation and competition during bacterial adaptation to a fungus.

To be submitted, preprint deposited in bioRxiv, 2023.03.27.534400.
doi:10.1101/2023.03.27.534400.

Enhanced niche colonisation and competition during bacterial adaptation to a fungus

Anne Richter^{1,2}, Felix Blei², Guohai Hu^{1,3,4,5}, Jan W. Schwitalla², Carlos N. Lozano-Andrade¹, Scott A Jarmusch⁶, Mario Wibowo⁶, Bodil Kjeldgaard¹, Surabhi Surabhi², Theresa Jautzus², Christopher B. W. Phippen⁶, Olaf Tyc⁷, Mark Arentshorst⁸, Yue Wang^{3,4}, Paolina Garbeva⁷, Thomas Ostenfeld Larsen⁶, Arthur F.J. Ram⁸, Cees A.M. van den Hondel⁸, Gergely Maróti⁹, Ákos T. Kovács^{1,2,8,*}

¹ Bacterial Interactions and Evolution Group, DTU Bioengineering, Technical University of Denmark, 2800 Lyngby, Denmark

² Terrestrial Biofilms Group, Institute of Microbiology, Friedrich Schiller University Jena, 07743 Jena, Germany

³ China National GeneBank, BGI-Shenzhen, 518120 Shenzhen, China

⁴ BGI-Shenzhen, 518083 Shenzhen, China

⁵ Shenzhen Key Laboratory of Environmental Microbial Genomics and Application, BGI-Shenzhen, 518083 Shenzhen, China

⁶ Natural Product Discovery Group, DTU Bioengineering, Technical University of Denmark, 2800 Lyngby, Denmark

⁷ Netherlands Institute of Ecology, 6708PB Wageningen, The Netherlands

⁸ Institute of Biology, Leiden University, Leiden, The Netherlands

⁹ Institute of Plant Biology, Biological Research Centre, Eötvös Loránd Research Network (ELKH), 6726 Szeged, Hungary

*For correspondence. E-mail a.t.kovacs@biology.leidenuniv.nl

Running title: Bacterial evolution in the presence of a fungus

Keywords: *Bacillus subtilis*, *Aspergillus niger*, adaptation, secondary metabolites, bacterial-fungal interaction, volatiles

Word count: 3284 (Introduction to Discussion); Number of Figures: 4

Current affiliations: FB, Department Pharmaceutical Microbiology, Hans-Knöll-Institute, Friedrich-Schiller-Universität, Jena, Germany; OT, Department of Internal Medicine I, Goethe University Hospital, Frankfurt, Germany; MW, Singapore Institute of Food and Biotechnology Innovation (SIFBI), Agency for Science, Technology and Research, Singapore, Republic of Singapore.

Abstract

Bacterial-fungal interactions (BFIs) influence microbial community performance of most ecosystems and elicit specific microbial behaviours, including stimulating specialised metabolite production. Using a simple BFI system encompassing the Gram-positive bacterium *Bacillus subtilis* and the black mould fungus *Aspergillus niger*, we established a co-culture experimental evolution method to investigate bacterial adaptation to the presence of a fungus. In the evolving populations, *B. subtilis* was rapidly selected for enhanced production of the lipopeptide surfactin and accelerated surface spreading ability, leading to inhibition of fungal expansion and acidification of the environment. These phenotypes were explained by specific mutations in the DegS-DegU two-component system. In the presence of surfactin, fungal hyphae exhibited bulging cells with delocalised secretory vesicles and RlmA-dependent cell wall stress induction. Increased surfactin production typically enhances the competitive success of bacteria against fungi, which likely explains the primary adaptation path in the presence of *A. niger*.

Introduction

Bacteria and fungi share diverse habitats and consequently, a wide span of interactions is observed between them ranging from mutualism to inhibition. These interactions not only influence the structure and ecology of the respective microbial community but also impact the development and evolution of the interacting species ^{1,2}. Bacteria and fungi can indirectly affect each other by sensing and responding to diffusible signals such as chemoattractants, quorum-sensing molecules, and volatile substances ³⁻⁵. However, several bacterial-fungal interactions (BFIs) require a close vicinity, and even direct contact between the interacting partners. In certain cases, the bacterium resides inside the cells of its fungal host ^{1,5}. Often, a combination of indirect influence and physical contact define a BFI. For example, the Gram-negative bacterium *Pseudomonas fluorescens* WCS365 exhibits chemotaxis towards fusaric acid secreted by *Fusarium oxysporum* f. sp. *radicis-lycopersici* hyphae in the rhizosphere of tomato plants ⁶. This leads to bacterial colonisation of the fungal mycelium and decreased infection by the fungus in tomato plants ^{6,7}. In addition to influencing short-term microbial development, BFIs can also impact the evolution of an organism over longer time scales ⁸. For example, a mutualistic relationship between fungus-growing ants, their fungal partner *Leucoagaricus gonglyophorus*, and associated actinobacteria was proposed to have existed for at least 45 million years ^{1,9}. Antimicrobials produced by actinomycetes protect the fungal gardens by selectively targeting parasitic fungi such as *Escovopsis* species ¹⁰⁻¹².

Investigating BFIs has led to the discovery of numerous secondary metabolites not produced under common laboratory cultivation conditions ¹². The direct co-cultivation of *Streptomyces rapamycinicus* with *Aspergillus nidulans* activates a silent gene cluster in the fungus and triggers the production of orsellinic acid ^{13,14}. The potential of BFIs has been

exploited to identify new antimicrobial compounds using co-cultivation methods, which are urgently needed due to the emergence of antibiotic-resistant bacteria ¹².

Mycelial networks usually cover a large area in soil, and they are used as a highway by bacteria to facilitate their movement along hyphae and thereby disperse and access favourable niches such as the plant endosphere ^{2,15-17}. In addition to transport, fungal hyphae can also function as attachment sites for bacterial biofilms ¹⁸. The presence of *Aspergillus niger* promotes the growth of *Salmonella enterica*, which forms a biofilm on the fungal mycelium and protects it against antifungal agents ^{19,20}. During colonisation of maize plants, co-inoculation of both strains leads to a higher reduction of plant growth than inoculation with each strain alone ¹⁹.

A direct interaction between the black mould-causing fungus *A. niger* and the plant growth-promoting Gram-positive bacterium *Bacillus subtilis* has previously been described^{18,21}. Both organisms are commonly found in soil, thus they potentially coexist in the same habitat and influence each other. Attachment of *B. subtilis* cells to fungal hyphae results in transcriptional changes. Specifically, the production of antimicrobial substances is downregulated in both microorganisms, including the *B. subtilis*-produced lipopeptide, surfactin. Furthermore, genes related to motility and aerobic respiration are also downregulated in the bacterium during attachment ²¹. Here, we investigated the effects of long-term cultivation of *B. subtilis* in the presence of *A. niger*, focusing on evolution of the bacterium. During this laboratory adaptation experiment, *B. subtilis* cells with enhanced surfactin production and spreading behaviour were selected, which was mimicked by incorporation of specific mutations in genes encoding a global two-component system. Increased surfactin production and niche colonisation by the bacterium disrupted fungal expansion and acidification of the medium, and caused cell wall stress in *A. niger*.

Results

Adaptation of *B. subtilis* to the presence of *A. niger* leads to enhanced bacterial surface colonisation. Utilising the ability of *B. subtilis* to colonise and grow on mycelia of the fungus *A. niger*^{18,21}, a simple bacterial-fungal co-culture system was established in which fungal spores and subsequently diluted planktonic bacterial cultures were streaked onto agar medium in a hashtag and square pattern. Areas where bacteria grew over fungal hyphae were dissected (Fig. 1a). This agar block was used to inoculate the bacterium on fresh medium, followed by planktonic growth for 24 h before initiating a new co-culture cycle. Importantly, *A. niger* was not evolved in this setup; a fresh batch of spores was used each time from the same fungal stock. Five parallel co-cultivated evolution BFIs (denoted CoEvo) were used in addition to five control lineages of the bacterium cultivated alone (denoted Bac) following otherwise identical isolation procedures (Supplementary Fig. 1a). After 10 weekly transfers, two endpoint isolates were collected from each lineage of both setups. These evolution endpoint bacterial isolates were tested for growth in the presence of the fungus and their ability to form a colony biofilm.

First, bacterial cultures were spotted between two lines of 1-day-grown *A. niger* mycelia. The ancestor bacterium grew and created a small colony almost surrounded by the fungus after 7 days (Fig. 1b). Most of the evolved isolates behaved similarly to the ancestor, but isolates from two CoEvo lineages, especially CoEvo2 and partially CoEvo4, displayed increased spreading that limited fungal growth and expansion (Fig. 1b, Supplementary Fig. 1b, and Supplementary Video 1 and 2). All Bac isolates behaved like the ancestor. To assess the influence of bacterial spreading on fungal physiology, bacterial cultures were spotted next to a 1-day-grown *A. niger* streak on lysogeny broth (LB) plates containing the pH dye Bromocresol

Purple that is purple above pH 6.8 and yellow below pH 5.2. When the fungus was cultivated alone, the entire agar medium displayed a yellow colour corresponding to the ability of *A. niger* to acidify its environment via excretion of citric acid^{22–24}. The ancestor bacterium and the CoEvo isolates restricted acidification, and the yellow coloration was apparent on the edge of the fungal streak, while the CoEvo2 isolate caused the strongest reduction in the remaining acidified area (Fig. 1b and Supplementary Fig. 1c). These results suggest increased niche colonisation by the CoEvo2 lineage in the presence of the fungus, whereas such adaptation wasn't observed for replicates of the Bac setup.

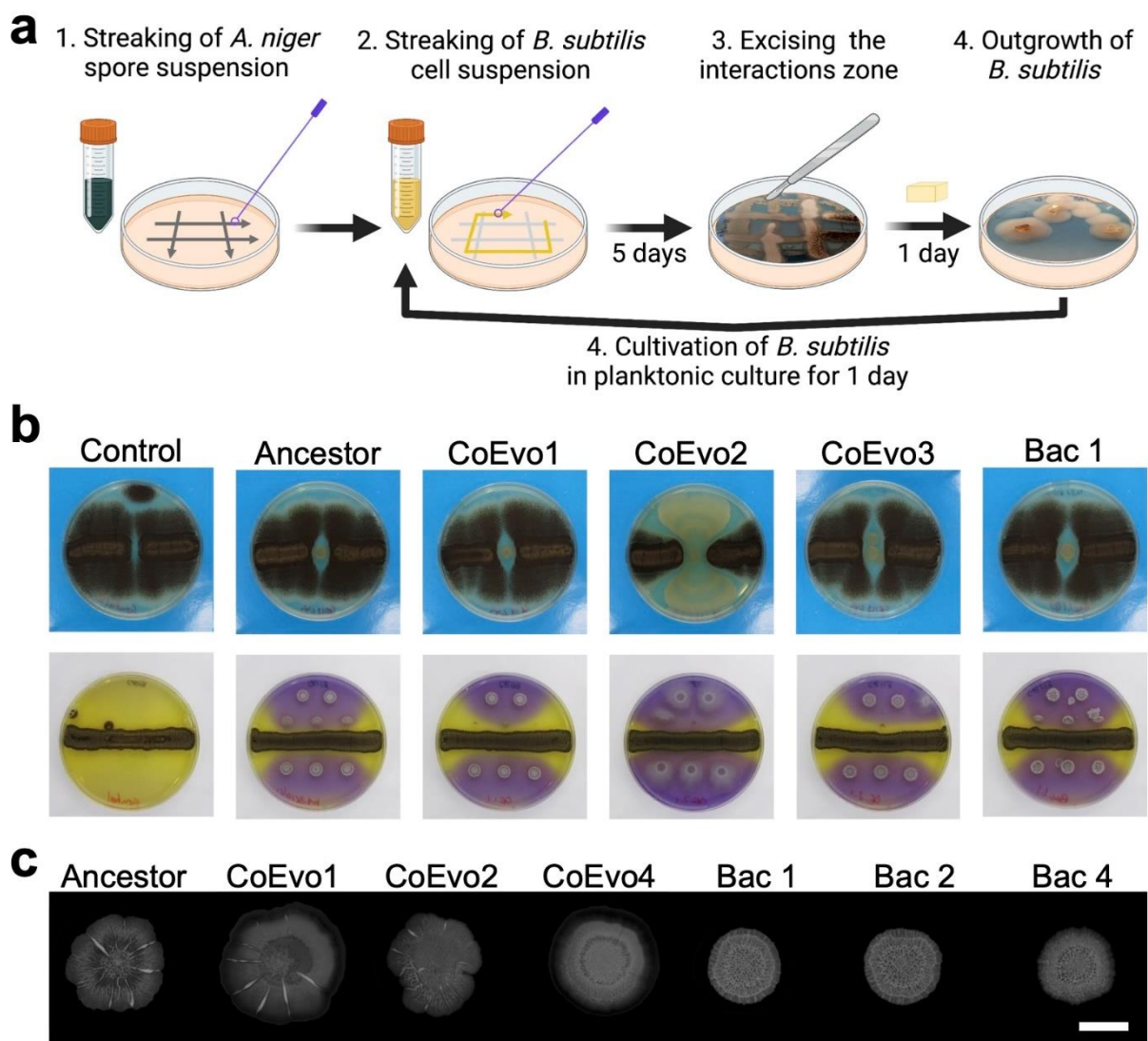


Fig. 1 | *B. subtilis* adaptation to the presence of *A. niger*. **a**, Schematic representation of the

evolution setup. **b**, Top panels showing bacterial growth spotted between two lines of fungal streaks, and lower panels showing the pH of the medium using Bromocresol Purple, where bacterial cultures were spotted next to a continuous fungal spore streak. Purple and yellow colours indicate pH >6.8 and pH <5.2, respectively. Plate size = 9 cm. CoEvo refers to co-culture evolved isolates, Bac denotes bacteria only evolved isolated. **c**, Biofilm colonies of selected evolved isolates. Scale bar = 10 mm. All isolates for panel b and c are shown in Supplementary Fig. 1.

Evolution of *B. subtilis* on agar medium selects for wrinkled variants. Unlike in the presence of a fungus, evolution of *B. subtilis* on a solid agar surface as pure cultures could potentially be driven by adapting biofilm complexity. Indeed, all but one replicate (Bac 3.2) of Bac isolates displayed increased architecture complexity (Fig. 1c and Supplementary Fig. 1d) reminiscent of biofilm matrix-overproducing wrinkled colonies observed in previous experimental evolution settings^{25–28}. In general, isolates from CoEvo lineages exhibited similar colony structure to the ancestor, with a slight increase in complexity of evolved isolate CoEvo 4.1 (Fig. 1c and Supplementary Fig. 1d).

Mutation of the global regulator DegU enhances spreading in the presence of the fungus. To dissect the mutational landscapes of *B. subtilis* adapted in the presence or absence of *A. niger*, sequential populations of each lineage at each transfer were subjected to high-coverage metagenome sequencing (except the first three timepoints of four Bac lineages). Single-nucleotide polymorphisms (SNPs) and short insertions and deletions (indels) were determined using the *breseq* pipeline^{29–31} which detected 142 and 157 mutations with >5% frequency in CoEvo and Bac populations, respectively (frequencies of each mutated gene in each lineage

are shown in Supplementary Fig. 2a and the mutation types are shown in Supplementary Dataset 1). Subsequently, the genealogical structure of each lineage was determined and visualised as lineage frequencies from shared, nested mutation trajectories over time, using *Lolipop*^{32,33}. This approach revealed both unique dominant mutations, including SNPs in *degU* and *degS* genes in lineages CoEvo2 and CoEvo3, respectively, and parallel genetic changes, such as specific SNPs in *sinR* of Bac lineages (Fig. 2a and Supplementary Dataset 1). In addition, certain genes were commonly mutated under both conditions, including *ywdH* and different *opp* genes. Importantly, while genetic diversity was comparable in both CoEvo and Bac lineages (Fig. 2b), parallelism was higher in control evolved lineages than fungal-adapted lines (Fig. 2c), based on the Jaccard index that reflects the likelihood that the same gene is mutated in two independent lineages³⁴. Subsequently, mutations in the genomes of the single endpoint isolates from each lineage were determined to corroborate population sequencing (Supplementary Dataset 1). CoEvo- and Bac-specific mutations were identified in addition to the few commonly mutated genes (Fig. 2d). SNPs in *sinR* were identified in Bac-evolved lineages that were previously associated with increased colony wrinkling^{26,28,35,36}. Interestingly, isolate Bac 3.2 lacking increased colony wrinkles harboured no unique SNPs other than those also present in CoEvo isolates. Isolates from lineages CoEvo 2 and 3 possessed SNPs in the genes coding for the two-component regulatory system, DegU and DegS, respectively. The serine to glycine substitution at position 202 of DegU is located at the edge of the helix-turn-helix domain involved in DNA binding (Supplementary Fig. 2b). Mutations in the vicinity (e.g. DegU^{R184C} in³⁷ and DegU^{I186M} and DegU^{H200Y} in³⁸) have been reported to alter the expression of DegU-regulated genes. The alanine to valine substitution at position 193 of DegS (Supplementary Fig. 2c) has been previously characterized and is known to abolish DegS protein kinase activity³⁹. Reduced phosphorylation of DegU by DegS

results in upregulation of genes related to motility and natural competence for DNA uptake, whereas genes encoding secreted degradative enzymes are upregulated by high levels of phosphorylated DegU^{37,39}. When *degU*^{S202G} and *degS*^{A193V} mutations were reintroduced into the ancestor, the engineered strains phenocopied the evolved isolates in the presence of *A. niger* (Fig. 2e). By contrast, deletion of *degU* was comparable to the wild-type ancestor (Fig. 2e), indicating that these mutations modified but did not abolish DegU activity.

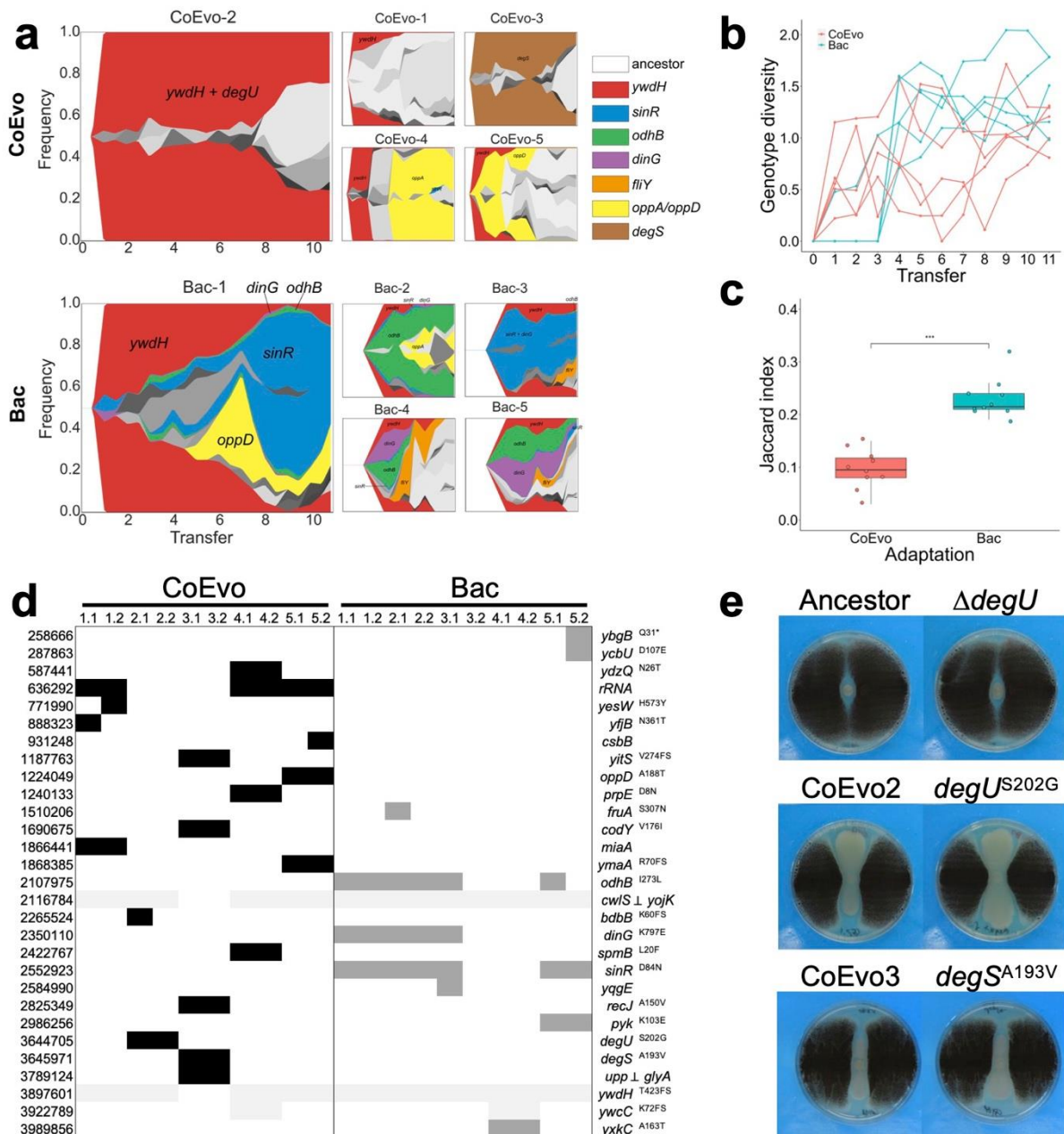


Fig. 2 | Genetic characterisation of *B. subtilis* adaptation to *A. niger*. a, Graphs showing the

genealogy and genotype frequencies throughout the transfers. Each colour or shade represents a distinct genotype. The vertical area corresponds to genotype frequency as inferred using Lolipop. Dominant genotypes with a high mutation gene frequency, which are shared in different populations, are highlighted by matching colours within both adaptation models. **b**, Genotype diversity. The dynamic distribution of genotype alpha diversity in each population of the two adaptation models over time was calculated using the Shannon method. **c**, Degree of parallelism within both conditions estimated by Jaccard index. Asterisks denote significant differences ($***p < 0.001$, Student's unpaired two-tailed t-test). Boxes indicate Q1–Q3, lines indicate the median and dots indicate the J value of each condition. **d**, Detected mutations in endpoint CoEvo and Bac isolates. Black indicates CoEvo-specific mutations, dark grey denotes Bac-specific SNPs and light grey represents common mutations found in both experimental setups. \perp indicates intergenic regions between the two genes depicted. * indicates an introduced stop codon. Amino acid changes are indicated unless synonymous mutations were determined. **e**, Bacterial colony growth between two lines of fungal streaks. Plate size = 9 cm.

Selected evolved isolates respond to fungal volatiles, resulting in reduced spreading. While isolating the CoEvo strains, increased spreading over the agar surface was observed compared with the ancestor strain. Intriguingly, while CoEvo2 isolates displayed increased spreading on 1% agar medium regardless of the presence of the fungus, the CoEvo3 clone was only able to expand on the agar surface in the absence of the fungus, even if separated from the fungus by a plastic barrier allowing only volatile-mediated interaction (Supplementary Fig. 3a). The recreated *degS*^{A193V} strain phenocopied the influence of *A. niger* volatiles on colony expansion (Supplementary Fig. 3b). Therefore, for the CoEvo 3 strain, the volatilomes of single and

separated co-cultures were determined at day 3 and day 7 after bacterial inoculation (see experimental setup in Supplementary Fig. 3c). Volatilomes contained dimethyl disulphide (DMS), pyrazine and 1-pentyne when *A. niger* was present but not when *B. subtilis* was cultured alone (for a full list see Supplementary Dataset 2). Supplementing either the pure compounds or the mixture of these volatile organic compounds (VOCs) reduced colony spreading of CoEvo 3 (Fig. 3a, one-way ANOVA, $F = 27.04$, $p < 0.001$, Tukey's HSD), demonstrating the volatile-mediated influence of *A. niger* on specific evolved isolates of *B. subtilis*. However, since these experiments were performed using a CoEvo 3 isolate, we cannot exclude the influence of these VOCs on the ancestor strain, which did not display enhanced surface spreading. Further experiments are needed to reveal the direct influence of the identified VOCs on the growth, physiology, or differentiation of *B. subtilis*.

Surfactin production is enhanced in evolved bacterial isolates. The lipopeptide surfactin plays an important role in *B. subtilis* expansion over semi-solid surfaces including swarming or sliding^{40–43}, and genes encoding the surfactin biosynthesis apparatus were downregulated during the initial attachment of *B. subtilis* to hyphae of *A. niger* in planktonic cultures²¹. Therefore, we hypothesised that surfactin production might be altered in the evolved strains during adaptation to the presence of the fungus. Direct semi-quantification of surfactin produced by the bacterium grown on agar medium confirmed an increase in surfactin production for several CoEvo isolates compared with the ancestor, especially lineages 2 and 3 (Fig. 3b, Student's t-test with Bonferroni-Holm correction), possibly facilitating the improved expansion of the bacterium. By contrast, surfactin production by Bac strains was not increased (Fig. 3b, Student's t-test with Bonferroni-Holm correction). Matrix-assisted laser desorption/ionisation-mass spectrometry imaging (MALDI-MSI) analysis of co-inoculated

bacteria-fungi samples further demonstrated increased surfactin production by CoEvo 2 compared with the ancestor strain (Fig. 3c). By contrast, production the lipopeptide plipastatin by CoEvo2 was comparable with the ancestor (Supplementary Fig. 3d).

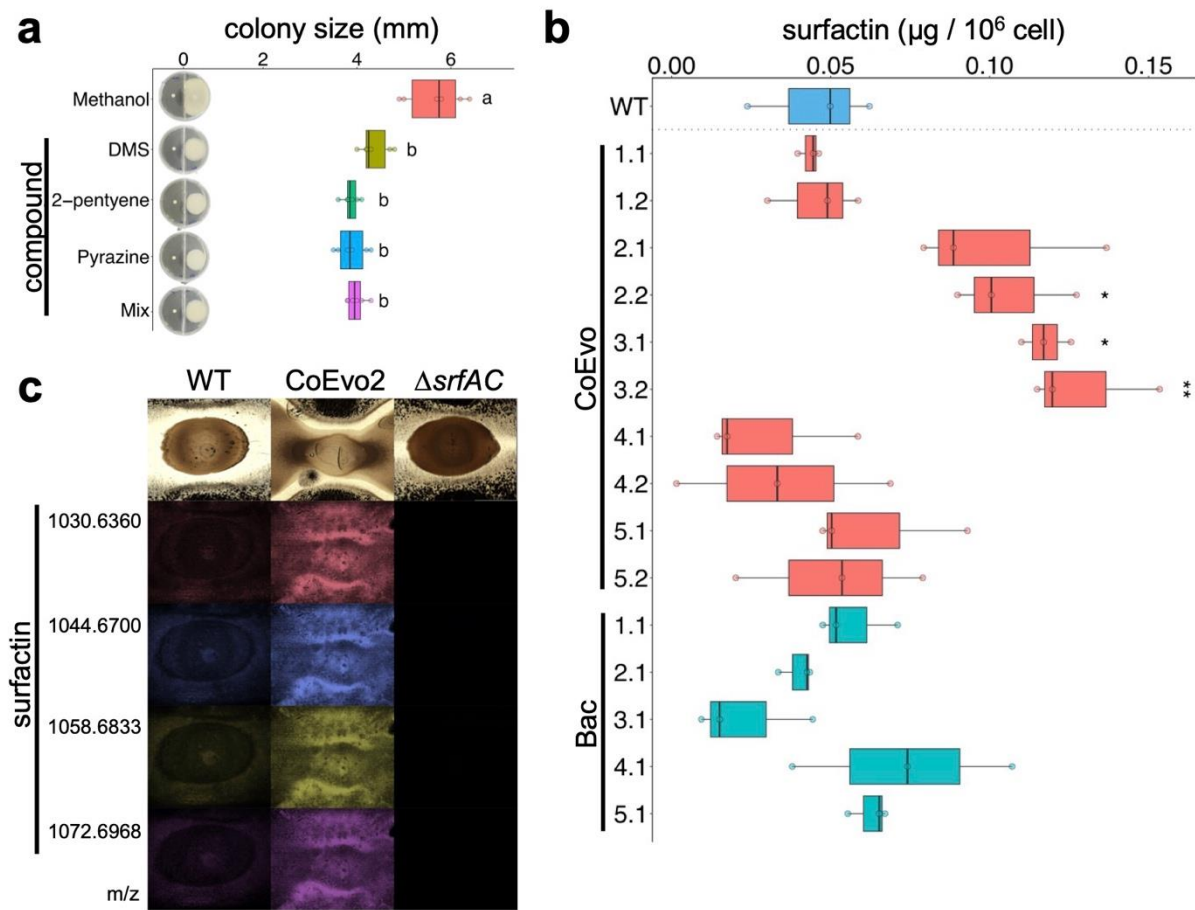


Fig. 3 | The effects of volatile compounds on *B. subtilis* growth, and detection of surfactin in evolved bacterial strains. **a**, Colony spreading of the CoEvo3 isolate recorded in the presence of methanol, dimethyl disulphide (DMS), 1-pentyne, pyrazine, or their mixture. One-way ANOVA was conducted to compare the effects of pure compounds and the mixture on CoEvo3 colony size. The results indicate a statistically significant difference in colony size between methanol treatment and other treatments ($F = 27.04$, $p < 0.001$). Tukey's HSD test was used to determine significant differences between means, which are denoted by letters. **b**, UHPLC-HRMS quantification of the produced surfactin normalised against the number of cells in colonies on agar medium. Student's t-test with Bonferroni-Holm correction was performed

(* $p_{\text{adjust}} < 0.05$, ** $p_{\text{adjust}} < 0.01$). **c**, MALDI-MSI spatial detection of surfactin isoforms in bacterial colonies (wild-type, CoEvo2, and the *surfAC* mutant from left to right) grown between two fungal streak lines. m/z values of surfactin isoforms are indicated on the left. Scale bars = 2 mm.

Surfactin causes hyphal bulging and cell wall stress in *A. niger*. The fungus-adapted bacterial isolate CoEvo2 displayed increased surfactin production and surface colonisation. In addition, acidification of the environment by *A. niger* was slightly reduced in the presence of CoEvo2. Therefore, we hypothesised that increased surfactin production not only stimulated spreading of bacterial colonies, but also influenced the fungus. Intriguingly, when planktonic cultures of *A. niger* were supplemented with bacterial cell-free supernatant from the *B. subtilis* ancestor, some fungal hyphae displayed bulging (Fig. 4a). However, bulbous fungal cells were absent when surfactin was not produced in the bacterial cultures due to deletion of either *surfAC* (encoding a subunit of the surfactin biosynthesis machinery) or *sfp* (encoding a phosphopantetheinyl transferase involved in activation of the peptidyl carrier protein domains of non-ribosomal synthetases; Fig. 4a). Supplementation the fungal culture with pure surfactin was sufficient to induce bulging (Fig. 4a), and bulbous hyphal cells were still present in mutants lacking the ability to synthesise other non-ribosomal proteins (plipastatin and bacillaene) unless surfactin biosynthesis was simultaneously disrupted (Supplementary Fig. 4a).

To investigate the influence of surfactin on fungal hyphae, we tested a series of fluorescent reporter strains for which specific cell components could be monitored. In the presence of bacterial cell-free supernatant the cell wall, mitochondria, and nuclei were comparable to those of untreated samples, while membranous components including

vacuoles, Golgi, and endoplasmic reticulum were aberrant (Supplementary Fig. 4b). In particular, secretory vesicle-specific soluble NSF attachment protein receptor SncA showed a homogenous distribution in bulged cells, and the secretory vesicles were mislocalised (Fig. 4b), unlike in untreated samples where these secretory vesicles are located close to the tips of hyphae to deliver cell wall components and secrete fungal enzymes ⁴⁴.

The surfactin-induced bulging of *A. niger* hyphae resembles the impact of Calcofluor White (CFW), a chitin and cellulose-binding fluorescent dye, on fungal mycelia ⁴⁵. CFW provokes cell wall stress in *A. niger* including upregulation of α -1,3-glucanase synthase encoded by the *agsA* gene ⁴⁵. Indeed, *agsA* transcription was induced in *A. niger* when treated with bacterial cell-free supernatant when monitoring using luciferase (Fig. 4c) or a fluorescence reporter (Supplementary Fig. 4c). Furthermore, induction was dependent on production of surfactin by *B. subtilis*, as it could also be promoted by supplementation of pure surfactin (Supplementary Fig. 4c and e). The cell wall stress-sensing pathway in *A. niger* includes the transcription factor RlmA that directly activates *agsA* transcription (Fig. 4d). Accordingly, deletion of the RlmA-binding box within the promoter region of the *agsA* reporter construct tempered induction by bacterial cell-free supernatant (Fig. 4c). Finally, disruption of *rlmA* amplified the number of bulbous hyphal cells in the presence of bacterial cell-free supernatant or purified surfactin (Fig. 4e). As expected, without surfactin in the cell-free culture supernatant, neither wild-type nor *rlmA* mutant *A. niger* hyphae displayed bulging (Fig. 4e).

These results demonstrate that the mode of action of *B. subtilis*-produced surfactin on *A. niger* involves hyphal bulging and inducing cell wall stress. Plipastatin, another lipopeptide synthesised by *B. subtilis*, did not provoke such changes in hyphal cell morphology (Supplementary Fig. 4a). Inhibition of *Fusarium* (another filamentous fungus) by *B. subtilis* is mediated by plipastatin but unaffected by deletion of surfactin ⁴⁶. Therefore, potential bulging

of *Fusarium* hyphae has been monitored and tested using *B. subtilis* strains lacking either surfactin or plipastatin. In line with the inhibitory activity of plipastatin against *Fusarium*, bulbous cell formation by *Fusarium culmorum* and *Fusarium oxysporum* was dependent on plipastatin in the cell-free supernatant (Supplementary Fig. 5).

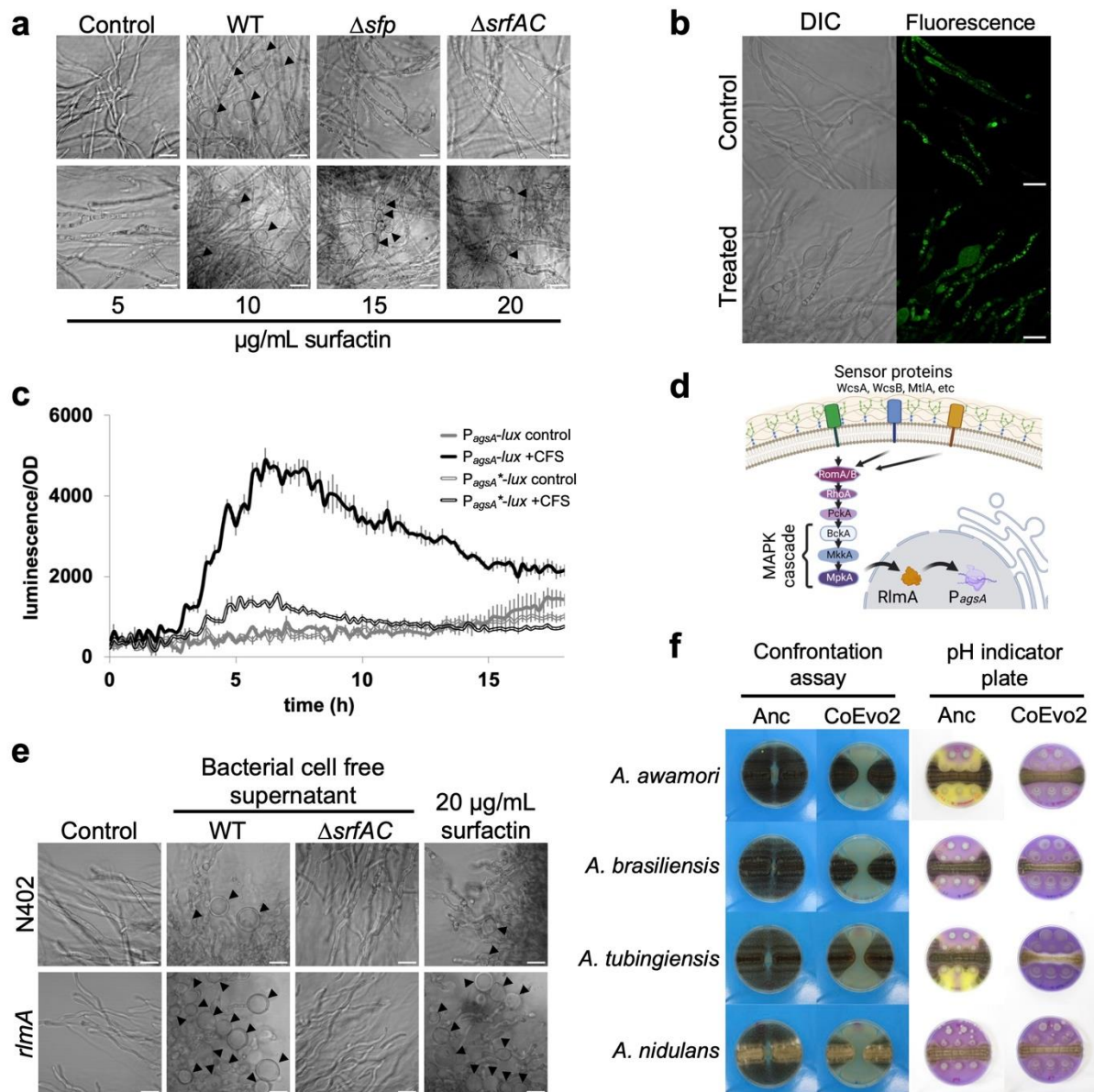


Fig. 4 | Influence of surfactin on fungal hyphae. **a**, Microscopy visualisation of bulging fungal hyphae with cell-free supernatant (CFS) of wild type (WT), *sfp* and surfactin mutants (top panels) or increasing amounts of surfactin (bottom panels). **b**, DIC (left) and green fluorescence (right) imaging of the *A. niger* FG7 strain ($P_{synA-GFP::SynA}$). Scale bar = 20 μm . **c**,

Luminescence reporter assay using *A. niger* strains MA297.3 and MA584.2 containing $P_{agsA(3\times RlmA\ box)}$ and $P_{agsA(RlmA\ box\ mutated)}$ before the promoter-less luciferase (grey and black lines, respectively). Cultures were treated with LB medium (double lines) or cell-free supernatant (CFS, filled lines). **d**, Schematic representation of cell wall stress perception in *A. niger* according to a previous report ⁴⁷. **e**, Influence of the cell-free supernatant from the WT strain and the surfactin mutant ($\Delta srfAC$), and 20 $\mu\text{g/ml}$ surfactin on bulbous hyphae formation in WT and *rlmA* mutant *A. niger* strains (top and bottom panels, respectively). **f**, Impact of the ancestor (Anc) and Coevo2 strains on *Aspergillus* species *A. awamori*, *A. brasiliensis*, *A. tubingiensis*, and *A. nidulans*. The two columns on the left show bacterial growth spotted between two lines of fungal streaks, while the two columns on the right depict the pH of the medium measured using Bromocresol Purple, where bacterial cultures were spotted next to a continuous fungal spore streak. Purple and yellow colours indicate pH >6.8 and pH <5.2, respectively. Plate diameter = 9 cm.

Spreading-mediated inhibition of other *Aspergillus* species. To reveal whether the ability of fungus-adapted *B. subtilis* to decrease *A. niger* growth was transferable to other *Aspergillus* species, the CoEvo 2 isolate was tested on them (Fig. 4f). In addition to *A. niger*, spreading enhanced by the CoEvo 2 strain was able to restrict the expansion of *Aspergillus awamori*, *Aspergillus brasiliensis*, *Aspergillus tubingiensis* and *A. nidulans*. Co-inoculation on medium containing a pH indicator revealed that CoEvo isolates could prevent fungal-mediated acidification of the medium during co-cultivation with several *Aspergillus* species (Fig. 4f), demonstrating a general advantage of increased spreading by *B. subtilis* during competition for space and nutrients on a surface.

Discussion

During prolonged co-cultivation with *A. niger*, selected lineages of *B. subtilis* adapted by increasing their surface spreading ability, which allows the bacterium to cover a larger area, reach more nutrients, and thus successfully compete against the fungus. The evolution of such elevated mobility might have been facilitated by the microhabitat generated by the fungal mycelium network. Zhang and colleagues observed rapid movement of single bacterial cells and subsequently groups of cells along a water film around fungal hyphae⁴⁸. The area surrounding a fungal hypha retains water and has a higher humidity than the wider environment, thereby generating conditions that promote bacterial movement even in a dry milieu^{48,49}. Spreading along a hypha might be advantageous for *B. subtilis* as the environment dehydrated over the 5-day incubation. Lack of a fungal microhabitat in control experiments may create drier conditions. Indeed, *B. subtilis* generally adapted by increasing matrix production in the absence of fungal mycelia. Investment in biofilm formation and smaller colony size might also be related to the dry environment since biofilms can act as water reservoirs^{50,51}.

Here, *B. subtilis* adaptation to the presence of *A. niger* increased competition, since in addition to enhanced spreading, several adapted lineages also produced more surfactin. Secondary metabolites such as lipopeptides are often involved in BFIs. These may act as cues to elicit a specific reaction or interfere directly with another microorganism via chemical warfare^{12,52}. While the higher surfactin level of certain adapted isolates likely increased the spreading behaviour^{41,43}, it also directly contributed to fungal inhibition via its antimicrobial properties^{53,54}. Importantly, we also revealed that the mode of action of surfactin on *A. niger* involves influencing membranous fungal cell components and provoking cell wall stress. By contrast, rapid adaptation of *B. subtilis* in a 15-day co-culture with the fungus *Setophoma*

terrestris was accompanied by reduced surfactin production, increased biofilm development, reduced swarming, and increased emission of anti-fungal volatile compounds⁵⁵. The distinct adaptation route could be potentially explained by differences in fungal partner sensitivity to antimicrobial compounds.

The fate of a BFI from mutualism and co-existence to competition and elimination of their companion is often not only determined by the specific influence of members on each other, but also influenced by their environment. For example, spatiotemporal organisation is crucial for a stable co-culture and the beneficial influence of *B. subtilis* on the fungus *Serendipita indica*⁵⁶. Interactions can also be influenced by environmental parameters including pH⁵⁵. *A. niger* acidifies its environment by citric acid secretion^{22,23}. One potential bacterial strategy to cope with a fungus-constructed niche includes adaptation to growth at low pH, thereby promoting survival in acidic soil, and hence co-occurrence with various fungal species, as reported previously^{57,58}. In our experiment, instead of adapting to a lower pH milieu, the evolved *B. subtilis* isolates possibly prevented medium acidification by *A. niger* rather than actively inhibiting the process. The increased spreading of *B. subtilis* could potentially lower nutrient availability for *A. niger*, surfactin could also inhibit the fungus, and a combination of both mechanisms could contribute to reduced growth and acidification by *A. niger*. This observation is further supported by the comparable influence of the evolved isolate on a set of *Aspergillus* species.

Overall, our study demonstrates the potential of combining co-culture and laboratory evolution experiments to deepen our understanding of BFIs. Such co-culture adaptation methodology could offer a general, genetically modified organism-free approach to enhance antifungal activities of biocontrol bacteria against pathogenic fungi.

Online methods

Media and cultivation conditions

B. subtilis DK1042 (a naturally competent derivative of the undomesticated biofilm-proficient NCIB3610 strain) and its derivatives were generally grown in lysogeny broth (LB; Lenox, Carl Roth, Germany) from a frozen stock for 18–20 h at 37°C with shaking at 220 rpm. To harvest conidia, *Aspergillus* strains were grown on malt extract agar (MEA) plates (Carl Roth, Germany) at 30°C for 1–2 weeks or on Complete Medium agar plates at 28°C for 3 days. After incubation, 10–20 ml of sterile Saline Tween solution (8 g/l NaCl with 0.005% Tween 80) was added, conidia were scraped off, and conidia-containing liquid was collected. The solution was vortexed, sterile filtered with Miracloth rewetted funnels and stored at 4°C. Interactions of *B. subtilis* and *A. niger* on plates were tested using LB medium supplemented with either 1% or 1.5% agar. To follow pH changes, LB agar medium was supplemented with 0.02 g/l Bromocresol Purple. Interactions of *B. subtilis* with different fungi in liquid cultures were tested in LB medium supplemented with 10 mM MgSO₄ and 1 mM MnCl₂ as previously reported²¹. Briefly, fungal spores were inoculated in LB medium and cultivated for 24 h. Subsequently, 1 ml cultures of the five fungal microcolonies were supplemented with 10 mM MgSO₄ and 1 mM MnCl₂ and overnight-grown *B. subtilis* was added at 1000-fold dilution in 24-well plates. Fungal cell morphology was assessed after 24 h of cultivation at 28°C with shaking at 120 rpm.

For luminescence reporter measurement, 7.5×10^4 fungal spores/ml were inoculated in 200 μ l LB medium containing 50 μ l luciferin (final concentration 0.5 mM) before either 50 μ l bacterial cell-free supernatant, CFW (final concentration 50 μ g/ml), LB medium or 1% methanol was added.

Strain construction

B. subtilis cells were transformed with genomic DNA (extracted from 168 *degU*) and selected on LB plates supplemented with kanamycin (10 µg/ml) to obtain the *degU* deletion mutant in the DK1042 background. Natural competence was used to transform *B. subtilis*⁵⁹. To obtain the single nucleotide-exchanged strain, DK1042 was first transformed with plasmids pTB693 and pTB694 (for *degU*^{S202G} and *degS*^{A193V}, respectively) and selected on LB agar plates containing 25 µg/ml lincomycin and 1 µg/ml erythromycin for macrolides (MLS) resistance. The obtained single recombinants were first verified using oligos specific for pMiniMad plasmid (oAR27 or oAR28) and flanking regions of *degU* (oAR25 and oAR26) or *degS* (oAR31 and oAR32) genes. The verified single recombinants were subsequently cultivated in liquid LB medium, cultures were plated on LB medium without antibiotics, single colonies were tested for the loss of integrated plasmid, and clones with specific SNPs (*degU*^{S202G} and *degS*^{A193V}) were selected. Plasmids pTB693 and pTB694 were obtained by cloning the PCR products obtained using oAR23 and oAR24 (*degU*^{S202G} from genomic DNA extracted from CoEvo3) and oAR30 and oAR41 (*degS*^{A193V} from genomic DNA extracted from CoEvo3) into plasmid pMiniMad⁶⁰ using restriction enzymes *Nco*I and *Bam*HI, and *Sal*I and *Bam*HI, respectively. Sequence of oligos are listed in Supplementary Table 1. Incorporation of the ancestor *degU* and *degS* alleles into the evolved variants was verified by sequencing. All other *B. subtilis* strains were constructed previously and the source is indicated in Supplementary Table 1.

The $P_{agsA(3\times RlmA\text{-}box)}\text{-}mluc\text{-}TtrpC$ cassette with *Not*I sites was PCR-amplified using plasmid pBN008 as template and primers PagsAP1f-*Not*I and TtrpCP2r-*Not*I. Plasmid pBN008 contains the $P_{agsA(3\times rlmA\text{-}box)}$ fragment from plasmid $P_{agsA(0.55\text{-}kb\text{-}rlm2add)\text{-}uidA\text{-}pyrG^*}$ ⁴⁵ and *mluc-TtrpC* from plasmid pVG4.1⁶¹. The $P_{agsA(3\times RlmA\text{-}box)}\text{-}mluc\text{-}TtrpC$ cassette with *Not*I sites was

ligated into pJet1.2 and verified by sequencing. The $P_{agsA(3\times RlmA\text{-box})}\text{-}mluc\text{-}TtrpC$ cassette was isolated with *NotI* and ligated into the *NotI*-digested plasmid pMA334⁶², yielding pMA348. The mutation in the RlmA box of the *agsA* promoter to generate the $P_{agsA(RlmA\text{-box mutated})}\text{-}mluc\text{-}TtrpC$ construct was introduced by PCR using primers PagsAP4f-*NotI* and PagsA-AF-R-mut-RlmA2 (211 bp) and primers PagsA-AF-F-mut-RlmA1 and PagsAP2r (441 bp) with genomic DNA from WT *A. niger* strain N402. Both PCR fragments were fused together by PCR with primers PagsAP4f-*NotI* and PagsAP2r (622 bp) and the fusion PCR product, containing a mutation in the RlmA box of the *agsA* promoter, was ligated into pJet1.2 and verified by sequencing. The mutated promoter was then isolated using *NotI* and *EcoRI* and ligated into corresponding sites of pBN008, yielding plasmid pMA368 $P_{agsA(RlmA\text{-box mutated})}\text{-}mluc\text{-}TtrpC$. The $P_{agsA(RlmA\text{-box mutated})}\text{-}mluc\text{-}TtrpC$ cassette with *NotI* sites was PCR-amplified using plasmid pMA368 as template and primers PagsAP1f-*NotI* and *TtrpC*2r-*NotI*, ligated into pJet1.2, and verified by sequencing. The $P_{agsA(RlmA\text{-box mutated})}\text{-}mluc\text{-}TtrpC$ cassette was isolated using *NotI* and ligated into the *NotI*-digested plasmid pMA334⁶², yielding pMA370. Plasmids pMA348 and pMA370 were digested with *Ascl* to release the complete $P_{agsA(3\times RlmA\text{-box})}\text{-}mluc\text{-}TtrpC\text{-}pyrG^{**}$ and $P_{agsA(RlmA\text{-box mutated})}\text{-}mluc\text{-}TtrpC\text{-}pyrG^{**}$ targeting cassettes and transformed into *A. niger* strain MA169.4⁶³ as described previously⁶⁴. Correct integration of the *pyrG*^{**} targeting construct was confirmed by Southern blot for MA297.3 and MA584.2.

Other *A. niger* strains were constructed previously and the source is indicated in Supplementary Table 1. Species identity of *Aspergillus* strains from the Jena Microbial Resource Collection (JMRC) was validated by sequencing their PCR-amplified calmodulin gene fragment⁶⁵ obtained using primers oBK7 and oBK8 (sequencing data included in Supplementary Dataset 3). *Fusarium* strains from the IBT Culture Collection were used as previously described⁴⁶.

Bacterial evolution in the presence of the fungus

For co-cultivation, filtered conidia solution of *A. niger* was streaked on solid 1.5% agar containing LB medium in a hashtag pattern (Fig. 1a) using an inoculation loop. Diluted culture of *B. subtilis* (1:100) was streaked as a square through the inoculation lines of *A. niger* and the plate was incubated for 5 days at 28°C. Small squares of the interaction zone of the bacterium and the fungus were excised and placed on a new LB plate to allow separation of *B. subtilis* by growing out from the old block of the medium over 1 day at 28°C. A sample of the isolated bacteria was collected and incubated overnight in liquid LB medium (shaking at 225 rpm), and the culture was used to incubate a new plate with freshly inoculated *A. niger*, and to create a cryo-stock that was stored at -80°C. Throughout the experiment, dilution of the bacterial culture was increased stepwise to 1:1000 to prevent overgrowth of the fungus by the evolved bacterial strains. As a control, *B. subtilis* was incubated without the fungus and the experiment was performed with five parallel replicates in each group. The experiment was conducted for 10 weeks after which the evolved bacterial populations were clean streaked and two single isolates per replicate were kept for further analysis.

Colony biofilm and surface spreading

To analyse changes in colony biofilm morphology, 2 µl of *B. subtilis* overnight culture was spotted on MSgg medium as previously described⁶⁶. Images of colony biofilms were recorded using an Axio Zoom V16 stereomicroscope (Carl Zeiss, Jena, Germany). A Zeiss CL 9000 LED light source and an AxioCam MRm monochrome camera were employed (Carl Zeiss).

To examine the spreading behaviour of *B. subtilis* in the presence or absence of *A. niger*, two-compartment plates with LB medium and 1% agar were dried for 15 min and 2 µl

of *B. subtilis* overnight culture was spotted in the middle of either one or both compartments. In the case of *A. niger* volatile challenge, fungal spores were inoculated in the other compartment 1 day before inoculation of bacterial cultures. The inoculated plates were dried for 10 min, incubated at 28°C, and expansion of strains was measured after 1 day.

To test the effects of volatile compounds on colony spreading of *B. subtilis*, 5 µl of 500 µM solution of either pyrazine, dimethyl disulphide (DMS), 2-pentyene, or their mixture was spotted on 5 mm filter paper discs placed in one side of the two-compartment plates. Next, 5 µl of an overnight culture of ancestor or CoEvo3 isolate, adjusted to an optical density at 600 nm (OD₆₀₀) of 1.0, was spotted in the second compartment and plates were dried for 10 min, sealed, and incubated for 96 h at 28°C. Every 24 h, 5 µl of each compound or the mixture was added onto the paper disc. The *B. subtilis* colony size was recorded and plates were photographed at the end of the experiment. The experiment was conducted twice with three biological replicates for each independent assay.

Direct bacterium-fungus interaction on plates

Spreading of *B. subtilis* in the presence of the fungus was analysed by pre-culturing two streaks of the *Aspergillus* strain with a gap of 10 mm in between for 1 day at 28°C. Afterwards, *B. subtilis* was spotted in the gap and the plates were incubated as described above.

To check for pH manipulation by *B. subtilis*, *A. niger* or other *Aspergillus* strains (see strain list and collection numbers in Supplementary Table 1), LB plates containing the pH indicator Bromocresol Purple (0.02 g/l) were prepared. The plates were inoculated with a streak of *Aspergillus* conidia in the middle next to 2 µl spots of *B. subtilis* culture and incubated at 28°C for 2 days.

Population metagenome sequencing and variant calling

For whole-population sequencing, frozen stocks of the evolved bacterial populations and ancestor were cultured for 16 h at 37°C and genomic DNA was extracted using a EURx Bacterial and Yeast Genomic DNA Kit. MGIEasy PCR-free Library Prep Set (MGI Tech) was used for creating acoustic fragmentation PCR-free libraries. Paired-end fragment reads (2 × 150 nucleotides) were generated on a DNBSEQ-Tx sequencer (MGI Tech) according to the manufacturer's procedures. Depth coverage >200× was obtained for all population samples before polymorphism calling.

Low-quality reads were filtered from the raw data using SOAPnuke (version 1.5.6)⁶⁷, including reads with >50% of bases with a quality score <12, >10% of unknown bases (N), and adaptor contamination-containing reads. The similar variants calling sensitivity was ensured by normalisation of the clean data to 200× depth for all population samples. Mutations were identified using breseq (version 0.35.7) with default parameters and the -p option for population samples^{29,30}. The default parameters called mutations only if they appeared at least twice on each strand and reached a frequency of at least 5% in the population. The reference genome used for population resequencing analysis was the NCIB 3610 genome and the pBS plasmid (GenBank accession no. NZ_CP020102 and NZ_CP020103, respectively). Mutations that were also detected in ancestor strains and in high polymorphism regions were omitted from the list to create the final table of mutations.

Genome resequencing of single evolved bacterial isolates

Genomic DNA of selected isolated strains was obtained as described above for evolved populations. An Illumina NextSeq sequencer was applied for generation of paired-end fragment reads (2 × 150 nucleotides) and bcl2fastq software (v2.17.1.14; Illumina) was applied

for primary data analysis (base-calling). SOAPnuke (version 1.5.6)⁶⁷ was initially used for removing low-quality reads as described for the population samples. In addition, the first 10 bases of each read were removed. Mutations were called using breseq (version 0.35.7) with default parameters and the -p option^{29,30}. Default parameters called mutations only if they appeared at least twice on each strand and reached a frequency of at least 5% in the sample, and mutations with a frequency <50% were removed. Mutation frequency data for each sequenced strain are included in Supplementary Dataset 1.

Quantification of surfactin production

Bacterial colonies cultivated on LB medium with 1% agar for 2 days were harvested by collecting a plug of agar from the edge of a bacterial colony and subsequently sonicating and diluting for colony-forming counts. PTFE-filtered supernatant was used for semi-quantifying the amount of surfactin. An Agilent Infinity 1290 UHPLC system (Agilent Technologies, Santa Clara, CA, USA) equipped with a diode array detector was used for ultra-high-performance liquid chromatography-high-resolution mass spectrometry (UHPLC-HRMS). An Agilent Poroshell 120 phenyl-hexyl column (2.1 × 250 mm, 2.7 μm) was used for separation using a linear gradient consisting of water (A) and acetonitrile (B) both buffered with 20 mM formic acid, starting at 10% B and increasing to 100% over 15 min, holding for 2 min, returning to 10% B in 0.1 min, and holding for 3 min (0.35 ml/min, 60°C). A 1 μl injection volume was applied. Mass spectra were recorded on an Agilent 6545 QTOF instrument equipped with an Agilent Dual Jet Stream electrospray ion source in positive ion mode as centroid data in the range m/z 85–1700, with an acquisition rate of 10 spectra/s. A drying gas temperature of 250°C, gas flow of 8 l/min, sheath gas temperature of 300°C and flow of 12 l/min were used. The capillary voltage and nozzle voltage were set to 4000 V and 500 V, respectively. Surfactin

A and its isoforms ($C_{53}H_{93}N_7O_{13}$) were semi-quantified using MassHunter quantitative analysis B.07.00 with the $[M + H]^+$ ion (m/z 1036.6904) and an isolation window of 10 ppm. A calibration curve was constructed using an authentic standard (Sigma-Aldrich).

Volatile assay and trapping of VOCs

For analysis and trapping of VOCs, two-compartment glass Petri-dishes⁶⁸ containing 1% LB agar were employed. *A. niger* was inoculated 24 h before addition of the bacterial strain on the left side of the two-compartment glass Petri dish and incubated overnight at 28°C (Extended Figure 3c). After CoEvo 3 was incubated overnight at 28°C in liquid LB medium, 2 μ l of culture was spotted on the opposite compartment of the fungal culture. The glass Petri dishes were kept open for 25 min to allow droplets to dry. Plates were then closed by a lid with an outlet connected to a steel trap containing 150 mg Tenax TA and 150 mg Carbopack B (Markes International Ltd., Llantrisant, UK) and incubated at 28°C. The Tenax steel traps were collected after 3 and 7 days of incubation and stored at 4°C until GC-Q-TOF analysis. Glass Petri dishes containing LB agar medium but without inoculated bacteria or fungi served as controls.

GC-Q-TOF measurement and volatile analysis

The trapped VOCs were analysed as described previously⁶⁹. Briefly, volatiles were desorbed from traps using a Unity TD-100 desorption unit (Markes International Ltd.) at 210°C for 12 min (He flow 50 ml/min) and trapped on a cold trap at -10°C. Volatiles were introduced into the GC-Q-TOF (Agilent 7890B GC and Agilent 7200A QTOF; Agilent Technologies) by heating the cold trap for 12 min to 250°C. The split ratio was 1:10 and the column was a 30 \times 0.25 mm ID RXI-5MS with a film thickness of 0.25 μ m (Restek 13424-6850, Bellefonte, PA, USA). The

temperature program was as follows: 39°C for 2 min, 39°C to 95°C at 3.5°C/min, 95°C to 165°C at 4°C/min, 165°C to 280°C at 15°C/min, 280°C to 320°C at 30°C/min, holding for 7 min. VOCs were ionised in EI mode at eV and mass spectra were acquired in full scan mode (30–400 U @ 5 scans/s). Mass spectra were extracted with MassHunter Qualitative Analysis Software V B.06.00 Build 6.0.633.0 (Agilent Technologies). The obtained mass spectra were transformed to netCDF files and imported into MZmine V2.20 (Copyright 2005–2012) MZmine Development Team) ⁷⁰. Compounds were identified via their mass spectra using the deconvolution function and local minimum search algorithm in combination with two mass spectral libraries, NIST 2014 V2.20 (National Institute of Standards and Technology, USA, <http://www.nist.gov>) and Wiley 7th edition spectral libraries, and by their linear retention index (LRI) calculated using AMDIS 2.72 (National Institute of Standards and Technology, USA). After deconvolution and mass identification, peak lists containing the mass features of each treatment were exported as csv files for further analysis.

MALDI-MSI

Petri dishes (5 cm diameter) were filled with ~4.5 mL of 1% LB and allowed to dry for 10 min. Subsequently, spores of *A. niger* were inoculated with a plastic loop drawing two separated lines and leaving a non-inoculated area at the centre of the plate. After 24 h of incubation at 28°C, 5 µL of *B. subtilis* ancestor, CoEvo2 or Δ *srfAC* were spotted onto the non-inoculated area. The plates were sealed with parafilm and incubated for 96 h. Samples were excised and mounted on an IntelliSlides conductive tin oxide glass slide (Bruker Daltonik GmbH) precoated with 0.25 ml of 2,5-dihydrobenzoic acid (DHB) by an HTX Imaging TM-Sprayer (HTX Technologies, USA). Slide images were subsequently taken using TissueScout (Bruker Daltonik GmbH) and a Braun FS120 scanner, followed by overnight drying in a desiccator. Subsequently,

samples were overlaid by spraying 1.75 ml of DHB (20 mg/ml in ACN/MeOH/H₂O (70:25:5, v/v/v)) in a nitrogen atmosphere and dried overnight in a desiccator prior to MSI measurement. Samples were analysed using a timsTOF flex mass spectrometer (Bruker Daltonik GmbH) for MALDI MSI acquisition in positive MS scan mode with 100 µm raster width and a mass range of 100–2000 Da. Calibration was performed using red phosphorus. The following settings were used in timsControl. Laser imaging 100 µm, Power Boost 3.0%, scan range 26 µm in the XY interval, laser power 90%; Tune Funnel 1 RF 300 Vpp, Funnel 2 RF 300 Vpp, Multipole RF 300 Vpp, isCID 0 eV, Deflection Delta 70 V, MALDI plate offset 100 V, quadrupole ion energy 5 eV, quadrupole loss mass 100 m/z, collision energy 10 eV, focus pre-TOF transfer time 75 µs, pre-pulse storage 8 µs. After data acquisition, SCiLS software was used for data analysis and all data were root mean square normalised.

Statistical analyses

Statistical analysis of volatile metabolite data was performed using MetaboAnalyst V3.0 (www.metaboanalyst.ca)⁷¹. Prior to statistical analysis, data normalisation was performed via log-transformation and data were mean-centred and divided by the standard deviation of each variable. To identify significant mass features, one-way analysis of variance (ANOVA) with post-hoc TUKEY test (HSD-test) and PLSD analysis were performed between datasets. Mass features were considered statistically significant at $p \leq 0.05$.

One-way ANOVA was conducted to compare the effect of pure compounds and the mixture on the colony size of CoEvo3. Tukey's HSD test was used to determine significant differences between means, which are denoted by letters.

To evaluate differences in surfactin production between strains and to explore the influence of *rImA* mutation in *A. niger*, Student's t-test with Bonferroni-Holm correction was performed. Student's unpaired two-tailed t-test was used for the Jaccard index.

Data availability

Population sequencing data have been deposited in the CNGB Sequence Archive (CNSA)⁷² of the China National GeneBank DataBase (CNGBdb)⁷³ under accession numbers CNP0002416 and CNP0003923. Data for the DK1042 ancestor strain are available under CNP0002416. Isolate sequencing data have been deposited at the NCBI Sequence Read Archive (SRA) database under BioProject accession numbers PRJNA625867 (ancestor) and PRJNA926387 (evolved clones). VOC data available on Metabolomics Workbench as project PR001621 (<http://dx.doi.org/10.21228/M85M6X>).

Data points are all included in Supplementary Datasets. All other data generated and analysed during this study are either available in Supplementary Dataset 4 or can be requested from the corresponding author.

References

1. Frey-Klett, P. *et al.* Bacterial-fungal interactions: hyphens between agricultural, clinical, environmental, and food microbiologists. *Microbiology and Molecular Biology Reviews* **75**, 583–609 (2011).
2. Deveau, A. *et al.* Bacterial-fungal interactions: Ecology, mechanisms and challenges. *FEMS Microbiol Rev* **42**, 335–352 (2018).
3. Lowery, C. A., Dickerson, T. J. & Janda, K. D. Interspecies and interkingdom communication mediated by bacterial quorum sensing. *Chem Soc Rev* **37**, 1337–1346 (2008).
4. Effmert, U., Kalderás, J., Warnke, R. & Piechulla, B. Volatile mediated interactions between bacteria and fungi in the soil. *J Chem Ecol* **38**, 665–703 (2012).
5. Sadiq, F. A. *et al.* Trans-kingdom interactions in mixed biofilm communities. *FEMS Microbiol Rev* **46**, fuac024 (2022).
6. de Weert, S., Kuiper, I., Lagendijk, E. L., Lamers, G. E. M. & Lugtenberg, B. J. J. Role of chemotaxis toward fusaric acid in colonization of hyphae of *Fusarium oxysporum* f. sp. *radicis-lycopersici* by *Pseudomonas fluorescens* WCS365. *Molecular Plant-Microbe Interactions* **17**, 1185–1191 (2004).
7. Bolwerk, A. *et al.* Interactions in the tomato rhizosphere of two *Pseudomonas* biocontrol strains with the phytopathogenic fungus *Fusarium oxysporum* f. sp. *radicis-lycopersici*. *Molecular Plant-Microbe Interactions* **16**, 983–993 (2003).
8. Zhang, M., Pereira e Silva, M. de C., Chaib De Mares, M. & van Elsas, J. D. The mycosphere constitutes an arena for horizontal gene transfer with strong evolutionary implications for bacterial-fungal interactions. *FEMS Microbiol Ecol* **89**, 516–526 (2014).
9. Mueller, U. G., Schultz, T. R., Currie, C. R., Adams, R. M. M. & Malloch, D. The origin of the attine ant-fungus mutualism. *Quarterly Review of Biology* **76**, 169–197 (2001).
10. Haeder, S., Wirth, R., Herz, H. & Spiteller, D. Candicidin-producing *Streptomyces* support leaf-cutting ants to protect their fungus garden against the pathogenic fungus *Escovopsis*. *Proc Natl Acad Sci U S A* **106**, 4742–4746 (2009).
11. Oh, D. C., Poulsen, M., Currie, C. R. & Clardy, J. Dentigerumycin: A bacterial mediator of an ant-fungus symbiosis. *Nat Chem Biol* **5**, 391–393 (2009).
12. Netzker, T. *et al.* Microbial interactions trigger the production of antibiotics. *Curr Opin Microbiol* **45**, 117–123 (2018).
13. Schroeckh, V. *et al.* Intimate bacterial-fungal interaction triggers biosynthesis of archetypal polyketides in *Aspergillus nidulans*. *Proceedings of the National Academy of Sciences* **106**, 14558–14563 (2009).
14. Nutzmann, H.-W. *et al.* Bacteria-induced natural product formation in the fungus *Aspergillus nidulans* requires Saga/Ada-mediated histone acetylation. *Proceedings of the National Academy of Sciences* **108**, 14282–14287 (2011).
15. Kohlmeier, S. *et al.* Taking the fungal highway: Mobilization of pollutant-degrading bacteria by fungi. *Environ Sci Technol* **39**, 4640–4646 (2005).

16. Simon, A., Hervé, V., Al-Dourobi, A., Verrecchia, E. & Junier, P. An *in situ* inventory of fungi and their associated migrating bacteria in forest soils using fungal highway columns. *FEMS Microbiol Ecol* **93**, 1–9 (2017).
17. van Overbeek, L. S. & Saikkonen, K. Impact of bacterial-fungal interactions on the colonization of the endosphere. *Trends Plant Sci* **21**, 230–242 (2016).
18. Kjeldgaard, B. *et al.* Fungal hyphae colonization by *Bacillus subtilis* relies on biofilm matrix components. *Biofilm* **1**, 100007 (2019).
19. Balbontín, R., Vlamakis, H. & Kolter, R. Mutualistic interaction between *Salmonella enterica* and *Aspergillus niger* and its effects on *Zea mays* colonization. *Microb Biotechnol* **7**, 589–600 (2014).
20. Brandl, M. T. *et al.* *Salmonella* biofilm formation on *Aspergillus niger* involves cellulose - chitin interactions. *PLoS One* **6**, e25553 (2011).
21. Benoit, I. *et al.* *Bacillus subtilis* attachment to *Aspergillus niger* hyphae results in mutually altered metabolism. *Environ Microbiol* **17**, 2099–2113 (2015).
22. Magnuson, J. K. & Lasure, L. L. Organic acid production by filamentous fungi. in *Advances in Fungal Biotechnology for Industry, Agriculture, and Medicine* 307–340 (2004). doi:10.1007/978-1-4419-8859-1_12.
23. Liaud, N. *et al.* Exploring fungal biodiversity: organic acid production by 66 strains of filamentous fungi. *Fungal Biol Biotechnol* **1**, 1 (2014).
24. Karaffa, L. & Kubicek, C. P. *Aspergillus niger* citric acid accumulation: Do we understand this well working black box? *Applied Microbiology and Biotechnology* vol. 61 189–196 Preprint at <https://doi.org/10.1007/s00253-002-1201-7> (2003).
25. Dragoš, A. *et al.* Evolution of exploitative interactions during diversification in *Bacillus subtilis* biofilms. *FEMS Microbiol Ecol* **94**, fix155 (2018).
26. Richter, A. *et al.* Hampered motility promotes the evolution of wrinkly phenotype in *Bacillus subtilis*. *BMC Evol Biol* **18**, 155 (2018).
27. Nordgaard, M. *et al.* Experimental evolution of *Bacillus subtilis* on *Arabidopsis thaliana* roots reveals fast adaptation and improved root colonization. *iScience* **25**, 104406 (2022).
28. Blake, C., Nordgaard, M., Maróti, G. & Kovács, Á. T. Diversification of *Bacillus subtilis* during experimental evolution on *Arabidopsis thaliana* and the complementarity in root colonization of evolved subpopulations. *Environ Microbiol* **23**, 6122–6136 (2021).
29. Barrick, J. E. *et al.* Identifying structural variation in haploid microbial genomes from short-read resequencing data using breseq. *BMC Genomics* **15**, 1039 (2014).
30. Deatherage, D. E. & Barrick, J. E. Identification of mutations in laboratory-evolved microbes from next-generation sequencing data using breseq. *Methods in Molecular Biology* **1151**, 165–188 (2014).
31. Hu, G. *et al.* Species and condition dependent mutational spectrum in experimentally evolved biofilms of *Bacilli*. *bioRxiv* <https://doi.org/10.1101/2022.12.07.519423> (2022).

32. Harris, K. B., Flynn, K. M. & Cooper, V. S. Polygenic adaptation and clonal interference enable sustained diversity in experimental *Pseudomonas aeruginosa* populations. *Mol Biol Evol* **38**, 5359–5375 (2021).
33. Scribner, M. R. *et al.* Parallel evolution of tobramycin resistance across species and environments. *mBio* **11**, e00932-20 (2020).
34. Bailey, S. F., Rodrigue, N. & Kassen, R. The effect of selection environment on the probability of parallel evolution. *Mol Biol Evol* **32**, 1436–1448 (2015).
35. Kampf, J. *et al.* Selective pressure for biofilm formation in *Bacillus subtilis*: Differential effect of mutations in the master regulator *sinR* on bistability. *mBio* **9**, e01464-18 (2018).
36. Leiman, S. A., Arboleda, L. C., Spina, J. S. & McLoon, A. L. SinR is a mutational target for fine-tuning biofilm formation in laboratory-evolved strains of *Bacillus subtilis*. *BMC Microbiol* **14**, 301 (2014).
37. Msadek, T. *et al.* Signal transduction pathway controlling synthesis of a class of degradative enzymes in *Bacillus subtilis*: Expression of the regulatory genes and analysis of mutations in *degS* and *degU*. *J Bacteriol* **172**, 824–834 (1990).
38. Barreto, H. C., Cordeiro, T. N., Henriques, A. O. & Gordo, I. Rampant loss of social traits during domestication of a *Bacillus subtilis* natural isolate. *Sci Rep* **10**, 18886 (2020).
39. Dahl, M. K., Msadek, T., Kunst, F. & Rapoport, G. The phosphorylation state of the DegU response regulator acts as a molecular switch allowing either degradative enzyme synthesis or expression of genetic competence in *Bacillus subtilis*. *Journal of Biological Chemistry* **267**, 14509–14514 (1992).
40. Grau, R. R. *et al.* A duo of potassium-responsive histidine kinases govern the multicellular destiny of *Bacillus subtilis*. *mBio* **6**, e00581-15 (2015).
41. Hölscher, T. & Kovács, Á. T. Sliding on the surface: bacterial spreading without an active motor. *Environ Microbiol* **19**, 2537–2545 (2017).
42. Jautzus, T., van Gestel, J. & Kovács, Á. T. Complex extracellular biology drives surface competition during colony expansion in *Bacillus subtilis*. *ISME J* **16**, 2320–2328 (2022).
43. Kearns, D. A field guide to bacterial swarming motility. *Nat Rev Microbiol* **8**, 634–644 (2010).
44. Kwon, M. J. *et al.* Molecular genetic analysis of vesicular transport in *Aspergillus niger* reveals partial conservation of the molecular mechanism of exocytosis in fungi. *Microbiology (N Y)* **160**, 316–329 (2014).
45. Damveld, R. A. *et al.* The *Aspergillus niger* MADS-box transcription factor RImA is required for cell wall reinforcement in response to cell wall stress. *Mol Microbiol* **58**, 305–319 (2005).
46. Kiesewalter, H. T. *et al.* Genomic and chemical diversity of *Bacillus subtilis* secondary metabolites against plant pathogenic fungi. *mSystems* **6**, e00770-20 (2021).
47. Yoshimi, A., Miyazawa, K. & Abe, K. Cell wall structure and biogenesis in *Aspergillus* species. *Bioscience, Biotechnology and Biochemistry* vol. 80 1–12 Preprint at <https://doi.org/10.1080/09168451.2016.1177446> (2016).

48. Zhang, Y., Kastman, E. K., Guasto, J. S. & Wolfe, B. E. Fungal networks shape dynamics of bacterial dispersal and community assembly in cheese rind microbiomes. *Nat Commun* **9**, 336 (2018).
49. Furuno, S. *et al.* Fungal mycelia allow chemotactic dispersal of polycyclic aromatic hydrocarbon-degrading bacteria in water-unsaturated systems. *Environ Microbiol* **12**, 1391–1398 (2010).
50. Seminara, A. *et al.* Osmotic spreading of *Bacillus subtilis* biofilms driven by an extracellular matrix. *Proc Natl Acad Sci U S A* **109**, 1116–1121 (2012).
51. Flemming, H. C. & Wuertz, S. Bacteria and archaea on Earth and their abundance in biofilms. *Nat Rev Microbiol* **17**, 247–260 (2019).
52. Kovács, Á. T. A fungal scent from the cheese. *Environ Microbiol* **22**, 4524–4526 (2020).
53. Heerklotz, H. & Seelig, J. Leakage and lysis of lipid membranes induced by the lipopeptide surfactin. *European Biophysics Journal* **36**, 305–314 (2007).
54. Carrillo, C., Teruel, J. A., Aranda, F. J. & Ortiz, A. Molecular mechanism of membrane permeabilization by the peptide antibiotic surfactin. *Biochim Biophys Acta Biomembr* **1611**, 91–97 (2003).
55. Albarracín Orio, A. G. *et al.* Fungal–bacterial interaction selects for quorum sensing mutants with increased production of natural antifungal compounds. *Commun Biol* **3**, 670 (2020).
56. Jiang, X. *et al.* Impact of spatial organization on a novel auxotrophic interaction among soil microbes. *ISME Journal* **12**, 1443–1456 (2018).
57. Stopnisek, N. *et al.* Molecular mechanisms underlying the close association between soil *Burkholderia* and fungi. *ISME Journal* **10**, 253–264 (2016).
58. Stopnisek, N. *et al.* Genus-wide acid tolerance accounts for the biogeographical distribution of soil *Burkholderia* populations. *Environ Microbiol* **16**, 1503–1512 (2014).
59. Anagnostopoulos, C. & Spizizen, J. Requirements for transformation in *Bacillus subtilis*. *J Bacteriol* **81**, 741–746 (1961).
60. Patrick, J. E. & Kearns, D. B. MinJ (YvjD) is a topological determinant of cell division in *Bacillus subtilis*. *Mol Microbiol* **70**, 1166–1179 (2008).
61. Meyer, V. *et al.* Fungal gene expression on demand: An inducible, tunable, and metabolism-independent expression system for *Aspergillus niger*. *Appl Environ Microbiol* **77**, 2975–2983 (2011).
62. Arentshorst, M., Legendijk, E. L. & Ram, A. F. A new vector for efficient gene targeting to the *pyrG* locus in *Aspergillus niger*. *Fungal Biol Biotechnol* **2**, 2 (2015).
63. Carvalho, N. D. S. P., Arentshorst, M., Jin Kwon, M., Meyer, V. & Ram, A. F. J. Expanding the ku70 toolbox for filamentous fungi: establishment of complementation vectors and recipient strains for advanced gene analyses. *Appl Microbiol Biotechnol* **87**, 1463–1473 (2010).
64. Arentshorst, M., Ram, A. F. J. & Meyer, V. Using non-homologous end-joining-deficient strains for functional gene analyses in filamentous fungi. *Methods in Molecular Biology* **835**, 133–150 (2012).

65. Samson, R. A. *et al.* Phylogeny, identification and nomenclature of the genus *Aspergillus*. *Stud Mycol* **78**, 141–173 (2014).
66. Gallegos-Monterrosa, R., Mhatre, E. & Kovács, Á. T. Specific *Bacillus subtilis* 168 variants form biofilms on nutrient-rich medium. *Microbiology (N Y)* **162**, 1922–1932 (2016).
67. Chen, Y. *et al.* SOAPnuke: A MapReduce acceleration-supported software for integrated quality control and preprocessing of high-throughput sequencing data. *Gigascience* **7**, gix120 (2018).
68. Garbeva, P., Hordijk, C., Gerards, S. & de Boer, W. Volatiles produced by the mycophagous soil bacterium *Collimonas*. *FEMS Microbiol Ecol* **87**, 639–649 (2014).
69. Tyc, O., Zweers, H., de Boer, W. & Garbeva, P. Volatiles in inter-specific bacterial interactions. *Front Microbiol* **6**, 1412 (2015).
70. Pluskal, T., Castillo, S., Villar-Briones, A. & Orešič, M. MZmine 2: Modular framework for processing, visualizing, and analyzing mass spectrometry-based molecular profile data. *BMC Bioinformatics* **11**, 395 (2010).
71. Xia, J., Sinelnikov, I. v., Han, B. & Wishart, D. S. MetaboAnalyst 3.0-making metabolomics more meaningful. *Nucleic Acids Res* **43**, W251-257 (2015).
72. Guo, X. *et al.* CNSA: A data repository for archiving omics data. *Database* **2020**, baaa055 (2020).
73. Chen, F. Z. *et al.* CNGBdb: China National GeneBank DataBase. *Hereditas* **42**, 799–809 (2020).

Acknowledgements

This work was supported by the Danish National Research Foundation (DNRF137) for the Center for Microbial Secondary Metabolites. Funding was provided by the Novo Nordisk Foundation for infrastructure “Imaging Microbial Language in Biocontrol (IMLiB)” (NNF19OC0055625). GH was supported by the China National GeneBank (CNGB). The authors thank Aaron J.C. Andersen and the DTU Bioengineering Metabolomics Core for support with LC-MS and MALDI-MSI.

Authors contributions

Á.T.K. conceived the project. A.R., F.B., J.W.S., B.K.S., S.B. and Á.T.K. performed the experiments. H.H and Y.W. performed bacterial population metagenomics experiments and corresponding data analysis. G.M. performed genome resequencing of the evolved bacterial clones. S.A.J. and M.W performed MALDI-MSI. O.T. and P.G. performed VOC identification. C.N.L.A. performed microbiology tests on VOCs. C.B.W.P. performed LC-MS on lipopeptides. T.O.L. contributed methods and instrumentation for lipopeptide analysis. M.A., A.F.J.R. and C.A.M.v.d.H. created fungal strains. T.J. and Á.T.K. wrote the manuscript with corrections from all authors.

Competing interests

The authors declare no competing interests.

Correspondence and requests for materials should be addressed to Á.T.K.

Datasets are available on bioRxiv:

<https://www.biorxiv.org/content/10.1101/2023.03.27.534400v1>

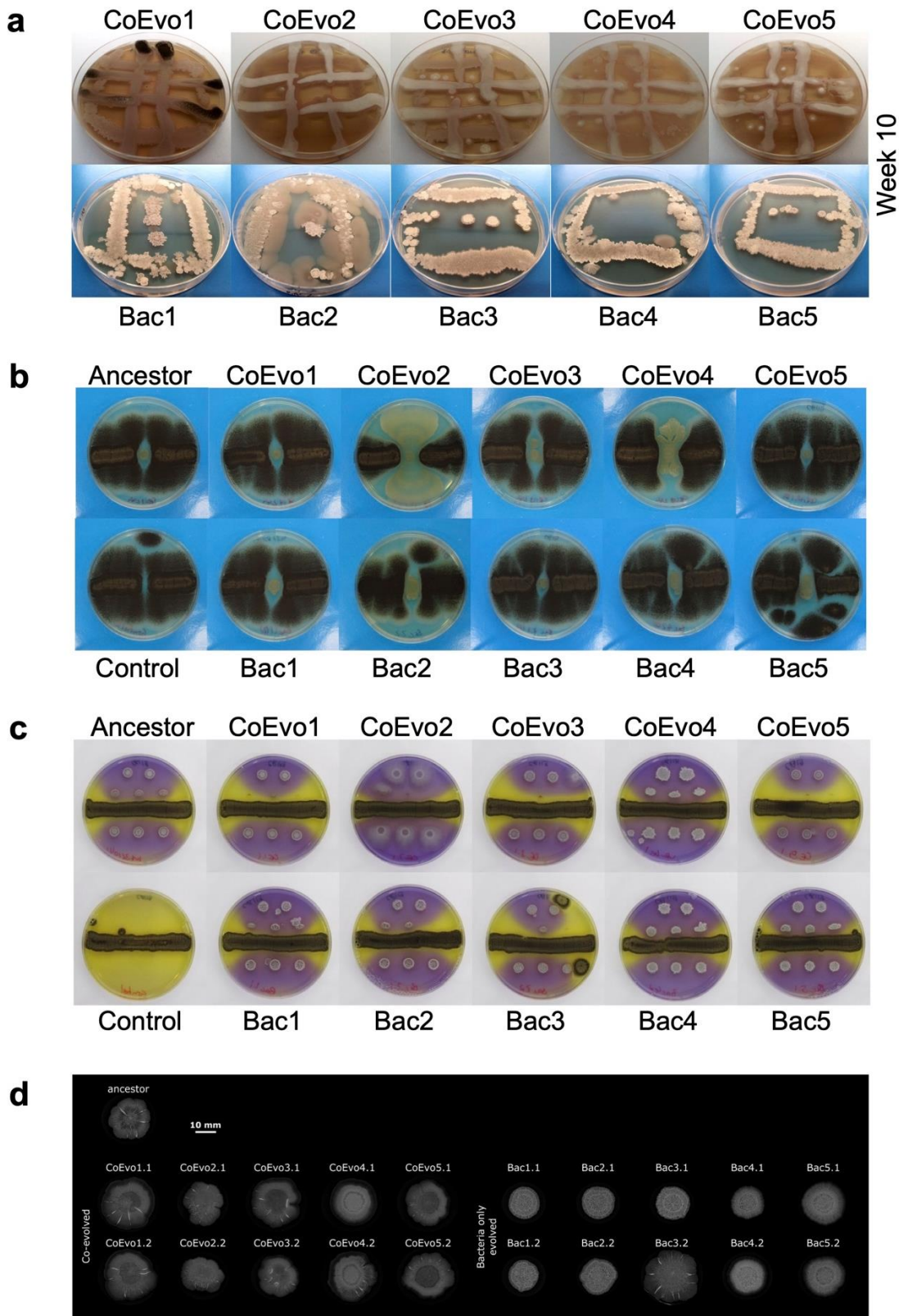


Fig. S1 | *B. subtilis* adaptation to the presence of *A. niger*. **a**, Experimental evolution plates at the 10th transfer, top panels showing *B. subtilis* evolved in the presence of *A. niger*, and lower panels showing bacteria only cultivations. **b**, Bacterial growth spotted between two lines of fungal streaks. **c**, Lower panels showing the pH of the medium using Bromocresol Purple, where bacterial cultures were spotted next to a continuous fungal spore streak. Purple and yellow colours indicate pH >6.8 and pH <5.2, respectively. In **b** and **c**, the plate size = 9 cm, CoEvo refers to co-culture evolved isolates, Bac denotes bacteria only evolved isolated. **d**, Biofilm colonies of evolved isolates on MSgg agar medium. Scale bar = 10 mm.

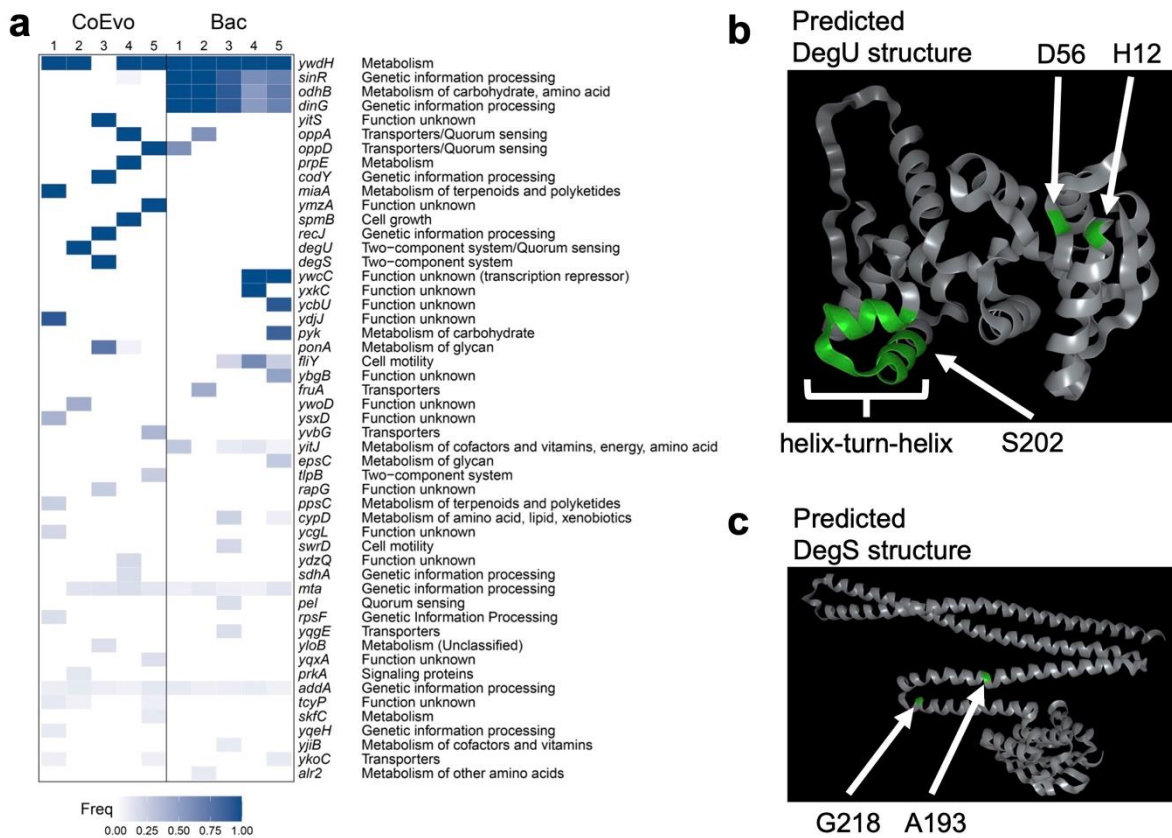


Fig. S2 | Genetic characterisation of *B. subtilis* adaptation to *A. niger*. **a**, Detected mutations in CoEvo and Bac populations. **b**, Predicted DegU structure based on AlphaFold (<https://alphafold.ebi.ac.uk/entry/P13800>). H12 and D56 amino acids are highlighted that were previously described to be involved in phosphorylation state of DegU. SNP in CoEvo2, S202 is also highlighted. **c**, Predicted DegS structure based on AlphaFold (<https://alphafold.ebi.ac.uk/entry/P13799>). G218 amino acid is highlighted that were previously described to be involved in phosphor-activity of DegS. SNP in CoEvo3, A193 is also highlighted.

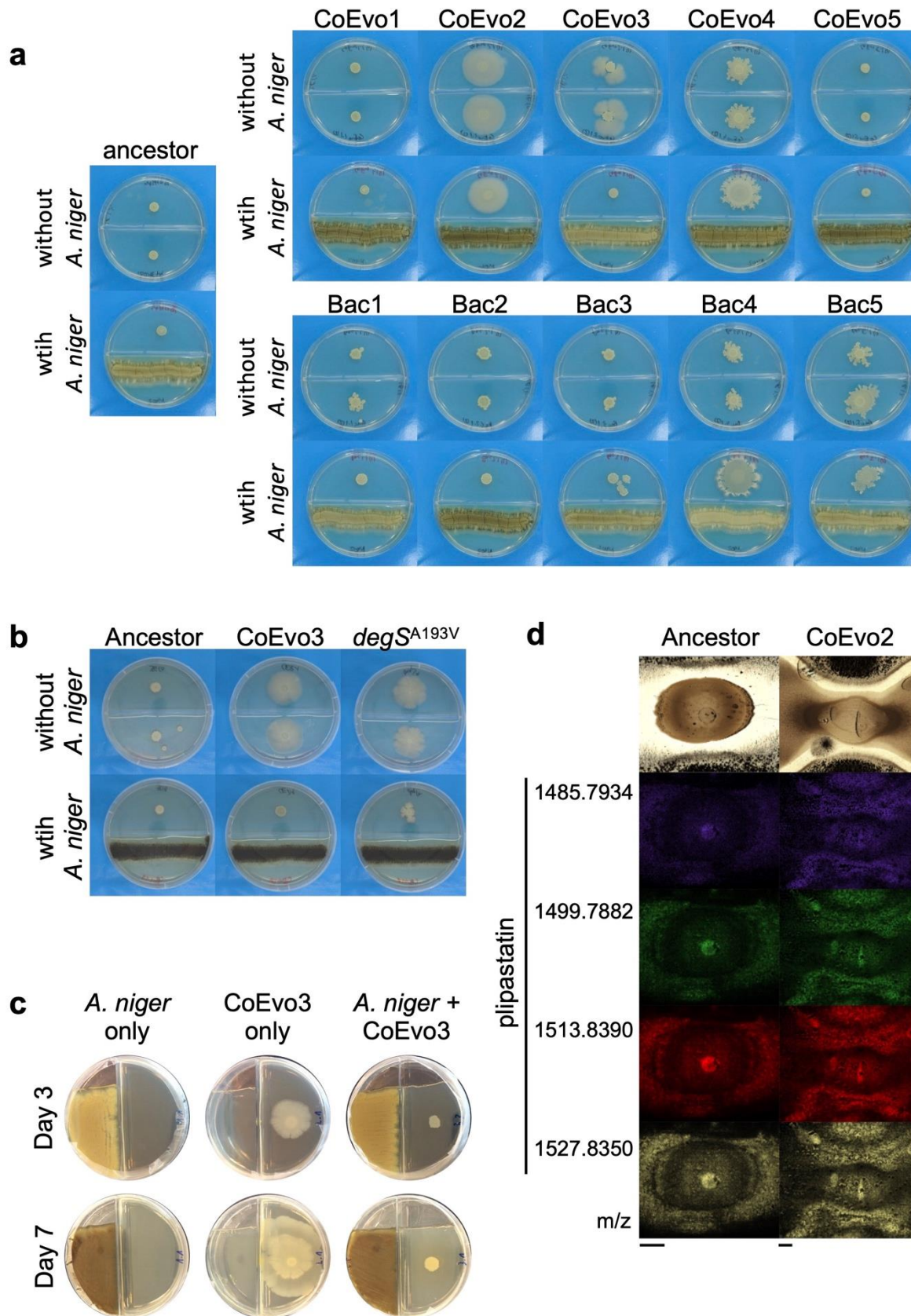


Fig. S3 | The effects of volatile compounds on *B. subtilis* growth, and spatial detection of plipastatin in CoEvo2. a, Colony spreading of the ancestor and evolved isolates in the absence (top panels) and presence of *A. niger* (lower panels). **b**, Colony spreading of the ancestor, CoEvo3 and *degS*^{A193V} mutant in the absence (top panels) and presence of *A. niger* (lower panels). **c**, Experimental setup used to trap VOCs at day 3 and 7. The empty space in the agar medium was used to place the steel traps containing 150 mg Tenax TA and 150 mg Carbopack B. **d**, MALDI-MSI spatial detection of plipastatin isoforms in bacterial colonies (wild-type and CoEvo2) grown between two fungal streak lines. m/z values of surfactin isoforms are indicated on the

left. Scale bars = 2 mm.

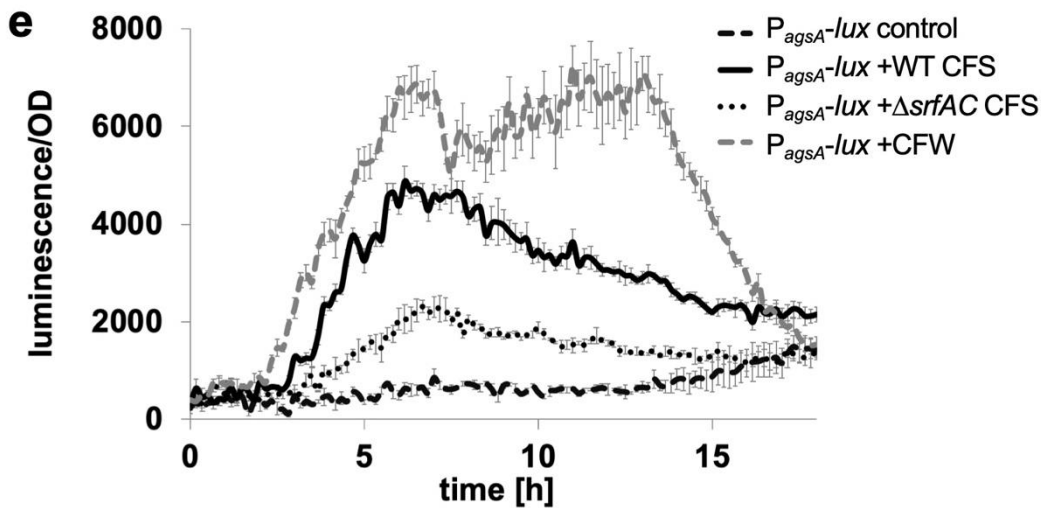
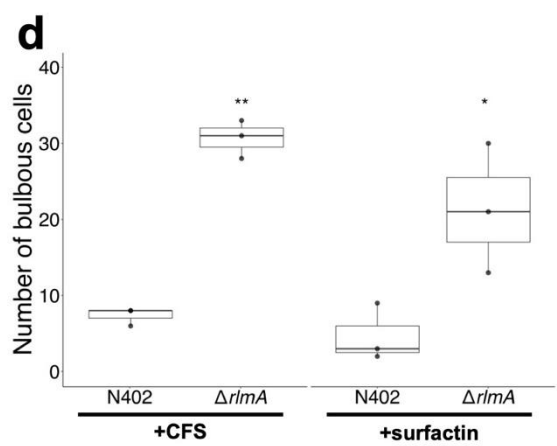
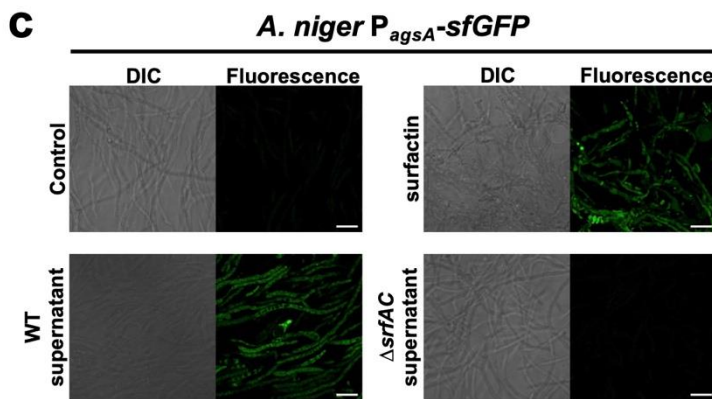
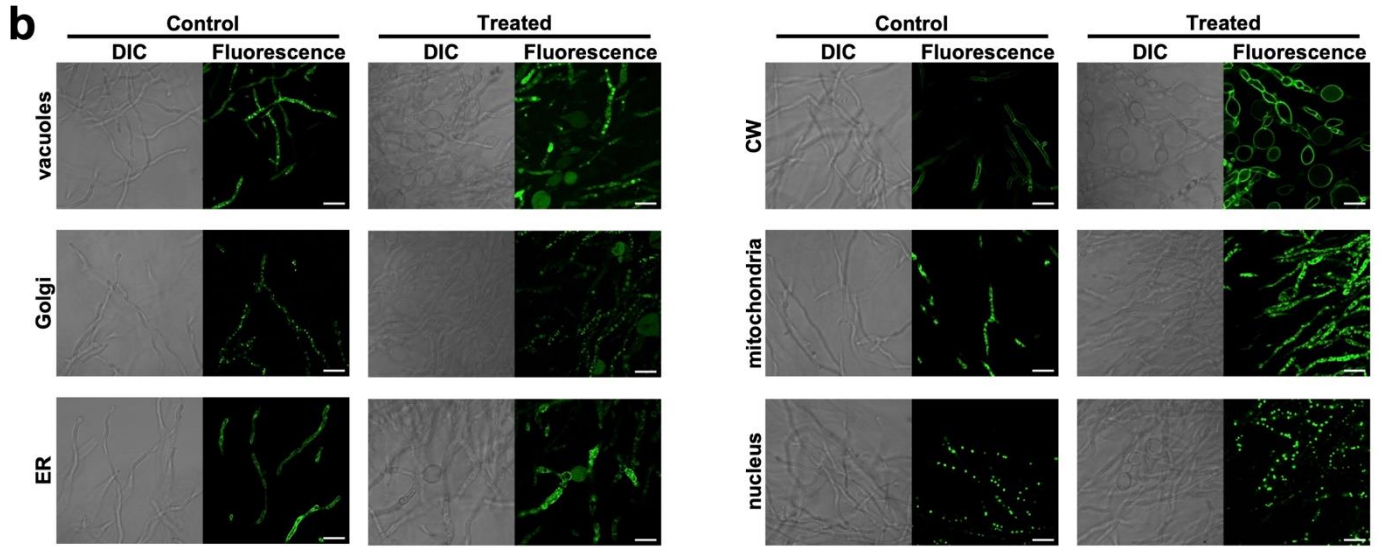
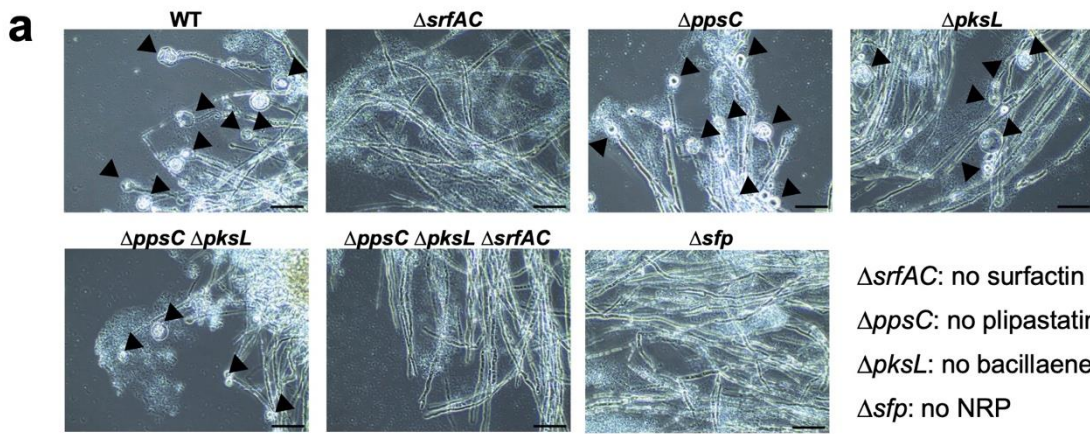


Fig. S4 | Influence of surfactin on fungal hyphae. **a**, Microscopy visualisation of bulging fungal hyphae with wild type (WT) and various mutants, including strain lacking surfactin ($\Delta srfAC$), plipastatin ($\Delta ppsC$), bacillaene ($\Delta pksL$), plipastatin and bacillaene ($\Delta ppsC \Delta pksL$), plipastatin, bacillaene, and surfactin ($\Delta ppsC \Delta pksL \Delta srfAC$), or all non-ribosomal peptides (Δsfp). Scale bar = 20 μ m. **b**, DIC (left) and green fluorescence (right) imaging of the *A. niger* MA23.1.1 strain for vacuoles (P_{gpdA} -CpyA::eGFP-TtrpC); Ren1.10 strain for Golgi (P_{gmtA} -eYFP::GMTA-TgmtA), MA141.1 strain for endoplasmic reticulum, ER (P_{gpdA} -glaA::sGFP-HDEL-TtrpC); ARO#11 strain for cell wall, CW (P_{gpdA} -glaA::sGFP-TtrpC); BN38.9 strain for mitochondria (P_{gpdA} -CitA::eGFP-TtrpC); and MA26.1 strain for nucleus (P_{gpdA} -H2B::eGFP-TtrpC) in the absence (Control) or presence (Treated) of bacterial cell free supernatant. Scale bar = 20 μ m. **c**, DIC (left) and green fluorescence (right) imaging of the *A. niger* JvD1.1 strain carrying P_{agsA} -eGFP-TtrpC for detection of *agsA* gene expression in the absence (control) and presence of cell-free WT supernatant, 20 μ g/ml surfactin, and cell-free $\Delta srfAC$ supernatant. Scale bar = 20 μ m. **d**, Number of bulbous cells by the wild-type N402 and $\Delta rlmA$ mutant *A. niger* in the presence of cell-free WT supernatant (CFS) or 20 μ g/ml surfactin. Student's t-test with Bonferroni-Holm correction was performed (* $p_{adjust} < 0.05$, ** $p_{adjust} < 0.01$). **e**, Luminescence reporter assay using *A. niger* strains MA297.3 containing $P_{agsA(3 \times RlmA \text{ box})}$ before the promoter-less luciferase. Cultures were treated with LB medium (black dashed line), cell-free WT supernatant (CFS, solid line), cell-free $\Delta srfAC$ supernatant ($\Delta srfAC$ CSF, dotted line), or Calcofluor White (CFW, grey dashed line).

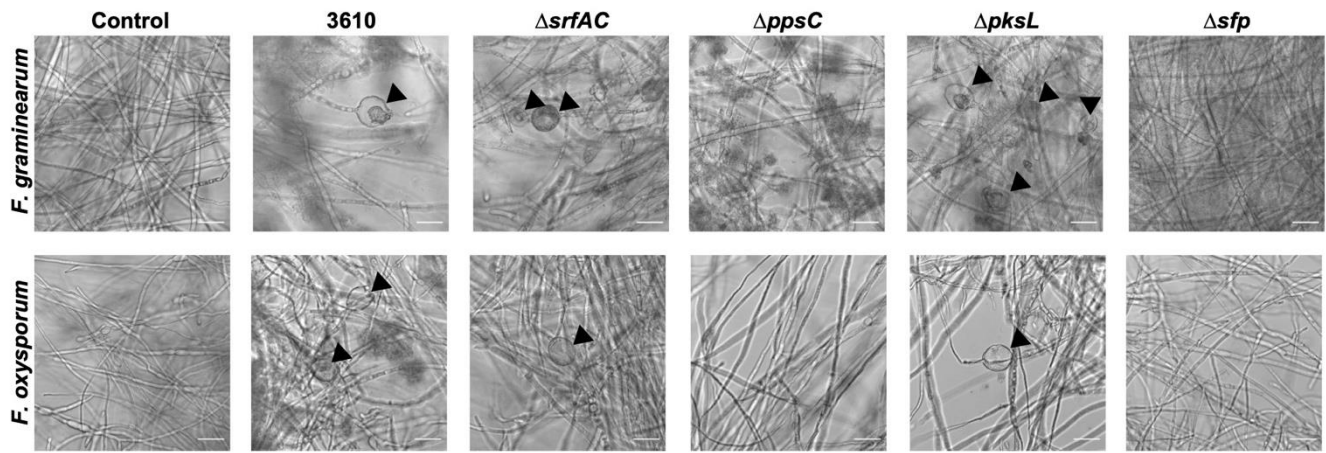


Fig. S5 | Influence of plipastatin on hyphae of *Fusarium* species. Microscopy visualisation of bulging *Fusarium* hyphae with wild type (WT) and various mutants, including strain lacking surfactin ($\Delta srfAC$), plipastatin ($\Delta ppsC$), bacillaene ($\Delta pksL$), or all non-ribosomal peptides (Δsfp). Scale bar = 25 μ m.

Supplementary Table 1 for strains, plasmids and oligos

<i>B. subtilis</i> strains	Genotype, description	Reference
NCIB 3610	undomesticated wild type strain	1,2
DK1042	NCIB 3610, but <i>comI</i> ^{Q12L} (naturally competent)	3
168 <i>degU</i>	<i>trpC</i> Δ <i>degU</i> ::Km ^R	4
TB742	DK1042 Δ <i>degU</i> ::Km ^R	This work
TB938	DK1042 <i>degU</i> ^{S202G}	This work
TB939	DK1042 <i>degS</i> ^{A193V}	This work
DS4085	NCIB 3610 Δ <i>pksL</i> ::Cm ^R	5
DS4114	NCIB 3610 Δ <i>ppsC</i> ::Tet ^R	5
DS1122	NCIB 3610 <i>srfAC</i> ::Tn10 Spec ^R	6
DS3337	NCIB 3610 Δ <i>sfp</i> ::Mls ^R	7
DS4113	NCIB 3610 Δ <i>ppsC</i> ::Tet ^R Δ <i>pksL</i> ::Cm ^R	5
DS4124	NCIB 3610 Δ <i>ppsC</i> ::Tet ^R Δ <i>pksL</i> ::Cm ^R <i>srfAC</i> ::Tn10 Spec ^R	5
<i>A. niger</i> strains	Genotype	Reference
N402	wild-type fungal strain	8
MA297.3	N402 P _{<i>agsA</i>(3×RlmA box)} - <i>mluc-TtrpC-pyrG</i> **	This work
MA584.2	N402 P _{<i>agsA</i>(RlmA box mutated)} - <i>mluc-TtrpC-pyrG</i> **	This work
Δ <i>rlmA</i>	N402 Δ <i>rlmA</i> :: <i>hyg</i> ^R	9
AR0#11	N402 P _{<i>gpdA</i>} - <i>glaA</i> ::sGFP- <i>TtrpC</i>	10
MA141.1	N402 P _{<i>gpdA</i>} - <i>glaA</i> ::sGFP-HDEL- <i>TtrpC</i>	11
Ren1.10	N402 P _{<i>gmtA</i>} -eYFP::GMTA- <i>TgmtA</i>	11
MA23.1.1	N402 P _{<i>gpdA</i>} - <i>CpyA</i> ::eGFP- <i>TtrpC</i>	12
FG7	N402 P _{<i>synA</i>} -eGFP::SynA- <i>TsynA</i>	13
BN38.9	N402 P _{<i>gpdA</i>} - <i>CitA</i> ::eGFP- <i>TtrpC</i>	14
MA26.1	N402 P _{<i>gpdA</i>} -H2B::eGFP- <i>TtrpC</i>	12
JvD1.1	N402 P _{<i>agsA</i>} -eGFP- <i>TtrpC</i>	15
Fungal strains		
<i>A. awamori</i>	FSU 11418	JMRC
<i>A. brasiliensis</i>	FSU 35902 (DSM 1988)	JMRC
<i>A. tubingiensis</i>	FSU 11408	JMRC
<i>A. nidulans</i>	HKI G034	JMRC
<i>F. graminearum</i>	IBT 41925	IBT
<i>F. oxysporum</i>	IBT 40872	IBT
JMRC: Jena Microbial Resource Collection at Leibniz Institute for Natural Product Research and Infection Biology Hans Knöll Institute, Jena, Germany (https://www.leibniz-hki.de/en/jena-microbial-resource-collection.html)		
IBT: IBT Culture Collection at DTU Bioengineering, Kongens Lyngby, Denmark (https://www.bioengineering.dtu.dk/research/strain-collections/ibt-culture-collection-of-fungi)		
Plasmids	description	Source
pMiniMad	<i>ori</i> ^{BsTs} <i>Amp</i> ^R <i>Mls</i> ^R	16
pTB693	pMiniMad with <i>degU</i> ^{S202G}	This work
pTB694	pMiniMad with <i>degS</i> ^{A193V}	This work
pMA334	vector with <i>pyrG</i> flanking regions	17

pBN008		vector with P _{agsA} (0.55-kb-rlm2add)-uidA-pyrG	9
pVG4.1		vector with mluc-TtrpC	18
pMA348		pMA334 with P _{agsA} (3×RlmA-box)-mluc-TtrpC-pyrG**	This work
pMA370		pMA334 with P _{agsA} (RlmA-box mutated)-mluc-TtrpC-pyrG**	This work
Oligos		sequence	gene targeted
oAR23	<i>NcoI</i>	ATCCATGGTGGCGGCTGAGAAGTCGTCG	<i>degU</i> in CoEvo2
oAR24	<i>BamHI</i>	GCGGATCCAAGAGGTTATCTGCTGAAAG	<i>degU</i> in CoEvo2
oAR30	<i>Sall</i>	CCGTCGACTTGGCGATAAACTTGAAGTG	<i>degS</i> in CoEvo3
oAR41	<i>BamHI</i>	ATGGATCCTGAAGAGCGCAACCTCAAAC	<i>degS</i> in CoEvo3
oAR25		AGACTTGCCAAGCTCTTC	<i>degU</i>
oAR26		GCTTGTAGAGCTGTATCC	<i>degU</i>
oAR31		TCAGGTCGAACCTTTAC	<i>degS</i>
oAR32		AACAGCTGGTCAAGAAC	<i>degS</i>
oAR27		TCCTCTGGCCATTGCTCTG	pMiniMad MCS
oAR28		CGAAGTTAGGCTGGTAAG	pMiniMad MCS
PagsAP1f-NotI		GCGGCCGCTCTAGAAGTACTAGT	
TtrpCP2r-NotI		AAGGAAAAAAGCGGCCGCTCTAGAAAGAAGGATTACCTC	
PagsAP4f-NotI		AAGGAAAAAAGCGGCCGCTGTCAGTAGTGGCGGCTGCTTC	
PagsA-AF-R-mut-RlmA2		CTCGGTGGTCCGCCGAGAAACGTCATATCAGGATAGC	
PagsA-AF-F-mut-RlmA1		ATATGACGTTTCTCGGCGGCGACCACCGAGAGTAGAGAATGA	
PagsAP2r		CTCGATCTTTCTGCGACCCATGATGGCAAGCGGCGTGTGGTA	
oBK7		CCGAGTACAAGGARGCCTTC	CaM
oBK8		CCGATRGAGGTCATRACGTGG	CaM

References

1. Branda, S. S., González-Pastor, J. E., Ben-Yehuda, S., Losick, R. & Kolter, R. Fruiting body formation by *Bacillus subtilis*. *Proc Natl Acad Sci U S A* **98**, 11621–11626 (2001).
2. Zeigler, D. R. *et al.* The origins of 168, W23, and other *Bacillus subtilis* legacy strains. *J Bacteriol* **190**, 6983–6995 (2008).
3. Konkol, M. A., Blair, K. M. & Kearns, D. B. Plasmid-encoded comI inhibits competence in the ancestral 3610 strain of *Bacillus subtilis*. *J Bacteriol* **195**, 4085–4093 (2013).
4. Kovács, Á. T. & Kuipers, O. P. Rok regulates *yuaB* expression during architecturally complex colony development of *Bacillus subtilis* 168. *J Bacteriol* **193**, 998–1002 (2011).
5. Müller, S. *et al.* Bacillaene and sporulation protect *Bacillus subtilis* from predation by *Myxococcus xanthus*. *Appl Environ Microbiol* **80**, 5603–5610 (2014).
6. Chen, R., Guttenplan, S. B., Blair, K. M. & Kearns, D. B. Role of the σ D-dependent autolysins in *Bacillus subtilis* population heterogeneity. *J Bacteriol* **191**, 5775–5784 (2009).
7. Patrick, J. E. & Kearns, D. B. Laboratory strains of *Bacillus subtilis* do not exhibit swarming motility. *J Bacteriol* **191**, 7129–7133 (2009).

8. Bos, C. J. *et al.* Genetic analysis and the construction of master strains for assignment of genes to six linkage groups in *Aspergillus niger*. *Curr Genet* **14**, 437–443 (1988).
9. Damveld, R. A. *et al.* The *Aspergillus niger* MADS-box transcription factor RlmA is required for cell wall reinforcement in response to cell wall stress. *Mol Microbiol* **58**, 305–319 (2005).
10. Gordon, C. L. *et al.* Glucoamylase::green fluorescent protein fusions to monitor protein secretion in *Aspergillus niger*. *Microbiology (N Y)* **146**, 415–426 (2000).
11. Carvalho, N. D. S. P. *et al.* Functional YFP-tagging of the essential GDP-mannose transporter reveals an important role for the secretion related small GTPase SrgC protein in maintenance of Golgi bodies in *Aspergillus niger*. *Fungal Biol* **115**, 253–264 (2011).
12. Weenink, X. O. Protein secretion in the filamentous fungus *Aspergillus niger*. (Leiden University, 2008).
13. Kwon, M. J. *et al.* Molecular genetic analysis of vesicular transport in *Aspergillus niger* reveals partial conservation of the molecular mechanism of exocytosis in fungi. *Microbiology (N Y)* **160**, 316–329 (2014).
14. Nitsche, B. M., Burggraaf-Van Welzen, A. M., Lamers, G., Meyer, V. & Ram, A. F. J. Autophagy promotes survival in aging submerged cultures of the filamentous fungus *Aspergillus niger*. *Appl Microbiol Biotechnol* **97**, 8205–8218 (2013).
15. Meyer, V. *et al.* Survival in the presence of antifungals: Genome-wide expression profiling of *Aspergillus niger* in response to sublethal concentrations of caspofungin and fenpropimorph. *Journal of Biological Chemistry* **282**, 32935–32948 (2007).
16. Patrick, J. E. & Kearns, D. B. MinJ (YvjD) is a topological determinant of cell division in *Bacillus subtilis*. *Mol Microbiol* **70**, 1166–1179 (2008).
17. Arentshorst, M., Lagendijk, E. L. & Ram, A. F. A new vector for efficient gene targeting to the *pyrG* locus in *Aspergillus niger*. *Fungal Biol Biotechnol* **2**, 2 (2015).
18. Meyer, V. *et al.* Fungal gene expression on demand: An inducible, tunable, and metabolism-independent expression system for *Aspergillus niger*. *Appl Environ Microbiol* **77**, 2975–2983 (2011).

Study 3

Kjeldgaard, B., Neves, A. R., Fonseca, C., Kovács, Á. T., and Domínguez-Cuevas, P. (2022).

Quantitative High-Throughput Screening Methods Designed for Identification of Bacterial Biocontrol Strains with Antifungal Properties.

Microbiology Spectrum. Vol. 10, Issue 2. doi:10.1128/spectrum.01433-21.



Quantitative High-Throughput Screening Methods Designed for Identification of Bacterial Biocontrol Strains with Antifungal Properties

 Bodil Kjeldgaard,^{a,b}  Ana Rute Neves,^{a*}  César Fonseca,^a  Ákos T. Kovács,^b  Patricia Domínguez-Cuevas^a

^aDiscovery, R&D, Chr. Hansen A/S, Hoersholm, Denmark

^bBacterial Interactions and Evolution Group, DTU Bioengineering, Technical University of Denmark, Kongens Lyngby, Denmark

ABSTRACT Large screens of bacterial strain collections to identify potential biocontrol agents often are time-consuming and costly and fail to provide quantitative results. In this study, we present two quantitative and high-throughput methods to assess the inhibitory capacity of bacterial biocontrol candidates against fungal phytopathogens. One method measures the inhibitory effect of bacterial culture supernatant components on the fungal growth, while the other accounts for direct interaction between growing bacteria and the fungus by cocultivating the two organisms. The antagonistic supernatant method quantifies the culture components' antifungal activity by calculating the cumulative impact of supernatant addition relative to the growth of a nontreated fungal control, while the antagonistic cocultivation method identifies the minimal bacterial cell concentration required to inhibit fungal growth by coinoculating fungal spores with bacterial culture dilution series. Thereby, both methods provide quantitative measures of biocontrol efficiency and allow prominent fungal inhibitors to be distinguished from less effective strains. The combination of the two methods sheds light on the types of inhibition mechanisms and provides the basis for further mode-of-action studies. We demonstrate the efficacy of the methods using *Bacillus* spp. with different levels of antifungal activities as model antagonists and quantify their inhibitory potencies against classic plant pathogens.

IMPORTANCE Fungal phytopathogens are responsible for tremendous agricultural losses on an annual basis. While microbial biocontrol agents represent a promising solution to the problem, there is a growing need for high-throughput methods to evaluate and quantify inhibitory properties of new potential biocontrol agents for agricultural application. In this study, we present two high-throughput and quantitative fungal inhibition methods that are suitable for commercial biocontrol screening.

KEYWORDS *Bacillus*, *Fusarium culmorum*, *Fusarium graminearum*, *Botrytis cinerea*, fungal growth inhibition method, quantification of antifungal properties, biocontrol agents, bacterial-fungal coinoculation, bioactive compounds, biocontrol screening, bioactive metabolites, fungal growth inhibition, high-throughput screening, antifungal agents, quantitative methods

On an annual basis, it is estimated that global crop production suffers losses between 20 to 40% due to pests and plant diseases (1). Plant diseases alone are predicted to cost the global economy a staggering \$220 billion per year (2). Among other plant pathogens, fungal phytopathogens contribute to considerable losses in agriculture and greatly impact food security in developing countries (3–5). Not only do fungal pathogens affect the yield, but fungal crop infections also lead to severe reductions of postharvest crop quality. For instance, the accumulation of high levels of mycotoxins renders crops unsafe for human consumption and for animal forage (6, 7). In modern intensified agriculture, fungal diseases are commonly fought using fungicides (8), but the rising fungicide resistance and chemical

Editor Lea Atanasova, University of Natural Resources and Life Sciences Vienna

Ad Hoc Peer Reviewer Sergio Casas-Flores, Instituto Potosino de Investigación Científica y Tecnológica, or Lidia Blaszczyk, Institute of Plant Genetics of the Polish Academy of Sciences

Copyright © 2022 Kjeldgaard et al. This is an open-access article distributed under the terms of the [Creative Commons Attribution 4.0 International license](https://creativecommons.org/licenses/by/4.0/).

Address correspondence to Patricia Domínguez-Cuevas, dkpacu@chr-hansen.com.

*Present address: Ana Rute Neves, Arla Foods Ingredients, Sønderhøj, Denmark.

The authors declare a conflict of interest. B.K., A.R.N., C.F. and P.D.-C. are or were employed by Chr. Hansen A/S, a global supplier of biocontrol strains for the Plant Health and Nutrition sector. The remaining author (Á.T.K) declares that the research was conducted in the absence of any commercial or financial relationships that could be construed as a potential conflict of interest.

Received 30 August 2021

Accepted 7 February 2022

pollution represent a challenge to the sustainable use of these chemicals in agriculture (9–12). In addition, many fungicides are hazardous to humans and may be implicated in developmental toxicity, reproductive defects, or cancer (13, 14). The application of microbial biocontrol agents represents a safe alternative to the intensive use of agrochemicals (11, 15). Biocontrol agents reside in close association with plant surfaces, i.e., leaves or roots, and protect the plant from phytopathogens by priming the plant defense response, competing for nutrients, and/or directly antagonizing the growth and development of the pathogenic intruders (16–18). Strains from the *Pseudomonas*, *Burkholderia*, *Streptomyces*, and *Bacillus* genera are well known for their antifungal capacity and for the production of a large variety of bioactive metabolites (15, 19–24). Although the inhibitory effect of specific soil bacteria is well documented and recognized, there is a lack of quantitative and high-throughput screening (HTS) procedures to identify competent biocontrol agents. Consequently, many potential biocontrol agents eventually fail to suppress plant diseases in field trials (25, 26). Classic antagonistic screens, which are referred to as dual culture, plate confrontation, or inhibition zone assays, assess the impact of the biocontrol candidates on the phytopathogen after coinoculation on solid media (25, 27). Such methods account for numerous factors, including nutrient or space competition, cell surface components, and the induced or constitutive secretion of volatile or soluble metabolites (21, 27–29). Other antagonistic assays evaluate the effect of individual inhibitory components, such as volatiles, polyketides, lipopeptides, siderophores, and lytic enzymes, including chitinases, glucanases, and proteases, on the phytopathogens' growth (21, 27). More complex antagonistic assays, such as leaf disc or seedling assays (30, 31), investigate the tripartite interaction between the biocontrol candidate, phytopathogen, and plant host, while nonantagonistic assays assess the importance of complementary inhibitory mechanisms, including niche colonization and priming of the plant immune response (27). Nevertheless, most screening systems are low throughput and provide only semiquantitative measurements of the inhibition potential against the fungus. Therefore, there is a need to develop more efficient screening methods combining quantitative measurements of antimicrobial activity with automation to increase the speed and reduce the resources required for the identification of good candidates.

Here, we describe two fungal inhibition methods to evaluate the antifungal potency of potential biocontrol agents. Both methods accommodate HTS of bacterial biocontrol candidates, allowing screening of a minimum of 1,000 strains per week, and provide accurate quantification of their inhibitory capacities. The major difference between the two methods is represented by the use of growing bacterial cells as opposed to (cell-inactive) culture supernatants. We demonstrate the efficacy of the methods using bacterial strains with different antifungal performance. Using the two novel methods, the antifungal properties of the bacteria were compared, and prominent fungal inhibitors were distinguished from less effective bacterial strains. Both methods were developed utilizing *Fusarium culmorum* as the model plant pathogen and *Bacillus* spp. as model antagonists. In addition, the methods were further applied for screening *Bacillus* spp. against other important phytopathogens, i.e., *Fusarium graminearum* and *Botrytis cinerea*, proving that our methods can readily be adjusted to other fungal species.

RESULTS

Coinoculation of fungal spores with bacterial dilution series facilitates quantification of inhibition potency. The so-called dual-culture assay is among the most common screening methods to identify potent fungal inhibitors from microbial collections (19, 23, 32–34). Typically, the assay is performed by inoculating potential biocontrol agents at a fixed distance from the pathogenic fungal inoculum on a petri dish, as illustrated in Fig. 1A. Subsequently, the biocontrol agent's ability to suppress fungal growth is manually assessed by measuring the radius of the mycelial growth relative to the control or by measuring the size of the inhibition zone (35–38). However, accurate comparison and subsequent ranking of large numbers of strains is difficult with this assay due to the format of the readout. To improve the evaluation and accurate quantification of antifungal potency, we developed an HT fungal inhibition assay based on direct coinoculation of bacterial cultures and fungal plant-pathogenic spores. Fungal spores rather than mycelium were used as the initial inoculum in the assay to allow assessment of the biocontrol agent's impact on both spore germination and fungal

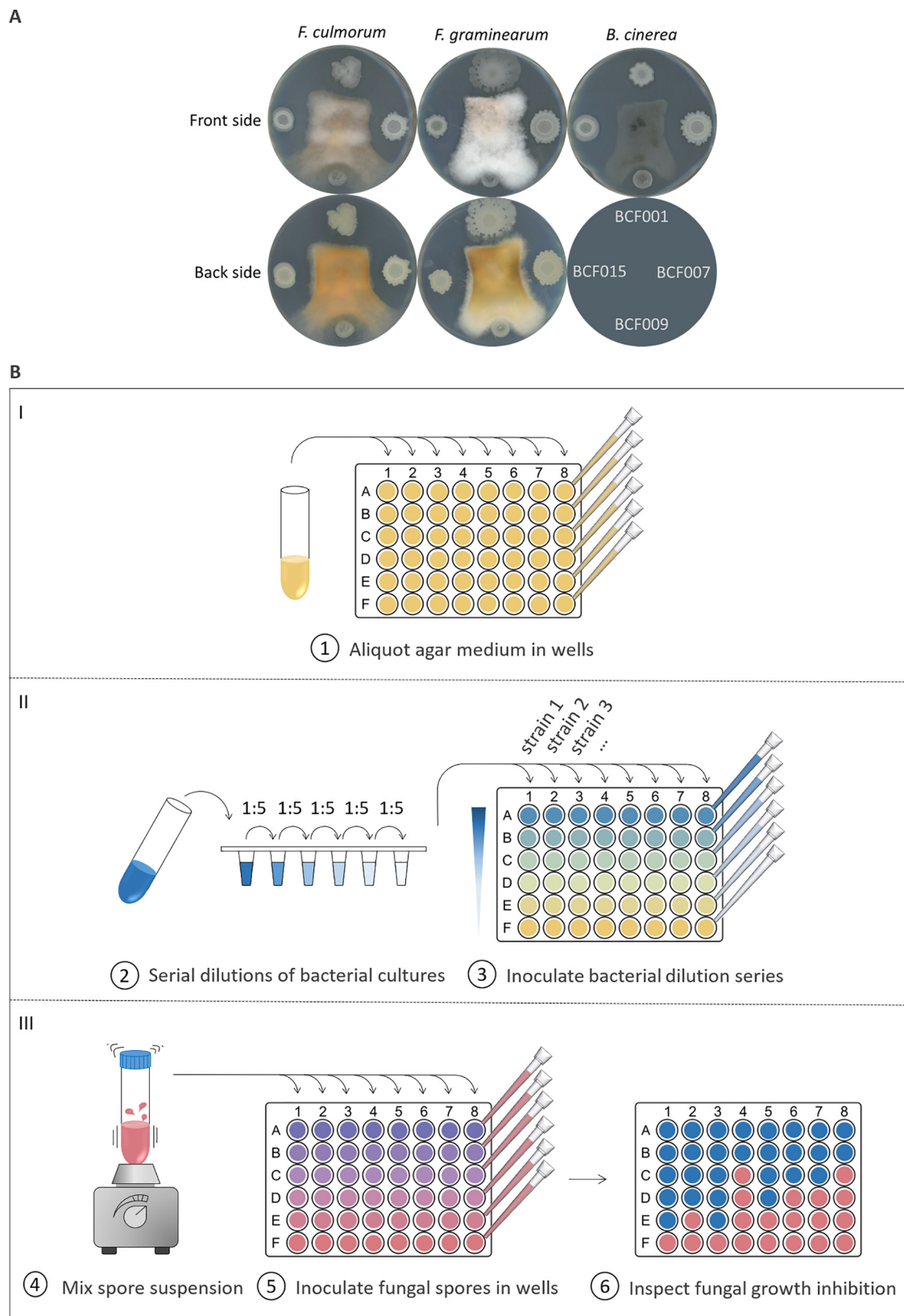

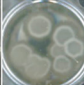
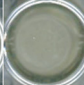
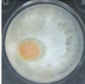
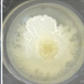
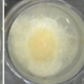

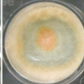
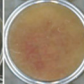


FIG 1 Fungal inhibition assays. (A) *B. subtilis* strain BCF001, *B. amyloliquefaciens* strain BCF007, *B. paralicheniformis* strain BCF009, and *B. velezensis* strain BCF015 were spotted around central inocula of *Fusarium culmorum*, *Fusarium graminearum*, and *Botrytis cinerea* on agar medium. Inhibition zones were observed 6 days postinoculation. The backside of the *B. cinerea* plate is not shown; the scheme shown instead indicates the positions of the inoculated strains. (B) In each well of a 48-well microtiter plate, molten

(Continued on next page)

A

Categories	Visual scoring			Growth score
No fungal growth				1
Weak growth				2
Fungal growth				3

B

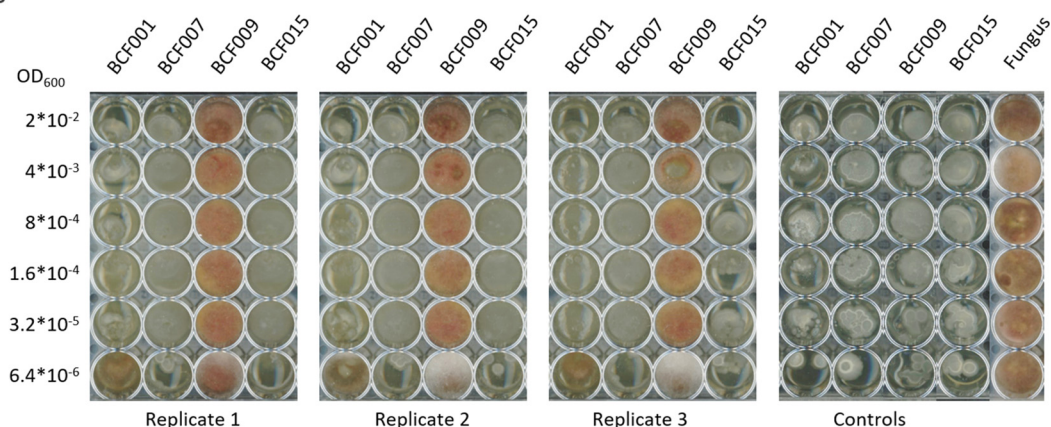


FIG 2 Comparison of *Bacillus* species inhibitory properties against *F. culmorum*. (A) *F. culmorum* growth was scored following a three-step scale, illustrated with three example images per category. The first category shown in the top row includes wells with absence of fungal growth, where only bacterial growth can be observed; the second category shown in the middle row includes wells with signs of co-growth of both species, while the third category shown in the bottom row includes wells with only fungal growth or mainly fungal growth. (B) Dilution series of *B. subtilis* BCF001, *B. amyloliquefaciens* BCF007, *B. paralicheniformis* BCF009, and *B. velezensis* BCF015 were prepared and inoculated in consecutive columns of a 48-well microtiter plate. A constant spore concentration of *F. culmorum* was inoculated in each well. ODs of serial dilutions are indicated on the left (OD_{600}). The rightmost panel shows the control plate, corresponding to the growth of bacterial serial dilutions in the absence of fungal spores and to fungal growth in the absence of bacteria.

growth. First, bacterial overnight cultures were normalized to the same optical density at 600 nm (OD_{600}) and 5-fold serial dilutions were prepared (down to an amount of approximately 300 to 500 bacterial cells inoculated). The OD_{600} of each strain used in the study was correlated with viable cell counts (CFU). A fungal spore suspension was prepared and mixed thoroughly to ensure a homogeneous spore distribution. Then, samples from the bacterial dilution series were coinoculated with a fixed quantity of fungal spores to determine the minimal inhibitory cell concentration (MICC) that abolished fungal growth (Fig. 1B). With this setup, a low MICC indicates a higher antifungal potency for a given bacterial strain. The assay was prepared on an appropriate agar medium for fungal cultivation in 48-well microtiter plates and incubated for 5 days at room temperature before assessing the fungal growth.

Four *Bacillus* strains of different species were selected based on their differential properties for fungal inhibition. The inhibitory capacities of the selected strains, *Bacillus subtilis* BCF001, *Bacillus amyloliquefaciens* BCF007, *Bacillus paralicheniformis* BCF009, and *Bacillus velezensis* BCF015, were quantified against *F. culmorum* DSM1094 using the developed method (Fig. 2B). The assay was conducted as three independent biological replicates, rendering very similar results, which indicates that the method is highly reproducible.

FIG 1 Legend (Continued)

PDA medium was aliquoted and allowed to solidify. Fivefold dilution series of *Bacillus* strains were prepared from cultures normalized to the same OD_{600} . In each column, consecutive wells were coinoculated with the *Bacillus* dilution series and a fixed quantity of fungal spores (constant volume of fungal spore suspension) on the agar surface. The spore suspensions were mixed thoroughly before aliquoting. Assay results were evaluated by visual inspection after 5 days of incubation at room temperature.

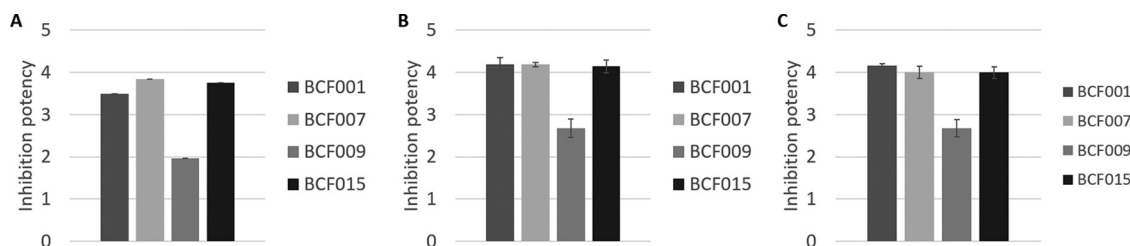


FIG 3 Inhibition potency of *Bacillus* species against fungal phytopathogens. The inhibition potencies of *B. subtilis* BCF001, *B. amyloliquefaciens* BCF007, *B. paralicheniformis* BCF009, and *B. velezensis* BCF015 were assigned numerical scores based on the minimal inhibitory cell concentration (MICC) against *F. culmorum* (A), *F. graminearum* (B), and *B. cinerea* (C). Inhibition scores were calculated by applying equation 1 (Materials and Methods). Error bars show standard deviations.

Fungal growth inhibition was scored as no growth (1), weak growth (2), and (positive) growth (3) (Fig. 2A). Fungal growth was defined by the presence of visible hyphae in the well, including those that were half-covered by fungal mycelia. No fungal growth was defined by the complete absence of visible fungal mycelia and clear presence of bacterial growth. Weak growth was defined by the presence of barely visible hyphae in all replicates or by the absence of growth in half of the replicates. The weak growth category included the wells where *F. culmorum* produced (orange) pigmentation, even in the absence of visible hyphae. The coinoculation of bacterial culture dilutions and fungal spores was used to distinguish the limits of the bacterial inhibition capacity.

Comparison of bacterial MICCs allowed ranking of the strains in accordance with their fungal inhibition properties (Fig. 3A, Table S1 in the supplemental material). The strains *B. amyloliquefaciens* BCF007 and *B. velezensis* BCF015 showed the most potent inhibition properties, and even at the highest dilution step (corresponding to an initial OD_{600} of 6.4×10^{-6} , equivalent to 340 to 500 CFU inoculated), the two strains were able to inhibit *F. culmorum*'s growth. Determining the MICC more accurately would require smaller dilution steps to be included in the assay. Nevertheless, the experimental setup is optimized for HTS of large strain collections. *B. subtilis* BCF001 also displayed potent fungal inhibition properties, abolishing fungal growth up to an OD_{600} of 3.2×10^{-5} , corresponding to 1,900 CFU inoculated. *B. paralicheniformis* BCF009, however, did not affect fungal growth even at the lowest dilution step, corresponding to an OD_{600} of 2×10^{-2} , or 3.89×10^4 CFU inoculated.

To generate visual and directly comparable plots of the inhibition results, we calculated a numerical inhibition score that reflects the inhibitory capacity of each strain. In brief, the lowest cell concentration that caused fungal growth inhibition was identified for each strain, and a numerical inhibition score was calculated based on the natural logarithm to the MICC by applying the empirical formula presented in equation 1 in Materials and Methods (Fig. 3A, Table S1). Plotting the inhibition scores clearly indicated that *B. amyloliquefaciens* BCF007 and *B. velezensis* BCF015 were the most efficient strains inhibiting the growth of *F. culmorum*. *B. subtilis* BCF001 also showed a high inhibition score, although smaller than the ones calculated for the two former strains. The scoring results for *B. paralicheniformis* BCF009 matched the low inhibitory activity of this strain against *F. culmorum*. The MICCs of all strains against *F. culmorum* were significantly different from each other (Table S2).

Evaluation of the inhibition method with additional fungal phytopathogens.

Using the newly developed method, the antifungal activities of *B. subtilis* BCF001, *B. amyloliquefaciens* BCF007, *B. paralicheniformis* BCF009, and *B. velezensis* BCF015 were also quantified against other phytopathogenic filamentous fungi, specifically *F. graminearum* and *B. cinerea* strains. Images acquired to record the experimental results and the calculated MICCs and inhibition scores can be found in Fig. S1 and Table S1. Interestingly, our inhibition assay proved applicable to these additional species of plant-pathogenic fungi. The initial spore concentration was the only parameter that required adjustment when testing growth inhibition against the new fungal strains.

The above-described scoring system was applied to the results obtained for the three fungal species (Fig. 3). While *B. amyloliquefaciens* BCF007 and *B. velezensis* BCF015 displayed

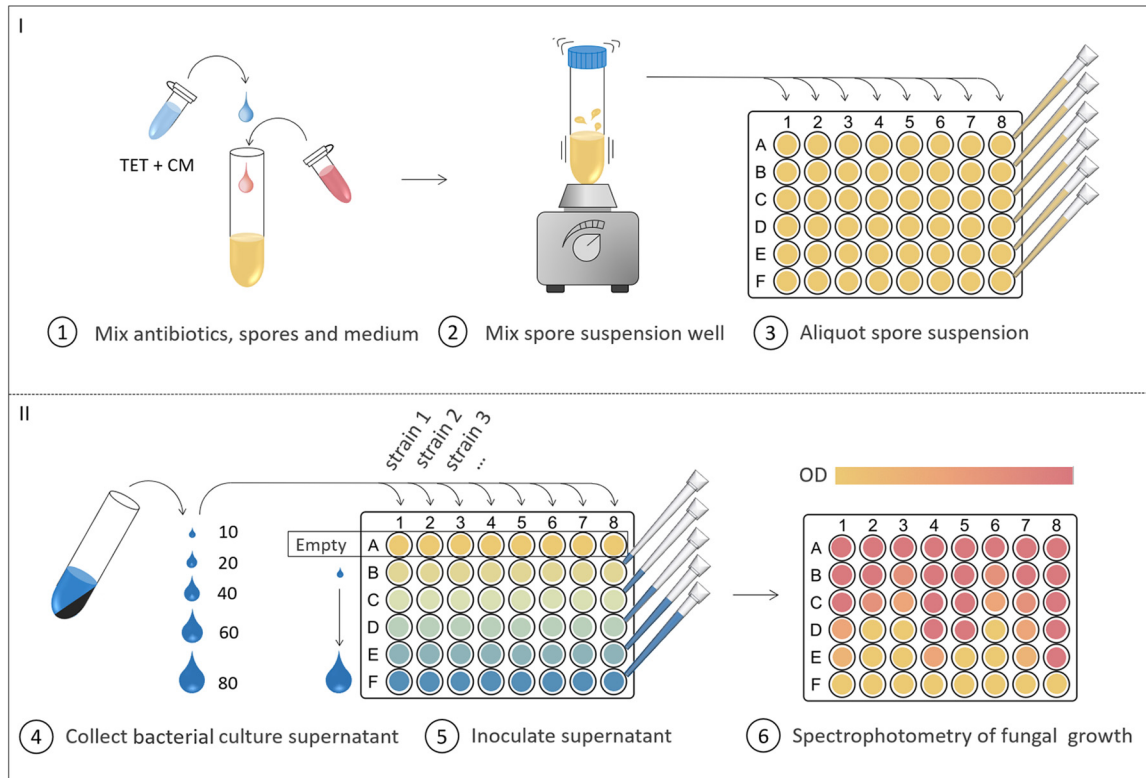


FIG 4 Supernatant inhibition method. A fungal spore suspension was prepared with PDB medium and the bacteriostatics tetracycline (TET) and chloramphenicol (CM). The suspension was mixed well and aliquoted into each well of a 48-well microtiter plate. *Bacillus* overnight cultures were adjusted to an OD_{600} of 2 and were subsequently centrifuged to collect the supernatants. In each column, a range of volumes of *Bacillus* supernatant (10 to 80 μ l) were added to consecutive wells. Fungal growth was evaluated by spectrophotometric measurements after 5 days of incubation at 25°C in darkness.

the most efficient growth inhibition of *F. culmorum*, the differences between them and *B. subtilis* BCF001 were minimal when assayed against *F. graminearum* DSM4528, and the MICCs were not significantly different (Table S2). Furthermore, *B. subtilis* BCF001 proved more efficient than *B. amyloliquefaciens* BCF007 and *B. velezensis* BCF015 against *B. cinerea* Kern B2. The inhibition scoring results obtained for *B. parlicheniformis* BCF009 were in accordance with the poor inhibitory properties of this strain, regardless of the fungal pathogen tested. For comparison between strains with similar inhibition potencies, the range of the dilution series can readily be adjusted to allow determination of a more accurate MICC.

Inoculation of fungal spores with bacterial culture supernatants validates the inhibitory importance of supernatant components. While the antagonistic coinoculation method assesses several inhibitory mechanisms, the use of cell-inactive supernatants accounts for the bioactivity of secreted metabolites, such as enzymes, lipopeptides, and polyketides, on the fungus. In the antagonistic supernatant method, fungal growth was estimated by OD_{600} measurements in liquid cultures, and therefore, reduced fungal growth in the presence of bacterial metabolites reflects greater inhibition potency of a given strain. For this method, bacterial cultures were grown overnight and normalized to the same OD_{600} value prior to collection of the culture supernatants by centrifugation (Fig. 4). A range of increasing supernatant volumes (10 to 80 μ l) were inoculated into fungal spore suspensions prepared in liquid medium in 48-well microtiter plates. To avoid any possibility of misreads arising from remaining bacterial cells present in the supernatants, bacteriostatic antibiotics were added to the fungal spore suspensions to prevent bacterial growth. The microtiter plates were incubated statically at 25°C in darkness. Subsequently, the fungal growth was quantified by spectrophotometric measurement. An area scan protocol (5 by 5 measurements) was used to account for empty spaces and clumps of fungal growth within the well. Optical density measurements were previously found to correlate to fungal dry weight (39–41). Dynamic

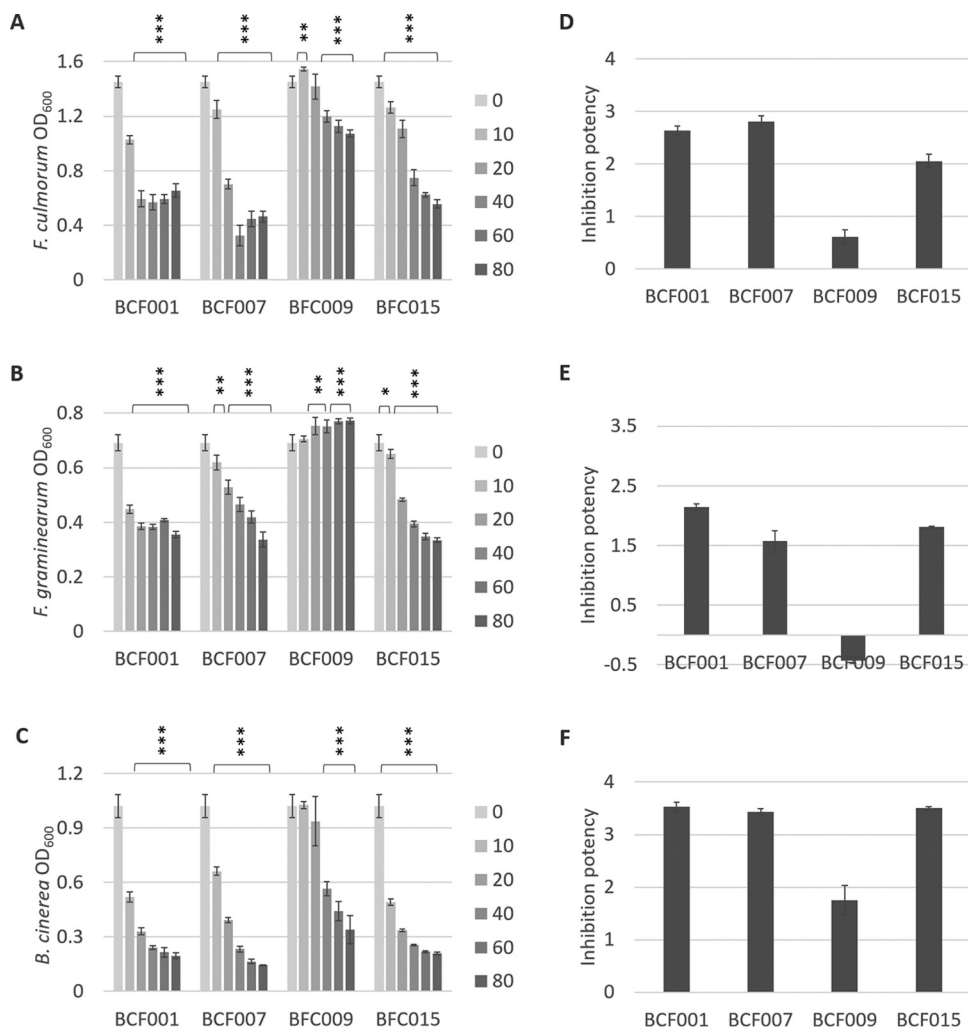


FIG 5 Fungal growth inhibition by *Bacillus* species culture supernatants. *Bacillus* species cultures were grown overnight in LB broth and normalized to an OD₆₀₀ of 2. Different volumes of cell-inactive supernatants (10, 20, 40, 60, and 80 μ l) were added to 48-well microtiter plates containing PDB medium and a fixed fungal spore concentration. Bacterial growth was inhibited by the presence of bacteriostatic antibiotics in the culture medium (50 μ g/mL chloramphenicol and 10 μ g/mL tetracycline). Plates were incubated at 25°C without shaking for 60 h (in darkness), and fungal growth was measured by spectrophotometry at 600 nm. Plots correspond to inhibition results for *F. culmorum* (A), *F. graminearum* (B), and *B. cinerea* (C). Statistical significance for each supernatant volume compared to the control was calculated based on biological triplicates. *, $P < 0.05$; **, $P < 0.005$; ***, $P < 0.0005$. For quantification of the culture supernatant inhibition potency, an inhibition score was assigned to each *Bacillus* strain by subtracting the accumulated relative fungal growth of *F. culmorum* (D), *F. graminearum* (E), and *B. cinerea* (F) in response to all supernatant volumes from the total potential growth according to equation 2 (Materials and Methods). Standard deviations were calculated based on biological triplicates.

assessment of fungal growth was done using this methodology, and fungal growth curves may be found in Fig. S2.

The inhibition assay demonstrated a reverse correlation between the added volume of bacterial cell-inactive supernatant and the growth of *F. culmorum*, *F. graminearum*, or *B. cinerea* (Fig. 5A to C). For the potent fungal inhibitory strains, including *B. subtilis* BCF001, *B. amyloliquefaciens* BCF007, and *B. velezensis* BCF015, increasing volumes of bacterial supernatant correlated with a progressive decrease of fungal growth. The addition of *B. paralicheniformis* BCF009 supernatant impacted fungal growth to a much lesser extent, which was in accordance with the results obtained with the coinoculation method. In some cases, a slight increase in fungal growth was observed in response to the addition of the largest supernatant volume (80 μ l culture supernatant), suggesting an effect of supplemented nutrients (not consumed by the bacteria) that outweighed the effect of the antifungal bioactive metabolites.

Scoring of supernatant inhibition potency. A numerical inhibition score was assigned to each strain by quantifying the fungal growth in response to supernatant addition (5 different volumes). The inhibition scores were calculated by subtracting the accumulated relative fungal growth from the total potential fungal growth under the 5 conditions tested (equation 2 in Materials and Methods).

The inhibition scores can be found in Table S1. Culture supernatants of *B. subtilis* BCF001 and *B. amyloliquefaciens* BCF007 showed the most effective growth inhibition of *F. culmorum* (Fig. 5A and D). Against *F. graminearum*, *B. subtilis* BCF001 culture supernatants proved the most inhibitory, while *B. subtilis* BCF001, *B. amyloliquefaciens* BCF007, and *B. velezensis* BCF015 all displayed similar inhibition potencies against *B. cinerea*. *B. paralicheniformis* BCF009 culture supernatants inhibited *F. culmorum* growth poorly.

It is worth mentioning that assays prepared from different fungal spore stock solutions showed small variations in final fungal growth (Fig. S3), possibly due to variations in the initial spore count or spore viability. These variations could be minimized either by prolonging the incubation time until readout or by preparing assays from a unique spore stock. For this reason, biological replicates were prepared with the same fungal spore solution. Nevertheless, the overall conclusions remained unchanged despite variations in the final fungal growth.

Comparison of methods to remove or inactivate cells from culture supernatants.

Typically, bacterial-cell-inactive supernatants are generated by filtration of the cell cultures (42–45). In contrast, in the setup proposed here, cell-inactive supernatants were generated by centrifugation to pellet bacterial cells. To avoid cell growth of remaining bacteria in suspension, we added the bacteriostatic antibiotics chloramphenicol and tetracycline. Plating of the fungal growth suspension on bacterium-selective medium after the endpoint measurement produced no bacterial growth (no colonies), indicating that the antibiotics effectively inhibited the growth of any putative remaining bacterial cells. The final fungal growth reached by *F. culmorum*, *F. graminearum*, and *B. cinerea* was somewhat affected by the addition of the respective antibiotics (Fig. S4). The results obtained with filtered supernatants with and without antibiotics revealed that the relative inhibition results remained unaltered, although the addition of antibiotics slightly but significantly reduced the fungal growth (Fig. S5, Table S3). Both filtration and antibiotic addition had generally no effect on the fungal inhibitory potency, suggesting that bioactive metabolites remained active after both procedures (Fig. S6, Table S3).

Comparison of the two methods proposed in the present study and the dual-culture assay. The two proposed quantitative HT methods were compared to the common dual-culture assay using plates inoculated with fungus and *Bacillus* strains (Fig. 1A). In accordance with the results from the two methods, zones of fungal growth inhibition were observed around the bacterial colonies of *B. subtilis* BCF001, *B. amyloliquefaciens* BCF007, and *B. velezensis* BCF0015, whereas the growth of *F. culmorum*, *F. graminearum*, and *B. cinerea* was nearly unaffected by *B. paralicheniformis* BCF009. The observed growth reduction from the dual-culture assay was in accordance with the calculated MICCs from the antagonistic coinoculation assay (Fig. 1A and 3, Table S1). Indeed, the traditional dual-culture assay allows the assessment of fungal inhibitory capacity and enables a quick and simple evaluation of biocontrol strains' potential, but the results lack the accurate quantification of the bacterial inhibition potency provided by the methods proposed here. By adjusting the range of the dilution series, genetically or phenotypically similar strains can be compared and ranked using the antagonistic coinoculation method. This allows the comparison of similarly potent biocontrol candidates. In addition, the simple numerical scoring systems allow easy comparison between a large number of strains. The throughput is approximately 1,000 strains per week for each of the two screening methods described, including preparation time and readout of the assays, but not taking incubation time into consideration. The cost of the assays includes the operation cost of the robot, pipette tips, growth medium, and one 48-well microtiter plate per 8 strains. Although the classical dual-culture assay is undoubtedly more cost-effective, the quantification aspect of the methods described in this study constitutes a great advantage when comparing biocontrol candidates, which is valuable for commercial screening.

While the antagonistic supernatant method specifically evaluates the inhibition potency of secreted metabolites, such as enzymes, lipopeptides, and polyketides, the antagonistic

coinoculation method quantifies the inhibitory effect of actively growing bacteria and, thereby, accounts for additional factors like competition for nutrients and space. Therefore, differences in results obtained by the two methods could provide insights into the mode of action and serve as the starting point for in-depth characterization of the molecular inhibitory mechanisms.

DISCUSSION

Despite the steadily growing market share of biocontrol products compared to the use of conventional pesticides (16, 46), plant pathogen management continues to rely heavily on chemical substances with associated risks to human health and the environment (47). Regardless of the increased (research) efforts on microbial biocontrol product development, their deployment into the market is difficult due to the absence of a harmonized global framework, public misinformation, and complex regulation and registration procedures, as well as the high costs of field trials (48–51). The application of reliable methods to identify and select potent biocontrol strains is of critical importance to reduce product development costs and accelerate their market implementation.

Large screens of strain collections are often laborious and expensive, with the cost being proportional to the complexity of the screening system (52). Simple HTS methods are cost-effective; however, they often fail to provide quantitative results for accurate comparison of the biocontrol strains. Furthermore, following the HTS and candidate selection, many strains eventually show low efficacy in field trials, demonstrating a discrepancy between *in vitro* laboratory conditions and *in planta* application experiments. To reduce costs and minimize failed tests, it is therefore crucial to identify biocontrol candidates in primary screens before moving on to complex experimental systems, such as greenhouse or field trials. Accordingly, the development of simple, reliable, and quantitative HTS methods is crucial for ranking and selection of the best biocontrol candidates.

In this study, bacterial strains were ranked according to their bioactivity against fungal plant pathogens by using two novel HTS methods: (i) an antagonistic cocultivation method based on the inoculation of a constant number of fungal spores together with bacterial dilution series on solid medium to generate a quantitative measurement of the minimal inhibitory (bacterial) cell concentration (MICC) of fungal growth and (ii) an antagonistic cell-inactive-supernatant method based on the inoculation of a constant number of fungal spores together with different volumes of bacterial culture supernatants in liquid medium to provide a quantitative measurement of fungal growth inhibition by secreted metabolites.

Although classic antagonistic methods that assess the adjacent growth of two species on agar plates allow the assessment of fungal inhibition potential (19, 32–34, 53–55), their accuracy is limited. Factors like the inoculum size, diffusion rate of metabolites, and differential conditions between agar plates contribute to the inaccuracy of classic antagonistic assays and impair the ranking of biocontrol candidates. The quantification provided by the antagonistic cocultivation method proposed here allows the ranking of biocontrol candidates according to their inhibitory strength by means of MICC values. In addition, the direct coinoculation of fungal spores with bacterial cells allows assessment not only of the impact on mycelial growth but also on fungal spore germination, contrary to the classic agar plate methods. This type of antagonistic method, employing direct coinoculation of biocontrol candidate and pathogen, has been developed for other applications; for instance, lactic acid biocontrol bacteria coinoculated with food spoilage fungi in studies of food products in the dairy industry (56, 57). However, these assays lack precise quantification of inhibition potency, regardless of the similarities to the coinoculation method described here.

Compared to simple dual-culture assays like ours, the more complex *in planta* assays include the tripartite interaction of the biocontrol candidate, phytopathogen, and plant host (30, 31, 58) and thereby attempt to mimic field settings. Despite the closer resemblance to natural conditions, the complexity of these screening systems limits the throughput (59) and leads to additional variation (60), which complicates the interpretation of results compared to our method. However, screens that consider the interaction between three biological systems

may be advantageous to apply to a subset of biocontrol candidates following an initial HTS (59, 61).

While the antagonistic cocultivation methods investigate the direct interaction between pathogen and biocontrol candidate, the antagonistic supernatant methods estimate the inhibition potency of secreted bioactive metabolites from the biocontrol candidate on the pathogen. The experimental setup can be either agar- or liquid-based, like the proposed antagonistic cell-inactive-supernatant method described in this study. Agar-based screens rely on the evaluation of fungal colony growth or inhibition zones in response to the addition of supernatants from the biocontrol candidates (34, 43, 62). Some assays allow a quantitative comparison of inhibition capacity between strains by calculating the reciprocal to the highest supernatant dilution that exhibits a clear zone of inhibition (43, 62). Even so, the scoring is notably laborious and low throughput compared to the proposed antagonistic supernatant method described in this study.

Liquid-based supernatant assays depend on the assessment of fungal morphology in response to the biocontrol supernatants by microscopy (62, 63), evaluation of fungal growth by dry weight (64), or spectrophotometry (36, 42, 55). The latter two share a great resemblance to the proposed cell-inactive-supernatant method and allow HTS and reproducible assessment of the potency of antifungal metabolites. However, the accurate quantification of antifungal capacity by determination of supernatant inhibition scores in the method proposed here allows easy benchmarking and comparison between biocontrol supernatants, which represents a major advantage over previously reported methods.

Both assays were initially developed utilizing *F. culmorum* as the model plant pathogen and different *Bacillus* species as model antagonists. Subsequently, the assays were validated with the relevant plant-pathogenic fungi *B. cinerea* and *F. graminearum*. The results demonstrated that the methods are robust and can readily be adapted for different fungal species. Moreover, the methods can be adapted to assess the potential for inhibiting bacterial plant pathogens. In agriculture, not only fungal plant pathogens but also bacterial plant pathogens contribute to significant yield losses (65). The adaptation of the proposed methods to quantify inhibition potency against plant-pathogenic bacteria simply requires a fluorophore-labeled bacterial pathogen, a bacterial pathogen with a selective marker (i.e., antibiotic resistance), or a pathogen-selective growth medium in order to make it applicable for HTS. For discrimination between bacterial strains with similar inhibition potencies, the antagonistic cocultivation method can be adjusted by using a smaller dilution factor. Furthermore, the dilution factors can be adjusted to fit more or less potent biocontrol candidates. Finally, the applicability of the methods may even be extended to other areas, such as biocontrol screens against human or animal pathogens or screens against food spoilage microorganisms.

Several previous studies employed combinatory screens with two or more assays for the identification of potent pathogen inhibitors (33, 35, 55, 58, 63, 66, 67). In this study, we propose the combination of two HT antagonistic methods to improve confident selection of potent biocontrol bacterial strains. While the antagonistic cocultivation method accounts for the entire repertoire of direct inhibitory mechanisms displayed by a biocontrol strain, such as bioactive compounds and competition for nutrients and space, the antagonistic supernatant method pinpoints the inhibitory effect of secreted metabolites, such as enzymes, lipopeptides, and polyketides. Thus, the two methods provide different results that in combination may aid further mechanistic elucidation. In addition, while the antagonistic coinoculation method may facilitate the identification of potent candidates ideal for in-furrow application or seed coating, where pathogens and biocontrol agents actively compete, the antagonistic supernatant method identifies high producers of bioactive metabolites that would be advantageous in a liquid formulation for foliar product application. In light of the results obtained and considering the different mechanistic aspects involved in pathogenic inhibition, we argue that the combination of our novel antagonistic cocultivation and supernatant methods constitutes an improved strategy for biocontrol strain identification. The combination of the two methods presented (i) confidently reflects the fungal inhibition capacity of biocontrol candidates, (ii) facilitates HTS of large strain collections, (iii)

TABLE 1 Fungal and bacterial strains used in the present study

Species	Strain	Source
Filamentous fungi		
<i>Fusarium culmorum</i>	DSM1094	DSMZ German collection
<i>Fusarium graminearum</i>	DSM4528	DSMZ German collection
<i>Botrytis cinerea</i>	Kern B2	University of California, Davis
Bacteria		
<i>Bacillus subtilis</i>	BCF001	Chr. Hansen A/S
<i>Bacillus amyloliquefaciens</i>	BCF007	Chr. Hansen A/S
<i>Bacillus paralicheniformis</i>	BCF009	Chr. Hansen A/S
<i>Bacillus velezensis</i>	BCF015	Chr. Hansen A/S

can provide valuable insights into types of inhibition mechanisms for further studies, and (iv) allows easy comparison of strains by accurate quantification of their inhibition potencies.

MATERIALS AND METHODS

Microbial species and growth conditions. The fungal and bacterial strains used in the inhibition assays are shown in Table 1. Fungal species were cultivated on potato dextrose agar (PDA) medium (4 g/L potato infusion, 20 g/L glucose, 15 g/L agar, pH 5.6 ± 0.2; Carl Roth). For inhibition assays on PDA, cultures were incubated at room temperature with natural light. For inhibition assays in broth, fungal spores were inoculated in potato dextrose broth (PDB) medium (6.5 g/L potato infusion, 20 g/L glucose, pH 5.6 ± 0.2; Carl Roth) and incubated at 25°C in darkness. Bacilli were grown overnight in lysogeny broth (10 g/L Bacto tryptone [Difco], 5 g/L yeast extract [Oxoid], 10 g/L NaCl [Merck], pH 7.2 ± 0.2) at 37°C with agitation at 250 rpm.

Fungal spore harvest. Spores were harvested as described by Benoit et al. (68) and Kjeldgaard et al. (69). In brief, PDA plates were inoculated with fungi and incubated at 22°C with 16-h-light/8-h-dark cycles for at least 2 weeks. Fungal spores were harvested from PDA plates using saline Tween solution (8 g/L NaCl, 0.05 mL/L Tween 80) and gentle scraping with an L-shaped spreader. The spore solution was filtered through double-layered Mira cloth (Millipore) and pelleted by centrifugation at 5,000 rpm for 10 min. The supernatant was discarded, and the spore pellet resuspended in saline Tween. Spore stocks were prepared by adding an appropriate concentration of glycerol. The spore concentration was determined by counting using a Fast-Read 102 counting chamber.

Quantification of fungal growth inhibition by coinoculation with bacterial dilution series. The fungal inhibition assay was prepared in 48-well microtiter plates with 0.5 mL PDA in each well. *Bacillus* cultures were adjusted to 2×10^{-2} or 8×10^{-4} at OD₆₀₀, and 5-fold dilution series were prepared with 6 steps using peptone saline as the diluent (maximum recovery diluent, 9.5 g/L; Millipore). Fifteen microliters of each bacterial dilution was inoculated in consecutive wells by spotting the solution in the center of each well. One strain was assigned per column. Next, a fungal spore solution was prepared with peptone saline and vortexed vigorously to disperse clumps of spores. Fifteen microliters of fungal spore solution was coinoculated with the bacterial dilutions in each well. The approximate final fungal spore concentrations of *F. culmorum*, *F. graminearum*, and *B. cinerea* were 5.5×10^6 spores/mL, 6.25×10^4 spores/mL, and 2×10^7 spores/mL, respectively. Coinoculated plates were sealed with 3M tape (0.5 cm; Millipore) to reduce growth differences between inner and peripheral wells and incubated at room temperature under natural light conditions. After 5 days, the fungal inhibition was evaluated by visual inspection and the plates were imaged by scanning (Epson Perfection V800 Photo). The minimal inhibitory cell concentration (MICC) was identified for each strain and averaged between technical duplicates and then between biological triplicates. The MICC (CFU) against each fungal species was converted to an inhibition score using equation 1, below, and statistical significance was calculated by the two-tailed Student's *t* test.

$$\text{Inhibition score} = 5 - \frac{\ln(\text{MICC})}{5} \quad (1)$$

Quantification of fungal inhibition potency by metabolites in bacterial (cell-inactive) supernatants. The fungal inhibition assay was prepared in 48-well microtiter plates with 0.5 mL PDB medium. Spores of *F. culmorum*, *F. graminearum*, or *B. cinerea* were added to a final concentration of 1.1×10^6 spores/mL, 1.25×10^4 spores/mL, or 2×10^6 spores/mL, respectively. The spore suspensions were mixed thoroughly by vortexing to ensure a homogeneous distribution. *Bacillus* species cultures were adjusted to an OD₆₀₀ of 2 and centrifuged to pellet the cells. The supernatants were collected, and the cell pellets discarded. Increasing volumes of bacterial supernatants (ranging from 10 to 80 μl) were inoculated into the fungal spore suspensions. Two approaches were implemented for sterilization of the supernatant to omit bacterial growth. Either the bacteriostatic antibiotics chloramphenicol and tetracycline were added to the fungal spore suspension to a final concentration of 50 μg/mL and 10 μg/mL, respectively, or the supernatants were sterilized by filtration (0.2-μm Minisart syringe filter; Sartorius) prior to coinoculation with the fungal spores. The plates were sealed with 3M tape and incubated at 25°C without shaking in the dark. The fungal growth was quantified by spectrophotometric measurements (OD₆₀₀) after 48 h for *F. graminearum* and *B. cinerea* inhibition assays and after 67 to 72 h

for *F. culmorum* inhibition assays. For more accurate fungal growth estimation, the OD₆₀₀ was measured using a 5-by-5 area-scanning matrix, resulting in 25 measurements per well, which were subsequently averaged. Following the evaluation of fungal growth, the supernatants were collected and plated on LB with fungicides (50 mg/L nystatin) to check for unwanted bacterial growth. Statistical analyses were done to compare the effects of (i) bacterial culture supernatants on fungal growth, (ii) filtration and antibiotics on the bacterial supernatants' potency, and (iii) prokaryotic antibiotics on fungal growth. Statistical significance was calculated by Student's *t* test (two tailed). A numerical inhibition score was assigned to each strain by quantifying the fungal growth in response to the addition of supernatant (5 volumes). The inhibition scores were calculated by subtracting the accumulated relative fungal growth from the total potential fungal growth (5 conditions tested) as shown in equation 2:

$$5 - \text{SUM (relative fungal growth)} \quad (2)$$

SUPPLEMENTAL MATERIAL

Supplemental material is available online only.

SUPPLEMENTAL FILE 1, PDF file, 0.5 MB.

ACKNOWLEDGMENTS

This project was supported by Chr. Hansen A/S and the Danish National Research Foundation (grant number DNR137) for the Center for Microbial Secondary Metabolites (DTU). B.K. was funded by a grant from the Innovation Fund Denmark (grant number 8053-00109B). The funders had no role in study design, data collection and interpretation, or the decision to submit the work for publication.

B.K., Á.T.K., A.R.N., and P.D.-C. designed the research, B.K. performed the research, B.K., Á.T.K., C.F., and P.D.-C. analyzed the data, and B.K., Á.T.K., C.F., and P.D.-C. wrote the manuscript; all authors approved the manuscript.

REFERENCES

- Food and Agriculture Organization, on behalf of the Secretariat of the International Plant Protection Convention. 2017. Plant health and food security. FAO, Rome, Italy.
- FAO. 2019. New standards to curb the global spread of plant pests and diseases. <http://www.fao.org/news/story/en/item/1187738/icode/>. Accessed 28 March 2020.
- Savary S, Ficke A, Aubertot JN, Hollier C. 2012. Crop losses due to diseases and their implications for global food production losses and food security. *Food Secur* 4:519–537. <https://doi.org/10.1007/s12571-012-0200-5>.
- Almeida F, Rodrigues ML, Coelho C. 2019. The still underestimated problem of fungal diseases worldwide. *Front Microbiol* 10:214. <https://doi.org/10.3389/fmicb.2019.00214>.
- Fisher MC, Henk DA, Briggs CJ, Brownstein JS, Madoff LC, McCraw SL, Gurr SJ. 2012. Emerging fungal threats to animal, plant and ecosystem health. *Nature* 484:186–194. <https://doi.org/10.1038/nature10947>.
- Hoffmann V, Jones K, Leroy JL. 2018. The impact of reducing dietary aflatoxin exposure on child linear growth: a cluster randomised controlled trial in Kenya. *BMJ Glob Health* 3:e000983. <https://doi.org/10.1136/bmjgh-2018-000983>.
- De Lucca AJ. 2007. Harmful fungi in both agriculture and medicine. *Rev Iberoam Micol* 24:3–13. [https://doi.org/10.1016/S1130-1406\(07\)70002-5](https://doi.org/10.1016/S1130-1406(07)70002-5).
- Lucas JA, Hawkins NJ, Fraaije BA. 2015. The evolution of fungicide resistance. *Adv Appl Microbiol* 90:29–92. <https://doi.org/10.1016/bs.aambs.2014.09.001>.
- Hahn M. 2014. The rising threat of fungicide resistance in plant pathogenic fungi: Botrytis as a case study. *J Chem Biol* 7:133–141. <https://doi.org/10.1007/s12154-014-0113-1>.
- Hellin P, King R, Urban M, Hammond-Kosack KE, Legrève A. 2018. The adaptation of *Fusarium culmorum* to DMI fungicides is mediated by major transcriptome modifications in response to azole fungicide, including the overexpression of a PDR transporter (FcABC1). *Front Microbiol* 9:1385. <https://doi.org/10.3389/fmicb.2018.01385>.
- Brauer VS, Rezende CP, Pessoni AM, De Paula RG, Rangappa KS, Nayaka SC, Gupta VK, Almeida F. 2019. Antifungal agents in agriculture: friends and foes of public health. *Biomolecules* 9:521. <https://doi.org/10.3390/biom9100521>.
- Zubrod JP, Bundschuh M, Arts G, Brühl CA, Imfeld G, Knäbel A, Payraudeau S, Rasmussen JJ, Rohr J, Scharmüller A, Smalling K, Stehle S, Schulz R, Schäfer RB. 2019. Fungicides: an overlooked pesticide class? *Environ Sci Technol* 53:3347–3365. <https://doi.org/10.1021/acs.est.8b04392>.
- Gupta PK. 2011. Herbicides and fungicides, p 503–521. In Gupta RC (ed), *Reproductive and developmental toxicology*. Academic Press, London, UK. <https://doi.org/10.1016/B978-0-12-382032-7.10039-6>.
- Kim KH, Kabir E, Jahan SA. 2017. Exposure to pesticides and the associated human health effects. *Sci Total Environ* 575:525–535. <https://doi.org/10.1016/j.scitotenv.2016.09.009>.
- Cawoy H, Bettiol W, Fickers P, Ongena M. 2011. Chapter 13. Bacillus-based biological control of plant diseases. In Stoytcheva M (ed), *Pesticides in the modern world—pesticides use and management*. IntechOpen, London, UK. <https://doi.org/10.5772/17184>.
- Prashar P, Kapoor N, Sachdeva S. 2013. Biocontrol of plant pathogens using plant growth promoting bacteria. *Sustain Agric Rev* 12:319–360. https://doi.org/10.1007/978-94-007-5961-9_10.
- Blake C, Christensen MN, Kovács ÁT. 2021. Molecular aspects of plant growth promotion and protection by *Bacillus subtilis*. *Mol Plant Microbe Interact* 34:15–25. <https://doi.org/10.1094/MPMI-08-20-0225-CR>.
- Lugtenberg B, Kamilova F. 2009. Plant-growth-promoting rhizobacteria. *Annu Rev Microbiol* 63:541–556. <https://doi.org/10.1146/annurev.micro.62.081307.162918>.
- Durairaj K, Velmurugan P, Park J-H, Chang W-S, Park Y-J, Senthilkumar P, Choi K-M, Lee J-H, Oh B-T. 2018. An investigation of biocontrol activity *Pseudomonas* and *Bacillus* strains against *Panax ginseng* root rot fungal phytopathogens. *Biol Control* 125:138–146. <https://doi.org/10.1016/j.biocontrol.2018.05.021>.
- Fira D, Dimkić I, Berić T, Lozo J, Stanković S. 2018. Biological control of plant pathogens by *Bacillus* species. *J Biotechnol* 285:44–55. <https://doi.org/10.1016/j.jbiotec.2018.07.044>.
- Cesa-Luna C, Baez A, Quintero-Hernández V, De La Cruz-Enríquez J, Castañeda-Antonio MD, Muñoz-Rojas J. 2020. The importance of antimicrobial compounds produced by beneficial bacteria on the biocontrol of phytopathogens. *Acta Biol Colomb* 25:140–154. <https://doi.org/10.15446/abc.v25n1.76867>.
- Penha RO, Vandenberghe LPS, Faulds C, Soccol VT, Soccol CR. 2020. Bacillus lipopeptides as powerful pest control agents for a more sustainable and healthy agriculture: recent studies and innovations. *Planta* 251:1–15. <https://doi.org/10.1007/s00425-020-03357-7>.
- Kiesewalter HT, Lozano-Andrade CN, Wibowo M, Strube ML, Maróti G, Snyder D, Sparholt Jørgensen T, Larsen TO, Cooper VS, Weber T, Kovács ÁT.

2020. Genomic and chemical diversity of *Bacillus subtilis* secondary metabolites against plant pathogenic fungi. *mSystems* 6:e00770-20. <https://doi.org/10.1128/mSystems.00770-20>.
24. Steinke K, Mohite OS, Weber T, Kovács ÁT. 2020. Phylogenetic distribution of secondary metabolites in the *Bacillus subtilis* species complex. *mSystems* 6:e00057-21. <https://doi.org/10.1128/mSystems.00057-21>.
 25. Pliego C, Ramos C, de Vicente A, Cazorla FM. 2011. Screening for candidate bacterial biocontrol agents against soilborne fungal plant pathogens. *Plant Soil* 340:505–520. <https://doi.org/10.1007/s11104-010-0615-8>.
 26. Folman LB, Postma J, Van Veen JA. 2003. Inability to find consistent bacterial biocontrol agents of *Pythium aphanidermatum* in cucumber using screens based on ecophysiological traits. *Microb Ecol* 45:72–87. <https://doi.org/10.1007/s00248-002-2013-0>.
 27. Raymaekers K, Ponet L, Holtappels D, Berckmans B, Cammue BPA. 2020. Screening for novel biocontrol agents applicable in plant disease management—a review. *Biol Control* 144:104240. <https://doi.org/10.1016/j.biocontrol.2020.104240>.
 28. Deketelaere S, Tyvaert L, França SC, Hofte M. 2017. Desirable traits of a good biocontrol agent against *Verticillium* wilt. *Front Microbiol* 8:1186. <https://doi.org/10.3389/fmicb.2017.01186>.
 29. Andrić S, Meyer T, Ongena M. 2020. *Bacillus* responses to plant-associated fungal and bacterial communities. *Front Microbiol* 11:1350. <https://doi.org/10.3389/fmicb.2020.01350>.
 30. Zhang X, Zhou Y, Li Y, Fu X, Wang Q. 2017. Screening and characterization of endophytic *Bacillus* for biocontrol of grapevine downy mildew. *Crop Prot* 96:173–179. <https://doi.org/10.1016/j.cropro.2017.02.018>.
 31. Latz MAC, Jensen B, Collinge DB, Lyngs Jørgensen HJ. 2020. Identification of two endophytic fungi that control *Septoria tritici* blotch in the field, using a structured screening approach. *Biol Control* 141:104128. <https://doi.org/10.1016/j.biocontrol.2019.104128>.
 32. Petatán-Sagahón I, Anducho-Reyes MA, Silva-Rojas HV, Arana-Cuenca A, Tellez-Jurado A, Cárdenas-Álvarez IO, Mercado-Flores Y. 2011. Isolation of bacteria with antifungal activity against the phytopathogenic fungus *Stenocarpella maydis* and *Stenocarpella macrospora*. *Int J Mol Sci* 12:5522–5537. <https://doi.org/10.3390/ijms12095522>.
 33. Wang L-Y, Xie Y-S, Cui Y-Y, Xu J, He W, Chen H-G, Guo J-H. 2015. Conjunctive screening of biocontrol agents (BCAs) against fusarium root rot and fusarium head blight caused by *Fusarium graminearum*. *Microbiol Res* 177:34–42. <https://doi.org/10.1016/j.micres.2015.05.005>.
 34. Jung SJ, Kim NK, Lee DH, Hong SI, Lee JK. 2018. Screening and evaluation of *Streptomyces* species as a potential biocontrol agent against a wood decay fungus, *Gloeophyllum trabeum*. *Mycobiology* 46:138–146. <https://doi.org/10.1080/12298093.2018.1468056>.
 35. Khan N, Martínez-Hidalgo P, Ice TA, Maymon M, Humm EA, Nejat N, Sanders ER, Kaplan D, Hirsch AM. 2018. Antifungal activity of bacillus species against fusarium and analysis of the potential mechanisms used in biocontrol. *Front Microbiol* 9:2363. <https://doi.org/10.3389/fmicb.2018.02363>.
 36. Besset-Manzoni Y, Joly P, Brutel A, Gerin F, Soudière O, Langin T, Prigent-Combaret C. 2019. Does in vitro selection of biocontrol agents guarantee success in planta? A study case of wheat protection against *Fusarium* seedling blight by soil bacteria. *PLoS One* 14:e0225655. <https://doi.org/10.1371/journal.pone.0225655>.
 37. Dai Y, Wu XQ, Wang YH, Zhu ML. 2021. Biocontrol potential of *Bacillus pumilus* HR10 against *Sphaeropsis* shoot blight disease of pine. *Biol Control* 152:104458. <https://doi.org/10.1016/j.biocontrol.2020.104458>.
 38. Kim YS, Lee Y, Cheon W, Park J, Kwon H-T, Balaraju K, Kim J, Yoon YJ, Jeon Y. 2021. Characterization of *Bacillus velezensis* AK-0 as a biocontrol agent against apple bitter rot caused by *Colletotrichum gloeosporioides*. *Sci Rep* 11:626. <https://doi.org/10.1038/s41598-020-80231-2>.
 39. Langvad F. 1999. A rapid and efficient method for growth measurement of filamentous fungi. *J Microbiol Methods* 37:97–100. [https://doi.org/10.1016/S0167-7012\(99\)00053-6](https://doi.org/10.1016/S0167-7012(99)00053-6).
 40. Broekaert WF, Terras FRG, Cammue BPA, Vanderleyden J. 1990. An automated quantitative assay for fungal growth inhibition. *FEMS Microbiol Lett* 69:55–59. [https://doi.org/10.1016/0378-1097\(90\)90412-J](https://doi.org/10.1016/0378-1097(90)90412-J).
 41. Banerjee UC, Chisti Y, Moo-Young M. 1993. Spectrophotometric determination of mycelial biomass. *Biotechnol Tech* 7:313–316. <https://doi.org/10.1007/BF00150905>.
 42. Kousser C, Clark C, Sherrington S, Voelz K, Hall RA. 2019. *Pseudomonas aeruginosa* inhibits *Rhizopus microsporus* germination through sequestration of free environmental iron. *Sci Rep* 9:1–14. <https://doi.org/10.1038/s41598-019-42175-0>.
 43. Shehata MG, Badr AN, El Sohaimy SA, Asker D, Awad TS. 2019. Characterization of antifungal metabolites produced by novel lactic acid bacterium and their potential application as food biopreservatives. *Ann Agric Sci* 64: 71–78. <https://doi.org/10.1016/j.aoas.2019.05.002>.
 44. Li Y, Héloir MC, Zhang X, Geissler M, Trouvelot S, Jacquens L. 2019. Surfactin and fengycin contribute to the protection of a *Bacillus subtilis* strain against grape downy mildew by both direct effect and defence stimulation. *Mol Plant Pathol* 20:1037–1050. <https://doi.org/10.1111/mpp.12809>.
 45. Arroyave-Toro JJ, Mosquera S, Villegas-Escobar V. 2017. Biocontrol activity of *Bacillus subtilis* EA-CB0015 cells and lipopeptides against postharvest fungal pathogens. *Biol Control* 114:195–200. <https://doi.org/10.1016/j.biocontrol.2017.08.014>.
 46. Robin DC, Marchand PA. 2019. Evolution of the biocontrol active substances in the framework of the European Pesticide Regulation (EC) no. 1107/2009. *Pest Manag Sci* 75:950–958. <https://doi.org/10.1002/ps.5199>.
 47. Barzman M, Bärberi P, Birch ANE, Boonekamp P, Dachbrodt-Saaydeh S, Graf B, Hommel B, Jensen JE, Kiss J, Kudsk P, Lamichhane JR, Messéan A, Moonen A-C, Ratnadass A, Ricci P, Sarah J-L, Sattin M. 2015. Eight principles of integrated pest management. *Agron Sustain Dev* 35:1199–1215. <https://doi.org/10.1007/s13593-015-0327-9>.
 48. Droby S, Wisniewski M, Teixidó N, Spadaro D, Jijakli MH. 2016. The science, development, and commercialization of postharvest biocontrol products. *Postharvest Biol Technol* 122:22–29. <https://doi.org/10.1016/j.postharvbio.2016.04.006>.
 49. Backer R, Rokem JS, Ilangumaran G, Lamont J, Praslickova D, Ricci E, Subramanian S, Smith DL. 2018. Plant growth-promoting rhizobacteria: context, mechanisms of action, and roadmap to commercialization of biostimulants for sustainable agriculture. *Front Plant Sci* 9:1473. <https://doi.org/10.3389/fpls.2018.01473>.
 50. Barratt BIP, Moran VC, Bigler F, van Lenteren JC. 2018. The status of biological control and recommendations for improving uptake for the future. *BioControl* 63:155–167. <https://doi.org/10.1007/s10526-017-9831-y>.
 51. Köhl J, Booi K, Kolnaar R, Ravensberg WJ. 2019. Ecological arguments to reconsider data requirements regarding the environmental fate of microbial biocontrol agents in the registration procedure in the European Union. *BioControl* 64:469–487. <https://doi.org/10.1007/s10526-019-09964-y>.
 52. Köhl J, Postma J, Nicot P, Ruocco M, Blum B. 2011. Stepwise screening of microorganisms for commercial use in biological control of plant-pathogenic fungi and bacteria. *Biol Control* 57:1–12. <https://doi.org/10.1016/j.biocontrol.2010.12.004>.
 53. Tao X, Zhang H, Gao M, Li M, Zhao T, Guan X. 2020. *Pseudomonas* species isolated via high-throughput screening significantly protect cotton plants against *verticillium* wilt. *AMB Expr* 10:1–12. <https://doi.org/10.1186/s13568-020-01132-1>.
 54. Leelasuphakul W, Hemmanee P, Chuenchitt S. 2008. Growth inhibitory properties of *Bacillus subtilis* strains and their metabolites against the green mold pathogen (*Penicillium digitatum* Sacc.) of citrus fruit. *Postharvest Biol Technol* 48:113–121. <https://doi.org/10.1016/j.postharvbio.2007.09.024>.
 55. Iqar I, Shinwari ZK, El-Sayed A, Ali GS. 2019. Bioactivity-driven high throughput screening of microbiomes of medicinal plants for discovering new biological control agents. *BioRxiv*. <https://doi.org/10.1101/611855>.
 56. Leyva Salas M, Thierry A, Lemaître M, Garric G, Harel-Oger M, Chatel M, Lê S, Mounier J, Valence F, Coton E. 2018. Antifungal activity of lactic acid bacteria combinations in dairy mimicking models and their potential as bioprotective cultures in pilot scale applications. *Front Microbiol* 9:1787. <https://doi.org/10.3389/fmicb.2018.01787>.
 57. Garnier L, Salas ML, Pinon N, Wiernasz N, Pawtowski A, Coton E, Mounier J, Valence F. 2018. Technical note: high-throughput method for antifungal activity screening in a cheese-mimicking model. *J Dairy Sci* 101: 4971–4976. <https://doi.org/10.3168/jds.2017-13518>.
 58. Han JH, Shim H, Shin JH, Kim KS. 2015. Antagonistic activities of *Bacillus* spp. strains isolated from tidal flat sediment towards anthracnose pathogens *Colletotrichum acutatum* and *C. gloeosporioides* in South Korea. *Plant Pathol J* 31:165–175. <https://doi.org/10.5423/PPJ.OA.03.2015.0036>.
 59. Haidar R, Roudet J, Bonnard O, Dufour MC, Corio-Costet MF, Fert M, Gautier T, Deschamps A, Fermaud M. 2016. Screening and modes of action of antagonistic bacteria to control the fungal pathogen *Phaeoaniella chlamydospora* involved in grapevine trunk diseases. *Microbiol Res* 192:172–184. <https://doi.org/10.1016/j.micres.2016.07.003>.
 60. Porter AS, Evans-FitzGerald C, McElwain JC, Yiotis C, Elliott-Kingston C. 2015. How well do you know your growth chambers? Testing for chamber effect using plant traits. *Plant Methods* 11:44. <https://doi.org/10.1186/s13007-015-0088-0>.
 61. Wang T, Liang Y, Wu M, Chen Z, Lin J, Yang L. 2015. Natural products from *Bacillus subtilis* with antimicrobial properties. *Chin J Chem Eng* 23: 744–754. <https://doi.org/10.1016/j.cjche.2014.05.020>.

62. Kilani-Feki O, Ben Khedher S, Dammak M, Kamoun A, Jabnoun-Khiareddine H, Daami-Remadi M, Tounsi S. 2016. Improvement of antifungal metabolites production by *Bacillus subtilis* V26 for biocontrol of tomato postharvest disease. *Biol Control* 95:73–82. <https://doi.org/10.1016/j.biocontrol.2016.01.005>.
63. Oh HS, Lee YH. 2000. A target-site-specific screening system for antifungal compounds on appressorium formation in *Magnaporthe grisea*. *Phytopathology* 90:1162–1168. <https://doi.org/10.1094/PHTO.2000.90.10.1162>.
64. Kilani-Feki O, Culioli G, Ortalo-Magné A, Zouari N, Blache Y, Jaoua S. 2011. Environmental *Burkholderia cepacia* strain Cs5 acting by two analogous alkyl-quinolones and a didecyl-phthalate against a broad spectrum of phytopathogenic fungi. *Curr Microbiol* 62:1490–1495. <https://doi.org/10.1007/s00284-011-9892-6>.
65. Mansfield J, Genin S, Magori S, Citovsky V, Sriariyanum M, Ronald P, Dow M, Verdier V, Beer SV, Machado MA, Toth I, Salmond G, Foster GD. 2012. Top 10 plant pathogenic bacteria in molecular plant pathology. *Mol Plant Pathol* 13:614–629. <https://doi.org/10.1111/j.1364-3703.2012.00804.x>.
66. Chen X, Wang Y, Gao Y, Gao T, Zhang D. 2019. Inhibitory abilities of *Bacillus* isolates and their culture filtrates against the gray mold caused by *Botrytis cinerea* on postharvest fruit. *Plant Pathol J* 35:425–436. <https://doi.org/10.5423/PPJ.OA.03.2019.0064>.
67. Xu W, Wang K, Wang H, Liu Z, Shi Y, Gao Z, Wang Z. 2020. Evaluation of the biocontrol potential of *Bacillus* sp. WB against *Fusarium oxysporum* f. sp. niveum. *Biol Control* 147:104288. <https://doi.org/10.1016/j.biocontrol.2020.104288>.
68. Benoit I, van den Esker MH, Patyshakuliyeva A, Mattern DJ, Blei F, Zhou M, Dijksterhuis J, Brakhage AA, Kuipers OP, de Vries RP, Kovács ÁT. 2015. *Bacillus subtilis* attachment to *Aspergillus niger* hyphae results in mutually altered metabolism. *Environ Microbiol* 17:2099–2113. <https://doi.org/10.1111/1462-2920.12564>.
69. Kjeldgaard B, Listian SA, Ramaswamhi V, Richter A, Kiesewalter HT, Kovács ÁT. 2019. Fungal hyphae colonization by *Bacillus subtilis* relies on biofilm matrix components. *Biofilm* 1:100007. <https://doi.org/10.1016/j.biofilm.2019.100007>.

1 **Supplementary material**

2 **Table S1.** The minimal inhibitory cell concentration (MICC) was determined for *B. subtilis* BCF001,
 3 *B. amyloliquefaciens* BCF007, *B. velezensis* BCF015 and *B. paralicheniformis* BCF009, as the lower
 4 number of cells (CFUs) that inhibit growth of *F. culmorum*, *F. graminearum* and *B. cinerea* by co-
 5 cultivation. The MICC against each fungal species was converted to an inhibition score by formula #1.
 6 For quantification of the culture supernatant inhibition potency, an inhibition score was calculated by
 7 formula #2 for each bacterial strain and for each experimental cell-inactivation method.

8

	BCF001	BCF007	BCF009	BCF015
MICC (CFU)				
<i>F. culmorum</i>	1903	<339	>3.89*10 ⁶	<497
<i>F. graminearum</i>	57	60	>1.09*10 ⁵	74
<i>B. cinerea</i>	67	150	>1.10*10 ⁵	153
Co-cultivation inhibition score				
<i>F. culmorum</i>	3.8	4.5	0.8	4.4
<i>F. graminearum</i>	3.4	3.4	0.4	3.3
<i>B. cinerea</i>	3.3	3.0	0.4	3.0
Supernatant inhibition score (antibiotics)				
<i>F. culmorum</i>	2.63	2.81	0.62	2.06
<i>F. graminearum</i>	2.14	1.57	-0.43	1.81
<i>B. cinerea</i>	3.53	3.43	1.75	3.50
Supernatant inhibition score (filtration)				
<i>F. culmorum</i>	2.52	2.64	0.46	2.13
<i>F. graminearum</i>	2.04	1.22	-0.50	1.81
<i>B. cinerea</i>	3.55	3.42	1.32	3.53
Supernatant inhibition score (filtration and antibiotics)				
<i>F. culmorum</i>	2.47	2.56	0.26	1.81
<i>F. graminearum</i>	2.35	1.37	-0.40	1.72
<i>B. cinerea</i>	3.50	3.35	0.81	3.50

9

10 **Table S2.** The significance of the minimal inhibitory cell concentration (MICC) against each fungus was
 11 determined for *B. subtilis* BCF001, *B. amyloliquefaciens* BCF007, *B. velezensis* BCF015 and

12 *B. paralicheniformis* BCF009 by students t-test comparison between the strains. Statistically significant
 13 values ($p < 0.05$) are indicated in red.

14

Compared strains	<i>F. culmorum</i>	<i>F. graminearum</i>	<i>B. cinerea</i>
BCF001/BCF007	0.00	0.45	0.10
BCF001/BCF009	$2 * 10^{-64}$	0.04	0.04
BCF001/BCF015	$2 * 10^{-66}$	0.32	0.15
BCF007/BCF009	$2 * 10^{-64}$	0.04	0.04
BCF007/BCF015	$1 * 10^{-62}$	0.32	0.48
BCF009/BCF015	$2 * 10^{-64}$	0.04	0.04

15

16 **Table S3.** Statistical significance of different *Bacillus* supernatant sterilization methods on fungal
 17 inhibition results. Statistical significance was calculated using student's t-test. Statistically significant
 18 values ($p < 0.05$) are indicated in red.

Filtered supernatants with antibiotics compared to supernatants with antibiotics						
Supernatant volume (μ l)		10	20	40	60	80
<i>F. culmorum</i>	BCF001	0.43	0.55	0.69	0.18	0.12
	BCF007	0.21	0.01	0.24	0.82	0.11
	BFC009	0.97	0.2	0.05	0.08	0.01
	BFC015	0.77	0.31	0.09	0.01	0.04
<i>F. graminearum</i>	BCF001	0.88	0.09	0.01	0	0.94
	BCF007	0.31	0.14	0.66	0.85	0.06
	BFC009	0.3	0.44	0.45	0.61	0.78
	BFC015	0.28	0.01	0.6	0.34	0.32
<i>B. cinerea</i>	BCF001	0.11	0.61	0.4	0.89	0.71
	BCF007	0.81	0.51	0.08	0.34	0.34
	BFC009	0.07	0.1	0.02	0.1	0.22
	BFC015	0.46	0.51	0.06	0.82	1
Filtered supernatants with antibiotics compared to filtered supernatants						
Supernatant volume (μ l)		10	20	40	60	80
<i>F. culmorum</i>	BCF001	0.77	0.04	0.97	0.52	0.84
	BCF007	0.02	0	0.06	0.02	0.87
	BFC009	0.07	0.13	0.62	0.97	0.09

	BFC015	0.42	0	0.18	0.09	0.04
<i>F. graminearum</i>	BCF001	0.39	0.2	0.01	0.03	0.32
	BCF007	0.42	0.75	0.08	0.05	0.98
	BFC009	0.29	0.8	0.04	0.91	0.37
	BFC015	0.09	0.93	0.71	0.63	0.72
<i>B. cinerea</i>	BCF001	0.55	0.71	0.52	0.35	0.27
	BCF007	0.46	0.82	0	0.11	0
	BFC009	0.24	0.01	0.47	0.22	0.33
	BFC015	0.15	0.89	0.03	0.35	0

Filtered supernatants compared to supernatants with antibiotics

Supernatant volume (μl)		10	20	40	60	80
<i>F. culmorum</i>	BCF001	0.38	0.29	0.7	0.04	0.16
	BCF007	0.31	0	0.23	0.01	0.41
	BFC009	0	0.71	0.07	0.07	0.13
	BFC015	0.58	0.61	0.47	0.69	0.27
<i>F. graminearum</i>	BCF001	0.42	0.82	0.16	0.81	0.37
	BCF007	0.19	0.12	0.18	0.03	0.07
	BFC009	0.19	0.54	0.14	0.42	0.24
	BFC015	0.2	0.19	0.53	0.81	0.16
<i>B. cinerea</i>	BCF001	0.2	0.32	0.35	0.5	0.44
	BCF007	0.03	0.47	0.04	0.36	0
	BFC009	0.29	0.47	0.06	0.13	0.56
	BFC015	0.32	0.7	0.06	0.19	0.01

19

20

21

22

23

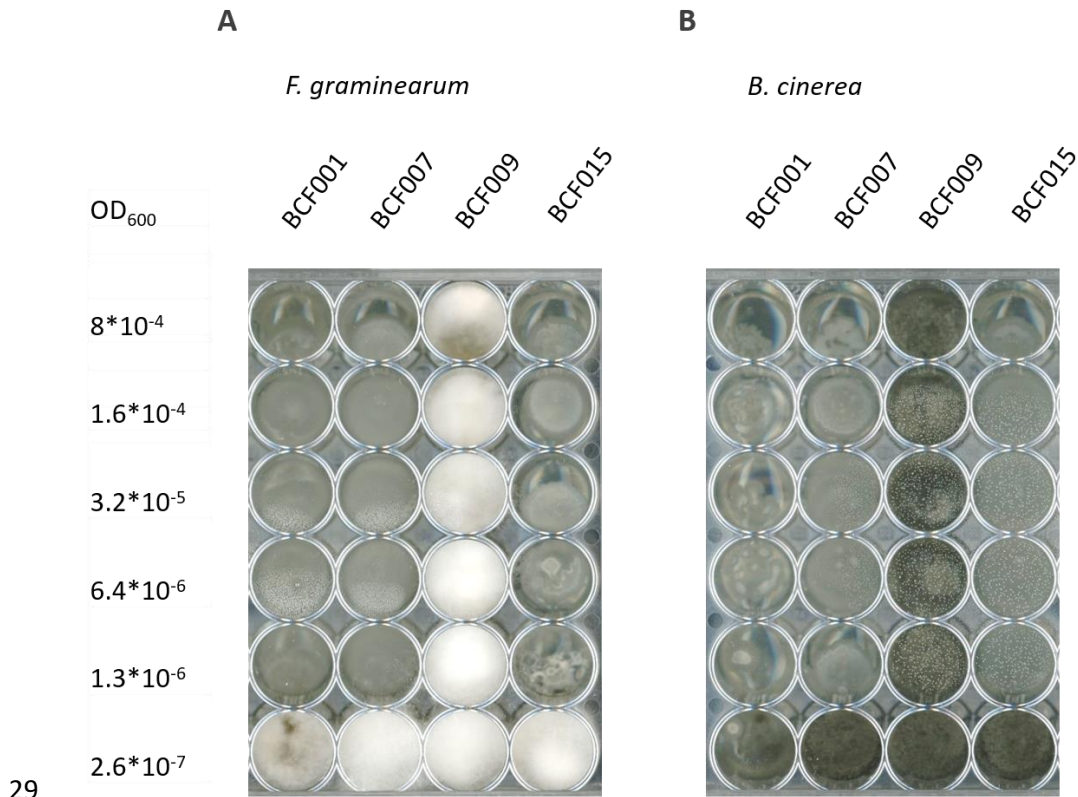
24

25

26

27 **Supplementary figures**

28

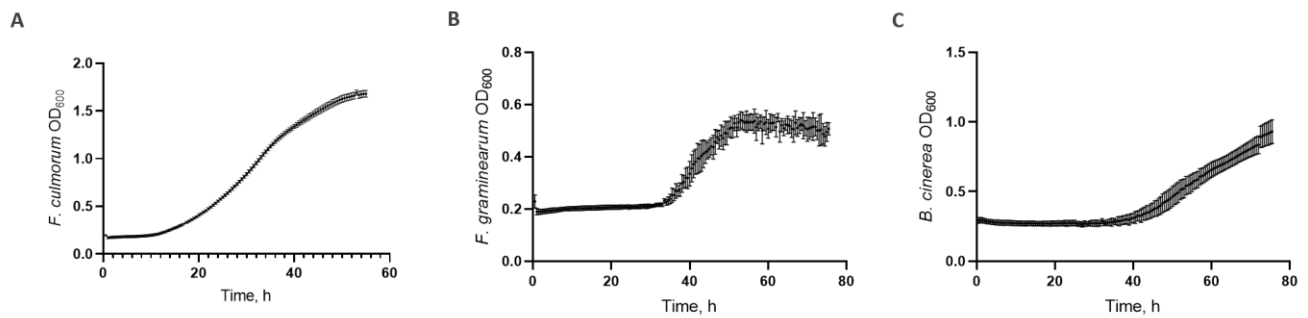


29

30

31 **Fig. S1.** Fungal inhibition assay with *Bacillus* dilution series. Dilution series of *B. subtilis* BCF001,
32 *B. amyloliquefaciens* BCF007, *B. paralicheniformis* BCF009 and *B. velezensis* BCF015 were prepared and
33 inoculated in consecutive columns of a 48-well microtiter plate. In each well, a constant spore
34 concentration was inoculated of (A) *F. graminearum* and (B) *B. cinerea*. Pictures are representative of
35 triplicates.

36

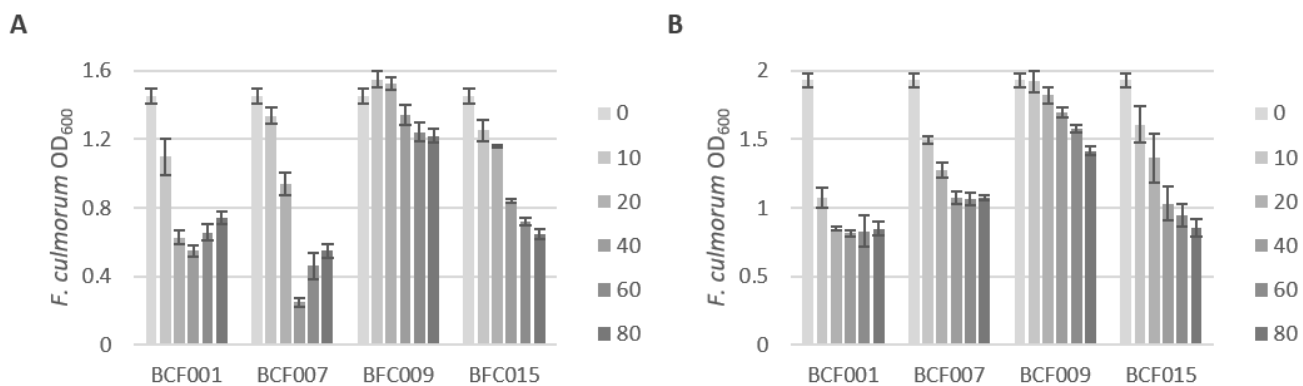


37

38

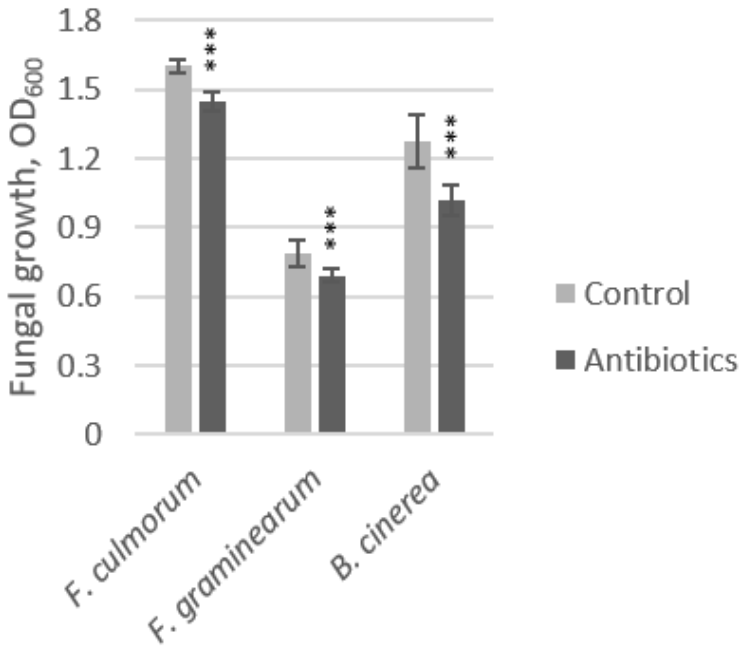
39 **Fig. S2.** Fungal growth monitored of A) *F. culmorum* B) *F. graminearum* and C) *B. cinerea* over 3 days by
 40 spectrophotometry using a 5x5 area scan protocol of each well. Subsequently the 25 measurements of
 41 each well were averaged.

42



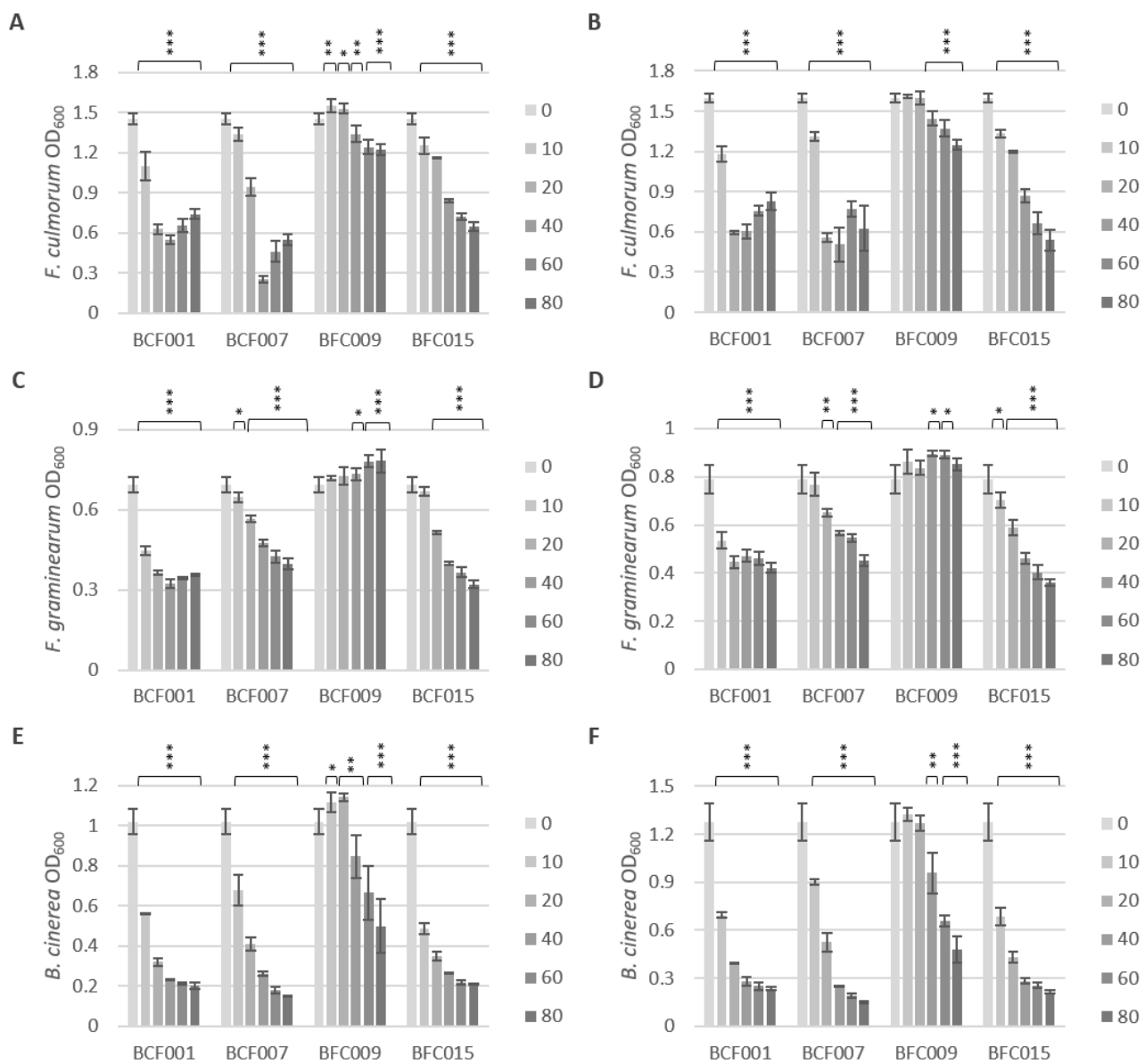
43

44 **Fig. S3.** Variation of *F. culmorum* growth with *Bacillus* supernatants. Inhibition assays with *F. culmorum*
 45 were prepared from different spore solutions and reached different final growth after 67h (A) and 72h
 46 (B) cultivation in PDB medium both with and without bacterial culture supernatants. Growth was
 47 evaluated by spectrophotometric measurements (OD₆₀₀). Standard deviations were calculated from
 48 biological triplicates.



49

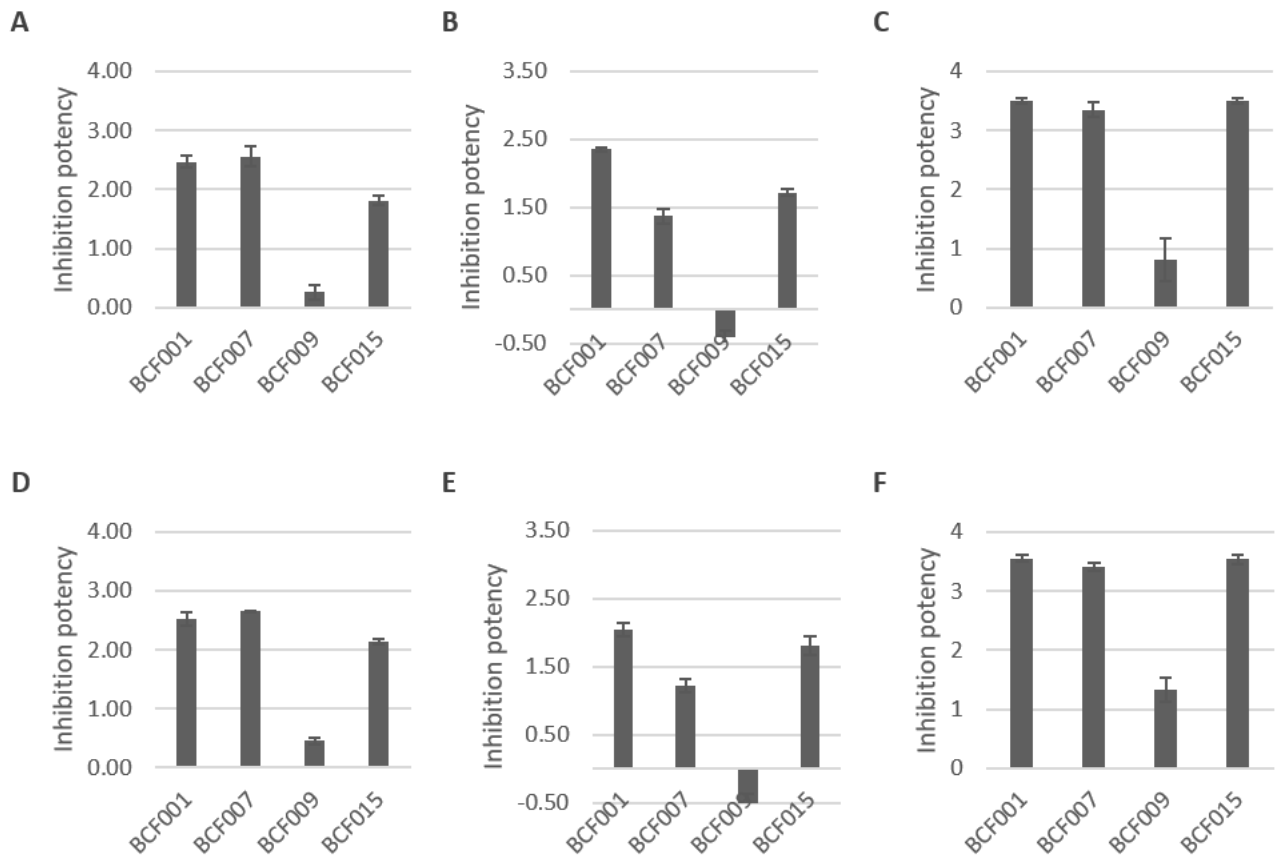
50 **Fig. S4.** Growth of *F. culmorum*, *F. graminearum* and *B. cinerea* without and without addition of
 51 antibiotics (50 µg/ml chloramphenicol and 10 µg/ml tetracycline). ***P<0.0005



52

53 **Fig. S5.** Comparison of methods to circumvent bacterial cell growth in fungal inhibition assays with
 54 bacterial supernatants. Fungal spore suspensions of *F. culmorum* (A,B), *F. graminearum* (C,D) and
 55 *B. cinerea* (E,F) were inoculated with filtered bacterial culture with antibiotics (A, C, and E) or without
 56 addition of antibiotics (B, D, and F). *P<0.05, **P<0.005, ***P<0.0005.

57



58

59 **Fig. S6.** Comparison of supernatant inhibition potencies using *Bacillus* cell inactivation by filtration and
 60 antibiotic addition or by filtration only. The culture supernatant inhibition potencies of *B. subtilis*
 61 BCF001, *B. amyloliquefaciens* BCF007, *B. paralicheniformis* BCF009 and *B. velezensis* BCF015 against
 62 *F. culmorum* (A,D), *F. graminearum* (B,E) and *B. cinerea* (C,F) were calculated by applying the formula
 63 #2. The effect of bacterial cell inactivation by filtration and antibiotic addition (A-C) was compared to
 64 bacterial cell inactivation by filtration (D-F).

65

Study 4

Kjeldgaard, B., Fonseca, C., Kovács, Á. T., and Domínguez-Cuevas, P.

Assessment of antifungal potential of natural *Bacillus* spp. isolates.

To be submitted.

Assessment of antifungal potential of natural *Bacillus* spp. isolates

Bodil Kjeldgaard^{1,2}, César Fonseca¹, Ákos T. Kovács², Patricia Domínguez- Cuevas^{1,3}

¹Discovery, R&D, Chr. Hansen A/S, Denmark

²Bacterial Interactions and Evolution Group, DTU Bioengineering, Technical University of Denmark

³Current affiliation: Scientific Integration, Early Innovation, Outreach and Alliances. Novo Nordisk A/S, Denmark

Abstract

Bacillus spp. are known for their potential to produce a vast array of specialized metabolites with various antimicrobial properties. Their bioactivity makes them excellent candidates for agricultural biocontrol applications. Here, we assess the inhibitory potential of different species of undomesticated *Bacillus* isolates using: i) genomic analysis of biosynthetic gene clusters (BGCs) related to the production of bioactive metabolites; ii) biochemical analysis of bacterial supernatants for the detection and relative quantification of lipopeptide/polyketide compounds, and iii) *in vitro* inhibition of fungal plant pathogens by bacterial cultures and/or respective supernatants. BGC mining revealed the genomic potential of the selected bacterial strains to produce antifungal metabolites, the LC-MS analysis of the culture supernatants evaluated the capacity of the strains to produce those metabolites, while the identities and levels of the metabolites were correlated with the *in vitro* fungal inhibition potency of the strains. The detection of high amounts of the antifungal iturins and fengycins from cultures of *Bacillus subtilis*, *Bacillus amyloliquefaciens* and *Bacillus velezensis* strains correlated with the observed prominent inhibition of *Fusarium culmorum*, *Fusarium graminearum* and *Botrytis cinerea*, while the absence of lipopeptide production aligned with the complete lack of fungal inhibition by a *Bacillus megaterium* (recently reclassified as *Priestia megaterium*) strain.

Importance

The bioactivity of a bacterial biocontrol strain greatly depends on the production of specialized metabolites. Therefore, genomic analysis, predicting the presence of BGCs, in combination with the biochemical identification of metabolites, respective levels in bacterial supernatants, and *in vitro* fungal inhibition with the same supernatants, ensures proper selection of good biocontrol candidate strains prior to more expensive experiments, for instance, green house or field trials. Here, we evaluated the potential of 14 undomesticated *Bacillus* isolates against important phytopathogens, including *F. culmorum*, *F. graminearum*, and *B. cinerea*. Biocontrol potential was assessed through three types of fungal inhibition assays: i) dual species plate confrontation, ii) inhibition by co-inoculation with *Bacillus* culture, and iii) inhibition by *Bacillus* cell-free culture supernatant.

Results

Prediction of biosynthetic gene clusters for the production of antifungal compounds

While some polyketides such as bacillaene or difficidin display antibacterial properties (1), cyclic lipopeptides are essential for fungal inhibition. In respect to growth inhibition of *Fusarium* and *Botrytis* species, specifically iturins and fengycins are important (2–5), whereas surfactins might have an additive synergistic effect in combination with fengycins/plipastatins against *B. cinerea* (6). Having access to whole genome sequences of many *Bacillus* strains, the genomic potential for biosynthesis of specialized metabolites can be estimated and provide valuable insight for natural product discovery and selection of biocontrol candidate strains (7). To elucidate the genomic potential of *Bacillus* isolates, antiSMASH, the web server tool for automatic genomic identification and analysis of biosynthetic gene clusters (8) was used in combination with compound annotation from Minimum Information about a Biosynthetic Gene cluster (MiBIG) (9) (Fig. 1). Mining of biosynthetic gene clusters (BGCs) predicted that all strains had the potential for biosynthesis of the antifungal compounds of the fengycin family of cyclic lipopeptides, and the siderophore bacillibactin, except for *Bacillus megaterium* (recently reclassified as *Priestia megaterium*) BCF008. This strain contained low similarity to the surfactin BGC and to a carotenoid BGC annotated from *Halobacillus halophilus*. The fengycin BGCs in *Bacillus subtilis* strains (BCF001, BCF002, BCF003, BCF004, BCF010) are most likely misidentified plipastatin BGCs, as a recent study demonstrated the specificity of the fengycin BGC to the *B. amyloliquefaciens* clade (10). Predictions also showed potential for bacillaene and bacilysin biosynthesis in most strains except *Bacillus paralicheniformis* (BCF005, BCF006, BCF009), whereas the polyketide macrolactin were specific to *Bacillus amyloliquefaciens* (BCF007) and *Bacillus velezensis* strains (BCF014, BCF015). The lichenysin and bacitracin BGCs were only predicted in *B. paralicheniformis* strains (BCF005, BCF006, BCF009) in accordance with genome mining studies (10). The findings of our BGC mining analysis align with the existing literature, which suggests that the co-occurrence of fengycin and bacitracin BGCs serves as a potential taxonomic marker for distinguishing *B. paralicheniformis* from *B. licheniformis*, as the fengycin operon is absent in the latter species (11, 12). In addition, difficidin was specific to BCF014 and BCF015 in accordance to a phylogenetic study of BGCs, where these compounds were mainly found in the *B. velezensis* clade (10). Additional BLAST search of *B. amyloliquefaciens* BCF007 and *B. velezensis* BCF015 identified the presence of iturin and bacillomycin BGCs, respectively, adjacent to the fengycin BCG, as previously reported (13). The proximity between the BCGs may explain why the iturin BGCs were not identified by AntiSMASH and MiBig genome mining and suggests that iturin BGCs may be found in the other *B. velezensis* strains (BCF12, BCF013, BCF014) as well.

BGC	Compound	BCF001 <i>B. subtilis</i>	BCF002 <i>B. subtilis</i>	BCF003 <i>B. subtilis</i>	BCF004 <i>B. subtilis</i>	BCF010 <i>B. subtilis</i>	BCF005 <i>B. paralicheniformis</i>	BCF006 <i>B. paralicheniformis</i>	BCF009 <i>B. paralicheniformis</i>	BCF012 <i>B. velezensis</i>	BCF013 <i>B. velezensis</i>	BCF014 <i>B. velezensis</i>	BCF015 <i>B. velezensis</i>	BCF007 <i>B. amyloliquefaciens</i>	BCF008 <i>P. (Bacillus) megaterium</i>
BGC0000433	Surfactin	43	78	43	43	43				91	47	91	91	82	13
BGC0001184	Bacilycin	100	100	100	100	100				100	100	100	100	100	
BGC0000407	Plipastatin	30		23											
BGC0000602	Subtilosin A	100	100	100	100	100									
BGC0000309	Bacillibactin	100	100	100	100	100	53	53	53	100	100	100	100	100	
BGC0000381	Lichenysin						100	100	100						
BGC0000310	Bacitracin						100	100	100						
BGC0000527	Mersacidin														100
BGC0000181	Macrolactin H									100	100	100	100	100	
BGC0000176	Difficidin									100	100	53	100		
BGC0001095	Fengycin	86	80	80	93	86	66	66	66	80	80	20	80	100	
BGC0001089	Bacilleane	100	100	100		100				100	100	100	100	100	
BGC0001114	Thailanstatin	10	10	10		10									
BGC0000693	Butirosin A/B						7	7	7	7	7	7	7	7	
BGC0000517	Haloduracin α/β						40	40	40						
BGC0000645	Carotenoid														50

Fig. 1. Genome mining of Biosynthetic Gene Clusters (BGCs) in selected *Bacillus* strains. Predicted known BGCs and the percental amino acid similarity were identified in each natural isolate and the potentially produced compound was annotated from MiBIG. Information about FZB42 BGCs were retrieved from literature and MiBig (Chen et al., 2007).

Semi-quantitative analysis of bioactive metabolites

LC-MS analysis confirmed the presence of the antifungal compound fengycin/plipastatin family in all *Bacillus* culture supernatants, except for *P. megaterium* BCF008 (Fig. 2). Fengycin/plipastatin were not differentiated, as distinction these metabolites cannot be performed by the LC-MS analysis. No lipopeptide or polyketide compounds were detected in samples from this *P. megaterium* strain making its antifungal potential questionable. High content of fengycin was detected in several cultures from the *Bacillus subtilis* strains (BCF001, BCF002, BCF003, BCF006, BCF010) and in the culture from *B. amyloliquefaciens* BCF007 raising their prospects for fungal inhibition. Surfactins were identified in all *B. subtilis*, *B. velezensis* and *B. amyloliquefaciens* strains (Fig. 2) in accordance with BCG predictions (Fig. 1). The lower percental similarity of surfactin BGCs in the *B. subtilis* strains may arise from the species origin of the MiBIG annotation (*B. velezensis* FZB42). The polyketides macrolactin, difficidin were specific to the *B. velezensis* and *B.*

amyloliquefaciens strains, in accordance with the BCG mining results. The *B. velezensis* strains BCF014 and BCF015 produced higher amounts of bacillomycin, whereas BCF007 produced the higher amount of iturin, both compounds with reported antifungal properties (14, 15). Although, the BGC for biosynthesis of bacillibactin was predicted in most natural isolates, not all strains produced the siderophore under the conditions tested, emphasizing that presence of a BGC does not necessarily equal production of the respective compound (16).

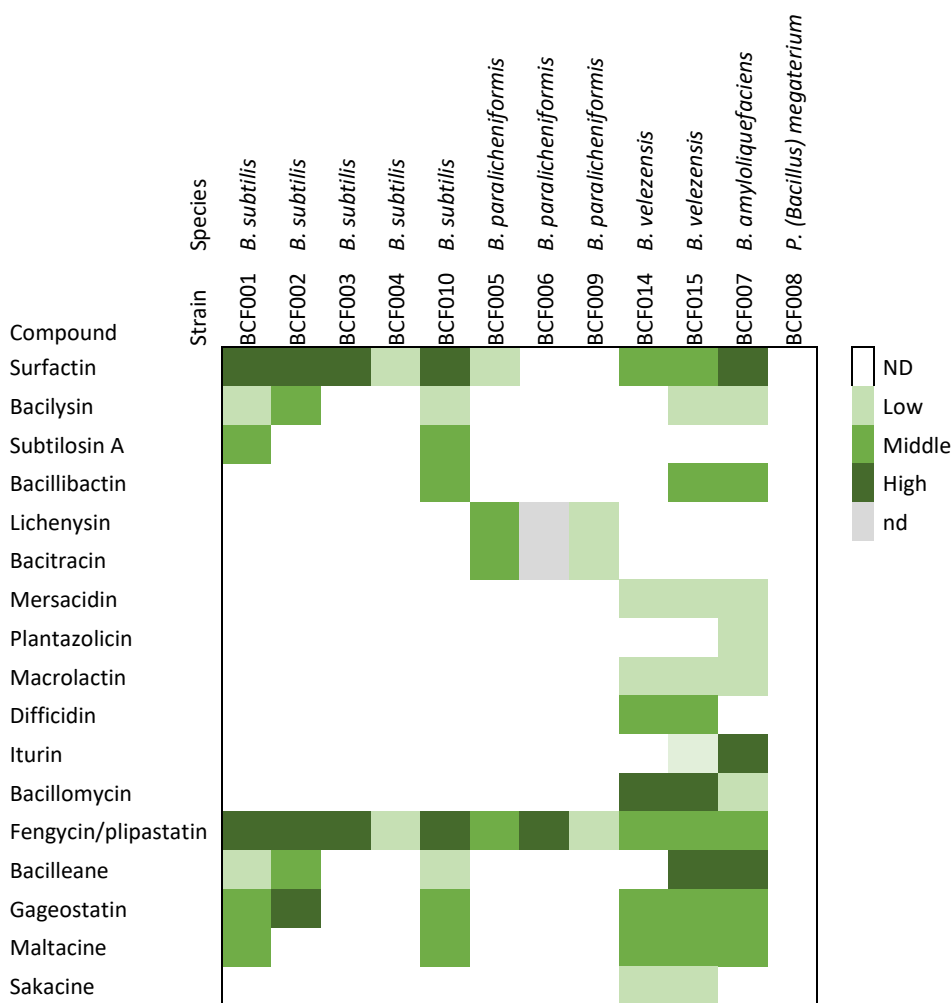


Fig. 2. Relative levels of specialized metabolites produced by selected *Bacillus* strains. LC-MS analysis of culture supernatants from *Bacillus* spp. grown for 24-48 h in PDB, LB, M2 or MSgg media at 37 °C. Color gradient, from light green (low levels) to dark green (high levels), refers to relative levels of bioactive metabolites from average peak areas of biological duplicates. Nd= no data.

Plate confrontation inhibition assays

The inhibition potency of 14 undomesticated isolates of various *Bacillus* species in addition to the well-described biocontrol strain *B. velezensis* FZB42 (17) and *B. subtilis* NCIB3610 (18) was evaluated against the phytopathogenic fungi *Fusarium culmorum* DSM1094, *F. graminearum* DSM4528, and *Botrytis cinerea* Kern

B2 by plate confrontation assays on LB and PDA media (Fig. 2, Fig. S1). The *Bacillus velezensis* (BCF012, BCF013, BCF014, BCF015, FZB42) and *B. amyloliquefaciens* (BCF007) strains displayed prominent inhibition of both *Fusarium* species by spreading (FZB42) or by secretion of bioactive metabolites into the medium creating a growth free zone surrounding the colony. Against all three fungal species, the *B. subtilis* strains BCF001, BCF002 and BCF010 showed considerable inhibition, while other *B. subtilis* strains were less inhibitory (BCF003, BCF004). *Bacillus paralicheniformis* strains (BCF005, BCF006, BCF009) inhibited fungal growth to a lesser degree, while *P. megaterium* strain BCF008 failed to impact *Fusarium* growth at all (not tested against *B. cinerea*).

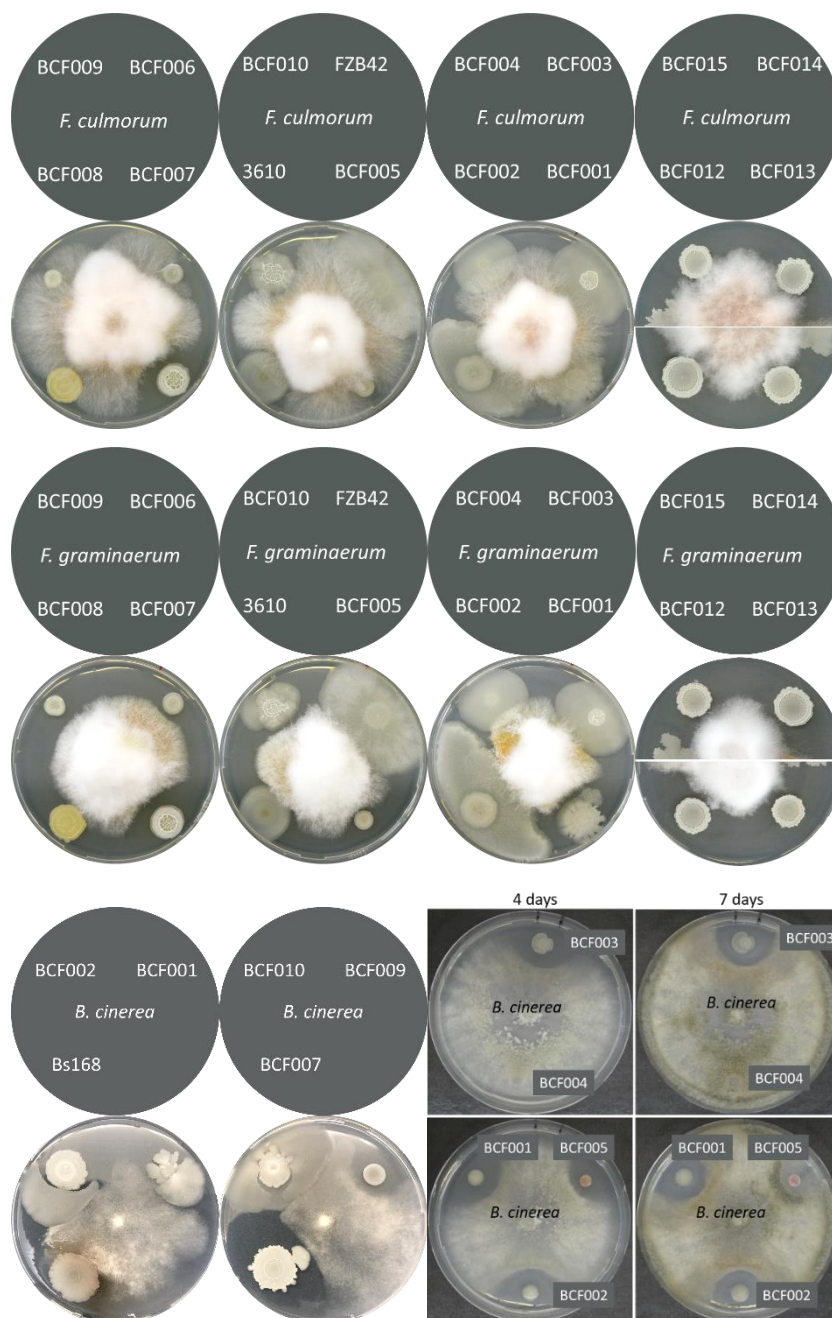


Fig. 3. Plate inhibition of fungi by selected *Bacillus* strains. Fourteen natural *Bacillus* isolates (*B. subtilis* BCF001, BCF002, BCF003, BCF004, BCF010, *B. paralicheniformis* BCF005, BCF006, BCF009, *B. amyloliquefaciens* BCF007, *B. velezensis* BCF012, BCF013, BCF014, BCF015, *P. megaterium* BCF008) and two benchmark strains (*B. velezensis* FZB42 and *B. subtilis* NCIB3610) were inoculated with a fixed distance to a central fungal inoculum on PDA medium. Growth of the fungi *F. culmorum*, *F. graminearum*, and *B. cinerea* and degree of inhibition was evaluated after 4-7 days incubation under natural light at room temperature. *Bacillus* strains and challenged fungus are indicated above plates or directly on image.

Fungal inhibition by co-inoculation with *Bacillus* cultures

To achieve comparable measures of inhibition potency, dilution series of *Bacillus* cultures were co-inoculated with a specific concentration of fungal spores and the minimal inhibitory dilution (MID) that prevented fungal growth was identified (Kjeldgaard et al., 2022, **Study 3**). For visualization and easy comparison between strains' potencies, the negative natural logarithm was calculated for the MIDs (equation 1#).

$$1\# \quad \text{Inhibition potency} = -\text{LN}(\text{MID})$$

Co-inoculation with *B. velezensis* strains (BCF012, BCF014, BCF015, FZB42) and *B. amyloliquefaciens* (BCF007) challenged *F. culmorum* growth most severely, while *B. subtilis* strains (BCF001, BCF002, BCF010) exhibited good inhibition and *B. paralicheniformis* BCF009 left the fungal growth unaffected (Fig. 3). When tested against *F. graminearum*, the inhibition potencies of *B. amyloliquefaciens* BCF007, *B. subtilis* BCF001 and *B. velezensis* FZB42 were similar to those observed against *F. culmorum*. Interestingly, *B. subtilis* strains (BCF001, BCF002, BCF010) appeared relatively more potent against *B. cinerea*, although *B. velezensis* strains (BCF015, FZB42) also inhibited the fungus effectively. In accordance with previous observations with *F. culmorum*, *F. graminearum* and *B. cinerea* growth remained unaffected when co-inoculated with *B. paralicheniformis* BCF009.

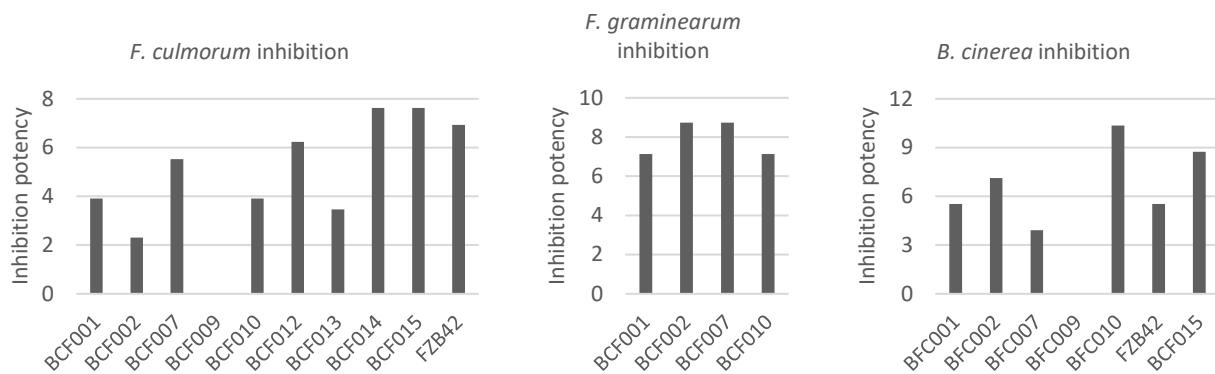


Fig. 4. Fungal inhibition potency by co-inoculation with *Bacillus* cultures. *Bacillus* culture dilution series were co-inoculated with fungal spores on PDA medium and incubated 3-5 days under natural light at room temperature. The minimal inhibitory dilution that abolished fungal growth was identified. The *Bacillus* inhibition potency was calculated by equation 1#.

Fungal inhibition by *Bacillus* culture supernatants

The inhibitory impact of secreted compounds was investigated by culture supernatant inhibition assays. To obtain comparable measures for supernatant inhibition, *Bacillus* supernatant dilution series were added to fungal spore suspensions. After incubation, the effect of culture addition on the fungal growth was evaluated by optical density measurements. This allowed calculation of the half-inhibitory dilution (ID50) that reduced fungal growth by 50% and enable easy comparison between natural isolates. Supernatants from all *B. subtilis* (BCF001, BCF002, BCF010), *B. amyloliquefaciens* (BCF007) and *B. velezensis* (BCF014, BCF0015) effectively inhibited *F. culmorum* growth in suspended static culture, with *B. amyloliquefaciens* BCF007 being the most effective inhibitor (selected strains, Fig. 5, top). Calculated ID50 values revealed that *B. subtilis* BCF002 and *B. amyloliquefaciens* BCF007 outperformed the other strains (selected strains, Fig. 5, top). Supernatant from *P. megaterium* BCF008 made no impact on *F. culmorum* growth, while *B. paralicheniformis* BCF009 showed minor inhibition (data not shown). Strains tested against *B. cinerea* challenged the fungus growth similarly (selected strains, Fig. 5, bottom). Calculated ID50 values revealed that *B. subtilis* (BCF002, BCF010) and *B. amyloliquefaciens* (BCF007) were superior *B. cinerea* inhibitors than the *B. velezensis* strains (BCF015, FZB42) (Fig. 5, bottom). Inhibition of *F. graminearum* growth was comparable between supernatants of *B. subtilis* BCF001, *B. subtilis* BCF010, *B. velezensis* BCF014 and *B. velezensis* BCF015, while *B. amyloliquefaciens* supernatants exhibited slightly stronger inhibition (data not shown).

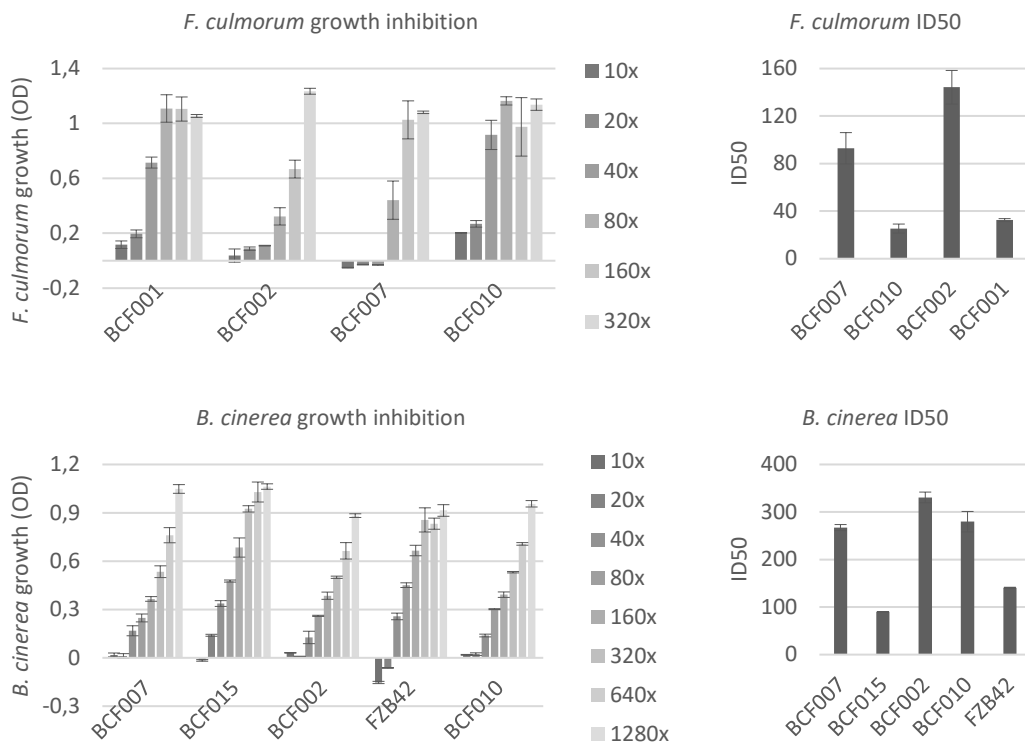


Fig. 5. Fungal inhibition potency by *Bacillus* culture supernatants. Fungal growth inhibition by culture supernatant dilution series (10-1280x) was assessed for selected *Bacillus* strains against *F. culmorum* and *B. cinerea*. *Bacillus* cultures were incubated for 48h at 37°C followed by collection of the supernatants. Dilution series of *Bacillus* culture supernatants were inoculated with fungal spore suspensions with a fixed spore concentration and incubated at 25°C 5-7 days. Fungal growth was measured by optical density and the half-inhibitory bacterial dilution (ID50), that reduced fungal growth by 50% was calculated by Hill slope regression. Error bars indicate standard deviation between biological duplicates.

Discussion

Bacillus species hold great potential as biocontrol strains due to their large capacity for bioactive compound production. In this study, we assessed the antifungal potential of natural isolates by i) genome mining of BGCs related to potential production of bioactive metabolites, ii) biochemical analysis of culture supernatants for the detection of bioactive metabolites, iii) plate inhibition assays, iv) co-inoculation inhibition assays, and v) supernatant inhibition assays. Some *Bacillus* strains appeared more potent in plate inhibition assays than in supernatant or co-inoculation inhibition assays (e.g., *B. subtilis* BCF001 against *F. culmorum*) (Fig. 6). The observed differences highlight the fact that each assay may reveal different inhibitory traits. The specific differences observed in the applied assays suggest that *Bacilli* may alter the biosynthesis of specialised metabolites in response to the interaction with the fungi (in co-cultures), as was previously demonstrated

(20, 21). Alternatively, other inhibition mechanisms can play a role, such as nutrient or space competition, which are not accounted in supernatant inhibition assays.

Summarizing conclusions were drawn based on inhibition potency results from the three types of inhibition assays (Fig. 6). Overall, *B. amyloliquefaciens* BCF007, *B. velezensis* strains BCF012, BCF013, BCF014, BCF015 and *B. subtilis* strains BCF001, BCF002, BCF003, BCF010 showed good inhibition against all three fungi, while *B. subtilis* BCF004 and *B. paralicheniformis* BCF005, BCF006, BCF009 exhibited minor antifungal properties. None of the fungal species were affected by the presence of *P. megaterium* BCF008 nor its supernatant contents. *Priestia (Bacillus) megaterium* species are recognized as effective plant growth promoters, facilitating phosphate solubilization (22, 23), still, their capacity as potent fungal inhibitors has not been reported. The identification of potent inhibitors largely correlated with specific antifungal lipopeptide levels. The potent *B. subtilis* strains (BCF001, BCF002, BCF003, BCF010) produced high amounts of fengycins/plipastatins, while the *B. velezensis* and *B. amyloliquefaciens* strains (BCF014, BCF015, BCF007) produced high amounts of iturins (iturin or bacillomycin). Poorer inhibitors such as *B. subtilis* BCF004 and *B. paralicheniformis* BCF009 produced low levels of bioactive metabolites, including fengycin, underlining to correlation between observed inhibition and bioactive metabolite production of antifungal compounds like fengycins and iturins.

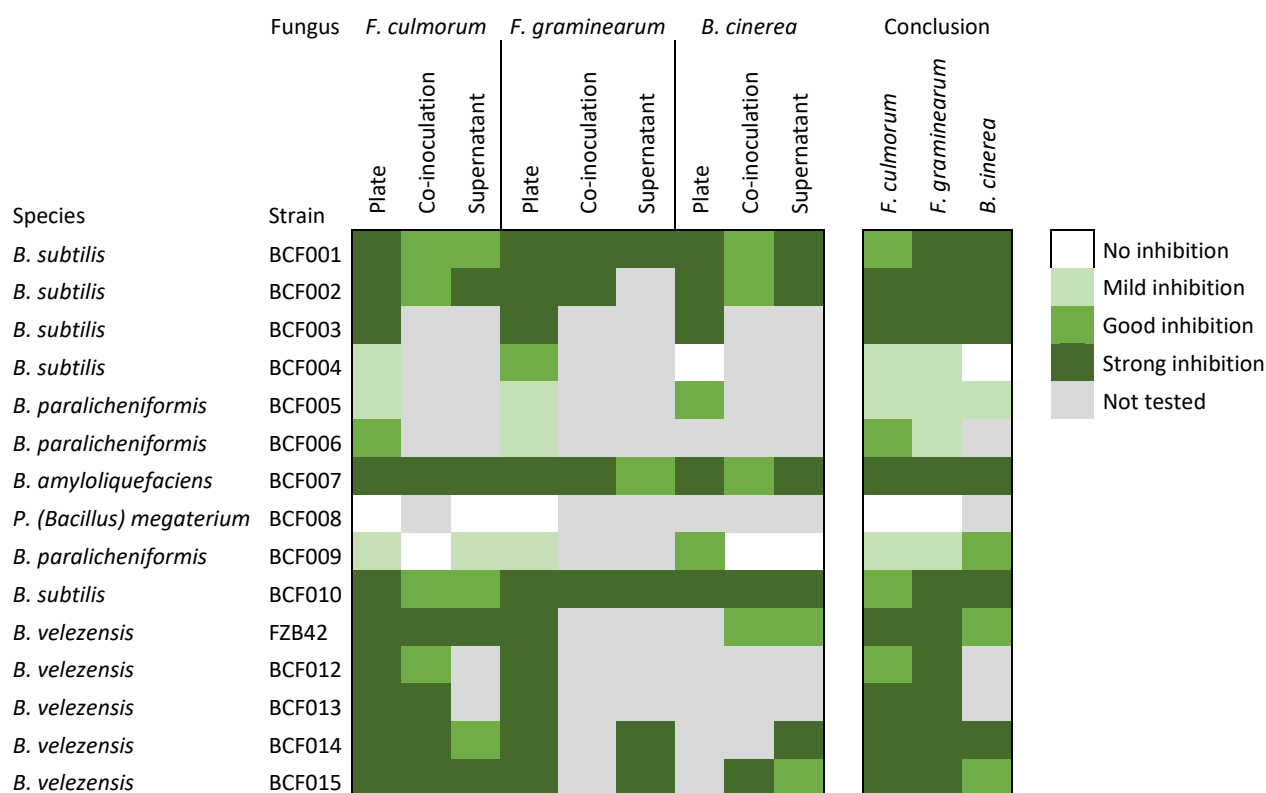


Fig. 6. Summary and conclusion of inhibition results. A summarizing conclusion on inhibition potency was drawn from the three types of fungal inhibition assays (plate confrontation, co-inoculation, culture supernatants).

Materials and methods

Species and strains

Species and strains	Number	Comment
Mold fungi		
<i>F. culmorum</i>	DSM1094	Phytopathogen isolated from wheat
<i>F. graminearum</i>	DSM4528	Phytopathogen isolated from maize
<i>B. cinerea</i>	Kern B2	Phytopathogen isolated from <i>A. thaliana</i>
Bacteria		
<i>B. subtilis</i>	BCF001	Chr. Hansen A/S strain
<i>B. subtilis</i>	BCF002	Chr. Hansen A/S strain
<i>B. subtilis</i>	BCF003	Chr. Hansen A/S strain
<i>B. subtilis</i>	BCF004	Chr. Hansen A/S strain
<i>B. paralicheniformis</i>	BCF005	Chr. Hansen A/S strain
<i>B. paralicheniformis</i>	BCF006	Chr. Hansen A/S strain
<i>B. amyloliquefaciens</i>	BCF007	Chr. Hansen A/S strain
<i>P. (Bacillus) megaterium</i>	BCF008	Chr. Hansen A/S strain
<i>B. paralicheniformis</i>	BCF009	Chr. Hansen A/S strain
<i>B. subtilis</i>	BCF010	Chr. Hansen A/S strain
<i>B. velezensis</i>	BCF012	Chr. Hansen A/S strain
<i>B. velezensis</i>	BCF013	Chr. Hansen A/S strain
<i>B. velezensis</i>	BCF014	Chr. Hansen A/S strain
<i>B. velezensis</i>	BCF015	Chr. Hansen A/S strain
<i>B. velezensis</i>	FZB42	<i>B. velezensis</i> model strain
<i>B. subtilis</i>	NCIB3610	<i>B. subtilis</i> model strain
<i>B. subtilis</i>	Bs168	<i>B. subtilis</i> laboratory strain

Medium and growth conditions. Bacilli were grown in lysogeny broth (LB) medium (10 g/L Bacto tryptone [Difco], 5 g/L yeast extract [Oxoid], 10 g/L NaCl [Merck], pH 7.2 ± 0.2). Fungi and bacterial-fungal co-growth were cultivated on potato dextrose agar (PDA) medium (4 g/L potato infusion, 20 g/L glucose, 15 g/L agar, pH 5.6 ± 0.2; [Carl Roth]) at room temperature or in potato dextrose broth (PDB) medium (6.5 g/L potato infusion, 20 g/L glucose, pH 5.6 ± 0.2 [Carl Roth]) at 25°C. When needed, *Bacillus* culture dilutions were prepared in peptone saline (pepsal) buffer (Maximum recovery diluent: peptone 1 g/L, sodium chloride 8.5 g/L, pH 7.0 ± 0.2, [Oxid]).

Genomic analysis of BGCs. Biosynthetic gene clusters (BGCs) were predicted using the automated pipeline *Antibiotics and Secondary Metabolites Analysis Shell* 5.0 (AntiSMASH) (8). Compounds were predicted and annotated from *Minimum Information about a Biosynthetic Gene cluster* (MIBiG, version 2) (9).

Plate confrontation inhibition assays. *Bacillus* culture (5 µl) was spotted on PDA plates at a fixed distance to the plate center, while 5 µl fungal spore solution (11×10^6 *F. culmorum* spores/ml, 1×10^5 *F. graminearum* spores/ml, 2×10^7 *B. cinerea* spores/ml) were spotted at the plate center. Plates were incubated under natural light for 4-7 days.

Fungal inhibition by *Bacillus* culture supernatants. Fungal spore suspensions were prepared in PDB supplemented with 50 µg/ml chloramphenicol and 10 µg/ml tetracycline to inhibit bacterial growth. The fungal spore suspensions were aliquoted into 48-well microtiter plates and *Bacillus* culture supernatants were added. The addition of *Bacillus* culture supernatants was either done according to (19) by adding a range of culture volumes (10-80 µl) to 400 µl fungal spore suspension or by preparing bacterial culture dilutions (10-1280x) in pepsal and adding 40 µl of each dilution to 360 µl fungal spore suspension. The assay plates were incubated statically at 25°C for 2-5 days before measuring the fungal growth by optical density at 600 nm using a 3x3 scanning matrix (9 points within each well). Half-inhibitory culture dilutions (ID50s) were determined using [inhibitor] vs. response regression in Graphpad Prism with variable slope fitting.

Fungal inhibition by co-inoculation with *Bacillus* cultures. Bacterial cultures were adjusted OD₆₀₀ 0.5 and 5x culture dilutions were prepared. From each dilution, a 5 µl volume was inoculated in each well of a 48-well microtiter plate with PDA. Fungal spore suspensions (11×10^6 *F. culmorum* spores/ml, 1×10^5 *F. graminearum* spores/ml, 2×10^7 *B. cinerea* spores/ml) were co-inoculated with the *Bacillus* dilution in each well. Plates were incubated under natural light for 3-5 days. Fungal growth and inhibition were assessed by visual inspection.

Biochemical analysis. LC-MS analysis of *Bacillus* culture supernatants were done according to Study 5.

Funding

This research was supported by Innovation Fund Denmark (8053-00109B) and Chr. Hansen A/S.

Acknowledgements

The authors would like to thank following contributors: Corinna Sachs, Signe Karlsen, Ricardo Almeida Faria.

References

1. Olishesvska S, Nickzad A, Déziel E. 2019. *Bacillus* and *Paenibacillus* secreted polyketides and peptides

involved in controlling human and plant pathogens. *Appl Microbiol Biotechnol* <https://doi.org/10.1007/s00253-018-9541-0>.

2. Hanif A, Zhang F, Li P, Li C, Xu Y, Zubair M, Zhang M, Jia D, Zhao X, Liang J, Majid T, Yan J, Farzand A, Wu H, Gu Q, Gao X. 2019. Fengycin produced by *Bacillus amyloliquefaciens* FZB42 inhibits *Fusarium graminearum* growth and mycotoxins biosynthesis. *Toxins (Basel)* 11.
3. Touré Y, Ongena M, Jacques P, Guiro A, Thonart P. 2004. Role of lipopeptides produced by *Bacillus subtilis* GA1 in the reduction of grey mould disease caused by *Botrytis cinerea* on apple. *J Appl Microbiol* 96:1151–1160.
4. Gong AD, Li HP, Yuan QS, Song XS, Yao W, He WJ, Zhang JB, Liao YC. 2015. Antagonistic mechanism of iturin a and plipastatin a from *Bacillus amyloliquefaciens* S76-3 from wheat spikes against *Fusarium graminearum*. *PLoS One* 10:e0116871.
5. Gu Q, Yang Y, Yuan Q, Shi G, Wu L, Lou Z, Huo R, Wu H, Borriss R, Gao X. 2017. Bacillomycin D produced by *Bacillus amyloliquefaciens* is involved in the antagonistic interaction with the plantpathogenic fungus *Fusarium graminearum*. *Appl Environ Microbiol* 83:e01075-17.
6. Kiesevalter HT, Lozano-Andrade CN, Wibowo M, Strube ML, Maróti G, Snyder D, Jørgensen TS, Larsen TO, Cooper VS, Weber T, Kovács ÁT. 2021. Genomic and Chemical Diversity of *Bacillus subtilis* Secondary Metabolites against Plant Pathogenic Fungi. *mSystems* 6.
7. Malit JJJ, Leung HYC, Qian PY. 2022. Targeted Large-Scale Genome Mining and Candidate Prioritization for Natural Product Discovery. *Mar Drugs*. Multidisciplinary Digital Publishing Institute (MDPI) <https://doi.org/10.3390/md20060398>.
8. Blin K, Shaw S, Steinke K, Villebro R, Ziemert N, Lee SY, Medema MH, Weber T. 2019. AntiSMASH 5.0: Updates to the secondary metabolite genome mining pipeline. *Nucleic Acids Res* 47:W81–W87.
9. Terlouw BR, Blin K, Navarro-Muñoz JC, Avalon NE, Chevrette MG, Egbert S, Lee S, Meijer D, Recchia MJJ, Reitz ZL, van Santen JA, Selem-Mojica N, Tørring T, Zaroubi L, Alanjary M, Aleti G, Aguilar C, Al-Salihi SAA, Augustijn HE, Avelar-Rivas JA, Avitia-Domínguez LA, Barona-Gómez F, Bernaldo-Agüero J, Bielinski VA, Biermann F, Booth TJ, Carrion Bravo VJ, Castelo-Branco R, Chagas FO, Cruz-Morales P, Du C, Duncan KR, Gavriilidou A, Gayraud D, Gutiérrez-García K, Haslinger K, Helfrich EJN, van der Hooft JJJ, Jati AP, Kalkreuter E, Kalyvas N, Kang K Bin, Kautsar S, Kim W, Kunjapur AM, Li Y-X, Lin G-M, Loureiro C, Louwen JJR, Louwen NLL, Lund G, Parra J, Philmus B, Pourmohsenin B, Pronk LJU, Rego A, Rex DAB, Robinson S, Rosas-Becerra LR, Roxborough ET, Schorn MA, Scobie DJ, Singh KS, Sokolova N, Tang X, Udway D, Vigneshwari A, Vind K, Vromans SPJM, Waschulin V, Williams SE, Winter JM, Witte TE, Xie H, Yang D, Yu J, Zdouc M, Zhong Z, Collemare J, Linington RG, Weber T, Medema MH. 2023. MIBiG 3.0: a community-driven effort to annotate experimentally validated biosynthetic gene

- clusters. *Nucleic Acids Res* 51:D603–D610.
10. Steinke K, Mohite OS, Weber T, Kovács ÁT. 2020. Phylogenetic Distribution of Secondary Metabolites in the *Bacillus subtilis* Species Complex. *mSystems* 6.
 11. Olajide AM, Chen S, LaPointe G. 2021. Markers to Rapidly Distinguish *Bacillus paralicheniformis* From the Very Close Relative, *Bacillus licheniformis*. *Front Microbiol* 11:3367.
 12. Du Y, Ma J, Yin Z, Liu K, Yao G, Xu W, Fan L, Du B, Ding Y, Wang C. 2019. Comparative genomic analysis of *Bacillus paralicheniformis* MDJK30 with its closely related species reveals an evolutionary relationship between *B. paralicheniformis* and *B. licheniformis*. *BMC Genomics* 20:283.
 13. Chen XH, Koumoutsis A, Scholz R, Schneider K, Vater J, Süßmuth R, Piel J, Borriss R. 2009. Genome analysis of *Bacillus amyloliquefaciens* FZB42 reveals its potential for biocontrol of plant pathogens. *J Biotechnol* 140:27–37.
 14. Koumoutsis A, Chen X-HH, Henne A, Liesegang H, Hitzeroth G, Franke P, Vater J, Borriss R. 2004. Structural and Functional Characterization of Gene Clusters Directing Nonribosomal Synthesis of Bioactive Cyclic Lipopeptides in *Bacillus amyloliquefaciens* Strain FZB42, p. 1084–1096. *In* *Journal of Bacteriology*. American Society for Microbiology Journals.
 15. Landy M, Warren GH, Rosenman SB, Colio LG. 1948. Bacillomycin: An Antibiotic from *Bacillus subtilis* Active against Pathogenic Fungi. *Proc Soc Exp Biol Med* 67:539–541.
 16. Zhang X, Hindra, Elliot MA. 2019. Unlocking the trove of metabolic treasures: activating silent biosynthetic gene clusters in bacteria and fungi. *Curr Opin Microbiol*. Elsevier Current Trends <https://doi.org/10.1016/j.mib.2019.03.003>.
 17. Fan B, Wang C, Song X, Ding X, Wu L, Wu H, Gao X, Borriss R. 2018. *Bacillus velezensis* FZB42 in 2018: The gram-positive model strain for plant growth promotion and biocontrol. *Front Microbiol*. Frontiers Media S.A. <https://doi.org/10.3389/fmicb.2018.02491>.
 18. Branda SS, González-Pastor JE, Ben-Yehuda S, Losick R, Kolter R. 2001. Fruiting body formation by *Bacillus subtilis*. *Proc Natl Acad Sci U S A* 98:11621–11626.
 19. Kjeldgaard B, Neves AR, Fonseca C, Kovács ÁT, Domínguez-Cuevas P. 2022. Quantitative High-Throughput Screening Methods Designed for Identification of Bacterial Biocontrol Strains with Antifungal Properties. *Microbiol Spectr* 10.
 20. Defilippi S, Groulx E, Megalla M, Mohamed R, Avis TJ. 2018. Fungal Competitors Affect Production of Antimicrobial Lipopeptides in *Bacillus subtilis* Strain B9–5. *J Chem Ecol* 44:374–383.
 21. Cawoy H, Debois D, Franzil L, De Pauw E, Thonart P, Ongena M. 2015. Lipopeptides as main ingredients for inhibition of fungal phytopathogens by *Bacillus subtilis/amyloliquefaciens*. *Microb Biotechnol* 8:281–295.

22. Kang SM, Radhakrishnan R, You YH, Joo GJ, Lee IJ, Lee KE, Kim JH. 2014. Phosphate Solubilizing *Bacillus megaterium* mj1212 Regulates Endogenous Plant Carbohydrates and Amino Acids Contents to Promote Mustard Plant Growth. *Indian J Microbiol* 54:427–433.
23. El-Komy HMA. 2005. Coimmobilization of *Azospirillum lipoferum* and *Bacillus megaterium* for successful phosphorus and nitrogen nutrition of wheat plants. *Food Technol Biotechnol* 43:19–27.

Supplemental material

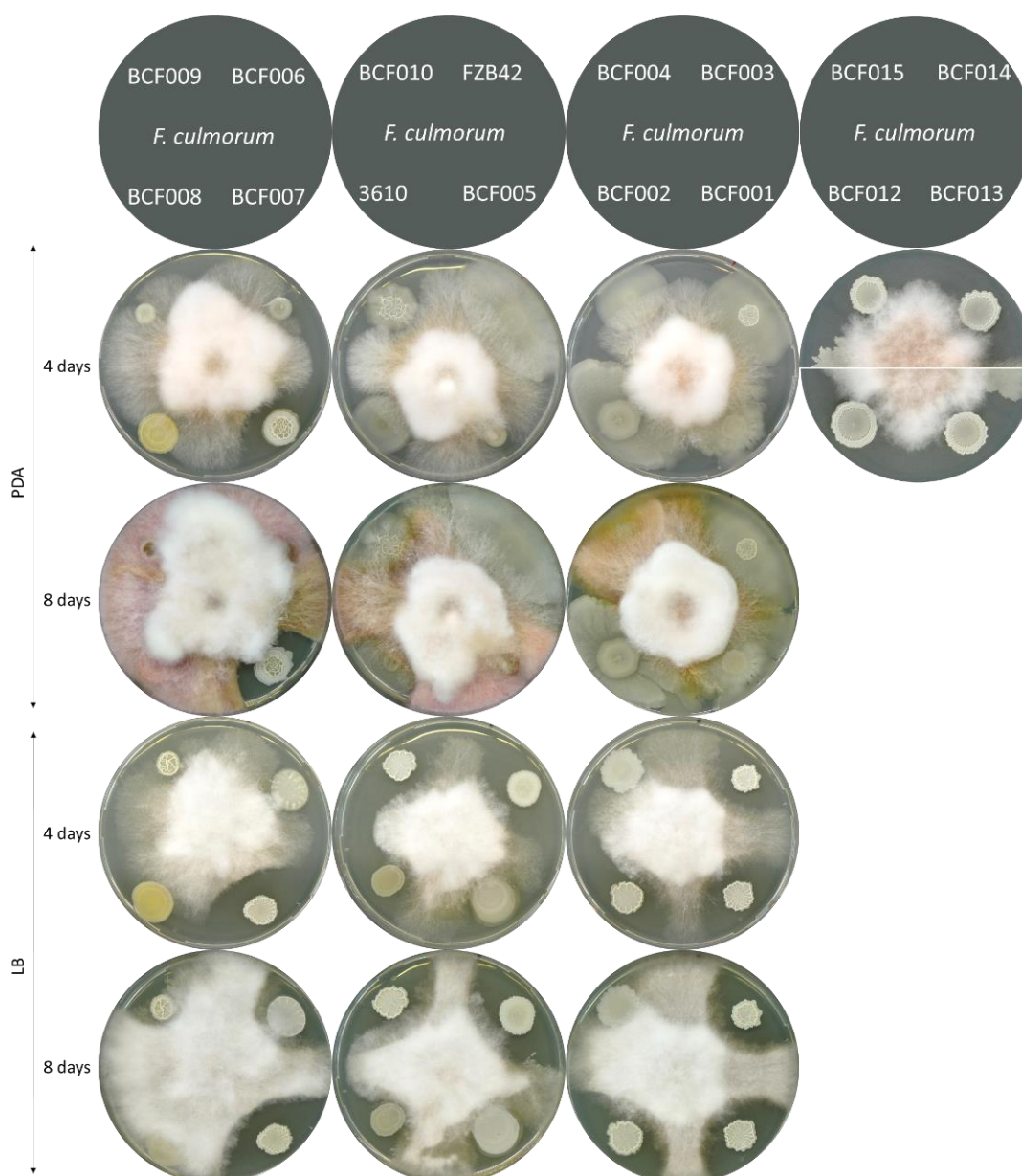


Fig. S 1. Plate inhibition of *Fusarium culmorum* by selected *Bacillus* strains. 14 *Bacillus* isolates and two benchmark strains (FZB42 and NCIB3610) were inoculated with a fixed distance to a central fungal inoculum on PDA and LB plates.

Fungal growth and degree of inhibition was evaluated after 4 days and 8 days incubation. *Bacillus* strains and challenged fungus are indicated above plates.

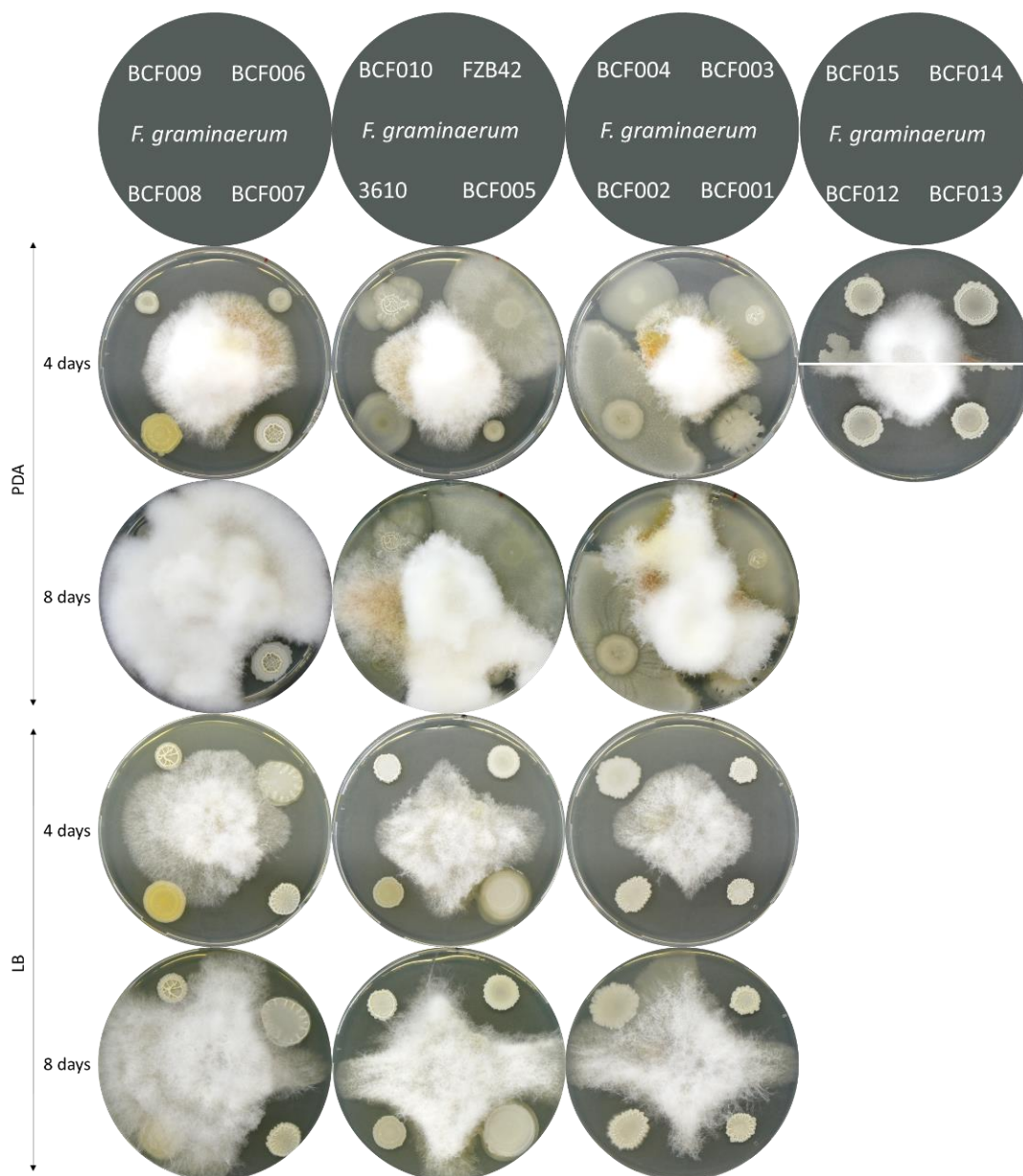


Fig. S 2. Plate inhibition of *Fusarium graminearum* by selected *Bacillus* strains. 14 *Bacillus* isolates and two benchmark strains (FZB42 and NCIB3610) were inoculated with a fixed distance to a central fungal inoculum on PDA and LB plates. Fungal growth and degree of inhibition was evaluated after 4 days and 8 days incubation. *Bacillus* strains and challenged fungus are indicated above plates.

Study 5

Kjeldgaard, B., Fonseca, C., Kovács, Á. T., and Domínguez-Cuevas, P.

Improving biocontrol ability of *Bacillus* spp. against *Fusarium culmorum*.

To be submitted.

Improving biocontrol ability of *Bacillus* spp. against *Fusarium culmorum*

Bodil Kjeldgaard^{1,2}, César Fonseca¹, Ákos T. Kovács², Patricia Domínguez- Cuevas^{1,3}

¹Discovery, R&D, Chr. Hansen A/S, Denmark

²Bacterial Interactions and Evolution Group, DTU Bioengineering, Technical University of Denmark

³Current affiliation: Scientific Integration, Novo Nordisk, Denmark

Abstract

Bacillus species produce a wide range of specialised metabolites with documented bioactivity against plant pathogenic fungi such as *Fusarium culmorum* that infects small-grain crops leading to detrimental agricultural damage. In this study, experimental evolution was employed of undomesticated species from the *B. subtilis* complex, subjecting them to repetitive co-cultivation cycles with the phytopathogen *F. culmorum* on solid growth medium. We show that the experimental evolution conditions targeted the quorum sensing system ComP-ComA, conferring changes to biofilm morphology, specialised metabolites biosynthesis, extracellular protease activity, poly- γ -glutamic acid production, and fungal inhibition potency. Notably, loss-of-function mutations in *comP* were intrinsic to reduced fungal inhibition potency of culture supernatants in accordance with reduced culture contents of cyclic lipopeptides. However, improved fungal inhibition potency was associated with increased space colonisation during confrontations with the fungus and an amplified effect of the *Bacillus* volatilome on fungal growth.

Introduction

Fusarium (*Gibberella*) comprises a large genus of ubiquitous filamentous fungi that inhabit soil or live in association with plants. The ascomycete causes plant infections known as *Fusarium* head blight (FHB), *Fusarium* root rot (FRR), vascular wilts, and yellowing disease in a wide range of commodity crops, from cereals to tropical fruits (1). The *Fusarium culmorum* species particularly infects important small-grain cereals including rice, wheat, barley, and oat. In addition, freshly harvested and inadequately dried grains are prone to post-harvest infection by *F. culmorum*. Together with other species from the *Fusarium graminearum* species complex, *F. culmorum* has been reported as a major pathogen of wheat causing FHB and FRR (2). *Fusarium culmorum* initiates infection of wheat at the spikelets, shoot germination site, or through stomata by secreting degradative enzymes to soften the tissue, permit invasion and acquire nutrients (1, 3), while the secretion of mycotoxins function as virulence factors to susceptible hosts (2). Among others, the specialised metabolites trichothecenes are important during infection and impose phytotoxicity by blocking protein synthesis leading to reduced plant germination, root- and shoot growth, while fusaric acid chelates ions and

induces plant cell death by increasing reactive oxygen species (1). Particularly, due to their production of a number of mycotoxins that accumulate in grains, species from the *F. graminearum* complex are of importance to food safety in crop production of cereals (4). High levels of accumulated mycotoxins may cause severe toxic effects in humans and livestock that consume the spoiled cultivar. Specifically, the *F. graminearum* species complex contaminate cereal grains with mycotoxins such as the trichothecenes deoxynivalenol (DON), the 10 times more toxic deoxynivalenol or the estrogenic analogue zearalenone (ZEN) (1, 3, 5). The accumulation of mycotoxin in grains leads to decreased harvest quality and yield (6). In addition, ingestion of grains contaminated with DON may lead to nausea, vomiting, diarrhea or fever, while ZEN contamination may confer reproductive disorders to female animals and cause precocious puberty in humans (4, 5, 7). *Fusarium culmorum* mycelium persists in plant debris or as chlamydospores in soil enabling the fungus to survive up to 4 years and impeding removal of the pathogen from infested agriculture (3). Triazoles are the most efficient chemical treatment of fusaria and function by inhibiting ergosterol synthesis. However, the emergence of resistant *F. culmorum* variants that have adapted to triazole application by overexpressing drug exporters request alternative methods for control of this phytopathogen (8). The application of microbial agents offers an environmentally safe alternative to chemical fungicides with a minimal risk of resistance development. Species from the *Bacillus subtilis* complex possess great potential as biocontrol agents due their immense genomic dedication to specialised metabolites of which the cyclic lipopeptides especially exhibit antifungal activity. In addition to inhibition of *Fusarium* growth and reduction of plant disease severity, the application of *Bacillus* spp. reduces mycotoxin accumulation in grains (9–11). Interestingly, studies of *Bacillus* spp. adaptation to the presence of fungi reveal improvement of antifungal properties seemingly mediated by alterations to cell differentiation regulators. In response to experimental evolution of *Bacillus* species in the presence of the filamentous fungi *Aspergillus niger* or *Setophoma terrestris*, genetic alterations occurred in genes encoding the DegU regulator as well as the quorum sensing system ComP-ComA leading to changes in specialised metabolites biosynthesis and volatilome, respectively (Albarracín Orió et al., 2020; Richter et al., 2023, Study 2). As several microorganisms, *Bacillus* spp. employ quorum sensing to monitor population density through exchange of signalling oligopeptides and coordinate transcription in a multicellular response (14, 15). In *Bacillus* spp. the peptide-mediated signalling is received by the two-component system ComP-ComA that responds, when threshold is reached (16–19). Quorum sensing enables *Bacillus* to coordinate multicellular behaviours such as complex biofilm formation, DNA uptake, onset of motility, sporulation, or secretion bioactive compounds (14, 15).

In this study, we aimed to improve the antifungal properties of selected *Bacillus* spp. against the phytopathogenic fungus *Fusarium culmorum* DSM1094 by utilizing adaptive laboratory evolution (ALE) as a strain optimization tool. Repetitive bacterial-fungal co-cultivation selected mutations affecting the gene

encoding the response regulator ComP, which impacted a multitude of phenotypes including pathogen inhibition potency, biofilm formation, and specialized metabolite production. Interestingly, the improved fungal inhibition observed by ALE derivatives carrying *comP* mutations was found associated with increased space competition and release of volatile antifungal compounds.

Results

Experimental design of adaptive laboratory evolution of *Bacillus* spp. with *F. culmorum*

Five *Bacillus* strains *Bacillus subtilis* BCF001, *B. subtilis* BCF002, *Bacillus amyloliquefaciens* BCF007, *Bacillus paralicheniformis* BCF009, and *B. subtilis* BCF010 were co-cultivated with the phytopathogen *F. culmorum* DSM1094 in iterative cycles for 16 weeks following a similar approach as described in (Richter et al., 2023, Study 2) (Fig. 1). In brief, bacterial culture was applied to the solid growth medium in a hashtag pattern, while fungal spore suspension was streaked in a square pattern. Each ancestor strain was co-cultivated with the fungus in triplicate ALE lineages (A, B, C) and, in addition, a control evolution lineage (X) was included for each ancestor strain that followed the same iterative cultivation cycle, but in absence of the fungus. The inclusion of evolved control lineages intended to single out genetic changes acquired during the adaptation to the growth conditions and not necessarily related to the presence of the plant pathogenic fungus. To avoid co-evolution of the fungus and promote competitive evolution of the *Bacillus* strains, passages from co-cultures entailed the exclusive transfer of the bacterial population, while fresh fungal inoculi were applied by each iteration. Stock samples were prepared from the evolved bacterial population by each transfer and the fungal inhibition potency of evolved populations was monitored over the time course of the ALE (Fig. S1). Strains evolved in the presence of *F. culmorum* will be referred to as co-evolved.

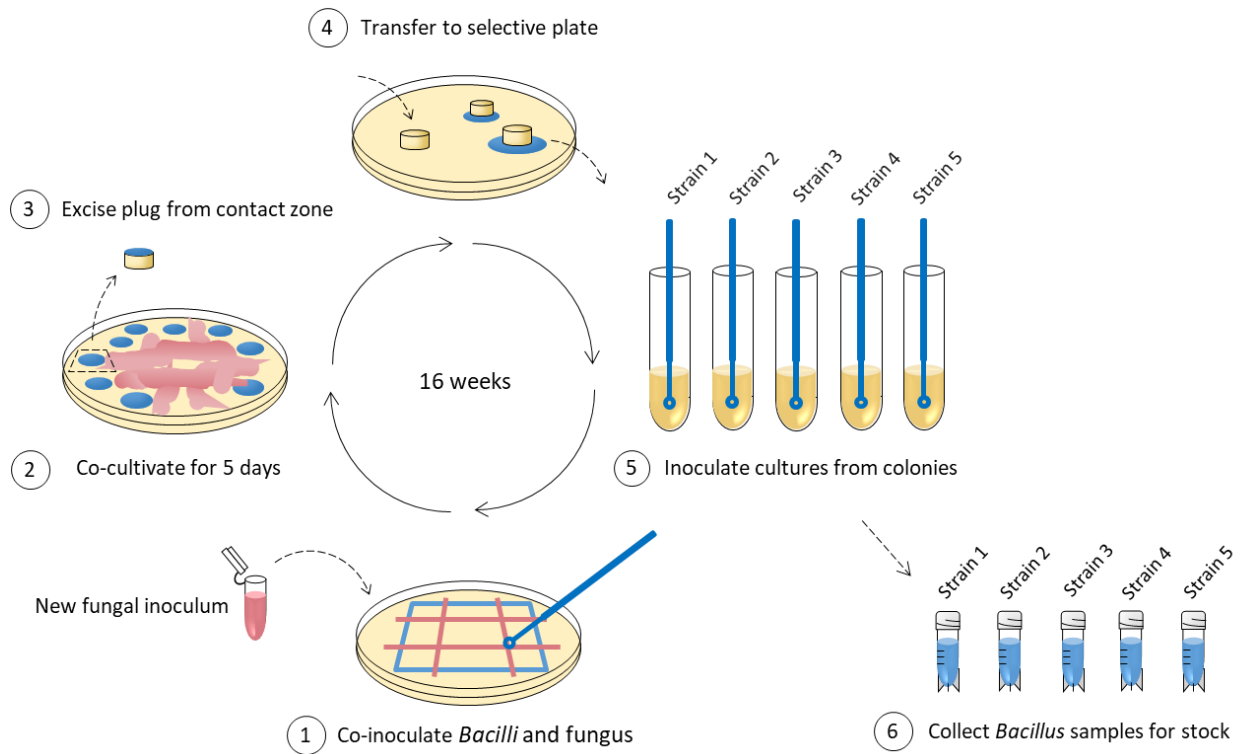


Fig. 1. Design of Adaptive Laboratory Evolution (ALE). *Bacillus* spp. and *F. culmorum*. *Bacillus* spp. (blue) and *F. culmorum* spores (red) were co-inoculated in a hashtag pattern onto the surface of a PDA growth plate. The species were co-cultivated for 5 days at room temperature, before an agar plug was excised from the growth contact zone and transferred to a bacterial selective medium. Overnight cultures (37°C) were inoculated from the outgrowing bacteria and stocks were prepared for later fitness screening. The co-cultivation cycle was repeated for 16 weeks, and bacterial stocks of the evolved populations were prepared following each transfer. Fresh fungal spores were used for the co-inoculations to prevent simultaneous evolution of the fungal strain. *Bacillus* control ALE lineages were grown under same conditions, but in absence of the fungus.

Already in the 3rd ALE week, morphological changes of *Bacillus* colonies were observed on the co-cultivation plates, in accordance with the rapid diversification of *Bacillus* spp. previously reported during experimental evolution experiments (20–22). Specific *B. amyloliquefaciens* BCF007 populations appeared slimy, wrinkled, or dry (data not shown) suggesting that changes in matrix composition had already occurred. Consistent with the previously reported ability of *Bacillus* spp. to colonize fungal hyphae (Benoit et al., 2015; Kjeldgaard et al., 2019, Study 1), areas with merging growth of *F. culmorum* and *Bacillus* spp. were evident from the beginning of the co-cultivation and persisted throughout the experimental evolution campaign (Fig. S2).

Screening of evolved *Bacillus* spp. isolates reveals tendency towards decreased fungal inhibition

Single colony derivatives were isolated from each of the evolved populations at progressive time points, specifically at week 5, 10 and 15, for fitness assessment in growth competition with *F. culmorum* according

to co-cultivation methods previously described (Kjeldgaard et al., 2022, Study 3). In brief, culture dilution series of each evolved *Bacillus* isolate were co-inoculated with a fixed fungal spore concentration on the surface of agar in consecutive columns of a 48-well microtiter plate (Fig. 2). As a measure of inhibition potency, the minimal bacterial dilution that inhibited fungal growth was identified and compared to that of the respective ancestor strain. A total of 1083 ALE derivatives were screened, and the potency was scored as *improved*, *neutral*, or *reduced* (Table S1).

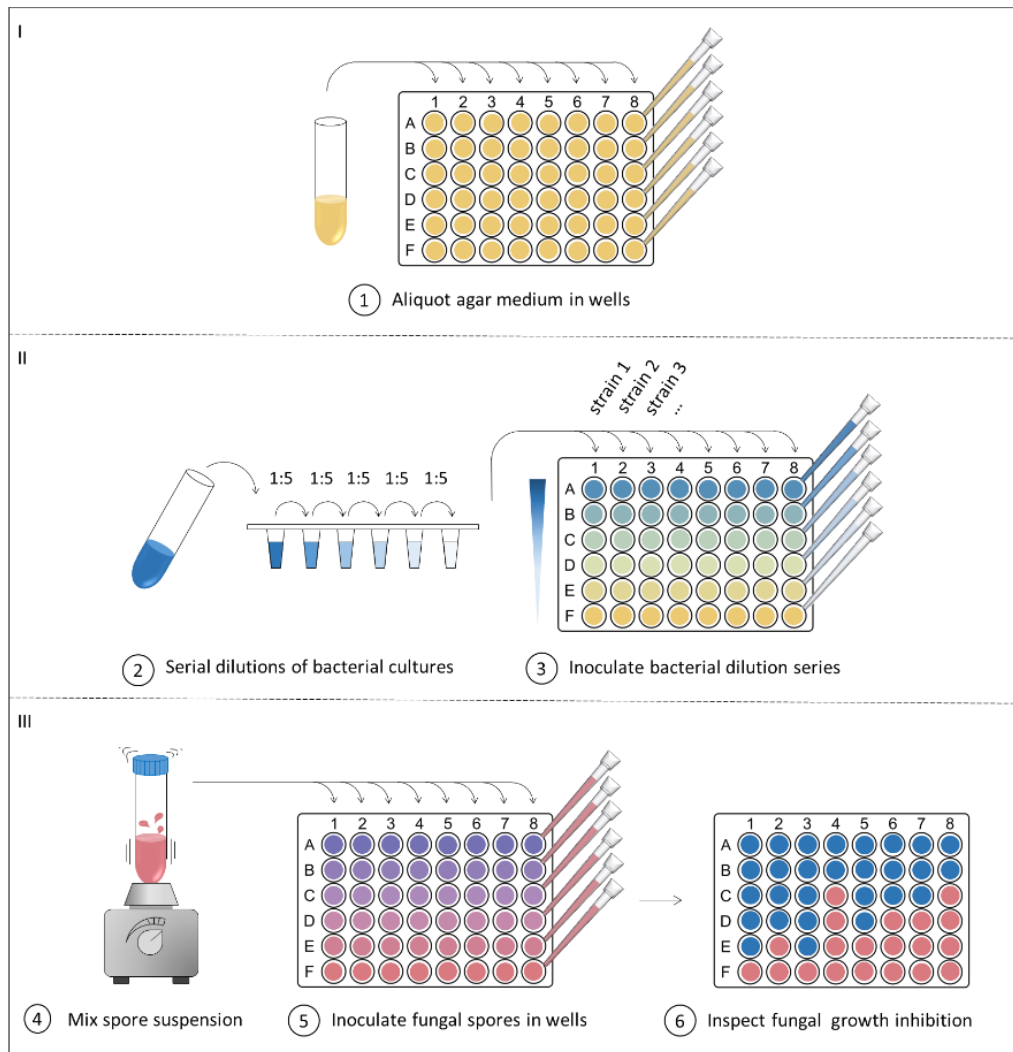


Fig. 2. Assessment of fungal inhibition potency of evolved *Bacillus* derivatives. In each well of a 48-well microtiter plate, molten PDA medium was aliquoted and let to solidify. Cultures dilution series of evolved *Bacillus* strains (blue) were prepared and inoculated in columns. In each well of the plate, a fixed quantity of fungal spores (red) (constant volume of fungal spore suspension) was co-inoculated with the *Bacillus* dilution series on the agar surface. The spore

suspensions were mixed thoroughly before aliquoting. Assay results were evaluated by visual inspection after 5 days incubation at room temperature. Text and figure adapted from (Kjeldgaard et al., 2022, Study 3).

The sum of improved derivatives reached 12-30% of the total number of tested *B. subtilis* isolates from BCF001, BCF002, or BCF010 (Fig. 3B), while the improved strains derived from *B. paralicheniformis* BCF009 summed up to staggering 57% of total tested isolates (Fig. 3A). The ancestors BCF001, BCF002, BCF007, and BCF010 had initial higher inhibition potencies in common, whereas *B. paralicheniformis* BCF009 showed a low inhibition capacity in competition against *F. culmorum* (Study 3). Especially, *B. amyloliquefaciens* BCF007 displayed initial prominent inhibition. Interestingly, the screening revealed a tendency for reduction in numbers of improved co-evolved derivatives from *B. subtilis* ancestor strains (BCF001, BCF002, BCF010) towards the endpoint of the campaign (Fig. 3B). The reduction of improved strains in progression with the ALE experiment was a tendency observed across all co-evolved *B. subtilis* populations (A, B, C) (Fig. S3). In contrast, co-evolved derivatives from the most potent ancestor strain *B. amyloliquefaciens* BCF007 failed to improve at all over the time course, whereas the co-evolved derivatives from *B. paralicheniformis* BCF009 showed significant increase in final potency. These results suggest that poor performing strains hold greater potential for fungal inhibition improvement, whereas potent inhibitors hold limited potential for optimization of their performance.

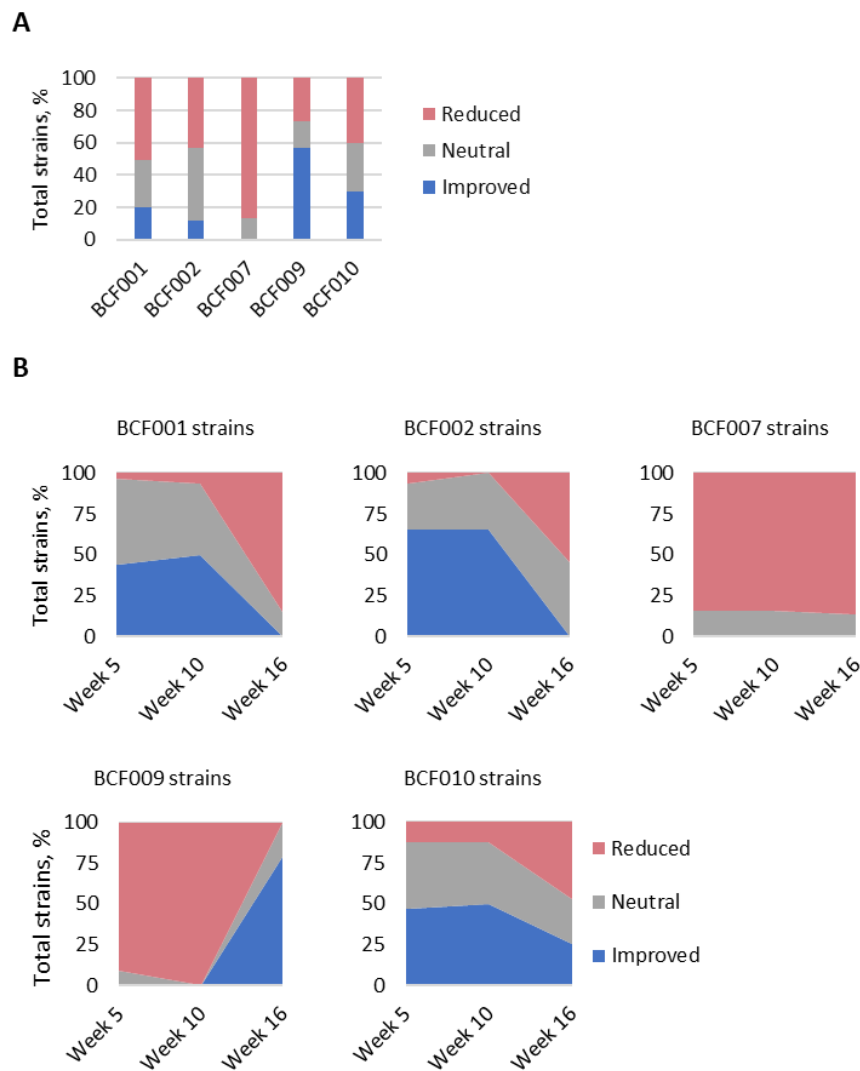


Fig. 3. Percental fitness improvement. A) The sum of co-evolved derivatives with *improved*, *neutral*, and *reduced* fungal inhibition potencies was calculated as percentage of the total number of screened ALE derivatives from each ancestor strain (BCF001, BCF002, BCF007, BCF009, BCF010). B) In addition, the percentage of evolved strains with *improved*, *neutral*, and *reduced* fungal inhibition potency was calculated relative to the total amount of screened strains per screening time point (week 5, week 10, week 15) during the ALE experiment from the respective ancestor.

Primary characterization enables selection of strains with different phenotypes

From the initial 1083 screened derivatives, 201 evolved strains were selected as candidates for whole genome sequencing (WGS). To enable selection of genotypically distinct derivatives for WGS, primary characteristics of the 201 evolved derivatives were determined in respect to: growth kinetics, sporulation capacity and colony morphology (Table S2). Colony morphology was scored 1-4 from more structure/less spread to less structure/more spread (Fig. 4) and sporulation as positive/negative (1/0). Interestingly, colony growth and morphological features on biofilm inducing medium revealed highly diverse phenotypes of

strains derived from the same parent, suggesting changes in matrix composition or production (Fig. S4-8). Also, differences in growth kinetics were revealed in respect to growth rate, maximum OD₆₀₀ and in some cases patterns indicating diauxic growth (Fig. S9). Sporulation negative derivatives (4/201) were discarded from further studies as they would not be suitable from the commercial point of view in the development of a biocontrol product formulation. Interestingly, sporulation negative strains appeared only on control populations (X09, X01).

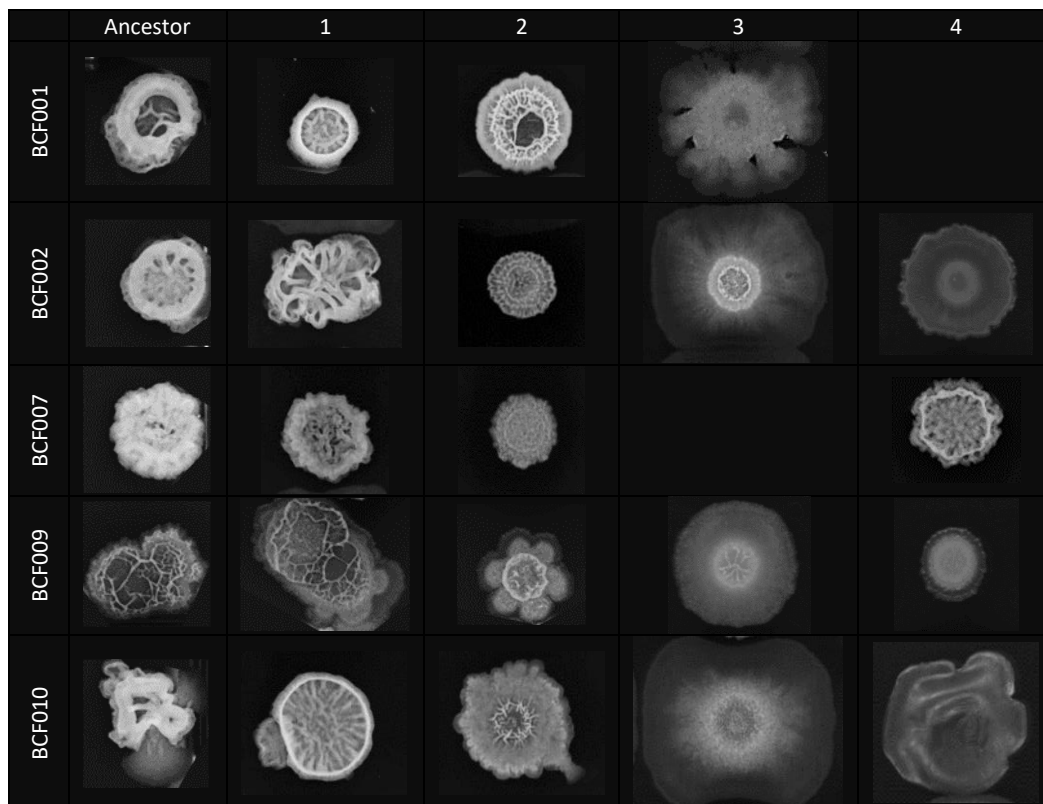


Fig. 4. Primary phenotypic characterization of colony morphology. Evolved derivatives were scored according to colony structure morphological similarity to the respective ancestors. Four different categories were established to enable grouping of the derivative strains: 1: Colonies showing complex structure and no spreading. 2: No spreading and reduces colony structure. 3: Bacterial colonies presenting a spreading phenotype, but still some structure. 4: Colonies showing both a spreading phenotype and lack of structure or mucoid texture. Examples are shown for each category from each ancestor. Empty fields denote lack of category representative from the respective ancestor.

Principle component analysis (PCA) of the acquired primary characterization data was used to compare strains and enabled selection of 52 phenotypic diverse strains for WGS. The inhibition score was considered as the primary selection criterion, while either colony structure phenotype or growth profile were considered, depending on what provided a better separation of derivatives (visualized by PCA plots). From each of the groups with high degree of similarity (colony structures, growth dynamics, inhibition scores and

isolation timepoint), only one representative strain was selected. The selection comprised: i. derivatives from different ancestors to compare mutations in different backgrounds, ii. derivatives from fungal co-evolved lines and evolved control lines to identify growth condition adaptations, iii. derivatives with improved inhibition, and iv. at least one derivative with weakened potency per ancestor, to identify essential mechanisms for fungal inhibition. In addition, few derivatives originating from the same population, but isolated at different timepoints were also included to investigate persistence of mutations (Table S2).

Mutation of *comP* provides increased competitive fitness

Whole genome sequencing (WGS) of the 52 selected ALE derivatives revealed surprisingly few acquired genetic changes (145 in total) and no selection for hypermutable strains was observed. Strains acquired mutations (111) mainly within open reading frames (ORFs) (i.e., nonsynonymous, insertions/deletions, and nonsense), while fewer genetic changes (34) were identified with no obvious effect (i.e., intergenic, synonymous, or affecting noncoding DNA regions). Mutations were evenly distributed among evolved populations and across ALE lines from different ancestor origins. However, the isolates from week 16 showed more genomic changes indicating that mutations accumulated over time with exception to *B. paralicheniformis* BCF009 derivatives (Fig. 5, Fig. S10). Specifically, strains derived from *B. subtilis* BCF001, BCF002, BCF010, *B. amyloliquefaciens* BCF007 acquired on average 1.2-2.2 mutations within 5 weeks experimental evolution, 1.6-2.75 mutations within 10 weeks experimental evolution, and 3.75-5 mutations within 16 weeks experimental evolution. Identical genetic changes concurred mainly within a population or in parallel populations derived from the same ancestor strain, albeit a few mutations were acquired in homologous loci in isolates derived from different ancestor origin (Fig. 6-10). WGS analysis also showed that some mutations persisted in the evolved populations throughout the ALE suggesting a fitness benefit for the specific growth conditions or for co-cultivation with *F. culmorum* (Fig. S11). The positive screening results of early isolates and negative screening results of late isolates suggest that the initial mutations correlate with the improved inhibition potency, whereas the late emerging mutations mask the beneficial effect and potentially lead to fitness decrease. Therefore, the late emerging mutations were considered less relevant in respect to improved fungal inhibition potency and were not investigated further. The majority of mutations occurred in non-unique loci (110 reoccurrences) (Table S3). Multiple mutations (73) affected proteins participating in the cell differentiation network that regulates the development into distinct cell types within a multicellular community upon reception of external signals (Table 1, extended Table S4). Specifically, genetic alterations affected Rap phosphatases (RapA, RapE) and histidine kinases (KinA, KinE) that influence the phosphorelay system. The phosphorelay system of *Bacilli* controls the activity of the global transcription regulator Spo0A, which regulates cell differentiations towards biofilm formation or sporulation (26–29). The

phosphorelay protein encoded by *spo0B* gained mutation as well (30). Moreover, mutations affected SinR, the transcription regulator of matrix genes encoded by the *tasA* and the large *eps* operon as well as the SinR inhibitor SinI affecting biofilm formation (31). Mutations also occurred in the genes coding for the quorum sensing regulatory pair ComP-ComA that induces surfactin production, Rap protein expression, and competence development (19, 32, 33). Furthermore, genes encoding the pheromone ComX that activates the quorum sensing system as well as ComQ that modifies ComX prior to secretion (19, 34) both acquired mutations during the ALE. Also, genes encoding the regulatory system DegS-DegU and DegQ that influence gene expression related to protease activity, onset of motility, biofilm formation, and specialised metabolite biosynthesis acquired mutations (35–43), as well as the phosphatase RapG that potentially prevents DNA-binding of DegU and inhibits ComA (44, 45). In addition, genetic changes influenced the Opp permease (OppB, OppC) that internalizes quorum sensing oligopeptides that inhibit specific Rap proteins (29, 46, 47).

Interestingly, *comP* encoding the quorum sensing response regulator was the most abundant mutated locus and the only locus targeted in derivatives across 4 of the 5 ancestors. Mutations in *comP* appeared already at week 5 and persisted throughout the ALE campaign, underlining the importance of these genetic changes (Fig. 5). Moreover, nearly all *comP* mutations disrupted the open reading frame by premature stop codons (nonsense), frameshifts (small deletion/insertion), or partial deletions. Albeit *comP* mutations seemed to provide a positive fitness effect in competition against *F. culmorum*, the mutations arose both in co-evolved and evolved control populations indicating a growth condition adaptation, rather than a fungal adaptation (Fig. 5). Nonetheless, the *comP* mutations yielded improved competitive potential in the HT-inhibition screen and proved beneficial for reduction of *F. culmorum* growth under these specific laboratory conditions.

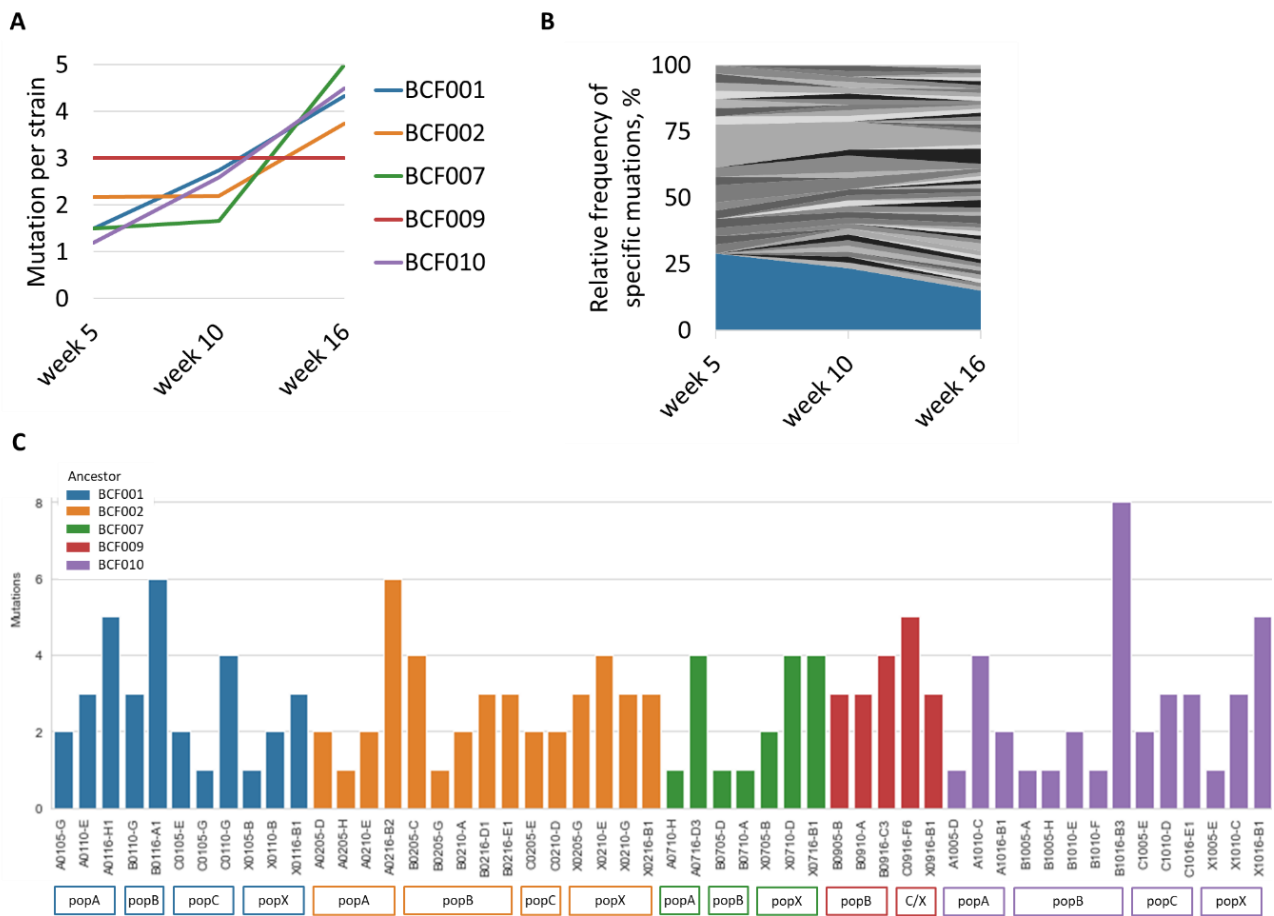


Fig. 5. Number and type of acquired mutations. **A)** Average number of mutations per strain derived from *B. subtilis* BCF001, BCF002, BCF010, *B. amyloliquefaciens* BCF007, *B. paralicheniformis* BCF009 timepoint week 5, 10, and 16. **B)** The relative frequency of each specific mutations was calculated relative to the total number of mutations at each given timepoint (week, 5, 10, 16) with the percental amount of *comp* mutation indicated in blue. Grey shades represent all other occurring mutations. **C)** Exact number of mutations per evolved strain. Population is indicated by the initial letter in the strain name (A, B, C, X), followed by number reference to ancestor strain (01, 02, 07, 09, 10). Final numbers refer to isolation timepoint (week 05, 10, 16). For instance, strain A0105-G originates from population A derived from ancestor BCF001 isolated at timepoint week 05.

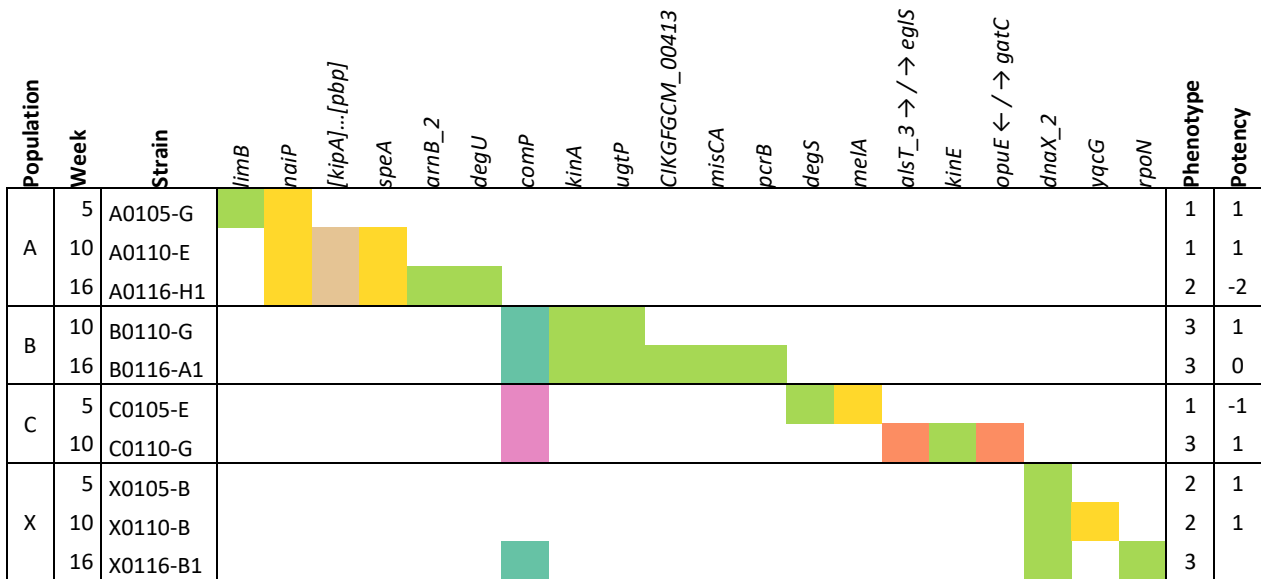


Fig. 6. Mutations identified in *B. subtilis* BCF001 background. The large deletion in strains A0110-E and A0116-H1 encompasses partially *kipA*, *kipR*, *lipC_1*, *CIKGF_{GCM}_00538*, *CIKGF_{GCM}_00539*, and partially *pbp*. Arrows indicate gene orientation in respect to intergenic mutation. Legend top-down; nonsynonymous SNP, small insert or deletion, synonymous SNP, nonsense SNP, intergenic SNP, noncoding SNP, large deletion.

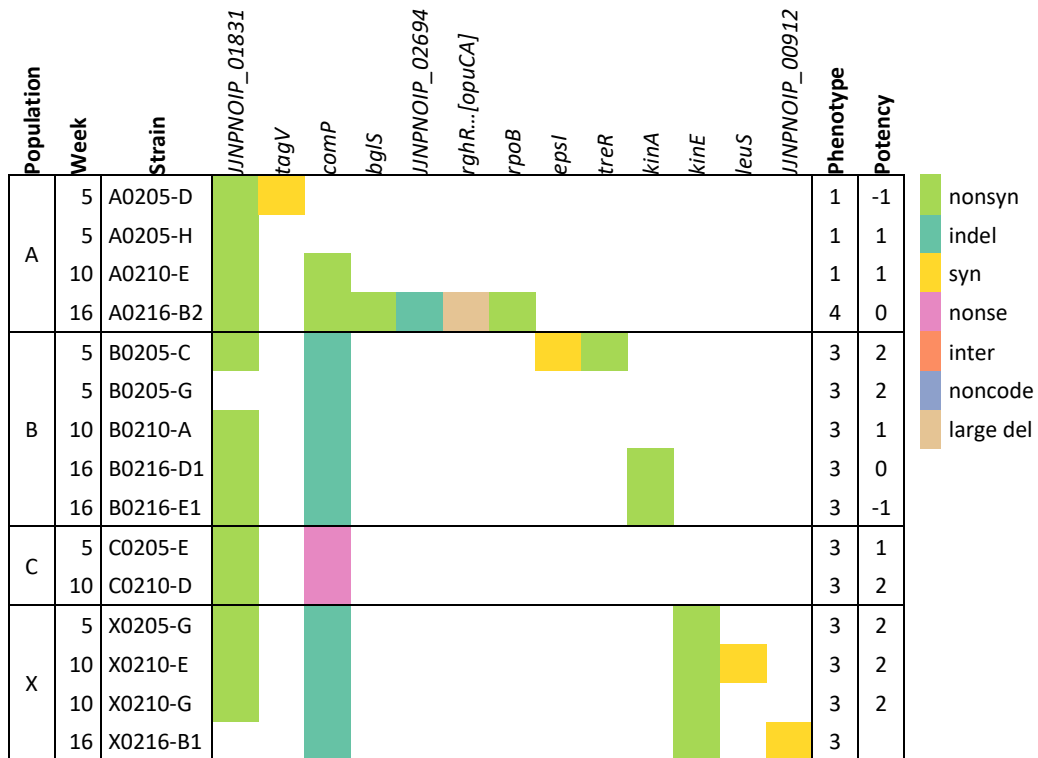


Fig. 7. Mutations identified in *B. subtilis* BCF002 background. The large deletion in strain A0216-B2 encompasses *rghR_1*, *rghR_2*, *yodB_2*, *mcpB_5*, *opuBD*, *opuBC*, *opuBB*, *opuBA_2*, *opcR_2*, *opuCD*, *opuCC*, *opuCB*, and partially *opuCA*.

Legend top-down; nonsynonymous SNP, small insert or deletion, synonymous SNP, nonsense SNP, intergenic SNP, noncoding SNP, large deletion.

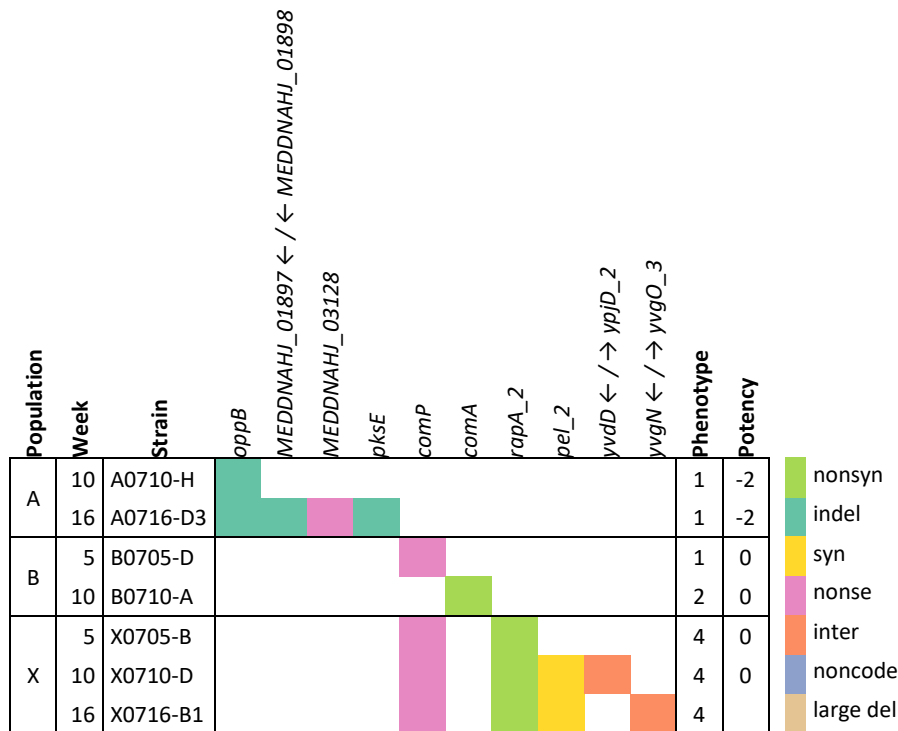


Fig. 8. Mutations identified in *B. amyloliquefaciens* BCF007 background. Arrows indicate gene orientation in respect to intergenic mutation. Legend top-down; nonsynonymous SNP, small insert or deletion, synonymous SNP, nonsense SNP, intergenic SNP, noncoding SNP, large deletion.

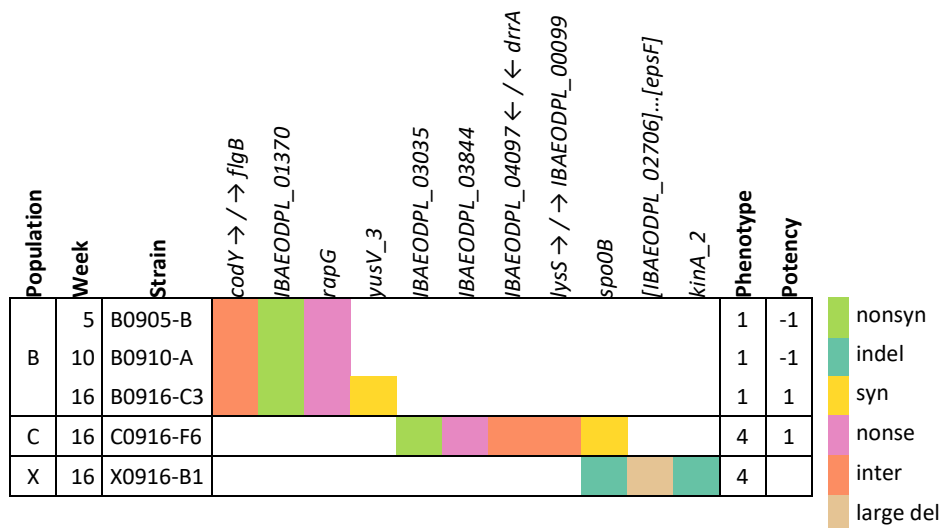


Fig. 9. Mutation identified in *B. paralicheniformis* BCF009 background. The large deletion in strain X0916-B1 encompasses partially *IBAEOPL_02706*, *sinI*, *sinR_1*, *tasA*, *sipW*, *IBAEOPL_02711*, *yqzG*, *IBAEOPL_02713*, *comGG*, *IBAEOPL_02715*, *IBAEOPL_02716*, *comGC*, and partially *epsF*. Arrows indicate gene orientation in respect to

intergenic mutation. Legend top-down; nonsynonymous SNP, small insert or deletion, synonymous SNP, nonsense SNP, intergenic SNP, large deletion.

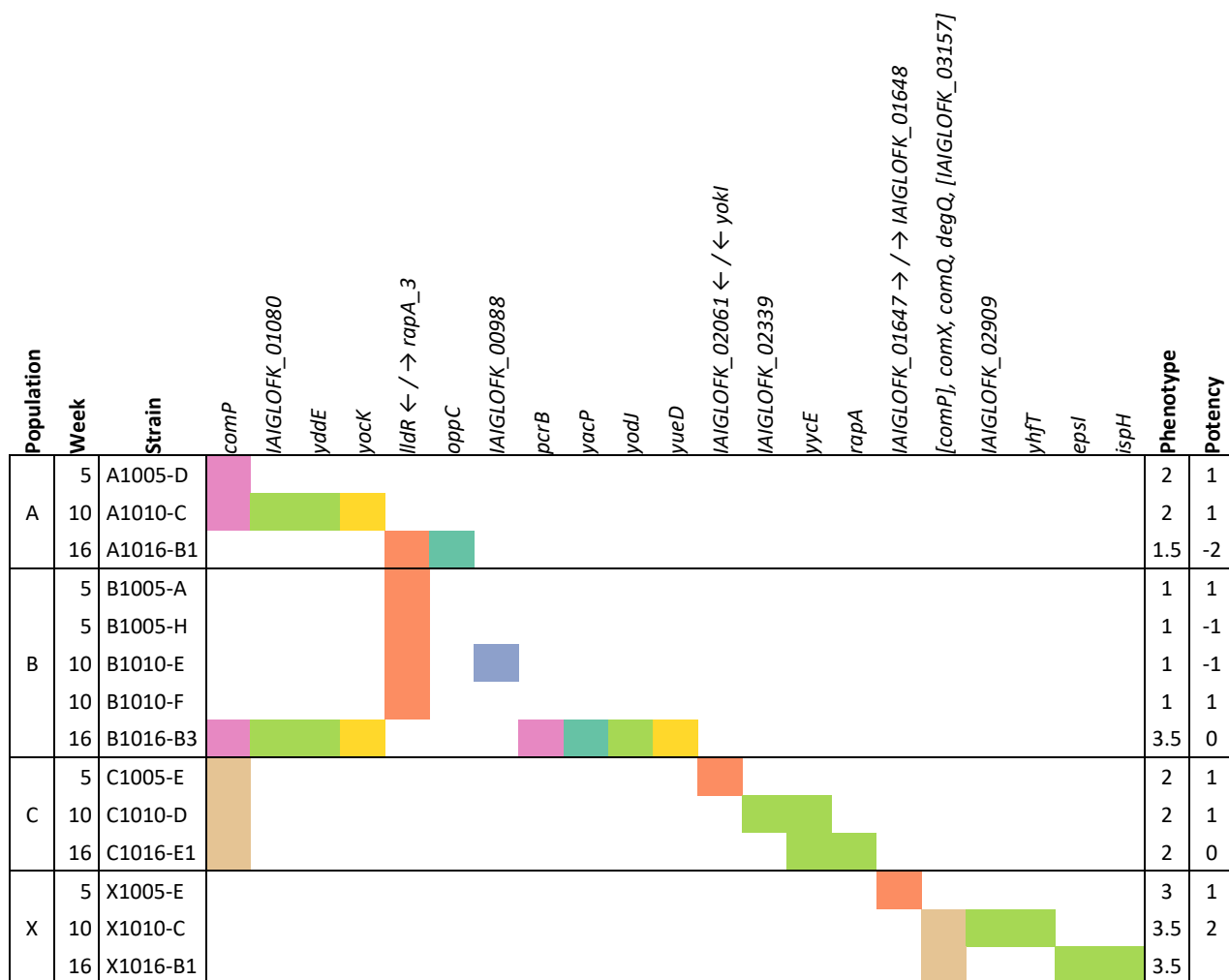
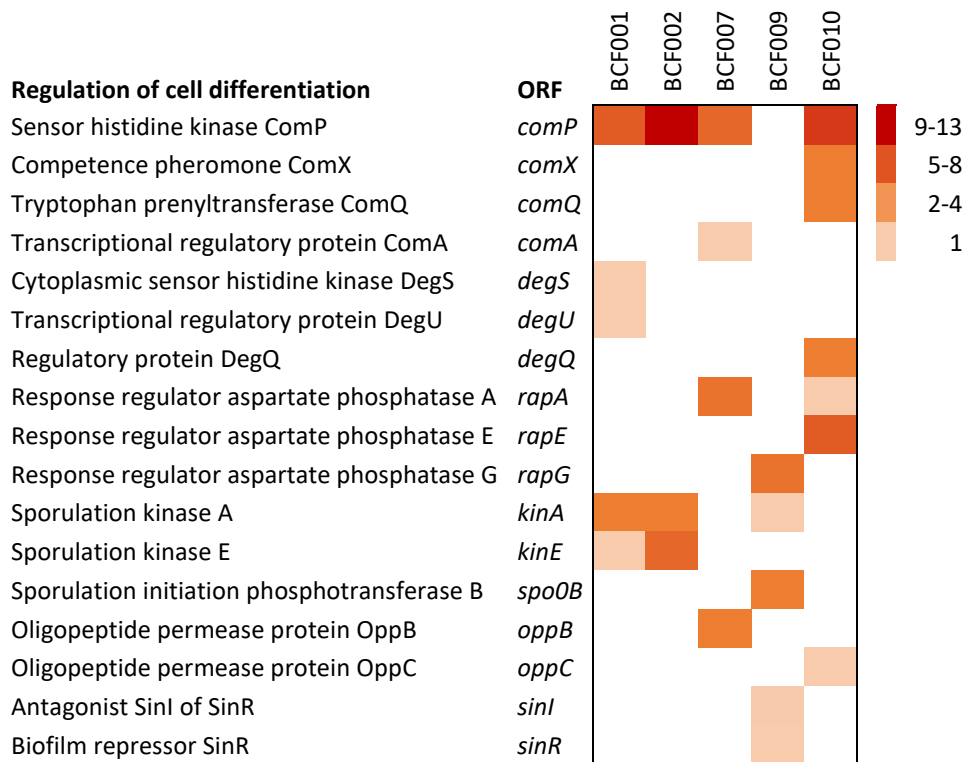


Fig. 10. Mutations identified in *B. subtilis* BCF010 background. The large deletion in strain X1010-C and X1016-B1 encompasses partially *comp*, *comX*, *comQ*, *degQ*, and partially *IAIGLOFK_03157*. Arrows indicate gene orientation in respect to intergenic mutation. Legend top-down; nonsynonymous SNP, small insert or deletion, synonymous SNP, nonsense SNP, intergenic SNP, noncoding SNP, large deletion.

Table 1. Mutations affecting ORFs related to cell differentiation. Multiple mutations were identified that affected the open reading frames (ORFs) of proteins involved in various cell differentiation pathways. Number of occurrences across strains is indicated by colour gradient scale.



From the primary characterization data and the insights of genomic changes, 12 derivatives were selected for further genotype to phenotype correlation studies mainly comprising strains with genetic changes in *compP*, but also *oppB/C*, *degS*, and *comA* (Table S6). Despite their significantly enhanced inhibition potency with respect to their ancestor, BCF009 derivatives were still outperformed by the other ancestor strains and their derivatives. Hence, no BCF009 derivatives were selected for further characterization.

***compP* mutations lead to loss of kinase function**

Analysis of the genetic changes identified within the *compP* coding sequence among 7 selected derivatives indicated most likely loss-of-function mutations, as either generated premature stop codons, large deletions or frameshifts in the open reading frame that result in truncated versions of the ComP sensor protein (Fig. 11).

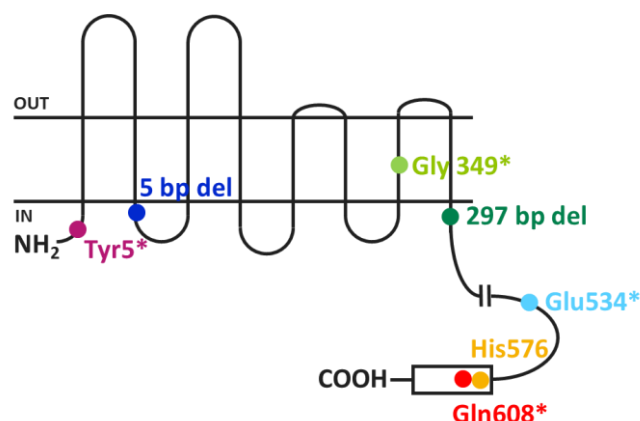


Fig. 11. ComP structural topology model with identified mutations from selected improved derivatives. Approximate positions of amino acid changes are indicated by coloured dots; Tyr5* (C0105-G) indicated in magenta, Δ 5bp deletion at position 409-413/2313 nt (B0205-G, X0205-G) indicated in dark blue, Gly349* (X0705-B) indicated in bright green, Δ 297bp deletion at position 1163-1459/2301 nt (C1005-E) indicated in dark green, Glu534* (A1005-D) indicated in light blue, and Gln608* (B0705-D) indicated in red. The conserved histidine kinase domain in ComP is indicated with a rectangle in the protein C-terminal end and the conserved autophosphorylation residue, His576 (16), is indicated in yellow. Figure inspired by (48).

Strain B0710-A harboured a substitution mutation (R183L) in the effector domain (147-212) of the response regulator ComA with possible impact on DNA binding, while strain C0105-E contained a substitution mutation (A247S) in the response regulator DegS not described in literature despite several mutagenesis studies of phosphorylation activity (36, 49, 50). The strains A0710-H, A0716-D3, and A1016-B1 showed decreased inhibition potency in the high throughput screening and acquired mutations disruption the reading frame of the pore forming proteins encoded by *oppB* (Δ 10, 528-537/936 nt) and *oppC* ((A)5 \rightarrow 4, 74/918 nt) known to participate in the oligopeptide transport systems (51, 52). These mutations possible affect the internalization of small signalling peptides by the oligopeptide transport system.

***comP* mutations are associated with decline in lipopeptide content**

Bioactive metabolites produced by a biocontrol strain greatly determine the potency of phytopathogen inhibition (53–55). Therefore, potent fungal inhibitor strains often synthesize high levels of bioactive metabolites. Especially the iturin (56–58) and fengycin lipopeptide families (11, 57–60) comprise potent antifungal compounds, but also surfactins may exhibit antifungal properties (59, 61). Surprisingly, ALE derivatives harbouring ComP loss-of-function mutations were associated with strong reduction in relative amounts of the cyclic lipopeptides fengycin and surfactin (Fig. 12A). In addition, relative amounts of the antibacterial polyketide bacillaene were reduced (Fig. S13C) and the *comP* mutants derived from

B. amyloliquefaciens BCF007 produced reduced relative amounts of the antifungal iturin lipopeptides (Fig. 12B). Interestingly, in line with these findings an experimental evolution study of *B. subtilis* co-cultivated with the fungal phytopathogen *Setophoma terrestris* also resulted in genetic alterations of *comP* leading to reduced biosynthesis of the fengycin/plipastatins and surfactin lipopeptides.

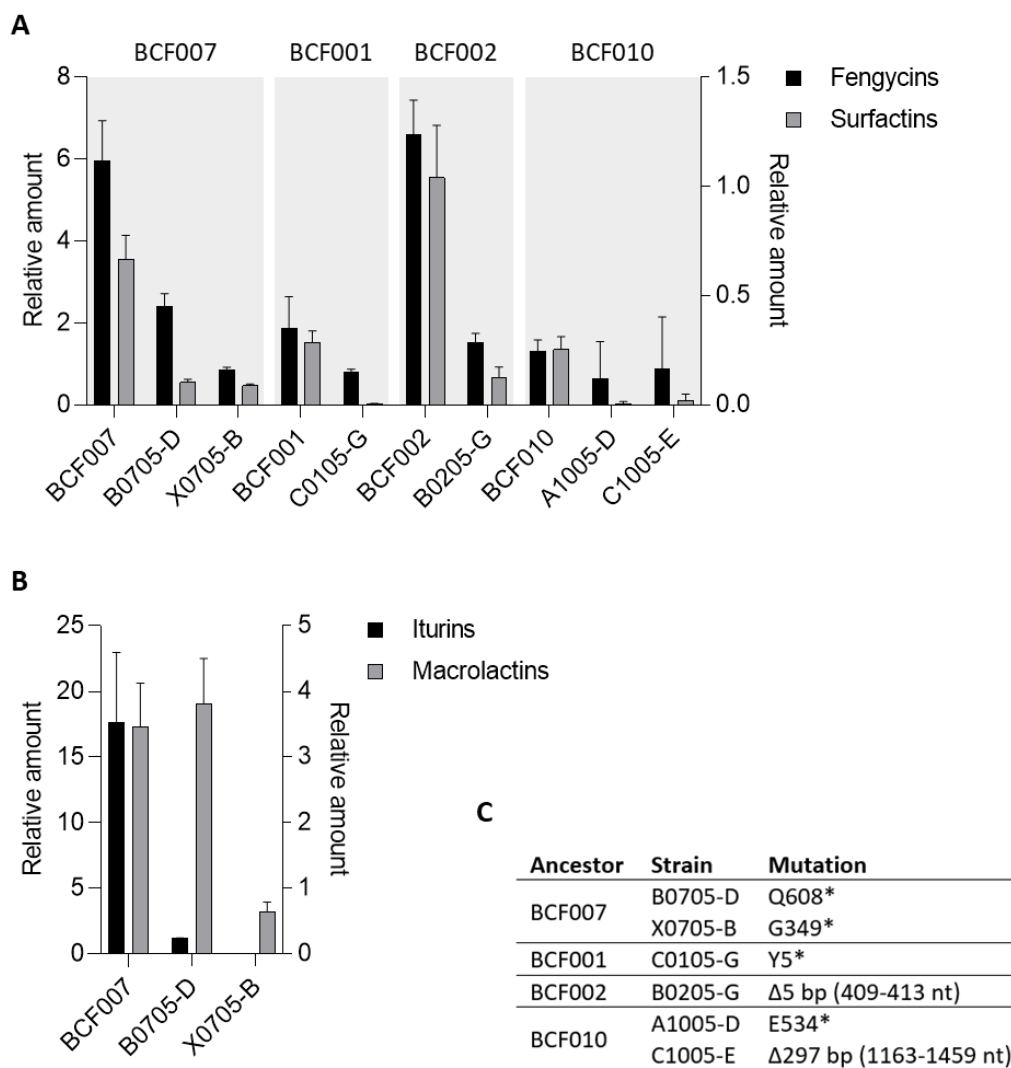


Fig. 12. Production of specialized metabolites by *comP* mutants. The lipopeptide and polyketide content of cultures from ALE derivatives containing *comP* mutations was analysed by LC-MS. Cultures were grown for 48h in PDB medium at 37°C with agitation to allow reaching the stationary growth phase. **A)** Fengycins/plipastatins (left axis) and surfactins (right axis) were analysed from cultures of evolved strains derived from *B. subtilis* BCF001, BCF002, BCF010, *B. amyloliquefaciens* BCF007. **B)** Additionally, relative amounts of iturins (left axis) and macrolactins (right axis) were analysed from *B. amyloliquefaciens* BCF007-derivatives. Error bars indicate standard deviation between biological duplicates. **C)** Overview of acquired *comP* mutations of respective evolved strains.

Fengycin culture contents of other mutants were reduced (*comA* mutant B0710-A, *degS* mutant C0105-E, *oppC* mutant A1016-B1, *oppB* mutants A0710-H and A0716-D3) (Fig. S13). The *oppB* mutants (A0710-H, A0716-D3) derived from *B. amyloliquefaciens* BCF007 retained production of surfactins and iturins, but showed reduced relative amounts of fengycins/plipastatins, while *comA* mutant B0710-A was severely affected in biosynthesis of all cyclic lipopeptide families. In addition, *degS* mutant C0105-E and *oppC* mutant A1016-B1 produced lower relative amounts of surfactin than the respective ancestors *B. subtilis* BCF001 and BCF010. Notably, evolved strains grew similarly to the respective ancestor with few exceptions; *opp* mutants A0710-H and A0716-D3 reached higher final OD₆₀₀ relative to the ancestor *B. amyloliquefaciens* BCF007, while the maximum growth rate of *comP* mutant A1005-D in exponential phase was inferior to the ancestor *B. subtilis* BCF010 (Fig. S12). Hence, the measured differences in specialised metabolite relative amounts could mainly be attributed to acquired mutations rather than growth differences.

Decreased fungal inhibition potency correlates to low lipopeptide contents

The half-inhibitory culture dilutions that reduced fungal growth by 50% (ID50) were determined. The fungal inhibitory potency of culture supernatants from *comP* mutants appeared significantly lower than the respective ancestor strains, correlating to a severe decrease in lipopeptide content (Fig. 13, Fig. S14). During the initial quantification of HT-screening in solid surface, *comP* mutants showed improved fungal inhibition potency. Contrary to our anticipation, this potency enhancement could not be assigned to components secreted into the extracellular medium as *comP* mutants displayed diminished ID50 in comparison to their ancestor strain.

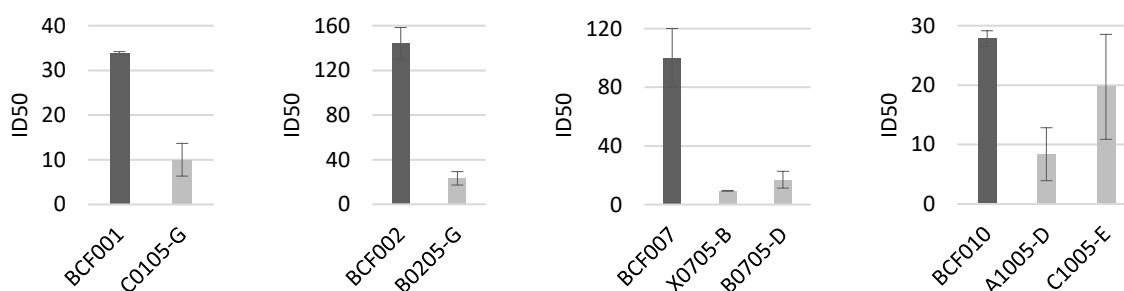


Fig. 13. Inhibition potency of *Bacillus* cultures on fungal growth. The half-inhibitory dilution (ID50) of *Bacillus* cultures that reduced *F. culmorum* growth to 50% was determined for *comP* mutants (light bars) and ancestor strains (dark bars). *Bacillus* culture dilution series were prepared and inoculated with a fixed fungal spore concentration. Bacteriostatic antibiotics were added to prevent bacterial growth. After 3 days incubation at 25°C, the fungal growth was quantified by spectrophotometry (OD₆₀₀) using an area scanning protocol. Results correspond to averages calculated from biological duplicates, with error bars indicating the standard deviation.

Culture addition of *comA* mutant B7010-A did not impact fungal growth, and therefore determination of ID50 was not possible (Fig. S14, Fig. S15). *oppB* mutants A0710-H and A0716-D3 showed prominent inhibition of *F. culmorum* growth, correlating to high lipopeptide content. However, ID50 values were slightly lower than those obtained with the ancestor strain *B. amyloliquefaciens* BCF007 in line with a lower fengycin/plipastatin content in the culture of those mutants. Both, *degS* mutant C0105-E and *oppC* mutant A1016-B1 affected fungal growth to a much lesser extent than their respective ancestor strains (BCF001, BCF010). ID50 values were drastically reduced, especially for A1016-B1 cultures, in accordance with reduced amounts of lipopeptides quantified in the bacterial cultures.

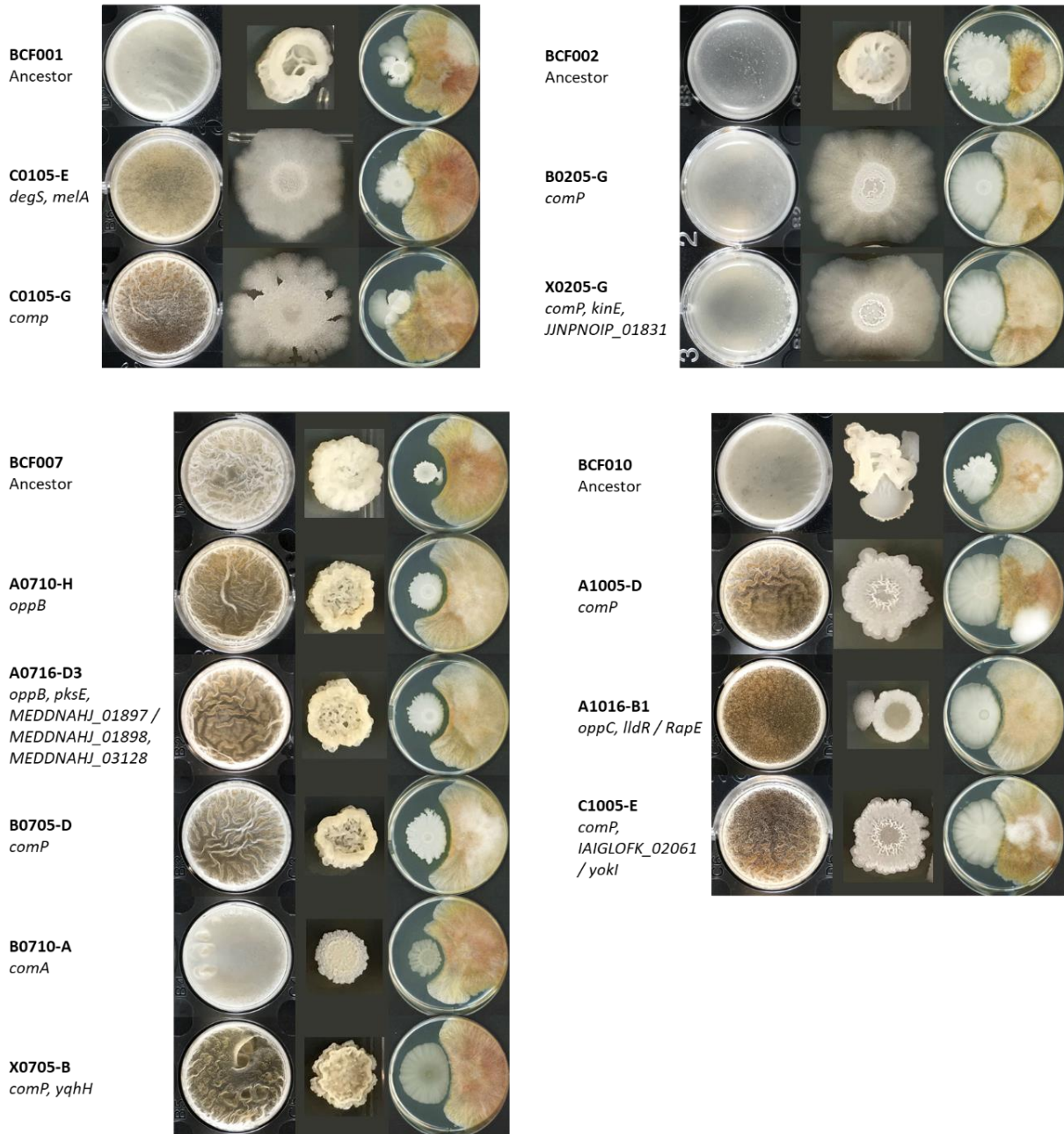
***comP* mutations alter biofilm structure and potentially improve competition for space**

The response regulatory system ComP-ComA influences the activation of biofilm formation (37). ComP-ComA may indirectly affect biofilm formation by induction of Rap phosphatase expression that control the activity of the sporulation/biofilm regulator Spo0A (29). Furthermore, the quorum sensing pair ComP-ComA induces the activity of two-component system DegS-DegU via DegQ, which affects biofilm formation and structure complexity in an undefined manner (42, 43, 62–64). To achieve more insights of the *comP* mutations' impact on biofilm formation, the ALE derivatives were cultured on solid biofilm inducing medium and their phenotypes compared to the respective ancestor strains in respect to structure, wrinkles, spreading, and mucoid/dry appearance. *B. subtilis comP* mutants displayed dry colony morphology with diminished biofilm structure in addition to increased colony expansion (Fig. 14). *B. amyloliquefaciens* BCF007 derived colonies remained more confined, but also displayed reduced complexity. In confrontation plate assays with *F. culmorum* on fungal growth medium, a spreading phenotype was observed leading to enhanced surface colonization (Fig. 14, Fig. S16). The increased colony expansion of *comP* mutants suggests that the improved antifungal activity detected during the initial screening may be explained by enhanced space competition of these strains. In some plates, the fungal colony growth reached the bacterial derivative colony. In contrast, the ancestor strains did not permit fungal growth in close proximity and created a growth free zone likely due to secretion and diffusion of bioactive compounds into the medium. The absence of an inhibition zone surrounding the bacterial derivative colonies in the plate confrontation assays suggests reduced secretion of bioactive compounds and is in accordance with the results obtained from lipopeptide quantification in liquid medium.

Bacillus spp. readily form biofilm on biotic as well as abiotic surfaces, but also have the ability transit from a motile live style in suspension to sessile biofilm-forming cells at the air-medium interphase. The pellicle morphologies of ALE derivatives were investigated to gain more insights of biofilm formation. Derivatives that acquired mutations in the *comP* gene showed altered pellicle phenotypes. A brown coloration of the

culture supernatant was observed, and, in most cases, the pellicles were wrinkled in comparison to ancestor strains, which suggest altered biofilm formation most likely linked to changes in synthesis of biofilm components (Fig. 14, Fig. S17).

A



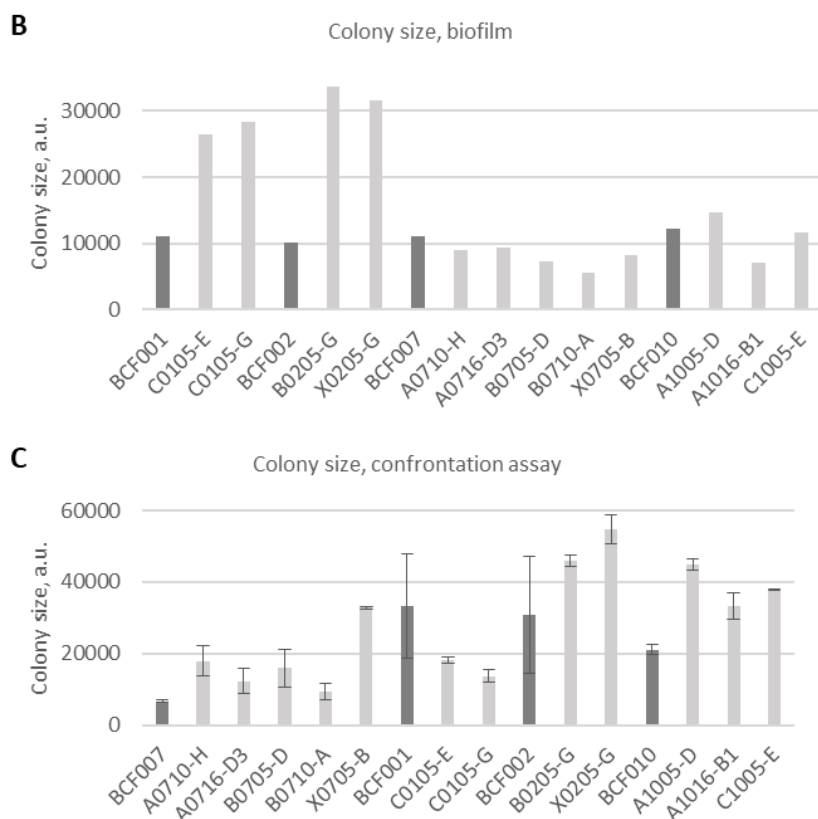


Fig. 14. Biofilm phenotypes of ALE derivatives. **A)** Biofilm phenotypes of ALE derivatives in comparison to their respective ancestor strains. Pellicle formation (biofilm at the medium-air interphase) was investigated in Mmsg medium after 3 days incubation at 30°C. Strains were incubated 2 days at 30°C on biofilm inducing medium to assess biofilm morphologies. *Bacillus* spp. and *F. culmorum* were co-inoculated on PDA medium to evaluate species confrontation. **B)** *Bacillus* colony expansion on biofilm inducing medium of derivatives (light bars) compared to the ancestor strains (dark bars). **C)** *Bacillus* colony expansion in confrontation with *F. culmorum* on PDA medium. Results correspond to averages calculated from biological duplicates, with error bars indicating the standard deviation.

Phenotypes of the *oppB* mutants (A0710-H, A0716-D3) were somewhat similar to the ancestor strain *B. amyloliquefaciens* BCF007, while *degS* mutant (C0105-E) showed reduced biofilm structure, enhanced colony spreading, altered pellicle, and coloration of pellicle supernatants in comparison to *B. subtilis* BCF001. *comA* mutant (B0710-A) derived from BCF007 was strongly affected in biofilm formation and displayed a structureless pellicle as well as colony with diminished biofilm complexity, but no increased colony expansion. Fungal growth was less affected in confrontation with the *comA* mutant and grew in close proximity to the colony in accordance the strain's reduced inhibition potency. *oppC* mutant (A1016-B1) derived from BCF010 displayed loss of biofilm structure and absence of spreading on biofilm inducing medium, but enhanced spreading in confrontation with *F. culmorum*.

Diminished poly- γ -glutamic acid (γ -PGA) production aligns with dry colony phenotype

In *Bacillus* spp. γ -PGA production requires ComPA as well as DegSU and DegQ (37, 65, 66). Therefore, the observed colony dryness of *comP* mutants is likely linked to reduced production of poly- γ -glutamic acid, which normally confers a mucoid aspect to the colonies (67). To test this hypothesis, the γ -PGA amount present in cell-free culture supernatants was quantified and compared between ALE derivatives and their ancestor strains. Indeed, *comP* ALE derivatives showed decreased levels of γ -PGA associated with the observed dry colony phenotype, with exception to strain B0205-G (Fig. 15).

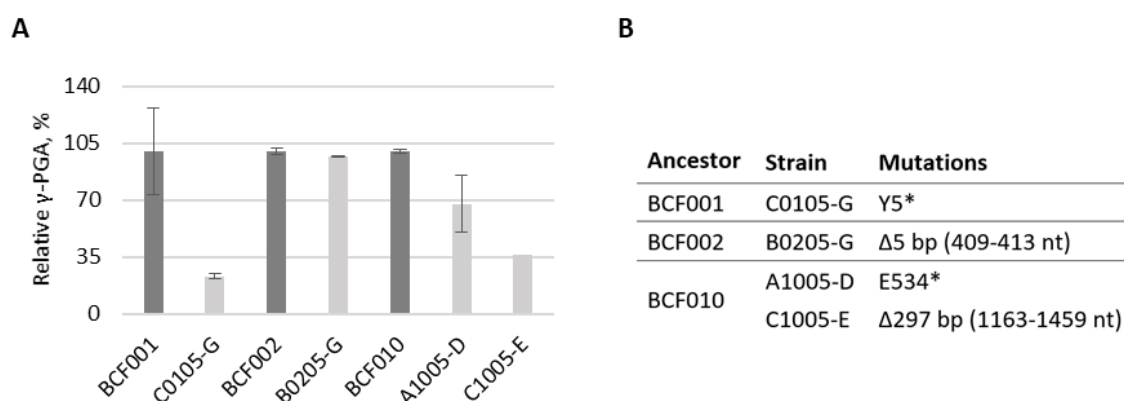


Fig. 15. γ -PGA quantification. **A)** The γ -PGA production was quantified and compared between ALE derivatives (light bars) and their ancestor strains (*B. subtilis* BCF010, BCF001, BCF002) (dark bars). The γ -PGA amount was calculated relative the respective ancestor strain in percentage. Results correspond to averages calculated from biological duplicates, with error bars indicating the standard deviation. **B)** Specific genetic changes of *comP* mutant ALE derivatives.

comP mutations hamper protease activity

Extracellular degradative enzymes recycle materials and scavenge amino acids from proteins or sugars from polysaccharides (68). In addition, extracellular proteases exert antifungal activity by degrading the hyphal cell wall and fungal signalling peptides, thereby benefitting the biocontrol potential of a strain (69, 70). Serine-class endo-protease activity was assessed by a colorimetric assay (described in materials and methods section) and the absorbance normalized to the signal from the corresponding ancestor strains (Fig. 16). All *comP* mutants showed significantly hampered protease activity when compared to the respective ancestor strains. Extracellular protease activity of *oppB* mutants (A0710-H, A0716-D3) showed minor reduction, while *comA* mutant B0710-A, *degS* mutant C0105-E and *oppC* mutant A1016-B1 showed a strong decrease of enzymatic activity (Fig. S18).

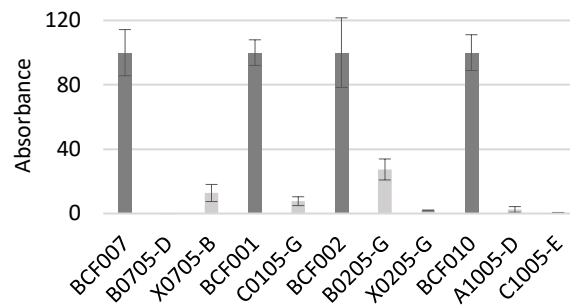


Fig. 16. Protease activity. The activity of serine-class endo-proteases was measured by a colorimetric assay. The absorbance from the derivatives (light bars) was normalized to the signal of the ancestor strains (dark bars). Results correspond to averages calculated from biological duplicates, with error bars indicating the standard deviation.

Swarming motility mainly unaffected

Swarming motility was assessed in semi-solid growth medium (LB 0.6% agar) to permit flagellar movement. The ALE derivatives swarmed similarly or slightly less compared to ancestor strains, except the *comP* mutant C0105-G derived from BCF001 and *comA* mutant B0710-A derived from BCF007, which appeared severely affected in swarming ability (Fig. 17, Fig. S19).

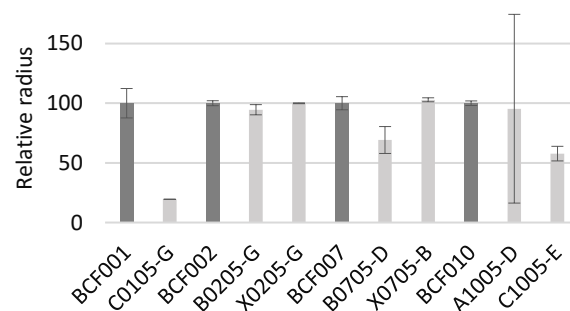


Fig. 17. Swarming motility. The radius of the swarming colonies was measured and normalized to that of the ancestor strains (dark). Swarming was assessed on semi-solid plates (0.6% agar). Results correspond to averages calculated from biological duplicates, with error bars indicating the standard deviation.

Quantitative evaluation of root colonization by evolved strains carrying *comP* mutations

It has been repeatedly documented that plant root colonization and plant pathogen biocontrol by *Bacillus* strongly depend and positively correlate with biofilm formation abilities (71, 72). Given the importance of matrix production for rhizosphere colonization (73) and the observed changes in colony phenotype of the ALE derivatives, we investigated root colonization abilities of *Arabidopsis thaliana* seedlings by *comP* mutants in comparison to their corresponding ancestor strains. While biological duplicates repeated on independent days showed a tendency towards reduced root colonization abilities of *comP* mutants derived from *B.*

amyloliquefaciens BCF007 and similar colonization by C0105-G to the ancestor *B. subtilis* BCF001, results for *comP* mutants derived from *B. subtilis* BCF010 were not reproducible (Fig. 18). Additional experiment repetitions are required to acquire significant data and confidently conclude on the root colonization capacity of the evolved strains. Due to the high variability, multiple repetition are required of root colonization assays, to draw reliable conclusions as previously demonstrated (74–76).

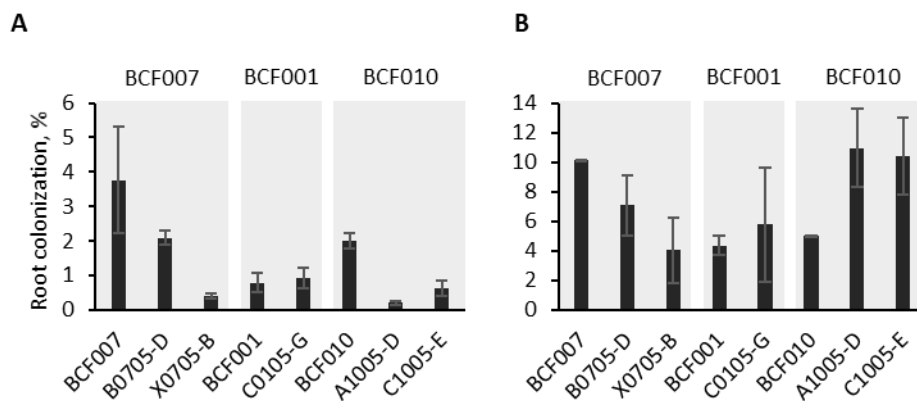


Fig. 18. Root colonization by *comP* mutants. *Bacillus* were inoculated with 7-9-day old *A. thaliana* seedlings in ½MS medium and incubated at 25°C. After 24 h, bacteria attached to the roots were removed by sonication pulses and dilution series were prepared and plated for CFU counting of spent medium as well as the sonicated samples. The root colonization was calculated by percentage attached cells relative to total cells (spent medium and attached). Root colonization was assessed in biological duplicates on two different days. **A)** Biological duplicate 1. **B)** Biological duplicate 2. Results correspond to averages calculated from biological duplicates, with error bars indicating the standard deviation.

Amplified effect of volatile organic compounds on fungal growth inhibition

Volatile organic compounds (VOCs) produced by *Bacilli* contribute to the interspecies chemical signalling. For instance, the production of the volatiles such as acetoin and 2,3-butanediol by *B. subtilis* stimulate plant growth in a cytokinin, ethylene, or auxin-dependent manner (77, 78). In addition to plant-growth promotion, VOCs contribute pathogen control by triggering induced system resistance in plants or by antibiosis of phytopathogenic species including fungi (79–81). To study the effect of bacterial volatiles on fungal growth, we implemented the use of volatile chambers. Volatile chambers were assembled by confronting two bottom Petri dishes to allow only VOC-mediated interaction between *Bacillus* strains and the fungal pathogen. *Bacillus* strains and *F. culmorum* were inoculated on bottom and top confronted plates, respectively. The fungal radial growth was measured in response to VOCs from the ancestor and derivatives and normalised to the fungal control (Fig. 18, Fig. S20). VOCs from all *comP* mutants displayed enhanced inhibitory effect on the fungal growth suggesting that VOCs contribute to the improved fungal inhibition.

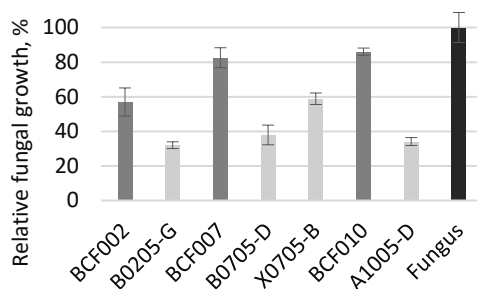


Fig. 19. In vitro percental of inhibition of *F. culmorum* by the *Bacillus volatilome*. *Bacillus* strains or *F. culmorum* spore suspension was inoculated in the centre of a petri dish on a filter paper disc. The plates were incubated 1.5 day before the sandwiching the bottoms of plates with the two species. The plate sandwich was sealed to prevent escape of volatiles and incubated at 25°C. The volatile compound effect of ALE derivatives (light grey) was calculated relative to the fungal control (fungus grown a petri dish compartment without bacteria) (black) and compared to the ancestor strains (BCF010, BCF007, BCF002, BCF001) (dark grey) after 48h.

Discussion

Adaptive laboratory evolution (ALE) is a powerful tool to gain insights into the molecular mechanisms of evolution and population dynamics (22, 82), but also for strain fitness optimization (74, 83, 84) and is yet to be fully explored for the purpose of developing new and potent biocontrol candidates for application in agriculture. In this study, we employed ALE for improving the antifungal properties of *Bacillus* strains against the devastating phytopathogen *F. culmorum* by iterative co-cultivation cycles. Subsequent HT-screening for antifungal properties revealed a reduced percentage of improved derivatives in progression with the ALE experiment. The decreasing numbers of improved derivatives may coordinate with previous reports of non-linear fitness improvement and steplike fitness increase in experimental evolution (85). The increased numbers of poor inhibitors may also be a sign of appearance of cheaters or exploiters that rely on other strains for antifungal properties, while saving energy on reduced production of those. *Bacillus* evolution studies report emergence of cheaters that shed the burden of costly productions and yet benefit from common goods from producing cells (86, 87). Another possibility is that the experimental design simply does not select for improved fungal inhibitors, but rather fungal mutualists leading to declining antifungal properties over time. In this respect, the screening results may reveal insights of a dynamic interaction between the species that is at first antagonistic and later becomes synergistic, as was the case of the plant-pathogenic *Pseudomonas protegens* that evolved into plant mutualists over repeated co-cultivation cycles with *A. thaliana* (88). Precautionary measures were taken to promote competitive evolution of the *Bacillus* strains and avoid simultaneous evolution of the fungi by applying fresh fungal inoculi at each experiment evolution passages.

Whole genome sequencing of selected improved strains from the HT-screening identified *comP* as the most frequently mutated ORF among ALE derivatives of co-evolved and evolved control populations (30/145 total mutations). Mutations occurring multiple times across ALE replicates are assumed to be adaptive (89), hence *comP* mutations are almost surely adaptive to the growth conditions. The occurrence in ALE control lines in the absence of fungus enabled us to conclude that *comP* mutations are not fungal co-cultivation adaptations, but rather general adaptations to the specific experimental conditions. Nonetheless, *comP* mutants were identified with improved inhibition fungal in the HT-screening demonstrating that mutation of *comP* indeed benefits *Bacillus* in competition against *F. culmorum* under laboratory growth conditions. The two-component system ComP-ComA plays part in a complex regulatory network that determines cell fate by regulating gene transcription in response to the external signals (17, 90). Upon increase in cell density, extracellular accumulation of the pheromone ComX activates the quorum sensing system ComP-ComA leading to a coordinated responsive behaviour across multiple cells (16, 19, 34, 91). Due to the influence of the regulatory pair ComP-ComA on cell differentiation (90), a variety of phenotypic characterization assays were undertaken. Among others, biofilm formation, specialised metabolite production, and culture inhibition potency was investigated to elucidate the impact of *comP* mutations.

To our surprise, the improved fitness could not be attributed to enhanced lipopeptide production as culture contents of potent antifungal compounds such as fengycins and iturins in addition to surfactins were reduced in *comP* mutants. These results suggest that the improved fungal inhibition depends on alternative mode-of-action than secretion of bioactive compounds. Indeed, in accordance with low lipopeptide content, fungal inhibition potency of the culture supernatant was decreased in *comP* mutants, while culture supernatant of the *comA* mutant failed to impact the *F. culmorum* growth. The hampered culture inhibition potency of the BCF007-derived *comA* mutant B0710-A correlates to a very low content of cyclic lipopeptides and indicates that the hitherto undescribed residue R183 is significant for ComA activity, further supporting the importance of ComA in the regulation of biosynthesis of bioactive compounds. *oppB* mutants (A0710-H, A0716-D3) retained production of surfactins and iturins, while fengycins/plipastatins were reduced. The preserved biosynthesis of specialised metabolites was reflected by the noteworthy culture supernatant inhibition of *F. culmorum* growth. Previous studies relate impaired biosynthesis of the antibiotic metabolite bacilylsin to the oligopeptide binding protein OppA by means of ComA, ComQ and the peptide pheromones PhrC and ComX, indicating that the permease possibly impacts specialised metabolite biosynthesis via the quorum sensing system ComP-ComA (92, 93). In contrast, bacilylsin production was considerably improved by *oppB* mutants in the present study, but impaired in *comP* and *comA* mutants (Fig. S13C).

Biosynthesis of fengycins (38, 39) and iturins (40, 41) is induced by the pleiotropic regulator DegQ. Transcription of DegQ itself is activated by phosphorylated ComP-ComA (43, 62). Therefore, the loss of ComP or ComA function likely leads to reduced transcription of fengycins and iturins due to impaired activation of DegQ. The surfactin non-ribosomal peptide synthase is encoded by the *srf* operon and induced by ComA upon phosphorylation by ComP (16, 18, 32). Thus, the loss of ComP function likely results in hampered activation of ComA and thereby reduced biosynthesis of surfactin, as was also observed in the evolution study of *B. subtilis* in the presence of the plant pathogenic fungus *S. terrestris* (12). Furthermore, deletion of the *srf* operon was previously shown to negatively impact biosynthesis of fengycin/plipastatin, linking the regulation of these lipopeptides (94).

Notably, matrix production by *comP* mutants appeared altered both on solid biofilm inducing medium and during pellicle formation at the air-medium interphase. Loss of biofilm structure, colony dryness, reflected by the declined poly- γ -glutamic acid (γ -PGA) production, and increased surface colonization was seemingly an effect of *comP* mutations in *B. subtilis* backgrounds. Simplified colony structure was also observed of the *B. amyloliquefaciens* BCF007 derivatives, but the colonies remained confined, indicating that loss of *comP* function impose less biofilm changes in this genetic background. The biofilm morphology of *comA* mutant B0710-A showed even lower degree of complexity, illustrating that ComA function is crucial for production of matrix components and biofilm structure, as demonstrated by previous studies (37).

Whereas surfactin is not essential for biofilm formation (95), this lipopeptide enables colony expansion across a surface (96–98). However, in the light of the reduced surfactin content in cultures, the increased colony expansion of *B. subtilis* derivatives cannot be assigned to the effects of this biosurfactant. In addition, colony spreading could arise from the passive expansive forces of a growing colony aided by the secretion of extracellular polysaccharides (99). ComP-ComA indirectly regulate matrix production by activation of Rap protein expression (29, 33, 100) and may influence colony expansion in this manner. Rap phosphatases control the phosphorylation state of the master response regulator Spo0A (101). At low phosphorylation levels, Spo0A triggers biofilm matrix production, whereas high Spo0A phosphorylation levels favour sporulation (102, 103). In addition, several studies suggest that DegU is required for complex biofilm architecture in a yet unknown manner, although its activity is necessary for expression of the biofilm hydrophobin BslA as well as the putative lipoprotein YvcA allegedly required for complex biofilm architecture (37, 42, 43, 63, 64). Furthermore, loss of DegQ has been associated with flat, structureless biofilm formation (38, 104). Both the two-component systems ComP-ComA and DegS-DegU seemingly induce transcription of DegQ (62), while DegQ itself stimulates phosphor-transfer from DegS to DegU (43). Interplay between the two-component systems have been hypothesized to occur via activation of DegQ transcription by ComP-

ComA upon high cell densities leading to induced phosphor-transfer from DegS to DegU (43). Studies show that DegU regulates different sets of genes dependent on its phosphorylation state. High levels of DegU~P onset its own transcription, biosynthesis of γ -PGA, and degradative enzymes. Intermediate levels of DegU~P onset biofilm formation in an undefined manner, whereas low levels of DegU~P induce flagella-driven motility (43, 63, 105, 106). Thus, we speculate that the loss of ComP function may affect matrix production, biofilm complexity and γ -PGA synthesis directly, through its hypothesized influence on the DegQSU regulatory pathway and/or through the Rap protein expression, leading to altered colony morphology. Furthermore, given the hypothesized influence of ComP-ComA on the activation of the DegQSU, loss of ComP-function may potentially affect pellicle phenotype, as initiation of pellicle formation requires motility, which is induced at low levels DegU~P (63, 107, 108). At the following stage, cells transit from motile to sessile matrix-producing cells (109), a process regulated by Spo0A and DegU as previously described. Further studies are required to elucidate the potential role of ComP in DegU phosphorylation. The dark coloration developed in supernatants of *comP* mutants (C0105-G, A1005-D, C1005-E, B0705-D) and *opp* mutants (A0710-H, A0716-D3, A1016-B1) pellicle assays could be related to accumulation of the iron chelator pulcherrimin. The iron-chelating compound pulcherrimin is secreted to the extracellular medium during biofilm formation (110) and has been shown to function as a growth inhibitor of competing microorganisms by creating an iron deficient zone (26). The pulcherriminic acid biosynthetic operon *yvmC-cypX* is regulated by PchR (YvmB), iron availability and the transcriptional repressor AbrB, the latter being induced itself by Spo0A (110, 111). Hence, it is possible that ComP indirectly affect pulcherriminic acid biosynthesis via its influence on Spo0A phosphorylation state. However, further studies are required to clarify this hypothesis. Another possibility is that the dark coloration arises from sporulating cells. *Bacillus* spp. enter the dormant spore state when nutrients become growth limiting and Spo0A phosphorylation gradually increases within the cells (102, 112). As ComP induces the Rap phosphatases that reduce the level of phosphorylated Spo0A, high Spo0A phosphorylation state and the sporulation pathway may be favoured in a *comP* mutant strain. Sporulation was of ALE derivatives was assessed in a HT assay that did not permit determination of efficiency.

Several changes in phenotypes were observed in *comP* mutants that are known to be controlled by the regulatory two-component system DegS-DegU in addition to ComP-ComA, which led us to further explore this regulon. Indeed, extracellular protease activity, regulated by DegQSU regulatory pathway (35, 36, 113, 114), was severely decreased in *comP*, *comA* and *degS* mutant ALE derivatives. Swarming motility was not affected notably in *comP* mutants in contrast to the results obtained for the *comA* mutant, where motility was severely impaired. In line with our finding, previous studies reported that ComP is dispensable for swarming motility, whereas ComA is essential (98). Generally, *comA* mutant phenotypes were impacted to a greater extent than *comP* mutant phenotypes both in respect to loss of biofilm structure, declined specialised

metabolite biosynthesis and hampered protease activity. These results suggest that ComA may retain some activity in absence of functional ComP, but genetic alterations of *comA* itself is detrimental to the assessed respective phenotypes. Motility of *degS* mutant C0105-E was not notably affected in accordance with literature. Swarming motility is known to be dependent on low levels of phosphorylated DegU to onset expression of flagellar genes, but independent of DegS activity (43, 67).

The *Bacillus* volatilome has proven effective against fusaria growth in several cases. For instance, previous studies demonstrate that secretion of the volatiles 2-nonanone and 2-heptanone produced by *B. amyloliquefaciens* L3 as well as 11 volatile compounds from *B. amyloliquefaciens* NJN-6 effectively inhibited growth of *F. oxysporum* (81, 115). Intriguingly, we found that VOCs produced by *comP* mutants significantly constrained fungal growth in comparison to the ancestor strains. The effect of quorum sensing (ComQPXA) mutations on production of VOCs (volatilome composition) has previously been reported in a similar study (12). With great resemblance to our findings, co-evolution of *Bacillus* with the fungus *Setophoma terrestris* led to reduced production of the cyclic lipopeptides surfactin and plipastatin, but concomitantly increased fungal growth inhibition by VOCs. The mechanism behind the influence of ComQPXA on VOC production is unknown, but the authors speculate that ComA may alter general metabolism in such way that degradation of branched amino acids favours biosynthesis of VOCs i.e., 2-heptanone and 2-octanone, or alternatively that ComA reduces transcription of *fapR*, the repressor of fatty acid synthesis encoded by the *fap* regulon. Thereby, mutations in *comA* could lead to increased fatty acid synthesis, where the decarboxylation of intermediate ketoacids potentially leads to 2-ketones formation. Additional experiments and repetitions of our initial approach are required to determine of volatilome of the ALE derivatives.

Concluding remarks

The present study investigated the prospects for developing potent fungal inhibitor strains by ALE in co-cultivation with fungi. The gene *comP*, encoding the response regulator of the quorum sensing system ComP-ComA was identified as the most frequently mutated ORF among derivatives with improved antifungal properties under laboratory conditions and characterization assays found several phenotypic traits associated with *comP* mutants (summarized in Table S6). These phenotypic traits largely align with the role of ComP-ComA in cell differentiation described in literature. In agreement with ComP's described regulatory influence, i) ComA-controlled surfactin production was affected, ii) biofilm matrix production was altered (possibly also sporulation) via regulation the Spo0A-phosphorelay system, and iii) phenotypes associated with DegQ activity and the two-component system DegSU were also affected including γ -PGA and lipopeptide production (fengycin and iturin), biofilm structure, extracellular degradative enzyme activity, and pellicle

formation. Finally, in terms of inhibitory fitness, results suggest that loss-of-ComP function leads to enhanced surface colonization in competition against fungus and in addition influences the volatilome composition via an unknown mechanism leading to improved fungal inhibition potency under the specific laboratory conditions.

Materials and methods

Microbial species, growth conditions and media: Bacterial and fungal species can be found in Table 3. Unless stated otherwise, *Bacillus* pre-cultures were grown in lysogeny broth (LB) medium (10 g/L Bacto tryptone [Difco], 5 g/L yeast extract [Oxoid], 10 g/L NaCl [Merck], pH 7.2 ± 0.2) at 37°C with 250 rpm agitation in culture tubes (3-4 ml) or in 96 deep-well plates. For growth in the BioLector I (m2p-labs), settings were; humidity 85%, shaking 1000, and O₂ 21%. Dilutions of bacterial cultures were prepared with peptone saline (pepsal) as diluent (Maximum recovery diluent: peptone 1 g/L, sodium chloride 8.5 g/L, pH 7.0 ± 0.2, [Oxid]). Fungus and bacterial-fungal co-inoculations were cultivated on potato dextrose agar (PDA) medium (4 g/L potato infusion, 20 g/L glucose, 15 g/L agar, pH 5.6 ± 0.2; [Carl Roth]) or in potato dextrose broth (PDB) medium (6.5 g/L potato infusion, 20 g/L glucose, pH 5.6 ± 0.2 [Carl Roth]).

Table 2. Microbial species. Bacterial and fungal species used in the present study.

Species and strains	Number	Source
Mold fungi		
<i>F. culmorum</i>	DSM1094	DSMZ German Collection
Bacteria		
<i>B. subtilis</i>	BCF001	Chr. Hansen A/S
<i>B. subtilis</i>	BCF002	Chr. Hansen A/S
<i>B. amyloliquefaciens</i>	BCF007	Chr. Hansen A/S
<i>B. paralicheniformis</i>	BCF009	Chr. Hansen A/S
<i>B. subtilis</i>	BCF010	Chr. Hansen A/S

Fungal spore harvesting: Fungal spores were harvested according to (24). In brief, fungal species were grown on PDA medium for 2-3 weeks at 28°C until sporulation. Spores were retrieved by adding saline Tween solution (8 g/L NaCl, 0.05 mL/L Tween 80) to the growth plates and gently scraping the mycelium. The spore suspension was filtered through Miracloth (Millipore) to remove hyphal debris and centrifuged at 5000 rpm for 10 minutes to collect spores. Spores were resuspended in saline Tween to an appropriate concentration.

ALE: Inspired by (Richter et al., 2023, Study 2), an ALE experiment with *Bacilli* and plant pathogenic fungus was established. The strains *B. subtilis* BCF001, *B. subtilis* BCF002, *B. amyloliquefaciens* BCF007, *B. paralicheniformis* BCF009, and *B. subtilis* BCF010 were co-cultivated in triplicate ALE-lines with

F. culmorum in iterative cycles for 16 weeks. First, *Bacillus* cultures were grown overnight in 3 ml LB and diluted 1:100, except strain BCF009. Two 10 μ l-loops of bacterial culture were streaked in a square pattern on PDA growth medium, while two loops of fungal spore suspension (1.1×10^6 spores/ml) were streaked in a hashtag pattern. For strain BCF009, a spore concentration of 1.1×10^7 spores/ml was used. The co-inoculated plates were incubated at room temperature with natural light for 5 days. An agar plug with *Bacillus* growth was excised from the contact zone between the two species and transferred to a selective medium for bacteria (LB supplemented with 50 mg/L nystatin) and incubated 24h. Cultures were inoculated from the bacterial outgrowth from the agar plug and incubated overnight. The cultures were once again used for co-inoculation with new fungal spores. The cycle was repeated for 16 weeks, and glycerol stocks were prepared from the *Bacillus* populations by each transfer and stored for later fitness screening. As controls, each of the strains BCF001, BCF002, BCF007, BCF009, and BCF010 were evolved by the described iterative cultivation cycles, but in the absence of fungus.

Competitive fungal inhibition screening: Using a Hamilton Microlab STAR Liquid Handling System, evolved *Bacillus* strains were screened for improved competitive growth against *F. culmorum* in a high throughput setup according to (25). In brief, strains were cultivated in 96-well microtiter plates at 30°C and the optical density (OD₆₂₀) adjusted. Except for BCF009 derivatives, all cultures were adjusted to OD₆₂₀ 0.02 and a 1:5 dilution series was prepared with 6 steps. BCF009 derivative cultures were adjusted to OD₆₂₀ 0.2 and a 1:2 dilution series was prepared. Each bacterial dilution series was inoculated in a column of a 48-well microtiter plate prepared with PDA. Of each dilution, 15 μ l was inoculated in consecutive rows. A fungal spore suspension was prepared with 3.5×10^3 spores/ml and 15 μ l was inoculated in each well of the 48-well microtiter plate. The co-inoculated plates were sealed with 3M tape and incubated at room temperature with natural light for 5 days. The fungal and bacterial growth was visually inspected. The dilution of each ALE derivative that inhibited fungal growth was identified and compared to that of the respective ancestor strain.

Colony morphology: *Bacillus* pre-cultures grown overnight at 28°C in 96-well plates were diluted 1:100 and 10 μ l culture was spotted on a Q-tray dish with biofilm inducing medium (LB agar, 0.1 mM MnCl₂, 1 % glycerol). The plates were incubated at 30°C for two days. The colony phenotypes were scored according to morphological similarity to the respective ancestor strains. 1: High structure and no spreading. 2: No spreading and less structure. 3: Spreading, but still some structure. 4: Spreading and no structure or mucoid texture.

Growth kinetics: *Bacillus* pre-cultures were diluted 1:100 in fresh PDB in 96-well plates and incubated in an EnzyScreen Growth Profiler 960 at 28°C with agitation in biological duplicates. The measured arbitrary G-values were converted to OD values using calibration curves from the respective ancestor strains.

Data analysis: Principal components analysis (PCA) was conducted to visualize the similarity of the isolates. PCA was performed using OD measurements (converted from arbitrary G-values) from time 0 to 16.5h, as well as the two variables *Phenotype* and *Score*, which were based on colony morphology categorization and fungal inhibition screening results. The OD measurements were standardized to have a mean of 0 and standard deviation of 1 within each experiment. Furthermore, standardized OD values were multiplied by 0.7 to obtain an optimal weighting of OD data and phenotype/score variables in the PCA analysis.

Whole genome sequencing, assembly, and SNP analysis: Using a Biomek i5 liquid handler (Beckman Coulter), genomic DNA for *de novo* short read WGS was extracted with Clean Blood & Tissue DNA Kit (NACBT-D0384). Tissue Lysis buffer was substituted with 200 μ L custom lysis buffer (1x PBS, 20 mg/mL lysozyme, 50 U/ μ L mutanolysin, 2 mg/mL RNase A). Genomic libraries were generated using NEBNext[®] Ultra[™] II FS DNA Library Prep Kit for Illumina[®] with NEBNext Multiplex Oligos for Illumina (Unique Dual Index UMI Adaptors DNA Set 1, New England Biolabs). Clean NGS beads (Clean NA) were used for double-sided post ligation size selection and one post-amplification clean-up to purify fragments at average size between 450 to 550 bp. Concentration of DNA libraries were measured by QubitFlex[®] Fluorimeter, while library size distribution was determined using the Agilent HS NGS Fragment (1-6000 bp) kit on the Agilent Fragment Analyzer (Agilent Technologies). Libraries were normalized and pooled in buffer (10 mM Tris-Cl, pH 8.0, 0.05 % Tween 20), prior to denaturation in 0.2N NaOH in ice-cold HT1 buffer. Denatured library was loaded onto the flow cell (NextSeq Reagent Mid Output) and sequenced on a NextSeq 550 platform (Illumina) with a paired-end protocol and read lengths of 151 nt. Ancestors were sequenced externally by GenXone using long read sequencing.

Illumina short reads were trimmed using AdapterRemoval version 2.2.4 with custom parameters ensuring minimum quality of 20 and discarding reads <30 base pairs. The genome of phi-X174 (NCBI accession id: J02482.1) was removed from the trimmed reads using bwa mem version 0.7.17-r1188. Trimmed short reads and raw ONT reads were assembled by Unicycler 0.4.7 with the parameter set to 'conservative'. Gene calling and functional annotation was done with prokka version 1.13. Single nucleotide polymorphism (SNP) analysis was conducted using breseq 0.34 on short reads with standard parameters and custom scripts against the ancestor reference genomes. Due to the repetitive nature of ribosomal RNA genes, mutation in those loci were filtered out. Also, identical mutations reoccurring in every derivative from an ancestor strain were considered to arise from the ancestor itself and filtered out.

Pellicle formation: MSgg medium was prepared according to (116) with 5 mM potassium phosphates buffer (pH 7), 100 mM MOPS, 2 mM MgCl₂, 700 μ M CaCl₂, 100 μ M MnCl₂, 50 μ M FeCl₃, 1 μ M ZnCl₂, 2 μ M thiamine, 0.5% glycerol, 0.5% glutamate, 50 μ M L-tryptophan, and 50 μ M L-phenylalanine. *Bacillus* cultures were

grown until OD₆₀₀ 1. Then 20 µl culture was inoculated into 1.5 ml MSgg medium in 24-well microtiter plates, which were incubated statically at 30°C for 3 days and imaged.

Plate confrontation: *Bacillus* pre-cultures grown overnight at 30°C were diluted 1:5. A fungal spore suspension was prepared with 1.76×10^4 spores/ml. 10 µl fungal spore suspension and 10 µl bacterial culture were inoculated on each side of a PDA growth plates 1.5 cm from the centre (total distance 3 cm). The plates were sealed with 3M tape and incubated at 25°C for 5-7 days in darkness.

Biochemical analysis: *Bacillus* strains were grown in PDB medium at 30°C in a BioLector for 48h and the samples submitted for biochemical analysis and for culture inhibition assessment. Metabolites were extracted by transferring 75µL of pure culture to a 1.5mL Eppendorf tube already containing 25µL of an internal standard, prepared by carbon 13 labelling a *Bacillus* culture, and 400µL of LC-MS grade methanol. Samples were mixed for 10 min in a rotatory mixer and sonicated for 5 min in ice water followed by centrifugation at 21 000 x g for 5 min at 4°C. The supernatant was transferred to a HPLC polypropylene tube before analysis in the LC-MS system by an Agilent 1290 Infinity LC equipped with an Agilent 6540UHD QTOF mass spectrometer. The LC separation was carried on a Waters CORTECS T3 Column, 120Å, 1.6 µm, 2.1 mm X 100 mm using Milli-Q waters + 0.1% Formic acid as solvent A and Acetonitrile + 0.1% Formic acid as eluent B. Mass spectrometry analysis was conducted in positive mode by using accurate mass analysis. Metabolites were quantified of lipopeptides (surfactins, iturins, fengycins/plipastatins), polyketides (bacillaenes, macrolactins, difficin), bacteriocins and other non-ribosomal peptides such as bacilysin, bacillibactin and bacitracin. As fengycins/plipastatins stereochemistry difference cannot be detected using LC-MS, only NMR, the results do not distinguish between these respective metabolites.

Fungal inhibition by bacterial cultures: Fungal inhibition by bacterial cultures was adapted from (Kjeldgaard et al., 2022, Study 3). In brief, a 1:2 dilution series with 8-steps was prepared from the *Bacillus* cultures. Fungal spore suspension was prepared with 5.28×10^2 spores/ml in PDB supplemented with 50 µg/ml chloramphenicol and 10 µg/ml tetracycline. The fungal spore suspension was inoculated in each well of a 48-well microtiter plate. The dilution series of bacterial cultures were inoculated in consecutive columns so that each row in the plate was assign to a strain. The growth plate was sealed with 3M tape and incubated statically at 25°C in darkness. The OD₆₀₀ was measured at timepoint 0 using a BioTek Synergy HI plate reader with a scanning matrix measuring 9 points within each well. The fungal growth was evaluated again after 3 days' incubation and the starting OD₆₀₀ was subtracted. The half-inhibitory dilution (ID50) was determined in Graphpad Prism by [inhibitor] vs. response regression using a variable slope fitting (Hill slope).

γ-PGA production: *Bacillus* pre-cultures were adjusted to OD₆₀₀ 0.2 in LB supplemented with 0.1 mM MnCl₂ and 1 % glycerol. Cultures were incubated 24h and the final growth measured by OD₆₀₀ before the

supernatant was harvested. γ -PGA was precipitated by addition of ethanol to a final concentration of 80% followed by incubation for 10 min at -20°C . The γ -PGA was harvested by centrifugation at 4°C , 5000 rpm for 30 min and the pellet was resuspended in 10 mM Tris-HCl pH 8.0 in a volume dependent on the final culture OD_{600} . The γ -PGA samples were run on 6-8% acrylamide gel and stained with 0.5% methylene blue in 3% acetic acid for 10 min while shaking. The gel was destained overnight with water and the γ -PGA bands were quantified in ImageJ fiji.

Fungal inhibition by bacterial VOCs: 5 μl fungal spore suspension (1.76×10^4 spores/ml) was inoculated on a filter paper disc in the centre of a PDA plate and incubated at 25°C for 1.5 day in darkness. *Bacillus* inoculum was prepared from pre-cultures adjusted to OD_{600} 1. A volume of 5 μl were inoculated on a filter paper disc in the centre of a PDA plate and the plate was incubated at 30°C overnight. The two plates containing respectively fungal and bacterial growth were sandwiched and sealed together with Petri-Seal. The plate sandwiches were incubated for 4 days at 25°C in darkness. The radial growth of the fungus was measured daily.

Seed preparation and growth: *A. thaliana* ecotype Col-0 seeds were stratified in MilliQ in the fridge at 4°C for 2 days and subsequently sterilized by; 1 minute washing in 1 ml 70% ethanol with regular inversion, removal of ethanol with 1 ml MilliQ, 3 minutes sterilizing in 1 ml 10% NaClO with regular inversion, and finally washing 3x in 1 ml MilliQ to remove residual ethanol and bleach. Seeds were resuspended in 0.1% agarose to enable separation of single seeds in droplets for sowing. *A. thaliana* seeds were grown on vertical plates with $\frac{1}{2}$ Murashige and Skoog ($\frac{1}{2}$ MS) medium (2.215 g/L [Sigma]) supplemented with 0.5% sucrose and 0.5% agar at 22°C with 16h light /8h dark cycles.

Root colonization: 7-9-day old *A. thaliana* seedlings were placed in $\frac{1}{2}$ MS medium in 12-well growth plates. *Bacillus* pre-cultures were prepared in root surrogate medium prepared as follows: Macronutrients: 175 g K_2HPO_4 , 75 g KH_2PO_4 , 12.5 g $\text{Na}_3\text{-Citrate}\cdot 2\text{H}_2\text{O}$, 2.5 g $\text{MgSO}_4\cdot 7\text{H}_2\text{O}$ per liter (autoclaved). Organic acids (20 mM final concentration): 0.12 g acetic acid, 0.96 g citric acid, 0.72 g lactic acid, 0.116 g fumaric acid, 0.268 g malic acid and 0.236 g succinic acid per liter (filter sterilized). Sugars: 2.52 g glucose, 1.08 g fructose, 2.74 g sucrose and 4.10 g maltose per liter (filter sterilized). Amino acids (10 mM final concentration): 0.08 g alanine, 0.348 g arginine, 0.25 g asparagine, 0.29 g glutamic, 0.11 g glycine, 0.2 g histidine, 0.66 g leucine and 0.9 g tyrosine per liter (filter sterilized). Trace elements: 0.190g MgCl_2 , 0.078g CaCl_2 , 0.006 g MnCl_2 , 0.008 g FeCl_3 , 0.0001 g ZnCl_2 per liter (filter sterilized). *Bacillus* cultures were inoculated to a final OD_{600} of 0.05 with the seedlings and incubated at 22°C with light and light shaking for 24h. Seedlings were transferred to PBS and sonicated (10 sec pulse of 40 A, 10 sec rest, 3 times repetition) to remove attached bacteria. Serial dilutions of the sonicated samples were prepared and plated for CFU count and quantification of attached bacteria.

Protease activity: Endo-protease activity was evaluated by a colorimetric assay. *Bacillus* cultures were inoculated to starting OD₆₀₀ 0.15 in PDB medium in 48-well MTP FlowerPlates and incubated in a BioLector for 18h until stationary to reach optimal protease expression (117). Culture supernatants were harvested and diluted 10x in pepsal. The synthetic endo-protease substrate N-succinyl-Ala-Ala-Pro-Phe-*para*-nitroanilide was dissolved in 0.2M Tris-HCl buffer pH 7.2 and added to the cultures in a 1:1 V/V ratio making a final dilution of 20x. The released product 4-nitroaniline was measured by absorbance (410 nm) at timepoint 0, 5, 10, and 20 min development. The timepoint 0 was subtracted from the accumulated absorbance and the accumulated absorbance was normalised to that of the respective ancestor strain.

Motility: Growth plates for motility assessment were prepared meticulously. Molten LB agar (0.6%) was poured into plates on a levelled surface. Plates were let to solidify with lids on and subsequently dried for the exact same amount of time. *Bacillus* pre-cultures were grown overnight at 30°C and adjusted to OD₆₀₀ 1. The agar was stabbed in the centre with a pipette tip and 5 µl culture was inoculated. The plates were incubated at room temperature overnight and next day the plates were transferred to 30°C until colony expansion was observed (few hours). Finally, the radius was measured.

Sporulation test: *Bacillus* sporulation medium was prepared with 8 g/L Difco Nutrient Broth, 1 g/L KCl, 0.25 g/L MgSO₄·7H₂O, 10 µM MnCl₂, 0.5 mM CaCl₂, and ammonium ferric citrate 4.4 µg/ml. *Bacillus* were inoculated to a starting OD₆₀₀ of 0.25 in sporulation medium and incubated for 36h. The cultures were diluted 1:100 and divided in two for 20 min heat treatment at 80°C and for direct plating. 10 µl of both heat-treated and non-treated samples were inoculated in wells of a 96-well microtiter plate filled with LB agar. The plates were incubated at 30°C and growth was evaluated after 24h.

Funding

This research was supported by Innovation Fund Denmark (8053-00109B) and Chr. Hansen A/S.

Acknowledgements

The authors gratefully acknowledge the contributions from Birgit Albrecht Svendsen, Tammi Vesth, Anna Koza, Kozai Al-Nakeeb, Ricardo Almeida Faria, Kristian Jensen, and Signe Karlsen.

References

1. Perincherry L, Lalak-Kańczugowska J, Stępień Ł. 2019. Fusarium-Produced Mycotoxins in Plant-Pathogen Interactions. *Toxins (Basel)* 11:664.
2. Aoki T, O'Donnell K, Geiser DM. 2014. Systematics of key phytopathogenic *Fusarium* species: Current

- status and future challenges. *J Gen Plant Pathol* 80:189–201.
3. Scherm B, Balmas V, Spanu F, Pani G, Delogu G, Pasquali M, Migheli Q. 2013. *Fusarium culmorum*: Causal agent of foot and root rot and head blight on wheat. *Mol Plant Pathol* 14:323–341.
 4. Desjardins AE, Proctor RH. 2007. Molecular biology of *Fusarium* mycotoxins. *Int J Food Microbiol* 119:47–50.
 5. Nguyen PA, Strub C, Fontana A, Schorr-Galindo S. 2017. Crop molds and mycotoxins: Alternative management using biocontrol. *Biol Control*. Academic Press <https://doi.org/10.1016/j.biocontrol.2016.10.004>.
 6. Bai GH, Plattner R, Desjardins A, Kolb F. 2001. Resistance to *Fusarium* head blight and deoxynivalenol accumulation in Virginia barley. *Plant Breed* 120:1–6.
 7. Sobrova P, Adam V, Vasatkova A, Beklova M, Zeman L, Kizek R. 2010. Deoxynivalenol and its toxicity. *Interdiscip Toxicol* 3:94–99.
 8. Hellin P, King R, Urban M, Hammond-Kosack KE, Legrève A. 2018. The adaptation of *Fusarium culmorum* to DMI fungicides is mediated by major transcriptome modifications in response to azole fungicide, including the overexpression of a PDR transporter (FcABC1). *Front Microbiol* 9:1385.
 9. Shi C, Yan P, Li J, Wu H, Li Q, Guan S, Shi C, Yan P, Li J, Wu H, Li Q, Guan S. 2014. Biocontrol of *Fusarium graminearum* Growth and Deoxynivalenol Production in Wheat Kernels with Bacterial Antagonists. *Int J Environ Res Public Health* 11:1094–1105.
 10. Abdallah MF, De Boevre M, Landschoot S, De Saeger S, Haesaert G, Audenaert K. 2018. Fungal endophytes control *Fusarium graminearum* and reduce trichothecenes and zearalenone in maize. *Toxins (Basel)* 10.
 11. Hanif A, Zhang F, Li P, Li C, Xu Y, Zubair M, Zhang M, Jia D, Zhao X, Liang J, Majid T, Yan J, Farzand A, Wu H, Gu Q, Gao X. 2019. Fengycin produced by *Bacillus amyloliquefaciens* FZB42 inhibits *Fusarium graminearum* growth and mycotoxins biosynthesis. *Toxins (Basel)* 11.
 12. Albarracín Orió AG, Petras D, Tobares RA, Aksenov AA, Wang M, Juncosa F, Sayago P, Moyano AJ, Dorrestein PC, Smania AM. 2020. Fungal–bacterial interaction selects for quorum sensing mutants with increased production of natural antifungal compounds. *Commun Biol* 3:1–9.
 13. Richter A, Blei F, Hu G, Schwitalla JW, Lozano-Andrade CN, Jarmusch SA, Wibowo M, Kjeldgaard B, Surabhi S, Jautzus T, Phippen CBW, Tyc O, Arentshorst M, Wang Y, Garbeva P, Larsen TO, Ram AFJ, Hondel CAM van den, Maroti G, Kovacs AT. 2023. Enhanced niche colonisation and competition during bacterial adaptation to a fungus. *bioRxiv* 2023.03.27.534400.
 14. Kalamara M, Spacapan M, Mandic-Mulec I, Stanley-Wall NR. 2018. Social behaviours by *Bacillus subtilis*: quorum sensing, kin discrimination and beyond. *Mol Microbiol*

<https://doi.org/10.1111/mmi.14127>.

15. Miller MB, Bassler BL. 2001. Quorum Sensing in Bacteria. *Annu Rev Microbiol* 55:165–199.
16. Weinrauch Y, Penchev R, Dubnau E, Smith E, Dubnau D. 1990. A *Bacillus subtilis* regulatory gene product for genetic competence and sporulation resembles sensor protein members of the bacterial two-component signal-transduction systems. *Genes Dev* 4:860–872.
17. Kunst F, Msadek T, Bignon J, Rapoport G. 1994. The DegS/DegU and ComP/ComA two-component systems are part of a network controlling degradative enzyme synthesis and competence in *Bacillus subtilis*. *Res Microbiol* 145:393–402.
18. Roggiani M, Dubnau D. 1993. ComA, a phosphorylated response regulator protein of *Bacillus subtilis*, binds to the promoter region of *srfA*. *J Bacteriol* 175:3182–3187.
19. Magnuson R, Solomon J, Grossman AD. 1994. Biochemical and genetic characterization of a competence pheromone from *B. subtilis*. *Cell* 77:207–216.
20. Leiman SA, Arboleda LC, Spina JS, McLoon AL. 2014. SinR is a mutational target for fine-tuning biofilm formation in laboratory-evolved strains of *Bacillus subtilis*. *BMC Microbiol* 14:1–10.
21. Richter A, Hölscher T, Pausch P, Sehr T, Brockhaus F, Bange G, Kovács ÁT. 2018. Hampered motility promotes the evolution of wrinkly phenotype in *Bacillus subtilis*. *BMC Evol Biol* 18:1–11.
22. Dragoš A, Lakshmanan N, Martin M, Horváth B, Maróti G, García CF, Lieleg O, Kovács ÁT. 2018. Evolution of exploitative interactions during diversification in *Bacillus subtilis* biofilms. *FEMS Microbiol Ecol* 94.
23. Kjeldgaard B, Listian SA, Ramaswamhi V, Richter A, Kiesewalter HT, Kovács ÁT. 2019. Fungal hyphae colonization by *Bacillus subtilis* relies on biofilm matrix components. *Biofilm* 1:100007.
24. Benoit I, van den Esker MH, Patyshakuliyeva A, Mattern DJ, Blei F, Zhou M, Dijksterhuis J, Brakhage AA, Kuipers OP, de Vries RP, Kovács ÁT. 2015. *Bacillus subtilis* attachment to *Aspergillus niger* hyphae results in mutually altered metabolism. *Environ Microbiol* 17:2099–2113.
25. Kjeldgaard B, Neves AR, Fonseca C, Kovács ÁT, Domínguez-Cuevas P. 2022. Quantitative High-Throughput Screening Methods Designed for Identification of Bacterial Biocontrol Strains with Antifungal Properties. *Microbiol Spectr* 10.
26. Arnaouteli S, Matoz-Fernandez DA, Porter M, Kalamara M, Abbott J, MacPhee CE, Davidson FA, Stanley-Wall NR. 2019. Pulcherrimin formation controls growth arrest of the *Bacillus subtilis* biofilm. *Proc Natl Acad Sci U S A* 116:13553–13562.
27. Molle V, Fujita M, Jensen ST, Eichenberger P, González-Pastor JE, Liu JS, Losick R. 2003. The Spo0A regulon of *Bacillus subtilis*. *Mol Microbiol* 50:1683–1701.
28. Jiang M, Shao W, Perego M, Hoch JA. 2000. Multiple histidine kinases regulate entry into stationary

- phase and sporulation in bacillus subtilis. *Mol Microbiol* 38:535–542.
29. Gallegos-Monterrosa R, Kovács ÁT. 2023. Phenotypic plasticity: The role of a phosphatase family Rap in the genetic regulation of Bacilli. *Mol Microbiol* <https://doi.org/10.1111/mmi.15060>.
 30. Hoch JA. 1993. Regulation of the phosphorelay and the initiation of sporulation in *Bacillus subtilis*. *Annu Rev Microbiol* 47:441–465.
 31. Cairns LS, Hogley L, Stanley-Wall NR. 2014. Biofilm formation by *Bacillus subtilis*: New insights into regulatory strategies and assembly mechanisms. *Mol Microbiol* 93:587–598.
 32. Nakano MM, Xia L, Zuber P. 1991. Transcription initiation region of the *srfA* operon, which is controlled by the *comP-comA* signal transduction system in *Bacillus subtilis*. *J Bacteriol* 173:5487–5493.
 33. Auchtung JM, Lee CA, Grossman AD. 2006. Modulation of the ComA-dependent quorum response in *Bacillus subtilis* by multiple rap proteins and Phr peptides. *J Bacteriol* 188:5273–5285.
 34. Ansaldi M, Marolt D, Stebe T, Mandic-Mulec I, Dubnau D. 2002. Specific activation of the *Bacillus* quorum-sensing systems by isoprenylated pheromone variants. *Mol Microbiol* 44:1561–1573.
 35. Kunst F, Pascal M, Lepesant-Kejzlarova J, Lepesant JA, Billault A, Dedonder R. 1975. Pleiotropic mutations affecting sporulation conditions and the syntheses of extracellular enzymes in *Bacillus subtilis* 168. *Biochimie* 56:1481–1489.
 36. Dahl MK, Msadek T, Kunst F, Rapoport G. 1991. Mutational analysis of the *Bacillus subtilis* DegU regulator and its phosphorylation by the DegS protein kinase. *J Bacteriol* 173:2539–2547.
 37. Stanley NR, Lazazzera BA. 2005. Defining the genetic differences between wild and domestic strains of *Bacillus subtilis* that affect poly- γ -DL-glutamic acid production and biofilm formation. *Mol Microbiol* 57:1143–1158.
 38. Wang P, Guo Q, Ma Y, Li S, Lu X, Zhang X, Ma P. 2015. DegQ regulates the production of fengycins and biofilm formation of the biocontrol agent *Bacillus subtilis* NCD-2. *Microbiol Res* 178:42–50.
 39. Tsume K, Ano T, Hirai M, Nakamura Y, Shoda M. 1999. The genes *degQ*, *pps*, and *lpa-8* (*sfp*) are responsible for conversion of *Bacillus subtilis* 168 to plipastatin production. *Antimicrob Agents Chemother* 43:2183–2192.
 40. Tsume K, Inoue S, Ano T, Itaya M, Shoda M. 2005. Horizontal transfer of *iturin* operon, *itu*, to *Bacillus subtilis* 168 and conversion into an *iturin* A producer. *Antimicrob Agents Chemother* 49:4641–4648.
 41. Koumoutsis A, Chen XH, Vater J, Borriss R. 2007. DegU and YczE positively regulate the synthesis of bacillomycin D by *Bacillus amyloliquefaciens* strain FZB42. *Appl Environ Microbiol* 73:6953–6964.
 42. Verhamme DT, Murray EJ, Stanley-Wall NR. 2009. DegU and Spo0A Jointly Control Transcription of Two Loci Required for Complex Colony Development by *Bacillus subtilis*. *J Bacteriol* 191:100–108.

43. Kobayashi K. 2007. Gradual activation of the response regulator DegU controls serial expression of genes for flagellum formation and biofilm formation in *Bacillus subtilis*. *Mol Microbiol* 66:395–409.
44. Hayashi K, Kensuke T, Kobayashi K, Ogasawara N, Ogura M. 2006. *Bacillus subtilis* RghR (YvaN) represses rapG and rapH, which encode inhibitors of expression of the srfA operon. *Mol Microbiol* 59:1714–1729.
45. Ogura M, Shimane K, Asai K, Ogasawara N, Tanaka T. 2003. Binding of response regulator DegU to the aprE promoter is inhibited by RapG, which is counteracted by extracellular PhrG in *Bacillus subtilis*. *Mol Microbiol* 49:1685–1697.
46. Perego M, Higgins CF, Pearce SR, Gallagher MP, Hoch JA. 1991. The oligopeptide transport system of *Bacillus subtilis* plays a role in the initiation of sporulation. *Mol Microbiol* 5:173–185.
47. Rudner DZ, LeDeaux JR, Ireton K, Grossman AD. 1991. The spo0K locus of *Bacillus subtilis* is homologous to the oligopeptide permease locus and is required for sporulation and competence. *J Bacteriol* 173:1388–1398.
48. Piazza F, Tortosa P, Dubnau D. 1999. Mutational analysis and membrane topology of ComP, a quorum-sensing histidine kinase of *Bacillus subtilis* controlling competence development. *J Bacteriol* 181:4540–4548.
49. Tanaka T, Kawata M, Mukai K. 1991. Altered phosphorylation of *Bacillus subtilis* DegU caused by single amino acid changes in DegS. *J Bacteriol* 173:5507–5515.
50. Jers C, Kobir A, Søndergaard EO, Jensen PR, Mijakovic I. 2011. *Bacillus subtilis* two-component system sensory kinase DegS is regulated by serine phosphorylation in its input domain. *PLoS One* 6:e14653.
51. Monnet V. 2003. Bacterial oligopeptide-binding proteins. *Cell Mol Life Sci* <https://doi.org/10.1007/s00018-003-3054-3>.
52. Slamti L, Lereclus D. 2019. The oligopeptide ABC-importers are essential communication channels in Gram-positive bacteria. *Res Microbiol* 170:338–344.
53. Cesa-Luna C, Baez A, Quintero-Hernández V, De La Cruz-Enríquez J, Castañeda-Antonio MD, Muñoz-Rojas J. 2020. The importance of antimicrobial compounds produced by beneficial bacteria on the biocontrol of phytopathogens. *Acta Biol Colomb* 25:140–154.
54. Penha RO, Vandenberghe LPS, Faulds C, Soccol VT, Soccol CR. 2020. *Bacillus* lipopeptides as powerful pest control agents for a more sustainable and healthy agriculture: recent studies and innovations. *Planta. Springer* <https://doi.org/10.1007/s00425-020-03357-7>.
55. Raymaekers K, Ponet L, Holtappels D, Berckmans B, Cammue BPA. 2020. Screening for novel biocontrol agents applicable in plant disease management – A review. *Biol Control* <https://doi.org/10.1016/j.biocontrol.2020.104240>.

56. Gu Q, Yang Y, Yuan Q, Shi G, Wu L, Lou Z, Huo R, Wu H, Borriss R, Gao X. 2017. Bacillomycin D produced by *Bacillus amyloliquefaciens* is involved in the antagonistic interaction with the plantpathogenic fungus *Fusarium graminearum*. *Appl Environ Microbiol* 83:e01075-17.
57. Koumoutsis A, Chen X-HH, Henne A, Liesegang H, Hitzeroth G, Franke P, Vater J, Borriss R. 2004. Structural and Functional Characterization of Gene Clusters Directing Nonribosomal Synthesis of Bioactive Cyclic Lipopeptides in *Bacillus amyloliquefaciens* Strain FZB42, p. 1084–1096. *In* *Journal of Bacteriology*. American Society for Microbiology Journals.
58. Cawoy H, Debois D, Franzil L, De Pauw E, Thonart P, Ongena M. 2015. Lipopeptides as main ingredients for inhibition of fungal phytopathogens by *Bacillus subtilis/amyloliquefaciens*. *Microb Biotechnol* 8:281–295.
59. Li Y, Héloir MC, Zhang X, Geissler M, Trouvelot S, Jacquens L, Henkel M, Su X, Fang X, Wang Q, Adrian M. 2019. Surfactin and fengycin contribute to the protection of a *Bacillus subtilis* strain against grape downy mildew by both direct effect and defence stimulation. *Mol Plant Pathol* 20:1037–1050.
60. Ongena M, Jacques P, Touré Y, Destain J, Jabrane A, Thonart P. 2005. Involvement of fengycin-type lipopeptides in the multifaceted biocontrol potential of *Bacillus subtilis*. *Appl Microbiol Biotechnol* 69:29–38.
61. Kiesewalter HT, Lozano-Andrade CN, Wibowo M, Strube ML, Maróti G, Snyder D, Jørgensen TS, Larsen TO, Cooper VS, Weber T, Kovács ÁT. 2021. Genomic and Chemical Diversity of *Bacillus subtilis* Secondary Metabolites against Plant Pathogenic Fungi. *mSystems* 6.
62. Msadek T, Kunst F, Klier A, Rapoport G. 1991. DegS-DegU and ComP-ComA modulator-effector pairs control expression of the *Bacillus subtilis* pleiotropic regulatory gene degQ. *J Bacteriol* 173:2366–2377.
63. Verhamme DT, Kiley TB, Stanley-Wall NR. 2007. DegU co-ordinates multicellular behaviour exhibited by *Bacillus subtilis*. *Mol Microbiol* 65:554–568.
64. Dergham Y, Sanchez-Vizueté P, Coq D Le, Deschamps J, Bridier A, Hamze K, Briandet R. 2021. Comparison of the genetic features involved in *Bacillus subtilis* biofilm formation using multi-culturing approaches. *Microorganisms* 9:1–17.
65. Tran L-SP, Nagai T, Itoh Y. 2000. Divergent structure of the ComQXPA quorum-sensing components: molecular basis of strain-specific communication mechanism in *Bacillus subtilis*. *Mol Microbiol* 37:1159–1171.
66. Nagai T, Phan Tran L-S, Inatsu Y, Itoh Y. 2000. A New IS 4 Family Insertion Sequence, IS 4Bsu 1, Responsible for Genetic Instability of Poly- γ -Glutamic Acid Production in *Bacillus subtilis*. *J Bacteriol* 182:2387–2392.

67. Chan JM, Guttenplan SB, Kearns DB. 2014. Defects in the flagellar motor increase synthesis of poly- γ -glutamate in *Bacillus subtilis*. *J Bacteriol* 196:740–753.
68. Msadek T. 1999. When the going gets tough: Survival strategies and environmental signaling networks in *Bacillus subtilis*. *Trends Microbiol.* *Trends Microbiol* [https://doi.org/10.1016/S0966-842X\(99\)01479-1](https://doi.org/10.1016/S0966-842X(99)01479-1).
69. Ling L, Cheng W, Jiang K, Jiao Z, Luo H, Yang C, Pang M, Lu L. 2022. The antifungal activity of a serine protease and the enzyme production of characteristics of *Bacillus licheniformis* TG116. *Arch Microbiol* 204.
70. Schönbichler A, Díaz-Moreno SM, Srivastava V, McKee LS. 2020. Exploring the Potential for Fungal Antagonism and Cell Wall Attack by *Bacillus subtilis* natto. *Front Microbiol* 11:521.
71. Beauregard PB, Chai Y, Vlamakis H, Losick R, Kolter R. 2013. *Bacillus subtilis* biofilm induction by plant polysaccharides. *Proc Natl Acad Sci* 110:E1621–E1630.
72. Chen Y, Yan F, Chai Y, Liu H, Kolter R, Losick R, Guo J. 2013. Biocontrol of tomato wilt disease by *Bacillus subtilis* isolates from natural environments depends on conserved genes mediating biofilm formation. *Environ Microbiol* 15:848–864.
73. Lugtenberg B, Kamilova F. 2009. Plant-growth-promoting rhizobacteria. *Annu Rev Microbiol* 63:541–556.
74. Blake C, Nordgaard M, Maróti G, Kovács ÁT. 2021. Diversification of *Bacillus subtilis* during experimental evolution on *Arabidopsis thaliana* and the complementarity in root colonization of evolved subpopulations. *Environ Microbiol* 23:6122–6136.
75. Nordgaard M, Mortensen RMR, Kirk NK, Gallegos-Monterrosa R, Kovács ÁT. 2021. Deletion of Rap-Phr systems in *Bacillus subtilis* influences in vitro biofilm formation and plant root colonization. *Microbiologyopen* 10:e1212.
76. Nordgaard M, Blake C, Maróti G, Hu G, Wang Y, Strube ML, Kovács ÁT. 2022. Experimental evolution of *Bacillus subtilis* on *Arabidopsis thaliana* roots reveals fast adaptation and improved root colonization. *iScience* 25:104406.
77. Blake C, Christensen MN, Kovács ÁT. 2021. Molecular Aspects of Plant Growth Promotion and Protection by *Bacillus subtilis*. *Mol Plant Microbe Interact* 34:15–25.
78. Ryu C-M, Farag MA, Hu C-H, Reddy MS, Wei H-X, Paré PW, Kloepper JW. 2003. Bacterial volatiles promote growth in *Arabidopsis*. *Proc Natl Acad Sci* 100:4927–4932.
79. Ryu CM, Farag MA, Hu CH, Reddy MS, Kloepper JW, Paré PW. 2004. Bacterial volatiles induce systemic resistance in *Arabidopsis*. *Plant Physiol* 134:1017–1026.
80. Chen H, Xiao X, Wang J, Wu L, Zheng Z, Yu Z. 2008. Antagonistic effects of volatiles generated by

Bacillus subtilis on spore germination and hyphal growth of the plant pathogen, *Botrytis cinerea*. *Biotechnol Lett* 30:919–923.

81. Yuan J, Raza W, Shen Q, Huang Q. 2012. Antifungal activity of *Bacillus amyloliquefaciens* NJN-6 volatile compounds against *Fusarium oxysporum* f. sp. *cubense*. *Appl Environ Microbiol* 78:5942–5944.
82. Kovács ÁT, Dragoš A. 2019. Evolved Biofilm: Review on the Experimental Evolution Studies of *Bacillus subtilis* Pellicles. *J Mol Biol* <https://doi.org/10.1016/j.jmb.2019.02.005>.
83. Dragosits M, Mattanovich D. 2013. Adaptive laboratory evolution - principles and applications for biotechnology. *Microb Cell Fact. BioMed Central* <https://doi.org/10.1186/1475-2859-12-64>.
84. Sandberg TE, Salazar MJ, Weng LL, Palsson BO, Feist AM. 2019. The emergence of adaptive laboratory evolution as an efficient tool for biological discovery and industrial biotechnology. *Metab Eng. Academic Press Inc.* <https://doi.org/10.1016/j.ymben.2019.08.004>.
85. Lenski RE, Rose MR, Simpson SC, Tadler SC. 1991. Long-Term Experimental Evolution in *Escherichia coli*. I. Adaptation and Divergence During 2,000 Generations. *Am Nat* 138:1315–1341.
86. Martin M, Dragoš A, Otto SB, Schäfer D, Brix S, Maróti G, Kovács ÁT. 2020. Cheaters shape the evolution of phenotypic heterogeneity in *Bacillus subtilis* biofilms. *ISME J* 14:2302–2312.
87. Martin M, Dragoš A, Hölscher T, Maróti G, Bálint B, Westermann M, Kovács ÁT. 2017. De novo evolved interference competition promotes the spread of biofilm defectors. *Nat Commun* 8:1–12.
88. Li E, de Jonge R, Liu C, Jiang H, Friman V-P, Pieterse CMJ, Bakker PAHM, Jousset A. 2021. Rapid evolution of bacterial mutualism in the plant rhizosphere. *Nat Commun* 12:3829.
89. Bailey SF, Rodrigue N, Kassen R. 2015. The effect of selection environment on the probability of parallel evolution. *Mol Biol Evol* 32:1436–1448.
90. Lopez D, Vlamakis H, Kolter R. 2009. Generation of multiple cell types in *Bacillus subtilis*. *FEMS Microbiol Rev* <https://doi.org/10.1111/j.1574-6976.2008.00148.x>.
91. Tortosa P, Logsdon L, Kraigher B, Itoh Y, Mandic-Mulec I, Dubnau D. 2001. Specificity and genetic polymorphism of the *Bacillus* competence quorum-sensing system. *J Bacteriol* 183:451–460.
92. Yazgan A, Özcengiz G, Marahiel MA. 2001. Tn10 insertional mutations of *Bacillus subtilis* that block the biosynthesis of bacilysin. *Biochim Biophys Acta - Gene Struct Expr* 1518:87–94.
93. Yazgan Karata° A, Çetin S, Özcengiz G, Karataş AY, Çetin S, Özcengiz G, Yazgan Karata° A, Çetin S, Özcengiz G. 2003. The effects of insertional mutations in *comQ*, *comP*, *srfA*, *spo0H*, *spo0A* and *abrB* genes on bacilysin biosynthesis in *Bacillus subtilis*. *Biochim Biophys Acta - Gene Struct Expr* 1626:51–56.
94. Vahidinasab M, Lilge L, Reinfurt A, Pfannstiel J, Henkel M, Morabbi Heravi K, Hausmann R. 2020. Construction and description of a constitutive plipastatin mono-producing *Bacillus subtilis*. *Microb*

Cell Fact 19:205.

95. Thérien M, Kieseewalter HT, Auria E, Charron-Lamoureux V, Wibowo M, Maróti G, Kovács ÁT, Beaugregard PB. 2020. Surfactin production is not essential for pellicle and root-associated biofilm development of *Bacillus subtilis*. *Biofilm* 2.
96. Angelini TE, Roper M, Kolter R, Weitz DA, Brenner MP. 2009. *Bacillus subtilis* spreads by surfing on waves of surfactant. *Proc Natl Acad Sci U S A* 106:18109–18113.
97. Kinsinger RF, Shirk MC, Fall R. 2003. Rapid surface motility in *Bacillus subtilis* is dependent on extracellular surfactin and potassium ion. *J Bacteriol* 185:5627–5631.
98. Hamze K, Julkowska D, Autret S, Hinc K, Nagorska K, Sekowska A, Holland IB, Sérór SJ. 2009. Identification of genes required for different stages of dendritic swarming in *Bacillus subtilis*, with a novel role for *phrC*. *Microbiology* 155:398–412.
99. Harshey RM. 2003. Bacterial Motility on a Surface: Many Ways to a Common Goal. *Annu Rev Microbiol*. Annual Reviews 4139 El Camino Way, P.O. Box 10139, Palo Alto, CA 94303-0139, USA <https://doi.org/10.1146/annurev.micro.57.030502.091014>.
100. Comella N, Grossman AD. 2005. Conservation of genes and processes controlled by the quorum response in bacteria: Characterization of genes controlled by the quorum-sensing transcription factor *ComA* in *Bacillus subtilis*. *Mol Microbiol* 57:1159–1174.
101. Pottathil M, Lazazzera BA. 2003. The extracellular PHR peptide-rap phosphatase signaling circuit of *bacillus subtilis*. *Front Biosci* <https://doi.org/10.2741/913>.
102. Fujita M, Losick R. 2005. Evidence that entry into sporulation in *Bacillus subtilis* is governed by a gradual increase in the level and activity of the master regulator *Spo0A*. *Genes Dev* 19:2236–2244.
103. Hamon MA, Lazazzera BA. 2001. The sporulation transcription factor *Spo0A* is required for biofilm development in *Bacillus subtilis*. *Mol Microbiol* 42:1199–1209.
104. McLoon AL, Guttenplan SB, Kearns DB, Kolter R, Losick R. 2011. Tracing the Domestication of a Biofilm-Forming Bacterium. *J Bacteriol* 193:2027–2034.
105. Ohsawa T, Tsukahara K, Ogura M. 2009. *Bacillus subtilis* response regulator *DegU* is a direct activator of *pgsB* transcription involved in γ -poly-glutamic acid synthesis. *Biosci Biotechnol Biochem* 73:2096–2102.
106. Do TH, Suzuki Y, Abe N, Kaneko J, Itoh Y, Kimura K. 2011. Mutations suppressing the loss of *DegQ* function in *Bacillus subtilis* (natto) poly- γ -glutamate synthesis. *Appl Environ Microbiol* 77:8249–8258.
107. Okshevsky M, Louw MG, Lamela EO, Nilsson M, Tolker-Nielsen T, Meyer RL. 2018. A transposon mutant library of *Bacillus cereus* ATCC 10987 reveals novel genes required for biofilm formation and implicates motility as an important factor for pellicle-biofilm formation. *Microbiologyopen* 7:e00552.

108. Kobayashi K. 2007. *Bacillus subtilis* pellicle formation proceeds through genetically defined morphological changes. *J Bacteriol* 189:4920–4931.
109. Vlamakis H, Chai Y, Beauregard P, Losick R, Kolter R. 2013. Sticking together: Building a biofilm the *Bacillus subtilis* way. *Nat Rev Microbiol* <https://doi.org/10.1038/nrmicro2960>.
110. Pisithkul T, Schroeder JW, Trujillo EA, Yeesin P, Stevenson DM, Chaiamarit T, Coon JJ, Wang JD, Amador-Noguez D. 2019. Metabolic remodeling during biofilm development of *Bacillus subtilis*. *MBio* 10:2021.
111. Randazzo P, Aubert-Frambourg A, Guillot A, Auger S. 2016. The MarR-like protein PchR (YvmB) regulates expression of genes involved in pulcherriminic acid biosynthesis and in the initiation of sporulation in *Bacillus subtilis*. *BMC Microbiol* 16.
112. Piggot PJ, Hilbert DW. 2004. Sporulation of *Bacillus subtilis*. *Curr Opin Microbiol*. Elsevier Current Trends <https://doi.org/10.1016/j.mib.2004.10.001>.
113. Yang M, Ferrari E, Chen E, Henner DJ. 1986. Identification of the pleiotropic *sacQ* gene of *Bacillus subtilis*. *J Bacteriol* 166:113–119.
114. Amory A, Kunst F, Aubert E, Klier A, Rapoport G. 1987. Characterization of the *sacQ* genes from *Bacillus licheniformis* and *Bacillus subtilis*. *J Bacteriol* 169:324–333.
115. Wu Y, Zhou J, Li C, Ma Y. 2019. Antifungal and plant growth promotion activity of volatile organic compounds produced by *Bacillus amyloliquefaciens*. *Microbiologyopen* 8:1–14.
116. Branda SS, González-Pastor JE, Ben-Yehuda S, Losick R, Kolter R. 2001. Fruiting body formation by *Bacillus subtilis*. *Proc Natl Acad Sci U S A* 98:11621–11626.
117. Barbieri G, Albertini AM, Ferrari E, Sonenshein AL, Belitsky BR. 2016. Interplay of CodY and ScoC in the Regulation of Major Extracellular Protease Genes of *Bacillus subtilis*. *J Bacteriol* 198:907–920.

Supplemental material

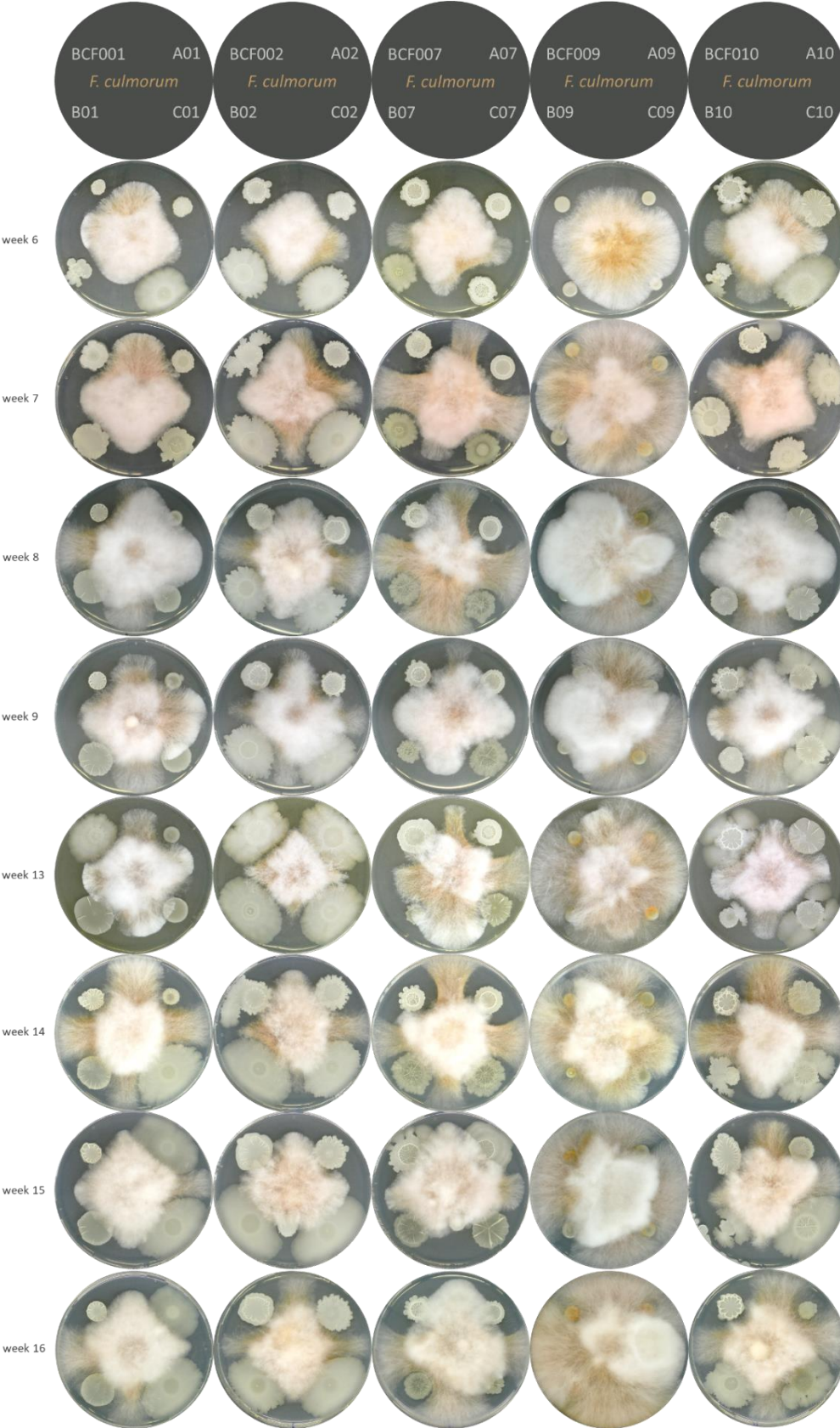


Fig. S 1. Fungal inhibition by evolved populations. Fungal inhibition was monitored over the ALE time course on co-evolved population level (A, B, C) from each ancestor strain (BCF001, BCF002, BCF007, BCF009, BCF010) against *F. culmorum* growth. Fungus was inoculated in the centre, while Bacilli were inoculated in the periphery around the fungal inoculum with a fixed distance.

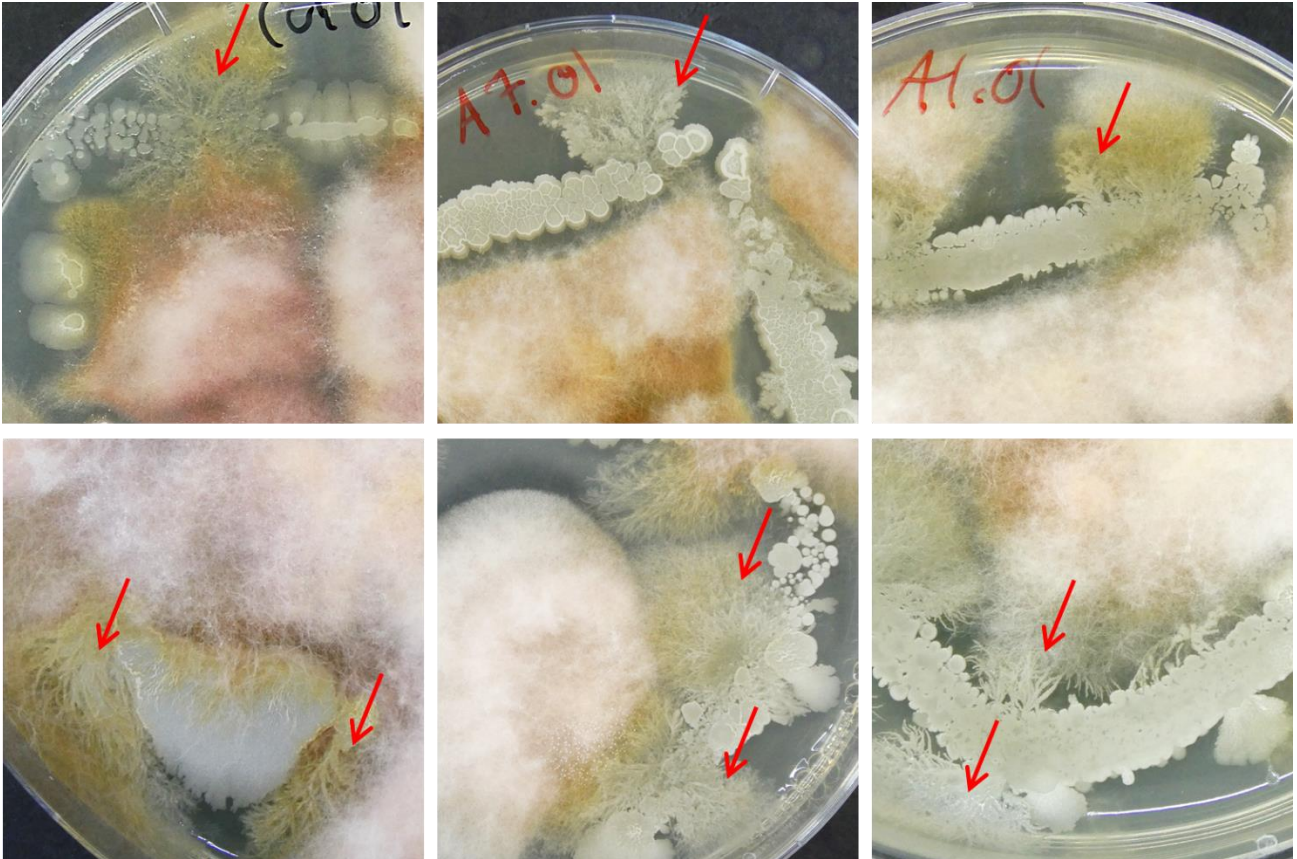


Fig. S 2. Merging growth. *F. culmorum* growth merging with growth of C0101 (BCF001 population C week 1), A0701 (BCF007 population A week 1), A0101 (BCF001 population A week 1), B0107 (BCF001 population B week 7), C0207 (BCF002 population C week 7), and A0107 (BCF001 population A week 7). Arrows indicate areas with overlapping growth of the two species.

Table S 1. Fitness screening results. Isolates from co-evolved populations (A, B, C) and the evolved control population (X) from the ancestor strains BCF001, BCF002, BCF007, BCF009, and BCF010 were screened for improved fungal inhibition potency at timepoint week 5, week 10, and week 16.

Ancestor	ALE	Week 5				Week 10				Week 16				Total			
		Improved	Reduced	Neutral	Total	Improved	Reduced	Neutral	Total	Improved	Reduced	Neutral	Total	Improved	Reduced	Neutral	Total
BCF001	A01	3		5	8	3		5	8		29	2	31	6	29	12	47
	B01	2		6	8	4	1	3	8		1	1	2	6	2	10	18
	C01	5	1	2	8	5	1	2	8		22	6	28	10	24	10	44
	X01	4		4	8	4		4	8					8	0	8	16
BCF002	A02	3	2	3	8	3		5	8		85	3	88	6	87	11	104
	B02	4		4	8	5		3	8		10	77	87	9	10	84	103
	C02	6		2	8	5		3	8					11	0	5	16
	X02	8			8	8			8					16	0	0	16
BCF007	A07		7	1	8		8		8		53	35	88	0	68	36	104
	B07		6	2	8		6	2	8		86		86	0	98	4	102
	C07		8		8		8		8		85		85	0	101	0	101
	X07		6	2	8		5	3	8					0	11	5	16
BCF009	A09		7	1	8		8		8			9	9	0	15	10	25
	B09		8		8		8		8	19		7	26	19	16	7	42
	C09		7	1	8		8		8	78		10	88	78	15	11	104
	X09		7	1	8		8		8					0	15	1	16
BCF010	A10	5	1	2	8	3	1	4	8	5	34	20	59	27	36	12	75
	B10	4	1	3	8	2	2	4	8	31	36	19	86	42	39	21	102
	C10	4	1	3	8	4	1	3	8					8	2	6	16
	X10	2	1	5	8	7		1	8					9	1	6	16
Total		50	63	47	160	53	65	42	160	152	441	170	763	255	569	259	1083

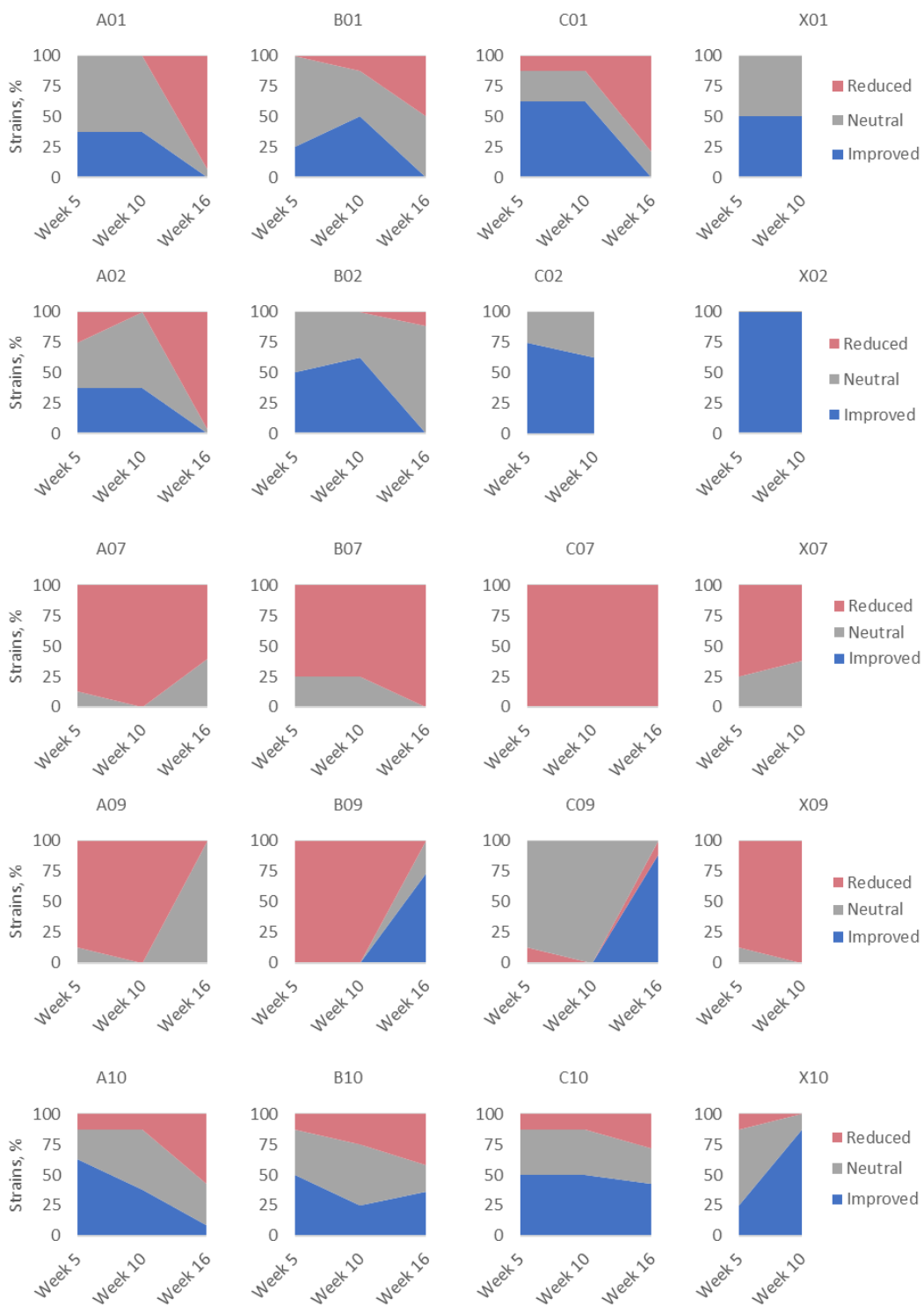


Fig. S 3. Percental fitness improvement. From each evolved population (A, B, C, X), the number of improved ALE derivatives were calculated relative to the total number of strains screened from the respective population at a given timepoint (week 5, week 10, and week 16) in percentage. 01 refers to BCF001 derived populations, 02 refers to BCF002 derived populations, 07 refers to BCF007 derived populations, 09 refers to BCF009 derived populations, and 10 refers to BCF010 derived populations.

Table S 2 Primary characterization. 201 selected strains were characterized in respect to colony morphology (Pheno, 1 to 4), fungal inhibition potency in high throughput screening (Score, -1 to 1), and sporulation capacity (Spo, 0 or 1). T denotes sampling point (week 5, 10 or 16) and Pop indicates population (co-evolved A, B, C, or evolved control X). The selection comprised 44 strains derived from BCF001, 53 strains derived from BCF002, 34 strains derived from BCF007, 21 strains derived from BCF009, and 49 strains derived from BCF010. Strains selected for whole genome sequencing are indicated in grey.

BCF001						BCF002						BCF007						BCF009						BCF010					
Strain	T	Pop	Pheno	Spo	Score	Strain	T	Pop	Pheno	Spo	Score	Strain	T	Pop	Pheno	Spo	Score	Strain	T	Pop	Pheno	Spo	Score	Strain	T	Pop	Pheno	Spo	Score
A0105-C	5	A01	1	1	1	A0205-B	5	A02	1	1	1	A0705-E	5	A07	1	1	0	A0905-A	5	A09	4	1	-1	A1005-A	5	A10	2	1	1
A0105-F	5	A01	1	1	1	A0205-C	5	A02	1	1	1	A0705-F	5	A07	1	1	-2	A0905-D	5	A09	4	1	0	A1005-B	5	A10	2	1	1
A0105-G	5	A01	1	1	1	A0205-D	5	A02	1	1	-1	A0710-H	10	A07	1	1	-2	A0910-A	10	A09	2	1	-1	A1005-C	5	A10	2	1	1
A0110-E	10	A01	1	1	1	A0205-G	5	A02	1	1	-1	A0716-E1	16	A07	1	1	0	A0916-D1	16	A09	4	1	-1	A1005-D	5	A10	2	1	1
A0110-F	10	A01	1	1	1	A0205-H	5	A02	1	1	1	A0716-H1	16	A07	1	1	-2	B0905-A	5	B09	2	1	-1	A1005-F	5	A10	2	1	1
A0110-G	10	A01	1	1	1	A0210-D	10	A02	2	1	1	A0716-C2	16	A07	1	1	-1	B0905-B	5	B09	1	1	-1	A1010-C	10	A10	2	1	1
A0116-F1	16	A01	2	1	0	A0210-E	10	A02	1	1	1	A0716-D3	16	A07	1	1	-2	B0910-A	10	B09	1	1	-1	A1010-D	10	A10	2	1	1
A0116-H1	16	A01	2	1	-2	A0210-G	10	A02	2	1	1	A0716-E5	16	A07	1	1	-1	B0916-C2	16	B09		1	1	A1010-H	10	A10	3.5	1	1
A0116-F4	16	A01	2	1	0	A0216-B1	16	A02	4	1	0	A0716-E9	16	A07	1	1	-1	B0916-F2	16	B09	3	1	0	A1016-B1	16	A10	1.5	1	-2
B0105-E	5	B01	1	1	1	A0216-B2	16	A02	4	1	0	B0705-B	5	B07	4	1	0	B0916-C3	16	B09	1	1	1	A1016-B2	16	A10	1.5	1	-2
B0105-F	5	B01	1	1	1	A0216-D10	16	A02	4	1	0	B0705-C	5	B07	1	1	-1	B0916-D3	16	B09	1	1	0	A1016-D4	16	A10	1.5	1	-1
B0110-A	10	B01	3	1	-1	B0205-A	5	B02	3	1	1	B0705-D	5	B07	1	1	0	C0916-C4	16	C09	4	1	1	A1016-H5	16	A10	1.5	1	-1
B0110-C	10	B01	1	1	1	B0205-C	5	B02	3	1	2	B0710-A	10	B07	2	1	0	C0916-C6	16	C09	4	1	1	A1016-B7	16	A10	1.5	1	-1
B0110-D	10	B01	1	1	1	B0205-D	5	B02	2	1	1	B0710-D	10	B07	2	1	0	C0916-D6	16	C09	4	1	1	A1016-C7	16	A10	1.5	1	-1
B0110-F	10	B01	3	1	1	B0205-F	5	B02	3	1	1	B0710-G	10	B07	2	1	-2	C0916-E6	16	C09	4	1	1	B1005-A	5	B10	1	1	1
B0110-G	10	B01	3	1	1	B0205-G	5	B02	3	1	2	B0716-A8	16	B07	2	1	-1	C0916-F6	16	C09	4	1	1	B1005-B	5	B10	1	1	1
B0116-A1	16	B01	3	1	0	B0210-A	10	B02	3	1	1	B0716-H8	16	B07	2	1	-1	X0905-A	5	X09	4	1	-1	B1005-C	5	B10	1	1	1
C0105-A	5	C01	3	1	0	B0210-B	10	B02	3	1	1	B0716-F9	16	B07	2	1	-1	X0905-D	5	X09	4	1	0	B1005-D	5	B10	1	1	1
C0105-B	5	C01	3	1	1	B0210-C	10	B02	3	1	1	B0716-A10	16	B07	2	1		X0910-A	10	X09	4	0	-1	B1005-H	5	B10	1	1	-1
C0105-D	5	C01	3	1	1	B0210-E	10	B02	3	1	1	B0716-B10	16	B07	2	1	-1	X0916-A1	16	X09	4	0		B1010-C	10	B10	1.5	1	1
C0105-E	5	C01	3	1	-1	B0210-F	10	B02	3	1	1	C0705-B	5	C07	2	1	-2	X0916-B1	16	X09	4	0		B1010-E	10	B10	1	1	-1
C0105-F	5	C01	3	1	1	B0216-D1	16	B02	3	1	0	C0710-H	10	C07	2	1	-1							B1010-F	10	B10	1	1	1
C0105-G	5	C01	3	1	1	B0216-E1	16	B02	3	1	-1	C0716-H3	16	C07	2	1	-1							B1016-B3	16	B10	3.5	1	0
C0110-A	10	C01	3	1	-1	B0216-C5	16	B02	3	1	-1	C0716-A4	16	C07	2	1	0							B1016-B4	16	B10	3.5	1	0
C0110-C	10	C01	3	1	1	B0216-D5	16	B02	3	1	0	C0716-H6	16	C07	2	1	0							B1016-B5	16	B10	3.5	1	0
C0110-E	10	C01	3	1	1	C0205-A	5	C02	3	1	1	X0705-C	5	X07	4	1	-1							B1016-B6	16	B10	3.5	1	0
C0110-F	10	C01	3	1	1	C0205-D	5	C02	3	1	1	X0705-B	5	X07	4	1	0							C1005-E	5	C10	2	1	1
C0110-G	10	C01	3	1	1	C0205-E	5	C02	3	1	1	X0705-E	5	X07	4	1	0							C1005-A	5	C10	2	1	-1

C0110-H	10	C01	3	1	1	C0205-F	5	C02	3	1	1	X0710-B	10	X07	4	1	0
C0116-G1	16	C01	3	1	0	C0205-G	5	C02	3	1	1	X0710-D	10	X07	4	1	0
C0116-A2	16	C01	3	1	0	C0205-H	5	C02	3	1	0	X0710-G	10	X07	4	1	-1
C0116-B2	16	C01	3	1	0	C0210-A	10	C02	3	1	1	X0710-H	10	X07	4	1	0
C0116-C2	16	C01	3	1	0	C0210-B	10	C02	3	1	1	X0716-A1	16	X07	4	1	
C0116-B4	16	C01	3	1	0	C0210-C	10	C02	3	1	1	X0716-B1	16	X07	4	1	
X0105-A	5	X01	2	1	0	C0210-D	10	C02	3	1	2						
X0105-B	5	X01	2	1	1	C0210-E	10	C02	3	1	1						
X0105-D	5	X01	2	1	1	X0210-A	10	X02	3	1	1						
X0105-H	5	X01	2	0	0	X0210-B	10	X02	3	1	1						
X0110-B	10	X01	2	1	1	X0210-C	10	X02	3	1	1						
X0110-C	10	X01	2	1	1	X0210-D	10	X02	3	1	1						
X0110-F	10	X01	2	1	1	X0210-E	10	X02	3	1	2						
X0110-G	10	X01	2	1	1	X0210-F	10	X02	3	1	1						
X0116-A1	16	X01	3	1		X0210-G	10	X02	3	1	2						
X0116-B1	16	X01	3	1		X0205-A	5	X02	3	1	1						
						X0205-B	5	X02	3	1	1						
						X0205-C	5	X02	3	1	1						
						X0205-D	5	X02	3	1	1						
						X0205-E	5	X02	3	1	1						
						X0205-F	5	X02	3	1	1						
						X0205-G	5	X02	3	1	2						
						X0205-H	5	X02	3	1	1						
						X0216-A1	16	X02	3	1							
						X0216-B1	16	X02	3	1							

C1005-B	5	C10	2	1	1												
C1005-C	5	C10	2	1	1												
C1005-D	5	C10	2	1	1												
C1010-D	10	C10	2	1	1												
C1010-E	10	C10	2	1	1												
C1010-F	10	C10	2	1	1												
C1010-H	10	C10	2	1	1												
C1016-E1	16	C10	2	1	0												
C1016-F1	16	C10	2	1	0												
C1016-G1	16	C10	2	1	0												
X1005-A	5	X10	1	1	1												
X1005-E	5	X10	3	1	1												
X1010-A	10	X10	3.5	1	0												
X1010-B	10	X10	3.5	1	1												
X1010-C	10	X10	3.5	1	2												
X1010-D	10	X10	3.5	1	1												
X1010-E	10	X10	3.5	1	1												
X1010-F	10	X10	3.5	1	1												
X1010-G	10	X10	3.5	1	1												
X1016-A1	16	X10	4	1													
X1016-B1	16	X10	3.5	1													

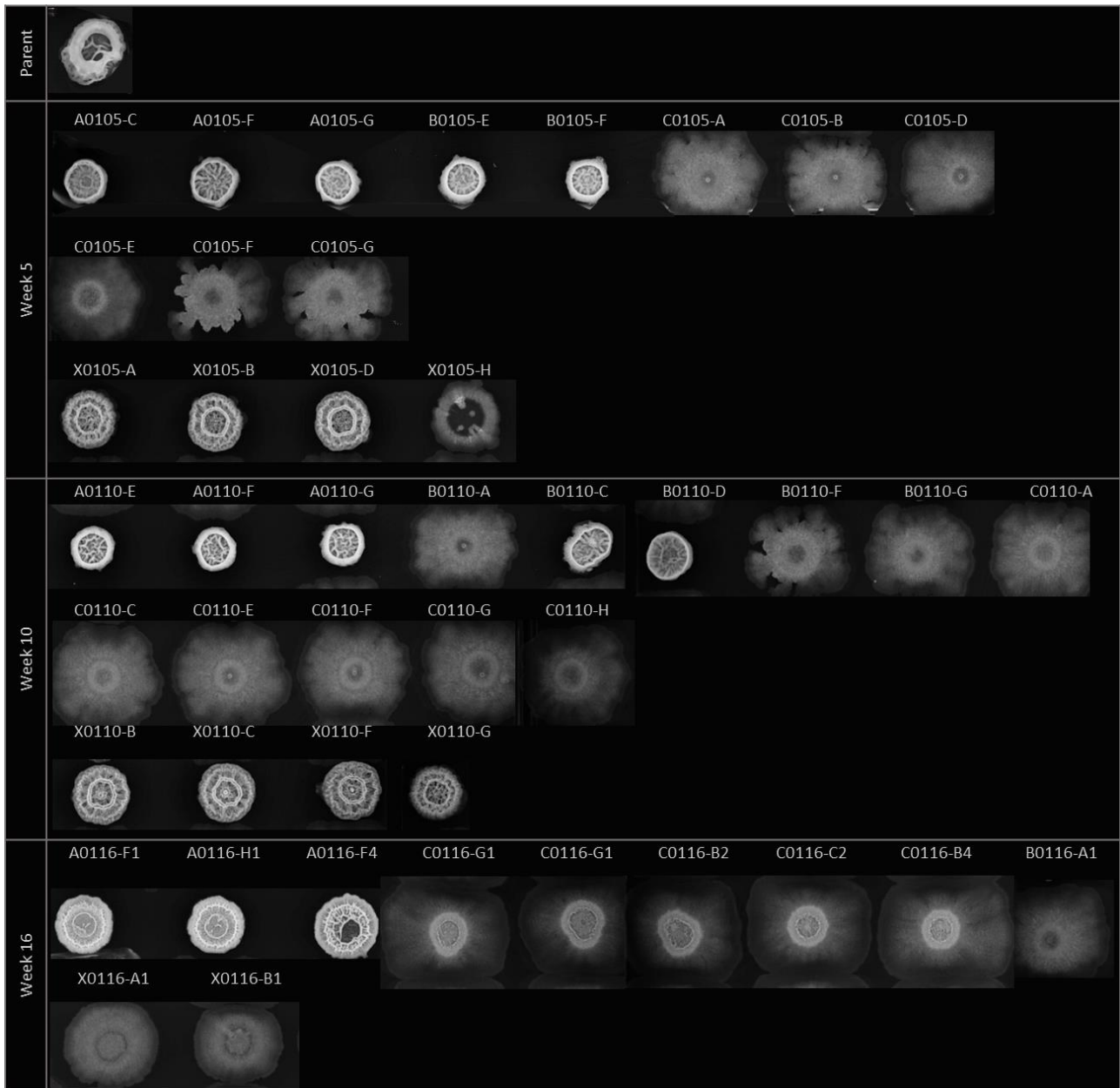


Fig. S 4. Colony morphology of BCF001 derivatives. Colony morphology of derivatives from BCF001 isolated at week 5, 10, and 16 from population A, B, C, and X was assessed on biofilm inducing medium. Population is indicated by the initial letter in strain name, followed by number reference to ancestor strain (01). Final numbers refer to isolation week (05, 10 or 16).

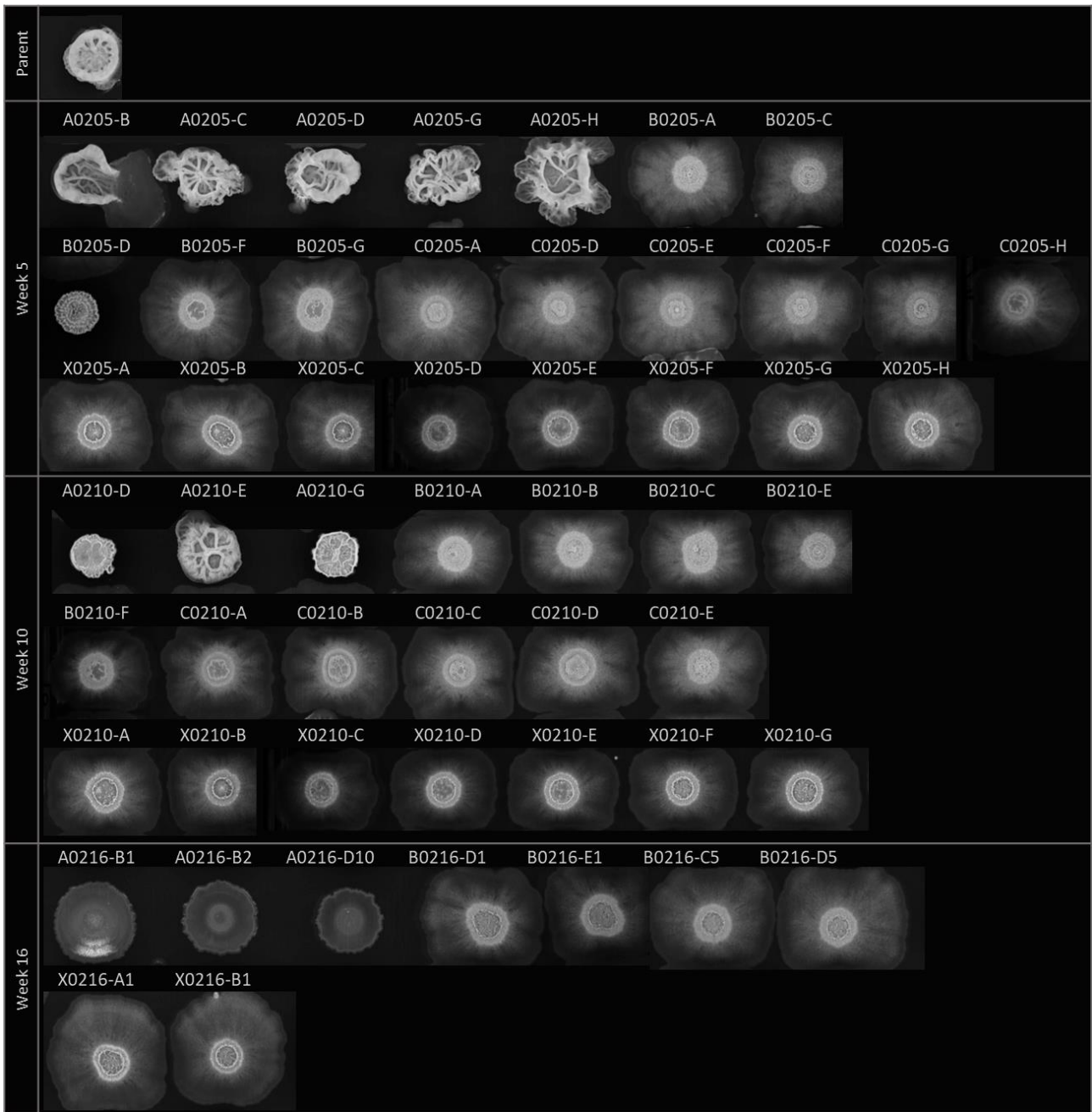


Fig. S 5. Colony morphology of BCF002 derivatives. Colony morphology of derivatives from BCF002 isolated at week, 5, 10, and 16 from population A, B, C, and X was assessed on biofilm inducing medium. Population is indicated by the initial letter in strain name, followed by number reference to ancestor strain (02). Final numbers refer to isolation week (05, 10 or 16).

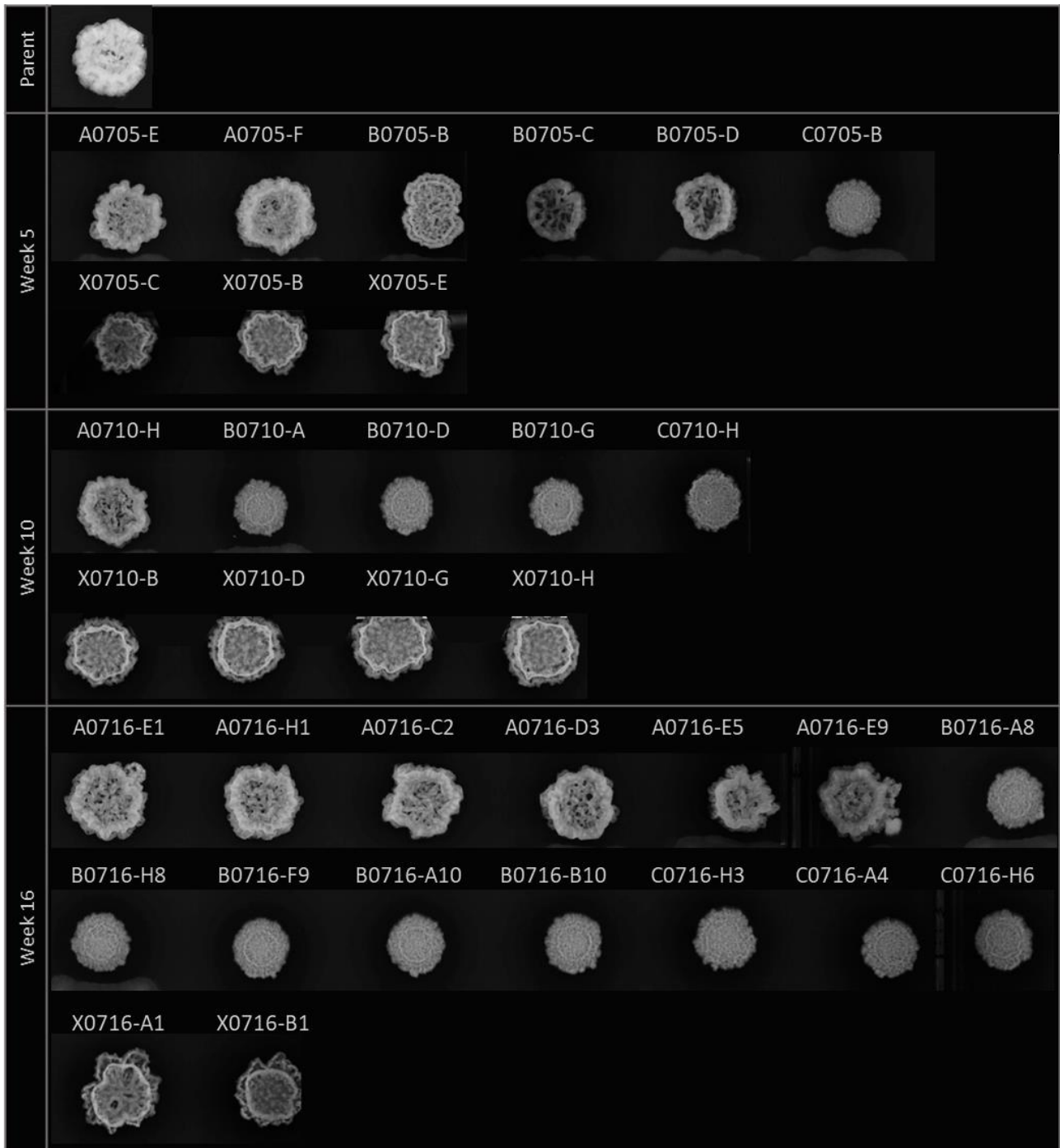


Fig. S 6. Colony morphology of BCF007 derivatives. Colony morphology of derivatives from BCF007 isolated at week, 5, 10, and 16 from population A, B, C, and X was assessed on biofilm inducing medium. Population is indicated by the initial letter in strain name, followed by number reference to ancestor strain (07). Final numbers refer to isolation week (05, 10 or 16).

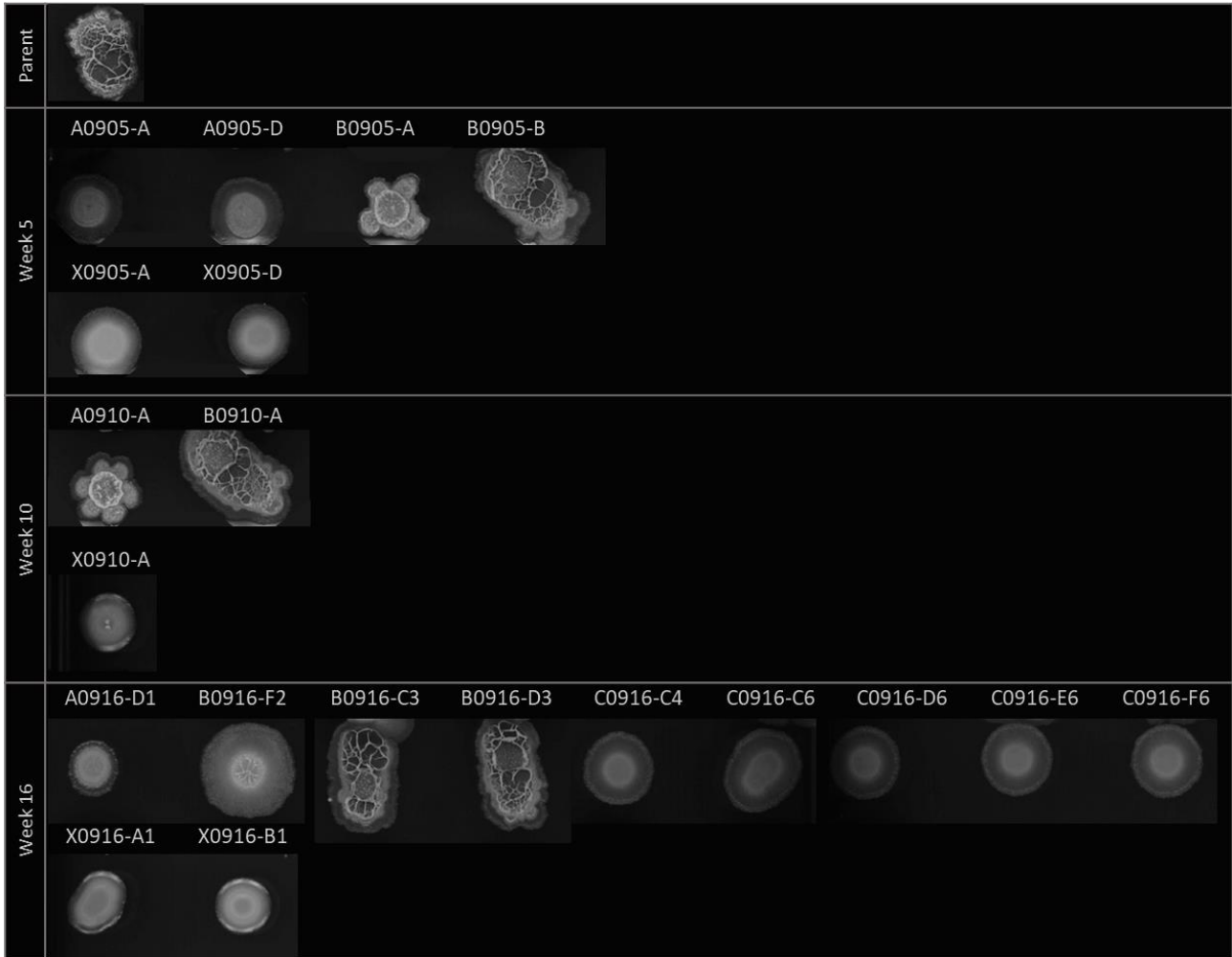


Fig. S 7. Colony morphology of BCF009 derivatives. Colony morphology of derivatives from BCF009 isolated at week, 5, 10, and 16 from population A, B, C, and X was assessed on biofilm inducing medium. Population is indicated by the initial letter in strain name, followed by number reference to ancestor strain (09). Final numbers refer to isolation week (05, 10 or 16).

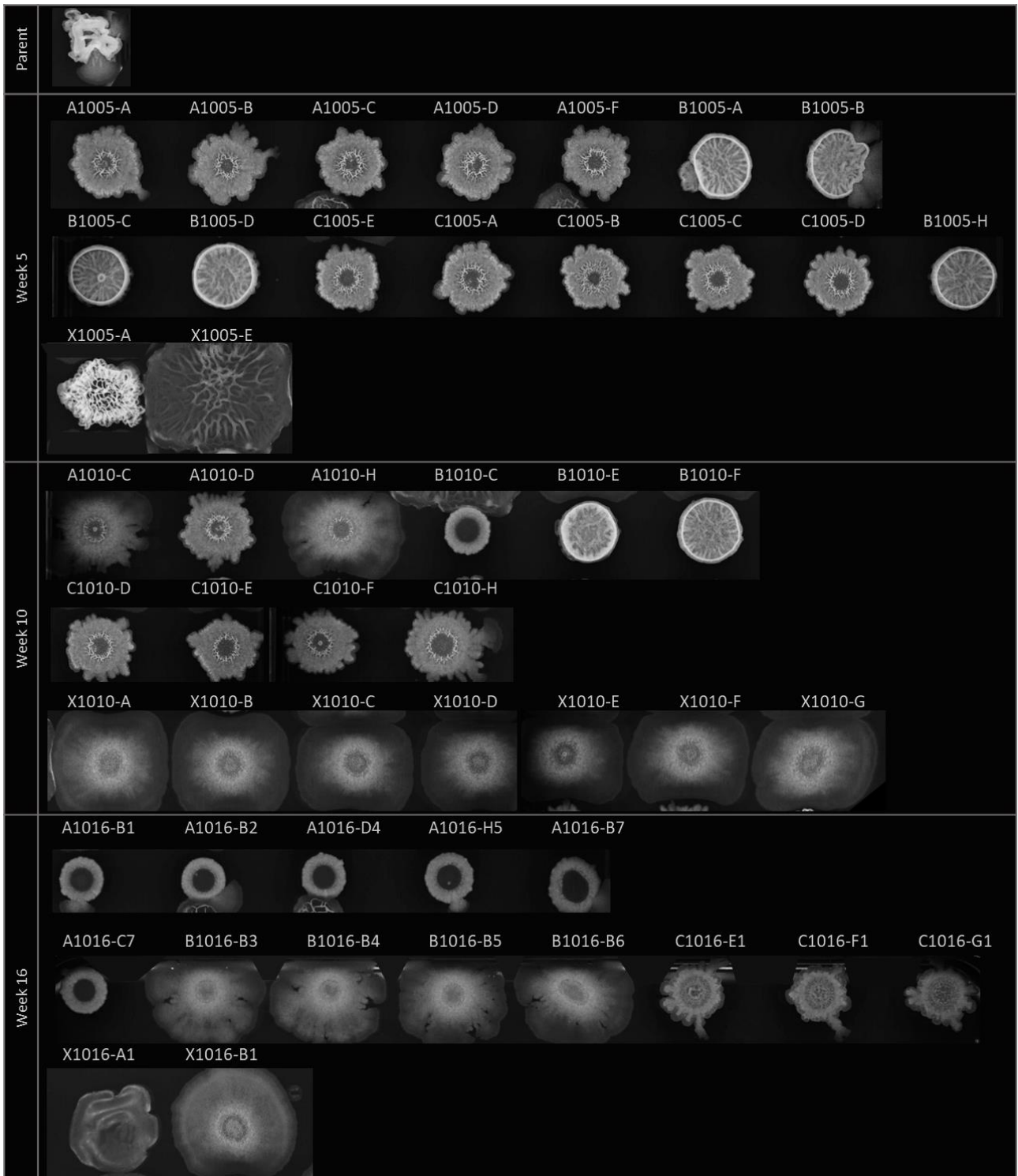


Fig. S 8. Colony morphology of BCF010 derivatives. Colony morphology of derivatives from BCF010 isolated at week, 5, 10, and 16 from population A, B, C, and X was assessed on biofilm inducing medium. Population is indicated by the initial letter in strain name, followed by number reference to ancestor strain (10). Final numbers refer to isolation week (05, 10 or 16).

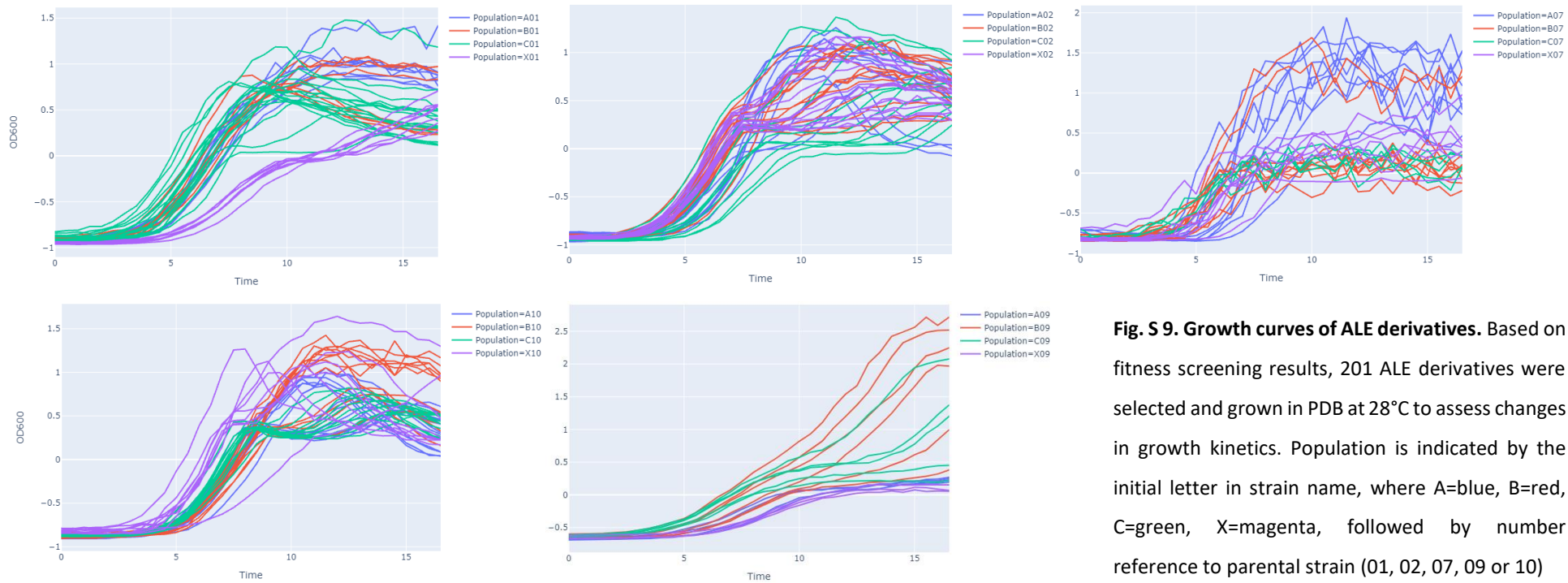


Fig. S 9. Growth curves of ALE derivatives. Based on fitness screening results, 201 ALE derivatives were selected and grown in PDB at 28°C to assess changes in growth kinetics. Population is indicated by the initial letter in strain name, where A=blue, B=red, C=green, X=magenta, followed by number reference to parental strain (01, 02, 07, 09 or 10)



7

Fig. S 10. Mutation per strain and types. The number of and types of mutations were identified for each evolved strain derived from the ancestors *B. subtilis* BCF001, BCF002, BCF010, *B. amyloliquefaciens* BCF007, *B. paralicheniformis* BCF009. Population is indicated by the initial letter in the strain name (A, B, C, X), followed by number reference to ancestor strain (01, 02, 07, 09, 10). Final numbers refer to isolation timepoint (week 05, 10, 16). For instance, strain A0105-G originates from population A derived from ancestor BCF001 isolated at timepoint week 05. Indel; insert/deletion. Intergenic; mutation in between ORFs. Nonsense; mutation leading to premature stop. Nonsynonymous; mutation leading to different amino acid. Synonymous; mutation changing codon, but not amino acid.

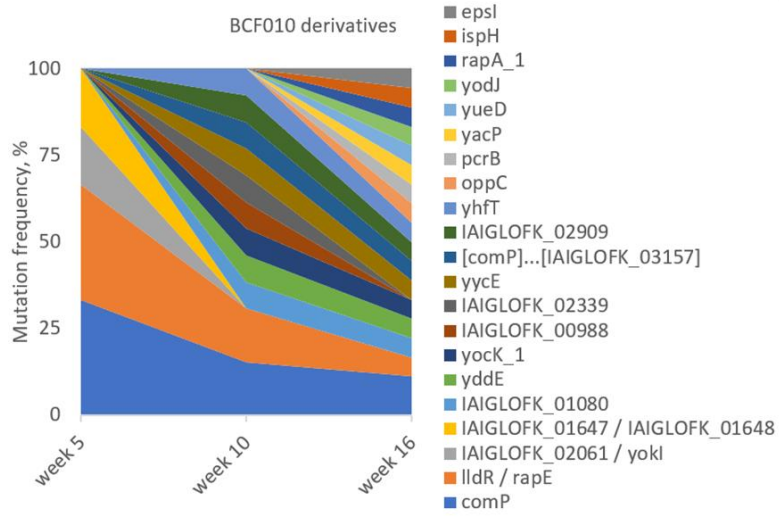
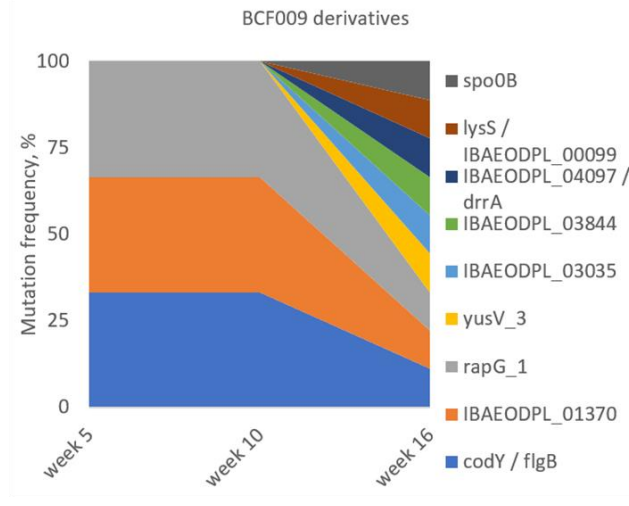
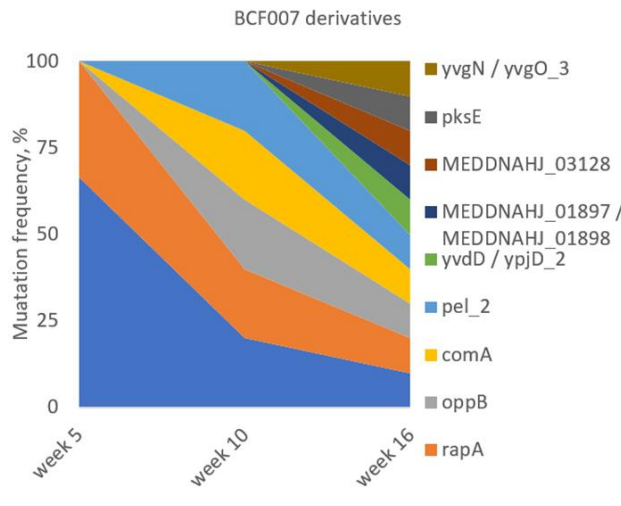
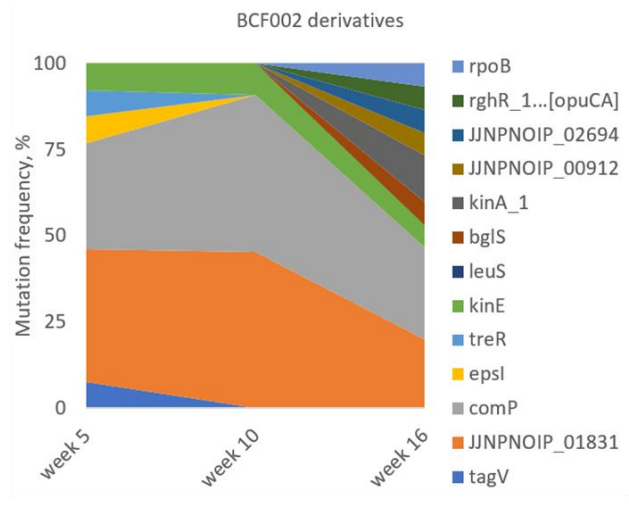
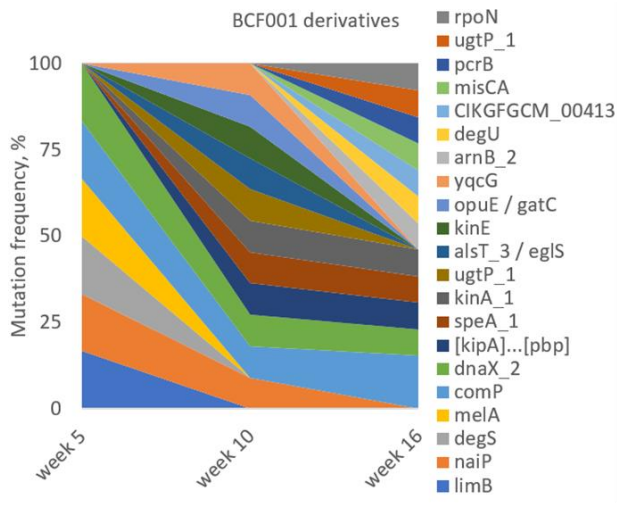


Fig. S 11. Relative mutation frequency. The frequency of each mutation was calculated based on mutation occurrences relative to the total number of mutations across all population from the respective ancestor (BCF001, BCF002, BCF007, BCF009, BCF010) at each timepoint (week, 5, 10, 16).

Table S 3. Reoccurring mutated loci. Mutations occurring in the same loci in several strains are listed. The SNPs are not necessarily identical. In strain names, initial letter refers to evolved population (A, B, C, X), following two number refer to ancestor strain (BCF001, BCF002, BCF007, BCF009, BCF010), and final two numbers refer to isolation timepoint (week 05, 10, 16).

ORF	Count	Derivatives
<i>[kipA]–[pbp]</i>	2	A0110-E, A0116-H1
<i>epsI</i>	2	B0205-C, X1016-B1
<i>mpfA</i>	2	A1010-C, B1016-B3
<i>sspl</i>	2	X1010-C, X1016-B1
<i>oppB</i>	2	A0710-H, A0716-D3
<i>pcrB</i>	2	B0116-A1, B1016-B3
<i>pel_2</i>	2	X0710-D, X0716-B1
<i>speA_1</i>	2	A0110-E, A0116-H1
<i>spo0B</i>	2	C0916-F6, X0916-B1
<i>ugtP_1</i>	2	B0110-G, B0116-A1
<i>yddE</i>	2	A1010-C, B1016-B3
<i>comQ</i>	2	X1010-C, X1016-B1
<i>comX</i>	2	X1010-C, X1016-B1
<i>degQ</i>	2	X1010-C, X1016-B1
<i>yhfT</i>	2	X1010-C, X1016-B1
<i>yocK_1</i>	2	A1010-C, B1016-B3
<i>yycE</i>	2	C1010-D, C1016-E1
<i>codY / flgB</i>	3	B0905-B, B0910-A, B0916-C3
<i>dnaX_2</i>	3	X0105-B, X0110-B, X0116-B1
<i>IBAEODPL_01370</i>	3	B0905-B, B0910-A, B0916-C3
<i>niaP</i>	3	A0105-G, A0110-E, A0116-H1
<i>yqhH</i>	3	X0705-B, X0710-D, X0716-B1
<i>rapG</i>	3	B0905-B, B0910-A, B0916-C3
<i>kinA</i>	5	B0110-G, B0116-A1, B0216-D1, B0216-E1, X0916-B1
<i>kinE</i>	5	C0110-G, X0205-G, X0210-E, X0210-G, X0216-B1
<i>lldR / rapE</i>	5	A1016-B1, B1005-A, B1005-H, B1010-E, B1010-F
<i>JJNPNOIP_01831</i>	13	A0205-D, A0205-H, A0210-E, A0216-B2, B0205-C, B0210-A, B0216-D1, B0216-E1, C0205-E, C0210-D, X0205-G, X0210-E, X0210-G
<i>comP</i>	30	A0210-E, A0216-B2, A1005-D, A1010-C, B0110-G, B0116-A1, B0205-C, B0205-G, B0210-A, B0216-D1, B0216-E1, B0705-D, B1016-B3, C0105-G, C0110-G, C0205-E, C0210-D, C1005-E, C1010-D, C1016-E1, X0116-B1, X0205-G, X0210-E, X0210-G, X0216-B1, X0705-B, X0710-D, X0716-B1, X1010-C, X1016-B1
Total reoccurrences	110	

Table S 4. Mutations affecting ORF related to cell differentiation. 66 mutations in ORFs regulating or impacting cell differentiation were identified. The cell differentiation pathway is indicated to the right. Count denotes number of occurrences across strains, where intergenic mutations are shown in brackets.

ORF	Protein	Count	Biofilm	Sporulation	Competence	Motility	Lytic enzymes
<i>comP</i>	Sensor histidine kinase ComP	30	✓	✓	✓		
<i>comX</i>	Competence pheromone ComX	2	✓	✓	✓		
<i>comQ</i>	Tryptophan prenyltransferase ComQ	2	✓	✓	✓		
<i>comA</i>	Transcriptional regulatory protein ComA	1	✓	✓	✓		
<i>degS</i>	Cytoplasmic sensor histidine kinase DegS	1	✓			✓	✓
<i>degU</i>	Transcriptional regulatory protein DegU	1	✓			✓	✓
<i>degQ</i>	Regulatory protein DegQ	2	✓			✓	✓
<i>rapA</i>	Response regulator aspartate phosphatase A	4(5)					
<i>rapE</i>	Response regulator aspartate phosphatase E	(5)	✓	✓			
<i>rapG</i>	Response regulator aspartate phosphatase G	3	✓	✓			
<i>kinA</i>	Sporulation kinase A	5	✓	✓			
<i>kinE</i>	Sporulation kinase E	5	✓	✓			
<i>spoOB</i>	Sporulation initiation phosphotransferase B	2	✓	✓			
<i>oppB</i>	Oligopeptide permease protein OppB	2	✓	✓	✓		
<i>oppC</i>	Oligopeptide permease protein OppC	1	✓	✓	✓		
<i>sinR</i>	Antagonist of SinR	1	✓				
<i>sinI</i>	Biofilm repressor SinR	1	✓				
Total		73					

Table S 5. Selected strains for phenotypic characterization. Strains were selected for phenotypic characterization in respect to; colony morphology, fungal confrontation inhibition, swarming motility, γ -PGA contents, secondary metabolite content, ID50, protease activity, VOC, and pellicle formation.

Ancestor	Week	Strain	Screen	Colony	Confront	Motility	γ -PGA	SecMet	ID50	Protease	VOC	Pellicle	ORFs
BCF001	5	C0105-G	1	3	0	-2	-1	-1	-2	-1		1	<i>comP</i>
	5	C0105-E	-1	3	0	0		-1	-1			0	<i>degS, melA</i>
BCF002	5	B0205-G	2	3	1	0	0	-1	-2	-1	1	1	<i>comP</i>
	5	X0205-G	2	3	1	0				-1		1	<i>comP, kinE, JJNPNOIP_01831</i>
BCF007	5	B0705-D	0	1	1	0		-1	-2	-1	1	0	<i>comP</i>
	10	A0710-H	-2	1	1	0		0	-1			0	<i>oppB</i>
	10	B0710-A	0	2	0	-2		-1	-2			-1	<i>comA</i>
	5	X0705-B	0	4	1	0		-1	-2	-1	1	0	<i>comP, yqhH</i>
	16	A0716-D3	-2	1	1	0		0	-1			0	<i>oppB, MEDDNAHJ_01897 / MEDDNAHJ_01898, MEDDNAHJ_03128, pksE</i>
BCF010	5	A1005-D	1	2	1	0	-1	-1	-2	-1	1	1	<i>comP</i>
	5	C1005-E	1	2	1	-1	-1	-1	-1	-1		1	<i>comP, IAIGLOFK_02061 / yoki</i>
	16	A1016-B1	-2	1.5	1	0		-1	-2			1	<i>oppC, lldR / rapE</i>

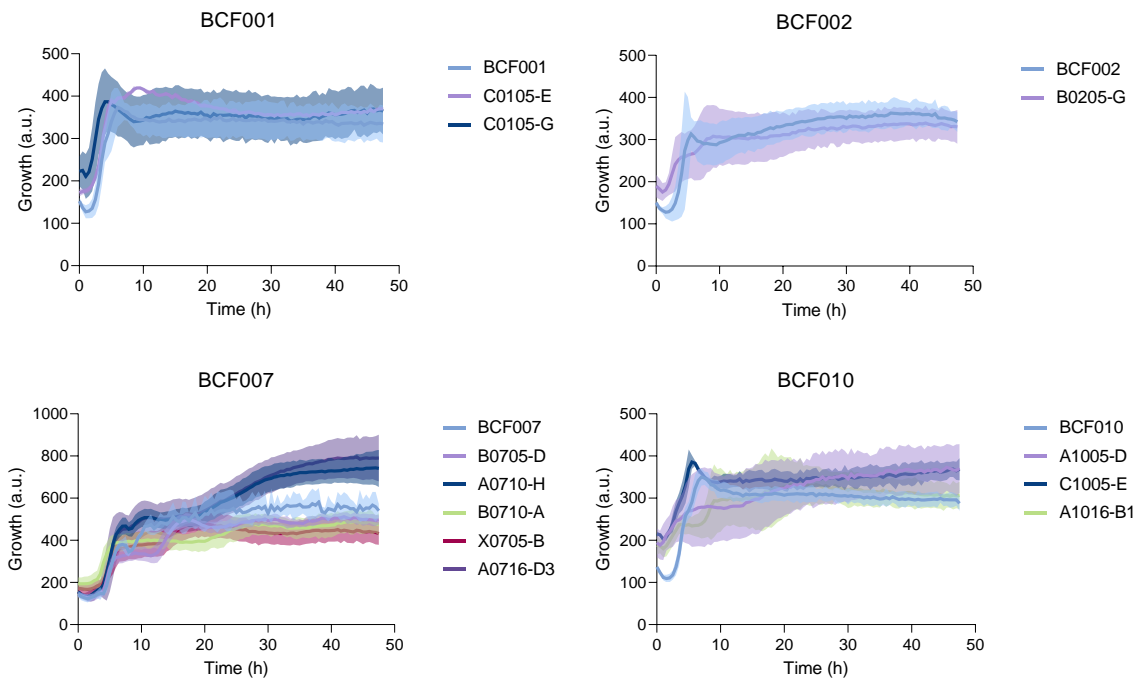


Fig. S 12. Culture growth. Evolved strains derived from *B. subtilis* BCF001, BCF002, BCF010, *B. amyloliquefaciens* BCF007, *B. paralicheniformis* BCF009 were grown for 48h at 37°C with agitation in PDB medium for analysis of specialised metabolite contents and for assessment of culture supernatant inhibition potency against *F. culmorum*.

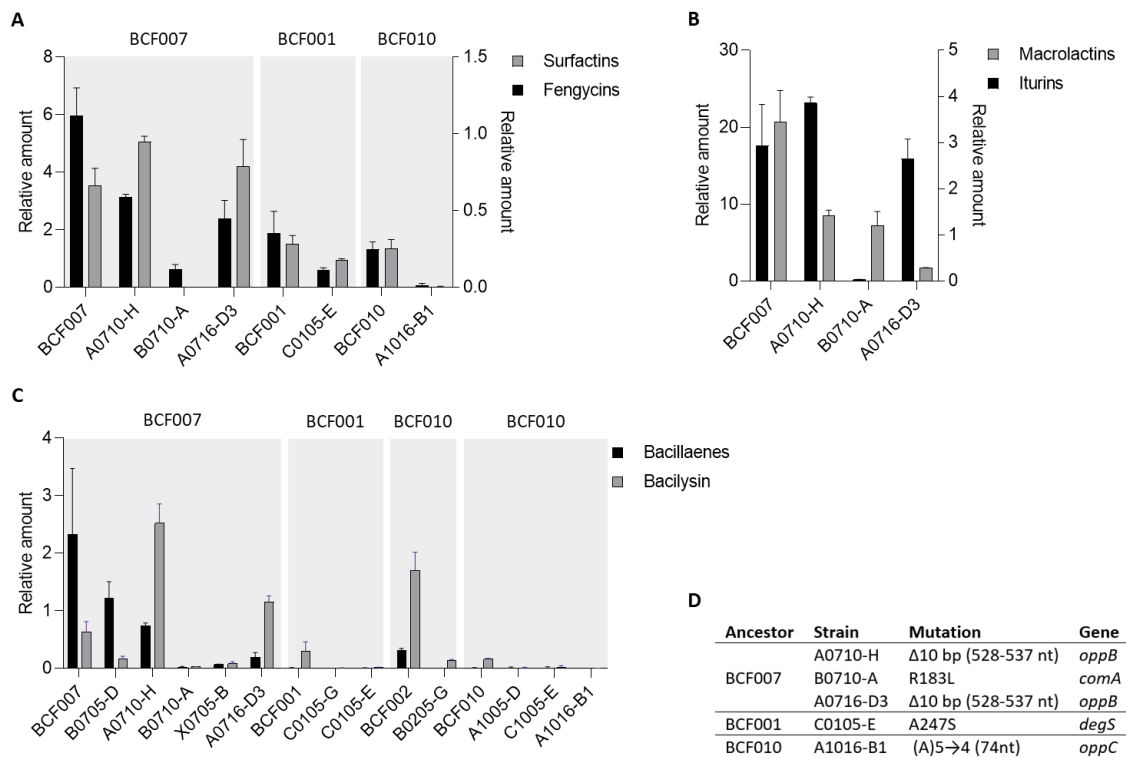


Fig. S 13. Bioactive metabolites content of *Bacillus* cultures. Lipopeptides and polyketides produced by mutants were analysed from cultures by LCMS of culture grown for 48h in PDB medium at 37°C with agitation to allow reaching the stationary growth phase. **A)** Fengycins (left axis) and surfactins (right axis) were analysed from cultures of evolved strains derived from *B. subtilis* BCF001, BCF002, BCF010, *B. amyloliquefaciens* BCF007. **B)** Additionally, relative amounts of iturins (left axis) and macrolactins (right axis) were analysed from *B. amyloliquefaciens* BCF007-derivatives. Error bars indicate standard deviation between biological duplicates. **C)** Relative amounts of produced bacillaene and bacilysin amounts. **E)** Overview of acquired mutations of respective evolved strains.

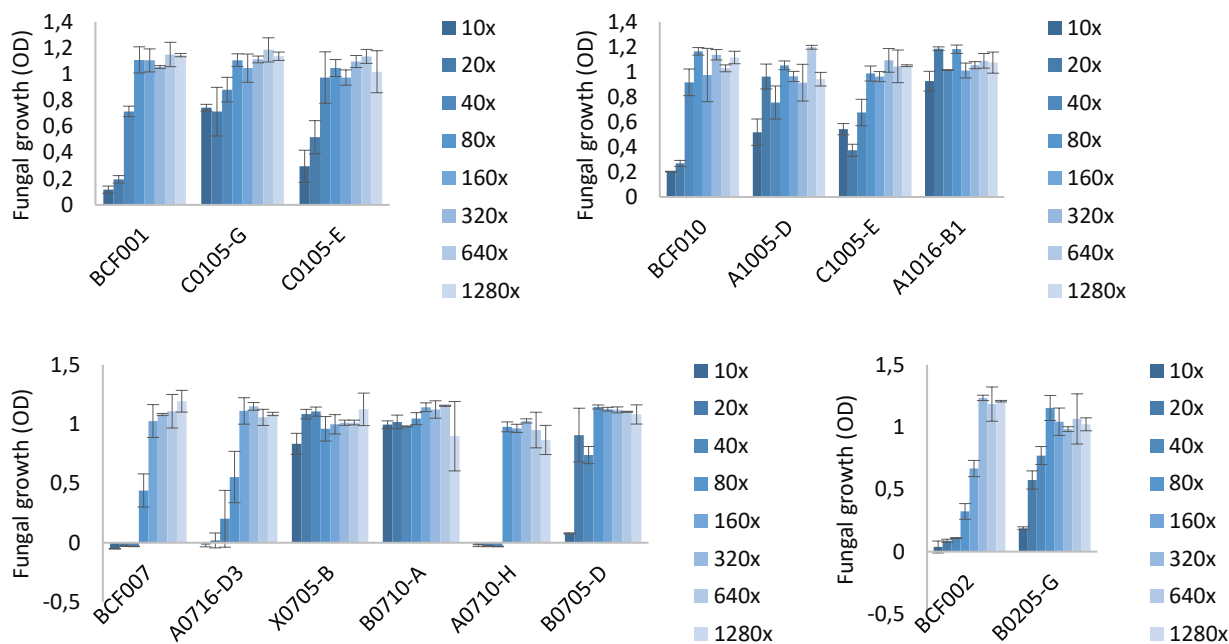


Fig. S 14. *F. culmorum* growth inhibition by *Bacillus* culture supernatants.

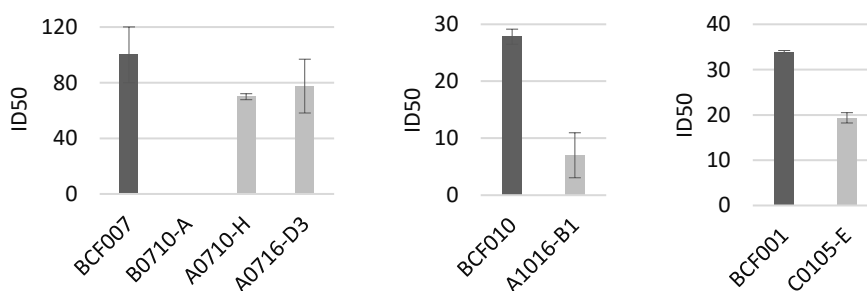


Fig. S 15. Inhibition potency of *Bacillus* cultures on fungal growth. The half inhibitory dilution (ID50) of *Bacillus* cultures that reduced *F. culmorum* growth to 50% was determined for ComA mutant B0710-A, oppB mutants A0710-H and A0716-D3, oppC mutant A1016-B1 and DegS mutant C0105-E (light) and ancestor strains (dark). *Bacillus* culture dilution series were prepared and inoculated with a fixed fungal spore concentration and bacteriostatic were added to prevent bacterial growth. Results correspond to averages calculated from biological duplicates, with error bars indicating the standard deviation.

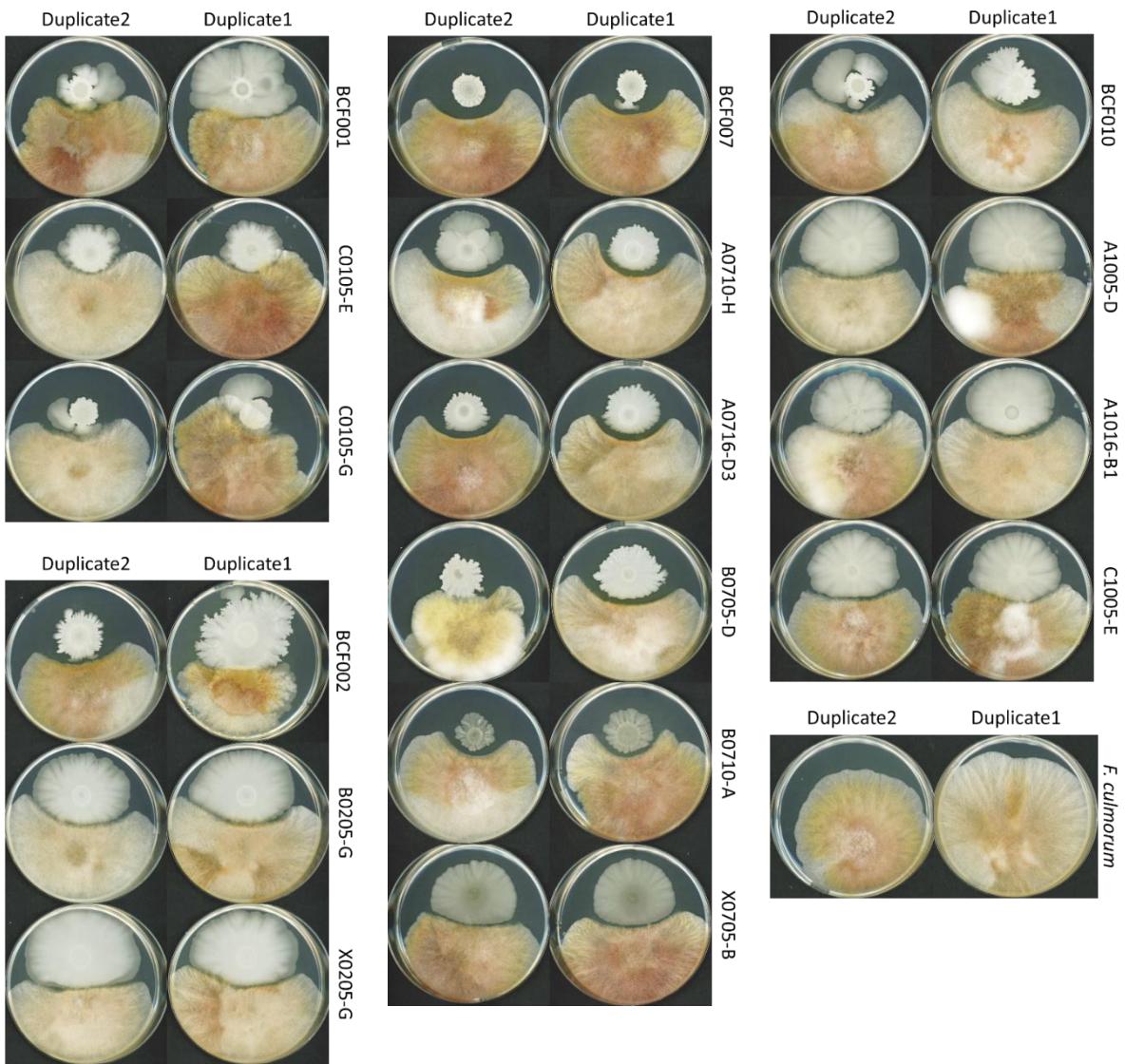


Fig. S 16. Dual species plate confrontation. *F. culmorum* growth was challenged by ALE derivatives confrontation. Fungal growth was imaged after 7 days incubation at 25°C.

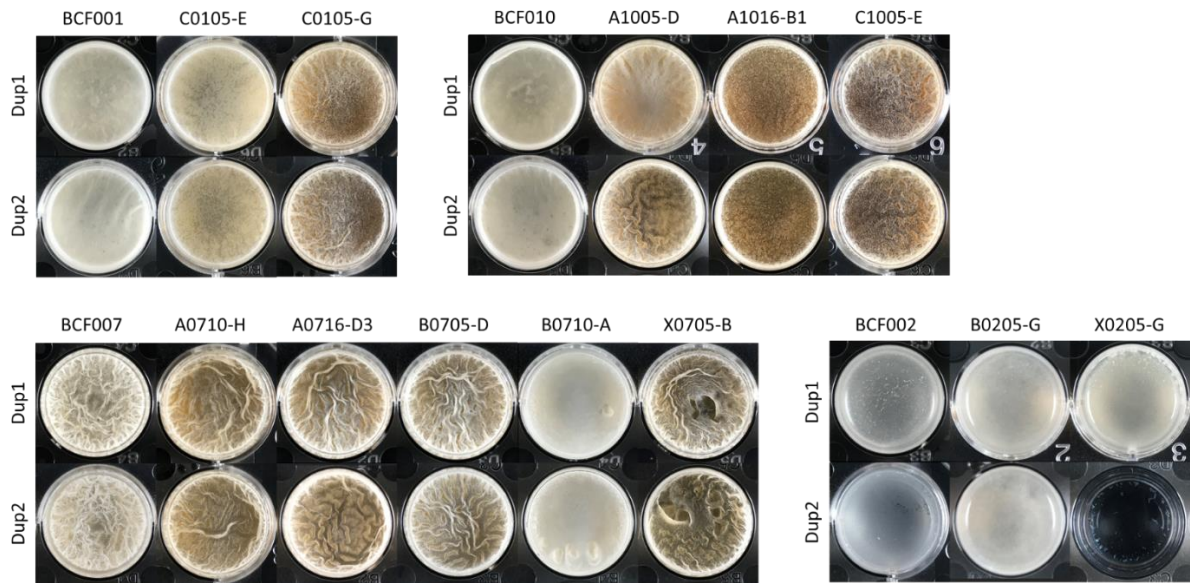


Fig. S 17. Pellicle phenotypes. Pellicle formation of selected derivatives was assessed in MSgg medium in biological duplicates.

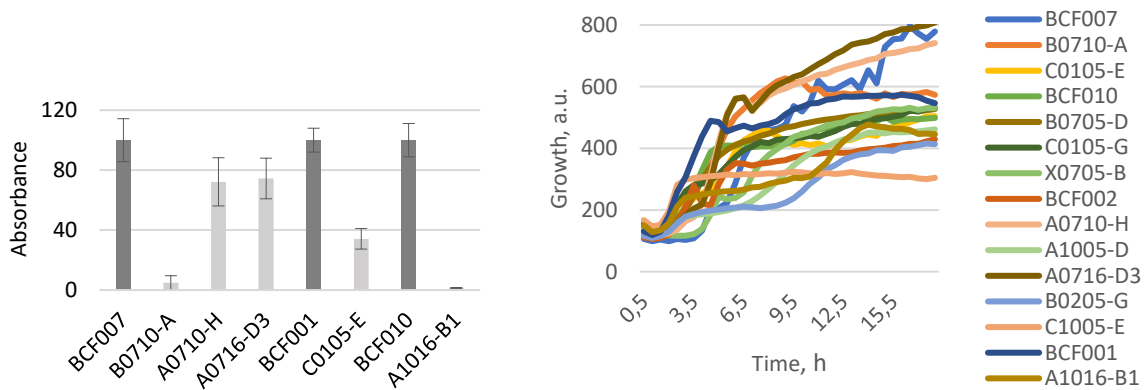


Fig. S 18. Protease activity. The activity of serine-class endo-proteases was measured by a colorimetric assay. **Left)** The absorbance from the *comA* mutant (B0710-A), *oppB* mutants (A0710-H, A0716-D3), *degS* mutant (C0105-E), and *oppC* (A1016-B1) (light bars) as normalized to the signal of the ancestor strains (dark bars). Error bars indicate standard deviation between biological duplicates. **Right)** Cultures were incubated for 18 h at 37°C before harvesting the supernatants by centrifugation.

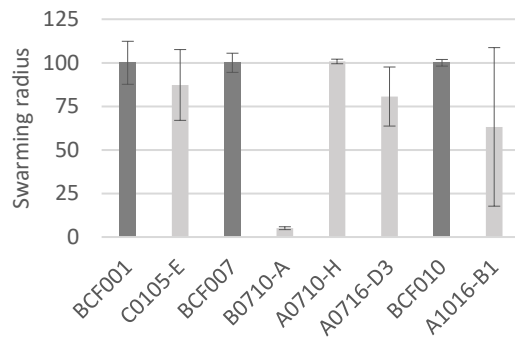


Fig. S 19. Swarming motility. The swarming motility of *degS* mutant C0105-E, *comA* mutant B0710-A, *oppB* mutants A0710-H, A0716-D3 and *oppC* mutant A1016-B1 was measured relative to the ancestors BCF001, BCF007, BCF010 on semi-solid growth plates.

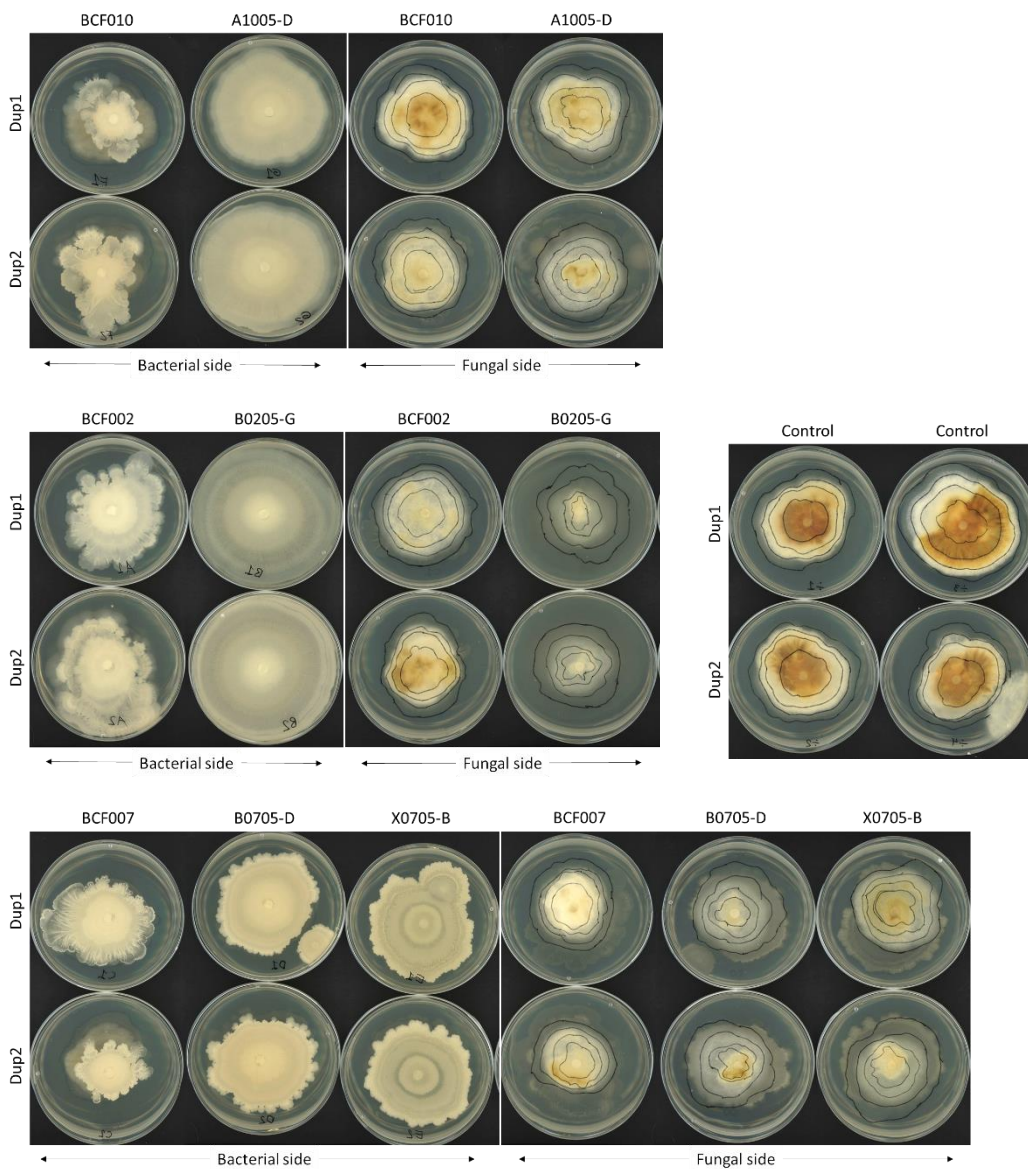


Fig. S 20. *Bacillus* volatile impact on fungal growth. The effect of *Bacillus* organic volatile compounds (VOCs) on fungal growth was evaluated by growing the species separately within the same compartment for 120h. Effects were visible already after 24h. *Dup* refers to biological replicate and *Control* refers to fungal growth in the absence of *Bacillus*.

Table S 6. Summary of ComP mutant phenotype. The ComP mutant phenotypes assessed in this study and the according results.

Phenotype assessed	<i>comP</i> mutant's phenotype
Colony morphology	Dry appearance, loss of structure, increased spreading
Dual-species confrontation	Increased surface colonization
Lipopeptide production	Reduced lipopeptide content
Culture supernatant inhibition	Reduced ID50 of culture supernatants
Pellicle formation	Altered pellicles with wrinkles and coloration
Swarming motility	Slightly reduced or similar motility
Poly- γ -glutamic acid (γ -PGA) production	Hampered γ -PGA production
Extracellular protease activity	Lower protease activity
Root colonization	Not improved root colonization
Volatile effect on fungal growth	Enhanced effect of volatile compounds

Study 6

Kjeldgaard, B., Fonseca, C., Kovács, Á. T., and Domínguez-Cuevas, P.

Adaptive evolution of *Bacillus* spp. against *Botrytis cinerea*.

To be submitted.

Adaptive evolution of *Bacillus* spp. against *Botrytis cinerea*

Bodil Kjeldgaard^{1,2}, César Fonseca¹, Ákos T. Kovács², Patricia Domínguez- Cuevas^{1,3}

¹Discovery, R&D, Chr. Hansen A/S, Denmark

²Bacterial Interactions and Evolution Group, DTU Bioengineering, Technical University of Denmark

³Current affiliation: Scientific Integration, Novo Nordisk, Denmark

Abstract

Botrytis cinerea, a notorious plant pathogen causing grey mold infections in a wide range of hosts, poses a significant threat to agriculture both during plant growth and post-harvest preservation. However, members of the *Bacillus subtilis* species complex hold great potential as biocontrol agents against grey mold disease. In this study, the adaptive response of undomesticated *Bacillus* spp. to the presence of the phytopathogenic fungus was investigated. We show that experimental evolution of planktonic *Bacillus*-fungal co-cultures was accompanied by bacterial adaptation to the laboratory growth conditions, characterized by accumulation of mutations in genes responsible for flagellum synthesis that drastically reduced motility. Furthermore, genetic alterations were detected in genes related to metal ion uptake and efflux, catabolite repression, and biosynthetic gene clusters for the production of specialized metabolites in certain ancestor backgrounds. These genotypes were associated with modification in biofilm morphology, fungal inhibition potency, production of poly- γ -glutamic acid (γ -PGA), extracellular protease activity and production of specialized metabolites.

Introduction

The air-borne phytopathogen *Botrytis cinerea* infects more than 200 plants, mainly belonging to dicotyledonous species, and causes grey mold disease in important cultivars including vegetables (cabbage, lettuce, broccoli, tomato), fruits (grape, berries, apple), seeds (chickpeas, sunflower, flax) and ornamental flowers (rose, gerbera). The fungus is particularly harmful to senescent plant structures and may remain idle within the healthy plant host before rapidly turning necrotrophic once favorable conditions appear, often during post-harvest storage. Habitually, infection initiates in mature leaves or flowers and subsequently spreads to adjacent fruits, but also manifests through infested seeds. *Botrytis*' virulence relies on production of oxalic acid and phytotoxins such as the sesquiterpene botrydial or the polyketide botcinin to induce apoptosis in host cells. Infection occurs by means of appressoria that secrete toxic metabolites as well as enzymes that kill and breach the plant surface tissue. The fungus potentially produces more than 200 carbohydrate-active enzymes. The release of these degradative enzymes during infection not only facilitates

entry, but also degenerates plant material for sequestration of nutrients to support fungal growth. The filamentous fungus persists as sclerotia (hardened mycelium) or survives in mycelial form in plant debris and later forms conidia that serve as primary inoculum of new plant tissue. *Botrytis cinerea* infestations are difficult to control due to the fungal dormancy in seemingly healthy plants, prolonged survival in dead plant material and variation of attack types (1–4). Accurate economical estimation of the disastrous crop damage caused by *B. cinerea* is difficult to calculate due to its broad host-range, but the fungus presumably eventuates a billion-dollar economic impact world-wide to pre- and post-harvest crops (5). A specific economic study suggests that in New Zealand only, *B. cinerea* infections impose a horticulture cost of NZ\$2578 per hectare (6). Commonly, *B. cinerea* grey mold disease is preventively treated by application of chemical fungicides. Despite the cellular fitness cost implications to the fungus (7, 8), *B. cinerea* develops resistance to fungicides by target site alteration or drug efflux improvement leading to significantly decline in treatment efficacy or complete failure of disease control (9). Discernibly, emergence of multiresistant *B. cinerea* populations has been reported globally including Chinese, European, Australian, South- and North American horticulture (8, 10–17). In addition, fungicides constitute a possible risk to human health and chemical leaching represent a potential source of pollution to aquatic ecosystems as well as natural soil environments (18–20).

Microbial biocontrol agents represent a safe and environmentally friendly alternative to the abundant usage of chemical fungicides in agriculture. Such microbes may reduce plant pathogen growth by competition for nutrients and growth niche, priming of plant defense, or by secretion of fungal inhibitory metabolites. Species from the *Bacillus* genera hold great potential as biocontrol agents due to their impressive capacity for biosynthesis of specialized metabolites with bioactivity and their natural occurrence in soil habitats. Especially, the cyclic lipopeptides from the fengycin and iturin families exert antifungal activity against several phytopathogens, including *B. cinerea* (21, 22). Previous studies show that *Bacillus* spp. among other mechanisms inhibit *B. cinerea* growth by plant induced systemic resistance (ISR) (23), production of lytic enzymes, biosynthesis of cyclic lipopeptides (24–27), secretion of volatiles (28) and siderophores (29). The *Bacillus* sporulation capacity provides an advantage for biocontrol product formulation and application, while the biofilm formation abilities enable proficient root colonization and niche occupation (30, 31). Together with the multifaceted inhibition mechanisms, these features make *Bacillus* spp. excellent candidates for agriculture biocontrol.

In this study, we explored adaptive laboratory evolution as a tool for *Bacillus* strain improvement by a bacterial-fungal co-culture system under planktonic growth conditions using *Bacillus* spp. and *B. cinerea*. Repetitive cycles of co-cultivation were continued for approximately 200 bacterial generations and *Bacillus*

evolved populations were sampled concurrently to the experimental evolution. High throughput screening of fungal inhibition potency enabled the selection of evolved strains for further genotype-phenotype investigation. Whole genome sequencing and analysis showed that evolved strains adapted to the laboratory growth conditions by acquiring mutations compromising flagellar-driven motility, whereas adaptations specific to the co-cultivation in the presence of fungi included changes in catabolism and metal ion transport.

Results

Experimental design of adaptive laboratory evolution of *Bacillus* spp. with *B. cinerea*

Five *Bacillus* strains, *B. subtilis* BCF001, BCF002, BCF010, *B. amyloliquefaciens* BCF007, and *B. velezensis* BCF015 were evolved in the presence of the grey mold fungus *Botrytis cinerea* Kern B2 by repeated co-cultivation cycles (Fig. 1). A simple adaptive laboratory evolution (ALE) setup was established with bacterial-fungal planktonic co-cultures. Owing to the rapid bacterial growth, the fungus was precultivated for 3 days to develop mycelium prior to co-inoculation of *Bacillus* cultures with concurrent nutrient supplementation. The bacterial-fungal co-cultures were incubated for 24 h, the fungal mycelium was removed from the *Bacillus* cultures by filtration, and new co-culture cycles were initiated using the pre-evolved bacterial cells. To avoid the concurrent adaption of the plant pathogenic fungus and facilitate an exclusive *Bacillus* evolution focus, the bacterial filtrates were collected and transferred, while the fungal mycelia were discarded and replaced with fresh fungal cultures from the same stock for each new evolution cycle. The bacterial growth was measured and adjusted by each transfer to the same optical density (OD₆₀₀ 0.01) (Fig. S1). All five ancestor strains were evolved in triplicate ALE lineages (G, H, I) in addition to a control lineage evolved in the absence of fungus (W). The addition of these control lineages allowed identification of genetic changes acquired during adaptation to the laboratory growth conditions unrelated to the fungus. The strains cultured in the presence of *B. cinerea* will be referred to as co-evolved strains (i.e., co-culture evolved populations) and the strains cultured in absence of the fungus will be referred to as evolved control strains.

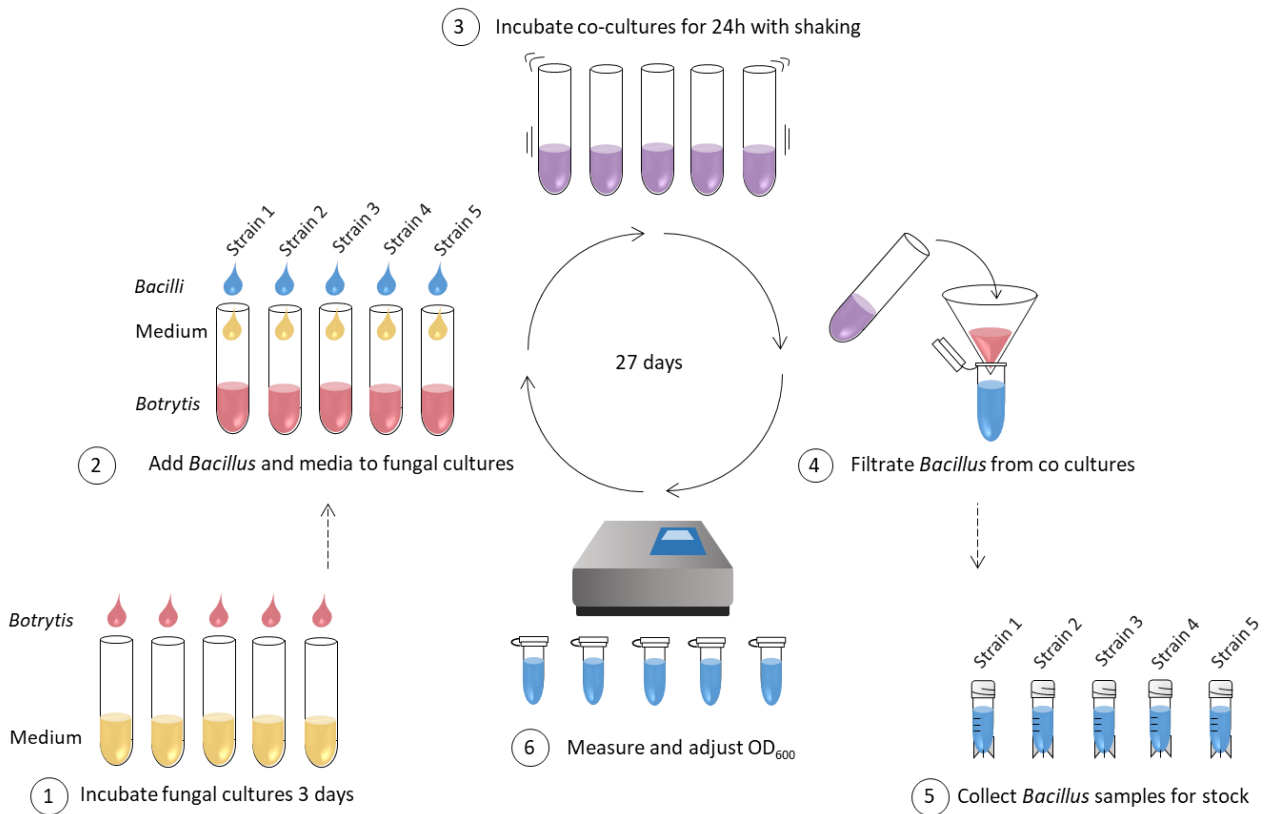


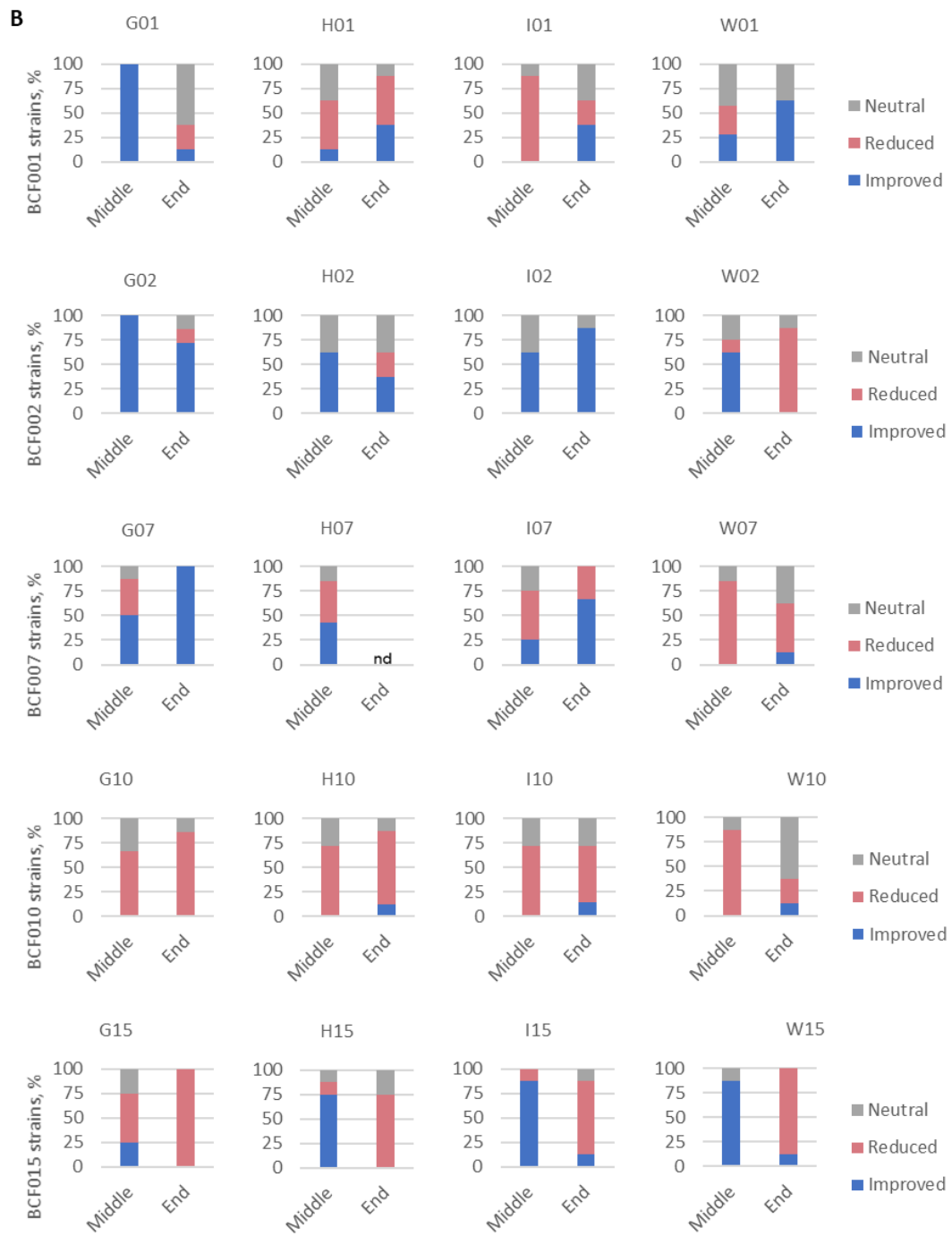
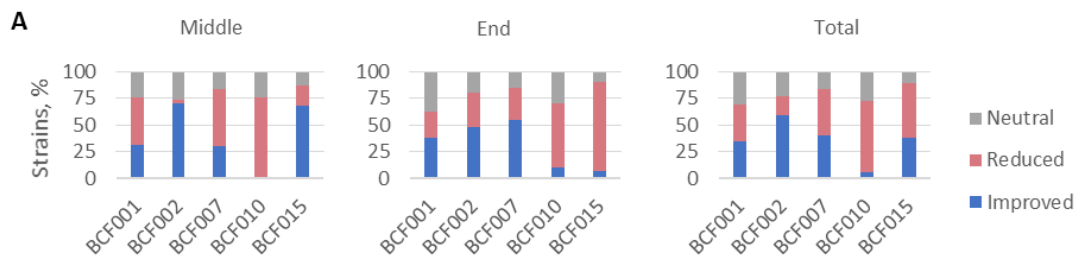
Fig. 1 Design of adaptive laboratory evolution (ALE) with *Bacillus* spp. and *Botrytis cinerea*. *Botrytis cinerea* spores were suspended in PDB medium and incubated 3 days prior to addition of *Bacillus* cultures. The co-cultures were incubated with agitation for 24h at 26°C. The bacteria were separated from the fungal mycelium by passing the co-culture through a filter and discarding the mycelium. The bacterial filtrate was adjusted to OD₆₀₀ 0.01 prior to co-inoculation with fresh fungal cultures. The co-culture cycle was repeated for 27 days (approximately 200 generations), and the evolved populations were sampled by each passage. Bacterial evolution control lineages were grown under the same conditions, but in the absence of *B. cinerea*.

Screening of evolved *Bacillus* derivatives

The high-throughput screening methodology previously developed to assess fungal inhibition potency of *Bacillus* strains (32) facilitated the screening of a large number of evolved derivatives. Approximately 300 strains were isolated from evolved populations at two timepoints of the ALE and screened for improved fungal inhibition properties against *B. cinerea*. In brief, dilution series of bacterial cultures were co-inoculated with a fixed fungal spore concentration onto agar medium in 48-well microtiter plates and the minimal inhibitory bacterial dilution (ID50) that prevented fungal growth was determined for each evolved derivative. The ID50 value served as a quantitative measure of inhibitory potency relative to the respective ancestor strains and enabled scoring of the evolved strains as follows; *improved*, *neutral*, or *reduced* (Table S1).

The screening of antifungal potency revealed no common tendency of fitness improvement or reduction across derivatives from different ancestors. The evolved strains derived from *B. subtilis* BCF001 and *B. amyloliquefaciens* BCF007 showed a total 1:1 distribution of improved and reduced fungal inhibition potency, while most strains derived from *B. subtilis* BCF002 showed improved potency and only a minority of strains derived from *B. subtilis* BCF010 and *B. velezensis* BCF015 were improved (Fig. 3A). Particularly, all evolved populations (G10, H10, I10, W10) derived from *B. subtilis* BCF010 contained a majority of strains with reduced inhibition potency, while most of the populations derived from *B. subtilis* BCF002 (G02, H02, I02, W02) comprised improved strains at both timepoints (Fig. 3B). Populations from *B. amyloliquefaciens* BCF007 showed a tendency towards more evolved strains with improved fungal inhibition potency at the end of the ALE, whereas BCF015 populations contained a higher proportion of improved derivatives in the middle of the ALE. Screening of the co-evolved derivatives revealed that some population such as H01, derived from BCF001, evolved predominantly poor inhibitors, while other populations such as I02, derived from BCF002, developed mainly improved fungal inhibitors. The control populations (W) also harbored improved derivatives.

Fig. 2. Distribution of evolved strains according to fungal inhibition potency in the middle and at the end of the ALE. **A)** The percentage of evolved derivatives with *improved*, *neutral*, and *reduced* fungal inhibition potencies was calculated from the total number of screened strains per timepoint (middle, end) from each co-evolved population (G, H, I) and control population (W) per ancestor (BCF001, BCF002, BCF007, BCF010, BCF015). **B)** The percental sum across population (G, H, I, W) per timepoint (middle, end) and in total was calculated per ancestor (BCF001, BCF002, BCF007, BCF010, BCF015). nd = no data.



Primary characterization of evolved derivatives enables strain selection

From the initially screened 293 ALE derivatives, 130 evolved strains were selected for primary characterization (Table S2) entailing investigation of colony morphology (Fig. S2), growth kinetics (Fig. S3), and sporulation ability. The primary characterization served to separate strains based on phenotypes and enabled selection of genotypically diverse strains for whole genome sequencing (WGS). Colony morphology features were categorized 1-4 from more to less structure and increasing colony expansion (Fig. 4), whereas sporulation was scored positive/negative (1/0). Interestingly, highly distinct morphological features were registered of evolved strains derived from the same ancestor (Fig. S2). Especially *B. subtilis* derivatives (BCF001, BCF002, BCF010) displayed diverse colony morphologies, whereas *B. amyloliquefaciens* BCF007 and *B. velezensis* BCF015 derivatives appeared more comparable to their respective ancestor. Interestingly, from the evolved derivatives tested, the co-evolved strains remained strikingly similar to the ancestor *B. amyloliquefaciens* BCF007, while the evolved control strains presented altered morphological structures (loss of structure complexity and spreading phenotype). Co-evolved and evolved control strains of *B. velezensis* BCF015 displayed close colony morphology resemblance to the ancestor and acquired few changes. However, to draw definitive conclusion, it is necessary to consider whether the observed morphological differences truly reflect biofilm variations or can be attributed to the limited number of derivatives (32) screened from each ancestor strain.

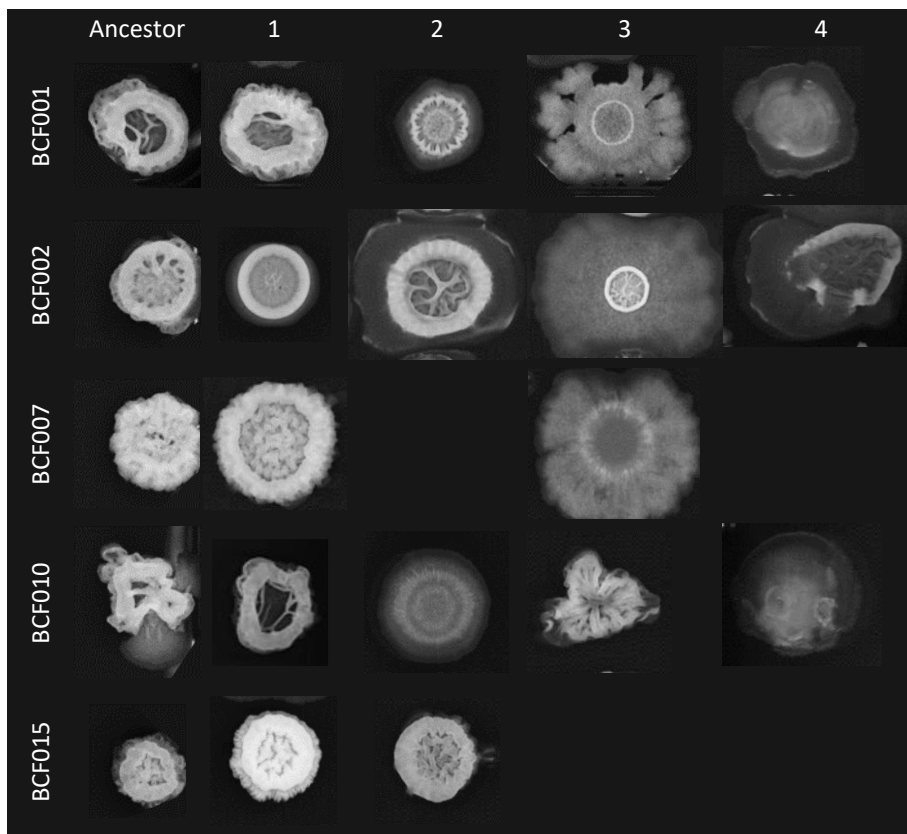


Fig. 3. Primary colony morphology categorization of evolved strains. Evolved derivatives were categorized based on colony structures relative to their respective ancestor. Specifically, derivatives were categorized based on the following criteria. 1: High colony structure complexity and no colony spreading. 2: Mitigated structure complexity and no colony spreading. 3: colony spreading and little structure. 4: Loss of structure or mucoid morphology and spreading colony. Each category (1-4) is represented by an example in addition to respective ancestors. Empty fields denote lack of category representative.

Only 4 out of the 130 evolved derivatives lost sporulation ability, identified in the evolved control populations (W01 and W10) of *B. subtilis* BCF001 and BCF010. Those strains were excluded from further characterization studies due to limited interest for biocontrol product formulation.

Principal component analysis (PCA) of the primary characterization data (inhibition score, growth kinetics, colony morphology categorization) permitted selection of 57 phenotypic distinct derivatives for WGS (Table S). The selection criteria emphasized: i. derivatives from different genetic backgrounds (BCF001, BCF002, BCF007, BCF010, BCF015), ii. derivatives from co-evolved (G, H, I) and control populations (W), iii. derivatives with both improved and reduced inhibition potency to identify genes essential to fungal inhibition, and iv. derivatives from both timepoints (middle, end of the ALE) derived from the same population to track persistence of mutations, albeit not all populations were represented in the selection.

Whole genome sequencing identified mutations in genes related to motility

Whole genome sequencing of 57 selected evolved derivatives followed by analysis of single nucleotide polymorphisms (SNPs) identified 193 genetic changes. Mutations appeared mainly within coding regions (164), while fewer mutations (29) were synonymous, intergenic, or non-coding (Fig. 6A-E). Derivatives from *B. subtilis* BCF001, *B. amyloliquefaciens* BCF007 and *B. velezensis* BCF015 accumulated mutations with the ALE progression, reflected by the increasing average of mutations per strain, whereas *Bacillus subtilis* BCF002 and BCF010-derived strains acquired equivalent average number of mutations regardless of the timepoint (middle, end) (Fig. 5). Generally, derivatives gained few mutations ranging from the minimal of 1 mutation (G0115-D from BCF001) to the maximum of 10 acquired mutations (H1530-B from BCF015) (Fig. 6A-E). Some mutations persisted in the evolved populations, such as the *cadA/copA* intergenic SNP in population I02 from *B. subtilis* BCF002, or the amino acid substitution of DegU in population W07 from *B. amyloliquefaciens* BCF007, whereas others were lost and not identified at the second timepoint (Fig. 7, 8, Fig. S5). Fewer mutations were unique (69), while the majority of mutations (124) occurred in derivatives from the same ancestor and often from the same population (Table. S3), indicating an early single mutation event. The most frequent mutations were identified in populations from all ancestors. Mutations in *swrAA*, encoding the flagellar biosynthesis master regulator, constituted 16.7% in BCF001 populations, while in BCF002

populations, *fliI*, encoding a flagellar-specific ATPase, constituted 15.7%. Genetic changes in *flgB* constituted 11.4% in BCF007 populations, whereas *yerO* encoding a putative TetR transcriptional regulator constituted 31.6% of all mutations in BCF010 populations. Lastly *fliM* encoding the flagellar motor switch protein constituted 17% of the mutations identified in BCF015 populations (Fig. S5). The few mutations arising across parallel populations include but are not limited to *flhA* from *B. subtilis* BCF001 encoding a flagellar biosynthesis protein (ALE lines I01, H01), *fliK* from *B. subtilis* BCF002 encoding flagellar hook-length control (ALE lines G02, H02) in addition to *flgB* from *B. amyloliquefaciens* BCF007 encoding the flagellar basal body rod protein (ALE lines G07, H07, I07) (Table S3). From the 57 sequenced ALE derivatives, 19 strains were selected for further phenotypic characterization (Table S4).

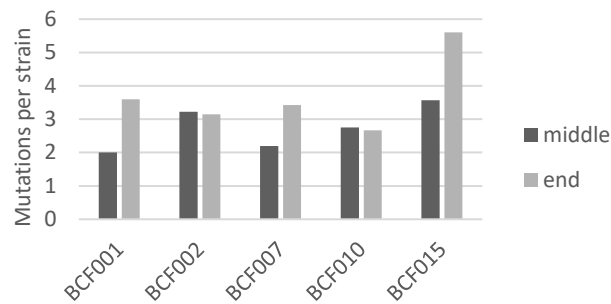
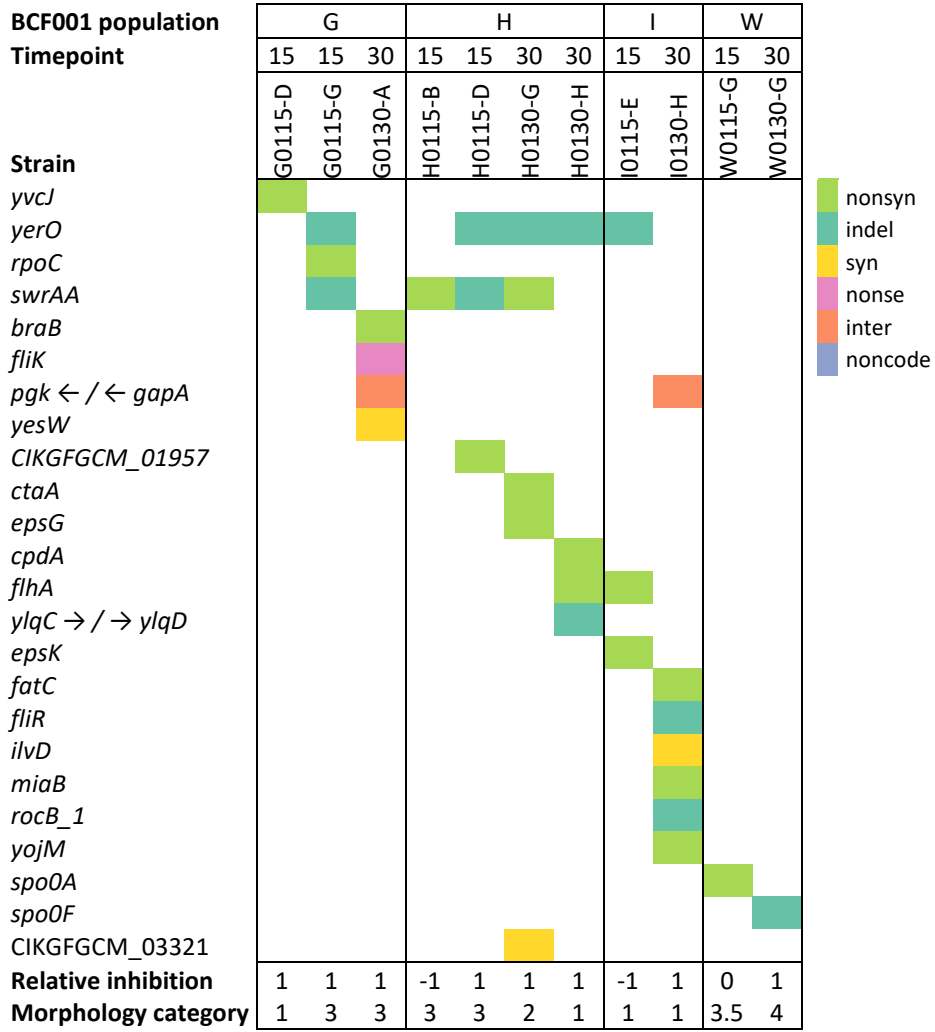


Fig. 4. Average number of mutations observed in evolved strains. The average mutation was determined per strain at the two timepoints (middle, end) derived from the ancestors *B. subtilis* BCF001, BCF002, BCF010, *B. amyloliquefaciens* BCF007, *B. velezensis* BCF015.

A



B

BCF002 population
Timepoint

Strain

czcD
fliI
hisS
rsbX
cstA
fliL
JJNPNOIP_01831
fliK
tpiA
yfhO
comA
resA_1
comP
czrA
prpD
ydgA \leftarrow / \rightarrow *ydgC*
yaaB $\rightarrow / \rightarrow$ *gyrB*
cadA \leftarrow / \leftarrow *copA*
ydjE
yafV_1
degU
fadD3 / bcd
flgG
vanW
flhA

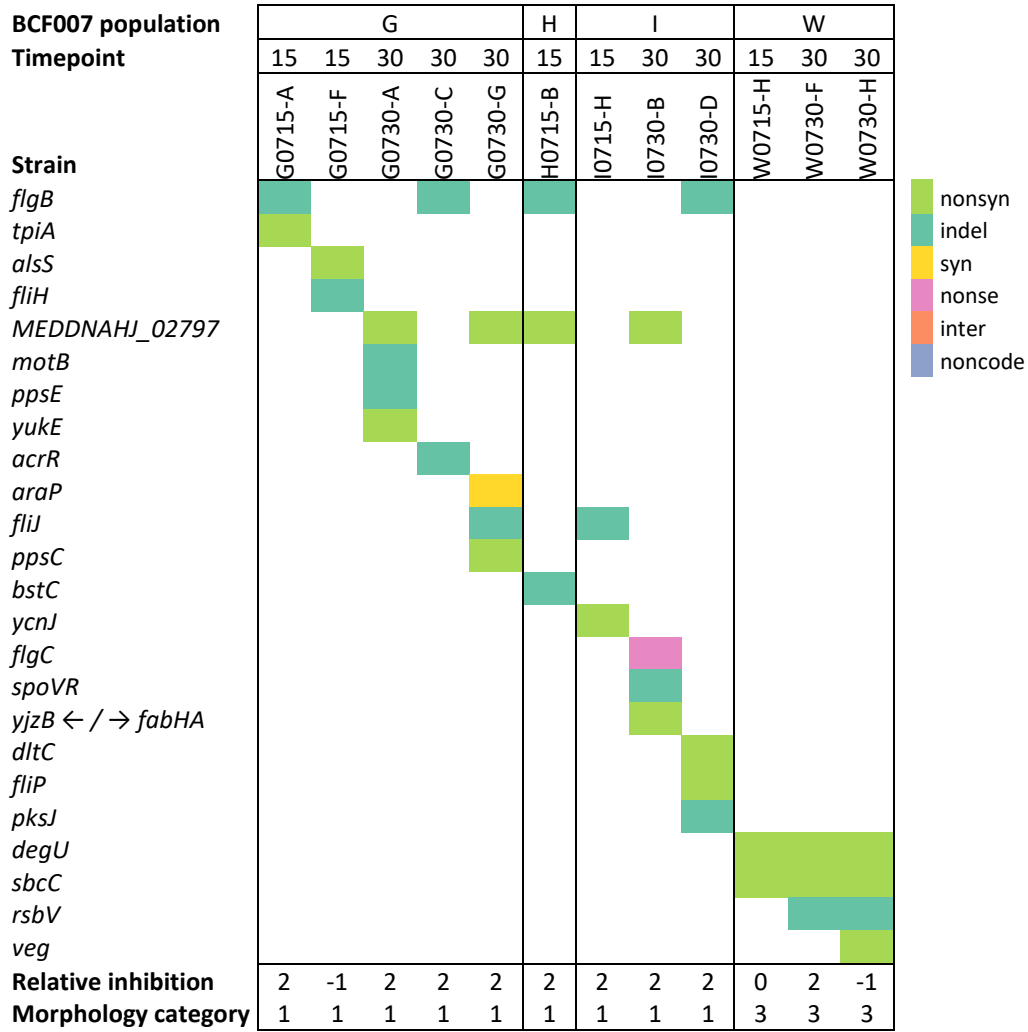
Relative inhibition

Morphology category

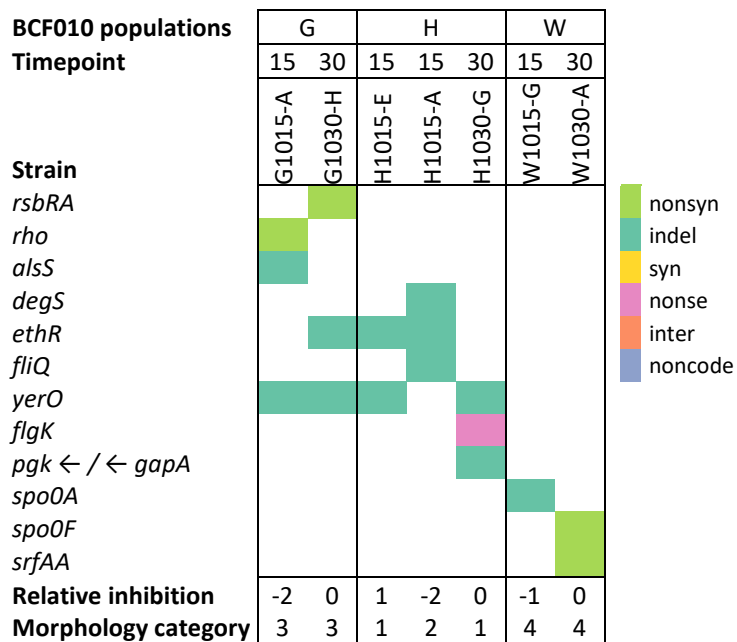
	G						H		I				W			
	15	15	15	15	30	30	15	30	15	30	30	30	15	15	15	
	G0215-C	G0215-D	G0215-F	G0215-H	G0230-B	G0230-F	H0215-F	H0230-A	I0215-F	I0230-D	I0230-E	I0230-F	W0215-B	W0215-F	W0215-G	
<i>czcD</i>	[nonsyn]															
<i>fliI</i>	[nonsyn]					[nonsyn]			[nonsyn]							
<i>hisS</i>	[nonsyn]					[nonsyn]										
<i>rsbX</i>	[syn]					[syn]									[nonsyn]	
<i>cstA</i>		[syn]														
<i>fliL</i>		[indel]														
<i>JJNPNOIP_01831</i>		[nonsyn]			[nonsyn]											
<i>fliK</i>				[indel]	[indel]		[indel]									
<i>tpiA</i>					[nonsyn]											
<i>yfhO</i>					[nonsyn]											
<i>comA</i>						[nonsyn]										
<i>resA_1</i>																
<i>comP</i>									[nonsyn]			[indel]				
<i>czrA</i>							[nonsyn]									
<i>prpD</i>							[nonsyn]									
<i>ydgA</i> \leftarrow / \rightarrow <i>ydgC</i>								[indel]								
<i>yaaB</i> $\rightarrow / \rightarrow$ <i>gyrB</i>								[inter]								
<i>cadA</i> \leftarrow / \leftarrow <i>copA</i>									[inter]	[inter]	[inter]	[inter]		[inter]		
<i>ydjE</i>									[nonsyn]							
<i>yafV_1</i>											[syn]					
<i>degU</i>													[nonsyn]			
<i>fadD3 / bcd</i>														[inter]		
<i>flgG</i>														[indel]		
<i>vanW</i>														[indel]		
<i>flhA</i>															[nonsyn]	
Relative inhibition	2	2	2	0	1	1	2	1	2	1	1	1	2	1	2	
Morphology category	2	4	3	2	2	3	2	2	2	3	2	2	1	4	2	

■ nonsyn
■ indel
■ syn
■ nonsense
■ inter
■ noncode

C



D



E

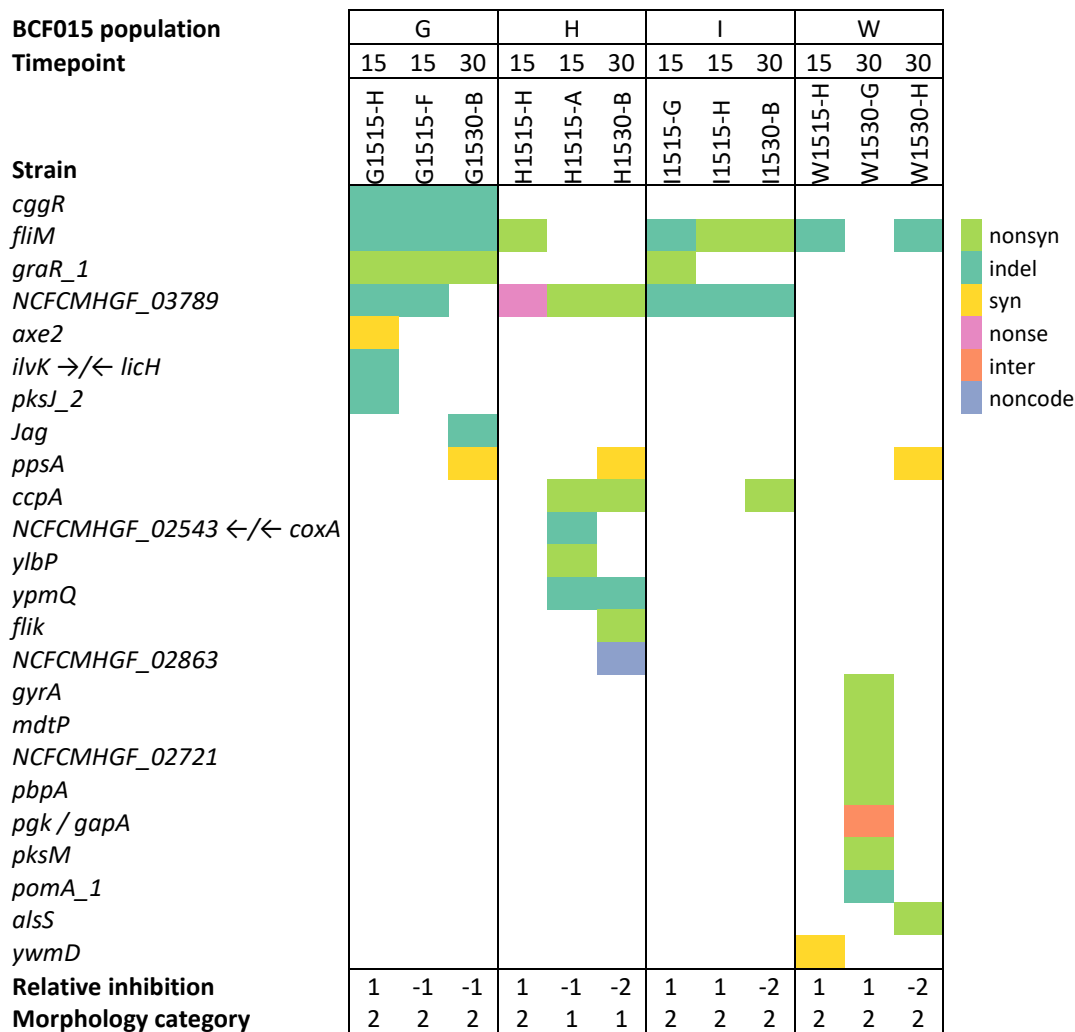


Fig. 5. Mutations observed in selected evolved strains. Mutations identified in different populations and ALE timepoints were linked to respective fungal inhibition potency and colony morphology. Mutations were identified in evolved strains derived from the ancestors **A)** *B. subtilis* BCF001, **B)** *B. subtilis* BCF002, **C)** *B. amyloliquefaciens* BCF007, **D)** *B. subtilis* BCF010, **E)** *B. velezensis* BCF015. Strains were sequenced from two timepoints of the ALE (middle=15, end=30) derived from the co-evolved populations (G, H, I) and evolved control populations (W). Legend top-down; nonsynonymous SNP, small insert or deletion, synonymous SNP, nonsense SNP, intergenic SNP, noncoding SNP. *Relative inhibition* denotes numerical antifungal potency from HT-screening and *Morphology category* denotes assigned colony biofilm morphology categorization.

Parallel evolution of motility-compromising mutations

Genetic alterations in motility-related genes accumulated in evolved populations originating from all five ancestors, demonstrating parallel adaptation. The genetic changes located in 18 distinct open reading frames (Table 1) and summed up to 26.9% of total mutations (52/193). The types comprised insertion/deletions with

impact on reading frame (28), nonsense mutations leading to premature stop codons (11), and missense mutations (13). The genetic changes occurred in genes required for the three architectural parts of the flagellar machinery (hook, filament, basal body) in addition to genes coding for flagella assembly, rotation and biosynthesis regulation (33). Mutations in regulatory genes were present in *swrAA* and *degU* encoding the two-component response regulator that governs motility by repressing the *fla/che* operon (34). The motility-related mutations were mainly detected within the large *fla/che* operon except for the genetic changes in *flgK*, *motB*, *degU* and *swrAA*.

Table 1. Motility-related mutations in evolved strains. Genetic alterations related to motility genes were identified across ancestors.

Protein	Gene	Occurrences
Flagellar basal body rod protein FlgC	<i>flgC</i>	1
Flagellar basal body rod protein FlgG	<i>flgG</i>	1
Flagellar hook associated protein 1	<i>flgK</i>	1
Flagellar biosynthetic protein FliP	<i>fliP</i>	1
Flagellar stator protein MotB	<i>motB</i>	1
Flagellar stator protein MotA	<i>motA</i>	1
Flagellar protein required for flagellar formation	<i>fliL</i>	1
Flagellum assembly	<i>fliR</i>	1
Flagellum and nanotube assembly	<i>fliQ</i>	1
Flagellar assembly protein	<i>fliH</i>	1
Flagellar FliJ protein	<i>fliJ</i>	2
Flagellar biosynthesis protein FlhA	<i>flhA</i>	3
Two-component response regulator DegU	<i>degU</i>	4
Flagellar basal body rod protein FlgB	<i>flgB</i>	4
Swarming motility protein	<i>swrAA</i>	4
Flagellar hook-length control	<i>fliK</i>	8
Flagellar-specific ATPase	<i>fliI</i>	8
Flagellar motor switch protein FliM	<i>fliM</i>	9
Total		52

Swarming of evolved derivatives was evaluated on semi-solid agar plates that revealed dramatic decline in motility abilities relative to the swarming-proficient ancestors (Fig. 8, Fig. S6). In accordance with previous studies (35), mutants of the flagellum machinery and mutants of motility regulators showed a radical reduction in colony expansion, beside the *srfAA* mutant that also displayed pronounced reduction in colony radius. Loss of motility has previously been reported from experimental evolution of bacterial cultures, where nutrients are rapidly distributed and the requirement for motility is limited (36–38). The same observation

applies to *B. subtilis* strains adapted to plant root colonization during experimental evolution under growth conditions with mild agitation (39, 40).

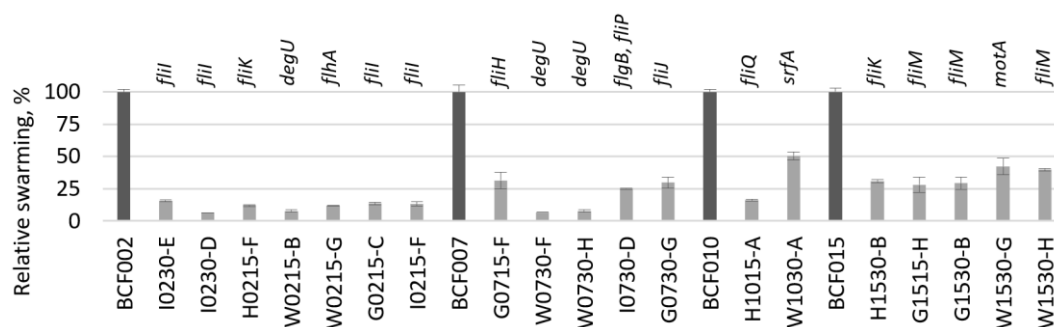


Fig. 6. Swarming motility of selected evolved strains. The radial swarming motility of selected derivatives (light bars) relative to their respective ancestors (dark bars) was assessed on semi-solid agar plates (LB 0.6 % agar). Motility-related mutations are indicated above the graph for each strain. Error bars indicate standard deviation between biological duplicates.

Metal ion transport related mutations were detected in the BCF002 populations

In *B. subtilis* BCF002 derivatives, several mutations were identified related to metal ion uptake and export (Table S5). In population G02, mutations were observed in *czcD* encoding a cation antiporter, while in population H02, *czrA* encoding a helix-turn-helix (HTH)-type transcriptional repressor was mutated, and finally in population I02, two intergenic mutations were detected between the *cadA/copA* genes encoding a Cd^{2+} , Zn^{2+} and Co^{2+} -transporting ATPase (41) and a copper-exporting P-type ATPase, respectively. CzcA acts as a transcriptional repressor, binding to the promoter regions, and relieves repression upon metal ion binding leading to expression of the antiporter CzcD and the P-type ATPase CadA, that facilitates copper export (42, 43). The *czrA* mutation resulted in an amino acid substitution (H64N) located within an HTH-motif in the DNA binding domain of the ArsR/SmtB transcription factor family ((Osman and Cavet, 2010), PROSITE annotation) and potentially alters repression. Interestingly, both intergenic mutations of *cadA/copA* (-78/+91 and -89/+80) co-located with a potential promoter binding site for CzcA (Harvie et al., 2006), which may affect DNA-binding (Fig. S7). CzcD catalyzes efflux of Zn^{2+} , Co^{2+} , and Cd^{2+} in exchange of K^+ or H^+ (44) and mutations were identified in the first transmembrane domain (12-32) and in the second cytoplasmic domain (64-83) (InterPro predictions) with unknown effects on the functionality of this antiporter.

Mutants of catabolite repression and carbon metabolism in BCF015 populations

Co-evolved populations (H15, I15) of *B. velezensis* BCF015 acquired substitutions with unknown effect in the catabolite control protein CcpA that regulates the expression of genes for to carbon acquisition and

metabolism by binding to DNA catabolite-responsive elements (*cre*) (45). Residues in proximity are known to be important for the allosteric switch (T62) of CcpA and for CcpA DNA binding (M17) (46). Furthermore, the co-evolved population G15 acquired mutations in *cggR* gene encoding for the repressor of essential glycolysis enzymes, which is antagonized high intracellular concentrations of fructose-1,6-bisphosphate forming during growth on glucose (47). The selection for genetic changes in CcpA and CggR may reflect nutrient competition or nutrient co-consumption by the *Bacillus* spp. and the fungus. Under the conditions used in the ALE (PDB medium, 28°C), the co-evolved strains with acquired *ccpA* or *cggR* mutations revealed a higher maximum growth rate and reached higher cell densities compared to the ancestor, which suggest acquired growth advantage in the respective medium (Fig. 7). However, this difference was not evident under cultivation at 30 or 37°C. Additionally, strains derived from other ancestors acquired mutations in the CggR regulon (*tpiA*, *pgk/gapA*).

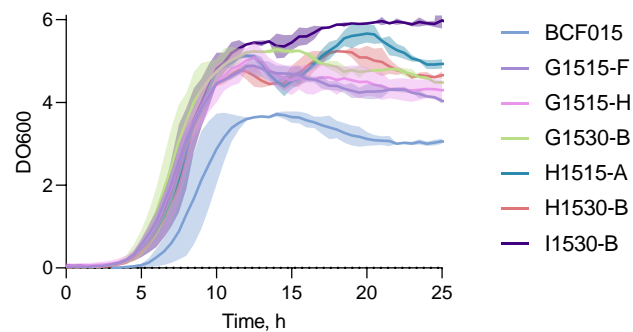


Fig. 7. Growth kinetics of selected evolved strains. Evolved strains derived from *B. velezensis* BCF015 with genetic changes in *ccpA* (H1515-A, H1530-B, I1530-B) and *cggR* (G1515-F, G1515-H, G1530-B) were grown in PDB medium in a biolector incubator at 28°C.

Interestingly, transcriptomic studies of *B. subtilis* strains' response to co-culture with *F. culmorum* revealed 310 differentially expressed genes, of which 68 genes belong to the large CcpA regulon, associated with carbohydrate acquisition and utilization (45, 48). Expression of genes repressed by CcpA was downregulated, whereas the genes induced by CcpA were upregulated in co-cultures compared to *Bacillus* control cultures (unpublished data, Table S7). This specific expression profile aligns with carbon catabolism of *Bacillus* in the presence of the preferred carbon source, glucose (47). The upregulated genes included the *ilvBCH* and *leuABCD* operons assigned to biosynthesis of branched-chain amino acids, while the downregulated genes included a variety of carbohydrate transport systems in addition to the corresponding hydrolases, which belong to the repressed CcpA regulon in the presence of glucose. Also, the genetic machinery for pyruvate conversion to acetoin (*alsSD*), the major extracellular fermentation product in the presence of excess glucose (49), was upregulated in co-culture. In accordance, expression was reduced of the *alsSD* operon repressor

AcoR, indicative of glucose-rich growth conditions (50). Furthermore, increased expression was observed of the *murQRP-amiE-nagZ-namZ* operon encoding the recycling systems of linked sugars N-acetylglucosamine (GlcNAc) and N-acetylmuramic acid (MurNAc) from peptidoglycan. As the fungal cell wall is mainly composed of polysaccharides glucan and chitin, a long chain polymer of N-acetylglucosamine, N-acetylglucosaminidases, NagZ could potentially function in nutrient acquisition from fungal debris or by degradation of mycelia (51, 52). Supporting this hypothesis, gene expression was increased for the major and minor extracellular serine proteases subtilisin (*aprE*) and Vpr, that facilitate degradation of extracellular proteins to supply amino acids for growth (53).

Specialized metabolites and fungal inhibition by culture supernatants

Multiple mutations occurred within biosynthetic gene clusters (BGCs) encoding for specialized metabolite biosynthesis (12/193) or in genes coding for possible regulators of specialized metabolites (5/ 193) (Table S6). Especially, strains derived from *B. amyloliquefaciens* BCF007 and *B. velezensis* BCF015 acquired mutations within those BGCs. Specifically, mutations were identified in the *pkxX* BGC encoding a hybrid polyketide/NRPS (54); the *pps* operon encoding the plipastatin/fengycin non-ribosomal peptide synthetase (NRPS) (55, 56); and the *srf* operon encoding surfactin NRPS (57). In addition, mutations occurred in regulator proteins with potential impact on antifungal properties i.e., the two component regulatory systems DegS-DegU

The eminent biocontrol properties of *Bacillus* spp. are largely assigned to their considerable variety and production of specialized metabolites (58–60). Especially, the cyclic lipopeptide families fengycin, iturin and to some extent surfactin are bioactive against fungal species (22, 27, 61–64) and important for the effectiveness of a biocontrol strain. To correlate levels of specialized metabolites in bacterial cultures to fungal inhibition potency, relative amounts of specialized metabolites in cultures were analyzed and the effect of culture supernatant dilution series addition to fungal spore suspensions was assessed as previously described (32) (Fig. S8). In brief, co-inoculation with bacterial culture dilutions enabled determination of minimal inhibitory dilution that reduced fungal growth to 50% (ID50) and facilitated comparison of inhibition potencies between strains.

Evolved strains from *B. velezensis* BCF015 produced reduced levels of the three cyclic lipopeptides fengycin/plipastatin, surfactin, the iturinic compound bacillomycin, as well as the polyketide macrolactin (Fig. 9A, B). Also, derivatives from *B. subtilis* BCF010 produced less fengycins and surfactins. In accordance with the decreased specialized metabolite levels, the culture supernatant inhibition potencies of the evolved strains were reduced in comparison to the ancestors *B. velezensis* BCF015 and *B. subtilis* BCF010 (Fig. 9D). Several *B. velezensis* BCF015 derivatives obtained mutations within the *pps* BGC, which highlights the

importance of specialized metabolites in fungal antibiosis. Derivatives from *B. subtilis* BCF010 acquired mutations in the BGC encoding surfactin NRPs (H1015-A), as well as *degS* (W1030-A), which presumably impacts biosynthesis of fengycins through the DegS-DegU two component system activated by DegQ (55, 65, 66). Cultures of the evolved strains G0715-F, W0730-F, W0730-H derived from *B. amyloliquefaciens* BCF007 contained reduced relative amounts of fengycins, surfactins, and in particular, of iturins (Fig. 9A, C), which particularly emphasizes the importance of iturins, in this genetic background, for fungal inhibition. Accordingly, culture inhibition assays revealed dramatically declined ID50 values of the respective strains (Fig. 9D). Besides motility-related genetic changes, both W0730-F and W0730-H acquired mutations in the DNA-binding domain of DegU (Fig. S10), while the AlsS protein sequence was altered in G0715-F. The derivative G0730-G acquired genetic changes in the plipastatin synthase subunit C and produced greater relative amounts of fengycins, iturins and surfactins, while I0730-D acquired genetic changes in the polyketide synthase *pksJ* and produced greater relative amounts of fengycins and the iron-chelating siderophore bacillibactin compared to the ancestor *B. amyloliquefaciens* BCF007, but decreased amounts of bacillaene, suggesting a redirection of metabolic flux. The increased specialized metabolite production by these derivatives was reflected by the improved inhibition of *B. cinerea* growth (Fig. 9A, C, D and Fig. S8-9). Further investigations are required to explore the relationship between these mutations and specialized metabolite biosynthesis, taking into consideration potential variations in growth kinetics. The evolved strains H0215-F, I0215-F, I0230-E, W0215-G showed comparable ID50 values to their ancestor *B. subtilis* BCF002 and produced comparable fengycins amounts, but decreased surfactin, indicating that fengycins are indeed more important for effective inhibition of *B. cinerea* growth (27, 67). G0215-C culture inhibition potency moderately exceeded that of the ancestor *B. subtilis* BCF002 accompanied by a minor increase in fengycin levels, further emphasizing the significance of fengycins in fungal inhibition. This strain acquired a mutation in *rsbX*, which potentially influences antifungal activity through SigB (68). The *comP* mutant strain I0230-D exhibited significantly reduced levels of cyclic lipopeptides, resulting in a substantially decreased culture inhibition potency (ID50) when compared to the ancestor strain *B. subtilis* BCF002. This decline in specialized metabolite production highlights the impact of the *comP* mutation on the strain's biochemical profile, as was demonstrated in **Study 5**.

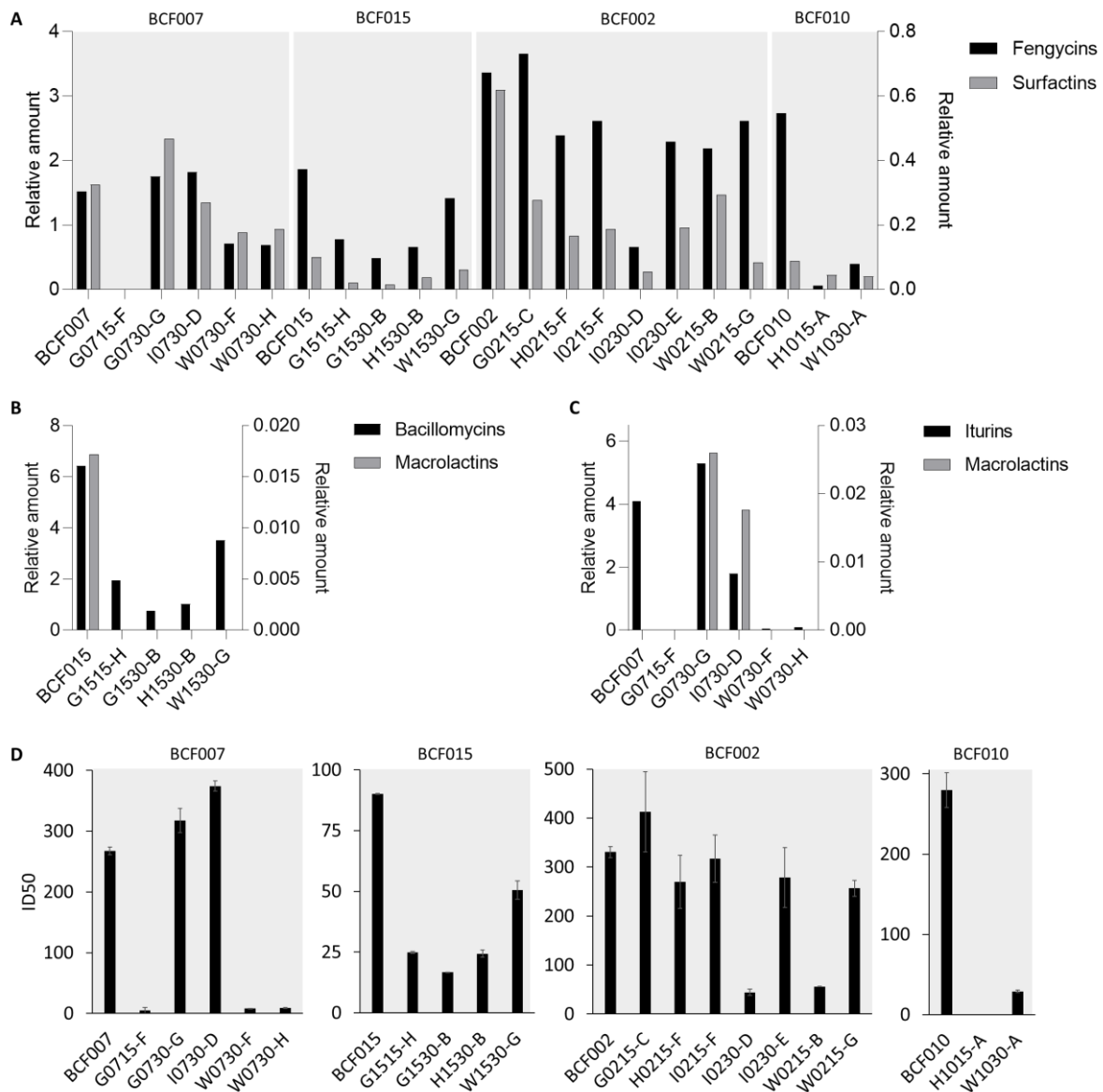


Fig. 8. Specialized metabolite production and culture supernatant inhibition potency of selected evolved strains. From all ALE derivative cultures, the relative amounts were analyzed of **A**) fengycins (left axis) and surfactins (right axis) in addition to bacillomycins (left axis), macrolactins (right axis) and iturins (left axis) in cultures of strains derived from **B**) *B. velezensis* BCF015 and **C**) *B. amyloliquefaciens* BCF007. *Bacillus* derivatives were cultured for 48 h at 30°C and pelleted prior to collection of supernatants for chemical analysis of specialized metabolites and **D**) fungal inhibition assays. Culture supernatant inhibitions potencies were evaluated against *B. cinerea* growth as previously reported (Kjeldgaard et al., 2022). The half-inhibitory dilution (ID50) that reduced the fungal growth to 50%, was determined by addition of *Bacillus* culture dilution series to fungal spore suspension. Fungal growth in response to the *Bacillus* culture supernatant components was quantified by optical density (OD₆₀₀) after 5 days' incubation. Results correspond to averages calculated from two biological duplicates, with error bars indicating the standard deviation.

Pellicle and biofilm formation by evolved strains

On biofilm-inducing medium, the ALE derivatives displayed varying degrees of colony structure complexity (Fig. 10). Strains derived from *B. subtilis* BCF002 with acquired motility mutations displayed mucoid morphologies and slightly reduced biofilm structures, whereas the *comP* mutant I0230-D displayed a dry, expanding colony with extreme loss of structure, as was also observed for *comP* mutants in co-evolved strains in the *Fusarium* ALE (Study 5). Weak pellicle formation (biofilm at the air-medium interphase) was observed for most strains with comparable appearance in relation to the ancestor (BCF002), except for *comP* mutant I0230-D, which formed a partial, submerged biofilm (Fig. 10, Fig. S11). Strain W1030-A produced a translucent colony as well as pellicle, a phenotype associated with reduced sporulation efficiency. This strain evolved from *B. subtilis* BCF010 and carried a missense mutation in *spoOF*, encoding a phosphotransferase of the sporulation initiation phosphorelay (69, 70). The derivatives H1015-A, W0215-B, W0730-F, W0730-H obtained mutations affecting the DegS-DegU response regulatory system, the pellicles and the flat colonies displayed minimal biofilm structures compared to their respective ancestor strains (BCF010, BCF002, BCF007). Indeed, the DegUS two-component system coordinate multicellular behavior in the transition from motile to sessile biofilm forming cells (Verhamme et al., 2007) and induce biosynthesis of matrix components upon high cell densities (71, 72). Accordingly, DegU influences biofilm complexity (72–75).

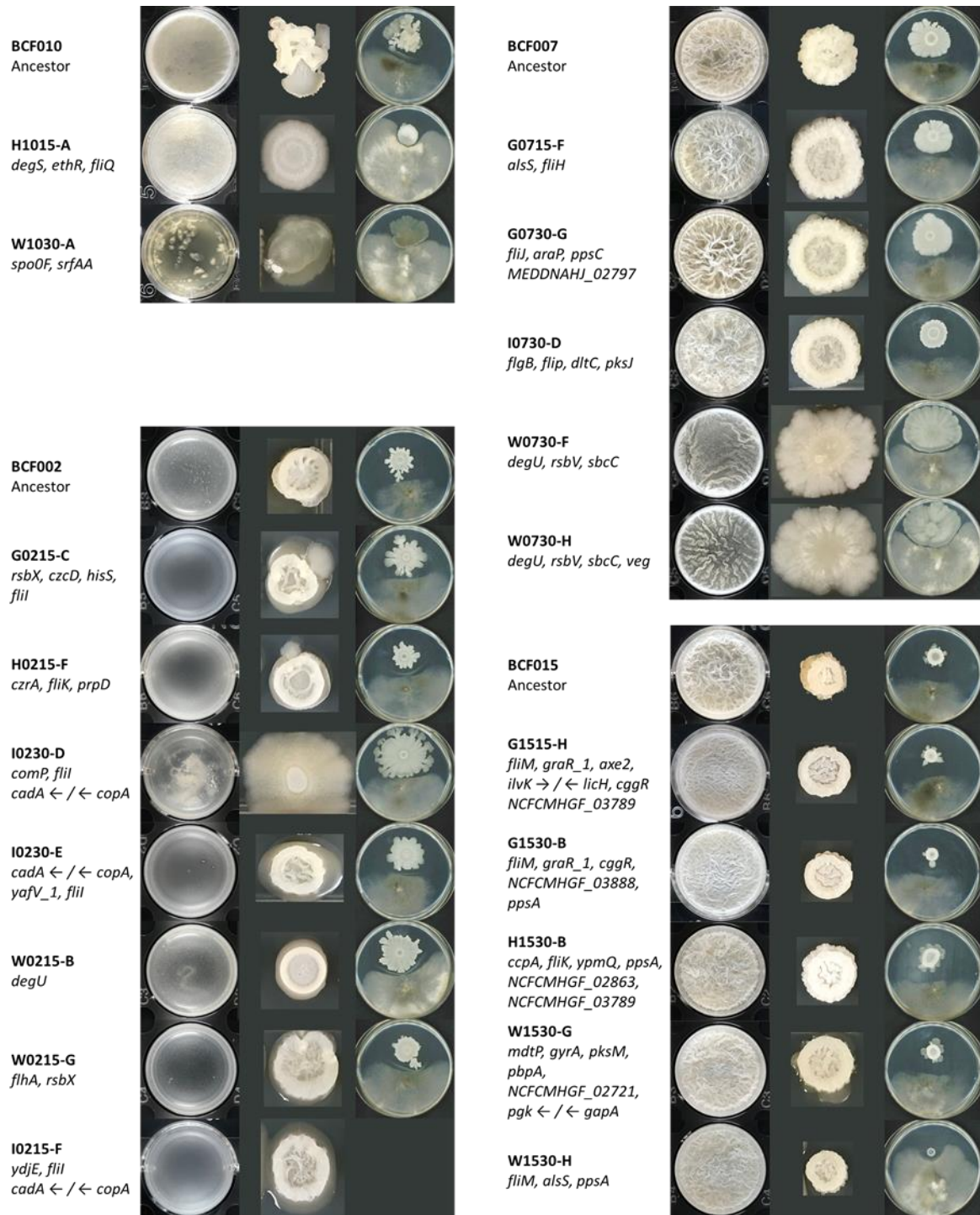


Fig. 9. Pellicle formation, colony morphology and *Bacillus-Botrytis* confrontation assays of selected evolved strains. The pellicle formation was assessed in MSgg medium after incubation at room temperature for 3 days (left panel). The colony morphology was assessed on biofilm inducing medium after 2 days' incubation at room temperature (central panel). The *Bacillus* colony growth and fungal inhibition were investigated in confrontation assays with *B. cinerea* on PDA-medium, for 7 days at 25°C (right panel). All phenotypic assays were performed in biological duplicates.

Confrontation between ALE derivatives and *B. cinerea*

Most evolved strains challenged *B. cinerea* growth comparably to their respective ancestor in bacterial-fungal confrontation assays, albeit a few derivatives hindered fungal growth to lesser extent (W0730-F, W0730-H, W1530-H, H1015-A, W1030-A) (Fig. 11, Fig. S12). Notably, the latter strains originated from control populations (W), suggesting that antifungal properties diminish during experimental evolution under the respective laboratory conditions. W1530-H derived from *B. velezensis* BCF015 produced a small and confined colony that had minor effects on the fungal growth in the confrontation assay. This strain harbored mutations shared with other yet inhibitory derivatives except for a unique amino acid substitution in the acetolactate synthase AlsS. The acetolactate synthase was proven to be essential for robustness of biofilms (76), which may explain the strain's hampered colony formation. W1030-A, derived from *B. subtilis* BCF010, gained a substitution mutation within *urfAA* that encodes a phosphotransferase important for sporulation/biofilm formation and part of the specialized metabolite synthetase for surfactin biosynthesis, which contributes to inhibition of *B. cinerea* growth on solid medium (27). H1015-A, also derived from *B. subtilis* BCF010, contained a frameshift mutation in *degS* leading to disruption of the histidine kinase domain and showed minor inhibition in confrontation with *B. cinerea* as the fungal colony expanded over most of the growth plate surface. The evolved control strains W0730-F and W0730-H both contained an amino acid substitution (F191C) possibly affecting the DNA binding domain of DegU. These derivatives formed spreading colonies with drastic reduction in architectural complexity on biofilm inducing medium. Similarly, the colonies expanded and occupied more area than the respective ancestor *B. amyloliquefaciens* BCF007 in confrontation with *B. cinerea*. Nonetheless, the fungal growth was not inhibited by the increased bacterial occupation of space. Rather, the fungal mycelium appeared denser and even seemed induced by confrontation with the evolved strains (W0730-F, W0730-H) compared to the fungal growth in confrontation with the ancestor (BCF007). These results suggest changed activity of the DegS-DegU regulatory system and that the potentially altered activity influences the inhibition efficiency of the fungal growth.

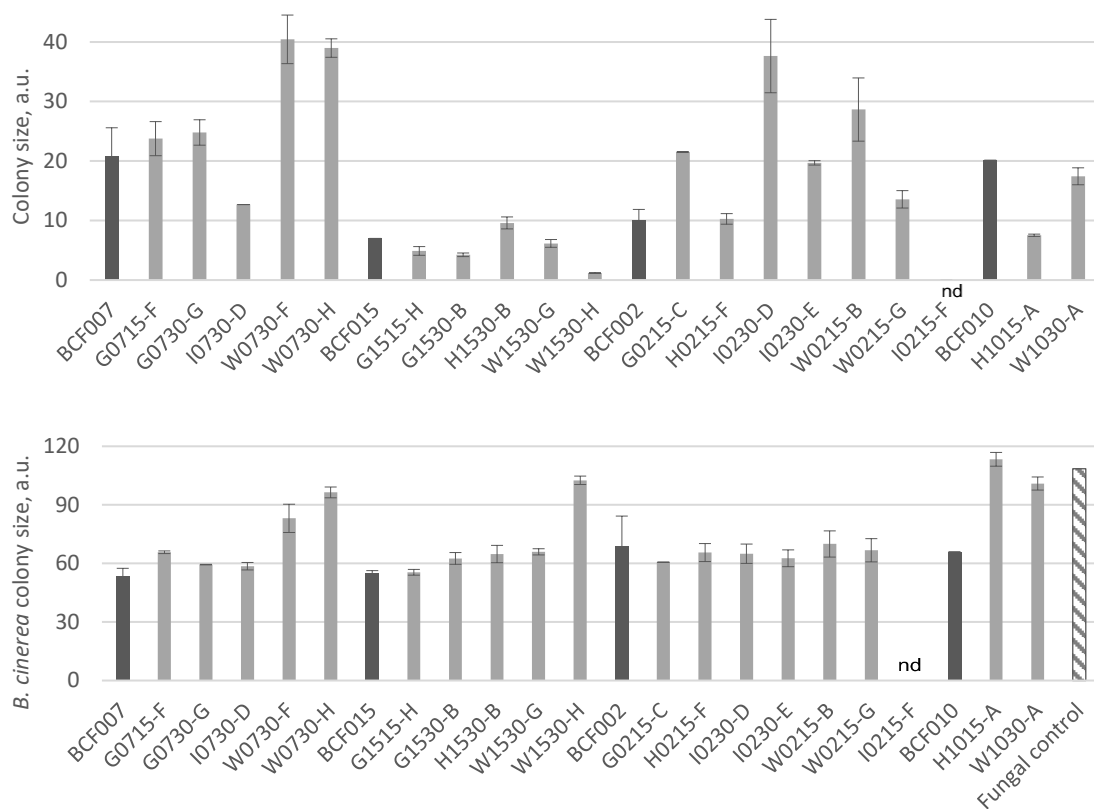


Fig. 10. Bacterial and fungal growth under *Bacillus-Botrytis* confrontation assays with selected evolved strains. Evolved *Bacillus* strains were confronted with *B. cinerea* on agar medium by inoculating the two species with a fixed distance. After 7 days incubation at 25°C, growth-occupied area was measured for selected evolved strains (light bars) relative to their respective ancestors (dark bars) (top panel), as well as the fungal growth in response to the selected evolved strains (light bars) in comparison to unchallenged fungal growth (dark bars) (bottom panel). Images of the confrontation plates can be found in Fig. S12. a.u. = arbitrary unit, nd = no data.

Increased poly- γ -glutamic acid of motility compromised strains

The levels of poly- γ -glutamic acid (γ -PGA) are known to be associated with mucoid colony morphology and defective flagellar motor function (77). The mucoid biofilm morphology of the BCF002 representative derivatives H0215-F and G0215-C, with acquired mutations in the flagella machinery, was linked to superior γ -PGA production by the co-evolved strains in planktonic cultures (Fig. 12). While γ -PGA is induced by phosphorylated DegU upon high cell densities (72, 78–80), motility onsets when DegU ceases repression of flagella genes at a low phosphorylation state and favors planktonic cell growth (72). Although direct antifungal properties of γ -PGA have not been documented, the polymer potentially contributes to improved biocontrol efficiency by aiding root colonization capacity and inducing plant defense mechanisms that reduce fungal disease severity in plants (81). Furthermore, the polymer possesses water holding capacity, which was

shown to positively influence the abundance of plant growth-promoting bacteria and benefit soil moisture contributing to drought resistance of maize seedling (82).

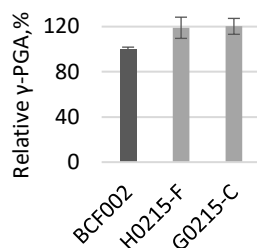


Fig. 11. Quantification of γ -PGA by selected evolved strains. The poly- γ -glutamic acid was quantified from the strains H0215-F and G0215-C (light bars) housing the mutations *czrA*, *fliK*, *prpD* and *rsbX*, *czcD*, *hisS*, *fliI*, respectively. γ -PGA amounts were evaluated relative to the that of the ancestor BCF002 (dark bar) in percentage. Error bars indicate standard deviation between biological duplicates.

Protease activity of evolved strains

Extracellular proteases degrade proteins to scavenge and recycle amino acids. In co-culture with fungi, such proteolytic enzymes also enable nutrient acquisition by deconstruction of fungal cell wall proteins, and it is documented that the secretion of proteases, as well as chitinases, is induced by exposure to fungal mycelium and cell debris (51, 83). As fungal cell wall degradation may contribute to the biocontrol efficiency of a strain, the protease activity of the ALE derivatives was assessed relative to the ancestors and normalized to growth (Fig. 13). As proteases production is induced by DegU~P at high cell densities (74), strains with poor growth were excluded from the analysis (Fig. S 13). Most of the evolved strains revealed a similar protease activity when compared to the ancestors, with exception to the *degS* mutant H1015-A, derived from BCF010, which presented negligible degradative activity, and to the *degU* mutant W0215-B, derived from BCF002, that displayed astonishing proteolytic activity, a trait that was previously associated with a hyperactive DegU and DegS mutant phenotypes (84). Also, strain W1030-A with amino acid substitutions in Spo0F and SfrAA displayed reduced protease activity. The measured protease activity of the evolved strains showed no clear correlation with the observed supernatant inhibition potency suggesting that the primary inhibitory mechanism likely arises from specialized metabolites.

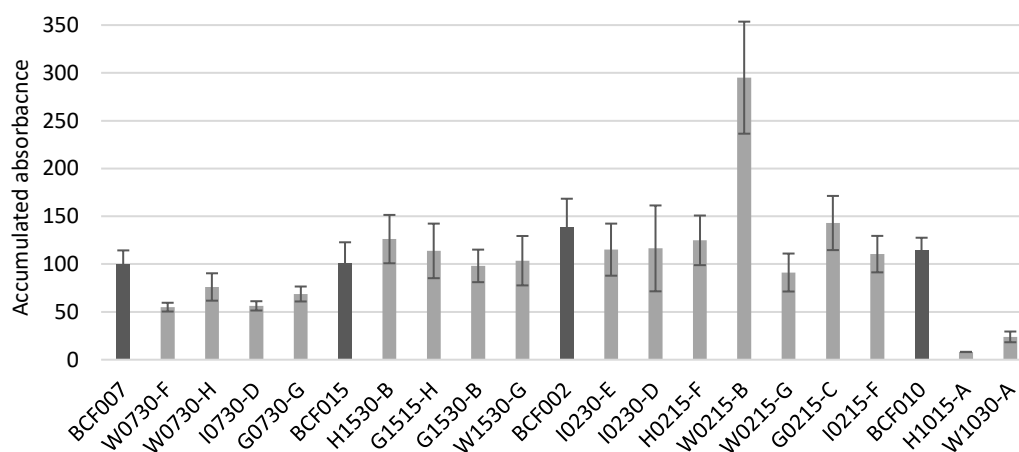


Fig. 12. Protease activity of selected evolved strains. The endo-protease activity of evolved strains (light bars) was measured relative to their respective ancestors (dark bars) and normalized to growth (area under the curve). Cultures were incubated 18 h until stationary phase and supernatants collected for protease activity measurements. Error bars indicate standard deviation between biological duplicates.

Discussion

In this study, *Bacillus* spp. were evolved in the presence of the phytopathogen *B. cinerea* by iterative co-cultivation cycles for the purpose of improving antifungal properties. The experimental design comprised suspended bacterial-fungal cultures in a rich growth medium with agitation. Predictably, repetitive cultivation under conditions with rapid distribution of nutrients selected against motility and led to impaired swarming of several evolved strains. Genetic alterations occurred in genes coding for flagellar regulation, architecture and rotation, in addition to changes affecting biosynthesis of the specialized metabolite surfactin that reduces surface tension and aids motility (85, 86). The rapid compromise of motility in continuously shaken cultures has been hypothesized to occur due the energetic cost of flagellar protein expression. Hence, loss of motility may provide mutants with a growth fitness advantage due to the shed energy burden (87, 88). This is exemplified by an experimental evolution study with *E. coli* on soft agar growth medium that selected for improved motility by enhanced velocity and increased flagella rotation, whereas the growth rate increased upon disruption of flagella genes (37). Also, experimental evolution by repeated passages of suspended cultures resulted in loss of motility of *Campylobacter jejuni* (38). Whereas compromised motility may provide a growth benefit to mutants under laboratory conditions, motility is suggested to be important during rhizosphere colonization of beneficial root-associated bacteria (89). Contrasting this believe, a trade-off between motility and biofilm formation, enabling enhanced root colonization under laboratory conditions, has repeatedly been observed for plant root-adapted *Bacilli* during experimental evolution with

mild agitation (39, 40, 90). Further experiments are required to elucidate the root colonization abilities of the motility-impaired evolved strains from the present study.

Domesticated bacterial species of *Pseudomonas aeruginosa*, *E. coli* and *B. subtilis* often display reduced abilities to form biofilm or, in other words, reduced multicellularity. Particularly, genetic changes of *epsC*, *swrAA*, *rapP* and *degQ* resulted in the inability of the domesticated model strain *B. subtilis* 168 to produce a robust biofilm, while introduction of specific SNPs restores biofilm complexity, production of exopolysaccharides, and γ -PGA (91–94). In addition, repetitive culture passage under laboratory conditions has been reported to target the biofilm regulator SinR, leading to biofilm morphological changes, in accordance with findings of Study 2 (Leiman et al., 2014; Richter et al., 2023, Study 2). Furthermore, *degU* is reportedly a mutational target during laboratory domestication (97). Within few experimental evolution passages, Barreto and colleagues detected accumulation of mutations in *degU*, which were coupled to several phenotypic traits i.e., cessation of swarming motility, reduced biofilm formation, loss of biofilm structure, reduced secretion of proteases and changed sporulation. Besides biofilm alterations, experimental evolution of *Bacillus* spp. under laboratory conditions has repeatedly been associated with decrease or loss of sporulation ability (97–100). In combination, these studies are indicative of selection against sporulation and mutational targeting of biofilm during propagation in rich growth medium.

In the present study, adaptation to the laboratory growth conditions by control populations targeted the response regulator DegU, the sporulation pathway, and BGCs for the production of specialized metabolites. In control populations (W01, W10) derived from *B. subtilis* BCF001 and BCF010, mutations were detected in sporulation related genes i.e., the master regulator of sporulation/biofilm Spo0A and the sporulation initiation phosphotransferase Spo0F, suggesting less dependency on the sporulation pathway for continuous propagation in rich medium, in accordance with previous studies. Further supporting this hypothesis, sporulation deficient strains originated exclusively from control populations.

Phenotypic changes similar to those reported by Barreto and colleagues i.e., cessation of swarming motility, reduced biofilm formation, loss of biofilm structure, and reduced secretion of proteases were observed *B. amyloliquefaciens* BCF007-derived *degU* mutants W0730-F, W0730-H harboring an amino acid substitution (F191C) in the DNA-binding domain (Fig. S10). In addition, these strains produced reduced amounts of fengycins and iturins. The *degU* mutant W0215-B, derived from *B. subtilis* BCF002, contained a different substitution in the signal receiver domain of DegU (D111G) (Fig. S14). Phenotypes associated with the mutant were significant loss of motility, reduced biofilm structure complexity, and strongly increased protease activity. These phenotypes are all indicative of high phosphorylation state of DegU (74). Overproduction of proteases (84, 101) and reduced expression of flagellar genes (34, 102) has previously been observed as a result of altering residue H12L, which extended the stability of phosphorylated DegU. In addition,

overproduction of the small proteins DegQ and DegR enhance expression of proteases (103, 104) in a DegU-dependent manner (105, 106). The phenotypic traits observed in hyperactive DegU protein align with those exhibited by the evolved strain W0215-B, implying alterations in the activity of its DegU protein.

The substitution (D111G) identified in strain W0215-B is localized in a putative pocket around Asp56 in $\beta 3$ (Fig. S), the known phosphorylation site for the cognate kinase DegS (84), which is conserved among response regulators (107), for example in CheY from *Escherichia coli* and VirG from *Agrobacterium tumefaciens* (108, 109). In *B. subtilis*, activation by phosphorylation of this residue is required for transcription of the motility related genes *hag*, *motA*, *ycaA* as well as *aprE* coding for the exoprotease subtilisin E (72). Other conserved aspartic acid residues include Asp51, Asp10 and Asp11, where the latter are suggested to be metal binding sites essential to phosphoryl group transfer by enhancing electrophilicity at the phosphorus center (107, 110). In *E. coli* these residues are suggested to form an aspartate acid pocket in a 3D structure (108), in proximity to D111G substitution. A conserved Lys residue in $\beta 5$ is important for the conformational changes triggered by phosphorylation. In addition, a conserved Thr/Ser residue in the $\beta 4$ sheet is thought to interact with the phosphorylation site (107). The metal binding sites (Asp10-11), the conserved interaction site (Ser84) and the essential residue to conformational changes (Lys106) in combination create a pocket around the phosphorylation site (Asp56). In W0215-B, the residue Asp111 is substituted with Gly. Along with Asp109 in helix $\alpha 5$, Asp111 could potentially participate in the pocket formation and aid metal ion coordination for the phosphoryl transfer and impact the conformational changes upon phosphorylation (Fig. S14). This could lead to altered phosphorylation pattern of DegU, which would impact its activity. Further investigation is required to characterize the specific impact of the substitution (D111G) on activity of the DegS-DegU regulatory response system. *Bacillus* proteases can effectively induce morphological abnormalities in hyphae of filamentous fungi including *Fusaria*, *Rhizoctonia solani*, and *B. cinerea* (83). Despite the significantly increased protease activity of W0215-B, the supernatant displayed reduced inhibition potency of *B. cinerea* growth. Except H1015-A comprising a frameshift deletion in *degS*, which showed hampered serine protease activity consistent with previous studies (104), most ALE derivatives showed comparable protease activity to the ancestors, despite altered fungal inhibition potency of their supernatants (reduced or improved). Collectively, the results suggest that protease activity plays a minor role in *B. cinerea* inhibition.

Evolved strains derived from *B. subtilis* BCF002 acquired mutations in genes related to metal ion uptake and efflux, which may indicate adaptation to the growth medium or potential ion competition with the fungus. While genetic changes of *czcD* encoding a cation antiporter and *czrA* encoding the transcriptional repressor of *cadA* occurred in co-evolved populations, the intergenic mutations potentially affecting *cadA* transcription also appeared in evolved control populations, suggesting that this group of mutations are growth conditioned adaptations. However, these derivatives inhibited *B. cinerea* growth better than the ancestor *B. subtilis*

BCF002, suggesting that the potential medium adaptation provided the strains with enhanced inter-species competition under these conditions. Notably, these mutants displayed mucoid biofilm morphology, which was positively correlated to γ -PGA acid content. Besides ion transport genes (*czcD*, *czrA*, *cadA/copA*), the derivatives shared genetic changes in flagellar genes (*fliI*, *fliK*). While no correlation has been demonstrated between these particular flagellum-related genes and the production of γ -PGA, expression of other motility-related genes is known to influence biosynthesis of the polymer. Expression of the *pgsBCAE* operon, coding for γ -PGA, requires low levels of DegU~P in addition to SwrAA (78, 111). Although SwrAA regulates motility genes, expression of the *fla/che* operon is dispensable for γ -PGA biosynthesis (78). However, defective flagellar motor protein increases γ -PGA production, inversely linking these two cell differentiations (77).

γ -PGA is an affective bioabsorbant and show great affinity towards both heavy metals and metal ions including Pb^{2+} , Cu^{2+} , Ni^{2+} , Cr^{3+} , Al^{3+} (112–114). Interestingly, growth medium contents of metal ions such as Zn^{2+} , Fe^{2+} influence the biosynthesis of γ -PGA. Specifically, studies show that Zn^{2+} induces expression of PgsE, while addition of Fe^{2+} improves the γ -PGA yield and Mn^{2+} is required for activity of PgsB (115–117). The membrane anchored PgsA shows sequence similarity to a serin/threonine phosphatase corresponding to sites for divalent cation coordination (118), suggesting yet another potential connection between the biopolymer and metal ions. Interestingly, the BCF002 derivatives devoid of mucoid biofilm morphology (I0230-D, W0215-B) showed reduced supernatant inhibition potency, suggesting a potential connection between mucoidy and fungal inhibition properties. Further experiments are required to correlate the mucoid biofilm morphology to specific mutations.

Specialized metabolites greatly contribute to the growth inhibition imposed on filamentous fungi by *Bacilli*. Particularly, the cyclic lipopeptides fengycin and iturin are effective against *B. cinerea* growth (22, 28), although surfactin may enhance the inhibitory effect (27). Furthermore, volatile organic compounds, such as O-anisaldehyde (28), and degradative enzymes, such as chitinases (119, 120), enable growth inhibition of *Botrytis* by *Bacillus* spp.

Chemical analysis showed that the specialized metabolite biosynthesis of evolved strains largely aligned with their culture supernatant fungal inhibition potencies (ID50s). Evolved strains with mutations in *degS*, *degU*, and BGCs produced lower relative amounts of specialized metabolites, which aligned with their reduced cell-free culture supernatant fungal inhibition potencies. Specifically, cultures from *degS* (H1015-A) and *degU* (W0730-F, W0730-H) mutants showed reduction of fengycins and iturins levels, indicating that the two-component regulatory system DegS-DegU influences biosynthesis of these compound families, as suggested in previous studies, via activation of phosphorylation by the pleiotropic regulator DegQ upon high cell concentration (55, 65, 66).

Albeit genetic alterations within the *pps* operon were mainly synonymous, the relative amounts of fengycins were reduced compared to the ancestor *B. velezensis* BCF015. The changes in fengycin biosynthesis may arise from the alternative codon usage affecting translation (121). Indeed, most synonymous mutations in *ppsA* resulted in a less frequent codons, which may impact translation (Table S7).

Few derivatives increased biosynthesis of specialized metabolites and displayed improved fungal inhibition potencies from culture supernatants when compared to the ancestor. The strain I0730-D acquired mutations disrupting the reading frame of *pksJ* encoding the bacillaene hybrid polyketide/NRPS (54) and showed impaired biosynthesis of the respective polyketide. Interestingly, the *pksJ* mutant displayed increased culture supernatant potency and increased production of the antifungal fengycin compounds, macrolactins and the siderophore bacillibactin that mediates iron-acquisition (122), previously shown to inhibit *B. cinerea* growth (29). These changes suggest redirection of available precursors to biosynthesis of alternative specialized metabolites, which may have provided the strain with improved antifungal properties in terms of enhanced iron competition or metabolite mediated antibiosis. Indeed, genomic deletion of other NRPS and polyketide synthases have been demonstrated to increase production of surfactin, illustrating that disruption of a biosynthesis pathway may alter the metabolic flux and lead to increased titer of other specialized metabolites (123). In addition, previous studies report modulated specialized metabolite production by *Bacillus* spp. upon interaction with different fungi (22, 124), illustrating that redirection of metabolic flux facilitates adjustment of antifungal activity.

Derivatives from *B. velezensis* BCF015 acquired genetic changes potentially affecting carbon metabolism i.e., *ccpA*, *cggR* and generated different growth curves under specific conditions. These growth changes of *ccpA* and *cggR* mutants in combination with the differential expression of the CppA regulon in *B. subtilis* co-cultured with *F. culmorum* suggest that the immediate response as well as the adapted response of *Bacillus* spp. to the presence of fungi may involve alterations to carbohydrate uptake and utilization. These responses potentially confer an advantage in nutrient competition and enable improved bacterial growth.

Moreover, carbon resource type and variety could influence the growth as well as production of specialized metabolites affecting pathogen inhibition as demonstrated in a co-cultivation study of *B. amyloliquefaciens* and phytopathogenic bacteria (125). While carbohydrates supported high cell densities, growth on amino acids or organic acids spawned enhanced biosynthesis of specialized metabolites. Thus, it is possible that *Bacilli* adapt carbon metabolism to enhance resource competition and/or optimize specialized metabolite production for antibiosis against fungi.

Carbon catabolite repression by CcpA is an important regulatory mechanism to achieve maximum growth on the preferred carbon source, when others sources are available (126). The reduced expression of a multitude

of carbohydrate transport and metabolism facilitation genes under control by CcpA suggest that *Bacilli* in co-culture with *F. culmorum* adapt to glucose supported growth. Notably, the *ilvBCH* and *leuABCD* coding for biosynthesis of branched-chain amino acids showed increased expression in addition to *murQRP-amiE-nagZ-namZ* operon that facilitates recycling of linked sugars N-acetylglucosamine (GlcNAc) and the major exoprotease subtilisin E. This differential expression suggests nutrient acquisition from other sources such as fungal debris, bacterial degradation of fungal cell wall, or breakdown products of complex medium polymers made accessible to the bacteria by fungal extracellular enzymes.

Concluding remarks

Propagation of undomesticated *Bacillus* spp. in PDB medium with agitation resulted in accumulation of mutations in flagellar genes, leading to impaired motility. Furthermore, several genetic alterations were detected affecting key regulators including DegU, CzrA, CcpA, and SwrAA. These mutations potentially affect entire regulons and represent a rapid adaptive mechanism compared to the relatively slower adaptation of protein function in the respective processes (127). The genetic adaptations primarily focused on energy conservation through the reduction or rewiring of specialized metabolite biosynthesis, altered protease production, and impaired motility. Few strains displayed improved *B. cinerea* inhibition by secreted compounds in the supernatants, which were correlated to increased amounts of lipopeptides and siderophores. Further studies are required to elucidate the inhibitory mechanism of these strains.

Materials and methods

Growth conditions and media: Fungal and bacterial stains used in the present study can be found in Table 2. *Bacillus* strains were cultured as described in Study 5 and *B. cinerea* was grown under similar conditions to *F. culmorum*. Media and solutions were prepared accordingly.

Table 2. Microbial species. Bacterial and fungal species used in the present study.

Species and strains	Number	Source
Mold fungi		
<i>B. cinerea</i>	Kern B2	University of California, Davis
Bacteria		
<i>B. subtilis</i>	BCF001	Chr. Hansen A/S
<i>B. subtilis</i>	BCF002	Chr. Hansen A/S
<i>B. amyloliquefaciens</i>	BCF007	Chr. Hansen A/S
<i>B. subtilis</i>	BCF010	Chr. Hansen A/S
<i>B. velezensis</i>	BCF015	Chr. Hansen A/S

Experimental evolution: The ancestor strains *B. subtilis* BCF001, BCF002, BCF010, *B. amyloliquefaciens* BCF007 and *B. velezensis* BCF015 were evolved with the fungus *Botrytis cinerea* in triplicate experimental evolutions lines. In addition, each ancestor was evolved under the exact same conditions, but in the absence of the fungus. Specifically, *Botrytis cinerea* spores were suspended in 2 ml fungal growth medium reaching a final concentration of spores/ml and incubated statically for 3 days at 25°C until mycelial structures were visible. Subsequently, fungal pre-grown cultures were co-inoculated with 30 µl *Bacillus* culture adjusted to OD₆₀₀ 1 in addition to 1 ml fresh medium. In total, the co-culture volume reached 3 ml and the initial bacterial OD₆₀₀ 0.01. The bacterial-fungal co-cultures were incubated with 200 rpm agitation at 26°C for 24h before separating the fungal mycelium from the *Bacillus* cells by filtration through double layered Miracloth (Millipore). *Bacillus* filtrates were OD-adjusted prior to initiating a new co-cultivation cycle. The dilution factor was approximately 150-250x, dependent on the final bacterial OD reached each day. Sample stocks were prepared by each transfer. The adaptive laboratory evolution was continued for 27 days corresponding to approximate 190-209 generations for co-evolved populations and 224-242 generations for control populations (Table S1). Generation number was calculated from the optical density measured daily by each transfer as follows; for all populations, the binary logarithm (log₂) of the initial OD relative to the final OD each day (*k*) was calculated and summed over total 27 days (*M*) (Equation 1).

$$Total\ generations = \sum_{k=1}^M \log_2 \left(\frac{initial\ OD_k}{final\ OD_k} \right) \quad (1)$$

Fitness screen: Fungal inhibition potency of evolved strains was assessed in a high-throughput screen implemented on a Hamilton Microlab STAR Liquid Handling System according to (Kjeldgaard et al., 2022) with minor changes. In brief, molten PDA was aliquoted in each well of a 48-well microtiter plate. *Bacillus* cultures were adjusted to OD₆₂₀ 0.2 and further diluted until OD₆₂₀ 10⁻⁵. From this concentration, a 1:2 dilution series was prepared with 6 steps. 15 µl of each dilution was inoculated in a separate well of a column in the microtiter plate and 15 µl fungal spore suspension with a concentration of 2 × 10⁷ spores/ml was co-inoculated in each well with the bacterial culture dilution series. The co-inoculated plates were sealed with 3M tape and incubated under natural light at room temperature for 5 days. Fungal growth was evaluated by visual inspection. All evolved derivatives were screened in biological duplicates.

Whole genome sequencing: Whole genome sequencing and SNP analysis was performed as described in detail in Study 5.

PCA: Principal component analysis of colony morphology, growth kinetics, and inhibition screening scores was done as described in Study 5.

Strain characterization assays: Following experimental work was done according to Study 5 with no changes: pellicle formation assay, colony morphology assessment, growth kinetics, biochemical analysis, γ -PGA quantification, protease activity, motility assay, and sporulation test. Plate confrontation and culture inhibition assays were prepared according to Study 5, but with *B. cinerea* 2×10^7 spores/ml instead of the *F. culmorum* spores in the protocol.

References

1. Elad Y. 2004. Botrytis: Biology, Pathology and Control. Springer.
2. Williamson B, Tudzynski B, Tudzynski P, Van Kan JAL. 2007. Botrytis cinerea: The cause of grey mould disease. Mol Plant Pathol 8:561–580.
3. Hua L, Yong C, Zhanquan Z, Boqiang L, Guozheng Q, Shiping T. 2018. Pathogenic mechanisms and control strategies of Botrytis cinerea causing post-harvest decay in fruits and vegetables. Food Qual Saf. Oxford Academic <https://doi.org/10.1093/fqsafe/fyy016>.
4. Bi K, Liang Y, Mengiste T, Sharon A. 2023. Killing softly: a roadmap of Botrytis cinerea pathogenicity. Trends Plant Sci 28:211–222.
5. Dean R, Van Kan JAL, Pretorius ZA, Hammond-Kosack KE, Di Pietro A, Spanu PD, Rudd JJ, Dickman M, Kahmann R, Ellis J, Foster GD. 2012. The Top 10 fungal pathogens in molecular plant pathology. Mol Plant Pathol <https://doi.org/10.1111/j.1364-3703.2011.00783.x>.
6. Hill GN, Jaksons P, Sharp JM, Hunt AG, Lewis KSJ. 2019. Investigating time and economic costs of botrytis bunch rot sampling using interpolated data. New Zeal Plant Prot 72:166–175.
7. Billard A, Fillinger S, Leroux P, Lachaise H, Beffa R, Debieu D. 2012. Strong resistance to the fungicide fenhexamid entails a fitness cost in Botrytis cinerea, as shown by comparisons of isogenic strains. Pest Manag Sci 68:684–691.
8. Chen SN, Luo CX, Hu MJ, Schnabel G. 2016. Fitness and Competitive Ability of Botrytis cinerea Isolates with Resistance to Multiple Chemical Classes of Fungicides. Phytopathology® 106:997–1005.
9. Hahn M. 2014. The rising threat of fungicide resistance in plant pathogenic fungi: Botrytis as a case study. J Chem Biol. Springer Verlag <https://doi.org/10.1007/s12154-014-0113-1>.
10. Baroffio CA, Siegfried W, Hilber UW. 2003. Long-Term Monitoring for Resistance of Botryotinia fuckeliana to Anilinopyrimidine, Phenylpyrrole, and Hydroxylanilide Fungicides in Switzerland. Plant Dis 87:662–666.
11. Fan F, Hamada MS, Li N, Li GQ, Luo CX. 2017. Multiple Fungicide Resistance in Botrytis cinerea from Greenhouse Strawberries in Hubei Province, China. Plant Dis 101:601–606.
12. Rupp S, Weber RWS, Rieger D, Detzel P, Hahn M. 2017. Spread of Botrytis cinerea Strains with Multiple

- Fungicide Resistance in German Horticulture. *Front Microbiol* 7:2075.
13. Baggio JS, Peres NA, Amorim L. 2018. Sensitivity of *Botrytis cinerea* Isolates from Conventional and Organic Strawberry Fields in Brazil to Azoxystrobin, Iprodione, Pyrimethanil, and Thiophanate-Methyl. *Plant Dis* 102:1803–1810.
 14. Alzohairy SA, Gillett J, Saito S, Naegele RN, Xiao CL, Miles TD. 2021. Fungicide Resistance Profiles of *Botrytis cinerea* Isolates From Michigan Vineyards and Development of a TaqMan Assay for Detection of Fenhexamid Resistance. *Plant Dis* 105:285–294.
 15. Shao W, Zhao Y, Ma Z. 2021. Advances in Understanding Fungicide Resistance in *Botrytis cinerea* in China. *Phytopathology*® 111:455–463.
 16. Harper LA, Paton S, Hall B, McKay S, Oliver RP, Lopez-Ruiz FJ. 2022. Fungicide resistance characterized across seven modes of action in *Botrytis cinerea* isolated from Australian vineyards. *Pest Manag Sci* 78:1326–1340.
 17. Malandrakis AA, Krasagakis N, Kavroulakis N, Ilias A, Tsagkarakou A, Vontas J, Markakis E. 2022. Fungicide resistance frequencies of *Botrytis cinerea* greenhouse isolates and molecular detection of a novel SDHI resistance mutation. *Pestic Biochem Physiol* 183:105058.
 18. Brauer VS, Rezende CP, Pessoni AM, De Paula RG, Rangappa KS, Nayaka SC, Gupta VK, Almeida F. 2019. Antifungal agents in agriculture: Friends and foes of public health. *Biomolecules* 9:521.
 19. Zubrod JP, Bundschuh M, Arts G, Brühl CA, Imfeld G, Knäbel A, Payraudeau S, Rasmussen JJ, Rohr J, Scharmüller A, Smalling K, Stehle S, Schulz R, Schäfer RB. 2019. Fungicides: An Overlooked Pesticide Class? *Environ Sci Technol* 53:3347–3365.
 20. Rasool S, Rasool T, Gani KM. 2022. A review of interactions of pesticides within various interfaces of intrinsic and organic residue amended soil environment. *Chem Eng J Adv* 11:100301.
 21. Ongena M, Jacques P. 2008. *Bacillus* lipopeptides: versatile weapons for plant disease biocontrol. *Trends Microbiol* 16:115–125.
 22. Cawoy H, Debois D, Franzil L, De Pauw E, Thonart P, Ongena M. 2015. Lipopeptides as main ingredients for inhibition of fungal phytopathogens by *Bacillus subtilis*/*amyloliquefaciens*. *Microb Biotechnol* 8:281–295.
 23. Stoll A, Salvatierra-Martínez R, González M, Araya M. 2021. The role of surfactin production by *Bacillus velezensis* on colonization, biofilm formation on tomato root and leaf surfaces and subsequent protection (ISR) against *botrytis cinerea*. *Microorganisms* 9:2251.
 24. Wang T, Liang Y, Wu M, Chen Z, Lin J, Yang L. 2015. Natural products from *Bacillus subtilis* with antimicrobial properties. *Chinese J Chem Eng* <https://doi.org/10.1016/j.cjche.2014.05.020>.
 25. Arroyave-Toro JJ, Mosquera S, Villegas-Escobar V. 2017. Biocontrol activity of *Bacillus subtilis* EA-

- CB0015 cells and lipopeptides against postharvest fungal pathogens. *Biol Control* 114:195–200.
26. Toral L, Rodríguez M, Béjar V, Sampedro I. 2018. Antifungal activity of lipopeptides from *Bacillus* XT1 CECT 8661 against *Botrytis cinerea*. *Front Microbiol* 9.
 27. Kieseewalter HT, Lozano-Andrade CN, Wibowo M, Strube ML, Maróti G, Snyder D, Jørgensen TS, Larsen TO, Cooper VS, Weber T, Kovács ÁT. 2021. Genomic and Chemical Diversity of *Bacillus subtilis* Secondary Metabolites against Plant Pathogenic Fungi. *mSystems* 6.
 28. Zhang X, Li B, Wang Y, Guo Q, Lu X, Li S, Ma P. 2013. Lipopeptides, a novel protein, and volatile compounds contribute to the antifungal activity of the biocontrol agent *Bacillus atrophaeus* CAB-1. *Appl Microbiol Biotechnol* 97:9525–9534.
 29. Dimopoulou A, Theologidis I, Benaki D, Koukounia M, Zervakou A, Tzima A, Diallinas G, Hatzinikolaou DG, Skandalis N. 2021. Direct Antibiotic Activity of Bacillibactin Broadens the Biocontrol Range of *Bacillus amyloliquefaciens* MBI600. *mSphere* 6.
 30. Beauregard PB, Chai Y, Vlamakis H, Losick R, Kolter R. 2013. *Bacillus subtilis* biofilm induction by plant polysaccharides. *Proc Natl Acad Sci* 110:E1621–E1630.
 31. Al-Ali A, Deravel J, Krier F, Béchet M, Ongena M, Jacques P. 2018. Biofilm formation is determinant in tomato rhizosphere colonization by *Bacillus velezensis* FZB42. *Environ Sci Pollut Res* 25:29910–29920.
 32. Kjeldgaard B, Neves AR, Fonseca C, Kovács ÁT, Domínguez-Cuevas P. 2022. Quantitative High-Throughput Screening Methods Designed for Identification of Bacterial Biocontrol Strains with Antifungal Properties. *Microbiol Spectr* 10.
 33. Mukherjee S, Kearns DB. 2014. The structure and regulation of flagella in *Bacillus subtilis*. *Annu Rev Genet* 48:319–340.
 34. Amati G, Bisicchia P, Galizzi A. 2004. DegU-P represses expression of the motility *fla-che* operon in *Bacillus subtilis*. *J Bacteriol* 186:6003–6014.
 35. Sanchez S, Snider E V, Wang X, Kearns DB. 2022. Identification of Genes Required for Swarming Motility in *Bacillus subtilis* Using Transposon Mutagenesis and High-Throughput Sequencing (TnSeq). *J Bacteriol* 204.
 36. Waters SM, Zeigler DR, Nicholson WL. 2015. Experimental Evolution of Enhanced Growth by *Bacillus subtilis* at Low Atmospheric Pressure: Genomic Changes Revealed by Whole-Genome Sequencing. *Appl Environ Microbiol* 81:7525–7532.
 37. Ni B, Ghosh B, Paldy FS, Colin R, Heimerl T, Sourjik V. 2017. Evolutionary Remodeling of Bacterial Motility Checkpoint Control. *Cell Rep* 18:866–877.
 38. Sher AA, Jerome JP, Bell JA, Yu J, Kim HY, Barrick JE, Mansfield LS. 2020. Experimental Evolution of *Campylobacter jejuni* Leads to Loss of Motility, *rpoN* (σ^{54}) Deletion and Genome Reduction. *Front*

Microbiol 11:2781.

39. Nordgaard M, Blake C, Maróti G, Hu G, Wang Y, Strube ML, Kovács ÁT. 2022. Experimental evolution of *Bacillus subtilis* on *Arabidopsis thaliana* roots reveals fast adaptation and improved root colonization. *iScience* 25:104406.
40. Hu G, Wang Y, Blake C, Nordgaard M, Liu X, Wang B, Kovács ÁT. 2023. Parallel genetic adaptation of *Bacillus subtilis* to different plant species. *bioRxiv* 2023.03.17.533125.
41. Gaballa A, Helmann JD. 2003. *Bacillus subtilis* CPx-type ATPases: characterization of Cd, Zn, Co and Cu efflux systems. *Biometals* 16:497–505.
42. Moore CM, Gaballa A, Hui M, Ye RW, Helmann JD. 2005. Genetic and physiological responses of *Bacillus subtilis* to metal ion stress. *Mol Microbiol* 57:27–40.
43. Harvie DR, Andreini C, Cavallaro G, Meng W, Connolly BA, Yoshida KI, Fujita Y, Harwood CR, Radford DS, Tottey S, Cavet JS, Robinson NJ. 2006. Predicting metals sensed by ArsR-SmtB repressors: Allosteric interference by a non-effector metal. *Mol Microbiol* 59:1341–1356.
44. Guffanti AA, Wei Y, Rood S V., Krulwich TA. 2002. An antiport mechanism for a member of the cation diffusion facilitator family: Divalent cations efflux in exchange for K⁺ and H⁺. *Mol Microbiol* 45:145–153.
45. Sonenshein AL. 2007. Control of key metabolic intersections in *Bacillus subtilis*. *Nat Rev Microbiol*. Nature Publishing Group <https://doi.org/10.1038/nrmicro1772>.
46. Detert Oude Weme R, Seidel G, Kuipers OP. 2015. Probing the regulatory effects of specific mutations in three major binding domains of the pleiotropic regulator CcpA of *Bacillus subtilis*. *Front Microbiol* 6:1051.
47. Fujita Y. 2009. Carbon catabolite control of the metabolic network in *Bacillus subtilis*. *Biosci Biotechnol Biochem* 73:245–259.
48. Blencke HM, Homuth G, Ludwig H, Mäder U, Hecker M, Stülke J. 2003. Transcriptional profiling of gene expression in response to glucose in *Bacillus subtilis*: Regulation of the central metabolic pathways. *Metab Eng* 5:133–149.
49. Lorca GL, Chung YJ, Barabote RD, Weyler W, Schilling CH, Saier MH. 2005. Catabolite repression and activation in *Bacillus subtilis*: Dependency on CcpA, HPr, and HprK. *J Bacteriol* 187:7826–7839.
50. Ali NO, Bignon J, Rapoport G, Debarbouille M. 2001. Regulation of the acetoin catabolic pathway is controlled by sigma L in *Bacillus subtilis*. *J Bacteriol* 183:2497–2504.
51. Schönbichler A, Díaz-Moreno SM, Srivastava V, McKee LS. 2020. Exploring the Potential for Fungal Antagonism and Cell Wall Attack by *Bacillus subtilis* natto. *Front Microbiol* 11:521.
52. A. Veliz E, Martínez-Hidalgo P, M. Hirsch A. 2017. Chitinase-producing bacteria and their role in

biocontrol. *AIMS Microbiol* 3:689–705.

53. Azrin NAM, Ali MSM, Rahman RNZRA, Oslan SN, Noor NDM. 2022. Versatility of subtilisin: A review on structure, characteristics, and applications. *Biotechnol Appl Biochem*. John Wiley & Sons, Ltd <https://doi.org/10.1002/bab.2309>.
54. Butcher RA, Schroeder FC, Fischbach MA, Straight PD, Kolter R, Walsh CT, Clardy J. 2007. The identification of bacillaene, the product of the PksX megacomplex in *Bacillus subtilis*. *Proc Natl Acad Sci U S A* 104:1506–1509.
55. Tsuge K, Ano T, Hirai M, Nakamura Y, Shoda M. 1999. The genes *degQ*, *pps*, and *lpa-8* (*sfp*) are responsible for conversion of *Bacillus subtilis* 168 to plipastatin production. *Antimicrob Agents Chemother* 43:2183–2192.
56. Vahidinasab M, Lilge L, Reinfurt A, Pfannstiel J, Henkel M, Morabbi Heravi K, Hausmann R. 2020. Construction and description of a constitutive plipastatin mono-producing *Bacillus subtilis*. *Microb Cell Fact* 19:205.
57. Nakano MM, Marahiel MA, Zuber P. 1988. Identification of a genetic locus required for biosynthesis of the lipopeptide antibiotic surfactin in *Bacillus subtilis*. *J Bacteriol* 170:5662–5668.
58. Cesa-Luna C, Baez A, Quintero-Hernández V, De La Cruz-Enríquez J, Castañeda-Antonio MD, Muñoz-Rojas J. 2020. The importance of antimicrobial compounds produced by beneficial bacteria on the biocontrol of phytopathogens. *Acta Biol Colomb* 25:140–154.
59. Penha RO, Vandenberghe LPS, Faulds C, Soccol VT, Soccol CR. 2020. *Bacillus* lipopeptides as powerful pest control agents for a more sustainable and healthy agriculture: recent studies and innovations. *Planta*. Springer <https://doi.org/10.1007/s00425-020-03357-7>.
60. Raymaekers K, Ponet L, Holtappels D, Berckmans B, Cammue BPA. 2020. Screening for novel biocontrol agents applicable in plant disease management – A review. *Biol Control* <https://doi.org/10.1016/j.biocontrol.2020.104240>.
61. Koumoutsis A, Chen X-HH, Henne A, Liesegang H, Hitzeroth G, Franke P, Vater J, Borriss R. 2004. Structural and Functional Characterization of Gene Clusters Directing Nonribosomal Synthesis of Bioactive Cyclic Lipopeptides in *Bacillus amyloliquefaciens* Strain FZB42, p. 1084–1096. *In* *Journal of Bacteriology*. American Society for Microbiology Journals.
62. Ongena M, Jacques P, Touré Y, Destain J, Jabrane A, Thonart P. 2005. Involvement of fengycin-type lipopeptides in the multifaceted biocontrol potential of *Bacillus subtilis*. *Appl Microbiol Biotechnol* 69:29–38.
63. Gu Q, Yang Y, Yuan Q, Shi G, Wu L, Lou Z, Huo R, Wu H, Borriss R, Gao X. 2017. Bacillomycin D produced by *Bacillus amyloliquefaciens* is involved in the antagonistic interaction with the plantpathogenic

- fungus *Fusarium graminearum*. *Appl Environ Microbiol* 83:e01075-17.
64. Hanif A, Zhang F, Li P, Li C, Xu Y, Zubair M, Zhang M, Jia D, Zhao X, Liang J, Majid T, Yan J, Farzand A, Wu H, Gu Q, Gao X. 2019. Fengycin produced by *Bacillus amyloliquefaciens* FZB42 inhibits *Fusarium graminearum* growth and mycotoxins biosynthesis. *Toxins (Basel)* 11.
 65. Tsuge K, Matsui K, Itaya M. 2007. Production of the non-ribosomal peptide plipastatin in *Bacillus subtilis* regulated by three relevant gene blocks assembled in a single movable DNA segment. *J Biotechnol* 129:592–603.
 66. Wang P, Guo Q, Ma Y, Li S, Lu X, Zhang X, Ma P. 2015. DegQ regulates the production of fengycins and biofilm formation of the biocontrol agent *Bacillus subtilis* NCD-2. *Microbiol Res* 178:42–50.
 67. Li Y, Héloir MC, Zhang X, Geissler M, Trouvelot S, Jacquens L, Henkel M, Su X, Fang X, Wang Q, Adrian M. 2019. Surfactin and fengycin contribute to the protection of a *Bacillus subtilis* strain against grape downy mildew by both direct effect and defence stimulation. *Mol Plant Pathol* 20:1037–1050.
 68. Bartolini M, Cogliati S, Vileta D, Bauman C, Ramirez W, Grau R. 2019. Stressresponsive alternative sigma factor SigB plays a positive role in the antifungal proficiency of *Bacillus subtilis*. *Appl Environ Microbiol* 85.
 69. Makroczyová J, Jamroškovič J, Krascšenitsová E, Labajová N, Barák I. 2016. Oscillating behavior of *Clostridium difficile* Min proteins in *Bacillus subtilis*. *Microbiologyopen* 5:387–401.
 70. Bongiorno C, Stoessel R, Perego M. 2007. Negative regulation of *Bacillus anthracis* sporulation by the Spo0E family of phosphatases. *J Bacteriol* 189:2637–2645.
 71. Kobayashi K. 2007. *Bacillus subtilis* pellicle formation proceeds through genetically defined morphological changes. *J Bacteriol* 189:4920–4931.
 72. Kobayashi K. 2007. Gradual activation of the response regulator DegU controls serial expression of genes for flagellum formation and biofilm formation in *Bacillus subtilis*. *Mol Microbiol* 66:395–409.
 73. Verhamme DT, Murray EJ, Stanley-Wall NR. 2009. DegU and Spo0A Jointly Control Transcription of Two Loci Required for Complex Colony Development by *Bacillus subtilis*. *J Bacteriol* 191:100–108.
 74. Verhamme DT, Kiley TB, Stanley-Wall NR. 2007. DegU co-ordinates multicellular behaviour exhibited by *Bacillus subtilis*. *Mol Microbiol* 65:554–568.
 75. Dergham Y, Sanchez-Vizueté P, Coq D Le, Deschamps J, Bridier A, Hamze K, Briandet R. 2021. Comparison of the genetic features involved in *Bacillus subtilis* biofilm formation using multi-culturing approaches. *Microorganisms* 9:1–17.
 76. Pisithkul T, Schroeder JW, Trujillo EA, Yeesin P, Stevenson DM, Chaiamarit T, Coon JJ, Wang JD, Amador-Noguez D. 2019. Metabolic remodeling during biofilm development of *Bacillus subtilis*. *MBio* 10:2021.

77. Chan JM, Guttenplan SB, Kearns DB. 2014. Defects in the flagellar motor increase synthesis of poly- γ -glutamate in bacillus subtilis. *J Bacteriol* 196:740–753.
78. Osera C, Amati G, Calvio C, Galizzi A. 2009. SwrAA activates poly- γ -glutamate synthesis in addition to swarming in *Bacillus subtilis*. *Microbiology* 155:2282–2287.
79. Ohsawa T, Tsukahara K, Ogura M. 2009. *Bacillus subtilis* response regulator DegU is a direct activator of pgsB transcription involved in γ -poly-glutamic acid synthesis. *Biosci Biotechnol Biochem* 73:2096–2102.
80. Do TH, Suzuki Y, Abe N, Kaneko J, Itoh Y, Kimura K. 2011. Mutations suppressing the loss of DegQ function in *Bacillus subtilis* (natto) poly- γ -glutamate synthesis. *Appl Environ Microbiol* 77:8249–8258.
81. Wang L, Wang N, Mi D, Luo Y, Guo J. 2017. Poly- γ -glutamic acid productivity of *Bacillus subtilis* BsE1 has positive function in motility and biocontrol against *Fusarium graminearum*. *J Microbiol* 55:554–560.
82. Yin A, Jia Y, Qiu T, Gao M, Cheng S, Wang X, Sun Y. 2018. Poly- γ -glutamic acid improves the drought resistance of maize seedlings by adjusting the soil moisture and microbial community structure. *Appl Soil Ecol* 129:128–135.
83. Ling L, Cheng W, Jiang K, Jiao Z, Luo H, Yang C, Pang M, Lu L. 2022. The antifungal activity of a serine protease and the enzyme production of characteristics of *Bacillus licheniformis* TG116. *Arch Microbiol* 204.
84. Dahl MK, Msadek T, Kunst F, Rapoport G. 1991. Mutational analysis of the *Bacillus subtilis* DegU regulator and its phosphorylation by the DegS protein kinase. *J Bacteriol* 173:2539–2547.
85. Peypoux F, Bonmatin JM, Wallach J. 1999. Recent trends in the biochemistry of surfactin. *Appl Microbiol Biotechnol* 51:553–563.
86. Kinsinger RF, Shirk MC, Fall R. 2003. Rapid surface motility in *Bacillus subtilis* is dependent on extracellular surfactin and potassium ion. *J Bacteriol* 185:5627–5631.
87. Edwards RJ, Sockett RE, Brookfield JFY. 2002. A simple method for genome-wide screening for advantageous insertions of mobile DNAs in *Escherichia coli*. *Curr Biol* 12:863–867.
88. Cooper TF, Rozen DE, Lenski RE. 2003. Parallel changes in gene expression after 20,000 generations of evolution in *Escherichia coli*. *Proc Natl Acad Sci U S A* 100:1072–1077.
89. Li E, Zhang H, Jiang H, Pieterse CMJ, Jousset A, Bakker PAHM, de Jonge R. 2021. Experimental-evolution-driven identification of arabidopsis rhizosphere competence genes in *pseudomonas protegens*. *MBio* 12:2020.12.01.407551.
90. Lin Y, Alstrup M, Pang JKY, Maróti G, Er-Rafik M, Tourasse N, Økstad OA, Kovács ÁT. 2021. Adaptation of *Bacillus thuringiensis* to Plant Colonization Affects Differentiation and Toxicity. *mSystems* 6.

91. Branda SS, González-Pastor JE, Ben-Yehuda S, Losick R, Kolter R. 2001. Fruiting body formation by *Bacillus subtilis*. *Proc Natl Acad Sci U S A* 98:11621–11626.
92. Stanley NR, Lazazzera BA. 2005. Defining the genetic differences between wild and domestic strains of *Bacillus subtilis* that affect poly- γ -DL-glutamic acid production and biofilm formation. *Mol Microbiol* 57:1143–1158.
93. Aguilar C, Vlamakis H, Losick R, Kolter R. 2007. Thinking about *Bacillus subtilis* as a multicellular organism. *Curr Opin Microbiol* 10:638–643.
94. McLoon AL, Guttenplan SB, Kearns DB, Kolter R, Losick R. 2011. Tracing the Domestication of a Biofilm-Forming Bacterium. *J Bacteriol* 193:2027–2034.
95. Leiman SA, Arboleda LC, Spina JS, McLoon AL. 2014. SinR is a mutational target for fine-tuning biofilm formation in laboratory-evolved strains of *Bacillus subtilis*. *BMC Microbiol* 14:1–10.
96. Richter A, Blei F, Hu G, Schwitalla JW, Lozano-Andrade CN, Jarmusch SA, Wibowo M, Kjeldgaard B, Surabhi S, Jautzus T, Phippen CBW, Tyc O, Arentshorst M, Wang Y, Garbeva P, Larsen TO, Ram AFJ, Hondel CAM van den, Maroti G, Kovacs AT. 2023. Enhanced niche colonisation and competition during bacterial adaptation to a fungus. *bioRxiv* 2023.03.27.534400.
97. Barreto HC, Cordeiro TN, Henriques AO, Gordo I. 2020. Rampant loss of social traits during domestication of a *Bacillus subtilis* natural isolate. *Sci Rep* 10.
98. Maughan H, Masel J, Birky CW, Nicholson WL. 2007. The Roles of Mutation Accumulation and Selection in Loss of Sporulation in Experimental Populations of *Bacillus subtilis*. *Genetics* 177:937–948.
99. Brown CT, Fishwick LK, Chokshi BM, Cuff MA, Jackson JM, Oglesby T, Rioux AT, Rodriguez E, Stupp GS, Trupp AH, Woollcombe-Clarke JS, Wright TN, Zaragoza WJ, Drew JC, Triplett EW, Nicholson WL. 2011. Whole-genome sequencing and phenotypic analysis of *Bacillus subtilis* mutants following evolution under conditions of relaxed selection for sporulation. *Appl Environ Microbiol* 77:6867–6877.
100. Zeigler DR, Nicholson WL. 2017. Experimental evolution of *Bacillus subtilis*. *Environ Microbiol* 19:3415–3422.
101. Dahl MK, Msadek T, Kunst F, Rapoport G. 1992. The phosphorylation state of the degU response regulator acts as a molecular switch allowing either degradative enzyme synthesis or expression of genetic competence in *Bacillus subtilis*. *J Biol Chem* 267:14509–14514.
102. Msadek T, Kunst F, Henner D, Klier A, Rapoport G, Dedonder R. 1990. Signal transduction pathway controlling synthesis of a class of degradative enzymes in *Bacillus subtilis*: Expression of the regulatory genes and analysis of mutations in degS and degU. *J Bacteriol* 172:824–834.
103. Yang M, Ferrari E, Chen E, Henner DJ. 1986. Identification of the pleiotropic sacQ gene of *Bacillus*

- subtilis*. J Bacteriol 166:113–119.
104. Tanaka T, Kawata M, Mukai K. 1991. Altered phosphorylation of *Bacillus subtilis* DegU caused by single amino acid changes in DegS. J Bacteriol 173:5507–5515.
 105. Henner DJ, Ferrari E, Perego M, Hoch JA. 1988. Location of the targets of the hpr-97, sacU32(Hy), and sacQ36(Hy) mutations in upstream regions of the subtilisin promoter. J Bacteriol 170:296–300.
 106. Mukai K, Kawata-Mukai M, Tanaka T. 1992. Stabilization of phosphorylated *Bacillus subtilis* DegU by DegR. J Bacteriol 174:7954–7962.
 107. Bourret RB. 2010. Receiver domain structure and function in response regulator proteins. Curr Opin Microbiol. Curr Opin Microbiol <https://doi.org/10.1016/j.mib.2010.01.015>.
 108. Bourret RB, Hess JF, Simon MI. 1990. Conserved aspartate residues and phosphorylation in signal transduction by the chemotaxis protein CheY. Proc Natl Acad Sci U S A 87:41–45.
 109. Jin S, Prusti RK, Roitsch T, Ankenbauer RG, Nester EW. 1990. Phosphorylation of the VirG protein of *Agrobacterium tumefaciens* by the autophosphorylated VirA protein: Essential role in biological activity of VirG. J Bacteriol 172:4945–4950.
 110. Allen KN, Dunaway-Mariano D. 2016. Catalytic scaffolds for phosphoryl group transfer. Curr Opin Struct Biol. Elsevier Current Trends <https://doi.org/10.1016/j.sbi.2016.07.017>.
 111. Calvio C, Osera C, Amati G, Galizzi A. 2008. Autoregulation of swrAA and Motility in *Bacillus subtilis*. J Bacteriol 190:5720–5728.
 112. Chunchart O, Kotabin N, Yadee N, Tahara Y, Issakul K. 2014. Effect of Lead and γ -Polyglutamic Acid Produced from *Bacillus subtilis* on Growth of *Brassica chinensis* L. APCBEE Procedia 10:269–274.
 113. Rajan YC, Inbaraj BS, Chen BH. 2014. In Vitro Adsorption of Aluminum by an Edible Biopolymer Poly(γ -glutamic acid). J Agric Food Chem 62:4803–4811.
 114. Yao J, Xu H, Wang J, Jiang M, Ouyang P. 2007. Removal of Cr(III), Ni(II) and Cu(II) by poly(γ -glutamic acid) from *Bacillus subtilis* NX-2. J Biomater Sci Polym Ed 18:193–204.
 115. Guo L, Lu L, Wang H, Zhang X, Wang G, Zhao T, Zheng G, Qiao C. 2023. Effects of Fe²⁺ addition to sugarcane molasses on poly- γ -glutamic acid production in *Bacillus licheniformis* CGMCC NO. 23967. Microb Cell Fact 22:37.
 116. Yamashiro D, Yoshioka M, Ashiuchi M. 2011. *Bacillus subtilis* pgsE (Formerly ywtC) stimulates poly- γ -glutamate production in the presence of zinc. Biotechnol Bioeng 108:226–230.
 117. Urushibata Y, Tokuyama S, Tahara Y. 2002. Characterization of the *Bacillus subtilis* ywsC gene, involved in γ -polyglutamic acid production. J Bacteriol 184:337–343.
 118. Ashiuchi M. 2010. Occurrence and Biosynthetic Mechanism of Poly-Gamma-Glutamic Acid, p. 77–93. *In* . Springer, Berlin, Heidelberg.

119. Huang C-J, Wang T-K, Chung S-C, Chen C-Y. 2005. Identification of an Antifungal Chitinase from a Potential Biocontrol Agent, *Bacillus cereus* 28-9. *BMB Rep* 38:82–88.
120. Kishore GK, Pande S. 2007. Chitin-supplemented foliar application of chitinolytic *Bacillus cereus* reduces severity of *Botrytis gray* mold disease in chickpea under controlled conditions. *Lett Appl Microbiol* 44:98–105.
121. Moszer I, Rocha EP, Danchin A. 1999. Codon usage and lateral gene transfer in *Bacillus subtilis*. *Curr Opin Microbiol* 2:524–528.
122. Hotta K, Kim CY, Fox DT, Koppisch AT. 2010. Siderophore-mediated iron acquisition in *Bacillus anthracis* and related strains. *Microbiology*. Microbiology Society <https://doi.org/10.1099/mic.0.039404-0>.
123. Wu Q, Zhi Y, Xu Y. 2019. Systematically engineering the biosynthesis of a green biosurfactant surfactin by *Bacillus subtilis* 168. *Metab Eng* 52:87–97.
124. Defilippi S, Groulx E, Megalla M, Mohamed R, Avis TJ. 2018. Fungal Competitors Affect Production of Antimicrobial Lipopeptides in *Bacillus subtilis* Strain B9–5. *J Chem Ecol* 44:374–383.
125. Yang C, Dong Y, Friman V, Jousset A, Wei Z, Xu Y, Shen Q. 2019. Carbon resource richness shapes bacterial competitive interactions by alleviating growth-antibiosis trade-off. *Funct Ecol* 33:868–875.
126. Görke B, Stülke J. 2008. Carbon catabolite repression in bacteria: Many ways to make the most out of nutrients. *Nat Rev Microbiol*. Nature Publishing Group <https://doi.org/10.1038/nrmicro1932>.
127. Elena SF, Lenski RE. 2003. Evolution experiments with microorganisms: The dynamics and genetic bases of adaptation. *Nat Rev Genet*. Nature Publishing Group <https://doi.org/10.1038/nrg1088>.

Supplemental material

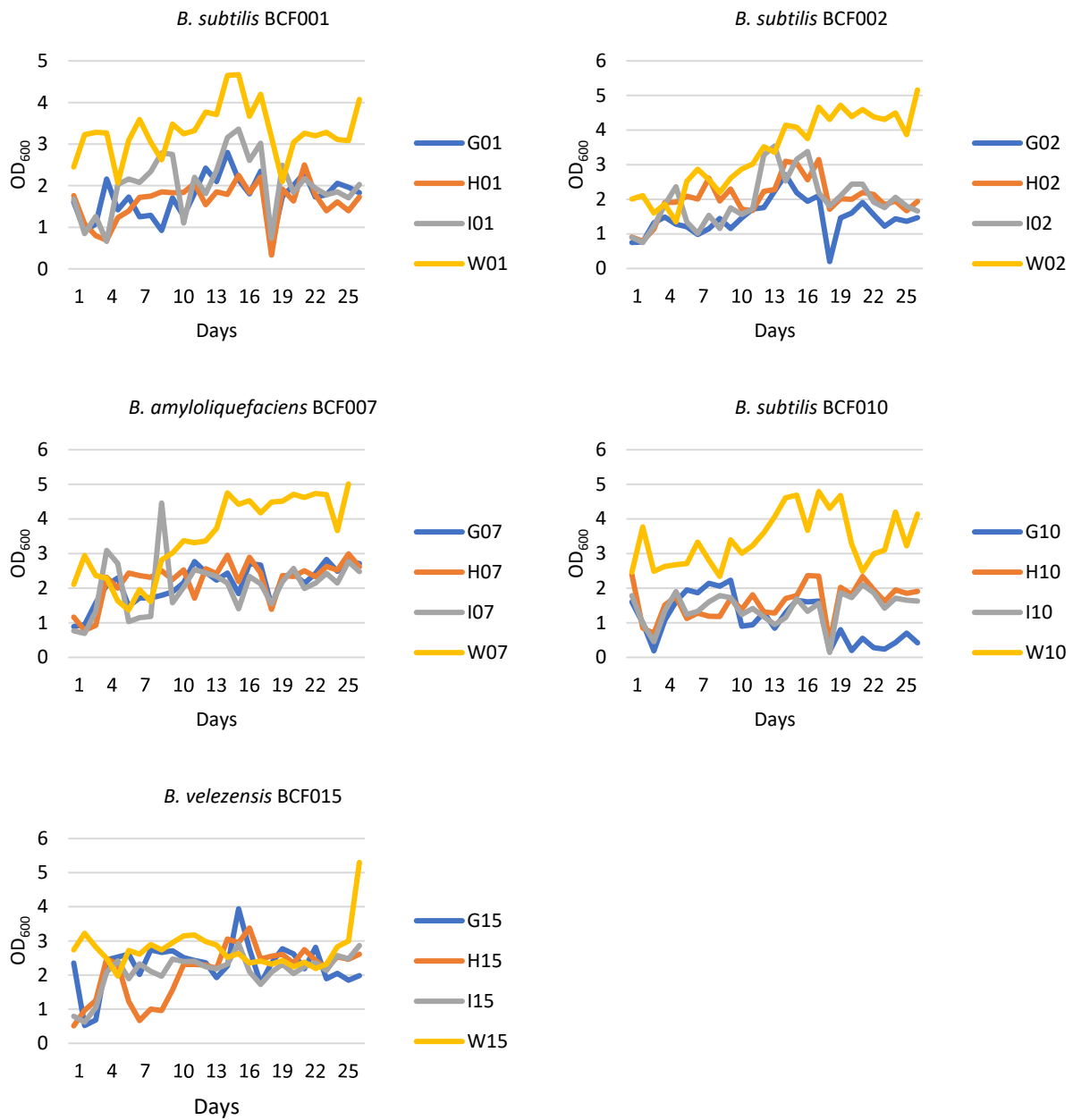


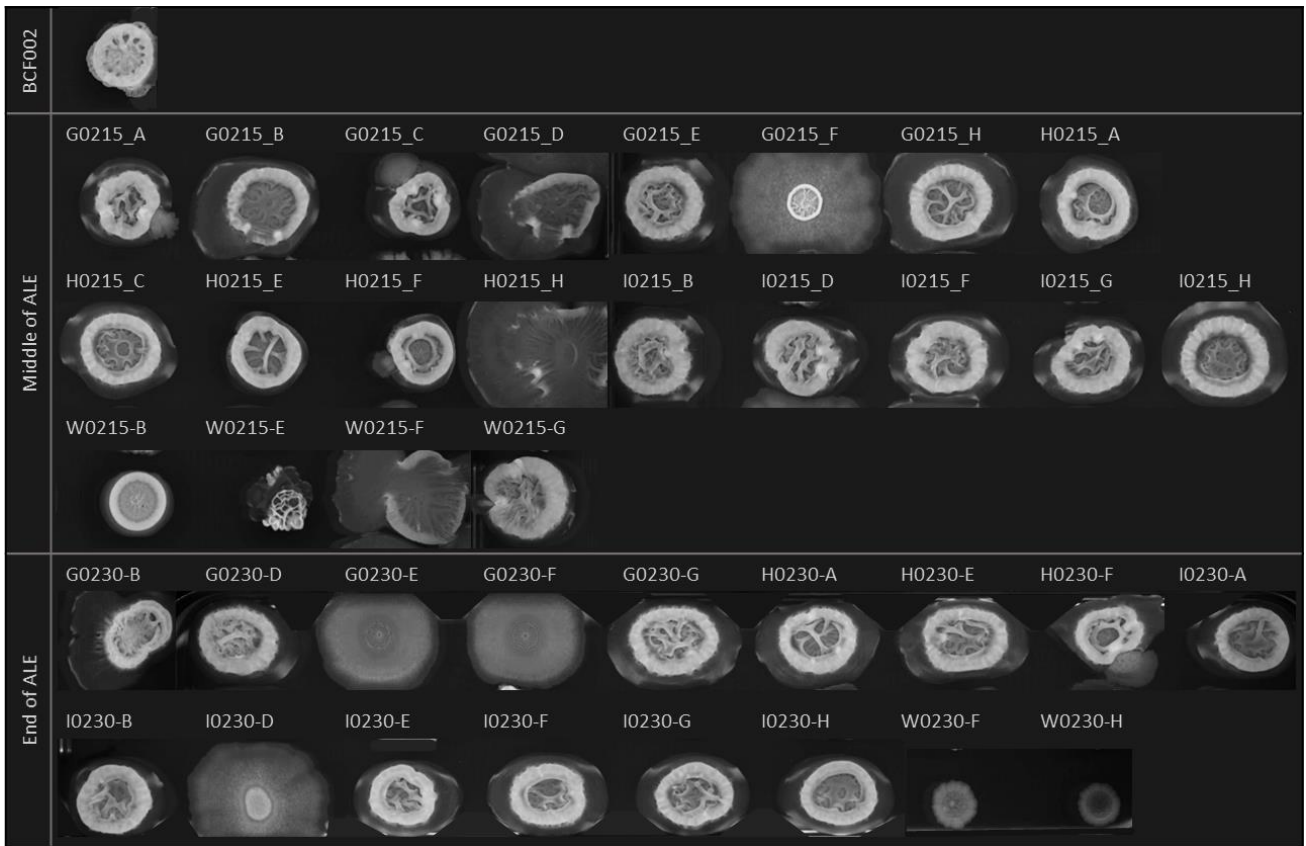
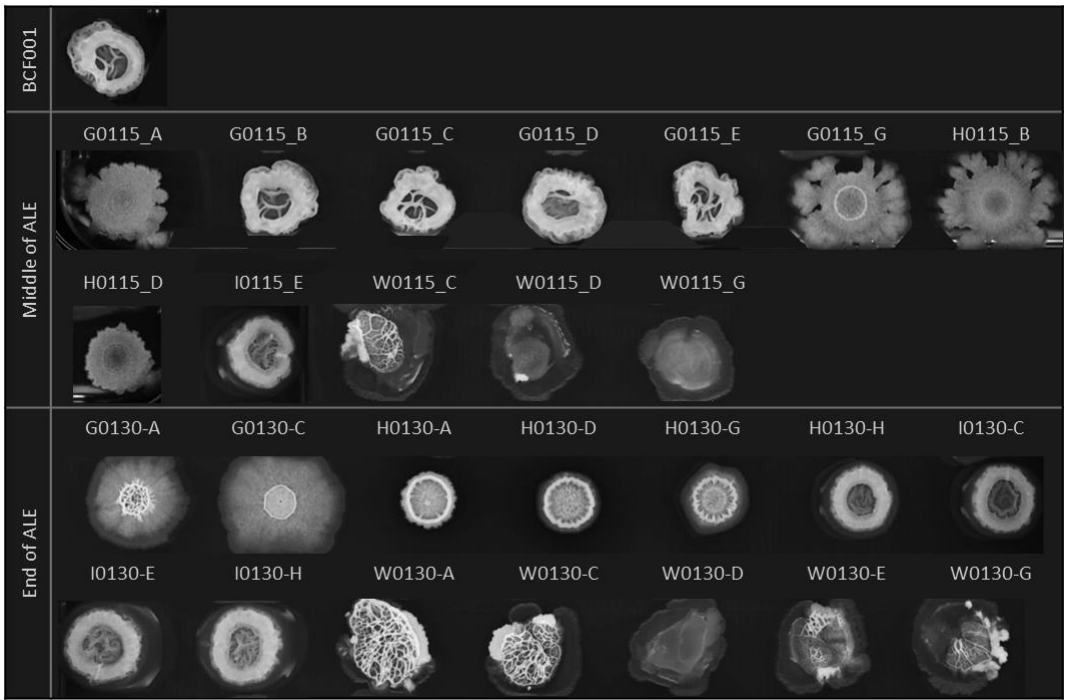
Fig. S 1. Growth of evolved strains. The growth of evolved control populations (W) and co-evolved populations (G, H, I) from the ancestors *B. subtilis* BCF001, BCF002, BCF010, *B. amyloliquefaciens* BCF007, *B. velezensis* BCF015 was measured and adjusted by optical density (OD₆₀₀) by each daily transfer over total 27 cycles. The evolved populations were named with a number reference to the parent (BCF001, BCF002, BCF007, BCF010, BCF015).

Table S 1. ALE generations. The total number of generations were calculated from optical density measurements for each evolved population (G, H, I, W) derived from the ancestors *B. subtilis* BCF001, BCF002, BCF010, *B. amyloliquefaciens* BCF007, *B. velezensis* BCF015.

Species	Ancestor	Population	Generations
<i>B. subtilis</i>	BCF001	G01	199
		H01	196
		I01	204
		W01	242
<i>B. subtilis</i>	BCF002	G02	191
		H02	205
		I02	203
		W02	239
<i>B. amyloliquefaciens</i>	BCF007	G07	207
		H07	209
		I07	204
		W07	232
<i>B. subtilis</i>	BCF010	G10	173
		H10	195
		I10	190
		W10	234
<i>B. velezensis</i>	BCF015	G15	209
		H15	204
		I15	207
		W15	224

Table S 2. Fitness screening result. Antifungal potency of strains from co-evolved populations (G, H, I) and evolved control populations (W) derived from the ancestors *B. subtilis* BCF001, BCF002, BCF010, *B. amyloliquefaciens* BCF007, *B. velezensis* BCF015 were evaluated by high-throughput screening. Both strains isolated in the middle and by the end of ALE experiment were screened. Stains' antifungal potencies were scored as; *Improved*, *Reduced*, or *Neutral* relative to the parental strains.

		Campaign middle				Campaign end				Total			
		Improved	Reduced	Neutral	Total	Improved	Reduced	Neutral	Total	Improved	Reduced	Neutral	Total
BCF001	G01	6			6	1	2	5	8	7	2	5	14
	H01	1	4	3	8	3	4	1	8	4	8	4	16
	I01		7	1	8	3	2	3	8	3	9	4	16
	W01	2	2	3	7	5		3	8	7	2	6	15
BCF002	G02	7			7	5	1	1	7	12	1	1	14
	H02	5		3	8	3	2	3	8	8	2	6	16
	I02	5		3	8	7		1	8	12	0	4	16
	W02	5	1	2	8		7	1	8	5	8	3	16
BCF007	G07	4	3	1	8	6			6	10	3	1	14
	H07	3	3	1	7					3	3	1	7
	I07	2	4	2	8	4	2		6	6	6	2	14
	W07		6	1	7	1	4	3	8	1	10	4	15
BCF010	G10		2	1	3		6	1	7	0	8	2	10
	H10		5	2	7	1	6	1	8	1	11	3	15
	I10		5	2	7	1	4	2	7	1	9	4	14
	W10		7	1	8	1	2	5	8	1	9	6	16
BCF015	G15	2	4	2	8		7		7	2	11	2	15
	H15	6	1	1	8		6	2	8	6	7	3	16
	I15	7	1		8	1	6	1	8	8	7	1	16
	W15	7		1	8	1	7		8	8	7	1	16
Total		62	55	30	147	43	68	33	144	105	123	63	291



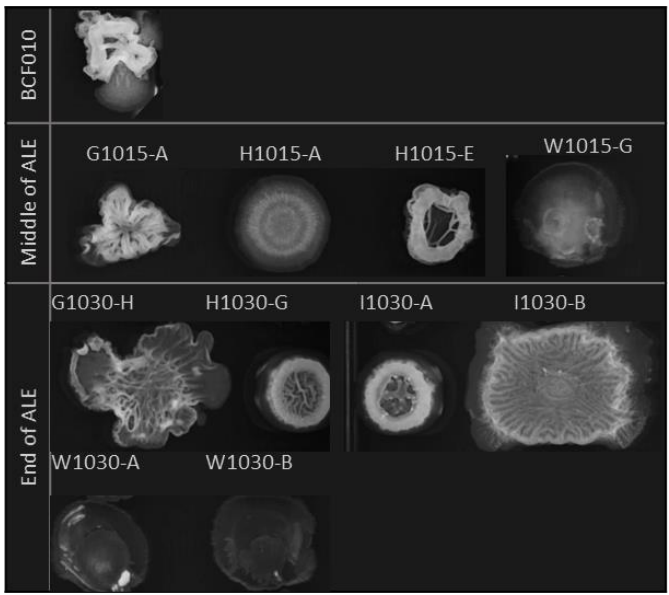
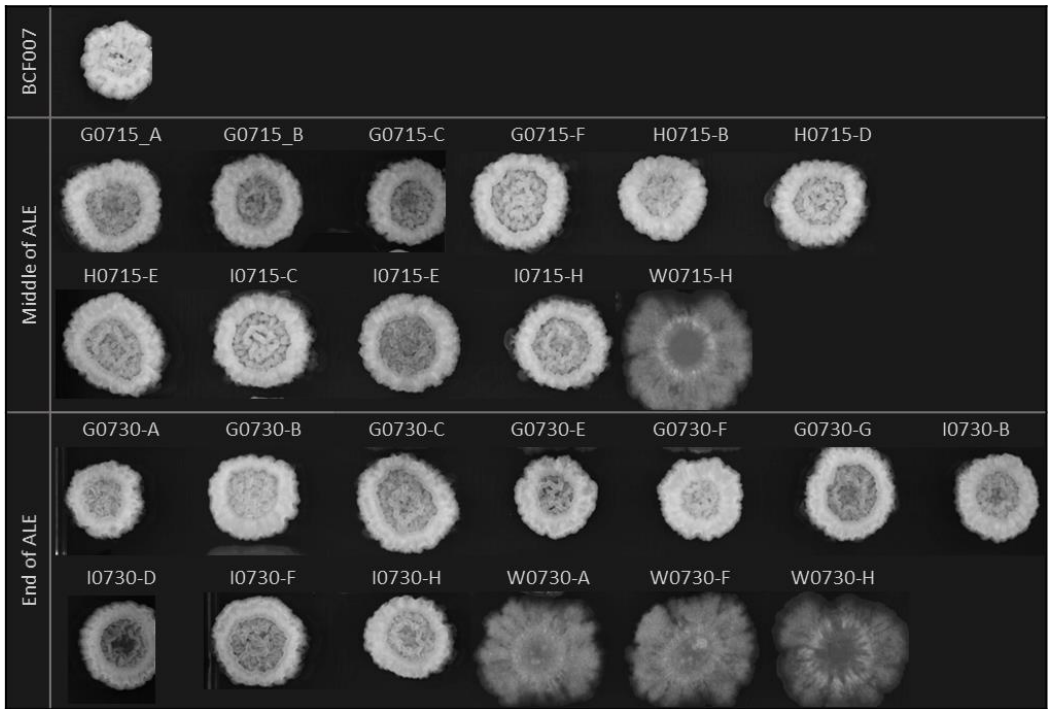




Fig. S 2. Colony morphology. The colony morphology of strains from co-evolved populations (G, H, I) and control populations (W) derived from the *B. subtilis* BCF001, BCF002, BCF010, *B. amyloliquefaciens* BCF007, *B. velezensis* BCF015 was evaluated on biofilm inducing medium.

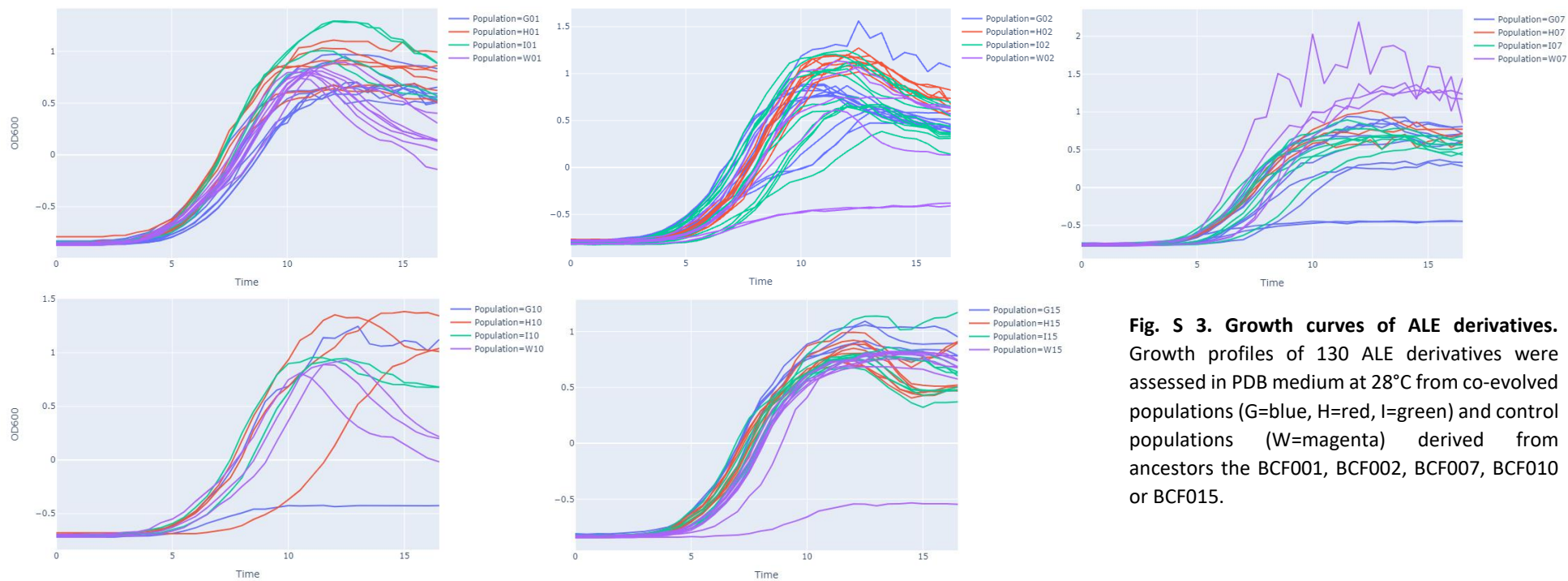


Fig. S 3. Growth curves of ALE derivatives. Growth profiles of 130 ALE derivatives were assessed in PDB medium at 28°C from co-evolved populations (G=blue, H=red, I=green) and control populations (W=magenta) derived from ancestors the BCF001, BCF002, BCF007, BCF010 or BCF015.

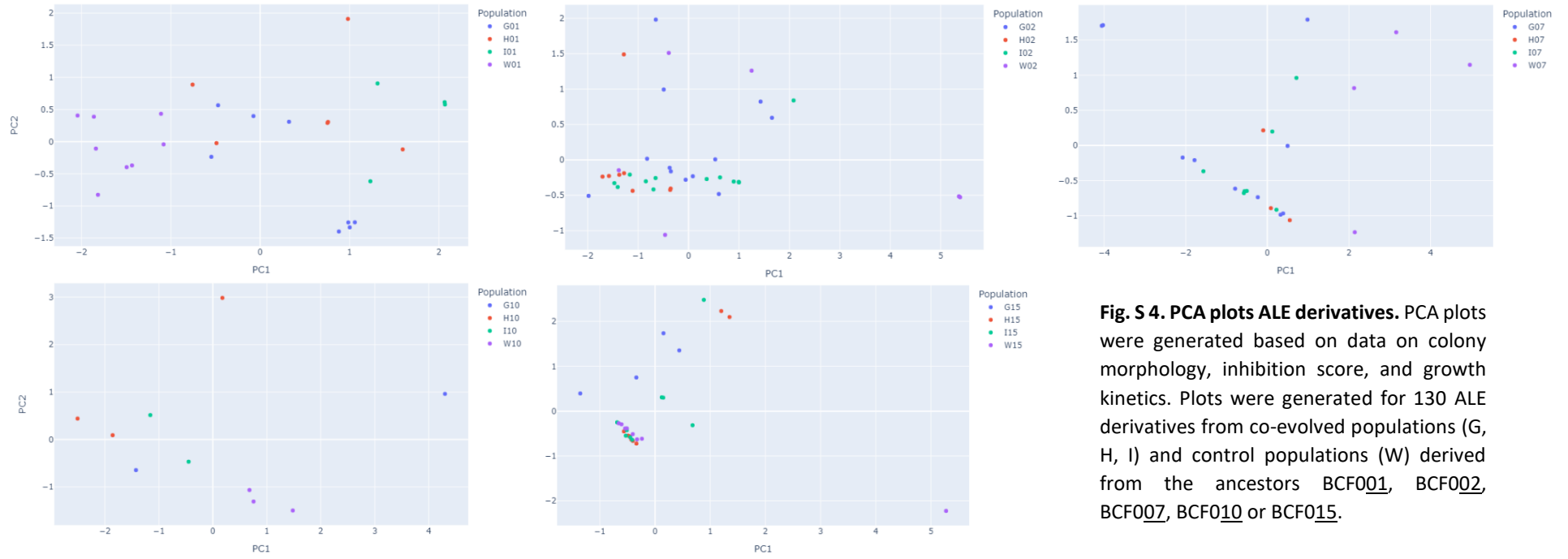


Fig. S 4. PCA plots ALE derivatives. PCA plots were generated based on data on colony morphology, inhibition score, and growth kinetics. Plots were generated for 130 ALE derivatives from co-evolved populations (G, H, I) and control populations (W) derived from the ancestors BCF001, BCF002, BCF007, BCF010 or BCF015.

Table S 3. Primary characterization. From the inhibition screen, 130 strains derived from the co-evolved populations (pop; G, H, I) or control populations (W) isolated from the middle or end of the ALE (T; 15 or 30) were selected for primary characterization regarding colony morphology (pheno; 1-4), inhibition potency (score; -1 to 1), sporulation (spo; 1 or 0). Strains selected for whole genome sequencing are indicated in grey.

BCF007						BCF015						BCF001						BCF002						BCF010					
Strain	T	Pop	Pheno	Spo	Score	Strain	T	Pop	Pheno	Spo	Score	Strain	T	Pop	Pheno	Spo	Score	Strain	T	Pop	Pheno	Spo	Score	Strain	T	Pop	Pheno	Spo	Score
G0715-A	15	G07	1	1	2	G1515-F	15	G15	2	1	-1	G0115-A	15	G01	2	1	0	G0215-A	15	G02	2	1	1	G1015-A	15	G10	3	1	-2
G0715-B	15	G07	1	1	2	G1515-G	15	G15	2	1	0	G0115-B	15	G01	1	1	1	G0215-B	15	G02	2	1	2	H1015-A	15	H10	2	1	-2
G0715-C	15	G07	1	1	1	G1515-H	15	G15	2	1	1	G0115-C	15	G01	1	1	1	G0215-C	15	G02	2	1	2	H1015-E	15	H10	1	1	1
G0715-E	15	G07	1	1	2	H1515-A	15	H15	1	1	-2	G0115-D	15	G01	1	1	1	G0215-D	15	G02	4	1	2	W1015-G	15	W10	4	1	-1
G0715-F	15	G07	1	1	-1	H1515-C	15	H15	2	1	1	G0115-E	15	G01	1	1	1	G0215-E	15	G02	2	1	2	G1030-A	30	G10	1	1	-2
H0715-B	15	H07	1	1	2	H1515-D	15	H15	2	1	1	G0115-G	15	G01	3	1	1	G0215-F	15	G02	3	1	2	G1030-H	30	G10	3	1	0
H0715-D	15	H07	1	1	2	H1515-E	15	H15	2	1	1	H0115-B	15	H01	3	1	-1	G0215-H	15	G02	2	1	0	H1030-G	30	H10	1	1	0
H0715-E	15	H07	1	1	1	H1515-F	15	H15	2	1	1	H0115-D	15	H01	3	1	1	H0215-A	15	H02	2	1	2	I1030-A	30	I10	1	1	-1
I0715-C	15	I07	1	1	1	H1515-G	15	H15	2	1	1	I0115-E	15	I01	1	1	-1	H0215-C	15	H02	2	1	2	I1030-B	30	I10	3	1	0
I0715-E	15	I07	1	1	0	H1515-H	15	H15	2	1	1	W0115-C	15	W01	3.5	1	0	H0215-E	15	H02	2	1	2	W1030-A	30	W10	4	0	0
I0715-H	15	I07	1	1	2	I1515-B	15	I15	2	1	1	W0115-D	15	W01	4	1	0	H0215-F	15	H02	2	1	2	W1030-B	30	W10	4	0	0
W0715-H	15	W07	3	1	0	I1515-C	15	I15	2	1	0	W0115-G	15	W01	4	0	0	H0215-H	15	H02	4	1	1						
G0730-A	30	G07	1	1	2	I1515-D	15	I15	2	1	1	G0130-A	30	G01	3	1	1	I0215-B	15	I02	2	1	1						
G0730-B	30	G07	1	1	1	I1515-E	15	I15	2	1	0	G0130-C	30	G01	3	1	0	I0215-D	15	I02	2	1	1						
G0730-C	30	G07	1	1	2	I1515-F	15	I15	2	1	1	H0130-A	30	H01	2	1	-1	I0215-F	15	I02	2	1	2						
G0730-E	30	G07	1	1	2	I1515-G	15	I15	2	1	1	H0130-D	30	H01	2	1	1	I0215-G	15	I02	2	1	1						
G0730-F	30	G07	1	1	1	I1515-H	15	I15	2	1	1	H0130-G	30	H01	2	1	1	I0215-H	15	I02	2	1	1						
G0730-G	30	G07	1	1	2	W1515-B	15	W15	2	1	1	H0130-H	30	H01	1	1	1	W0215-B	15	W02	1	1	2						
I0730-B	30	I07	1	1	2	W1515-C	15	W15	2	1	1	I0130-C	30	I01	1	1	1	W0215-E	15	W02	3.5	1	1						
I0730-D	30	I07	1	1	2	W1515-D	15	W15	2	1	1	I0130-E	30	I01	1	1	1	W0215-F	15	W02	4	1	1						
I0730-F	30	I07	1	1	2	W1515-E	15	W15	2	1	1	I0130-H	30	I01	1	1	1	W0215-G	15	W02	2	1	2						
I0730-H	30	I07	1	1	2	W1515-G	15	W15	2	1	1	W0130-A	30	W01	3.5	1	1	G0230-B	30	G02	2	1	1						
W0730-A	30	W07	3	1	-1	W1515-H	15	W15	2	1	1	W0130-C	30	W01	3.5	1	1	G0230-D	30	G02	2	1	1						
W0730-F	30	W07	3	1	2	W1515-I	15	W15	2	1	1	W0130-D	30	W01	4	0	1	G0230-E	30	G02	3	1	0						
W0730-H	30	W07	3	1	-1	G1530-B	30	G15	2	1	-1	W0130-E	30	W01	3.5	1	1	G0230-F	30	G02	3	1	1						
						H1530-B	30	H15	1	1	-2	W0130-G	30	W01	3.5	1	1	G0230-G	30	G02	2	1	1						
						I1530-B	30	I15	2	1	-2							H0230-A	30	H02	2	1	1						
						I1530-H	30	I15	2	1	0							H0230-E	30	H02	2	1	1						
						W1530-G	30	W15	2	1	1							H0230-F	30	H02	2	1	1						
						W1530-H	30	W15	2	1	-2							I0230-A	30	I02	2	1	1						
																	I0230-B	30	I02	2	1	1							
																	I0230-D	30	I02	3	1	1							
																	I0230-E	30	I02	2	1	1							
																	I0230-F	30	I02	2	1	1							
																	I0230-G	30	I02	2	1	1							
																	I0230-H	30	I02	2	1	1							
																	W0230-F	30	W02	2	1	-2							
																	W0230-H	30	W02	2	1	-2							

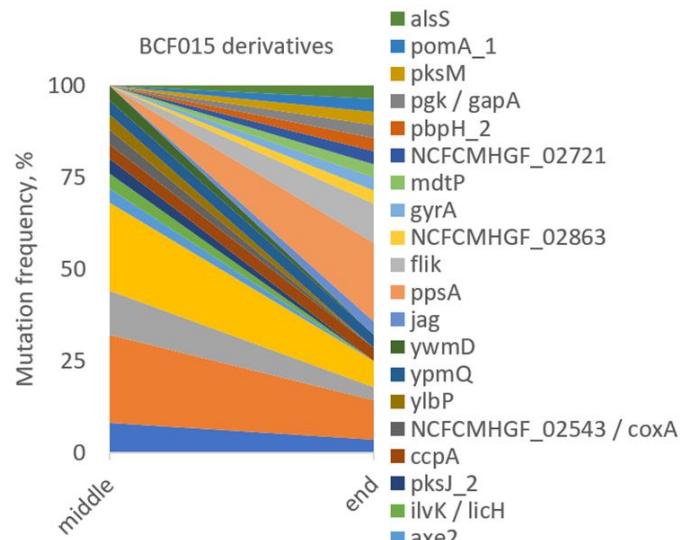
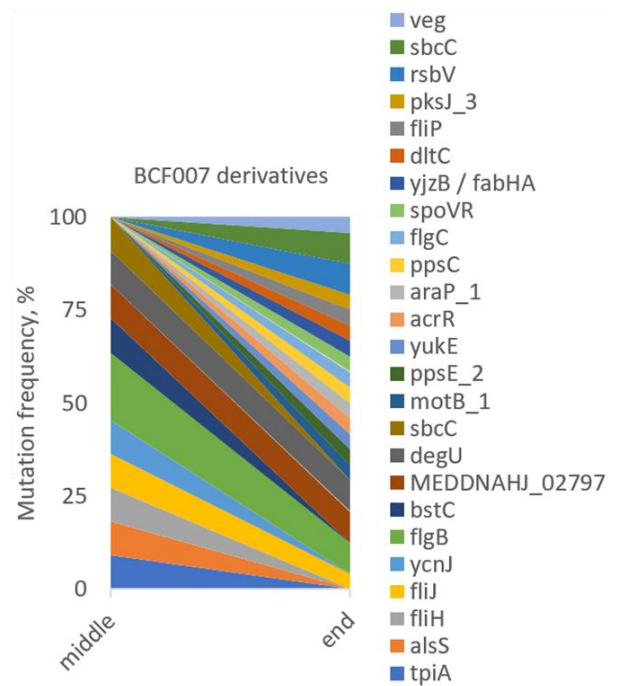
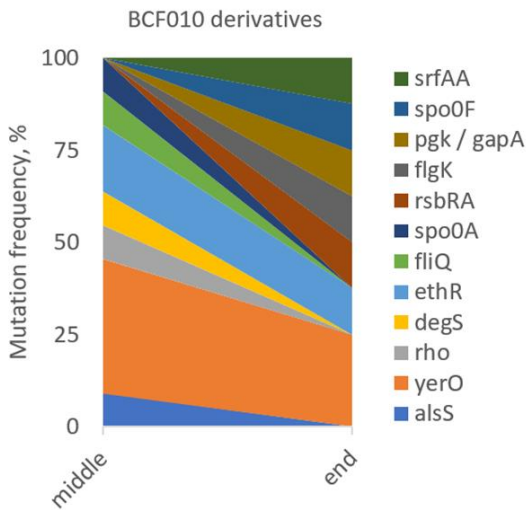
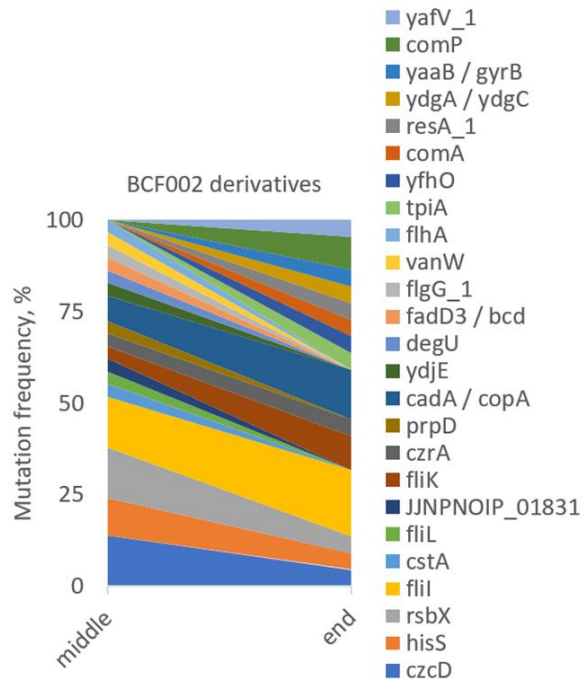
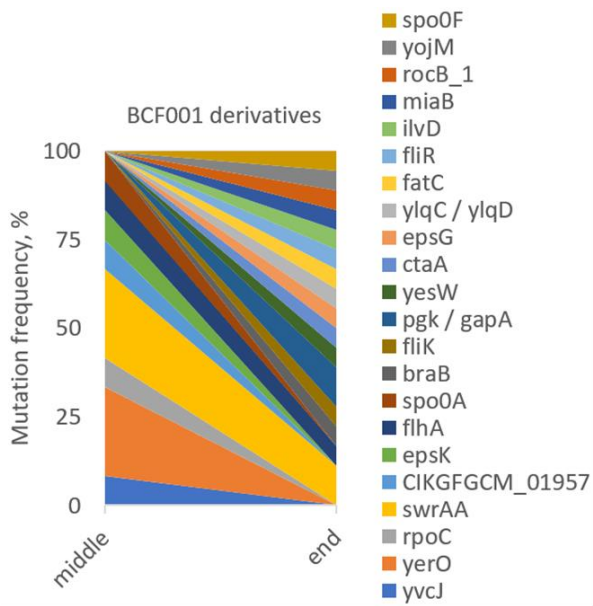


Fig. S 5. Occurrence and persistence of mutations. Genetic changes were analysed in 57 derivatives from co-evolved populations (G, H, I) and control populations (W) derived from the ancestors BCF001, BCF002, BCF007, BCF010 or BCF015 from two timepoints (middle, end).

Table S 4. Non-unique mutations. Mutations occurred in derivatives from the same ancestor or in homologues loci from different ancestors.

Protein	Gene	Occurrences
Sensor histidine kinase ComP	<i>comP</i>	2
HTH-type transcriptional repressor CzrA	<i>czrA</i>	2
Flagellar FljI protein	<i>fliJ</i>	2
hypothetical protein	<i>JJNPNOIP-01831</i>	2
Anti-sigma-B factor antagonist	<i>rsbV</i>	2
Stage 0 sporulation protein A	<i>spo0A</i>	2
Sporulation initiation phosphotransferase F	<i>spo0F</i>	2
Triosephosphate isomerase	<i>tpiA</i>	2
SCO1 protein	<i>ypmQ</i>	2
Acetolactate synthase	<i>alsS</i>	3
Catabolite control protein A	<i>ccpA</i>	3
Central glycolytic genes regulator	<i>cggR</i>	3
HTH-type transcriptional regulator EthR	<i>ethR</i>	3
Flagellar biosynthesis protein FlhA	<i>flhA</i>	3
Plipastatin synthase subunit A	<i>ppsA</i>	3
Nuclease SbcCD subunit C	<i>sbcC</i>	3
Transcriptional regulatory protein DegU	<i>degU</i>	4
Flagellar basal body rod protein FlgB	<i>flgB</i>	4
Response regulator protein GraR	<i>graR-1</i>	4
Histidine--tRNA ligase	<i>hisS</i>	4
Unknown protein	<i>yotI</i>	4
Phosphoglycerate kinase/Glyceraldehyde-3-phosphate dehydrogenase 1	<i>pgk / gapA</i>	4
Swarming motility protein	<i>swrAA</i>	4
Cadmium, zinc and cobalt-transporting ATPase/Copper-exporting P-type ATPase	<i>cadA / copA</i>	5
Cadmium, cobalt and zinc/H(+)-K(+) antiporter	<i>czcD</i>	5
Phosphoserine phosphatase RsbX	<i>rsbX</i>	5
Flagellar-specific ATPase	<i>fliI</i>	8
Flagellar hook-length control	<i>fliK</i>	8
unknown protein	<i>NCFCMHGF-03789</i>	8
Flagellar motor switch protein FliM	<i>fliM</i>	9
Unknown tetR transcriptional regulator	<i>yerO</i>	9
	Total	124

Table S 5. Strains selected for phenotypic characterization.

Ancestor	Strain	Inhib.	Morph.	Tp	Mutated loci
BCF007	G0715-F	-1	1	15	<i>alsS, fliH</i>
	G0730-G	2	1	30	<i>fliJ, araP_1, MEDDNAHJ_02797, ppsC</i>
	I0730-D	2	1	30	<i>flgB, fliP, dltC, pksJ</i>
	W0730-F	2	3	30	<i>degU, rsbV, sbcC</i>
	W0730-H	-1	3	30	<i>degU, rsbV, sbcC, veg</i>
BCF015	G1515-H	1	2	15	<i>fliM, graR_1, axe2, cggR, ilvK → / ← lich, NCFCMHGF_03789</i>
	G1530-B	-1	2	30	<i>fliM, graR_1, cggR, NCFCMHGF_03888, ppsA</i>
	H1530-B	-2	1	30	<i>ccpA, fliK, NCFCMHGF_02863, NCFCMHGF_03789, ppsA, ypmQ</i>
	W1530-G	1	2	30	<i>mdtP, gyrA, NCFCMHGF_02721, pbpH_2, pgk ← / ← gapA, pksM</i>
	W1530-H	-2	2	30	<i>fliM, alsS, ppsA</i>
BCF002	G0215_C	2	2	15	<i>rsbX, czcD, hisS, flil</i>
	H0215_F	2	2	15	<i>czrA, fliK, prpD</i>
	I0215_F	2	2	15	<i>ydjE, cadA ← / ← copA, flil</i>
	I0230-D	1	3	30	<i>comP, cadA ← / ← copA, flil</i>
	I0230-E	1	2	30	<i>cadA ← / ← copA, yafV_1, flil</i>
	W0215-B	2	1	15	<i>degU</i>
	W0215-G	2	2	15	<i>flhA, rsbX</i>
BCF010	H1015-A	-2	2	15	<i>degS, ethR, fliQ</i>
	W1030-A	0	4	30	<i>spo0F, srfAA</i>

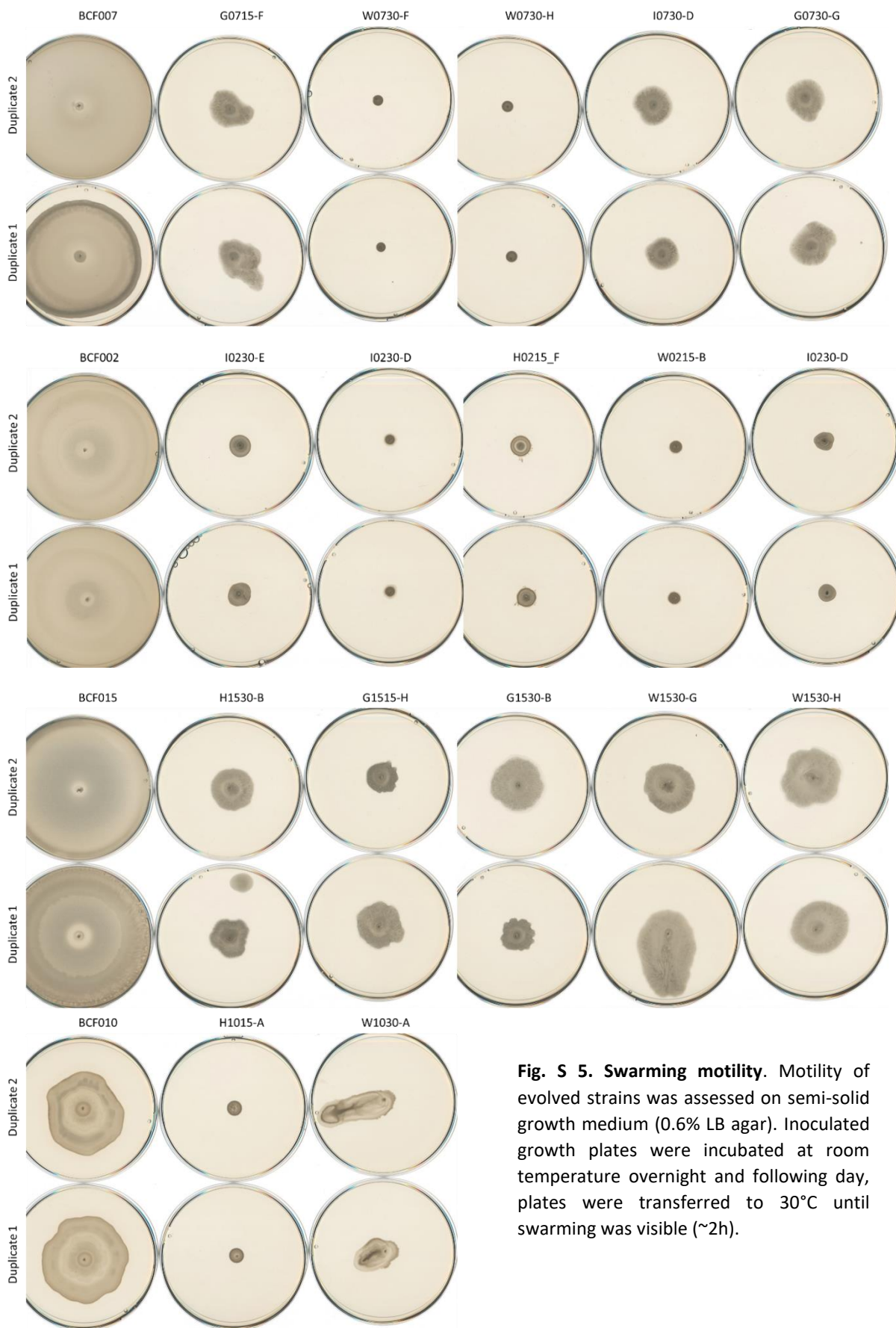


Fig. S 5. Swarming motility. Motility of evolved strains was assessed on semi-solid growth medium (0.6% LB agar). Inoculated growth plates were incubated at room temperature overnight and following day, plates were transferred to 30°C until swarming was visible (~2h).

Table S 6. Mutations related to metal ion homeostasis. Genetic alterations were identified related to uptake and efflux of metal ions.

Ancestor	Pop	Strain	Gene	Protein
BCF002	G02	G0215-C	<i>czcD</i>	Cadmium, cobalt and zinc/H(+)-K(+) antiporter
		G0215-D		
		G0215-F		
		G0215-H		
H02	H0215-F	<i>czrA</i>	HTH-type transcriptional repressor CzrA	
	H0230-A			
I01	I0215-F	<i>cadA</i> ←/← <i>copA</i>	Cadmium, zinc and cobalt-transporting ATPase/Copper-exporting P-type ATPase	
	I0230-D			
	I0230-E			
I0230-F				
W02	W0215-F			
BCF007	H07	H0715-B	<i>bstC</i>	Bacillithiol S-transferase
	I07	I0715-H	<i>ycnJ</i>	Copper transport protein YcnJ

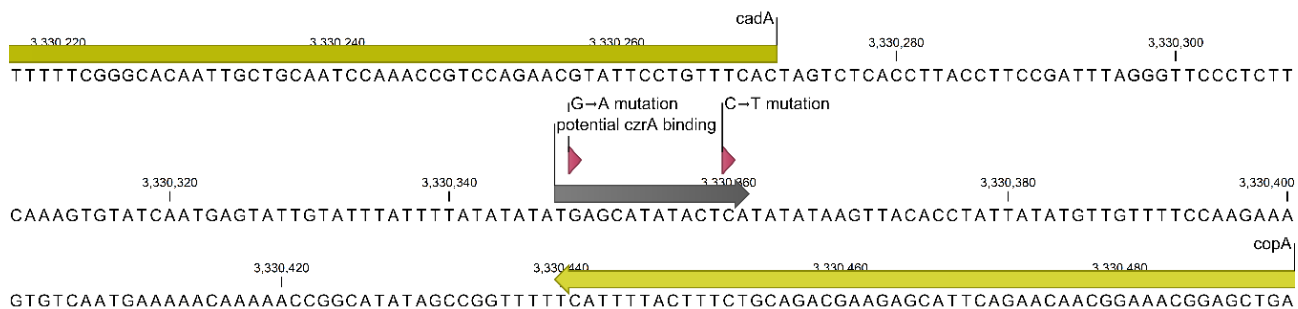


Fig. S 6. Potential CzrA binding site. In the intergenic region of *cadA/copA*, a potential CzrA binding site (grey) was identified that coincided with two acquired substitution mutations (G→A and C→T, red) on the antisense strand in the positions -78/+91 and -89/+80 relative to the open reading frames of *cadA* and *copA* (yellow).

Table S 7. Selected differentially expressed regulons. The transcriptome of *B. subtilis* strains was investigated in response to co-cultivation with *F. culmorum*. *Bacillus* exponential culture was added to pre-grown fungal cultures and co-inoculated for approximately 2h until reaching exponential phase. The differentially expressed genes were identified relative to *Bacillus* control cultures grown in the absence of fungi until exponential phase.

Regulons	Operons/genes	Function	Expression
CcpA repression	<i>levDEFG-sacC</i>	Fructan PTS and utilization	Down
	<i>acoR</i>	Regulation of acetoin utilization	Down
	<i>araABDLMNPQ-abfA</i>	Arabinose utilization	Down
	<i>rbsRDACBK</i>	Ribose ABC transporter and utilization	Down
	<i>licABCH</i>	Lichenan PTS	Down
	<i>gmuBACDREFG</i>	PTS and kinases for utilization of glucomannan	Down
	<i>trePAR</i>	Trehalose PTS and utilization	Down
	<i>ioIABCDEFGHJ</i>	Catabolism of inositol	Down
	<i>yesLMN</i>	Uncharacterized protein, histidine kinase, and uncharacterized transcriptional regulatory	Down
	<i>mleN</i>	Malate-lactate antiporter	Down
	<i>glpFKD, glpTQ</i>	Glycerol uptake and utilization	Up/down
	<i>cccA</i>	Small cytochrome c550 active in respiration	Down
	<i>cwlS</i>	Peptidoglycan hydrolase active in cell separation	Up
	<i>abn2</i>	Arabinan degradation	Up
	<i>resDE</i>	Regulation of aerobic and anaerobic respiration	Up
	<i>cstA</i>	Peptide transporter	Down
	<i>ganSPQAB</i>	Uptake and utilization of galactan	Down
<i>mtlR</i>	Regulation of mannitol utilization	Up	
<i>manR</i>	Regulation of mannose utilization	Down	
<i>bglHP-yxiE</i>	Glucoside uptake and utilization	Down	
<i>rapA-phrA</i>	Control of sporulation initiation	Up	
CcpA activation	<i>ilvBHC-leuABCD</i>	Biosynthesis of branched-chain amino acids	Up

Table S 8. Specialised metabolite-related mutations. Mutations in biosynthetic gene clusters or genes related to regulation thereof appeared in strains derived from different ancestors.

Ancestor	Protein	Gene	Occurrences
BCF007	Polyketide synthase PksJ	<i>pksJ</i>	1
	Plipastatin synthase subunit C	<i>ppsC</i>	1
	Plipastatin synthase subunit E	<i>ppsE</i>	1
	Two-component response regulator	<i>degU</i>	4
BCF015	Polyketide synthase PksJ	<i>pksJ_2</i>	1
	Polyketide synthase PksM	<i>pksM</i>	1
	Plipastatin synthase subunit A	<i>ppsA</i>	6
BCF010	Two-component sensor kinase	<i>degS</i>	1
	Surfactin synthase subunit 1	<i>srfAA</i>	1
Total			17

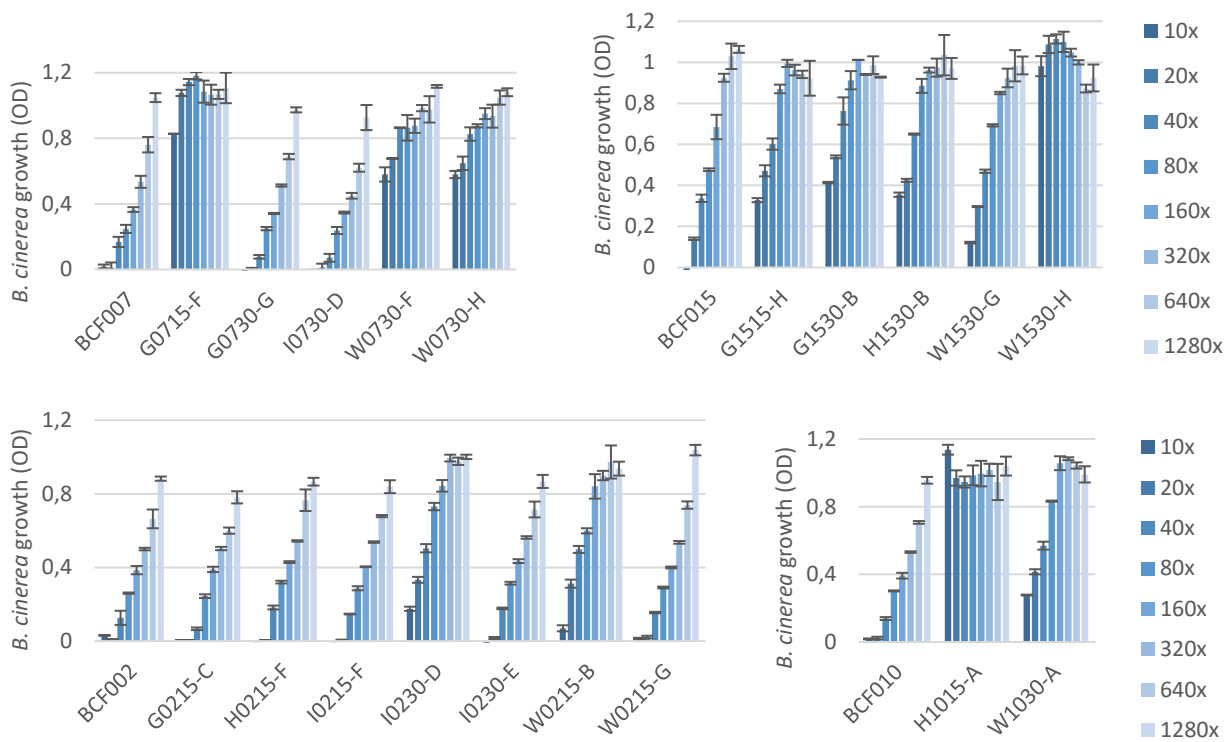


Fig. S 7. Culture supernatant inhibition. The fungal growth in response to addition of culture supernatant dilution series (10-1280x) was evaluated after 5 days incubation by optical density (OD₆₀₀). *Bacillus* cultures were incubated 48 h prior to co-inoculation with fungal spore suspension and addition of bacteriostatic compounds. Fungal spore suspensions were incubated statically at 25°C.

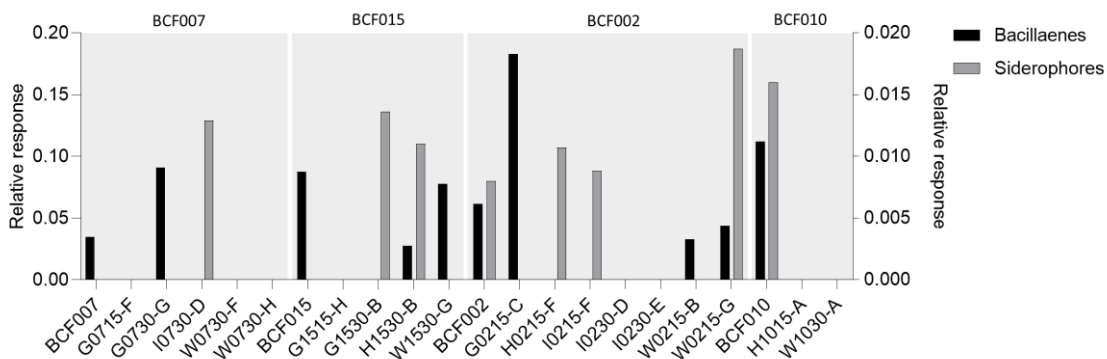


Fig. S 8. Relative amounts of specialised metabolites. Relative amounts of bacillaene and siderophores in culture supernatants of evolved strains from *B. amyloliquefaciens* BCF007, *B. velezensis* BCF015, *B. subtilis* BCF002 and BCF010.

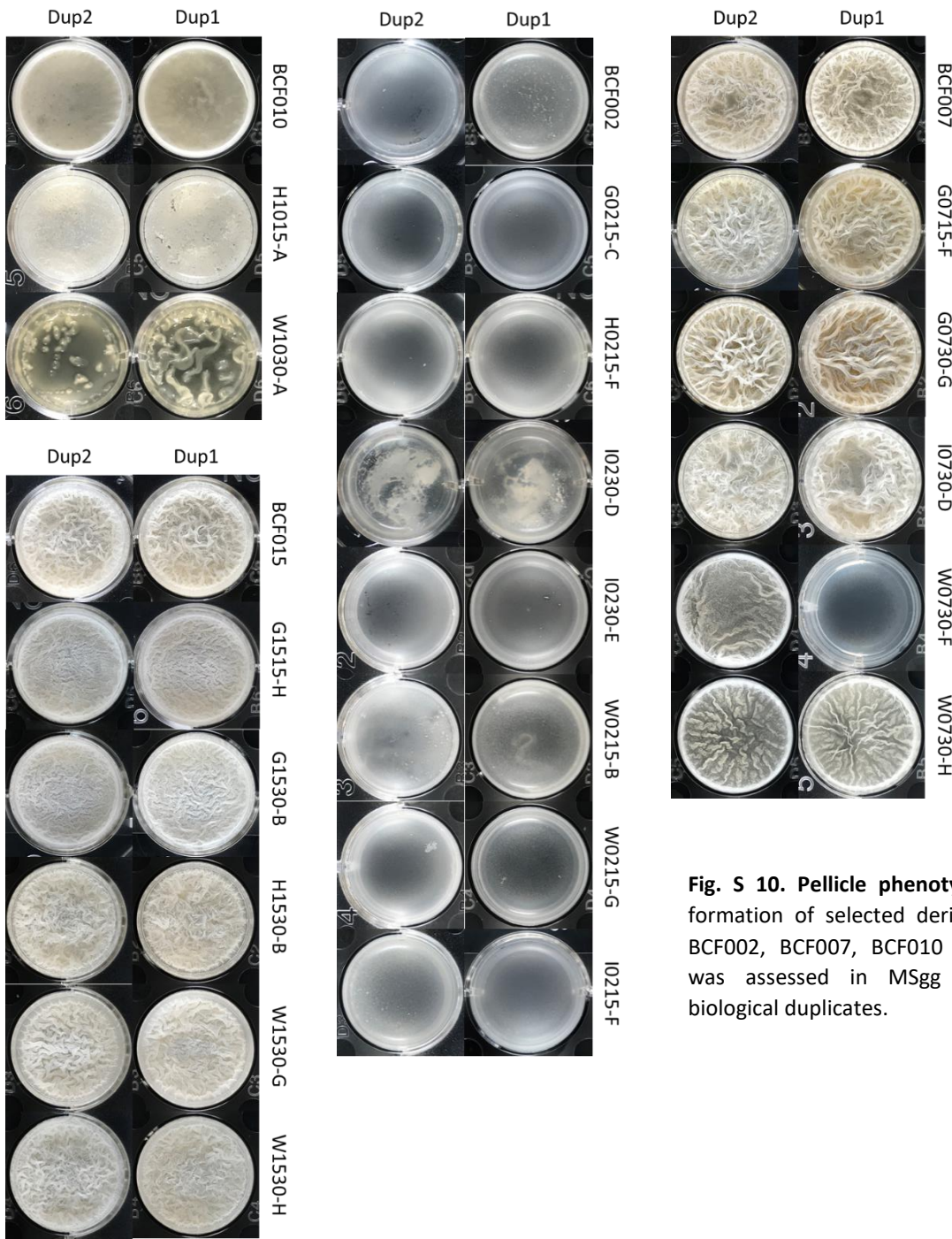


Fig. S 10. Pellicle phenotypes. Pellicle formation of selected derivatives from BCF002, BCF007, BCF010 and BCF015 was assessed in MSgg medium in biological duplicates.

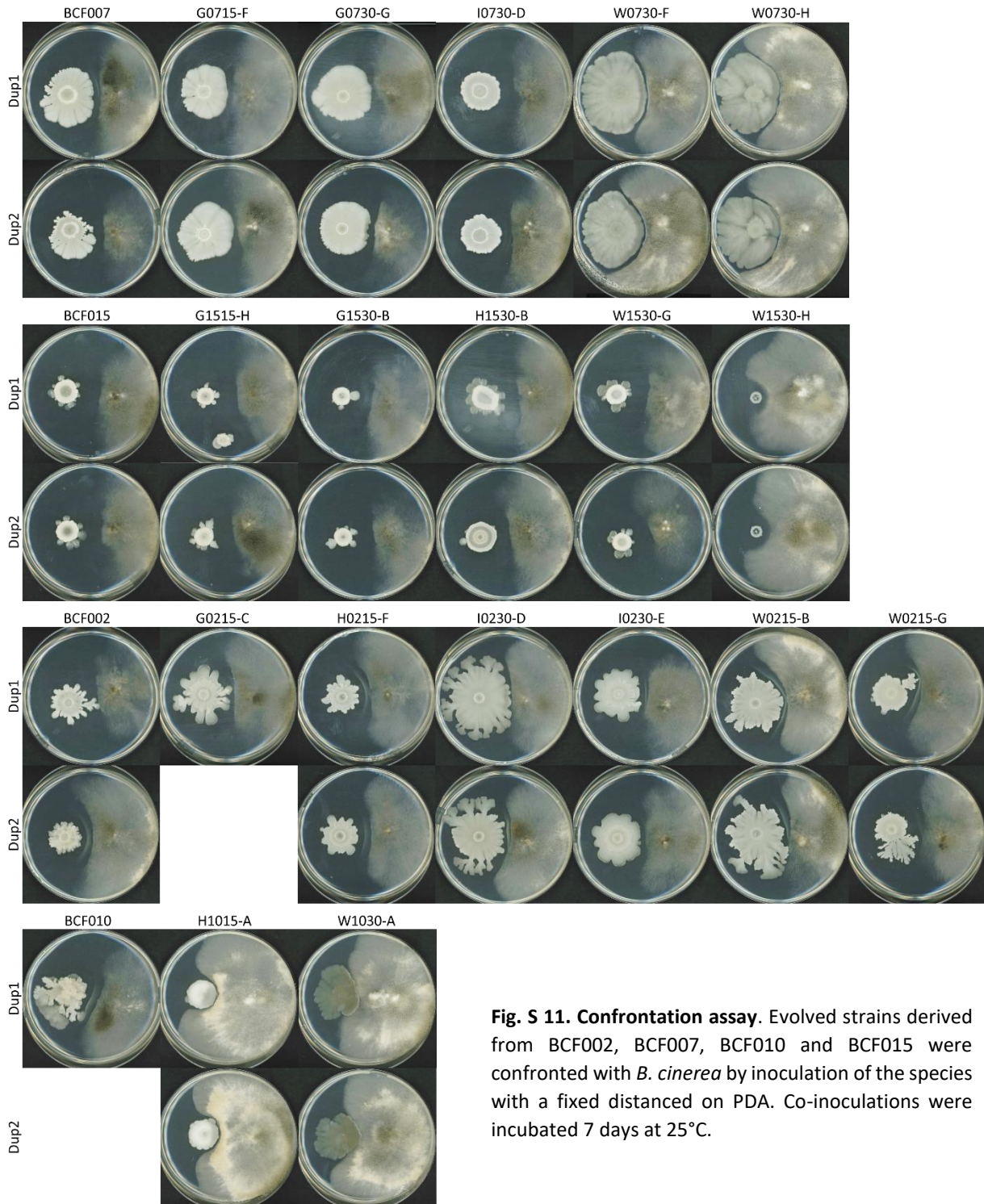


Fig. S 11. Confrontation assay. Evolved strains derived from BCF002, BCF007, BCF010 and BCF015 were confronted with *B. cinerea* by inoculation of the species with a fixed distance on PDA. Co-inoculations were incubated 7 days at 25°C.

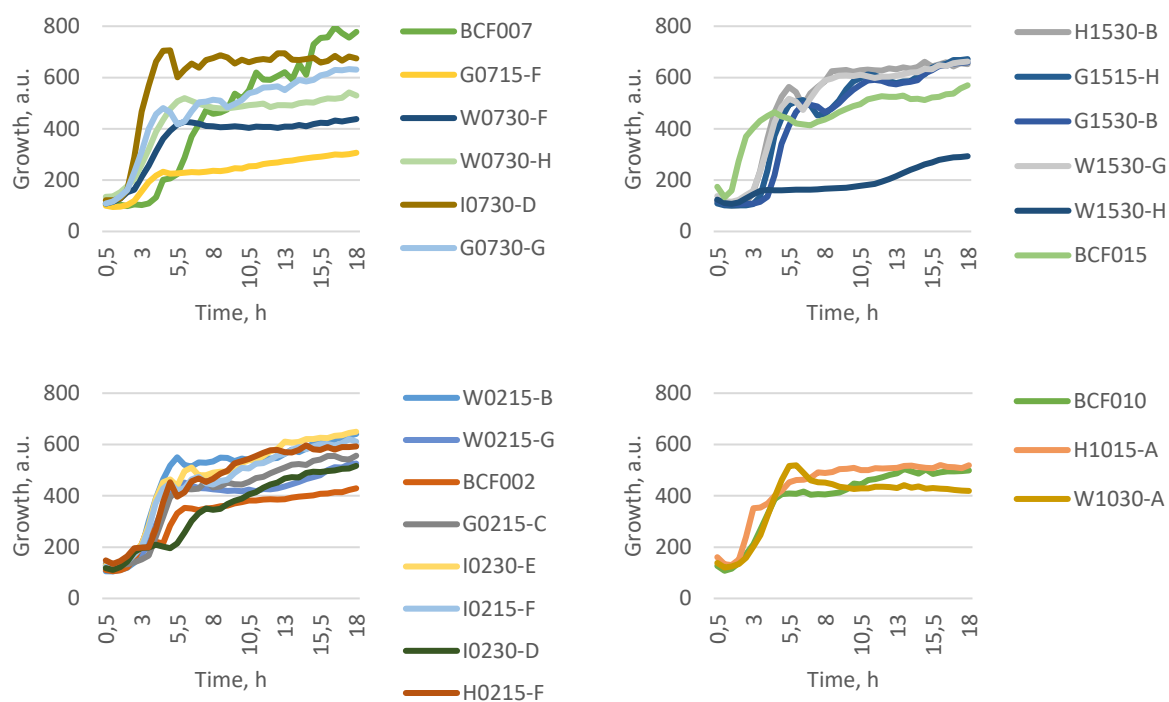


Fig. S 12. Growth of cultures for protease activity. Strains were cultured in PDB medium at 37°C for 18h and pelleted to collect supernatants for protease activity assays. Strains with poor growth were not included in the analysis (G0715-F, W1530-H).

Table S 9 Codon usage in *B. subtilis*. The synonymous mutations in *ppsA* leading to different codons and their estimated frequency per thousand.

Gene	Amino acid	Codon change	Frequency	Derivatives
<i>ppsA</i>	Glutamic acid (E)	GAA→GAG	48.1 → 22.6	H1530-B
<i>ppsA</i>	Leucine (L)	CUC→CUU	10.7 → 21.8	H1530-B, W1530-H
<i>ppsA</i>	Serine (S)	UCA→UCG	14.6 → 6.5	G1530-B, H1530-B, W1530-H

		Sheet	Helix	Sheet	Helix	Sheet	
W0215B	MTKVNIVII	DDHQLFREGVKRILDFEPTFEVVAEGDDGDEAARIVEHYHPDVVIM					60
BCF002	MTKVNIVII	DDHQLFREGVKRILDFEPTFEVVAEGDDGDEAARIVEHYHPDVVIM					60
VraR	--TIKVLV	DDHEMVRIGISSYLSIQSDIEVVGEGASGKEATAKAHELKPDILML					58
	**::.* *:. * : .***.** .*** ... :*:::**: *					
		Helix	Sheet	Helix	Sheet	Helix	
W0215B	NVNGVEATKQLVELYPESKVIIL	SIHDDENYVTHALKTGARGYLLKEMDAGTLIEAVKV					120
BCF002	NVNGVEATKQLVELYPESKVIIL	SIHDDENYVTHALKTGARGYLLKEMDADTLIEAVKV					120
VraR	DMDGVEATTQIKKDL	PQIKVLMISFIEDKEVYRALDAGVDSYILKTTSAKDIADAVRKT					118
		:::*****.*: : * : **::*:. . : : * : **.*. .***. * : : **:					
		Sheet					
W0215B	AEGGSYLHPKVTHNLVNEFRR	LATSGVSAHPQHEVYPEIRRPLHILTRRECEVLQMLADG					180
BCF002	AEGGSYLHPKVTHNLVNEFRR	LATSGVSAHPQHEVYPEIRRPLHILTRRECEVLQMLADG					180
VraR	SRGESVFEPEVLVKMRNR	MKKR-----AELYEMLTEREMEILLIAK					161
		::* * :.*:* : : *::: . .***.** *:* :.*:					
		DNA binding					
W0215B	KSNRGIGESLFISEKTVKNHVS	NILQKMNVDRTQAVVVAIKNGWVEMR					229
BCF002	KSNRGIGESLFISEKTVKNHVS	NILQKMNVDRTQAVVVAIKNGWVEMR					229
VraR	YSNQEI	ASASHITIKTVKTHVSNILSKLEVQDR					208
		** : *... .* : ****.*****.*:*.*****: *::: . :					

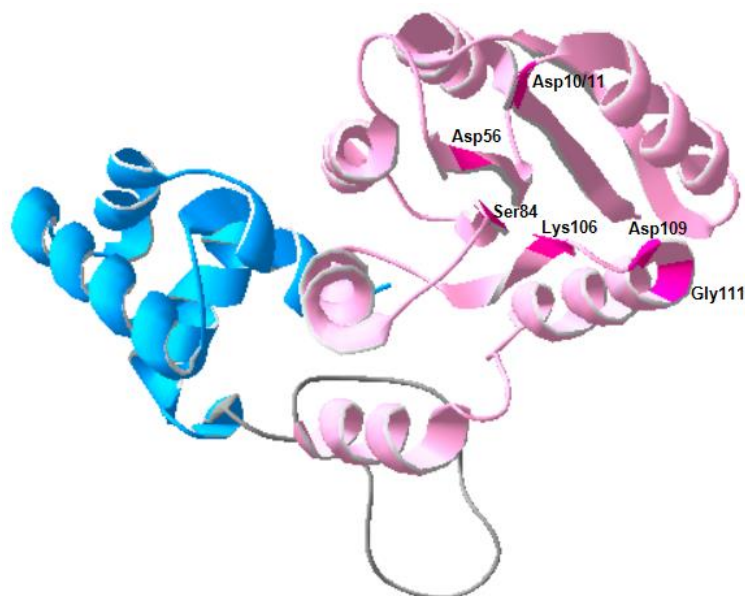


Fig. S 13. DegU alignment and structure model. Top) DegU protein sequence from W0215-B and its ancestor *B. subtilis* BCF002 were aligned with VraA from *S. aureus*. The substituted amino acid (Asp111Gly) is indicated with an arrow, residues participating in the active site in the receiver domain are boxed in green and the sequence motifs are indicated above sequence. **Bottom)** Protein model of W0215-B DegU. The 3D structure of the DegU protein was modelled based on the resolved structure of VraR from *S. aureus* in Swiss Model. Important amino acids: metal binding sites (Asp10-11), conserved interaction site (Ser84), essential residue to conformational changes (Lys106) and phosphorylation site (Asp56), were highlighted in SwissPdbViewer to visualize proximity to the mutated residue Gly111. The receiver domain is indicated in pink, while the DNA binding domain is indicated in blue.